

**BASE- AND VISIBLE LIGHT-PROMOTED ACTIVATION OF ARYL
HALIDES UNDER TRANSITION-METAL-FREE CONDITIONS:
APPLICATIONS AND MECHANISTIC STUDIES**

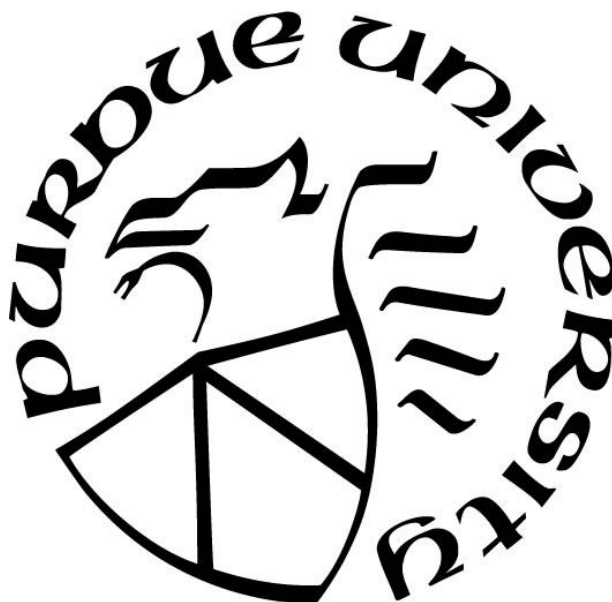
by
Lei Pan

A Dissertation

Submitted to the Faculty of Purdue University

In Partial Fulfillment of the Requirements for the degree of

Doctor of Philosophy



Department of Chemistry and Chemical Biology at IUPUI

Indianapolis, Indiana

December 2021

THE PURDUE UNIVERSITY GRADUATE SCHOOL
STATEMENT OF COMMITTEE APPROVAL

Dr. Sébastien Laulhé, Chair

Department of Chemistry and Chemical Biology

Dr. Eric Long

Department of Chemistry and Chemical Biology

Dr. Martin J. O'Donnell

Department of Chemistry and Chemical Biology

Dr. Mingji Dai

Department of Chemistry and Center for Cancer Research, PUWL

Approved by:

Dr. Eric Long

To my parents

This work would not have been possible without your unwavering love and support.

ACKNOWLEDGMENTS

First and foremost, I would like to express my sincere appreciation to my supervisor, Dr. Sébastien Laulhé, for accepting me into his group, and his guidance and dedication. It was an honor to be his first PhD student. I thank him for providing me opportunities for chemistry research. Without his guidance and persistent help this dissertation would not have been possible.

I also wish to thank my committee members, Dr. Martin O'Donnell, Dr. Eric Long, Dr. Mingji Dai and my former advisor Dr. Haibo Ge who have been more than generous with their expertise and precious time.

I acknowledge the former and current members of my the research group for their many helpful suggestions and comments on the studies performed for this dissertation. I truly enjoyed my time working with them. In addition, I thank my friends and relatives. They have helped me to solve all kinds of problems and provided me great support in life and study.

Finally, I would like to thank my parents. They have always been there cheering me up and supporting me in every possible way.

TABLE OF CONTENTS

LIST OF TABLES.....	7
LIST OF FIGURES.....	8
LIST OF SCHEMES.....	9
ABSTRACT.....	11
CHAPTER 1. A REVIEW OF PHOTO-INDUCED TRANSITION-METAL-FREE ACTIVATION OF ARYL HALIDES UNDER CATALYST-FREE CONDITIONS.....	12
1.1 Introduction.....	12
1.2 UV-Induced Activation of Aryl Halides.....	16
1.3 Base-Promoted Activation of Aryl Halides.....	20
1.3.1 Early Examples: Base-Promoted Heat-Induced Activations.....	20
1.3.2 Base-Promoted Photo-Induced Activation of Aryl Halides.....	22
1.4 Conclusions.....	30
1.5 References.....	31
CHAPTER 2. DIMSYL ANION ENABLES VISIBLE-LIGHT-PROMOTED CHARGE TRANSFER IN CROSS-COUPPLING REACTIONS OF ARYL HALIDES.....	35
2.1 Introduction.....	35
2.2 Results and Discussion.....	37
2.3 Summary.....	46
2.4 Acknowledgements.....	47
2.5 Experimental.....	47
2.6 References.....	64
CHAPTER 3. BASE-MEDIATED PHOTO-INDUCED BORYLATION AND PHOSPHONATION OF ARYL HALIDES.....	67
3.1 Introduction.....	67
3.2 Results and Discussion.....	68
3.3 Summary.....	75
3.4 Experimental.....	75
3.5 References.....	84

CHAPTER 4. MILD PHOTO-INDUCED PHOSPHONATION OF ARYL IODIDES USING DIPEA AND TRIALKYL PHOSPHITES.....	87
4.1 Introduction.....	87
4.2 Results and Discussion.....	88
4.3 Summary.....	93
4.4 Experimental.....	94
4.5 References.....	105
CHAPTER 5. PHOTOCHEMICAL REGIOSELECTIVE C(SP ³)–H AMINATION OF AMIDES USING <i>N</i> -HALOIMIDES.....	107
5.1 Introduction.....	107
5.2 Results and Discussion.....	109
5.3 Summary.....	119
5.4 Acknowledgements.....	119
5.5 Experimental.....	119
5.6 References.....	134
APPENDIX A. NMR SPECTRA.....	137
APPENDIX B. GC-MS SPECTRA.....	314
APPENDIX C. COMPUTATIONAL CALCULATIONS.....	324
PUBLICATIONS.....	349

LIST OF TABLES

Table 2.1. Optimization of reaction conditions ^a	38
Table 3.1. Optimization of reaction conditions. ^a	69
Table 4.1. Optimization of reaction conditions. ^a	89
Table 5.1. Optimization of reaction conditions. ^a	109

LIST OF FIGURES

Figure 2.1. Bioactive drugs and polymer materials.....	35
Figure 2.2. The influence of different bases.....	60
Figure 2.3. The influence of the equivalence of KO ^t Bu.....	60
Figure 2.4. The combinations of 2.1a and 2.2a.....	61
Figure 2.5. The combinations of 2.1a, 2.2a and KO ^t Bu.....	62
Figure 2.6. The influence of X in aryl halides.....	62
Figure 2.7. The influence of NaH to 4-iodoanisole after 1 h activation at 50 °C.....	63
Figure 2.8. The combinations of 2.1a, KO ^t Bu in DMSO.....	63
Figure 4.1. Examples of Aromatic Phosphonates in Pharmaceutical Agents.....	87
Figure 4.2. Proposed reaction mechanism.....	93
Figure 5.1. Representative biologically active compounds containing amido aminal functional group.....	107

LIST OF SCHEMES

Scheme 1.1. Early ways to activate aryl halides.....	13
Scheme 1.2. Traditional transition-metal-catalyzed cross-coupling reactions.....	13
Scheme 1.3. The merger of transition metal catalysis and photocatalysis.....	14
Scheme 1.4. Transition-metal-free organic photocatalysts cross-coupling reactions under visible light.....	15
Scheme 1.5. Iodination of aryl halides under UV irradiation.....	16
Scheme 1.6. Borylation of aryl halides under UV.....	17
Scheme 1.7. The synthesis of aryl trimethylstannanes from aryl halides under UV.....	18
Scheme 1.8. Transition-metal-free arylation of pyrimidines under UV.....	19
Scheme 1.9. Catalyst-free aminosulfonylation of aryl halides under UV.....	20
Scheme 1.10. Traditional transition-metal-free activation of aryl halides.....	22
Scheme 1.11. Arylation of aryl halides by using KO ^t Bu.....	23
Scheme 1.12. Photo-induced direct C–H arylation of alkenes.....	24
Scheme 1.13. Phosphinylation of heteraryl halides by using KO ^t Bu.....	25
Scheme 1.14. Transition-metal-free cross-coupling of aryl halides with H-phosphonates.....	26
Scheme 1.15. KO ^t Bu-promoted dehalogenation of aryl halides.....	27
Scheme 1.16. Visible light-promoted intermolecular charge transfer between the thiolate-aryl halides.....	28
Scheme 1.17. Synthesis of S-aryl dithiocarbamates by using Cs ₂ CO ₃ under CFL.....	29
Scheme 1.18. Synthesis of thiochromane derivatives.....	30
Scheme 2.1. Current and proposed approaches to generate diaryl sulfides and selenides.....	37
Scheme 2.2. Aryl halide and aryl disulfide scope. ^a	40
Scheme 2.3. Aryl diselenide and ditelluride scope. ^a	41
Scheme 2.4. Selected UV-Vis experiments.....	43
Scheme 2.5. Control experiments and calculated EDA complex.....	44
Scheme 2.6. Proposed mechanism and Ongoing work.....	46
Scheme 3.1. Current and proposed approaches to generate aryl boronic esters and aryl phosphonate esters.....	68

Scheme 3.2. Substrate scope of aryl halides.....	71
Scheme 3.3. Scope of the phosphonation reaction.....	72
Scheme 3.4. Control Experiments.....	73
Scheme 3.5. Proposed mechanism and EDA complex calculation.....	74
Scheme 4.1. Approaches for C-P Bond Formation.....	88
Scheme 4.2. Substrate scope. ^a	92
Scheme 4.3. Control experiments.....	93
Scheme 5.1. A. Current methods to access the amido aminal functional group require the use of catalysts and strong oxidants at high temperatures. B. Presented photoexcited C–H activation under mild reaction conditions.....	108
Scheme 5.2. Amination of amides with <i>N</i> -Bromophthalimide. ^{a,b}	111
Scheme 5.3. Amination of amides by <i>N</i> -halosaccharins. ^{a,b}	112
Scheme 5.4. Amination of Boc-protected amines. ^{a,b}	114
Scheme 5.5. A. radical trapping experiments. B. Control experiments. C. Proposed mechanism.....	116
Scheme 5.6. UV-vis spectroscopic measurements.....	117
Scheme 5.7. Energy reaction pathways (kCal/mol) of <i>N</i> -bromophthalimide 5.1a with <i>tert</i> -butoxide through computational simulations using B3LYP/6-311+G(d,p)/MWB28 (Br) level of theory.....	118
Scheme 5.8. Additional substrate scope.....	122

ABSTRACT

Aromatic rings are universal motifs in natural products, pharmaceuticals, agrochemicals, and wide variety of organic materials. Aromatic halides are widely used as synthetic precursors in all these applications. Therefore, tremendous effort has been devoted to activate aryl halides in the past decades. The common methods to activate aryl halides require the use of transition-metals either in the form of Grignard reagents or through the use of transition-metal catalysis. Over the past decade, photoredox catalysis has attracted significant attention as a cogent tool to develop greener synthetic processes and enable new molecular activation pathways under mild conditions. The most common of these approaches uses a photoredox/nickel dual catalytic cycle. While this technology has greatly expanded the toolbox of organic chemists, this method still requires expensive rare-metal-based catalysts. Herein, we present a series of visible light-induced methods that are transition-metal-free. These new base-promoted transformations and their mechanistic work will be discussed in the following order:

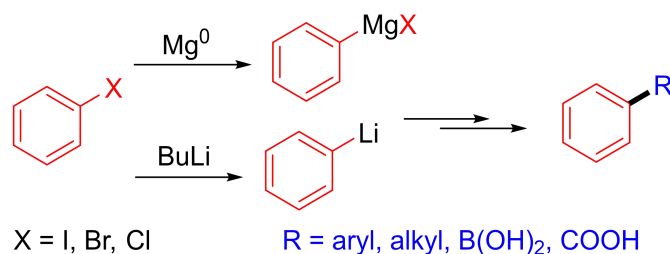
We will first present our discovery that the dimsyl anion enables visible-light-promoted charge transfer in cross-coupling reactions of aryl halides. This work was applied to the synthesis of unsymmetrical diaryl chalcogenides. This method has a broad scope and functional group tolerance. An electron-donor-acceptor (EDA) complex between a dimsyl anion and the aryl halide is formed during the reaction and explains the observed aryl radical reactivity observed. Then, a visible-light-induced borylation and phosphorylation of aryl halides under mild conditions was developed. Inspired by the mechanistic breakthroughs observed in the previous work. The mechanism of this reaction also involves an aryl radical that is presumed to be formed also via an EDA complex. In other work, a photo-induced phosphonation of ArI using *N,N*-diisopropylethylamine (DIPEA) and trialkyl phosphites was developed. This method uses very mild conditions, which allowed the preparation a wide variety of functionalized aromatic phosphonates derivatives, including natural products and medicinal compounds. Finally, a photochemical amination of amides was developed via a C(sp³)-H bond functionalization process under visible light irradiation. This reaction showed good functional group compatibility without the use of external radical initiators, strong oxidants, or heat source. An EDA complex between *N*-bromophthalimide and LiOtBu is formed during the reaction.

CHAPTER 1. A REVIEW OF PHOTO-INDUCED TRANSITION-METAL-FREE ACTIVATION OF ARYL HALIDES UNDER CATALYST-FREE CONDITIONS

1.1 Introduction

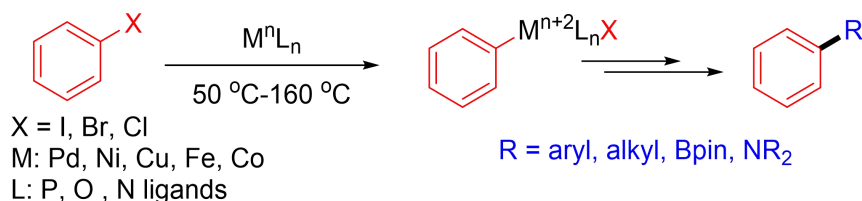
Aromatic rings are universal motifs in natural products ranging from endogenous neurotransmitters (serotonin and dopamine) to vitamins (riboflavin, tocopherol, and phyloquinone). A recent analysis of the database from Pfizer, AstraZeneca, and GlaxoSmithKline showed that 99% of over 3,500 compounds explored for medicinal purposes contained at least one aromatic moiety.^{1a} In addition, aromatic rings are the most frequently used rings in small molecule drugs listed in the FDA Orange Book.^{1b} Aromatic rings are also important motifs in the material sciences, such as organic electrode materials, due to their ultra-stable configurations with highly delocalized sp^2 -hybridized electrons.^{1c} The appeal of aromatic systems in medicinal chemistry stems from the rigid scaffolds they generate as well as the many interactions they create with biological systems through π - π , π -cation, and π -anion interactions.² Finally, aromatic rings benefit from enormous methods and synthetic strategies that allow for their straightforward modifications, either through traditional electrophilic aromatic substitutions or through cross-coupling reactions.³ Compared to selective activation of C-H bonds, which need the additional steps of installing and removing directing groups, prefunctionalization of the aromatic ring as an aryl halides is much easier and leads to regioselective functionalization. As a result, directly activating C-X in organic synthesis, pharmaceuticals, agrochemicals, and polymers remains mainstream.

Early methods for the activation of aryl halides require stoichiometric amounts of magnesium to generate the corresponding Grignard reagents, or the use of highly reactive *n*-butyl lithium to generate organolithium reagents (Scheme 1.1). Beyond the environmental implications of using large quantities of metals to activate aryl halides using these approaches, a major disadvantage of Grignard and organolithium reagents come from their high reactivity, limited selectivity, corrosivity, flammability and their sensitivity towards moisture, which makes scalability problematic.⁴



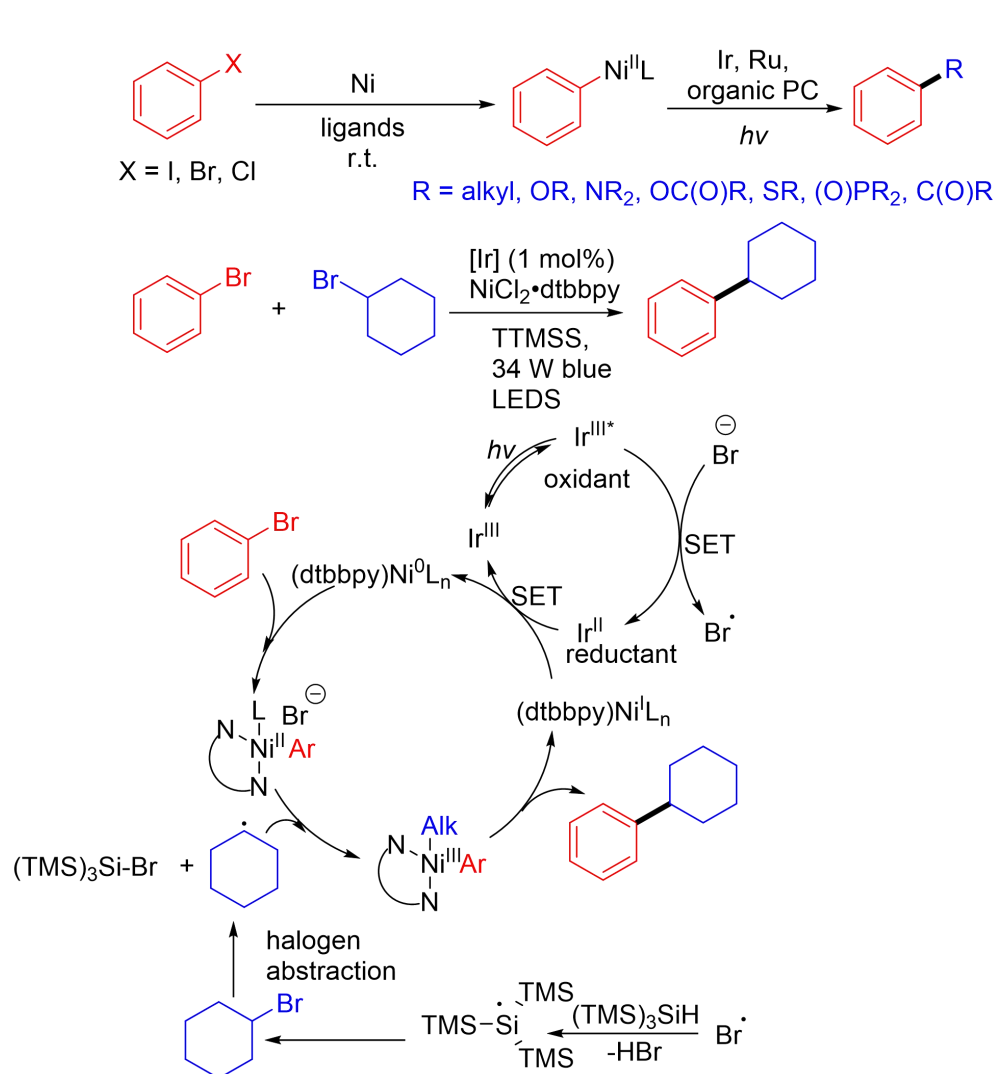
Scheme 1.1. Early ways to activate aryl halides.

Development of transition-metal-catalyzed methods enabled a major transformation in the activation of aryl halides. These methods avoid the use of stoichiometric amounts of metals and significantly improved functional group compatibility compared to Grignard and organolithium reagents. Importantly, these transition-metal-catalyzed cross-coupling reactions enabled facile $\text{C}(\text{sp}^2)\text{--C}(\text{sp}^2)$ bond formations and a major expansion in the synthesis of biaryl compounds. Many reviews comprehensively summarize transition-metal-catalyzed cross-coupling reactions using metals such as Pd, Cu, Ni, Fe, and Co (Scheme 1.2).⁵ Of particular interest, palladium-catalyzed transformations revolutionized the activation of aryl halides. The Suzuki-Miyaura and the Negishi cross-coupling reactions are one of the most important and most cited methodologies in medicinal chemistry,^{6d} and these discoveries awarded Drs. Suzuki, Negishi, and Heck the Nobel Prize in Chemistry in 2010.⁶



Scheme 1.2. Traditional transition-metal-catalyzed cross-coupling reactions.

Transition-metal-catalyzed reactions still, however, have limitations and disadvantages that need to be tackled. Firstly, most transition-metal catalysts, and their required structurally distinct ligands, are very expensive. Secondly, all metals have some intrinsic toxicity and it is problematic to remove trace amounts of catalyst residues from reaction mixtures in pharmaceutical compounds.⁷ Additionally, many transition-metal catalysts are usually sensitive to oxygen and moisture, which requires special manipulation and reaction conditions.⁸ Moreover, most reactions need to be performed under harsher conditions (50–160 °C).

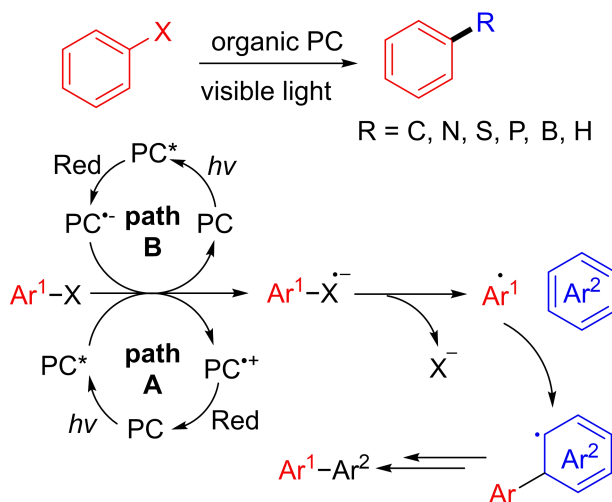


Scheme 1.3. The merger of transition metal catalysis and photocatalysis.

Recently, the merger of transition-metal catalysis and photocatalysis has appeared as a new, highly enabling synthetic methodology due to its mild reaction conditions (Scheme 1.3).⁹ This merger tolerates a wide range of functional groups, and allows direct coupling of non-traditional nucleophilic partners through radical mechanisms. Some of these transformations can also be achieved using only metal photocatalysts.¹⁰ However, the importance of ruthenium (>\$151/g Sigma Aldrich) and iridium polypyridyl photocatalysts (> \$1500/g Sigma Aldrich) is diminished by their extreme high costs, potential toxicity, and scarcity.¹¹ Indeed, large consumption of transition-metals around the world and difficulty to dispose of them does not meet requirements of sustainable development, with current estimates indicating that rare metals, such as Rh, Ir, Pd and Pt, may become very scarce long before petroleum.¹² Therefore, the development of mild

transition-metal-free alternative cross-coupling methodologies are significant in academia and industry.

While these transition-metal-based methods involve oxidative addition of the metal into the C–X bond, more recently, a radical pathway for the activation of aryl halides has been gaining traction. In this approach, a photocatalyst, often organic-based, is used to reduce aryl halides under visible-light and generate a reactive aryl radical. A large number of organic photoredox catalysts have been exploited in photoredox-catalyzed radical-mediated C–X bond cleavage reactions.¹³ In these processes, photocatalysts donate an electron to the aryl halide through a single electron transfer (SET) and generate an aryl radical anion. After loss of the halogen, an aryl radical is formed that can react with a wide variety of coupling partners (Scheme 1.4). Compared to the UV light irradiation pathway, the excited state of the photocatalysts or photocatalyst radical anions would act as the electron donor. However, most of the organic photocatalysts required for these transformations are moisture sensitive, air sensitive, expensive, and are difficult to synthesize and store.



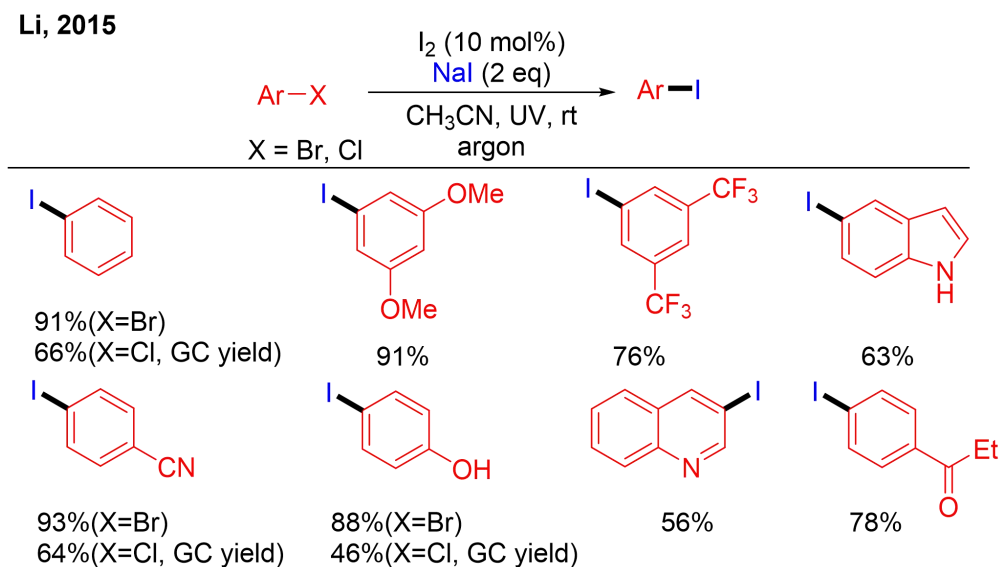
Scheme 1.4. Transition-metal-free organic photocatalysts cross-coupling reactions under visible light.

Performing aryl halide activations under transition-metal-free conditions and in the absence of photocatalysts have been significantly less studied. Development of such methods could improve the environmental footprint of these reactions, while reducing costs. For these reasons, our focus has been placed in the study and development of methods that use commercially available bases in presence of light irradiation to activate aryl halides.

1.2 UV-Induced Activation of Aryl Halides

Early methods focused on cleavage of the aryl halides using UV-light irradiation to generate aryl radicals in the absence of catalysts.¹⁴ Aryl halides may dissociate homolytically to generate aryl and halide radicals. In other cases, the aryl radical is generated through a $S_{RN}1$ mechanism, in which a photo-induced electron transfer from the anion of the nucleophile, or the base, is donated to the aryl halide, forming an aryl halide radical anion. Subsequently, the aryl halide radical anion cleaves to generate the aryl radical and the halide anion. The reactive aryl radical intermediate can then couple with the nucleophile to provide the target molecule.

In 2015, the Li group reported a photo-induced transition-metal-free iodination of aromatic bromides and chlorides under mild conditions (Scheme 1.5).^{14a} Functionalized aryl iodides are very valuable reagents in organic synthesis due to their high reactivity, which makes them easy to further modify through cross-coupling transformations. This iodination method was also applied to vinyl halides starting materials. Iodine (I_2) catalyst was not necessary for the transformation to occur but the addition of 10 mol% I_2 increased yields. Given the strength of the UV irradiation, a mechanism involving the light-induced homolytic cleavage of the C–X (X = Br or Cl) bonds of aryl halides was proposed as the initiating step to form aryl radicals.

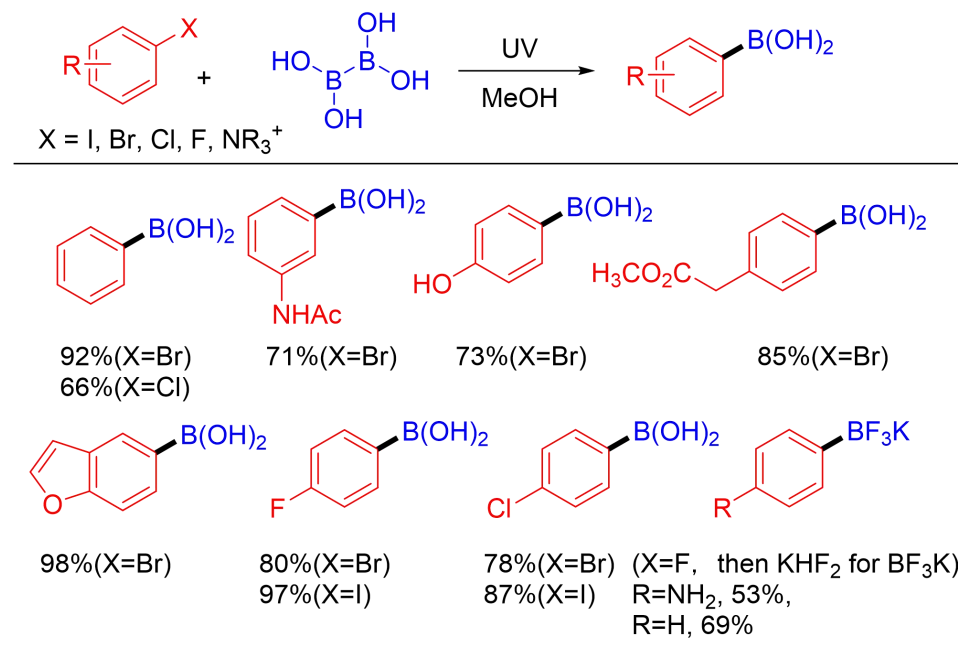


Scheme 1.5. Iodination of aryl halides under UV irradiation.

In 2016, Larionov and coworkers reported a simple, metal- and additive-free, photo-induced borylation of haloarenes (Scheme 1.6).^{14b} This method proceeded in methanol with a

wide variety of aryl halides including aryl iodides, bromides, chlorides, electron-rich fluorides, as well as aryl ammonium salts. This borylation method has a broad scope and functional group tolerance. Similarly to Li's work, the Larionov group proposed the formation of an aryl radical through the homolytic cleavage of the C–X bond.

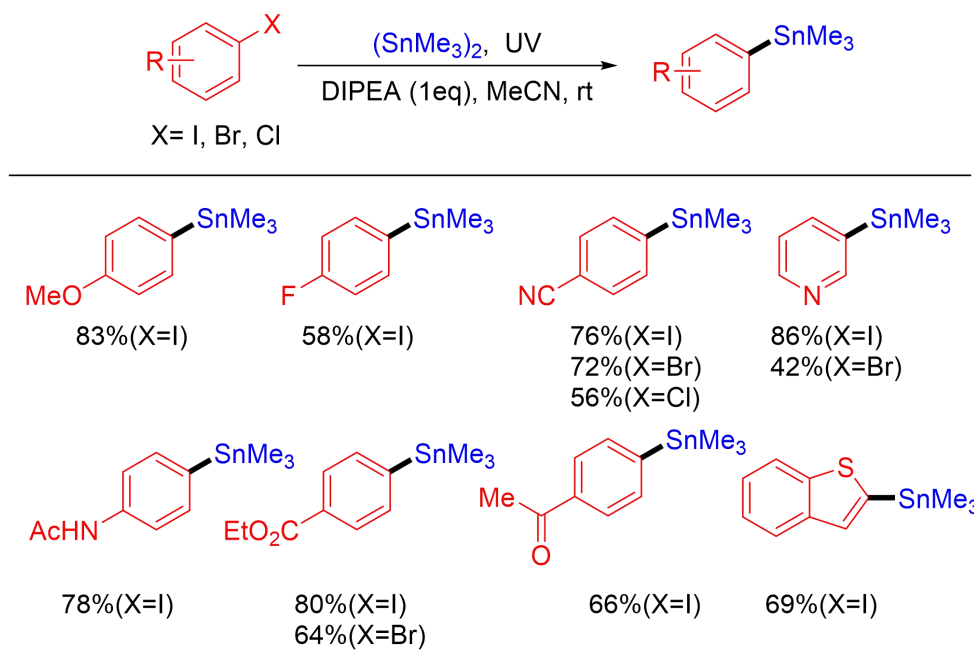
Larionov, 2016



Scheme 1.6. Borylation of aryl halides under UV.

In the same year, the Li group discovered a transition-metal-free photochemical method to synthesize aryl trimethylstannanes with broad functional group tolerance, mild reaction conditions and short reaction times (Scheme 1.7).^{14c} A photo-initiated radical chain mechanism was proposed based on preliminary mechanistic studies. The excited state of the aryl iodides may be rendered by UV light and then undergo homolytic C–I bond cleavage to generate the aryl radical and an iodine atom radical. Then aryl radicals may react with hexamethyldistannane to obtain the stannylation product.

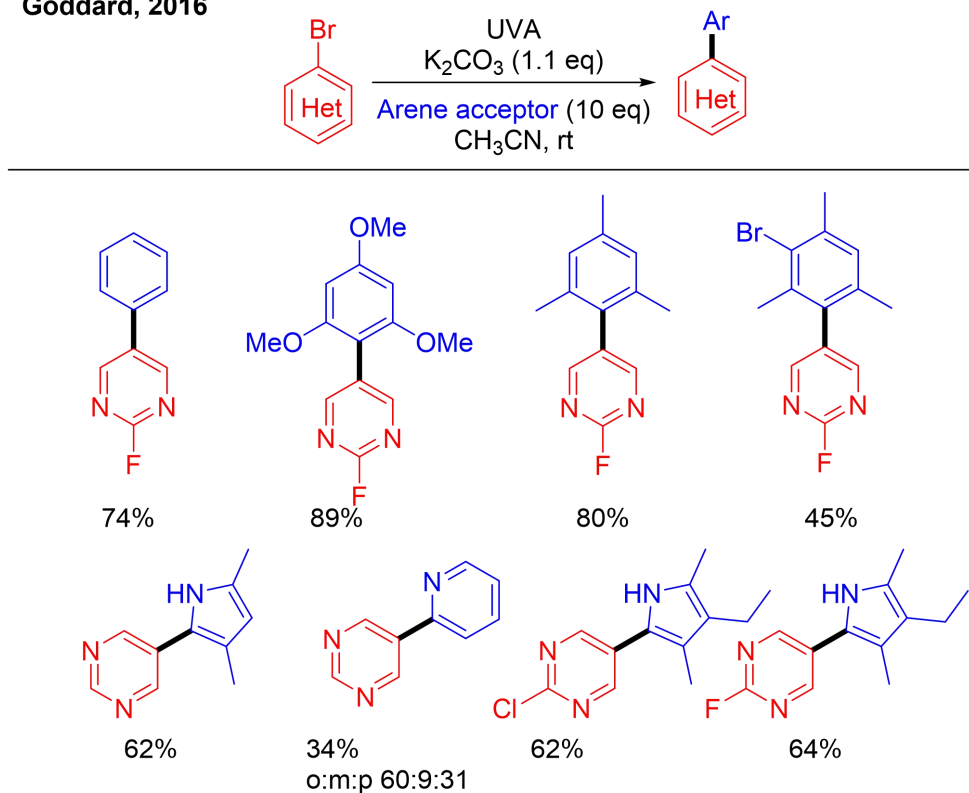
Li, 2016



Scheme 1.7. The synthesis of aryl trimethylstannanes from aryl halides under UV.

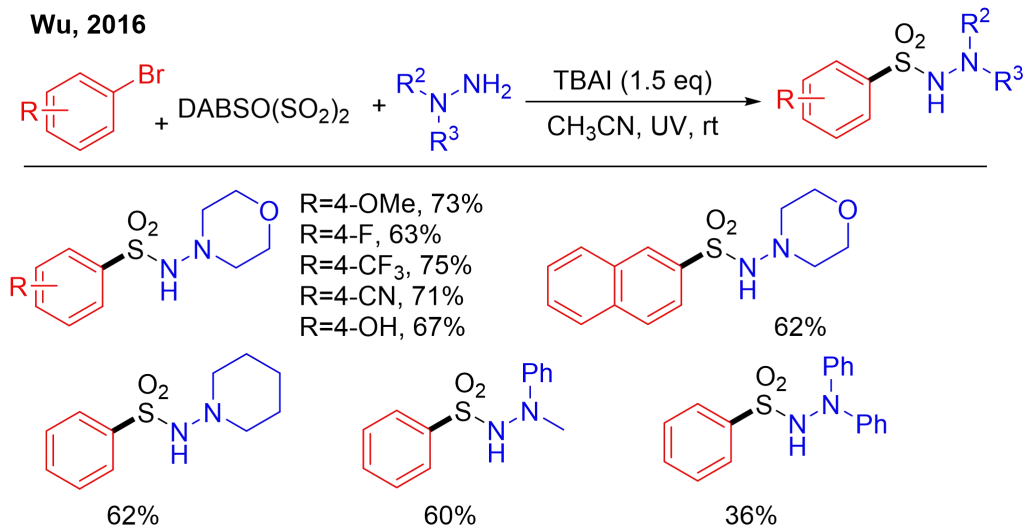
In 2016, Goddard and coworkers reported a transition-metal-free arylation of pyrimidines through photochemical process with the assistance of K_2CO_3 (Scheme 1.8).^{14d} In this work, pyrimidinyl and pyrazinyl radicals were generated by homolytic cleavage under UV irradiation conditions, and proved to promptly undergo C–C bond formation processes. This method avoided large excess of arenes or using arenes as solvent. Using only 10 equivalents of arene coupling partner in CH_3CN as solvent, hetero-biaryl derivatives were obtained in good to excellent yields. However, functional group compatibility was limited to the use of electron deficient pyrimidine halides as starting materials. Further, heteroarenes could also be used as arene acceptors. The 5-pyrimidinyl radical was trapped by TEMPO.

Goddard, 2016



Scheme 1.8. Transition-metal-free arylation of pyrimidines under UV.

In 2016, Wu group reported a catalyst-free aminosulfonylation through insertion of sulfur dioxide with aryl/alkyl halides (including aryl bromides and aryl chlorides) under UV irradiation (Scheme 1.9).^{14c} The reaction proceeded in the absence of metals or photoredox catalysts. This is a three-component reaction between aryl/alkyl halides, DABCO·(SO₂)₂, and hydrazines. The corresponding *N*-aminosulfonamides are afforded in good to excellent yields. A broad reaction scope is demonstrated with good functional group tolerance (OMe, F, CF₃, CN, OH). Additionally, alkyl halides are good substrates as well during the insertion of sulfur dioxide. A possible mechanism involving a homolytic cleavage of the C–X bond to form aryl and alkyl radicals was proposed.



Scheme 1.9. Catalyst-free aminosulfonylation of aryl halides under UV.

While all these UV-induced methods enable remarkable transformations, the use of specialized high-energy UV reactors is dangerous and difficult to implement in academic and industrial laboratories. Additionally, the use of high-energy UV-irradiation is incompatible with many functional groups and can easily generate unwanted byproducts or lead to decomposition of the final products. Therefore, the use of less energetic visible-light to enable similar transformations would enable scalability and promote adoption while reducing costs. Visible-light irradiation sources such as LEDs or household lamps are ubiquitous, affordable and do not require special safety handling. To date, many outstanding reports have been published on the use of metal-free organic photocatalysts to activate aryl halides.¹³ However, most of these complicated organic photocatalysts above are moisture sensitive, air sensitive, and are difficult to synthesize and store. Additionally, performing the reactions under visible-light without photocatalysts has been less studied.

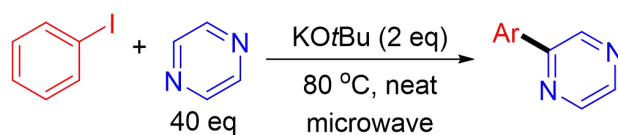
1.3 Base-Promoted Activation of Aryl Halides

1.3.1 Early Examples: Base-Promoted Heat-Induced Activations

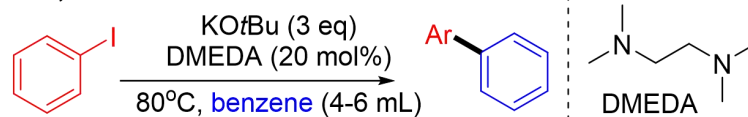
Transition-metal-free coupling reactions have attracted some attention over the past decade.¹⁵ Itami and co-workers were the first to disclose such a reaction involving aryl halides in 2008 (Scheme 1.10).¹⁶ The transformation used potassium *tert*-butoxide (KO^{*t*}Bu) at high

temperatures to enable the direct C–H arylation of electron-deficient arenes with aryl halides. It was then proposed that the *tert*-butoxide anion ($^-\text{OtBu}$) behaves as a strong electron donor capable of performing a single electron transfer (SET) into the aryl iodide. Later, in 2010,¹⁷ the Lei and the Hayashi groups independently discovered that aryl halides could be coupled to unactivated benzene through the use of KO*t*Bu or NaO*t*Bu in the presence of catalytic amounts of amine-based ligands, such as *N,N'*-dimethylethylenediamine (DMEDA) and phenantroline at high temperatures (80–155 °C). These reactions were proposed to proceed via a SET from a base-ligand complex to the aryl halides, however the exact nature of the active species and its mechanism remained unclear. It was only in 2016 that Tuttle and Murphy¹⁸ provided the first compelling explanation of the mechanism of these transition-metal-free transformations. It was determined that in most cases KO*t*Bu is not involved in the SET step. Instead, they identified various electron-donating species, generated *in situ*, that were performing the SET to aryl halides at high temperatures.

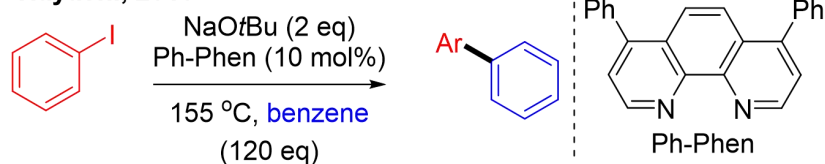
Itami, 2008



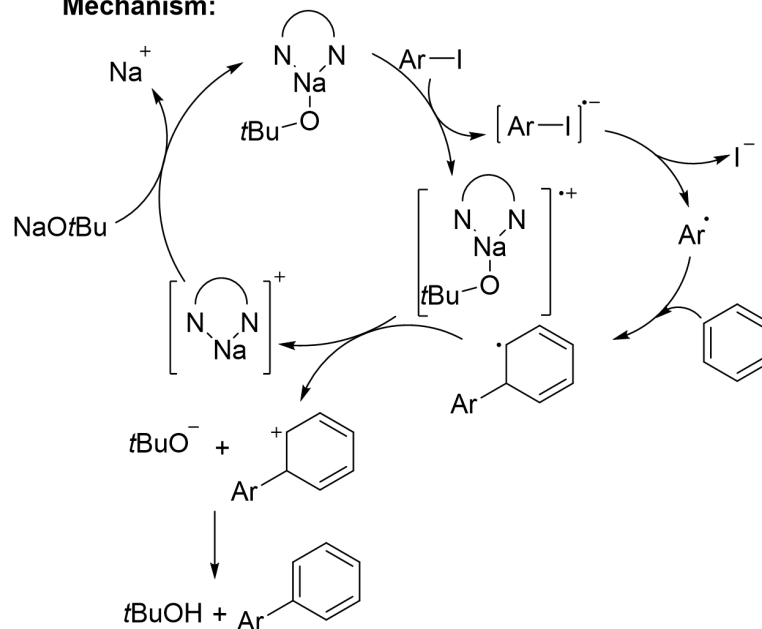
Lei, 2010



Hayashi, 2010



Mechanism:

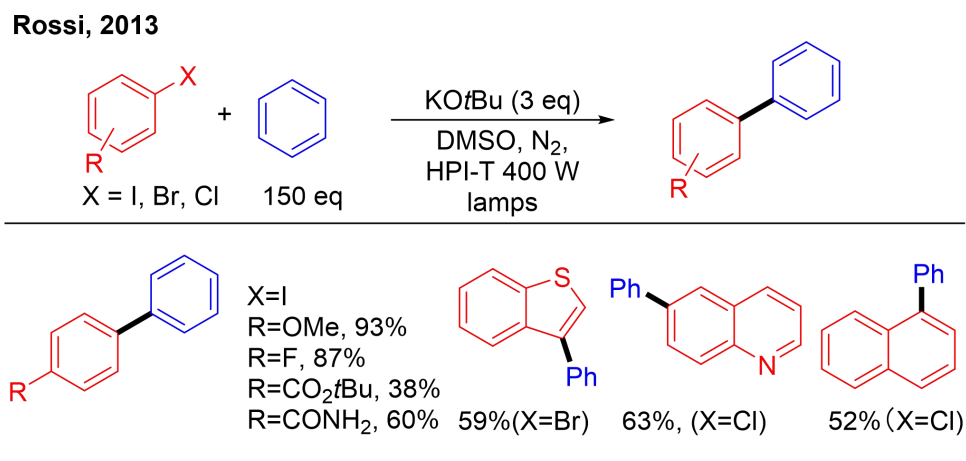


Scheme 1.10. Traditional transition-metal-free activation of aryl halides.

1.3.2 Base-Promoted Photo-Induced Activation of Aryl Halides

Base-promoted photo-induced functionalizations of aryl halides are the most common methods used for the activation of aryl halides under catalyst-free conditions. Alkali metal *tert*-butoxides have been used to help the single electron transfer process to aryl halides and generate aryl halides radical anions that upon fragmentation form aryl radicals and halide ions.¹⁹ In 2013,

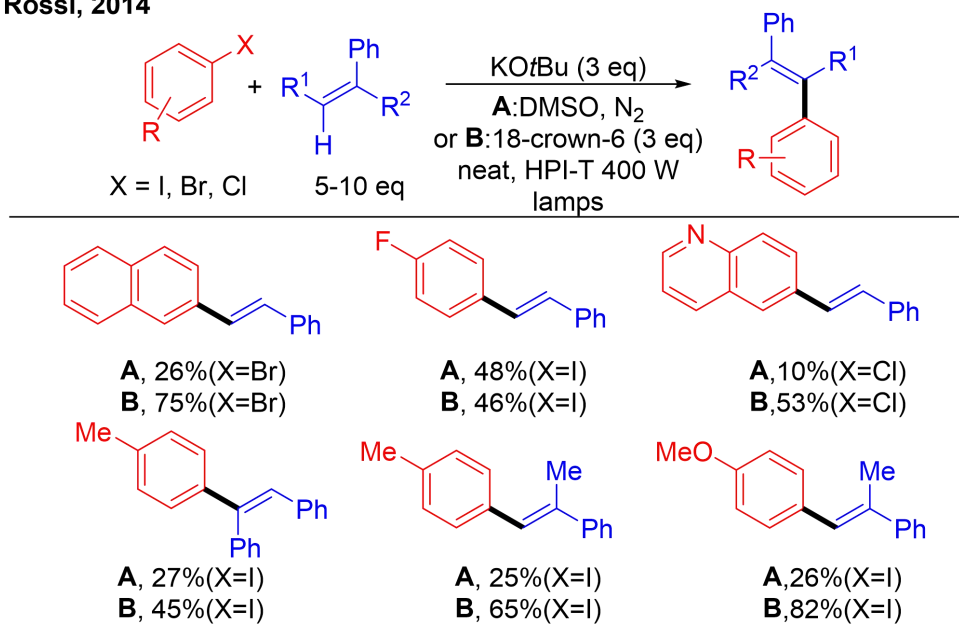
Rossi group reported the arylation of aryl halides (including ArI, ArBr, and even ArCl) by using KO^tBu in dimethyl sulfoxide (DMSO) (Scheme 1.11).^{19a} This reaction requires two HPI-T (white light, high-pressure mercury-iodine-vapour lamp) 400 W lamps. A large excess (150 equiv) of benzene (or arene) is required, which limits the scope of substrates.



Scheme 1.11. Arylation of aryl halides by using KO^tBu.

The following year, the same group reported a photo-induced direct C–H arylation of activated alkenes at room temperature (Scheme 1.12). This transformation afforded *E*-stilbene moieties by using KO^tBu, with a broad range of aryl halides, including ArI, ArBr, and even ArCl.^{19b} In this work, two conditions were tested. One used DMSO as solvent like in their previous work and the other one used neat conditions, but 18-crown-6 ether was used as an additive.

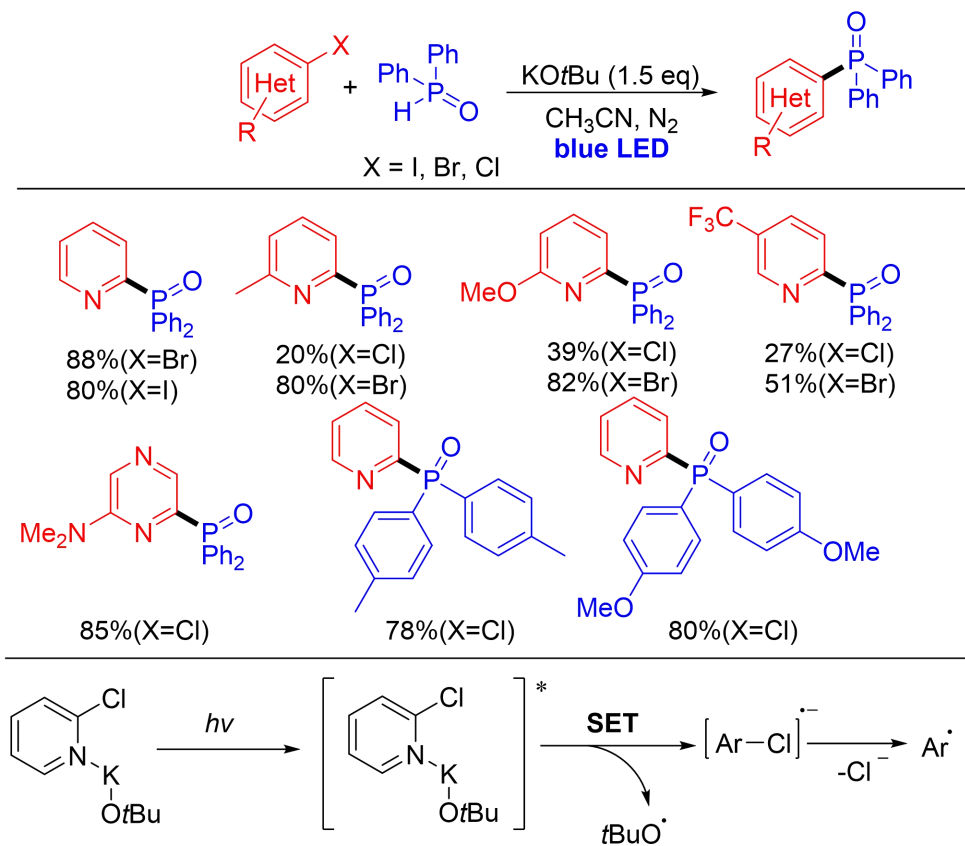
Rossi, 2014



Scheme 1.12. Photo-induced direct C–H arylation of alkenes.

More recently, the Che group showed a phosphinylation of heteroaryl halides by using KOtBu in anhydrous CH₃CN.^{19c} Heteroaryl phosphine oxides were synthesized in moderate to excellent yields. The Che group was the first to propose the possibility of an EDA complex between the KOtBu and heteroaryl halides (Scheme 1.13). Aryl radicals could be generated by a single electron transfer between the heteroaryl halides and KOtBu.

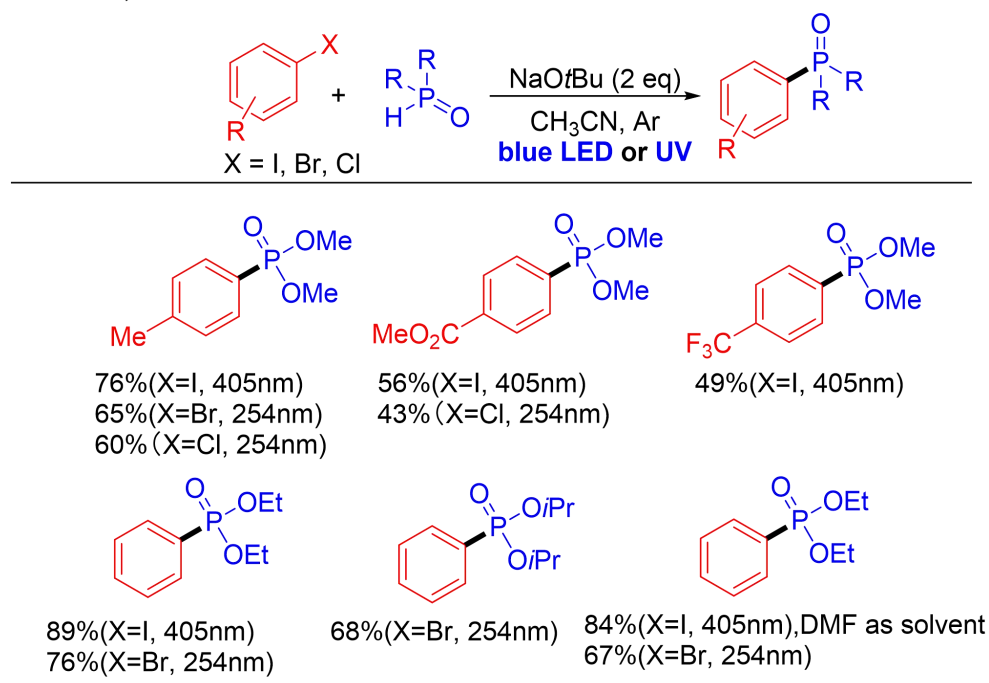
Che, 2018



Scheme 1.13. Phosphinylation of heteraryl halides by using K⁺OtBu.

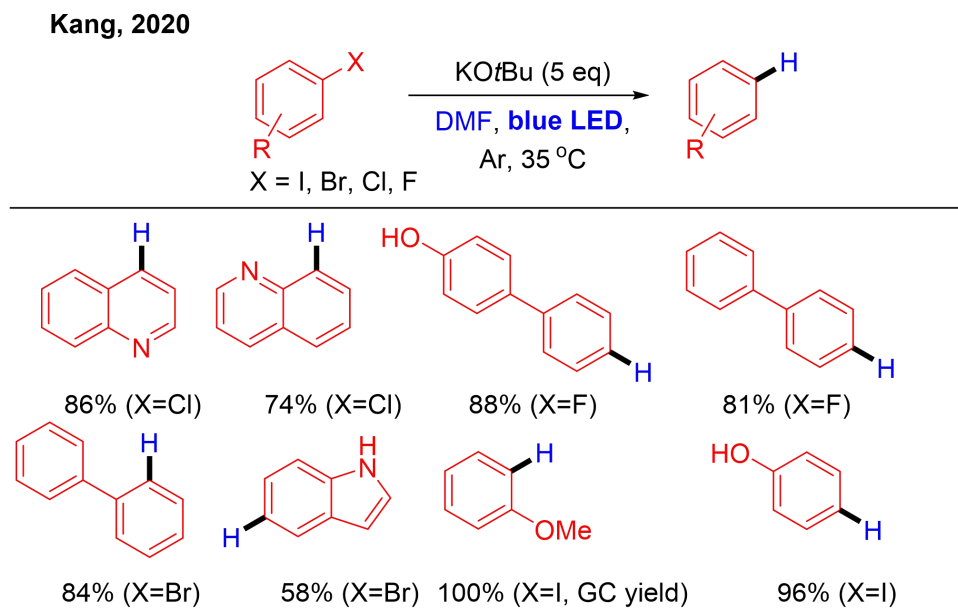
In 2009, the Li group reported a photo-induced transition-metal-free cross-coupling of aryl halides with H-phosphonates (Scheme 1.14).^{19d} The scope of aryl halides includes Ar-Cl, Ar-Br, and Ar-I, however, UV light was required for aryl bromides and aryl chlorides. In addition, the scope of H-phosphonates includes dialkyl phosphonates, and diarylphosphine oxides. They proposed two tentative mechanisms. One is homolytic cleavage of the C-X bond. The other one is by a weak halogen-metal bonding intermediate to form aryl radicals.

Li, 2019



Scheme 1.14. Transition-metal-free cross-coupling of aryl halides with H-phosphonates.

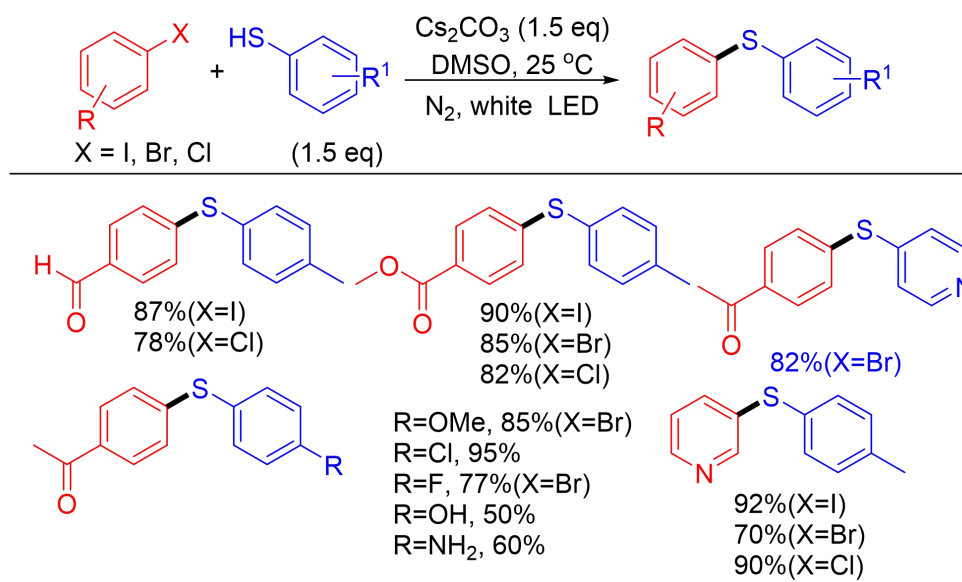
Recently, Kang and coworkers reported the dehalogenation of a variety of aryl halides, including aryl fluorides, chlorides, bromides, and iodides (Scheme 1.15). Aryl halides could be reduced to the corresponding (hetero)arenes with moderate to excellent yields under mild conditions. And they used deuterated *N,N*-dimethylformamide (DMF) to produce the deuterated dehalogenated aryl product, which led them to propose that KO*t*Bu may be deprotonating DMF and indicated that DMF was the hydrogen source in this transformation.^{19c}



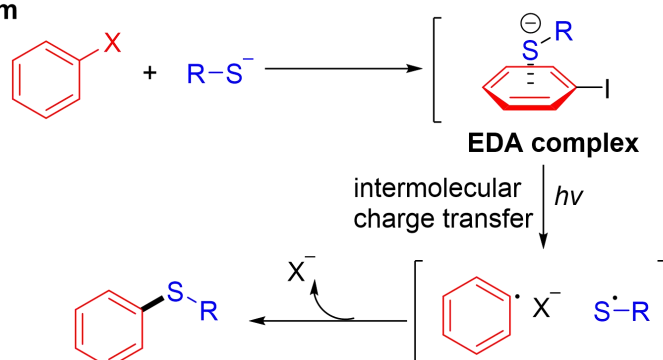
Scheme 1.15. KOtBu-promoted dehalogenation of aryl halides.

Another pathway to produce aryl radicals could be achieved by base-promoted formation of an electron-donor-acceptor complex (EDA) between aryl halides (including ArI, ArBr and ArCl) and thiolates under visible light.²⁰ In 2017, Miyake and coworkers described a visible light-promoted C–S bond forming transformation using aryl halides and thiophenols with the assistance of Cs_2CO_3 . Mechanistic work showed that an intermolecular charge transfer was responsible for this reactivity. The thiolate anion forms an EDA complex with the aryl halide.^{20a} This EDA complex allowed the aryl halides and arylthiophenol to form aryl radicals and sulfur radicals (Scheme 1.16). A wide range of unsymmetrical diaryl sulfides were constructed in this work. However, the scope of electron-neutral or rich aryl iodides was limited.

Miyake, 2017

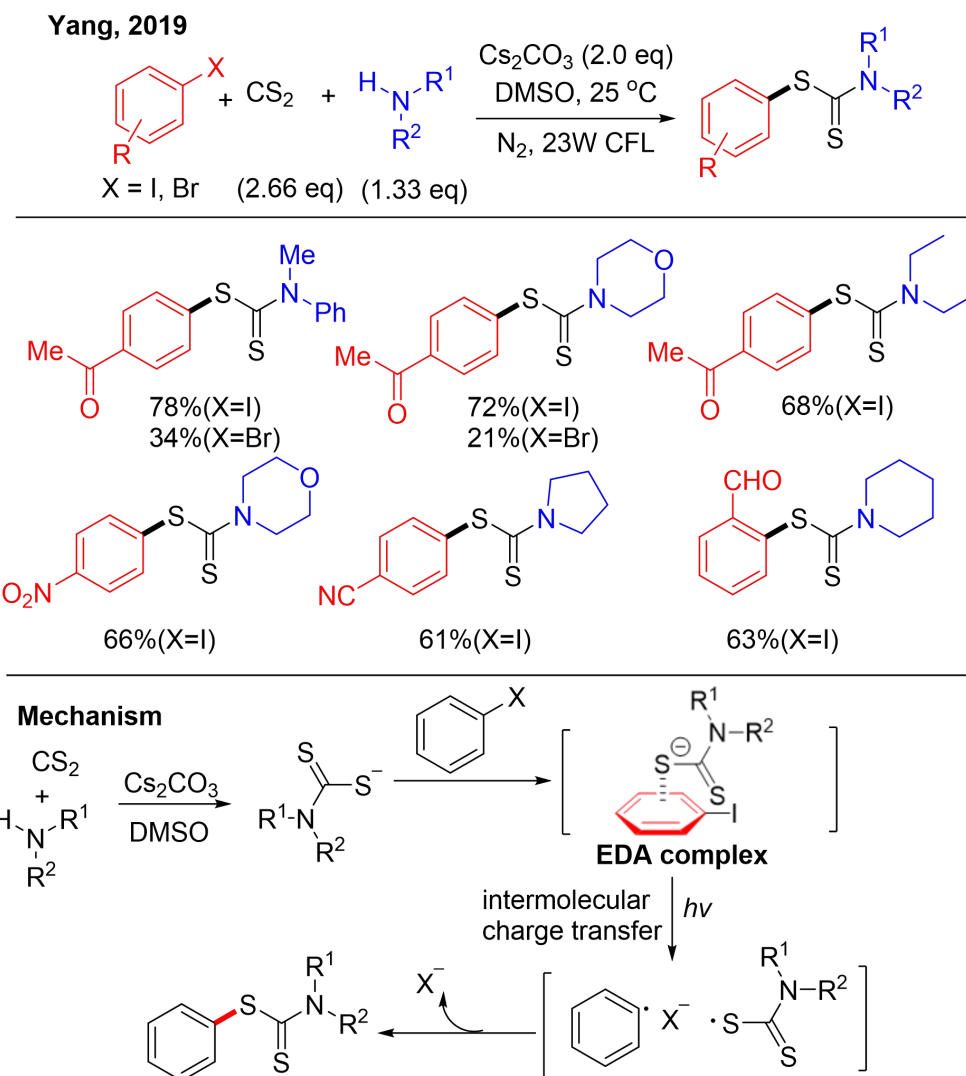


Mechanism



Scheme 1.16. Visible light-promoted intermolecular charge transfer between the thiolate-aryl halides.

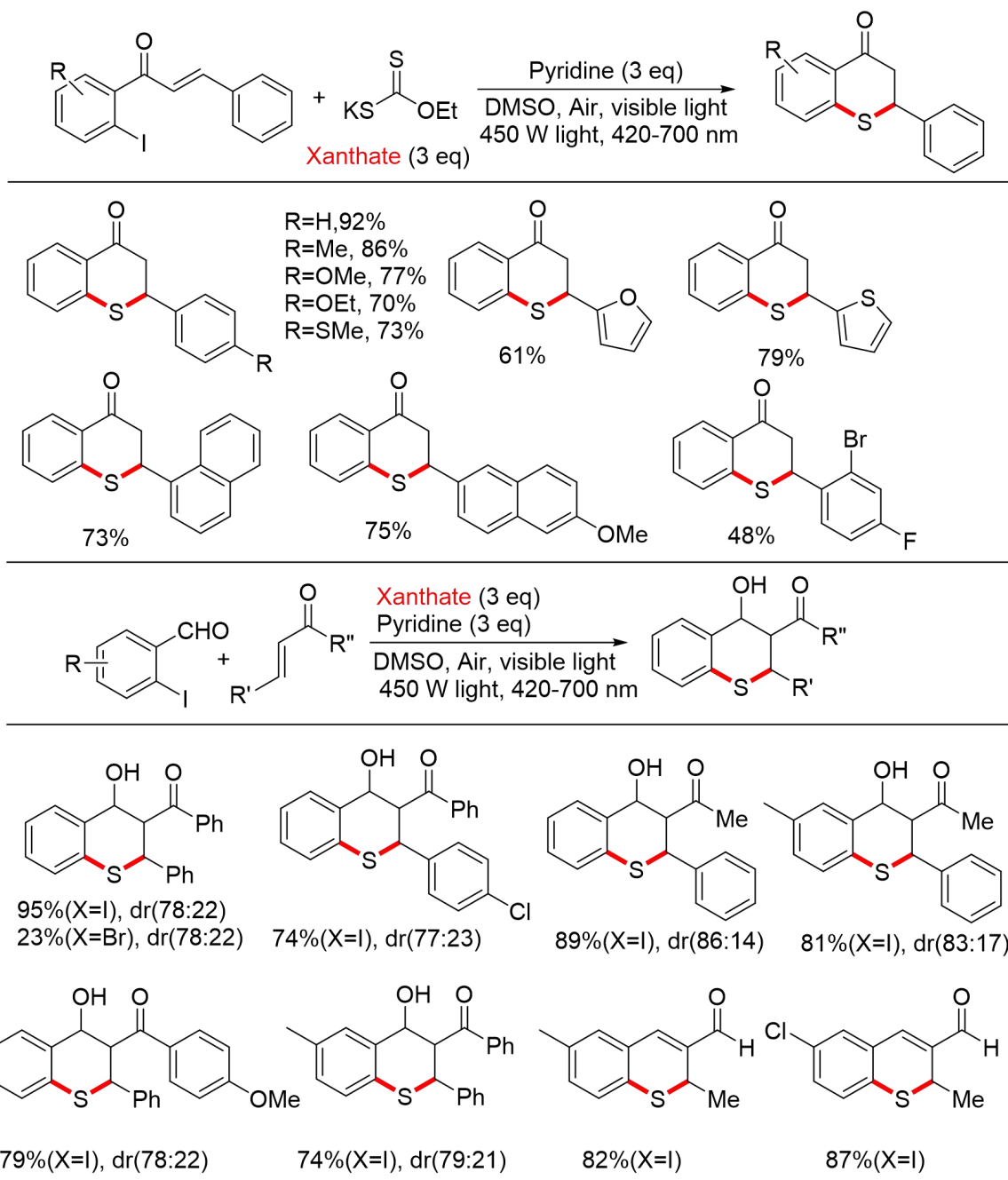
The Yang group reported a multi-component reaction protocol to synthesize aryl dithiocarbamates by using Cs_2CO_3 under compact fluorescent lamp (CFL) (Scheme 1.17).^{20b} In this reaction, CS_2 is presumed to react with amines in the presence of Cs_2CO_3 to form the corresponding thiolate that then reacts with aryl halides. Aryl halides with electron-withdrawing groups displayed high reactivity, while those with electron-donating ones were found to be poor substrates. Such results suggest the formation of an EDA complex involving the aryl halides and thiolate. The authors observed that aryl radicals and sulfur radicals were formed during the reaction.



Scheme 1.17. Synthesis of S-aryl dithiocarbamates by using Cs_2CO_3 under CFL.

In 2021, the Sekar group reported the synthesis of thiochromane derivatives by a photocatalyst free C–S cross-coupling reaction using xanthate as a sulfur surrogate with pyridine as base (Scheme 1.18).^{20c} The reaction proceeds via the formation of an EDA complex between aryl halides and xanthate to form the C–S bond. Moreover, C–S bond formation can be followed by inter or intra-molecular sulfa-Michael addition and then aldol reaction to access multisubstituted thiochromanes. The use of inodorous solid potassium ethyl xanthate in place of arenethiols as sulfur surrogates makes this domino strategy environmentally benign and convenient.

Sekar, 2021



Scheme 1.18. Synthesis of thiochromane derivatives.

1.4 Conclusions

Activation of aryl halides is an important synthetic strategy to construct C–C, C–N, C–S, C–B and C–P bonds. Most of the traditional methods require transition-metal catalysts or harsh

conditions. Even most of the photochemical methods require expensive and complicated organic photocatalysts. Limited examples of catalyst-free methods were reported in photochemistry. Part of these catalyst-free methods need special and expensive high energy UV irradiation, which may cause issues such as forming undesired byproducts. Additionally, UV light is potentially harmful if not used properly. Thus, visible-light-induced transition-metal-free photochemistry under catalyst-free conditions deserves to be explored as an alternative.

In this dissertation, we will report our work on visible-light-induced transition-metal-free activation of aryl halides or sp^3 C–H bonds.

1.5 References

1. (a) Poleto, M. D.; Rusu, V. H.; Grisci, B. I.; Dorn, M.; Lins, R. D.; Verli, H. Aromatic Rings Commonly Used in Medicinal Chemistry: Force Fields Comparison and Interactions With Water Toward the Design of New Chemical Entities. *Front. Pharmacol.* **2018**, *9*, 395–395. (b) Taylor, R. D.; MacCoss, M.; Lawson, A. D. G. Rings in Drugs. *J. Med. Chem.* **2014**, *57*, 5845–5859. (c) Liu, Y.; Zhao, X.; Fang, C.; Ye, Z.; He, Y.; Lei, D.; Yang, J.; Zhang, Y.; Li, Y.; Liu, Q.; Huang, Y.; Zeng, R.; Kang, L.; Liu, J.; Huang, Y. Activating aromatic rings as Na-ion storage sites to achieve high capacity. *Chem* **2018**, *4*, 2463–2478.
2. (a) Meyer, E. A.; Castellano, R. K.; Diederich, F. Interactions with Aromatic Rings in Chemical and Biological Recognition. *Angew. Chem. Int. Ed.* **2003**, *42*, 1210–1250. (b) Salonen, L. M.; Ellermann, M.; Diederich, F. Aromatic Rings in Chemical and Biological Recognition: Energetics and Structures. *Angew. Chem., Int. Ed.* **2011**, *50*, 4808–4842.
3. (a) Davies, H. M. L.; Morton, D. Recent Advances in C–H Functionalization. *J. Org. Chem.* **2016**, *81*, 343–350. (b) Shawn, D. W.; Timothy, E. B.; Joseph, R. M.; Stephen, L. B. A Rationally Designed Universal Catalyst for Suzuki-Miyaura Coupling Processes. *Angew. Chem., Int. Ed.* **2004**, *43*, 1871–1876. (c) Huang, X.; Anderson, K. W.; Zim, D.; Jiang, L.; Klapars, A.; Buchwald, S. L. Expanding Pd-Catalyzed Bond-Forming Processes: the First Amidation of Aryl Sulfonates, Aqueous Amination, and Complementarity with Cu-Catalyzed Reactions. *J. Am. Chem. Soc.* **2003**, *125*, 6653–6655.
4. (a) Peltzer, R. M.; Gauss, J.; Eisenstein, O.; Cascella, M. The Grignard Reaction – Unraveling a Chemical Puzzle. *J. Am. Chem. Soc.* **2020**, *142*, 2984–2994. (b) Seyferth, D. The Grignard Reagents. *Organometallics* **2009**, *28*, 1598–1605. (c) Schwindeman, J. A.; Woltermann, C. J.; Letchford, R. J. Safe handling of organolithium compounds in the laboratory. *Chem. Health Saf.* **2002**, *9*, 6–11. (d) Juhász, K.; Magyar, Á.; Hell, Z. Transition-Metal-Catalyzed Cross-Coupling Reactions of Grignard Reagents. *Synthesis* **2021**, *53*, 983–1002. (e) Shimizu, M. Lithium Compounds in Cross-Coupling Reactions. *Lithium Compounds in Organic Synthesis*, **2014**, 463–490.

5. (a) Biffis, A.; Centomo, P.; Del Zotto, A.; Zecca, M. Pd metal catalysts for cross-couplings and related reactions in the 21st century: A critical review. *Chem. Rev.* **2018**, *118*, 2249–2295. (b) Buskes, M. J.; Blanco, M. J. Impact of cross-coupling reactions in drug discovery and development. *Molecules* **2020**, *25*, 3493. (c) Pérez Sestelo, J.; and Sarandeses, L.A. . Advances in Cross-Coupling Reactions. *Molecules* **2020**, *25*, 4500. (d) Johansson Seechurn, C.C.C.; Kitching, M.O.; Colacot, T.J.; Snieckus, V. Palladium-catalyzed cross-coupling: A historical contextual perspective to the 2010 Nobel prize. *Angew. Chem. Int. Ed.* **2012**, *51*, 5062–5085. (e) Amal Joseph, P. J.; Priyadarshini, S. Copper-mediated C-X functionalization of aryl halides. *Org. Process Res. Dev.* **2017**, *21*, 1889–1924. (f) Campeau, L.-C.; Hazari, N. Cross-coupling and related reactions: Connecting past success to the development of new reactions for the future. *Organometallics* **2019**, *38*, 3–35. (g) Haas, D.; Hammann, J.M.; Greiner, R.; Knochel, P. Recent developments in Negishi cross-coupling reactions. *ACS Catal.* **2016**, *6*, 1540–1552.
6. (a) Negishi, E.-i. Magical Power of Transition Metals: Past, Present, and Future (Nobel Lecture). *Angew. Chem., Int. Ed.* **2011**, *50*, 6738–6764. (b) Suzuki, A. Cross-Coupling Reactions Of Organoboranes: An Easy Way To Construct C–C Bonds (Nobel Lecture). *Angew. Chem., Int. Ed.* **2011**, *50*, 6722–6737. (c) Seechurn, C. C. C. J.; Kitching, M. O.; Colacot, T. J.; Snieckus, V. Palladium-Catalyzed Cross-Coupling: A Historical Contextual Perspective to the 2010 Nobel Prize. *Angew. Chem., Int. Ed.* **2012**, *51*, 5062–5085. (d) Brown, D.G.; Bostrom, J. Analysis of past and present synthetic methodologies on medicinal chemistry: Where have all the new reactions gone? *J. Med. Chem.* **2016**, *59*, 4443–4458.
7. (a) Nair, D.; Scarpello, J.; White, L.; Freista dos Santos, L.; Vankelecom, I.; Livingston, A. Semi-Continuous Nanofiltration-Coupled Heck Reactions as a New Approach to Improve Productivity of Homogeneous Catalysts. *Tetrahedron Lett.* **2001**, *42*, 8219–8222. (b) Garrett, C.; Prasad, K. The Art of Meeting Palladium Specifications in Active Pharmaceutical Ingredients Produced by Pd-Catalyzed Reactions. *Adv. Synth. Catal.* **2004**, *346*, 889–900. (c) Jana, R.; Pathak, T. P.; Sigman, M. S. Advances in Transition Metal (Pd,Ni,Fe)-Catalyzed Cross-Coupling Reactions Using Alkyl Organometallics as Reaction Partners. *Chem. Rev.* **2011**, *111*, 1417–1492.
8. (a) Gansäuer, A.; Bluhm, H. Reagent-Controlled Transition-Metal-Catalyzed Radical Reactions. *Chem. Rev.* **2000**, *100*, 2771–2788. (b) Wang, C.; Xi, Z. Co-operative Effect of Lewis Acids with Transition Metals for Organic Synthesis. *Chem. Soc. Rev.* **2007**, *36*, 1395–1406. (c) Ackermann, L. Carboxylate-Assisted Transition-Metal-Catalyzed C–H Bond Functionalizations: Mechanism and Scope. *Chem. Rev.* **2011**, *111*, 1315–1345.
9. (a) Skubi, K. L.; Blum, T. R.; Yoon, T. P. Dual Catalysis Strategies in Photochemical Synthesis. *Chem. Rev.* **2016**, *116*, 10035–10074. (b) Zhang, H.-H.; Chen, H.; Zhu, C.; Yu, S. A Review of Enantioselective Dual Transition Metal/Photoredox Catalysis. *Sci. China: Chem.* **2020**, *63*, 637–647. (c) Twilton, J.; Le, C.; Zhang, P.; Shaw, M. H.; Evans, R. W.; MacMillan, D. W. C. The Merger of Transition Metal and Photocatalysis. *Nat. Rev. Chem.* **2017**, *1*, 0052. (d) Toth, B. L.; Tischler, O.; Novak, Z. Recent Advances in Dual Transition Metal-Visible Light Photoredox Catalysis. *Tetrahedron Lett.* **2016**, *57*, 4505–4513. (e) Zhang, P.; Le, C. C.; MacMillan, D. W. C. Silyl Radical Activation of Alkyl Halides in Metallaphotoredox Catalysis: A Unique Pathway for Cross-Electrophile Coupling. *J. Am. Chem. Soc.* **2016**, *138*, 8084–8087.

10. (a) Jiang, M.; Li, H.; Yang, H.; Fu, H. Room-Temperature Arylation of Thiols: Breakthrough with Aryl Chlorides. *Angew. Chem., Int. Ed.* **2017**, *56*, 874–879. (b) Korvorapun, K.; Struwe, J.; Kuniyil, R.; Zangarelli, A.; Casnati, A.; Waeterschoot, M.; Ackermann, L. PhotoInduced Ruthenium-Catalyzed C–H Arylations at Ambient Temperature. *Angew. Chem., Int. Ed.* **2020**, *59*, 18103–18109. (c) Sagadevan, A.; Charitou, A.; Wang, F.; Ivanova, M.; Vuagnat, M.; Greaney, M. F. Ortho C–H arylation of arenes at room temperature using visible light ruthenium C–H activation. *Chem. Sci.* **2020**, *11*, 4439–4443.
11. Sigma-Aldrich: <https://www.sigmaaldrich.com>. (checked on 10/2021)
12. (a) Gerst, M. D.; Graedel, T. E. In-Use Stocks of Metals: Status and Implications. *Environ. Sci. Technol.* **2008**, *42*, 7038–7045. (b) Gordon, R. B.; Bertram, M.; Graedel, T. E. Metal Stocks and Sustainability. *Proc. Natl. Acad. Sci. U. S. A.*, **2006**, *103*, 1209–1214. (c) Johnson, J.; Harper, E. M.; Lifset, R.; Graedel, T. E. Dining at the Periodic Table: Metals Concentrations as They Relate to Recycling. *Environ. Sci. Technol.*, **2007**, *41*, 1759–1765. (d) Dunn, P. J. The Importance of Green Chemistry in Process Research and Development. *Chem. Soc. Rev.* **2012**, *41*, 1452–1461. (e) Anastas, P. T.; Warner, J. C. *Green Chemistry: Theory and Practice*; Oxford University Press: New York, **1998**. (f) Horváth, I. T. Introduction: Sustainable Chemistry. *Chem. Rev.* **2018**, *118*, 369–371. (g) Li, C.-J.; Trost, B. M. Green Chemistry for Chemical Synthesis. *Proc. Natl. Acad. Sci. U.S.A.* **2008**, *105*, 13197–13202.
13. Selected examples of organic photo catalysts: (a) Ghosh, I.; Ghosh, T.; Bardagi, J. I.; König, B. Reduction of Aryl Halides by Consecutive Visible Light-Induced Electron Transfer Processes. *Science* **2014**, *346*, 725–728. (b) Shaikh, R. S.; Düsel, S. J. S.; König, B. Visible-Light Photo-Arbuzov Reaction of Aryl Bromides and Trialkyl Phosphites Yielding Aryl Phosphonates. *ACS Catal.* **2016**, *6*, 8410–8414. (c) Zhu, D.-L.; Wu, Q.; Li, H.-Y.; Li, H.-X.; Lang, J.-P. Hantzsch Ester as a Visible-Light Photoredox Catalyst for Transition-Metal-Free Coupling of Arylhalides and Arylsulfonates. *Chem. - Eur. J.* **2020**, *26*, 3484–3488. (d) Jin, S.; Dang, H. T.; Haug, G. C.; He, R.; Nguyen, V. D.; Nguyen, V. T.; Arman, H. D.; Schanze, K. S.; Larionov, O. V. Visible LightInduced Borylation of C–O, C–N, and C–X Bonds. *J. Am. Chem. Soc.* **2020**, *142*, 1603–1613.
14. UV light references: (a) Li, L.; Liu, W.; Zeng, H.; Mu, X.; Cosa, G.; Mi, Z.; Li, C.-J. Photoinduced Metal-Catalyst-Free Aromatic Finkelstein Reaction. *J. Am. Chem. Soc.* **2015**, *137*, 8328–8331. (b) Mfuh, A. M.; Doyle, J. D.; Chhetri, B.; Arman, H. D.; Larionov, O. V. Scalable, Metal-and Additive-Free, Photoinduced Borylation of Haloarenes and Quaternary Arylammonium Salts. *J. Am. Chem. Soc.* **2016**, *138*, 2985–2988. (c) Chen, K.; He, P.; Zhang, S.; Li, P. Synthesis of aryl trimethylstannanes from aryl halides: an efficient photochemical method. *Chem. Commun.* **2016**, *52*, 9125–9128. (d) Ruch, J.; Aubin, A.; Erbland, G.; Fortunato, A.; Goddard, J.-P. Metal-free arylation of pyrimidines through a photochemical process. *Chem. Commun.* **2016**, *52*, 2326–2329. (e) Li, Y.; Zheng, D.; Li, Z.; Wu, J. *Org. Chem. Front.* **2016**, *3*, 574–578.
15. (a) Mehta, V. P.; Punji, B. Recent Advances in Transition-Metal-Free Direct C–C and C–Heteroatom Bond Forming Reactions. *RSC Adv.*, **2013**, *3*, 11957–11986. (b) Sun, C.-L.; Shi, Z.-J. Transition-Metal-Free Coupling Reactions. *Chem. Rev.* **2014**, *114*, 9219–9280. (c) Li, G.; Nieves-Quinones, Y.; Zhang, H.; Liang, Q.; Su, S.; Liu, Q.; Kozłowski, M. C.; Jia, T.

Transition-Metal-Free Formal Cross-Coupling of Aryl Methyl Sulfoxides and Alcohols via Nucleophilic Activation of C-S Bond. *Nat. Commun.* **2020**, *11*, 2890.

16. Yanagisawa, S.; Ueda, K.; Taniguchi, T.; Itami, K. Potassium t-Butoxide Alone Can Promote the Biaryl Coupling of Electron-Deficient Nitrogen Heterocycles and Haloarenes. *Org. Lett.*, **2008**, *10*, 4673–4676.
17. (a) Shirakawa, E.; Itoh, K.-I.; Higashino, T.; Hayashi, T. tert-Butoxide-Mediated Arylation of Benzene with Aryl Halides in the Presence of a Catalytic 1,10-Phenanthroline Derivative. *J. Am. Chem. Soc.* **2010**, *132*, 15537–15539. (b) Liu, W.; Cao, H.; Zhang, H.; Zhang, H.; Chung, H. K.; He, C.; Wang, H.; Kwong, F. Y.; Lei, A. Organocatalysis in Cross-Coupling: DMEDA-Catalyzed Direct C–H Arylation of Unactivated Benzene. *J. Am. Chem. Soc.* **2010**, *132*, 16737–16740.
18. Barham, J. P.; Coulthard, G.; Emery, K. J.; Doni, E.; Cumine, F.; Nocera, G.; John, M. P.; Berlouis, L. E. A.; McGuire, T.; Tuttle, T.; Murphy, J. A. KOtBu: A Privileged Reagent for Electron Transfer Reactions? *J. Am. Chem. Soc.* **2016**, *138*, 7402–7410.
19. (a) Budén M. E.; Guastavino, J. F.; Rossi, R. A. Room-Temperature Photoinduced Direct C–H-Arylation via Base-Promoted Homolytic Aromatic Substitution. *Org. Lett.*, **2013**, *15*, 1174–1177. (b) Guastavino, J. F.; Budén M. E.; Rossi, R. A. Room-Temperature and Transition-Metal-Free Mizoroki–Heck-type Reaction. Synthesis of E-stilbene by Photoinduced C–H Functionalization. *J. Org. Chem.* **2014**, *79*, 9104–9111. (c) Yuan, J.; To, W.-P.; Zhang, Z.-Y.; Yue, C.-D.; Meng, S.; Chen, J.; Liu, Y.; Yu, G.-A.; Che, C.-M. Visible-Light-Promoted Transition-Metal-Free Phosphinylation of Heteroaryl Halides in the Presence of Potassium tert-Butoxide. *Org. Lett.* **2018**, *20*, 7816–7820. (d) Zeng, H.; Dou, Q.; Li, C.-J. Photoinduced Transition-Metal-Free CrossCoupling of Aryl Halides with H-Phosphonates. *Org. Lett.* **2019**, *21*, 1301–1305. (e) Ding, T.-H.; Qu, J.-P.; Kang, Y.-B. Visible-Light-Induced, Base-Promoted Transition-Metal-Free Dehalogenation of Aryl Fluorides, Chlorides, Bromides, and Iodides. *Org. Lett.* **2020**, *22*, 3084–3088.
20. (a) Liu, B.; Lim, C.-H.; Miyake, G. M. Visible-light-promoted C–S cross-coupling via intermolecular charge transfer. *J. Am. Chem. Soc.* **2017**, *139*, 13616–13619. (b) Li, G.; Yan, Q.; Gan, Z.; Li, Q.; Dou, X.; Yang, D. Photocatalyst-Free VisibleLight-Promoted C(sp²)-S Coupling: A Strategy for the Preparation of S-Aryl Dithiocarbamates. *Org. Lett.* **2019**, *21*, 7938–7942. (c) Sundaravelu, N.; Nandy, A.; Sekar, G. Visible Light Mediated Photocatalyst Free C–S Cross Coupling: Domino Synthesis of Thiochromane Derivatives via Photoinduced Electron Transfer. *Org. Lett.* **2021**, *23*, 3115–3119.

CHAPTER 2. DIMSYL ANION ENABLES VISIBLE-LIGHT-PROMOTED CHARGE TRANSFER IN CROSS-COUPLING REACTIONS OF ARYL HALIDES

(Reproduced in part with permission from Pan L.; Cooke MV.; Spencer A.; Laulhé S. “Dimsyl Anion Enables Visible-Light-Promoted Charge Transfer in Cross-Coupling Reactions of Aryl Halides”, *Adv.Synth.Catal.* **2021**, DOI: 10.1002/adsc.202101052. Copyright 2021 John Wiley & Sons, Inc.)

2.1 Introduction

Diaryl sulfides, selenides, and tellurides are valuable moieties across all chemical sectors from pharmaceuticals to material sciences (Figure 2.1).¹

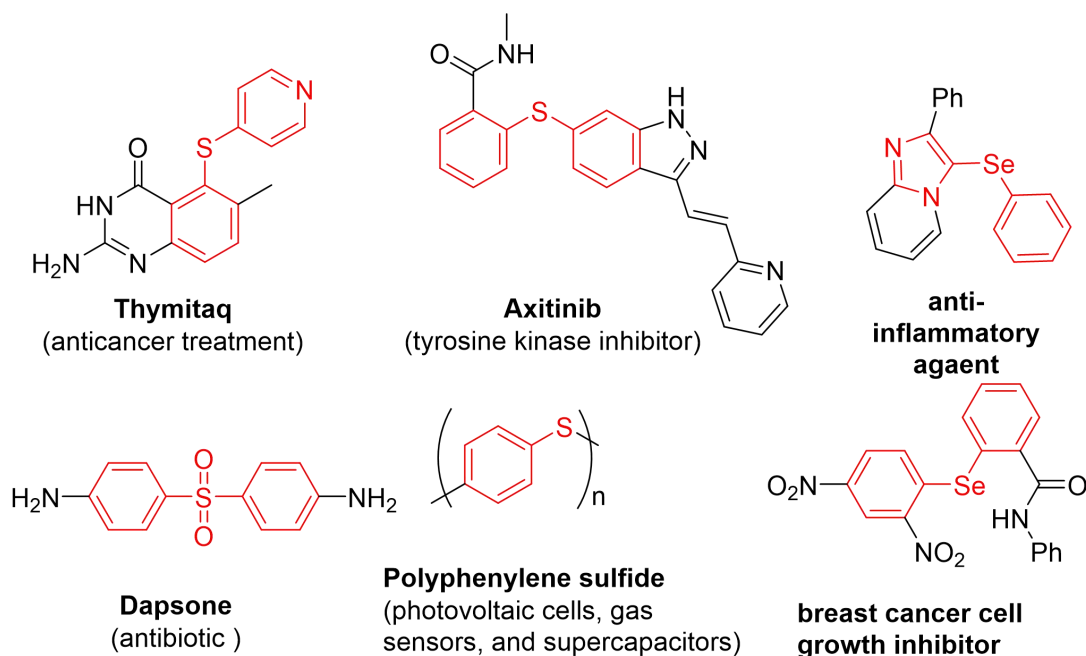


Figure 2.1. Bioactive drugs and polymer materials.

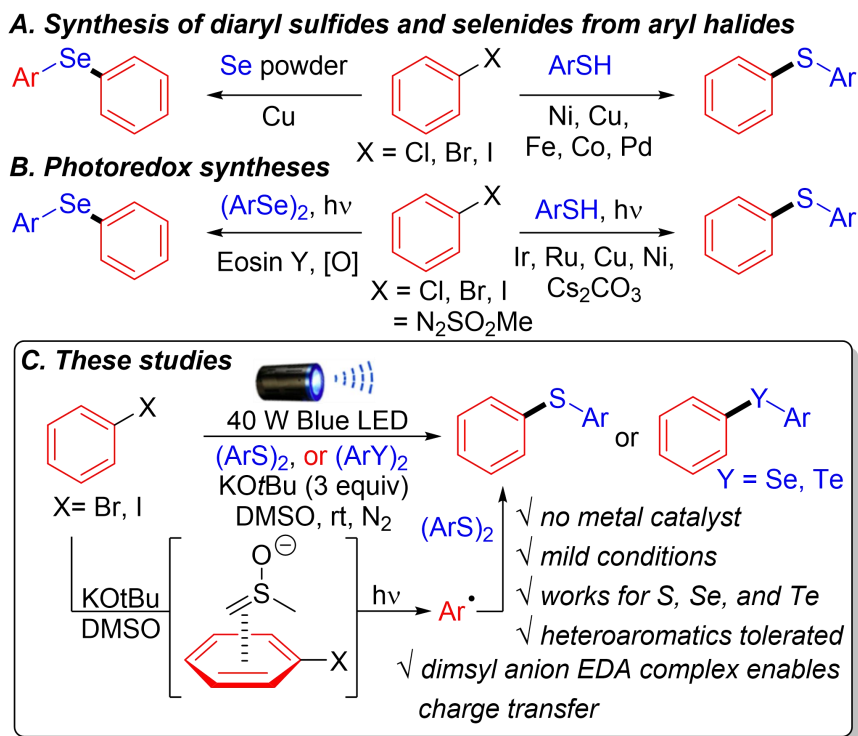
Consequently, the construction of these carbon-chalcogenide bonds has attracted significant interest.² Most methods rely on transition-metal catalysis for the cross-coupling of aryl halides^{3,4} with aryl chalcogenides (Scheme 2.1A). High temperatures and expensive ligands are often required to avoid thiolate-induced catalyst deactivation and poisoning.⁵ Additionally,

the thiols and selenols used in these reactions are unstable, have strong unpleasant odors,⁶ and some derivatives, such as stannyl selenides,⁷ have increased toxicity making them unsuitable for large-scale reactions. Milder reaction conditions using photoredox strategies have been developed (Scheme 2.1B),^{8,9} but these methods often require the use of expensive photocatalysts. A limited number of catalyst-free photo-induced methodologies for C–S bond formation from aryl halides exist,^{2d,10} but they were not shown to work across group 16 elements.

Over the past decade, there has been an emergence of transition-metal-free cross-coupling reactions of aryl halides utilizing *tert*-butoxides (OtBu). Initial observations demonstrated that KOtBu in the presence of ligands¹¹ at high temperatures enabled the direct C–H arylation of benzene with aryl halides. In the presence of visible-light, similar transformations of aryl halides have been achieved at room temperature,¹² often using dimethyl sulfoxide (DMSO) as solvent.

Tuttle and Murphy contributed significantly in elucidating the mechanism of these metal-free transformations,¹³ and it was determined that in most cases KOtBu is not involved in the single electron transfer (SET) step. Instead, they identified various electron-donating species, such as the dimethyl anion, that are capable of performing a SET to aryl halides at high temperatures (135 °C).¹⁴ However, this work did not provide an explanation for the photo-induced activation of aryl halides in DMSO in the absence of additives. Recently, the Rossi group proposed that the dimethyl anion can be photo-excited to initiate a SET to alkyl halides,¹⁵ but an electron-donor-acceptor (EDA) complex was not observed.

Our interest in photoinduced SET performed by KOtBu , recently led us to identify a halogen-bonded EDA complex capable of C–H aminations.¹⁶ Herein, an unprecedented EDA complex between dimethyl anion and aryl halides is reported that is responsible for a photo-induced activation of aryl halides and enables a visible-light-promoted C–S, C–Se, and C–Te cross-coupling with diaryl dichalcogenides (Scheme 2.1C). The reaction proceeds at room temperature in the absence of catalysts generating the desired products in good to excellent yields across a range of substrates. The involvement of this EDA complex is supported by UV-Vis spectroscopy, time-dependent density functional theory (DFT) calculations, and experimental controls. The observation of this EDA complex provides a compelling mechanistic explanation for the SET that initiates this reaction and possibly other photo-induced transformations of aryl halides that use DMSO in the presence of base.



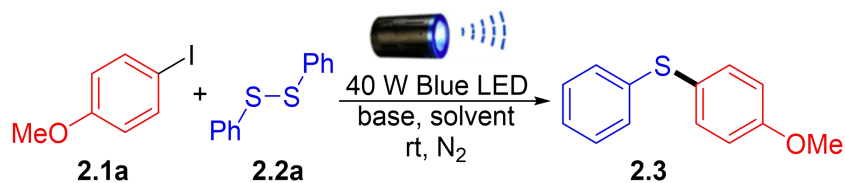
Scheme 2.1. Current and proposed approaches to generate diaryl sulfides and selenides.

2.2 Results and Discussion

We selected 4-iodoanisole (**2.1a**) and diphenyl disulfide (**2.2a**) as model reagents to optimize the reaction. No product was detected in the absence of base under inert atmosphere with DMSO as the solvent (Table 2.1, entry 1). In the presence of three equivalents of KO*t*Bu the reaction provided the desired product in 88% isolated yield (entry 2). Using NaO*t*Bu or LiO*t*Bu as base resulted in lower yields (entries 3, 4) indicating the importance of solubility of the base. Other solvents such as acetonitrile (CH₃CN) or dichloromethane (CH₂Cl₂) (entries 5, 6) also gave lower yields. Inorganic and organic bases (Cs₂CO₃, DABCO (1,4-diazabicyclo[2.2.2]octane), and Et₃N) were explored to further understand the potential role of the base in this transformation (Table 2.1, entries 7–9). Unfortunately, the yields for these reactions were low. The poor performance with Cs₂CO₃ (entry 7) further emphasizes that a different mechanism is at play compared to previously proposed transformations.^{2d} Reducing the amount of **2.2a** to 1.5 equivalent (entry 11) did not affect the reaction. Further reducing **2.2a** to 1.1 equivalent (entry 12) lowered the yield. When the reaction was performed in dark (entry 13) no product was formed, which highlights the fundamental role of photons. Importantly, a

decrease in yield was also observed when the reaction was carried out in air (entry 14). Finally, a time study showed that for the reaction was completed in 4h (entry 15).

Table 2.1. Optimization of reaction conditions^a

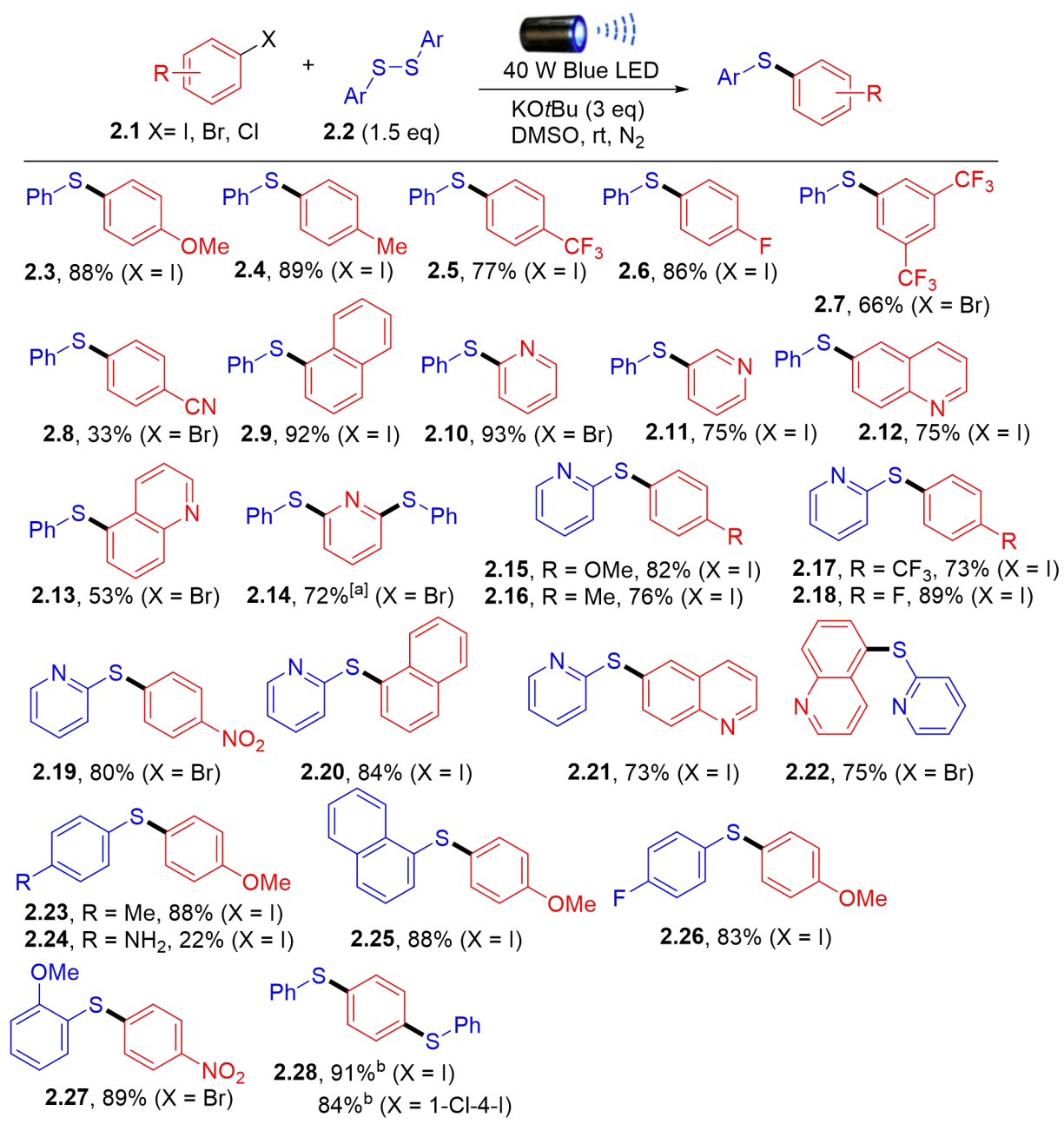


entry	base (equiv.)	2.2a (equiv.)	solvent (mL)	yield (%) ^b
1	–	2.0	DMSO (1.0)	–
2 ^a	KOtBu (3.0)	2.0	DMSO (1.0)	85 (88) ^c
3	NaOtBu (3.0)	2.0	DMSO (1.0)	76
4	LiOtBu (3.0)	2.0	DMSO (1.0)	63
5	KOtBu (3.0)	2.0	CH ₃ CN (1.0)	12
6	KOtBu (3.0)	2.0	CH ₂ Cl ₂ (1.0)	–
7	Cs ₂ CO ₃ (3.0)	2.0	DMSO (1.0)	35
8	DABCO (3.0)	2.0	DMSO (1.0)	38
9	Et ₃ N (3.0)	2.0	DMSO (1.0)	trace
10	KOtBu (2.0)	2.0	DMSO (1.0)	25
11 ^a	KOtBu (3.0)	1.5	DMSO (1.0)	83
12	KOtBu (3.0)	1.1	DMSO (1.0)	59
13 ^d	KOtBu (3.0)	1.5	DMSO (1.0)	–
14 ^e	KOtBu (3.0)	1.5	DMSO (1.0)	53
15 ^f	KOtBu (3.0)	1.5	DMSO (1.0)	82

a. Conditions: **2.1a** (0.2 mmol), **2.2a**, base, solvent, room temperature around reaction flask was 35 °C (heating caused by the LED lamp), under N₂, 24h. b. Yields are based on **2.1a**, determined by ¹H-NMR using dibromomethane as internal standard. c. Isolated yield. d. The reaction was performed in dark covered by aluminum foil. e. The reaction was performed in the air. f. 4h reaction.

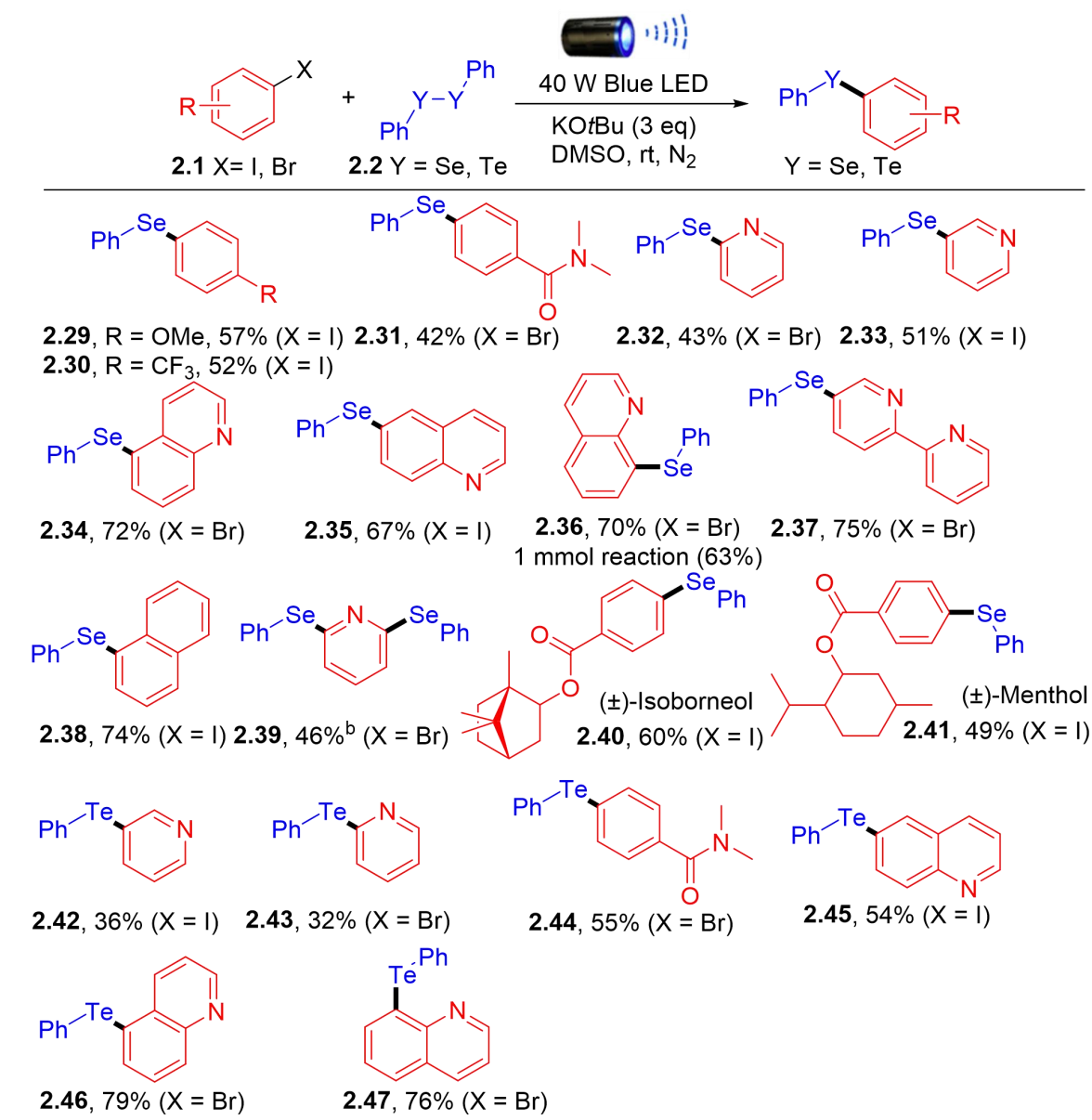
We continued our study investigating the substrate scope for this transformation. The scope of aryl halides is quite broad (Scheme 2.2, products **2.1–2.14**). Both electron-donating (OMe, Me) and electron-withdrawing (CF₃, F) groups at the *para* positions afforded the desired cross-coupled products **2.3–2.6** in good to excellent yields (77–89%). Highly electron-poor substrates such as 1-bromo-3,5-ditrifluoromethylbenzene also gave desired product **2.7** albeit in slightly lower yields (66%). The presence of an aryl nitrile afforded product **2.8** (33%), primarily due to hydrolysis of the cyano group. Acidic or easily hydrolysable functional groups were not well tolerated. Excellent yields were obtained when 1-iodonaphthalene and 2-bromopyridine were used as coupling partners affording products **2.9** and **2.10** (92% and 93%). This promising result led us to explore other heteroaromatic halides, particularly those with privileged frameworks in bioactive compounds. 3-Iodopyridine and 6-iodoquinoline provided desired products **2.11** and **2.12** in good yield (75%). 5-Bromoquinoline afforded product **2.13** in 53% yield. Finally, 2,6-dibromopyridine was efficiently coupled at both halogen sites giving product **2.14** in a single step (72%).

Various aryl disulfides were also investigated (Scheme 2.2, products **2.15–2.28**). Product scope was extended to heteroaromatic moieties present on the disulfide, which complements those in the aryl halides. For example, 2,2'-dipyridyldisulfide reacted readily in good to excellent yields with both electron-rich aryl iodides (**2.15, 2.16**) and electron-poor aryl halides (**2.17–2.19**, 73–80%) even tolerating highly electron deficient aromatic rings containing nitro (NO₂) functionalities. Having heteroaromatic moieties on both coupling partners does not negatively affect the yield affording products **2.21** and **2.22** in 73% and 75% yields, respectively. Both electron-rich and electron-poor aromatic rings are well tolerated in the disulfide to give products **2.23, 2.26, and 2.27** (88%, 83%, and 89%). However, the presence of aniline affected product formation **2.24** (22%). Finally, disubstituted product **2.28** was generated in one step in excellent yields (91%) from 1,4-diiodobenzene, and 84% from 1-chloro-4-iodobenzene, further indicating that selected chlorinated substrates can be coupled (Scheme 2.2). Unfortunately, other aryl chlorides provided poor yields, presumably because they do not form EDA complexes with the dimsyl anion.



Scheme 2.2. Aryl halide and aryl disulfide scope.^a

a. Conditions: **2.1** (0.2 mmol), **2.2** (1.5 equiv.), KOtBu (3 equiv.), DMSO (1 mL), room temperature around reaction flask was 35 °C (heating caused by the LED lamp), under N₂, 24h. b. **2.2** (3 equiv.).



Scheme 2.3. Aryl diselenide and ditelluride scope.^a

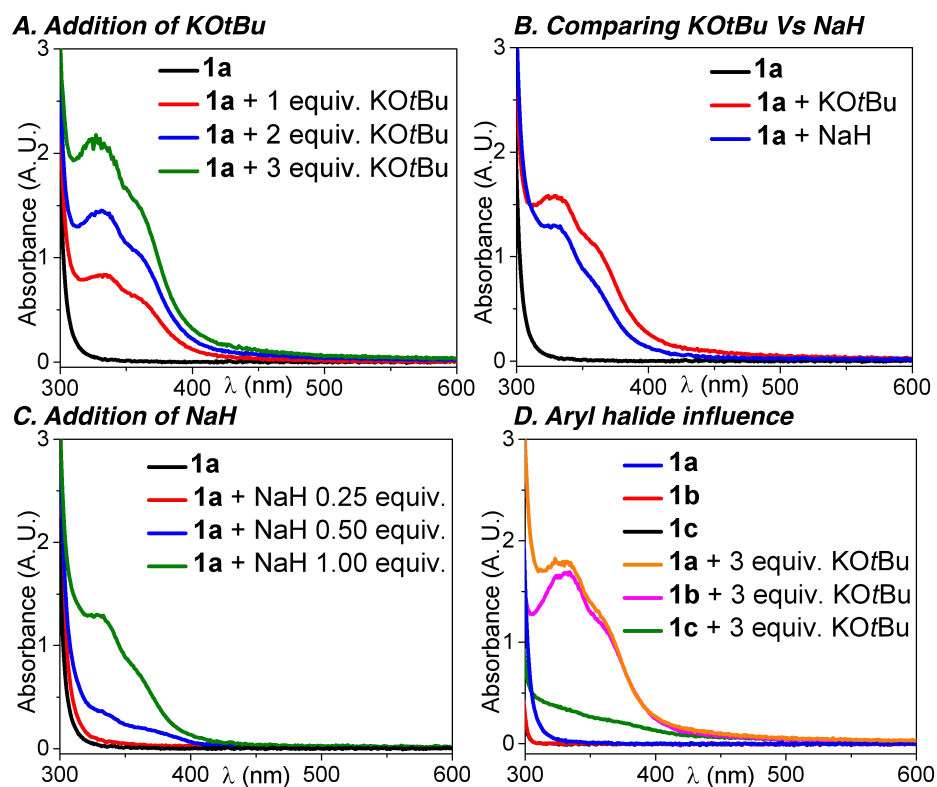
a. Conditions: **2.1** (0.2 mmol), **2.2** (1.5 equiv.), KOtBu (3 equiv.), DMSO (1 mL), room temperature around reaction flask was 35 °C (heating caused by the LED lamp), under N₂, 24h. b. **2.2** (3 equiv.).

Other commercially available aryl dichalcogenides (Scheme 2.3) were investigated. Using diphenyl diselenide, electron-rich (**2.29**) and electron-poor (**2.30**) aryl iodides were coupled in moderate yields (57% and 52%). Amide functionality on the *para* position was tolerated to give **2.31** (42%). Importantly, heteroaromatic halides also cross-coupled in moderate to good yields. Indeed 2-bromopyridine and 3-iodopyridine afforded products **2.32** and **2.33**

(43% and 51%). Quinolines and bipyridines were well-tolerated affording products **2.34–2.37** in moderate to good yields, emphasizing potential application of this method to drug discovery. One-step disubstitution of 2,6-dibromopyridine also provided product **2.39** in moderate yield (46%). Attempting to cross-couple aryl iodides with complex ester functionalities and natural product moieties also proved to be successful, generating isoborneol (**2.40**) and menthol (**2.41**) derivatives (60% and 49%). Finally, diphenyl ditelluride was also investigated as a coupling partner and afforded desired products **2.42–2.47** (32–79%), further demonstrating that the method presented herein works across group 16 elements. Importantly the synthesis of these diaryl tellurides tolerated heteroatoms, amide functionalities, and worked for both aryl bromides and iodides (Scheme 2.3).

To investigate the mechanism of this transformation we performed UV-Vis spectroscopy experiments on various samples of 4-iodoanisole (**2.1a**) and *tert*-butoxides and NaH in DMSO (Scheme 2.4). As we increased the equivalency of KO*t*Bu in our solution of **2.1a** in DMSO (Scheme 2.4A), we observed the formation of a new peak ($\lambda_{\text{max}} = 329$ nm; shoulder: $\lambda = 360$ nm). Importantly, an identical peak was formed when KO*t*Bu was replaced with NaH ($\lambda_{\text{max}} = 328$ nm; shoulder: $\lambda = 360$ nm) (Scheme 2.4B), indicating that the resulting EDA complex formed herein does not involve K⁺ or [−]O*t*Bu. Instead, we propose that this peak results from the absorption of an EDA complex between the dimsyl anion and the aryl halide **2.1a**.

Also, as shown in Scheme 2.4D, not all aryl halides efficiently engage with the dimsyl anion to form an EDA complex. Indeed, 4-iodoanisole (**2.1a**) and 4-bromoanisole (**2.1b**) generate an intense absorption band when mixed with KO*t*Bu in DMSO, while 4-chloroanisole (**2.1c**) has a significantly smaller absorption band under identical conditions. This observation serves as a possible explanation for the lower reactivity of aryl chloride substrates.

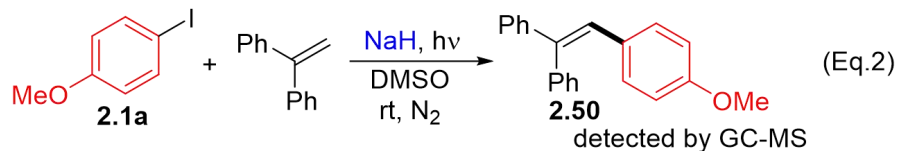


Scheme 2.4. Selected UV-Vis experiments.

1a, **1b**, and **1c** is the abbreviation of corresponding **2.1a**, **2.1b** and **2.1c**.

We performed additional experiments to verify that aryl halide radical initiation can take place in the absence of thiolates^{2d} or KOtBu (Scheme 2.5A, Eq.1 & Eq.2). A mixture of **2.1a** and KOtBu in DMSO under blue-light irradiation generates aryl radicals trapped using 1,1-diphenylethylene (1,1-DPE) to form product **2.50**. Replacing KOtBu by NaH under identical conditions also generated the desired aryl radicals. The use of radical quenchers, such as TEMPO and 1,1-DPE (Scheme 2.5B), lead to lower yields for the desired product **2.3**. However, using NaH as a base did not significantly affect the C–S cross-coupling reaction and afforded the desired product in 71% yield. These results further suggest that an EDA complex between dimsyl anion and aryl halide is responsible for the observed reactivity.

A. Radical initiation experiments

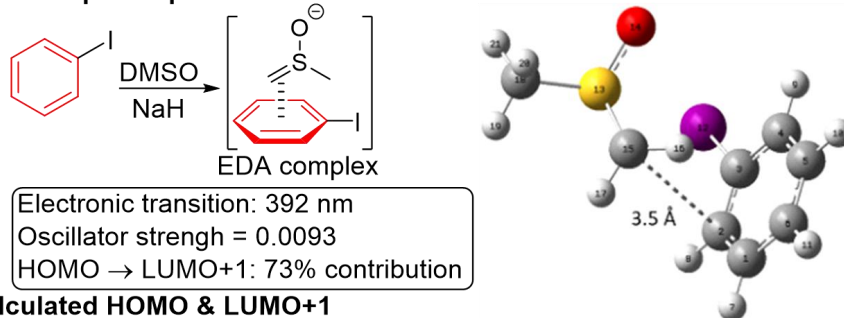


B. Control reactions

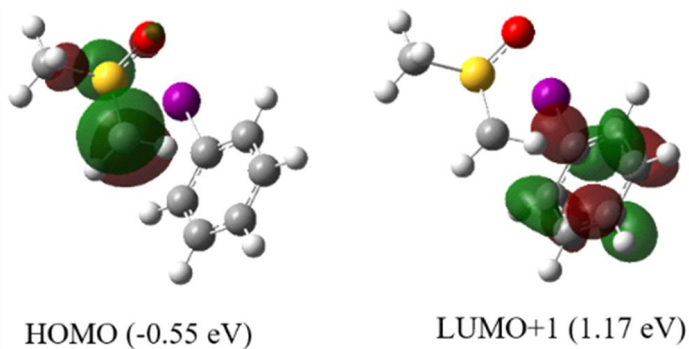


entry	additives (equiv.)	base (equiv.)	yield (%)
1	—	KOtBu (3.0)	88
2	TEMPO (2.0)	KOtBu (3.0)	53
3	1,1-DPE (2.0)	KOtBu (3.0)	43
4	—	NaH (3.0)	71

C. EDA complex representation and calculated



D. Calculated HOMO & LUMO+1



Scheme 2.5. Control experiments and calculated EDA complex.

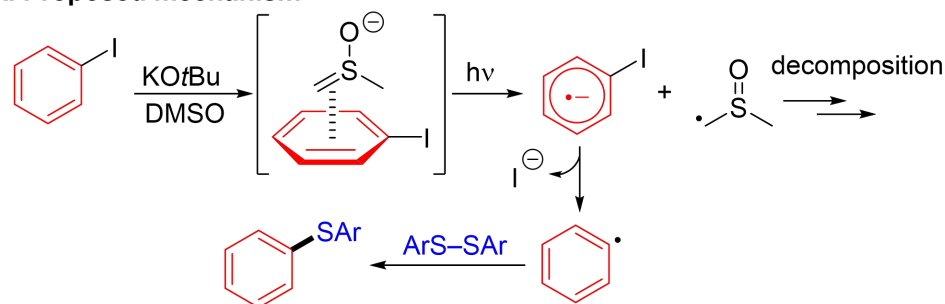
Finally, to support these observations, we performed time dependent-density functional theory (TD-DFT) calculations involving a π - π interaction between the dimsyl anion and the aryl halide where the shortest distance between the moieties is 3.5 Å (Scheme 2.5C and 2.5D).

Results show that the least energetic electronic transition appears at 392 nm and is responsible for the observed visible-light absorption. This transition has a charge-transfer excitation character originating from the dimsyl anion molecular orbital (MO) π_{HOMO} to the aryl halide MOs σ_{LUMO} , $\pi_{\text{LUMO}+1}$ and $\pi_{\text{LUMO}+2}$ with a 14%, 74%, and 8% contribution, respectively. Based on previous reports of KO t Bu performing SET,^{11, 16} we performed various DFT calculations with analogous complexes involving $^-$ O t Bu and aryl iodide. Unfortunately, neither halogen-bonded intermediates nor anion- π complexes modeled in our study had charge-transfer character, further eroding a potential involvement of $^-$ O t Bu in the SET step.

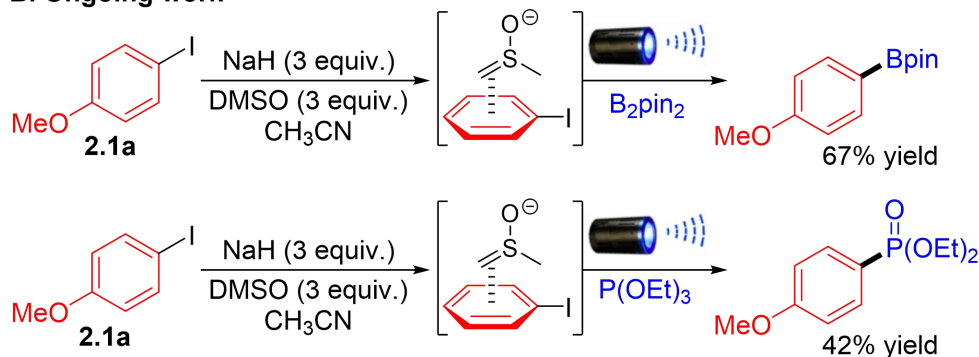
Based on the calculations and mechanistic experiments presented above, we propose that in presence of base, DMSO generates dimsyl anions capable of forming an EDA complex with the aromatic halide (Scheme 2.6A). A charge-transfer from the dimsyl anion to the aryl halide forms aryl radical anion and dimsyl radical. Loss of iodide generates aryl radical that then couples with disulfide or thiyl radical to give the desired product. Decomposition of the dimsyl radical via reactions with *tert*-butanol, disulfide or by other processes lead to the formation of minor impurities.

Finally, to further demonstrate the value of the proposed mechanism and open the door to future work and other possible transformations, we demonstrated that similar metal-free reaction conditions that generate dimsyl anion can be used to generate new C-B and C-P bonds from (Scheme 2.6B). Indeed, starting from **2.1a** in presence of B₂pin₂ or P(OEt)₃ (Scheme 2.6B, Eq.3 & Eq.4) and NaH in CH₃CN with 3 equivalents of DMSO generated the desired aryl-Bpin and aryl-phosphate in good unoptimized yields (67% and 42%, respectively). These two additional examples suggest that our EDA complex strategy can be applied to other functional group interconversions and that DMSO can be used as a reagent and not as a solvent. These examples also further demonstrate that KO t Bu is not required as a reagent and it is therefore not involved in the SET step. While more work and further optimization is required for these two reactions, we believe other valuable transformations that generate aryl radicals from aryl halides via EDA complexes are possible.

A. Proposed mechanism



B. Ongoing work^[a]



Scheme 2.6. Proposed mechanism and Ongoing work.

A. Proposed Mechanism. B. Ongoing transformations utilizing same mechanism. a. Reaction conditions: **2.1a** (0.2 mmol, 1 equiv.), NaH (3 equiv.), DMSO (3 equiv.), CH₃CN (1 mL), B₂pin₂ or P(OEt)₃ (3 equiv.) room temperature around reaction flask was 35 °C (heating caused by the LED lamp), under N₂, 24h.

2.3 Summary

In summary, we have developed a simple and efficient visible-light-induced cross-coupling reaction between aryl halides and diaryl disulfide, diselenides, and ditellurides to form unsymmetrical diaryl chalcogenides without using transition-metal catalysts, a photocatalyst, or added ligands. The transformation proceeds under mild reaction conditions, exhibits good tolerance of functional groups, and can be applied to cross-couplings of heteroaromatic halides. We also have postulated a novel mechanism to account for these transformations based on control experiments, a UV-Vis spectroscopy investigation, and TD-DFT calculations. We surmise that an EDA complex between dimsyl anion and the aryl halide is formed during the reaction. Upon absorbance of visible light, the EDA complex undergoes a charge transfer that leads to loss of halide and formation of an aryl radical. From this observation, we envision future dimsyl anion enabled cross-coupling reactions of aryl halides with different aryl radical trapping agents.

2.4 Acknowledgements

This publication was made possible, with support from the National Institute of Dental & Craniofacial Research grant number 5R21DE029156-02. This research was supported in part by Lilly Endowment, Inc. through its support for the Indiana University Pervasive Technology Institute. The authors also want to acknowledge Drs. M. K. Brown and S. Cook (IU Bloomington) and graduate student S. K. Dorn for helping with compound characterization.

2.5 Experimental

General Information: All the solvents and commercially available reagents were purchased from commercial sources (Acros Organics, TCI, Alfa Aesar, Sigma-Aldrich, Oakwood) and used directly. DMSO was purchased from Fisher Chemical (LOT 163913) with assay (99.9%) and water (0.02%). Thin layer chromatography (TLC) was performed on EMD precoated plates (silica gel 60 F254, Art 5715) and visualized by fluorescence quenching under UV light or stains for TLC Plates. Column chromatography was performed on EMD Silica Gel 60 (200–300 Mesh) using a forced flow of 0.5–1.0 bar. The ^1H and ^{13}C NMR spectra were obtained on a Bruker AVANCE III-400 or 500 spectrometer. ^1H NMR data was reported as: chemical shift (δ ppm), multiplicity, coupling constant (Hz), and integration. ^{13}C NMR data was reported in terms of chemical shift (δ ppm), multiplicity, and coupling constant (Hz). Melting point was obtained using MPA160 Melting Point Apparatus. High Resolution Mass Spectrometry (HRMS) analysis was obtained using Agilent Technologies 6520 Accurate-Mass Q-TOF LC/MS system. UV-Vis was obtained using Thermo Scientific Evolution 600 UV-Vis Spectrophotometers and fisherbrand macro quartz cuvettes (cat. No. 14-958-112). A Kessil (427 or 456nm) Blue LED lamp 40W was used for this light-promoted reaction. The vial was placed approximately 4 cm away from the Blue LED, with the LED shining directly at the side of the vial. 10 mL microwave reaction vial secured by 20mm aluminum seals with 0.125-inch thick, blue PTFE / white silicone septa was used for the reaction.

General procedure for the preparation of diaryl disulfides:

Procedure A: A mixture of thiol (1.0 mmol), potassium carbonate (1.0 mmol) in acetonitrile (5 mL) is stirred at room temperature and access to atmosphere in a glass reactor equipped without an air purge. The completion of reaction is monitored by GC-MS. The reaction

mixture is filtered, and evaporation of the filtrate under reduced pressure followed by preparative thin layer chromatography on silica gel afforded the pure products **2.2**.

Procedure B: Under ambient condition, a sample vial was charged with 0.2 mmol of thiols, then 1.0 mL of 0.01M *t*BuOK THF solution was added. The vial was sealed at room temperature and stirred. The completion of reaction is monitored by GC-MS. Isolated products **2.2** were obtained after flash chromatography using petroleum ether as eluent.

General procedure for the preparation of starting materials: To a solution of acid (2 mmol), alcohol (0.8 equiv) and 4-dimethylaminopyridine (0.1 equiv) in dichloromethane (0.5 mmol/mL) was added *N,N*-dicyclohexylcarbodiimide (0.8 equiv) at 0 °C. After the reaction mixture was allowed to stir at ambient temperature overnight. The completion of reaction is monitored by GC-MS. Isolated products were obtained after flash chromatography.

General procedure for the synthesis of unsymmetrical dichalcogenides: A 10 mL microwave vial was charged with aryl halides (0.2 mmol), KO*t*Bu (0.6 mmol), diaryl dichalcogenides (0.3 mmol), 1.0 mL DMSO and capped with 20 mm microwave crimp caps with septa. After using acetone-dry ice cooling bath to freeze the mixture, the vial was evacuated and filled with N₂ three times. Remove the reaction mixture from cooling bath and let it warm to room temperature. And then then put the vial approximately 4 cm away from the Blue LED lamp and stirred. After the completion of reaction, the product was determined by thin layer chromatography and GC-MS. The reaction mixture was quenched with DI water and diluted and extracted with EtOAc. The organic layer was filtered through a pad of Celite, and the filtrate was concentrated in vacuo. Then the residue was purified by flash chromatography (ethyl acetate/hexane) on silica gel to yield the desired product.

1 mmol scale detailed method included for one-step transformations: A 10 mL microwave vial was charged with 8-bromoquinoline (208 mg, 1.0 mmol), KO*t*Bu (336 mg, 3.0 mmol), diphenyl diselenide (468 mg, 1.5 mmol), 3.0 mL DMSO and capped with 20 mm microwave crimp caps with septa. After using acetone-dry ice cooling bath to freeze the mixture, the vial was evacuated and filled with N₂ three times. Remove the reaction mixture from cooling bath and let it warm to room temperature. And then then put the vial approximately 4 cm away from the Blue LED lamp and stirred. After the completion of reaction, the product was determined by thin layer chromatography and GC-MS. The reaction mixture was quenched with DI water and diluted and extracted with EtOAc. The organic layer was filtered through a pad of

Celite, and the filtrate was concentrated in vacuo. Then the residue was purified by flash chromatography (ethyl acetate/hexane=1/50) on silica gel to yield the desired product **2.36** as a pale yellow solid (179 mg, 63 %). m.p:115-118 °C

Analytical Data of Compounds:

(4-methoxyphenyl)(phenyl)sulfane (2.3) Conditions: 1-iodo-4-methoxybenzene (47 mg, 0.2 mmol), KO^tBu (67 mg, 0.6 mmol), diphenyl disulfide (66 mg, 0.3 mmol), 1.0 mL DMSO, 24h. The product was isolated by flash chromatography (ethyl acetate/hexane= 1/50) as a pale yellow oil (38.0 mg, 88%). ¹H NMR (400 MHz, CDCl₃) δ 7.47 – 7.43 (m, 2H), 7.29 – 7.24 (m, 2H), 7.22 – 7.14 (m, 3H), 6.96 – 6.90 (m, 2H), 3.85 (s, 3H). ¹³C NMR (101 MHz, CDCl₃) δ 159.9 (s), 138.6(s), 135.4 (s), 128.9 (s), 128.3 (s), 125.8 (s), 124.4 (s), 115.0 (s), 55.4 (s).

phenyl(p-tolyl)sulfane (2.4) Conditions: 1-iodo-4-methylbenzene (44 mg, 0.2 mmol), KO^tBu (67 mg, 0.6 mmol), diphenyl disulfide (66 mg, 0.3 mmol), 1.0 mL DMSO, 24h. The product was isolated by flash chromatography (hexane) as a colorless oil (35.6 mg, 89%). ¹H NMR (400 MHz, CDCl₃) δ 7.30 (t, *J* = 6.1 Hz, 2H), 7.28 – 7.17 (m, 5H), 7.14 (d, *J* = 7.9 Hz, 2H), 2.35 (s, 3H). ¹³C NMR (101 MHz, CDCl₃) δ 137.6 (s), 137.2 (s), 132.3 (s), 131.4 (s), 130.1 (s), 129.9 (s), 129.1 (s), 126.4 (s), 21.1 (s).

phenyl(4-(trifluoromethyl)phenyl)sulfane (2.5) Conditions: 1-iodo-4-(trifluoromethyl)benzene (54 mg, 0.2 mmol), KO^tBu (67 mg, 0.6 mmol), diphenyl disulfide (66 mg, 0.3 mmol), 1.0 mL DMSO, 24h. The product was isolated by flash chromatography (hexane) as a pale yellow oil (39.2 mg, 86%). ¹H NMR (400 MHz, CDCl₃) δ 7.46 (dd, *J* = 7.6, 2.1 Hz, 4H), 7.40 – 7.33 (m, 3H), 7.27 – 7.23 (m, 2H). ¹³C NMR (101 MHz, CDCl₃) δ 142.9 (s), 133.5 (s), 132.6 (s), 129.7 (s), 128.7 (s), 128.3 (s), 128.1 (q, *J* = 34 Hz), 125.8 (q, *J* = 3.8 Hz), 124.1 (q, *J* = 270 Hz). ¹⁹F NMR (377 MHz, CDCl₃) δ -62.47 (s).

(4-fluorophenyl)(phenyl)sulfane (2.6) Conditions: 1-fluoro-4-iodobenzene (44 mg, 0.2 mmol), KO^tBu (67 mg, 0.6 mmol), diphenyl disulfide (66 mg, 0.3 mmol), 1.0 mL DMSO, 24h. The product was isolated by flash chromatography (hexane) as a pale yellow oil (35.1 mg, 86%). ¹H NMR (400 MHz, CDCl₃) δ 7.32 – 7.26 (m, 2H), 7.22 – 7.16 (m, 4H), 7.15 – 7.10 (m, 1H), 6.97 – 6.91 (m, 2H). ¹³C NMR (101 MHz, CDCl₃) δ 162.4 (d, *J* = 246 Hz), 136.7 (s), 134.1 (d, *J* = 8.2 Hz), 130.3 (d, *J* = 3.3 Hz), 130.0 (s), 129.2 (s), 126.8 (s), 116.5 (s), 116.3 (s). ¹⁹F NMR (377 MHz, CDCl₃) δ -113.96 – -114.06 (m).

(3,5-bis(trifluoromethyl)phenyl)(phenyl)sulfane (2.7) Conditions: 1-bromo-3,5-bis(trifluoromethyl)benzene (59 mg, 0.2 mmol), KOtBu (67 mg, 0.6 mmol), diphenyl disulfide (66 mg, 0.3 mmol), 1.0 mL DMSO, 24h. The product was isolated by flash chromatography (ethyl acetate/hexane= 1/50) as a colorless oil (42.5 mg, 66%). ¹H NMR (400 MHz, CDCl₃) δ 7.63 (s, 1H), 7.57 (s, 2H), 7.49 (qd, *J* = 3.7, 1.4 Hz, 2H), 7.44 (dd, *J* = 6.6, 2.7 Hz, 3H). ¹³C NMR (101 MHz, CDCl₃) δ 141.7 (s), 133.8 (s), 132.3 (q, *J* = 33.4 Hz), 131.2 (s), 130.0 (s), 129.4 (s), 123.0 (q, *J* = 271 Hz), 119.6 (dt, *J* = 7.6, 3.8 Hz). ¹⁹F NMR (377 MHz, CDCl₃) δ -63.14 (s).

4-(phenylthio)benzonitrile (2.8) Conditions: 4-bromobenzonitrile (36 mg, 0.2 mmol), KOtBu (67 mg, 0.6 mmol), diphenyl disulfide (66 mg, 0.3 mmol), 1.0 mL DMSO, 24h. The product was isolated by flash chromatography (ethyl acetate/hexane= 1/50) as a pale yellow oil (27.9 mg, 33%). ¹H NMR (400 MHz, CDCl₃) δ 7.54 – 7.50 (m, 2H), 7.49 (d, *J* = 1.8 Hz, 1H), 7.47 (s, 1H), 7.45 – 7.41 (m, 3H), 7.19 – 7.14 (m, 2H). ¹³C NMR (101 MHz, CDCl₃) δ 145.7 (s), 134.5 (s), 132.4 (s), 130.9 (s), 129.9 (s), 129.4 (s), 127.4 (s), 118.8 (s), 108.8 (s).

naphthalen-1-yl(phenyl)sulfane (2.9) Conditions: 1-iodonaphthalene (51 mg, 0.2 mmol), KOtBu (67 mg, 0.6 mmol), diphenyl disulfide (66 mg, 0.3 mmol), 1.0 mL DMSO, 24h. The product was isolated by flash chromatography (hexane) as a pale yellow oil (43.4 mg, 92%). ¹H NMR (400 MHz, CDCl₃) δ 8.45 (dd, *J* = 6.3, 3.4 Hz, 1H), 7.98 – 7.87 (m, 2H), 7.73 (d, *J* = 7.2 Hz, 1H), 7.57 (dq, *J* = 6.7, 3.4 Hz, 2H), 7.48 (t, *J* = 7.7 Hz, 1H), 7.32 – 7.18 (m, 5H). ¹³C NMR (101 MHz, CDCl₃) δ 137.0 (s), 134.3 (s), 133.7 (s), 132.6 (s), 131.3 (s), 129.2 (s), 129.1 (s), 129.1 (s), 128.6 (s), 127.0 (s), 126.5 (s), 126.2 (s), 125.9(s), 125.7(s).

2-(phenylthio)pyridine (2.10) Conditions: 2-bromopyridine (32 mg, 0.2 mmol), KOtBu (67 mg, 0.6 mmol), diphenyl disulfide (66 mg, 0.3 mmol), 1.0 mL DMSO, 24h. The product was isolated by flash chromatography (ethyl acetate/hexane= 1/30) as a pale yellow oil (34.8 mg, 93%). ¹H NMR (400 MHz, CDCl₃) δ 8.42 (dd, *J* = 4.8, 1.0 Hz, 1H), 7.63 – 7.55 (m, 2H), 7.48 – 7.37 (m, 4H), 6.99 (ddd, *J* = 7.4, 4.9, 0.9 Hz, 1H), 6.88 (d, *J* = 8.1 Hz, 1H). ¹³C NMR (101 MHz, CDCl₃) δ 161.5 (s), 149.6 (s), 136.7 (s), 134.9 (s), 131.1 (s), 129.6 (s), 129.1 (s), 121.4 (s), 119.9 (s).

3-(phenylthio)pyridine (2.11) Conditions: 3-iodopyridine (41 mg, 0.2 mmol), KOtBu (67 mg, 0.6 mmol), diphenyl disulfide (66 mg, 0.3 mmol), 1.0 mL DMSO, 24h. The product was isolated by flash chromatography (ethyl acetate/hexane= 1/30) as a pale yellow oil (28.1 mg, 75%). ¹H NMR (400 MHz, CDCl₃) δ 8.58 (d, *J* = 1.5 Hz, 1H), 8.48 (d, *J* = 3.9 Hz, 1H), 7.65 –

7.58 (m, 1H), 7.43 – 7.28 (m, 5H), 7.23 (dd, $J = 8.0, 4.8$ Hz, 1H). ^{13}C NMR (101 MHz, CDCl_3) δ 151.1 (s), 147.8 (s), 137.9 (s), 133.9 (s), 133.7 (s), 131.8 (s), 129.5 (s), 127.9 (s), 123.9 (s).

6-(phenylthio)quinoline (2.12) Conditions: 6-iodoquinoline (51 mg, 0.2 mmol), KOtBu (67 mg, 0.6 mmol), diphenyl disulfide (66 mg, 0.3 mmol), 1.0 mL DMSO, 24h. The product was isolated by flash chromatography (ethyl acetate/hexane= 1/30) as a yellow oil (35.6 mg, 75%). ^1H NMR (400 MHz, CDCl_3) δ 8.86 (d, $J = 3.0$ Hz, 1H), 8.00 (d, $J = 8.7$ Hz, 2H), 7.69 (d, $J = 1.4$ Hz, 1H), 7.59 (dd, $J = 8.8, 1.6$ Hz, 1H), 7.44 (d, $J = 7.0$ Hz, 2H), 7.34 (dt, $J = 9.4, 5.3$ Hz, 4H). ^{13}C NMR (101 MHz, CDCl_3) δ 150.3 (s), 147.2 (s), 135.3 (d, $J = 1.8$ Hz), 134.5 (s), 132.1 (s), 131.5 (s), 130.3 (s), 129.5 (s), 128.7 (s), 128.0 (s), 127.8 (s), 121.7 (s).

5-(phenylthio)quinoline (2.13) Conditions: 5-bromoquinoline (42 mg, 0.2 mmol), KOtBu (67 mg, 0.6 mmol), diphenyl disulfide (66 mg, 0.3 mmol), 1.0 mL DMSO, 24h. The product was isolated by flash chromatography (ethyl acetate/hexane= 1/30) as a pale yellow oil (25.2 mg, 53%). ^1H NMR (400 MHz, CDCl_3) δ 8.86 (dd, $J = 4.1, 1.4$ Hz, 1H), 8.60 (d, $J = 8.5$ Hz, 1H), 8.04 (d, $J = 8.2$ Hz, 1H), 7.67 – 7.55 (m, 2H), 7.34 (dd, $J = 8.5, 4.2$ Hz, 1H), 7.19 – 7.07 (m, 5H). ^{13}C NMR (101 MHz, CDCl_3) δ 150.8 (s), 149.0 (s), 136.3 (s), 134.0 (s), 132.8 (s), 131.8 (s), 130.6 (s), 129.3 (s), δ 129.25 (d, $J = 1.2$ Hz), 129.0 (s), 126.6 (s), 121.7 (s). HRMS (ESI) m/z : $[\text{M}+\text{Na}]^+$ calcd for $\text{C}_{15}\text{H}_{11}\text{NNaS}$ 260.0504; found 260.0523.

2,6-bis(phenylthio)pyridine (2.14) Conditions: 2,6-dibromopyridine (47 mg, 0.2 mmol), KOtBu (133 mg, 1.2 mmol), diphenyl disulfide (131 mg, 0.6 mmol), 1.0 mL DMSO, 24h. The product was isolated by flash chromatography (ethyl acetate/hexane= 1/30) as a white solid (42.5 mg, 72%). ^1H NMR (400 MHz, CDCl_3) δ 7.59 (dd, $J = 6.4, 3.1$ Hz, 4H), 7.44 – 7.36 (m, 6H), 7.19 (t, $J = 7.9$ Hz, 1H), 6.54 (d, $J = 7.9$ Hz, 2H). ^{13}C NMR (101 MHz, CDCl_3) δ 161.7 (s), 137.0 (s), 135.2 (s), 130.8 (s), 129.6 (s), 129.1 (s), 117.0 (s).

2-((4-methoxyphenyl)thio)pyridine (2.15) Conditions: 1-iodo-4-methoxybenzene (47 mg, 0.2 mmol), KOtBu (67 mg, 0.6 mmol), 2,2'-dithiodipyridine (66 mg, 0.3 mmol), 1.0 mL DMSO, 24h. The product was isolated by flash chromatography (ethyl acetate/hexane= 1/20) as a white solid (35.6 mg, 82%). ^1H NMR (400 MHz, CDCl_3) δ 8.40 (dd, $J = 4.8, 0.9$ Hz, 1H), 7.56 – 7.50 (m, 2H), 7.41 (ddd, $J = 9.4, 7.8, 1.9$ Hz, 1H), 6.99 – 6.92 (m, 3H), 6.78 (d, $J = 8.1$ Hz, 1H), 3.85 (s, 3H). ^{13}C NMR (101 MHz, CDCl_3) δ 162.8 (s), 160.7 (s), 149.4 (s), 137.3 (s), 136.6 (s), 121.2 (s), 120.4 (s), 119.5 (s), 115.3 (s), 55.4 (s).

2-(p-tolylthio)pyridine (2.16) Conditions: 1-iodo-4-methylbenzene (44 mg, 0.2 mmol), KOtBu (67 mg, 0.6 mmol), 2,2'-dithiodipyridine (66 mg, 0.3 mmol), 1.0 mL DMSO, 24h. The product was isolated by flash chromatography (ethyl acetate/hexane= 1/30) as a pale yellow oil (30.6 mg, 76%). ¹H NMR (400 MHz, CDCl₃) δ 8.41 (dd, *J* = 4.8, 1.0 Hz, 1H), 7.49 (d, *J* = 8.1 Hz, 2H), 7.42 (td, *J* = 8.0, 1.9 Hz, 1H), 7.23 (d, *J* = 7.9 Hz, 2H), 6.96 (ddd, *J* = 7.4, 4.9, 0.9 Hz, 1H), 6.84 (d, *J* = 8.1 Hz, 1H), 2.39 (s, 3H). ¹³C NMR (101 MHz, CDCl₃) δ 162.2 (s), 149.5 (s), 139.5 (s), 136.6 (s), 135.3 (s), 130.5 (s), 127.3 (s), 120.9 (s), 119.6 (s), 21.3 (s).

2-((4-(trifluoromethyl)phenyl)thio)pyridine (2.17) Conditions: 1-iodo-4-(trifluoromethyl)benzene (54 mg, 0.2 mmol), KOtBu (67 mg, 0.6 mmol), 2,2'-dithiodipyridine (66 mg, 0.3 mmol), 1.0 mL DMSO, 24h. The product was isolated by flash chromatography (ethyl acetate/hexane= 1/30) as a pale yellow oil (37.3 mg, 73%). ¹H NMR (400 MHz, CDCl₃) δ 8.48 – 8.45 (m, 1H), 7.68 – 7.59 (m, 4H), 7.54 (td, *J* = 7.9, 1.9 Hz, 1H), 7.13 – 7.06 (m, 2H). ¹³C NMR (101 MHz, CDCl₃) δ 158.8 (s), 150.1 (s), 137.1 (s), 133.5 (s), 130.4 (q, *J* = 32.7 Hz), 126.2 (q, *J* = 3.7 Hz), 123.9 (q, *J* = 271 Hz), 123.1 (s), 121.0 (s). ¹⁹F NMR (377 MHz, CDCl₃) δ -62.74 (s).

2-((4-fluorophenyl)thio)pyridine (2.18) Conditions: 1-fluoro-4-iodobenzene (44 mg, 0.2 mmol), KOtBu (67 mg, 0.6 mmol), 2,2'-dithiodipyridine (66 mg, 0.3 mmol), 1.0 mL DMSO, 24h. The product was isolated by flash chromatography (ethyl acetate/hexane= 1/30) as a pale yellow oil (36.5 mg, 89%). ¹H NMR (400 MHz, CDCl₃) δ 8.41 (dd, *J* = 4.8, 0.9 Hz, 1H), 7.63 – 7.55 (m, 2H), 7.46 (td, *J* = 7.9, 1.9 Hz, 1H), 7.17 – 7.08 (m, 2H), 7.02 – 6.96 (m, 1H), 6.87 (d, *J* = 8.1 Hz, 1H). ¹³C NMR (101 MHz, CDCl₃) δ 164.7 (s), 161.7 (d, *J* = 87.7 Hz), 149.7 (s), 137.3 (d, *J* = 8.5 Hz), 136.8 (s), 126.2 (d, *J* = 3.5 Hz), 121.1 (s), 120.0(s), 116.8 (d, *J* = 22.0 Hz). ¹⁹F NMR (377 MHz, CDCl₃) δ -111.43 (s).

2-((4-nitrophenyl)thio)pyridine (2.19) Conditions: 1-bromo-4-nitrobenzene (40 mg, 0.2 mmol), KOtBu (67 mg, 0.6 mmol), 2,2'-dithiodipyridine (66 mg, 0.3 mmol), 1.0 mL DMSO, 24h. The product was isolated by flash chromatography (ethyl acetate/hexane= 1/30) as a yellow solid (37.2 mg, 80%). ¹H NMR (400 MHz, CDCl₃) δ 8.51 (dd, *J* = 4.8, 0.9 Hz, 1H), 8.17 (dd, *J* = 9.2, 2.2 Hz, 2H), 7.67 – 7.55 (m, 3H), 7.30 (d, *J* = 8.0 Hz, 1H), 7.21 – 7.14 (m, 1H). ¹³C NMR (101 MHz, CDCl₃) δ 156.6 (s), 150.5 (s), 147.0 (s), 142.4 (s), 137.4 (s), 131.9 (s), 124.9 (s), 124.2 (s), 122.0 (s).

2-(naphthalen-1-ylthio)pyridine (2.20) Conditions: 1-iodonaphthalene (51 mg, 0.2 mmol), KOtBu (67 mg, 0.6 mmol), 2,2'-dithiodipyridine (66 mg, 0.3 mmol), 1.0 mL DMSO, 24h. The product was isolated by flash chromatography (ethyl acetate/hexane= 1/30) as a pale yellow oil (39.9 mg, 84%). ¹H NMR (400 MHz, CDCl₃) δ 8.48 – 8.37 (m, 2H), 8.04 – 7.90 (m, 3H), 7.61 – 7.51 (m, 3H), 7.31 (ddd, *J* = 11.4, 6.4, 2.6 Hz, 1H), 6.96 (ddd, *J* = 7.4, 4.9, 0.9 Hz, 1H), 6.57 (d, *J* = 8.1 Hz, 1H). ¹³C NMR (101 MHz, CDCl₃) δ 161.7 (s), 149.5 (s), 136.7 (s), 135.7 (s), 134.6 (s), 134.5 (s), 130.9 (s), 128.7 (s), 127.8 (s), 127.4 (s), 126.6 (s), 126.0 (s), 120.7 (s), 119.6 (s).

6-(pyridin-2-ylthio)quinoline (2.21) Conditions: 6-iodoquinoline (51 mg, 0.2 mmol), KOtBu (67 mg, 0.6 mmol), 2,2'-dithiodipyridine (66 mg, 0.3 mmol), 1.0 mL DMSO, 24h. The product was isolated by flash chromatography (ethyl acetate/hexane= 1/30) as a pale yellow solid (34.8 mg, 73%). ¹H NMR (400 MHz, CDCl₃) δ 8.94 (dd, *J* = 4.2, 1.7 Hz, 1H), 8.48 – 8.41 (m, 1H), 8.16 – 8.04 (m, 3H), 7.80 (dd, *J* = 8.8, 2.0 Hz, 1H), 7.52 – 7.38 (m, 2H), 7.03 (ddd, *J* = 11.1, 6.9, 3.1 Hz, 2H). ¹³C NMR (101 MHz, CDCl₃) δ 160.2 (s), 151.3 (s), 149.9 (s), 148.0 (s), 136.9 (s), 135.9 (s), 134.8 (s), 133.5 (s), 130.7 (s), 130.0 (s), 128.8 (s), 122.2 (s), 121.8 (s), 120.5 (s).

5-(pyridin-2-ylthio)quinoline (2.22) Conditions: 5-bromoquinoline (42 mg, 0.2 mmol), KOtBu (67 mg, 0.6 mmol), 2,2'-dithiodipyridine (66 mg, 0.3 mmol), 1.0 mL DMSO, 24h. The product was isolated by flash chromatography (ethyl acetate/hexane= 1/30) as a pale yellow oil (35.7 mg, 75%). ¹H NMR (400 MHz, CDCl₃) δ 8.94 (dd, *J* = 4.2, 1.6 Hz, 1H), 8.66 (dd, *J* = 8.5, 0.6 Hz, 1H), 8.41 – 8.34 (m, 1H), 8.23 (d, *J* = 8.5 Hz, 1H), 7.98 (dd, *J* = 7.2, 1.0 Hz, 1H), 7.76 (dd, *J* = 8.5, 7.2 Hz, 1H), 7.42 (dd, *J* = 8.6, 4.2 Hz, 1H), 7.34 (td, *J* = 7.8, 1.9 Hz, 1H), 6.96 (ddd, *J* = 7.4, 4.9, 0.9 Hz, 1H), 6.60 (d, *J* = 8.1 Hz, 1H). ¹³C NMR (101 MHz, CDCl₃) δ 160.8 (s), 150.9 (s), 149.7 (s), 149.1 (s), 136.8 (s), 135.9 (s), 134.5 (s), 132.3 (s), 130.2 (s), 129.5 (s), 128.2 (s), 122.2 (s), 121.0 (s), 120.0 (s). HRMS (ESI) *m/z*: [M+Na]⁺ calcd for C₁₄H₁₀N₂NaS 261.0457; found 261.0436.

(4-methoxyphenyl)(p-tolyl)sulfane (2.23) Conditions: 1-iodo-4-methoxybenzene (47 mg, 0.2 mmol), KOtBu (67 mg, 0.6 mmol), p-Tolyl disulfide (74 mg, 0.3 mmol), 1.0 mL DMSO, 24h. The product was isolated by flash chromatography (ethyl acetate/hexane= 1/50) as a pale yellow oil (40.5 mg, 88%). ¹H NMR (400 MHz, CDCl₃) δ 7.38 – 7.34 (m, 2H), 7.16 – 7.11 (m, 2H), 7.07 (d, *J* = 8.1 Hz, 2H), 6.89 – 6.85 (m, 2H), 3.81 (s, 3H), 2.30 (s, 3H). ¹³C NMR (101 MHz, CDCl₃) δ 159.5 (s), 136.1 (s), 134.4 (s), 133.5 (s), 129.8 (s), 129.4 (s), 125.7 (s), 114.9 (s), 55.4 (s), 21.0 (s).

4-((4-methoxyphenyl)thio)aniline (2.24) Conditions: 1-iodo-4-methoxybenzene (47 mg, 0.2 mmol), KO^tBu (67 mg, 0.6 mmol), 4,4'-disulfanediyl dianiline (75 mg, 0.3 mmol), 1.0 mL DMSO, 24h. The product was isolated by flash chromatography (ethyl acetate/hexane= 1/50) as a yellow oil (10.2 mg, 22%). ¹H NMR (400 MHz, CDCl₃) δ 7.22 (d, *J* = 2.3 Hz, 2H), 7.20 (d, *J* = 2.0 Hz, 2H), 6.81 (d, *J* = 8.8 Hz, 2H), 6.63 (d, *J* = 8.5 Hz, 2H), 3.77 (s, 5H). ¹³C NMR (101 MHz, CDCl₃) δ 158.6 (s), 146.1 (s), 134.0 (s), 131.5 (s), 128.8 (s), 123.6 (s), 115.8 (s), 114.6 (s), 55.4 (s).

(4-methoxyphenyl)(naphthalen-1-yl)sulfane (2.25) Conditions: 1-iodo-4-methoxybenzene (47 mg, 0.2 mmol), KO^tBu (67 mg, 0.6 mmol), 1,2-di(naphthalen-1-yl)disulfane (96 mg, 0.3 mmol), 1.0 mL DMSO, 24h. The product was isolated by flash chromatography (ethyl acetate/hexane= 1/50) as a yellow solid (46.9 mg, 88%). ¹H NMR (400 MHz, CDCl₃) δ 8.42 – 8.34 (m, 1H), 7.86 (dd, *J* = 6.9, 2.5 Hz, 1H), 7.77 – 7.70 (m, 1H), 7.57 – 7.48 (m, 2H), 7.40 – 7.30 (m, 4H), 6.91 – 6.82 (m, 2H), 3.80 (s, 3H). ¹³C NMR (101 MHz, CDCl₃) δ 159.4 (s), 134.7 (s), 134.0 (s), 133.8 (s), 132.3 (s), 128.5 (s), 128.5 (s), 127.4 (s), 126.5 (s), 126.3 (s), 125.8 (s), 125.2 (s), 124.9 (s), 115.0 (s), 55.4 (s).

(4-fluorophenyl)(4-methoxyphenyl)sulfane (2.26) Conditions: 1-iodo-4-methoxybenzene (47 mg, 0.2 mmol), KO^tBu (67 mg, 0.6 mmol), 1,2-bis(4-fluorophenyl)disulfane (76 mg, 0.3 mmol), 1.0 mL DMSO, 24h. The product was isolated by flash chromatography (ethyl acetate/hexane= 1/50) as a pale yellow oil (38.9 mg, 83%). ¹H NMR (400 MHz, CDCl₃) δ 7.39 – 7.32 (m, 2H), 7.20 (ddd, *J* = 6.7, 5.2, 2.1 Hz, 2H), 7.00 – 6.92 (m, 2H), 6.91 – 6.85 (m, 2H), 3.81 (s, 3H). ¹³C NMR (101 MHz, CDCl₃) δ 161.6 (d, *J* = 246.1 Hz), 159.7 (s), 134.5 (s), 133.1 (d, *J* = 3.2 Hz), 131.1 (d, *J* = 7.9 Hz), 125.3 (s), 116.1 (d, *J* = 22.0 Hz), 115.0 (s), 55.4 (s). ¹⁹F NMR (377 MHz, CDCl₃) δ -116.07 – -116.26 (m).

(2-methoxyphenyl)(4-nitrophenyl)sulfane (2.27) Conditions: 1-bromo-4-nitrobenzene (40 mg, 0.2 mmol), KO^tBu (67 mg, 0.6 mmol), 1,2-bis(2-methoxyphenyl)disulfane (84 mg, 0.3 mmol), 1.0 mL DMSO, 24h. The product was isolated by flash chromatography (ethyl acetate/hexane= 1/50) as a yellow solid (46.5 mg, 89%). ¹H NMR (400 MHz, CDCl₃) δ 8.08 – 8.00 (m, 2H), 7.55 – 7.45 (m, 2H), 7.16 – 7.09 (m, 2H), 7.04 (dd, *J* = 11.8, 4.4 Hz, 2H), 3.82 (s, 3H). ¹³C NMR (101 MHz, CDCl₃) δ 159.7 (s), 148.0 (s), 145.2 (s), 136.9 (s), 132.0 (s), 126.2 (s), 123.9 (s), 121.7 (s), 117.7 (s), 111.8 (s), 56.0 (s).

1,4-bis(phenylthio)benzene (2.28) Conditions: 1,4-diiodobenzene (66 mg, 0.2 mmol), KO^tBu (133 mg, 1.2 mmol), diphenyl disulfide (132 mg, 0.6 mmol), 1.0 mL DMSO, 24h. The product was isolated by flash chromatography (hexane) as a white solid (53.6 mg, 91%). ¹H NMR (400 MHz, CDCl₃) δ 7.44 – 7.27 (m, 14H). ¹³C NMR (101 MHz, CDCl₃) δ 135.1 (s), 135.0 (s), 131.5 (s), 131.2 (s), 129.3 (s), 127.4 (s).

(4-methoxyphenyl)(phenyl)selane (2.29) Conditions: 1-iodo-4-methoxybenzene (47 mg, 0.2 mmol), KO^tBu (67 mg, 0.6 mmol), diphenyl diselenide (94 mg, 0.3 mmol), 1.0 mL DMSO, 24h. The product was isolated by flash chromatography (ethyl acetate/hexane= 1/50) as a pale yellow oil (30.0 mg, 57%). ¹H NMR (400 MHz, CDCl₃) δ 7.56 – 7.48 (m, 2H), 7.36 – 7.31 (m, 2H), 7.25 – 7.16 (m, 3H), 6.90 – 6.83 (m, 2H), 3.82 (s, 3H). ¹³C NMR (101 MHz, CDCl₃) δ 159.8 (s), 136.5 (s), 133.2 (s), 130.9 (s), 129.2 (s), 126.5 (s), 120.0 (s), 115.2 (s), 55.3 (s).

phenyl(4-(trifluoromethyl)phenyl)selane (2.30) Conditions: 1-iodo-4-(trifluoromethyl)benzene (54 mg, 0.2 mmol), KO^tBu (67 mg, 0.6 mmol), diphenyl diselenide (94 mg, 0.3 mmol), 1.0 mL DMSO, 24h. The product was isolated by flash chromatography (hexane) as a pale yellow oil (31.3 mg, 52%). ¹H NMR (400 MHz, CDCl₃) δ 7.60 – 7.55 (m, 2H), 7.45 (q, *J* = 8.6 Hz, 4H), 7.39 – 7.32 (m, 3H). ¹³C NMR (101 MHz, CDCl₃) δ 137.8 (d, *J* = 1.4 Hz), 134.9 (s), 131.0 (s), 129.7 (s), 128.8 (s), 128.6 (s), 125.9 (q, *J* = 3.8 Hz), 124.1 (q, *J* = 273 Hz). ¹⁹F NMR (377 MHz, CDCl₃) δ -62.60 (s).

***N,N*-dimethyl-4-(phenylselanyl)benzamide (2.31)** Conditions: 4-bromo-*N,N*-dimethylbenzamide (46 mg, 0.2 mmol), KO^tBu (67 mg, 0.6 mmol), diphenyl diselenide (94 mg, 0.3 mmol), 1.0 mL DMSO, 24h. The product was isolated by flash chromatography (ethyl acetate/hexane= 1/30) as a yellow oil (25.6 mg, 42%). ¹H NMR (400 MHz, CDCl₃) δ 7.55 – 7.49 (m, 2H), 7.42 (d, *J* = 8.2 Hz, 2H), 7.33 – 7.27 (m, 5H), 3.03 (s, 6H). ¹³C NMR (126 MHz, CDCl₃) δ 171.1 (s), 134.9 (s), 134.0 (d, *J* = 2.6 Hz), 131.8 (s), 129.9 (s), 129.6 (s), 128.0 (s), 128.0 (s), 39.6 (s), 35.5 (s).

2-(phenylselanyl)pyridine (2.32) Conditions: 2-bromopyridine (32 mg, 0.2 mmol), KO^tBu (67 mg, 0.6 mmol), diphenyl diselenide (94 mg, 0.3 mmol), 1.0 mL DMSO, 24h. The product was isolated by flash chromatography (ethyl acetate/hexane= 1/50) as a pale yellow oil (20.1 mg, 43%). ¹H NMR (400 MHz, CDCl₃) δ 8.46 – 8.42 (m, 1H), 7.74 – 7.68 (m, 2H), 7.44 – 7.35 (m, 4H), 7.05 – 6.97 (m, 2H). ¹³C NMR (101 MHz, CDCl₃) δ 158.9 (s), 149.9 (s), 136.7 (s), 136.2 (s), 129.7 (s), 128.9 (s), 127.9 (s), 124.3 (s), 120.4 (s).

3-(phenylselanyl)pyridine (2.33) Conditions: 3-iodopyridine (41 mg, 0.2 mmol), KOtBu (67 mg, 0.6 mmol), diphenyl diselenide (94 mg, 0.3 mmol), 1.0 mL DMSO, 24h. The product was isolated by flash chromatography (ethyl acetate/hexane= 1/50) as a pale yellow oil (23.9 mg, 51%). ¹H NMR (400 MHz, CDCl₃) δ 8.66 (d, *J* = 1.6 Hz, 1H), 8.48 (dd, *J* = 4.7, 1.2 Hz, 1H), 7.74 (dt, *J* = 7.9, 1.8 Hz, 1H), 7.50 (dd, *J* = 6.3, 3.1 Hz, 2H), 7.34 – 7.28 (m, 3H), 7.19 (dd, *J* = 7.9, 4.8 Hz, 1H). ¹³C NMR (101 MHz, CDCl₃) δ 152.5 (s), 148.1 (s), 140.2 (s), 133.6 (s), 129.6 (s), 129.5 (s), 129.0 (s), 128.1 (s), 124.3 (s).

5-(phenylselanyl)quinoline (2.34) Conditions: 5-bromoquinoline (42 mg, 0.2 mmol), KOtBu (67 mg, 0.6 mmol), diphenyl diselenide (94 mg, 0.3 mmol), 1.0 mL DMSO, 24h. The product was isolated by flash chromatography (ethyl acetate/hexane= 1/30) as a pale yellow oil (40.9 mg, 72%). ¹H NMR (400 MHz, CDCl₃) δ 8.92 (dd, *J* = 4.2, 1.5 Hz, 1H), 8.65 (d, *J* = 8.5 Hz, 1H), 8.13 (d, *J* = 8.5 Hz, 1H), 7.85 (d, *J* = 7.2 Hz, 1H), 7.63 (dd, *J* = 8.3, 7.4 Hz, 1H), 7.41 (dd, *J* = 8.5, 4.2 Hz, 1H), 7.36 – 7.28 (m, 2H), 7.24 – 7.15 (m, 3H). ¹³C NMR (101 MHz, CDCl₃) δ 150.7 (s), 148.8 (s), 136.2 (s), 134.5 (s), 131.6 (s), 131.3 (s), 130.7 (s), 129.7 (s), 129.6 (s), 129.5 (s), 127.1 (s), 121.8 (s). HRMS (ESI) *m/z*: [M+Na]⁺ calcd for C₁₅H₁₁NNaSe 307.9949 ; found 307.9944.

6-(phenylselanyl)quinoline (2.35) Conditions: 6-iodoquinoline (51 mg, 0.2 mmol), KOtBu (67 mg, 0.6 mmol), diphenyl diselenide (94 mg, 0.3 mmol), 1.0 mL DMSO, 24h. The product was isolated by flash chromatography (ethyl acetate/hexane= 1/30) as a yellow oil (38.1 mg, 67%). ¹H NMR (400 MHz, CDCl₃) δ 8.92 – 8.84 (m, 1H), 8.04 – 7.95 (m, 2H), 7.86 (d, *J* = 1.7 Hz, 1H), 7.70 (dd, *J* = 8.8, 1.8 Hz, 1H), 7.58 – 7.50 (m, 2H), 7.37 (dd, *J* = 8.3, 4.2 Hz, 1H), 7.34 – 7.28 (m, 3H). ¹³C NMR (101 MHz, CDCl₃) δ 150.4 (s), 147.3 (s), 135.4 (s), 133.8 (s), 133.5 (s), 130.6 (s), 130.5 (s), 130.2 (s), 129.6 (s), 128.9 (s), 128.0(s), 121.6 (s).

8-(phenylselanyl)quinoline (2.36) Conditions: 8-bromoquinoline (42 mg, 0.2 mmol), KOtBu (67 mg, 0.6 mmol), diphenyl diselenide (94 mg, 0.3 mmol), 1.0 mL DMSO, 24h. The product was isolated by flash chromatography (ethyl acetate/hexane= 1/30) as a pale yellow solid (39.8 mg, 70%). ¹H NMR (400 MHz, CDCl₃) δ 8.97 (dd, *J* = 4.2, 1.5 Hz, 1H), 8.14 (dd, *J* = 8.3, 1.5 Hz, 1H), 7.80 (dd, *J* = 7.6, 1.5 Hz, 2H), 7.59 (d, *J* = 8.1 Hz, 1H), 7.49 – 7.41 (m, 4H), 7.28 (dd, *J* = 11.2, 4.2 Hz, 1H), 7.13 (d, *J* = 7.4 Hz, 1H). ¹³C NMR (101 MHz, CDCl₃) δ 149.4 (s), 145.7 (s), 137.8 (s), 137.5 (s), 136.4 (s), 129.8 (s), 129.0 (s), 128.3 (s), 127.6 (d, *J* = 3.5 Hz),

127.1 (s), 124.9 (s), 121.8 (s). HRMS (ESI) m/z : $[M+K]^+$ calcd for $C_{15}H_{11}NKSe$ 323.9688; found 323.9684.

5-(phenylselanyl)-2,2'-bipyridine (2.37) Conditions: 5-bromo-2,2'-bipyridine (47 mg, 0.2 mmol), $KOtBu$ (67 mg, 0.6 mmol), diphenyl diselenide (94 mg, 0.3 mmol), 1.0 mL DMSO, 24h. The product was isolated by flash chromatography (ethyl acetate/hexane= 1/30) as a yellow oil (46.7 mg, 75%). 1H NMR (500 MHz, $CDCl_3$) δ 8.69 (d, J = 2.1 Hz, 1H), 8.66 (d, J = 4.7 Hz, 1H), 8.37 (d, J = 8.0 Hz, 1H), 8.31 (d, J = 8.3 Hz, 1H), 7.85 (dd, J = 8.3, 2.2 Hz, 1H), 7.79 (td, J = 7.8, 1.8 Hz, 1H), 7.57 – 7.49 (m, 2H), 7.37 – 7.27 (m, 4H). ^{13}C NMR (126 MHz, $CDCl_3$) δ 155.6 (s), 154.7 (s), 151.9 (s), 149.2 (s), 140.9 (s), 137.0 (s), 133.6 (s), 129.7 (s), 129.6 (s), 129.4 (s), 128.1 (s), 123.9 (s), 121.7 (s), 121.0 (s).

naphthalen-1-yl(phenyl)selane (2.38) Conditions: 1-iodonaphthalene (51 mg, 0.2 mmol), $KOtBu$ (67 mg, 0.6 mmol), diphenyl diselenide (94 mg, 0.3 mmol), 1.0 mL DMSO, 24h. The product was isolated by flash chromatography (hexane) as a pale yellow oil (35.3 mg, 74%). 1H NMR (400 MHz, $CDCl_3$) δ 8.38 – 8.31 (m, 1H), 7.89 – 7.84 (m, 2H), 7.78 (d, J = 7.1 Hz, 1H), 7.55 – 7.48 (m, 2H), 7.41 – 7.32 (m, 3H), 7.24 – 7.18 (m, 3H). ^{13}C NMR (101 MHz, $CDCl_3$) δ 134.2 (s), 134.1 (s), 133.9 (s), 131.7 (s), 129.4 (s), 129.3 (s), 129.2 (s), 128.6 (s), 127.7 (s), 126.9 (d, J = 12.4 Hz), 126.4 (s), 126.0 (s).

2,6-bis(phenylselanyl)pyridine (2.39) Conditions: 2,6-dibromopyridine (47 mg, 0.2 mmol), $KOtBu$ (131 mg, 0.6 mmol), diphenyl diselenide (188 mg, 0.6 mmol), 1.0 mL DMSO, 24h. The product was isolated by flash chromatography (ethyl acetate/hexane= 1/20) as a pale yellow solid (35.8 mg, 46%). 1H NMR (400 MHz, $CDCl_3$) δ 7.70 (dd, J = 7.8, 1.4 Hz, 4H), 7.44 – 7.34 (m, 6H), 7.08 (t, J = 7.9 Hz, 1H), 6.67 (d, J = 7.8 Hz, 2H). ^{13}C NMR (101 MHz, $CDCl_3$) δ 159.4 (s), 136.9 (s), 136.4 (s), 129.7 (s), 129.0 (s), 127.7 (s), 120.5 (s).

1,7,7-trimethylbicyclo[2.2.1]heptan-2-yl 4-(phenylselanyl)benzoate (2.40) Conditions: 1,7,7-trimethylbicyclo[2.2.1]heptan-2-yl 4-iodobenzoate (77 mg, 0.2 mmol), $KOtBu$ (67 mg, 0.6 mmol), diphenyl diselenide (94 mg, 0.3 mmol), 1.0 mL DMSO, 24h. The product was isolated by flash chromatography (ethyl acetate/hexane= 1/30) as a pale yellow oil (39.7 mg, 60%). 1H NMR (500 MHz, $CDCl_3$) δ 7.85 (d, J = 8.3 Hz, 2H), 7.58 (dd, J = 7.4, 1.6 Hz, 2H), 7.40 – 7.32 (m, 5H), 4.90 (dd, J = 7.5, 3.9 Hz, 1H), 1.95 – 1.83 (m, 2H), 1.79 (t, J = 4.1 Hz, 1H), 1.77 – 1.69 (m, 1H), 1.64 – 1.56 (m, 1H), 1.28 – 1.20 (m, 1H), 1.17 – 1.12 (m, 1H), 1.09 (s, 3H), 0.91 (s, 3H), 0.88 (s, 3H). ^{13}C NMR (126 MHz, $CDCl_3$) δ 165.7 (s), 139.4 (s), 135.0 (s), 134.4 (s), 130.4 (s), 130.1 (s),

129.7 (s), 129.1 (s), 129.0 (s), 128.8 (s), 128.5 (s), 128.4 (s), 81.6 (s), 49.0 (s), 47.0 (s), 45.1 (s), 38.9 (s), 33.8 (s), 27.1 (s), 20.2 (s), 20.1 (s), 11.6 (s). HRMS (ESI) m/z : $[M+K]^+$ calcd for $C_{23}H_{26}KO_2Se$ 453.0730; found 453.0720.

2-isopropyl-5-methylcyclohexyl 4-(phenylselanyl)benzoate (2.41) Conditions: 2-isopropyl-5-methylcyclohexyl 4-iodobenzoate (77 mg, 0.2 mmol), $KOtBu$ (67 mg, 0.6 mmol), diphenyl diselenide (94 mg, 0.3 mmol), 1.0 mL DMSO, 24h. The product was isolated by flash chromatography (ethyl acetate/hexane= 1/30) as a pale yellow oil (40.7 mg, 49%). 1H NMR (500 MHz, $CDCl_3$) δ 7.88 (d, J = 8.3 Hz, 2H), 7.58 (dd, J = 7.3, 1.4 Hz, 2H), 7.40 – 7.30 (m, 5H), 4.91 (td, J = 10.9, 4.4 Hz, 1H), 2.11 (d, J = 11.6 Hz, 1H), 1.93 (dtd, J = 13.9, 6.9, 2.6 Hz, 1H), 1.77 – 1.68 (m, 2H), 1.61 – 1.48 (m, 2H), 1.18 – 1.03 (m, 2H), 0.91 (dd, J = 9.5, 6.8 Hz, 7H), 0.78 (d, J = 7.0 Hz, 3H). ^{13}C NMR (126 MHz, $CDCl_3$) δ 165.8 (s), 139.3 (s), 134.9 (s), 134.4 (s), 130.5 (s), 130.2 (s), 129.7 (s), 129.1 (s), 129.0 (s), 128.9 (s), 128.5 (s), 74.9 (s), 47.3 (s), 41.0 (s), 34.3 (s), 31.5 (s), 26.5 (s), 23.7 (s), 22.1 (s), 20.8 (s), 16.6 (s). HRMS (ESI) m/z : $[M+K]^+$ calcd for $C_{23}H_{28}KO_2Se$ 455.0886; found 455.0897.

3-(phenyltellanyl)pyridine (2.42) Conditions: 3-iodopyridine (41 mg, 0.2 mmol), $KOtBu$ (67 mg, 0.6 mmol), diphenyl ditelluride (123 mg, 0.3 mmol), 1.0 mL DMSO, 24h. The product was isolated by flash chromatography (ethyl acetate/hexane= 1/30) as a yellow oil (20.4 mg, 36%). 1H NMR (500 MHz, $CDCl_3$) δ 8.78 (d, J = 1.1 Hz, 1H), 8.43 (dd, J = 4.7, 1.4 Hz, 1H), 7.88 (dt, J = 7.8, 1.7 Hz, 1H), 7.65 (d, J = 7.1 Hz, 2H), 7.25 (t, J = 7.4 Hz, 1H), 7.17 (dd, J = 13.8, 6.2 Hz, 2H), 7.07 (dd, J = 7.8, 4.8 Hz, 1H). ^{13}C NMR (126 MHz, $CDCl_3$) δ 157.0 (s), 148.7 (s), 145.0 (s), 138.5 (s), 129.8 (s), 128.4 (s), 124.7 (s), 113.4 (s), 112.5 (s).

2-(phenyltellanyl)pyridine (2.43) Conditions: 2-bromopyridine (32 mg, 0.2 mmol), $KOtBu$ (67 mg, 0.6 mmol), diphenyl ditelluride (123 mg, 0.3 mmol), 1.0 mL DMSO, 24h. The product was isolated by flash chromatography (ethyl acetate/hexane= 1/50) as a yellow oil (18.1 mg, 32%). 1H NMR (500 MHz, $CDCl_3$) δ 8.47 (dd, J = 4.8, 1.0 Hz, 1H), 7.96 (dd, J = 7.9, 1.0 Hz, 2H), 7.42 (t, J = 7.4 Hz, 1H), 7.36 – 7.27 (m, 3H), 7.19 (d, J = 7.9 Hz, 1H), 7.02 (ddd, J = 7.4, 4.9, 1.0 Hz, 1H). ^{13}C NMR (126 MHz, $CDCl_3$) δ 150.7 (s), 146.4 (s), 140.6 (s), 136.1 (s), 130.3 (s), 129.9 (s), 128.9 (s), 121.1 (s), 113.8 (s).

***N,N*-dimethyl-4-(phenyltellanyl)benzamide (2.44)** Conditions: 4-bromo-*N,N*-dimethylbenzamide (46 mg, 0.2 mmol), $KOtBu$ (67 mg, 0.6 mmol), diphenyl ditelluride (123 mg, 0.3 mmol), 1.0 mL DMSO, 24h. The product was isolated by flash chromatography (ethyl

acetate/hexane= 1/20) as a yellow oil (38.8 mg, 55%). ¹H NMR (500 MHz, CDCl₃) δ 7.66 (d, *J* = 7.1 Hz, 2H), 7.58 (d, *J* = 8.0 Hz, 2H), 7.34 – 7.14 (m, 5H), 3.01 (s, 3H), 2.89 (s, 3H). ¹³C NMR (126 MHz, CDCl₃) δ 171.1 (s), 138.7 (s), 137.1 (s), 135.6 (s), 129.6 (d, *J* = 22.6 Hz), 128.3 (d, *J* = 8.2 Hz), 128.0 (s), 127.1 (s), 117.2 (s), 114.0 (s), 39.6 (s), 35.4 (s). HRMS (ESI) *m/z*: [M+K]⁺ calcd for C₂₃H₂₈KO₂Se 393.9847; found 393.9862.

6-(phenyltellanyl)quinoline (2.45) Conditions: 6-iodoquinoline (51 mg, 0.2 mmol), KO^tBu (67 mg, 0.6 mmol), diphenyl ditelluride (123 mg, 0.3 mmol), 1.0 mL DMSO, 24h. The product was isolated by flash chromatography (ethyl acetate/hexane= 1/30) as a yellow oil (36.0 mg, 54%). ¹H NMR (500 MHz, CDCl₃) δ 8.80 (dd, *J* = 4.0, 1.3 Hz, 1H), 8.04 (s, 1H), 7.92 (dd, *J* = 8.3, 1.3 Hz, 1H), 7.83 (d, *J* = 8.8 Hz, 2H), 7.69 (d, *J* = 7.1 Hz, 2H), 7.29 (dd, *J* = 8.3, 4.2 Hz, 1H), 7.25 (t, *J* = 7.4 Hz, 1H), 7.17 (dd, *J* = 10.3, 4.7 Hz, 2H). ¹³C NMR (126 MHz, CDCl₃) δ 150.7 (s), 147.6 (s), 138.6 (s), 137.9 (s), 136.6 (s), 135.3 (s), 130.2 (s), 129.8 (s), 129.3 (s), 128.3 (s), 121.5 (s), 114.2(s), 113.7 (s). HRMS (ESI) *m/z*: [M+Na]⁺ calcd for C₁₅H₁₂NNaTe 357.9846; found 357.9863.

5-(phenyltellanyl)quinoline (2.46) Conditions: 5-bromoquinoline (42 mg, 0.2 mmol), KO^tBu (67 mg, 0.6 mmol), diphenyl ditelluride (123 mg, 0.3 mmol), 1.0 mL DMSO, 24h. The product was isolated by flash chromatography (ethyl acetate/hexane= 1/30) as a yellow oil (52.6 mg, 79%). ¹H NMR (500 MHz, CDCl₃) δ 8.79 (dd, *J* = 4.2, 1.5 Hz, 1H), 8.44 (d, *J* = 8.4 Hz, 1H), 8.06 – 7.98 (m, 2H), 7.50 – 7.42 (m, 3H), 7.30 (dd, *J* = 8.5, 4.2 Hz, 1H), 7.15 (dd, *J* = 13.8, 6.4 Hz, 1H), 7.06 (t, *J* = 7.5 Hz, 2H). ¹³C NMR (126 MHz, CDCl₃) δ 150.8 (s), 148.6 (s), 140.4 (s), 139.8 (s), 137.2 (s), 131.5 (s), 131.2 (s), 130.2 (s), 129.7 (s), 127.9 (s), 122.1 (s), 117.6 (s), 114.5 (s). HRMS (ESI) *m/z*: [M+Na]⁺ calcd for C₁₅H₁₂NNaTe 357.9846; found 357.9832.

8-(phenyltellanyl)quinoline (2.47) Conditions: 8-bromoquinoline (42 mg, 0.2 mmol), KO^tBu (67 mg, 0.6 mmol), diphenyl ditelluride (123 mg, 0.3 mmol), 1.0 mL DMSO, 24h. The product was isolated by flash chromatography (ethyl acetate/hexane= 1/30) as a yellow solid (50.6 mg, 76%). ¹H NMR (500 MHz, CDCl₃) δ 8.91 (dd, *J* = 4.2, 1.5 Hz, 1H), 8.14 (dd, *J* = 8.2, 1.4 Hz, 1H), 8.10 – 8.04 (m, 2H), 7.63 (dd, *J* = 7.5, 1.5 Hz, 1H), 7.51 (t, *J* = 7.5 Hz, 1H), 7.46 (dd, *J* = 8.2, 4.3 Hz, 1H), 7.40 (t, *J* = 7.5 Hz, 2H), 7.29 (ddd, *J* = 9.7, 7.3, 2.1 Hz, 2H). ¹³C NMR (126 MHz, CDCl₃) δ 149.3 (s), 148.0 (s), 142.0 (s), 136.3 (s), 132.3 (s), 129.8 (s), 128.9 (s), 128.0 (s), 127.8 (s), 126.5 (s), 125.6 (s), 121.8 (s), 113.3 (s). HRMS (ESI) *m/z*: [M+H]⁺ calcd for C₁₅H₁₂N⁺Te 336.0026; found 336.0030.

UV-Vis Spectra:

A stock solution of **2.1a** in DMSO was prepared with a concentration of 0.1 mmol/mL. All bases were taken straight from the glovebox and we weighed 0.3 mmol of each base in scintillation vials and we added 1 mL of the stock solution to each vial. Afterwards, all spectra were taken with a concentration of 5×10^{-3} mmol/mL of **2.1a**. (**1a** in the figure is the abbreviation of **2.1a**)

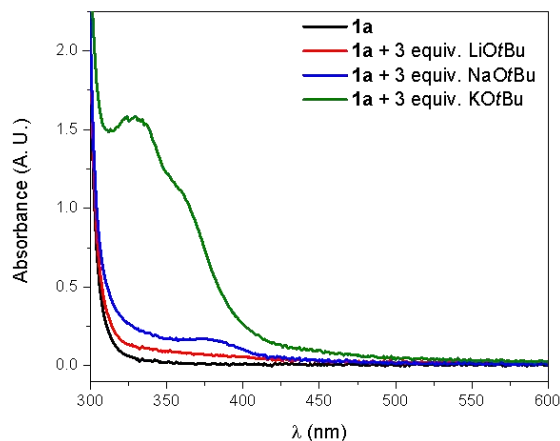


Figure 2.2. The influence of different bases.

A stock solution of **2.1a** in DMSO was prepared with a concentration of 0.1 mmol/mL. KOtBu was taken straight from the glovebox and we weighed 0.1, 0.2, 0.3, 0.4 and 0.5 mmol in different scintillation vials and we added 1 mL of the stock solution to each vial. Afterwards, all spectra were taken with a concentration of 5×10^{-3} mmol/mL of **2.1a**. (**1a** in the figure is the abbreviation of **2.1a**)

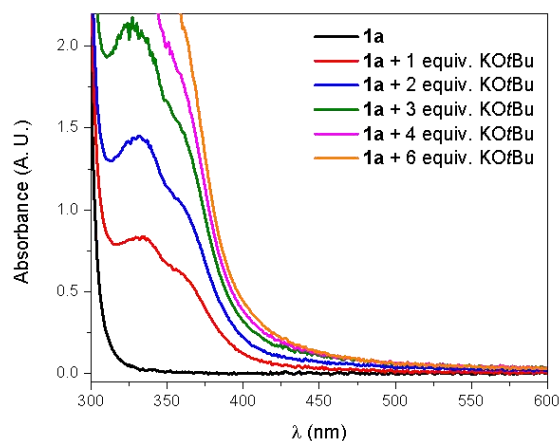


Figure 2.3. The influence of the equivalence of KOtBu.

We prepared a solution of **2.1a** in DMSO with a concentration of 0.2 mmol/mL, a solution of **2.2a** with a concentration of 0.3 mmol/mL and a third solution combining the two with a concentration of 0.2 mmol/mL for **2.1a** and 0.3 mmol/mL for **2.2a**. Afterwards, the spectra was taken with a concentration of 1×10^{-3} mmol/mL for **2.1a**, 7.5×10^{-4} mmol/mL and the spectra of **2.2a** and the combination had a concentration of 5×10^{-4} mmol/mL for **2.1a** and 7.5×10^{-4} mmol/mL for **2.2a**. (**1a** and **2a** in the figure is the abbreviation of **2.1a** and **2.2a**)

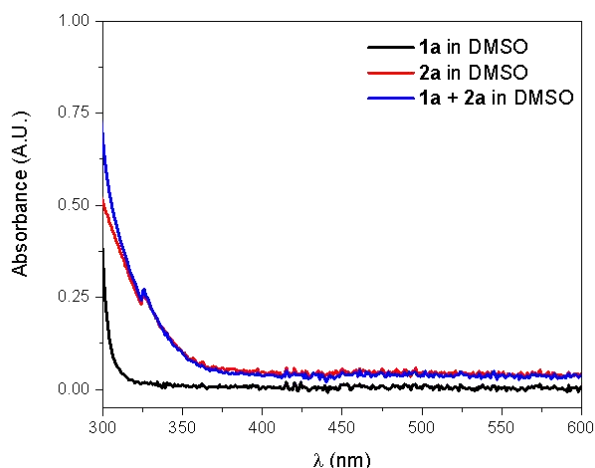


Figure 2.4. The combinations of **2.1a** and **2.2a**.

A stock solution of **2.1a** in DMSO was prepared with a concentration of 0.1 mmol/mL. KO t Bu was taken straight from the glovebox and we weighed 0.3 mmol in a scintillation vial and we added 1 mL of the stock solution. We also prepared a solution of **2.2a** with a concentration of 0.3 mmol/mL and a solution of **2.2a** with KO t Bu at a concentration of 0.3 mmol/mL and 0.6 mmol/mL, respectively. Afterwards, the spectra were taken at a concentration of 5×10^{-3} mmol/mL for **2.1a** and **2.1a** + KO t Bu, and at 7.5×10^{-4} mmol/mL for **2.2a** and **2.2a** + KO t Bu. (**1a** and **2a** in the figure is the abbreviation of **2.1a** and **2.2a**)

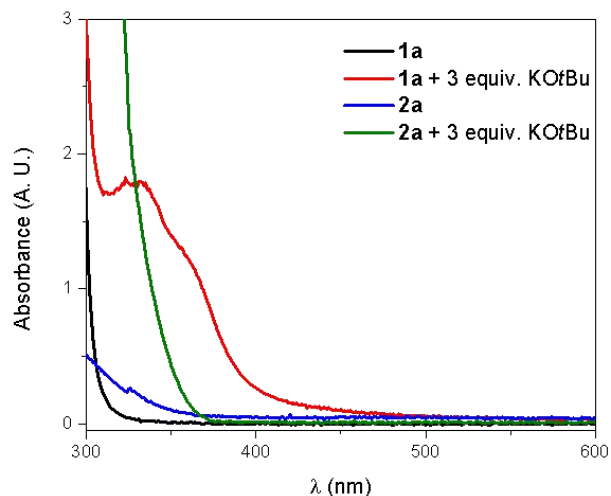


Figure 2.5. The combinations of **2.1a**, **2.2a** and KOtBu.

Stock solutions of 4-chloroanisole, 4-bromoanisole and 4-iodoanisole in DMSO were prepared with a concentration of 0.1 mmol/mL. KOtBu was taken straight from the glovebox and we weighed 0.3 mmol in different scintillation vials and we added 1 mL of each stock solution to each vial. Afterwards, all spectra were taken with a concentration of 5×10^{-3} mmol/mL of the anisoles.

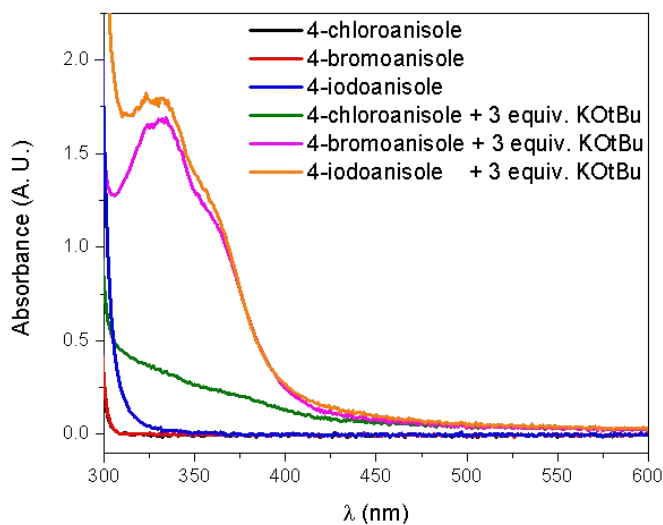


Figure 2.6. The influence of X in aryl halides.

NaH was washed with hexanes to remove the mineral oils and placed inside the glovebox. In three microwave vials we weighed **2.1a** (0.2 mmol) and NaH (0.25, 0.5 and 1 equiv.) and capped inside the glovebox. Next, we added 1 mL of DMSO to each one via syringe and heated

the solution at 50 °C for 1 hour. After that, all spectra were taken with a concentration of 1×10^{-2} mmol/mL of **2.1a**. (**1a** in the figure is the abbreviation of **2.1a**)

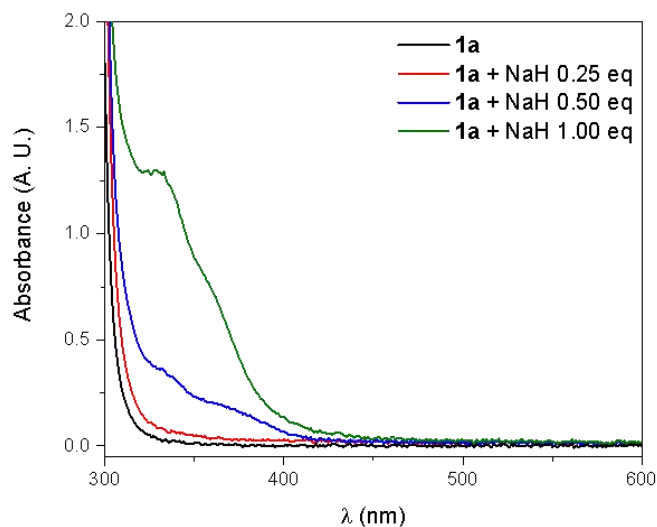


Figure 2.7. The influence of NaH to 4-iodoanisole after 1 h activation at 50 °C.

A stock solution of **2.1a** in DMSO was prepared with a concentration of 0.1 mmol/mL. KO^tBu was taken straight from the glovebox and we weighed 0.3 mmol of each base in scintillation vials and we added 1 mL of the stock solution to one vial and 1 mL of DMSO to the other. Afterwards, all spectra were taken with a concentration of 5×10^{-3} mmol/mL of **2.1a** and 15×10^{-3} mmol/mL of KO^tBu. (**1a** in the figure is the abbreviation of **2.1a**)

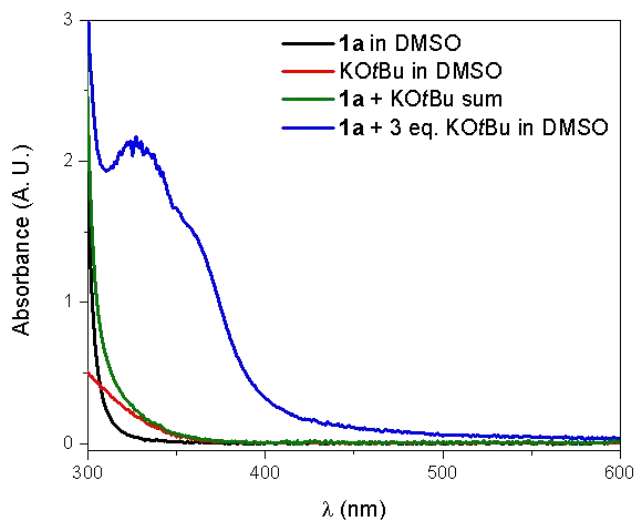


Figure 2.8. The combinations of **2.1a**, KO^tBu in DMSO.

2.6 References

- (a) Feng, M.; Tang, B.; Liang, S.H.; Jiang, X. Sulfur in Medicinal Chemistry. *Curr. Top. Med. Chem.* **2016**, *16*, 1200–1216. (b) Banerjee, B.; Koketsu, M. Recent Developments in the Synthesis of Biologically Relevant Selenium-Containing Scaffolds. *Coord. Chem. Rev.* **2017**, *339*, 104–127. (c) Nogueira, C. W.; Zeni, G.; Rocha, J. B. T. Organoselenium and Organotellurium Compounds: Toxicology and Pharmacology. *Chem. Rev.* **2004**, *104*, 6255–6285. (d) Devendar, P.; Yang, G.-F. Sulfur-Containing Agrochemicals. *Top. Curr. Chem.* **2017**, *375*, 82. (e) Rahate, A. S.; Nemade, K. R.; Waghuley, S. A. Polyphenylene Sulfide (PPS): State of the Art and Applications. *Rev. Chem. Eng.* **2013**, *29*, 471–489.
- (a) Beletskaya, I. P.; Ananikov, V. P. Transition-Metal-Catalyzed C–S, C–Se, and C–Te Bond Formation via Cross-Coupling and Atom-Economic Addition Reactions. *Chem. Rev.* **2011**, *111*, 1596–1636. (b) Liu, J.; Tian, M.; Li, Y.; Shan, X.; Li, A.; Lu, K.; Fagnoni M.; Protti, S.; Zhao, X. Metal-Free Synthesis of Unsymmetrical Aryl Selenides and Tellurides via Visible Light-Driven Activation of Arylazo Sulfones. *Eur. J. Org. Chem.* **2020**, 7358–7367. (c) Wang, H.; Chen, S.; Liu, G.; Guan, H.; Zhong, D.; Cai, J.; Zheng, Z.; Mao, J.; Walsh, P. J. Synthesis of Diaryl Selenides via Palladium-Catalyzed Debenzylative Cross-Coupling of Aryl Benzyl Selenides with Aryl Bromides. *Organometallics* **2018**, *37*, 4086–4091. (d) Liu, B.; Lim, C.-H.; Miyake, G. M. Visible-light-promoted C–S cross-coupling via intermolecular charge transfer. *J. Am. Chem. Soc.* **2017**, *139*, 13616–13619. (e) Lemir, I. D.; Castro-Godoy, W. D.; Heredia, A. A.; Schmidt, L. C.; Arguello, J. E. Metal- and Photocatalyst-Free Synthesis of 3-Selenylindoles and Asymmetric Diarylselenides Promoted by Visible Light. *RSC Adv.* **2019**, *9*, 22685–22694.
- For thiol coupling to aryl halides: (a) Jones, K. D.; Power, D. J.; Bierer, D.; Gericke, K. M.; Stewart, S. G. Nickel Phosphite/Phosphine-Catalyzed C–S Cross-Coupling of Aryl Chlorides and Thiols. *Org. Lett.* **2018**, *20*, 208–211. (b) Correa, A.; Carril, M.; Bolm, C. Iron-Catalyzed S-Arylation of Thiols with Aryl Iodides. *Angew. Chem., Int. Ed.* **2008**, *47*, 2880–2883. (c) Wong, Y.-C.; Jayanth, T. T.; Cheng, C.-H. Cobalt-Catalyzed Aryl Sulfur Bond Formation. *Org. Lett.* **2006**, *8*, 5613–5616. (d) Fernandez-Rodriguez, M. A.; Shen, Q.; Hartwig, J. F. A General and Long-Lived Catalyst for the Palladium-Catalyzed Coupling of Aryl Halides with Thiols. *J. Am. Chem. Soc.* **2006**, *128*, 2180–2181. (e) Itoh, T.; Mase, T. A General Palladium-Catalyzed Coupling of Aryl Bromides/Triflates and Thiols. *Org. Lett.* **2004**, *6*, 4587–4590.
- For selenide coupling to aryl halides: (a) Wu, S.; Shi, J.; Zhang, C.-P. Cu-Mediated Arylselenylation of Aryl Halides with Trifluoromethyl Aryl Selenonium Ylides. *Org. Biomol. Chem.* **2019**, *17*, 7468–7473. (b) Hu, D. Liu, M. Wu, H.; Gao, W.; Wu, G. Copper-catalyzed diarylation of Se with aryl iodides and heterocycles. *Org. Chem. Front.* **2018**, *5*, 1352–1355. (c) Gao, C.; Wu, G.; Min, L.; Liu, M.; Gao, W.; Ding, J.; Chen, J.; Huang, X.; Wu, H. Copper-Catalyzed Three-Component Coupling Reaction of Azoles, Se Powder, and Aryl Iodides. *J. Org. Chem.* **2017**, *82*, 250–255.
- Hegedus, L. L.; McCabe, R. W. Catalyst Poisoning; Marcel Dekker: New York, **1984**.
- Node, M.; Kajimoto, T. Development of Odorless Organosulfur Reagents and Asymmetric Reaction Using Odorless Thiols. *Heteroat. Chem.* **2007**, *18*, 572–683.

7. (a) Beletskaya, I. P.; Sigeev, A. S.; Peregudov, A. S.; Petrovskii, P. V. New approaches to the synthesis of unsymmetrical diaryl selenides. *J. Organomet. Chem.* **2000**, *605*, 96–101. (b) Nishiyama, Y.; Tokunaga, K.; Sonoda, N. New Synthetic Method of Diorganyl Selenides: Palladium-Catalyzed Reaction of PhSeSnBu₃ with Aryl and Alkyl Halides. *Org. Lett.* **1999**, *1*, 1725–1727.
8. (a) Li, Y.; Wang, M.; Jiang, X. Controllable Sulfoxidation and Sulfenylation with Organic Thiosulfate Salts via Dual Electron- and Energy-Transfer Photocatalysis. *ACS Catal.* **2017**, *7*, 7587–7592. (b) Jiang, M.; Li, H.; Yang, H.; Fu, H. Room-Temperature Arylation of Thiols: Breakthrough with Aryl Chlorides. *Angew. Chem., Int. Ed.* **2017**, *56*, 874–879. (c) Johnson, M. W.; Hannoun, K. I.; Tan, Y.; Fu, G. C.; Peters, J. C. A Mechanistic Investigation of the Photoinduced, Copper-Mediated Cross-Coupling of an Aryl Thiol with an Aryl Halide. *Chem. Sci.* **2016**, *7*, 4091–4100. (d) Oderinde, M. S.; Frenette, M.; Robbins, D. W.; Aquila, B.; Johannes, J. W. Photoredox Mediated Nickel Catalyzed Cross-Coupling of Thiols With Aryl and Heteroaryl Iodides via Thiyl Radicals. *J. Am. Chem. Soc.* **2016**, *138*, 1760–1763. (e) Jouffroy, M.; Kelly, C. B.; Molander, G. A. Thioetherification via Photoredox/Nickel Dual Catalysis. *Org. Lett.* **2016**, *18*, 876–879. (f) Uyeda, C.; Tan, Y.; Fu, G. C.; Peters, J. C. A New Family of Nucleophiles for Photoinduced, Copper-Catalyzed Cross-Couplings via Single-Electron Transfer: Reactions of Thiols with Aryl Halides Under Mild Conditions (0 °C). *J. Am. Chem. Soc.* **2013**, *135*, 9548–9552.
9. (a) Bu, M.-J.; Lu, G.-P.; Jiang, J.; Cai, C. Merging Visible-Light Photoredox and Micellar Catalysis: Arylation Reactions with Anilines Nitrosated *in situ*. *Catal. Sci. Technol.* **2018**, *8*, 3728–3732. (b) Kundu, D.; Ahammed, S.; Ranu, B. C. Visible Light Photocatalyzed Direct Conversion of Aryl/Heteroarylamines to Selenides at Room Temperature. *Org. Lett.* **2014**, *16*, 1814–1817. (c) Kobiki, Y.; Kawaguchi, S.-i.; Ohe, T.; Ogawa, A. Photoinduced Synthesis of Unsymmetrical Diaryl Selenides from Triarylbiismuthines and Diaryl Diselenides. *Beilstein J. Org. Chem.* **2013**, *9*, 1141–1147.
10. Bunnett, J. F.; Creary, X. Nucleophilic Replacement of Two Halogens in Dihalobenzenes Without the Intermediacy of Monosubstitution Products. *J. Org. Chem.* **1974**, *39*, 3611–3612.
11. (a) Yanagisawa, S.; Ueda, K.; Taniguchi, T.; Itami, K. Potassium *t*-Butoxide Alone Can Promote the Biaryl Coupling of Electron-Deficient Nitrogen Heterocycles and Haloarenes. *Org. Lett.*, **2008**, *10*, 4673–4676. (b) Shirakawa, E.; Itoh, K.-I.; Higashino, T.; Hayashi, T. *tert*-Butoxide-Mediated Arylation of Benzene with Aryl Halides in the Presence of a Catalytic 1,10-Phenanthroline Derivative. *J. Am. Chem. Soc.* **2010**, *132*, 15537–15539. (c) Liu, W.; Cao, H.; Zhang, H.; Zhang, H.; Chung, H. K.; He, C.; Wang, H.; Kwong, F. Y.; Lei, A. Organocatalysis in Cross-Coupling: DMEDA-Catalyzed Direct C–H Arylation of Unactivated Benzene. *J. Am. Chem. Soc.* **2010**, *132*, 16737–16740. (d) Roman, D. S.; Takahashi, Y.; Charette, A. B. Potassium *tert*-Butoxide Promoted Intramolecular Arylation via a Radical Pathway. *Org. Lett.*, **2011**, *13*, 3242–3245.

12. (a) Budén M. E.; Guastavino, J. F.; Rossi, R. A. Room-Temperature Photoinduced Direct C–H Arylation via Base-Promoted Homolytic Aromatic Substitution. *Org. Lett.*, **2013**, *15*, 1174–1177. (b) Guastavino, J. F.; Budén M. E.; Rossi, R. A. Room-Temperature and Transition-Metal-Free Mizoroki–Heck-type Reaction. Synthesis of *E*-stilbene by Photoinduced C–H Functionalization. *J. Org. Chem.* **2014**, *79*, 9104–9111. (c) Yuan, J.; To, W.-Pong.; Zhang, Z.-Y.; Yue, C.-D.; Meng, S.; Chen, J.; Liu, Y.; Yu, G.-A.; Che, C.-M. Visible-Light-Promoted Transition-Metal-Free Phosphinylation of Heteroaryl Halides in the Presence of Potassium tert-Butoxide. *Org. Lett.* **2018**, *20*, 7816–7820. (d) Ding, T.-H.; Qu, J.-P.; Kang, Y.-B. Visible-Light-Induced, Base-Promoted Transition-Metal-Free Dehalogenation of Aryl Fluorides, Chlorides, Bromides, and Iodides. *Org. Lett.* **2020**, *22*, 3084–3088.
13. Barham, J. P.; Coulthard, G.; Emery, K. J.; Doni, E.; Cumine, F.; Nocera, G.; John, M. P.; Berlouis, L. E. A.; McGuire, T.; Tuttle, T.; Murphy, J. A. KOt Bu: A Privileged Reagent for Electron Transfer Reactions? *J. Am. Chem. Soc.* **2016**, *138*, 7402–7410.
14. Rohe, S.; Révol, G.; Marmin, T.; Barriault, D.; Barriault L. Single-Electron Transfer from Dimsyl Anion in the Alkylation of Phenols. *J. Org. Chem.* **2020**, *85*, 2806–2813.
15. Budén M. E.; Guastavino, J. F.; Puiatti M.; Rossi, R. A. Initiation in Photoredox C–H Functionalization Reactions. Is Dimsyl Anion a Key Ingredient? *J. Org. Chem.* **2017**, *82*, 8325–8333.
16. Pan, L.; Elmasry, J.; Osscorma, T.; Cooke, M. V.; Laulhé, S. Photochemical Regioselective C(sp³)–H Amination of Amides Using *N*-haloimides. *Org. Lett.* **2021**, *23*, 3389–3393.

CHAPTER 3. BASE-MEDIATED PHOTO-INDUCED BORYLATION AND PHOSPHONATION OF ARYL HALIDES

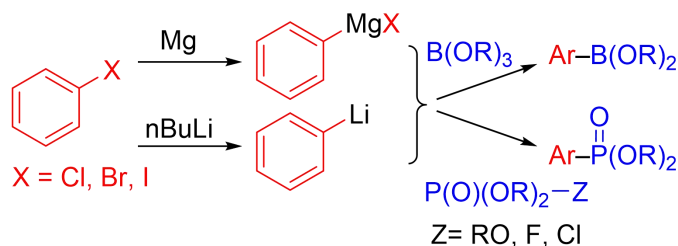
3.1 Introduction

Aryl boronic esters are valuable moieties in organic synthesis and drug manufacturing as they are essential reagents for the Suzuki-Miyaura cross-coupling reaction.¹ Similarly, aryl phosphonate esters are found in a wide variety of compounds including pharmaceuticals, agrochemicals, and in ligands for metal catalysis.² Aryl halides are the most commonly used precursors to access these moieties given their commercial availability and stability. Traditional methods use highly reactive Grignard and organolithium reagents to activate the aryl halide into coupling with trialkyl boranes³ or phosphorus reagents (Scheme 3.1-A).⁴ Transition-metal-catalyzed methods have been successful at increasing functional group compatibility with the help of metals such as Pd, Co, Zn, Ni, Cu and Fe (Scheme 3.1-B).⁵ However, these methods often require high temperatures and expensive ligands. Additionally, the cost associated with metal residue removal, in selective industrial applications, further reduces cost-efficiency of some of these reactions.⁶ While metal-free borylations have been reported,⁷ they often require the use of uncommon silylborane reagents.

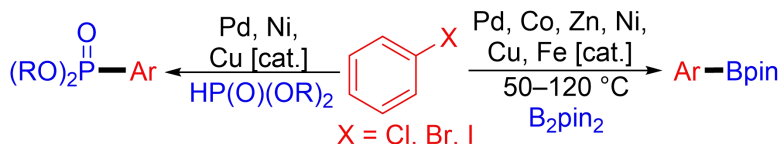
Recently, photoredox pathways have been reported to generate aryl boronates⁸ and aryl phosphonates⁹ from aryl halides using rare metal-based photocatalysts or toxic organic dyes. Catalyst-free photo-induced borylations¹⁰ and phosphonations¹¹ have been gaining attention over the past decades due to their low environmental footprint and mild reaction conditions, but these methods often require the use of dangerous UV radiation, which limit scalability and broad adoption (Scheme 3.1-C).

Our interest in catalyst-free photo-induced transformations,¹² recently led us to discover the ability of aryl halides to form electron-donor-acceptor (EDA) complexes with the dimsyl anion, which enabled the synthesis of chalcogenides. Inspired by that discovery and its mechanistic breakthrough, herein, we report a catalyst-free visible-light-induced borylation and phosphonation of aryl iodides that is proposed to also involve an EDA complex between aryl halides and anions generated in situ (Scheme 3.1-D).

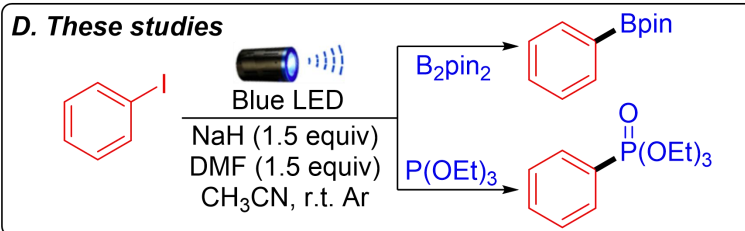
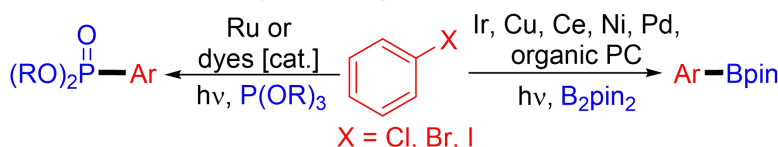
A. Traditional borylation and phosphonation



B. Transition-metal catalysis approaches



C. Photoredox-catalyzed and photo-induced reactions



Scheme 3.1. Current and proposed approaches to generate aryl boronic esters and aryl phosphonate esters.

3.2 Results and Discussion

We selected 4-iodoanisole (**3.1a**), bis(pinacolato)diboron (**3.2a**) as model reagents to optimize the reactions (Table 3.1). Based on our previous work,¹² we showed that KO t Bu is not involved in the single electron activation of aryl halides. Therefore, we initiated our screens using a non-nucleophilic base like sodium hydride (NaH) in different solvents (entries 1–3). While DMSO and *N,N*-dimethylacetamide (DMA) did not afford the desired product in significant yield, *N,N*-dimethylformamide (DMF) afforded the borylated product in 30% yield. To improve solubility, the use of a co-solvent system was investigated (entries 4–5). The yield of the reaction increased to 69% when DMF/CH₃CN solvent system was used (entry 4). The use of THF as a co-solvent was however deleterious and decreased yield to 8% (entry 5). Replacing the base to DIPEA, DBU or NaO t Bu negatively affected the yield (entries 6, 7 and 8) affording the borylated product in yields ranging from 11–32%. Reducing the amount of NaH and DMF from

3 equivalents to 1.5 equivalents (entry 9) further improved the yield (84%). However, reducing these ratios further to 1.1 equivalents (entry 10) lowered yields (69%). In the absence of DMF, the reaction still provides the desired product (entry 11) albeit in lower yield (68%), indicating that both acetonitrile and DMF promote the reaction and are possibly involved in the mechanism. Control experiments show that no product was formed in the absence of base (entry 12) and that in the absence of light (entry 13) the yield decrease to 8% despite the use of heat, showing that this reaction requires both photons and base. Reducing **3.2a** to 2.0 equivalent (entry 14) did have a deleterious effect on yield (57%). Importantly, a small decrease in yield was observed when the reaction was carried out in air (entry 15). Finally, screening of different wavelengths (entries 16, 17) showed that 390 nm light provided much improved yields (95%), while increasing the wavelength to 440 nm slightly reduced yields (72%) compared to 427 nm.

Table 3.1. Optimization of reaction conditions.^a



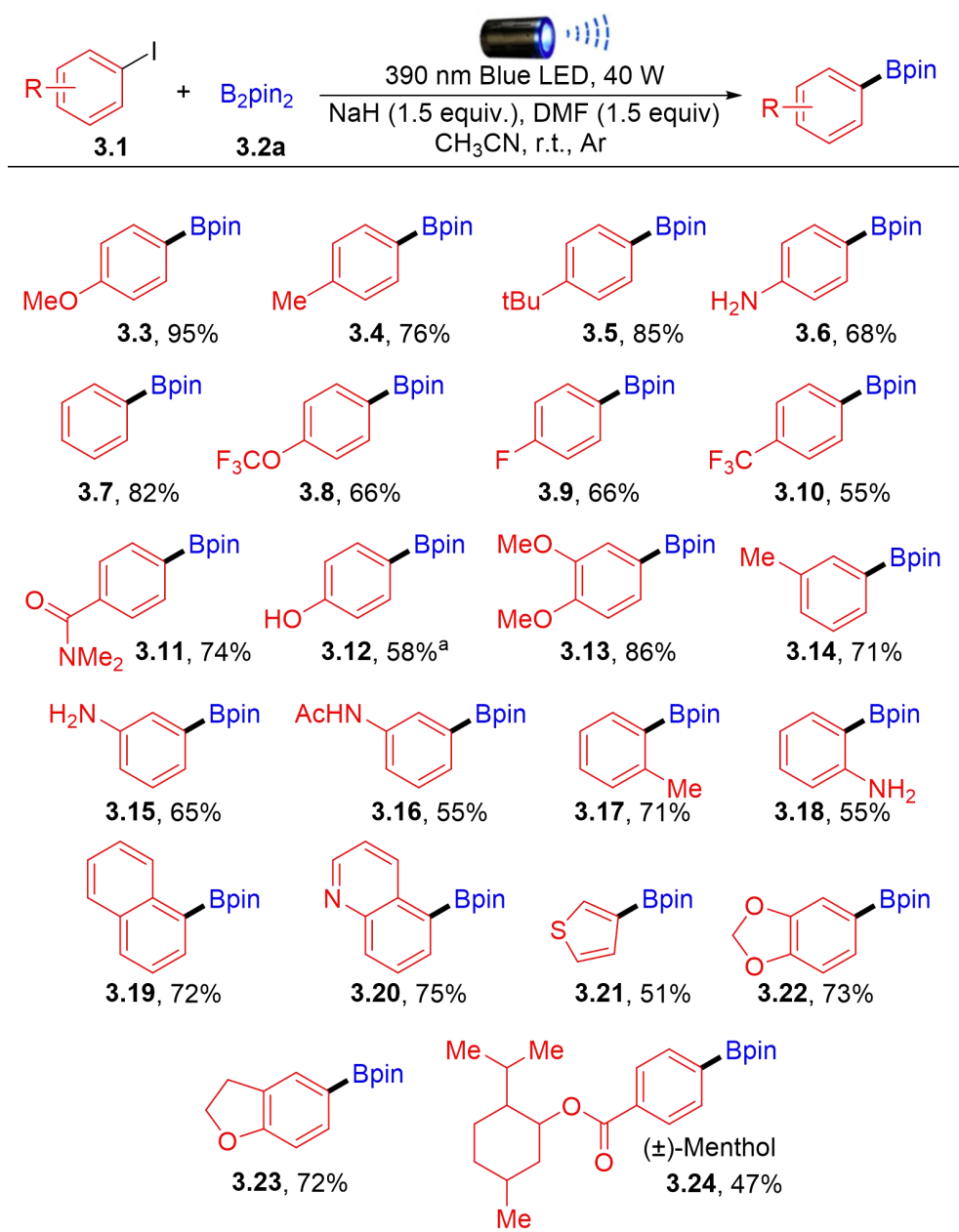
entry	base (equiv.)	3.2a (equiv.)	solvent (mL)	yield (%) ^b
1	NaH (3.0)	3.0	DMSO (1.0)	trace
2	NaH (3.0)	3.0	DMA (1.0)	4
3	NaH (3.0)	3.0	DMF (1.0)	30
4	NaH (3.0)	3.0	DMF/ CH_3CN (0.1/0.9)	69
5	NaH (3.0)	3.0	DMF/THF (0.1/0.9)	8
6	DIPEA (3.0)	3.0	DMF/ CH_3CN (0.1/0.9)	32
7	DBU (3.0)	3.0	DMF/ CH_3CN (0.1/0.9)	29
8	NaOtBu (3.0)	3.0	DMF/ CH_3CN (0.1/0.9)	11
9	NaH (1.5)	3.0	DMF/ CH_3CN (1.5eq/1.0)	84
10	NaH (1.1)	3.0	DMF/ CH_3CN (1.1eq/1.0)	69
11	NaH (1.5)	3.0	CH_3CN (1.0)	68
12	-	3.0	DMF/ CH_3CN (2 eq/1.0)	-

Table 3.1. Continued.

13 ^c	NaH (2.0)	3.0	DMF/CH ₃ CN (2 eq/1.0)	8
14	NaH (1.5)	2.0	DMF/CH ₃ CN (1.5 eq/1.0)	57
15 ^d	NaH (1.5)	3.0	DMF/CH ₃ CN (1.5 eq/1.0)	79
16 ^e	NaH (1.5)	3.0	DMF/CH ₃ CN (1.5 eq/1.0)	95
17 ^f	NaH (1.5)	3.0	DMF/CH ₃ CN (1.5 eq/1.0)	72

a Reaction conditions: **1a** (0.2 mmol, 1 equiv), **2a**, base, solvent, temperature around reaction flask was 35 °C (heating caused by the 427 nm LED lamp), under Ar, 24h. b Yields are based on **1a**, determined by ¹H-NMR using dibromomethane as internal standard. c The reaction was performed in dark covered by aluminum foil at 40 °C. d The reaction was performed in the air. e 390 nm. f 440 nm.

Following reaction optimization, we continued our study investigating the substrate scope for this transformation. We began by exploring the scope of aryl iodides compatible with B₂pin₂ under the optimal reaction conditions (Scheme 3.2). Electron-donating aryl iodides (OMe, Me, *t*Bu) afforded products **3.3–3.5** in good to excellent yields (76–95%). 4-Iodoaniline afforded borylated product **3.6** in lower but respectable yield (68%), showing that this methodology is compatible with amine functional groups. Electron-neutral iodobenzene also reacted efficiently to give product **3.7** in good yield (82%). Electron-withdrawing iodoarenes (OCF₃, F, CF₃) gave desired products **3.8–3.10** in lower yields (55–66%). The method was well tolerated in presence of primary amide (**3.11**, 74%). Trimethylsilyl (TMS) protected 4-iodophenol generated product **3.12** in moderate yield (58%), but was deprotected during column chromatography purification. Steric hindrance in *meta* position was also tolerated affording products **3.13–3.16** in moderate to good yields (55–86%) in the presence electron-rich groups, anilines, and secondary amides. *Ortho* substituents were also tolerated giving borylated products **3.17** and **3.18** in 71% and 55% yields, respectively. 1-Iodonaphthalene afforded product **3.19** in good yield (72%). Heteroaromatic iodides such as quinoline and thiophene gave products **3.20** and **3.21** in moderate to good yields (51–75%). Bioactive 1,3-benzodioxole and 2,3-dihydrobenzofuran afforded products **3.22** and **3.23** in good yields (72–73%). Finally, natural product containing substrate **3.24**, which contains an ester moiety, was obtained in 47% yield.

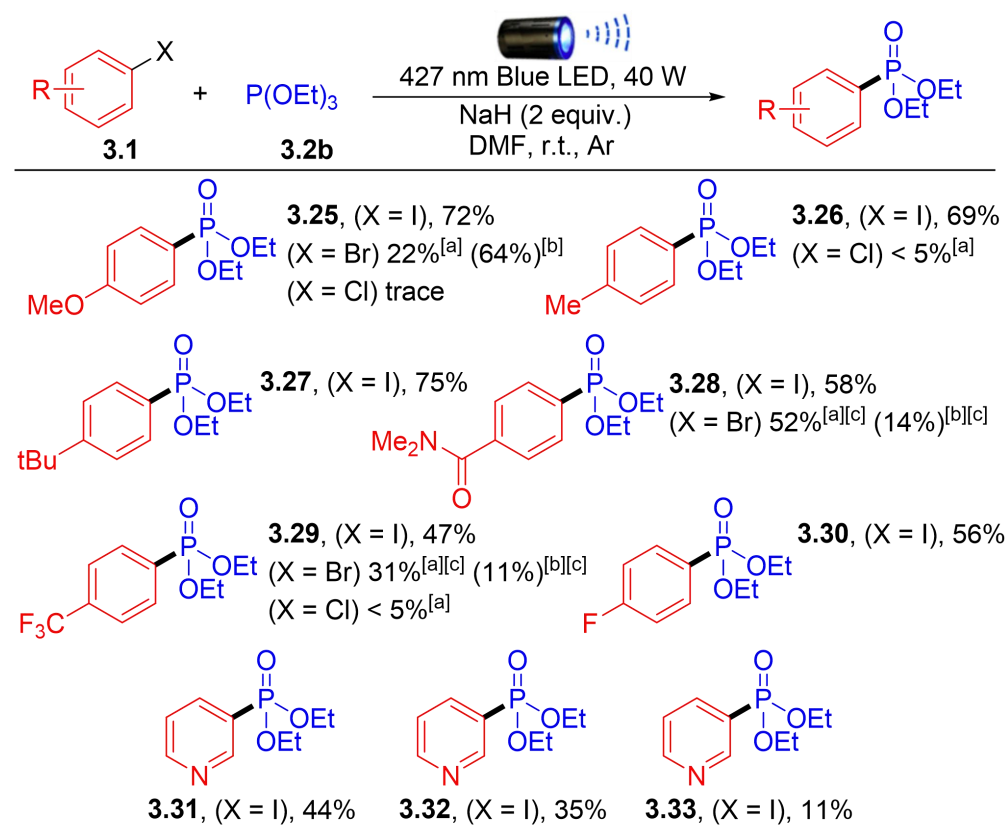


Scheme 3.2. Substrate scope of aryl halides.

Reaction conditions: **3.1** (0.2 mmol, 1 equiv), **3.2a** (0.6 mmol, 3 equiv), NaH (1.5 equiv), DMF (1.5 equiv), CH₃CN (1 mL), temperature around reaction flask was 35 °C (heating caused by the 390 nm LED lamp), under Ar, 24h. Yields are for isolated products. a R=OTMS, deprotected after flash column chromatography.

We continued our study using triethyl phosphite as a phosphonation reagent (Scheme 3.3). Optimal conditions for the phosphonation reaction were found to be slightly different than for borylation. The use of DMF as sole solvent in presence of 2 equivalents of NaH under 427 nm

light irradiation afforded the best transformation. Aryl iodides with electron-donating functional groups (OMe, Me, *t*Bu) afforded phosphonated products **3.25**–**3.27** in good yields (69–75%). 4-Bromoanisole afforded product **3.25** in low yield (22%), but 64% of the starting material remained unreacted. Unfortunately, aryl chlorides only afforded products in very low yield. Tertiary amide was tolerated and gave product **3.28** in moderate yield (52–58%) using both aryl iodide and bromide. Similarly to the borylation reaction, electron-withdrawing groups (CF₃, F) generated the desired products in moderate yields (31–56%). Finally, several heterocyclic iodides were also tested (products **3.31**–**3.33**) but gave the phosphonated products in low to moderate yields (11–44%).

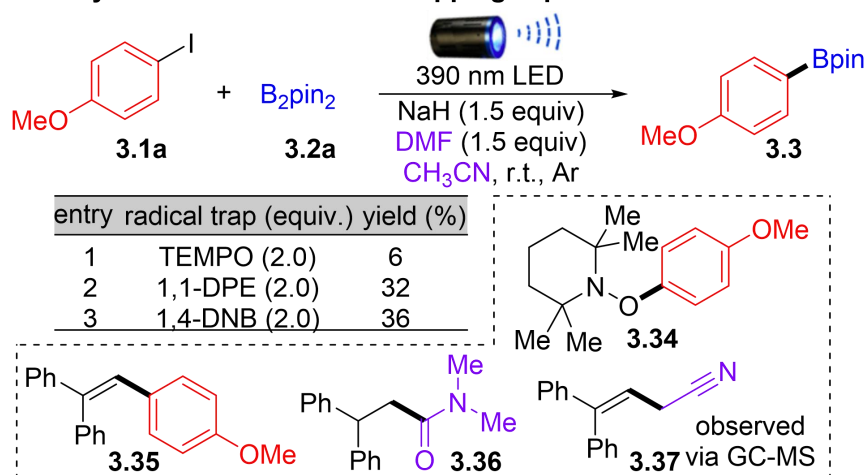


Scheme 3.3. Scope of the phosphonation reaction.

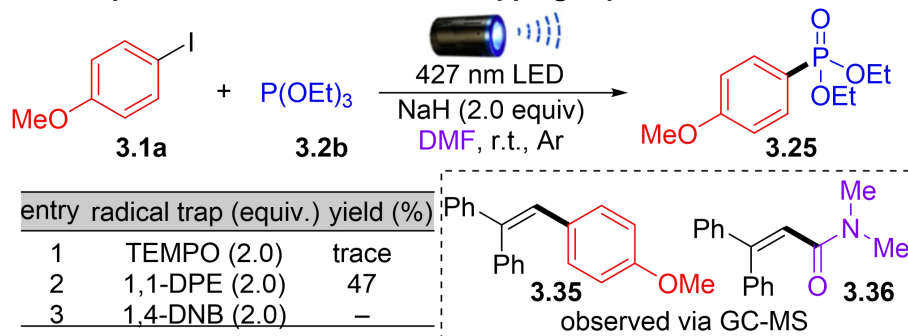
Reaction conditions: **3.1** (0.2 mmol, 1 equiv), **3.2b** (3 equiv), NaH (2 equiv), DMF (1 mL), room temperature around reaction flask was 35 °C (heating caused by the 427 nm LED lamp), under Ar, 24h. Isolated yields unless otherwise noted. a. Yields are based on **3.1**, determined by ¹H-NMR using dibromomethane as internal standard. b. Yields of unreacted starting materials, determined by ¹H-NMR using dibromomethane as internal standard. c. 48h reaction.

To investigate the mechanism of these two transformations we performed several control experiments using different radical trapping agents (Scheme 3.4). Addition of 2,2,6,6-tetramethylpiperidinyloxy (TEMPO), 1,1-diphenylethylene (1,1-DPE), and 1,4-dinitrobenzene (1,4-DNB) to both the borylation reaction (Scheme 3.4A) and the phosphonation reaction (Scheme 3.4B) reduced product formation, which suggests that the reaction probably goes through a radical pathway. It is worth noting that for the borylation reaction (Scheme 3.4A) four different radical intermediates were trapped and observed via GC-MS. The aryl radical intermediate was trapped both as a TEMPO adduct (**3.34**) and a 1,1-DPE adduct (**3.35**). Additionally, DMF (**3.36**) and CH₃CN radicals (**3.37**) were also trapped as 1,1-DPE adducts.

A. Borylation reaction: radical trapping experiment



B. Phosphonation reaction: radical trapping experiment



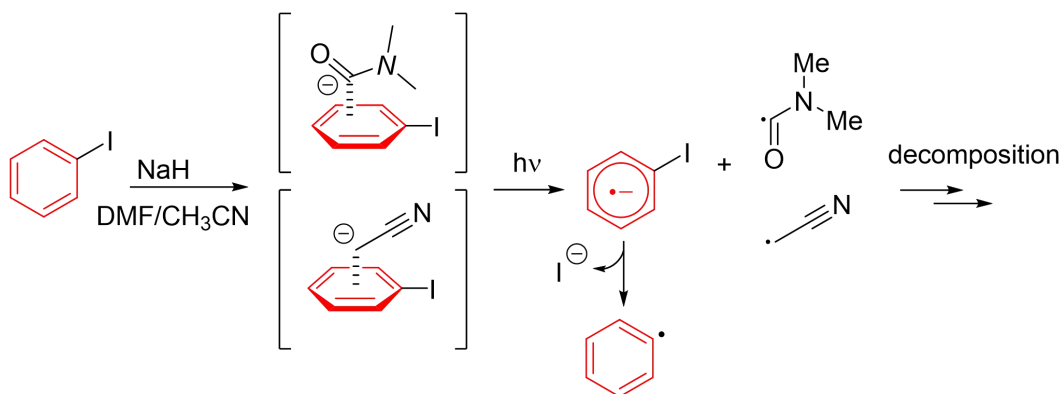
Scheme 3.4. Control Experiments.

Similarly, the phosphonation reaction in presence of radical trapping agents saw a dramatic decrease in yield and the aryl radical intermediate was observed via GC-MS as a 1,1-DPE adduct (**3.35**) as well as the DMF radical (**3.36**) (Scheme 3.4B). It is worth noting that the fragmentation

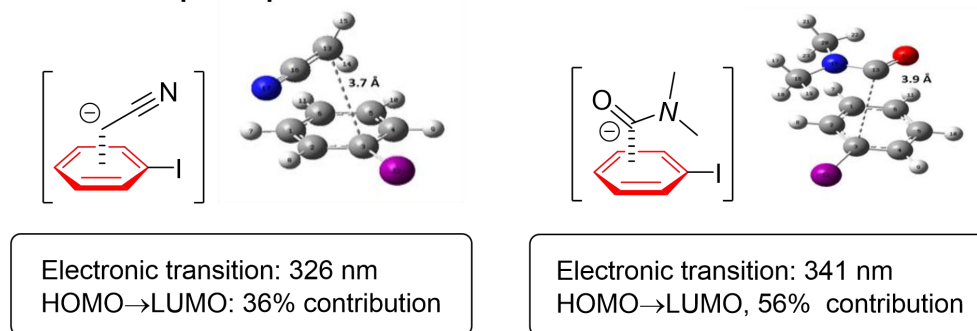
patterns in GC-MS confirm the structure of the observed DMF adduct **3.36**, which suggests the presence of the acyl radical.

Given our previous findings of the dimsyl anion forming an EDA complex with aryl halides, we hypothesize that a similar mechanism could be at play in this transformation, but proceed through a DMF anion or an acetonitrile anion (Scheme 3.5A). To verify the possibility of these EDA complexes we performed time dependent-density functional theory (TD-DFT) calculations. Results show that the acetonitrile anion and the DMF anion can form EDA complexes with aryl iodides where the shortest distance between the moieties is 3.7 Å and 3.9 Å, respectively (Scheme 3.5B). The calculations also show that the least energetic electronic transition between these two complexes appear at 326 nm and 341 nm, respectively, and they may be responsible for the observed visible-light absorption. However, more mechanistic work and experimental results are needed to confirm this possibility.

A. Proposed mechanism



B. EDA complex representation and calculation



Scheme 3.5. Proposed mechanism and EDA complex calculation.

3.3 Summary

In summary, we have developed a visible-light photoredox cross coupling reaction between aryl halides and bis(pinacolato)diboron or triethyl phosphite to synthesize arylboronates and arylphosphonates under mild conditions. Based on control experiments, the mechanism of this work involves a radical pathway. Further studies to determine the mechanistic details of this process and to expand the applications of this synthetic strategy are ongoing in our laboratory.

3.4 Experimental

General Information: All the solvents and commercially available reagents were purchased from commercial sources (Acros Organics, TCI, Alfa Aesar, Sigma-Aldrich, Oakwood) and used directly. Thin layer chromatography (TLC) was performed on EMD precoated plates (silica gel 60 F254, Art 5715) and visualized by fluorescence quenching under UV light or stains for TLC Plates. Column chromatography was performed on EMD Silica Gel 60 (200–300 Mesh) using a forced flow of 0.5–1.0 bar. The ^1H and ^{13}C NMR spectra were obtained on a Bruker AVANCE III-400 or 500 spectrometer. ^1H NMR data was reported as: chemical shift (δ ppm), multiplicity, coupling constant (Hz), and integration. ^{13}C NMR data was reported in terms of chemical shift (δ ppm), multiplicity, and coupling constant (Hz). High Resolution Mass Spectrometry (HRMS) analysis was obtained using Agilent Technologies 6520 Accurate-Mass Q-TOF LC/MS system. UV-Vis was obtained using GENESYS™ 10S UV-Vis Spectrophotometer and fisherbrand macro quartz cuvettes (cat. No. 14-958-112). Two Kessil (390 nm or 427nm, 40W) Blue LED lamps were used for this light-promoted reaction. The vial was placed approximately 3 cm away from the Blue LEDs, with the LEDs shining directly at the side of the vial as shown in following picture. Six reactions could be set up at the same time. A fan above the reaction vials kept the temperature around 35 °C. 10 mL microwave reaction vials secured by 20mm aluminum seals with 0.125-inch thick, blue PTFE / white silicone septa were used for the reaction.

General procedure for the preparation of starting materials: A 25 mL round bottom flask equipped with a stir bar was charged with acid (3 mmol), alcohol (2 mmol), DCC (0.6 g, 3 mmol) and 12 mL of CH_2Cl_2 . Then 4-DMAP (0.4 mmol) was added in one portion. The reaction

was stirred for 4 h at room temperature. After filtration, the solution was concentrated under reduced pressure. The residue was purified by flash column chromatography to give product.

General procedure for the synthesis of arylboronates A: A 10 mL microwave vial was charged with solid aryl halide (0.2 mmol) and bis(pinacolato)diboron **3.2a** (0.6 mmol, 152 mg). Put the vial into the glove box. Add sodium hydride (7 mg, 1.5 eq), and capped with 20 mm microwave crimp caps with septa. Go out of the glove box. Add DMF (23 μ L, 1.5 eq) and CH₃CN (1mL) by syringe. And then put the vial approximately 3 cm away from the LED and stirred. After 24h, the product was determined by GC-MS. The reaction mixture was quenched by di-water and diluted and extracted the reaction mixture to a scintillation vial with EtOAc. The reaction mixture was concentrated in vacuo and yield was determined by ¹HNMR using dibromomethane as internal standard. Then the residue was purified by flash chromatography on silica gel.

General procedure for the synthesis of arylboronates B: A 10 mL microwave vial was charged with bis(pinacolato)diboron **3.2a** (0.6 mmol, 152 mg). Put the vial into the glove box. Add sodium hydride (7 mg, 1.5 eq), and capped with 20 mm microwave crimp caps with septa. Go out of the glove box. Add liquid aryl halides (0.2 mmol), DMF (23 μ L, 1.5 eq) and CH₃CN (1mL) by syringe. And then put the vial approximately 3 cm away from the LED and stirred. After 24h, the product was determined by GC-MS. The reaction mixture was quenched by di-water and diluted and extracted the reaction mixture to a scintillation vial with EtOAc. The reaction mixture was concentrated in vacuo and yield was determined by ¹HNMR using dibromomethane as internal standard. Then the residue was purified by flash chromatography on silica gel.

General procedure for the synthesis of aromatic phosphonates A: A 10 mL microwave vial was charged with solid aryl halides (0.2 mmol). Put the vial into the glove box. Add sodium hydride (10 mg, 2 eq), and capped with 20 mm microwave crimp caps with septa. Go out of the glove box. Add triethyl phosphite (100 mg, 0.6 mmol) and DMF (1.0 ml) by syringe. And then put the vial approximately 3 cm away from the LED and stirred. After 24h, the product was determined by GC-MS. The reaction mixture was quenched by di-water and diluted and extracted the reaction mixture to a scintillation vial with EtOAc. The reaction mixture was concentrated in vacuo and yield was determined by flash chromatography on silica gel.

General procedure for the synthesis of aromatic phosphonates B: Put a 10 mL microwave vial into the glove box. Add sodium hydride (10 mg, 2 eq), and capped with 20 mm microwave crimp caps with septa. Go out of the glove box. Add liquid aryl halides (0.2 mmol), triethyl phosphite (100 mg, 0.6 mmol) and DMF (1.0 ml) by syringe. And then put the vial approximately 3 cm away from the LED and stirred. After 24h, the product was determined by GC-MS. The reaction mixture was quenched by di-water and diluted and extracted the reaction mixture to a scintillation vial with EtOAc. The reaction mixture was concentrated in vacuo and yield was determined by flash chromatography on silica gel.

Analytical Data of Compounds:

2-(4-methoxyphenyl)-4,4,5,5-tetramethyl-1,3,2-dioxaborolane (3.3) Conditions: 1-iodo-4-methoxybenzene (47 mg, 0.2 mmol), bis(pinacolato)diboron (0.6 mmol, 152 mg), sodium hydride (7 mg, 1.5 eq), DMF (23 μ L, 1.5 eq), CH₃CN (1.0 ml), 24h. The product was isolated by flash chromatography (ethyl acetate/hexane= 1/50) as a colorless oil (95%). ¹H NMR (400 MHz, CDCl₃) δ 7.76 (d, *J* = 8.6 Hz, 2H), 6.90 (d, *J* = 8.6 Hz, 2H), 3.83 (s, 3H), 1.34 (s, 12H). ¹³C NMR (101 MHz, CDCl₃) δ 162.2 (s), 136.5 (s), 113.3 (s), 83.6 (s), 55.1 (s), 24.9 (s).

4,4,5,5-tetramethyl-2-(p-tolyl)-1,3,2-dioxaborolane (3.4) Conditions: 1-iodo-4-methylbenzene (44 mg, 0.2 mmol), bis(pinacolato)diboron (0.6 mmol, 152 mg), sodium hydride (7 mg, 1.5 eq), DMF (23 μ L, 1.5 eq), CH₃CN (1.0 ml), 24h. The product was isolated by flash chromatography (ethyl acetate/hexane= 1/50) as a colorless oil (76%). ¹H NMR (400 MHz, CDCl₃) δ 7.71 (d, *J* = 7.8 Hz, 2H), 7.19 (d, *J* = 7.6 Hz, 2H), 2.37 (s, 3H), 1.34 (s, 12H). ¹³C NMR (101 MHz, CDCl₃) δ 141.4 (s), 134.8 (s), 128.5 (s), 83.6 (s), 24.9 (s), 21.7 (s).

2-(4-(tert-butyl)phenyl)-4,4,5,5-tetramethyl-1,3,2-dioxaborolane (3.5) Conditions: 1-(tert-butyl)-4-iodobenzene (52 mg, 0.2 mmol), bis(pinacolato)diboron (0.6 mmol, 152 mg), sodium hydride (7 mg, 1.5 eq), DMF (23 μ L, 1.5 eq), CH₃CN (1.0 ml), 24h. The product was isolated by flash chromatography (ethyl acetate/hexane= 1/50) as a white solid (85%). ¹H NMR (400 MHz, CDCl₃) δ 7.78 (d, *J* = 8.2 Hz, 2H), 7.42 (d, *J* = 8.3 Hz, 2H), 1.35 (s, 12H), 1.34 (s, 9H). ¹³C NMR (101 MHz, CDCl₃) δ 154.5 (s), 134.7 (s), 124.7 (s), 83.6 (s), 34.9 (s), 31.2 (s), 24.9 (s).

4-(4,4,5,5-tetramethyl-1,3,2-dioxaborolan-2-yl)aniline (3.6) Conditions: 4-iodoaniline (44 mg, 0.2 mmol), bis(pinacolato)diboron (0.6 mmol, 152 mg), sodium hydride (7 mg, 1.5 eq), DMF (23 μ L, 1.5 eq), CH₃CN (1.0 ml), 24h. The product was isolated by flash chromatography

(ethyl acetate/hexane= 1/10) as a light yellow solid (68%). ^1H NMR (400 MHz, CDCl_3) δ 7.62 (d, J = 8.3 Hz, 2H), 6.66 (d, J = 8.4 Hz, 2H), 3.82 (s, 2H), 1.32 (s, 12H). ^{13}C NMR (101 MHz, CDCl_3) δ 149.3 (s), 136.4 (s), 114.1 (s), 83.3 (s), 24.9 (s).

4,4,5,5-tetramethyl-2-phenyl-1,3,2-dioxaborolane (3.7) Conditions: iodobenzene (41 mg, 0.2 mmol), bis(pinacolato)diboron (0.6 mmol, 152 mg), sodium hydride (7 mg, 1.5 eq), DMF (23 μL , 1.5 eq), CH_3CN (1.0 ml), 24h. The product was isolated by flash chromatography (ethyl acetate/hexane= 1/50) as a colorless oil (82%). ^1H NMR (400 MHz, CDCl_3) δ 7.79 – 7.70 (m, 2H), 7.43 – 7.35 (m, 1H), 7.29 (dd, J = 11.3, 4.3 Hz, 2H), 1.28 (s, 12H). ^{13}C NMR (101 MHz, CDCl_3) δ 134.8 (s), 131.3 (s), 127.7 (s), 83.8 (s), 24.9 (s).

4,4,5,5-tetramethyl-2-(4-(trifluoromethoxy)phenyl)-1,3,2-dioxaborolane (3.8) Conditions: 1-iodo-4-(trifluoromethoxy)benzene (58 mg, 0.2 mmol), bis(pinacolato)diboron (0.6 mmol, 152 mg), sodium hydride (7 mg, 1.5 eq), DMF (23 μL , 1.5 eq), CH_3CN (1.0 ml), 24h. The product was isolated by flash chromatography (ethyl acetate/hexane= 1/50) as a colorless oil (66%). ^1H NMR (400 MHz, CDCl_3) δ 7.84 (d, J = 8.6 Hz, 2H), 7.20 (dd, J = 8.6, 0.9 Hz, 2H), 1.34 (s, 12H). ^{19}F NMR (377 MHz, CDCl_3) δ -57.57 (s). ^{13}C NMR (101 MHz, CDCl_3) δ 151.7 (s), 136.5 (s), δ 120.4 (q, J = 257.5 Hz), 119.9 (s), 84.1 (s), 24.9 (s).

2-(4-fluorophenyl)-4,4,5,5-tetramethyl-1,3,2-dioxaborolane (3.9) Conditions: 1-fluoro-4-iodobenzene (44 mg, 0.2 mmol), bis(pinacolato)diboron (0.6 mmol, 152 mg), sodium hydride (7 mg, 1.5 eq), DMF (23 μL , 1.5 eq), CH_3CN (1.0 ml), 24h. The product was isolated by flash chromatography (ethyl acetate/hexane=1/50) as a colorless oil (66%). ^1H NMR (400 MHz, CDCl_3) δ 7.80 (dd, J = 8.4, 6.3 Hz, 2H), 7.08 – 7.01 (m, 2H), 1.34 (s, 12H). ^{19}F NMR (377 MHz, CDCl_3) δ -108.49 (dd, J = 10.8, 4.6 Hz). ^{13}C NMR (101 MHz, CDCl_3) δ 165.1 (d, J = 250.4 Hz), 137.0 (d, J = 8.2 Hz), 114.8 (d, J = 20.2 Hz), 83.9 (s), 24.9 (s).

4,4,5,5-tetramethyl-2-(4-(trifluoromethyl)phenyl)-1,3,2-dioxaborolane (3.10) Conditions: 1-iodo-4-(trifluoromethyl)benzene (54 mg, 0.2 mmol), bis(pinacolato)diboron (0.6 mmol, 152 mg), sodium hydride (7 mg, 1.5 eq), DMF (23 μL , 1.5 eq), CH_3CN (1.0 ml), 24h. The product was isolated by flash chromatography (ethyl acetate/hexane=1/50) as a white solid (55%). ^1H NMR (400 MHz, CDCl_3) δ 7.91 (d, J = 7.8 Hz, 2H), 7.61 (d, J = 7.9 Hz, 2H), 1.36 (s, 12H). ^{19}F NMR (376 MHz, CDCl_3) δ -63.06 (s). ^{13}C NMR (101 MHz, CDCl_3) δ 135.0 (s), 132.8 (q, J = 32.0 Hz), 124.3 (q, J = 3.8 Hz), 124.1 (q, J = 274 Hz), 84.3 (s), 24.9 (s).

***N,N*-dimethyl-4-(4,4,5,5-tetramethyl-1,3,2-dioxaborolan-2-yl)benzamide (3.11)**

Conditions: 4-iodo-*N,N*-dimethylbenzamide (55 mg, 0.2 mmol), bis(pinacolato)diboron (0.6 mmol, 152 mg), sodium hydride (7 mg, 1.5 eq), DMF (23 μ L, 1.5 eq), CH₃CN (1.0 ml), 24h. The product was isolated by flash chromatography (ethyl acetate/hexane= 1/2) as a light yellow solid (74%). ¹H NMR (400 MHz, CDCl₃) δ 7.82 (d, *J* = 8.0 Hz, 2H), 7.39 (d, *J* = 8.0 Hz, 2H), 3.02 (d, *J* = 65.1 Hz, 6H), 1.34 (s, 12H). ¹³C NMR (101 MHz, CDCl₃) δ 171.5 (s), 138.9 (s), 134.7 (s), 126.2 (s), 84.0 (s), 39.4 (s), 35.3 (s), 24.9 (s).

4-(4,4,5,5-tetramethyl-1,3,2-dioxaborolan-2-yl)phenol (3.12) Conditions:

(4-iodophenoxy)trimethylsilane (58 mg, 0.2 mmol), bis(pinacolato)diboron (0.6 mmol, 152 mg), sodium hydride (7 mg, 1.5 eq), DMF (23 μ L, 1.5 eq), CH₃CN (1.0 ml), 24h. The product was isolated by flash chromatography (ethyl acetate/hexane= 1/10) as a white solid (58%). ¹H NMR (400 MHz, CDCl₃) δ 7.71 (d, *J* = 8.5 Hz, 2H), 6.85 – 6.77 (m, 2H), 5.40 (s, 1H), 1.33 (s, 12H). ¹³C NMR (101 MHz, CDCl₃) δ 158.4 (s), 136.8 (s), 114.8 (s), 83.7 (s), 24.8 (s).

2-(3,4-dimethoxyphenyl)-4,4,5,5-tetramethyl-1,3,2-dioxaborolane (3.13) Conditions:

4-iodo-1,2-dimethoxybenzene (53 mg, 0.2 mmol), bis(pinacolato)diboron (0.6 mmol, 152 mg), sodium hydride (7 mg, 1.5 eq), DMF (23 μ L, 1.5 eq), CH₃CN (1.0 ml), 24h. The product was isolated by flash chromatography (ethyl acetate/hexane= 1/20) as a white solid (86%). ¹H NMR (400 MHz, CDCl₃) δ 7.42 (dd, *J* = 8.0, 1.2 Hz, 1H), 7.29 (d, *J* = 1.0 Hz, 1H), 6.88 (d, *J* = 8.0 Hz, 1H), 3.92 (s, 3H), 3.90 (s, 3H), 1.34 (s, 12H). ¹³C NMR (101 MHz, CDCl₃) δ 151.7 (s), 148.4 (s), 128.6 (s), 116.7 (s), 110.6 (s), 83.7 (s), 55.9 (s), 55.8 (s), 24.9 (s).

4,4,5,5-tetramethyl-2-(*m*-tolyl)-1,3,2-dioxaborolane (3.14) Conditions:

1-iodo-3-methylbenzene (44 mg, 0.2 mmol), bis(pinacolato)diboron (0.6 mmol, 152 mg), sodium hydride (7 mg, 1.5 eq), DMF (23 μ L, 1.5 eq), CH₃CN (1.0 ml), 24h. The product was isolated by flash chromatography (ethyl acetate/hexane= 1/50) as a colorless oil (71%). ¹H NMR (400 MHz, CDCl₃) δ 7.63 (dd, *J* = 9.9, 4.8 Hz, 2H), 7.28 (dd, *J* = 3.7, 1.5 Hz, 2H), 2.36 (s, 3H), 1.35 (s, 12H). ¹³C NMR (101 MHz, CDCl₃) δ 137.1 (s), 135.4 (s), 132.0 (s), 131.8 (s), 127.7 (s), 83.7 (s), 24.9 (s), 21.3 (s).

3-(4,4,5,5-tetramethyl-1,3,2-dioxaborolan-2-yl)aniline (3.15) Conditions:

3-iodoaniline (44 mg, 0.2 mmol), bis(pinacolato)diboron (0.6 mmol, 152 mg), sodium hydride (7 mg, 1.5 eq), DMF (23 μ L, 1.5 eq), CH₃CN (1.0 ml), 24h. The product was isolated by flash chromatography (ethyl acetate/hexane=1/10) as a light yellow solid (65%). ¹H NMR (400 MHz, CDCl₃) δ 7.24 –

7.11 (m, 3H), 6.79 (ddd, $J = 7.6, 2.5, 1.4$ Hz, 1H), 1.34 (s, 12H). ^{13}C NMR (101 MHz, CDCl_3) δ 145.7 (s), 128.8 (s), 125.1 (s), 121.2 (s), 118.1 (s), 83.7 (s), 24.9 (s).

***N*-(3-(4,4,5,5-tetramethyl-1,3,2-dioxaborolan-2-yl)phenyl)acetamide (3.16)** Conditions: *N*-(3-iodophenyl)acetamide (52 mg, 0.2 mmol), bis(pinacolato)diboron (0.6 mmol, 152 mg), sodium hydride (7 mg, 1.5 eq), DMF (23 μL , 1.5 eq), CH_3CN (1.0 ml), 24h. The product was isolated by flash chromatography (ethyl acetate/hexane= 1/4) as a light yellow solid (55%). ^1H NMR (400 MHz, CDCl_3) δ 7.88 (d, $J = 7.8$ Hz, 1H), 7.62 (s, 1H), 7.54 (d, $J = 7.3$ Hz, 1H), 7.34 (t, $J = 7.7$ Hz, 1H), 7.21 (s, 1H), 2.16 (s, 3H), 1.33 (s, 12H). ^{13}C NMR (101 MHz, CDCl_3) δ 168.2 (s), 137.4 (s), 130.6 (s), 128.6 (s), 125.8 (s), 123.1 (s), 83.9 (s), 24.9 (s), 24.6 (s).

4,4,5,5-tetramethyl-2-(*o*-tolyl)-1,3,2-dioxaborolane (3.17) Conditions: 1-iodo-2-methylbenzene (44 mg, 0.2 mmol), bis(pinacolato)diboron (0.6 mmol, 152 mg), sodium hydride (7 mg, 1.5 eq), DMF (23 μL , 1.5 eq), CH_3CN (1.0 ml), 24h. The product was isolated by flash chromatography (ethyl acetate/hexane= 1/50) as a colorless oil (71%). ^1H NMR (400 MHz, CDCl_3) δ 7.79 – 7.74 (m, 1H), 7.32 (td, $J = 7.5, 1.5$ Hz, 1H), 7.17 (dd, $J = 9.4, 3.6$ Hz, 2H), 2.55 (s, 3H), 1.35 (s, 12H). ^{13}C NMR (101 MHz, CDCl_3) δ 144.8 (s), 135.9 (s), 130.8 (s), 129.9 (s), 124.7 (s), 83.4 (s), 24.9 (s), 22.2 (s).

2-(4,4,5,5-tetramethyl-1,3,2-dioxaborolan-2-yl)aniline (3.18) Conditions: 2-iodoaniline (44 mg, 0.2 mmol), bis(pinacolato)diboron (0.6 mmol, 152 mg), sodium hydride (7 mg, 1.5 eq), DMF (23 μL , 1.5 eq), CH_3CN (1.0 ml), 24h. The product was isolated by flash chromatography (ethyl acetate/hexane= 1/10) as a light yellow solid (55%). ^1H NMR (400 MHz, CDCl_3) δ 7.61 (dd, $J = 7.4, 1.4$ Hz, 1H), 7.24 – 7.17 (m, 1H), 6.67 (t, $J = 7.3$ Hz, 1H), 6.60 (d, $J = 8.1$ Hz, 1H), 4.73 (s, 2H), 1.34 (s, 12H). ^{13}C NMR (101 MHz, CDCl_3) δ 153.6 (s), 136.8 (s), 132.7 (s), 116.9 (s), 114.8 (s), 83.5 (s), 24.9 (s).

4,4,5,5-tetramethyl-2-(naphthalen-1-yl)-1,3,2-dioxaborolane (3.19) Conditions: 1-iodonaphthalene (51 mg, 0.2 mmol), bis(pinacolato)diboron (0.6 mmol, 152 mg), sodium hydride (7 mg, 1.5 eq), DMF (23 μL , 1.5 eq), CH_3CN (1.0 ml), 24h. The product was isolated by flash chromatography (ethyl acetate/hexane= 1/50) as a white solid (72%). ^1H NMR (400 MHz, CDCl_3) δ 8.79 (d, $J = 8.4$ Hz, 1H), 8.10 (dd, $J = 6.8, 1.1$ Hz, 1H), 7.95 (d, $J = 8.2$ Hz, 1H), 7.85 (d, $J = 7.7$ Hz, 1H), 7.55 (ddd, $J = 8.4, 6.8, 1.4$ Hz, 1H), 7.52 – 7.45 (m, 2H), 1.44 (s, 12H). ^{13}C NMR (101 MHz, CDCl_3) δ 137.0 (s), 135.7 (s), 133.3 (s), 131.6 (s), 128.5 (s), 128.4 (s), 126.4 (s), 125.5 (s), 125.0 (s), 83.8 (s), 25.0 (s).

6-(4,4,5,5-tetramethyl-1,3,2-dioxaborolan-2-yl)quinoline (3.20) Conditions: 6-iodoquinoline (51 mg, 0.2 mmol), bis(pinacolato)diboron (0.6 mmol, 152 mg), sodium hydride (7 mg, 1.5 eq), DMF (23 μ L, 1.5 eq), CH₃CN (1.0 ml), 24h. The product was isolated by flash chromatography (ethyl acetate/hexane= 1/5) as a colorless oil (75%). ¹H NMR (400 MHz, CDCl₃) δ 8.94 (dd, J = 4.2, 1.6 Hz, 1H), 8.34 (s, 1H), 8.19 (dd, J = 8.3, 1.5 Hz, 1H), 8.08 (s, 2H), 7.40 (dd, J = 8.3, 4.2 Hz, 1H), 1.39 (s, 12H). ¹³C NMR (101 MHz, CDCl₃) δ 151.4 (s), 149.8 (s), 136.7 (s), 136.1 (s), 134.3 (s), 128.5 (s), 127.7 (s), 121.1 (s), 84.2 (s), 24.9 (s).

4,4,5,5-tetramethyl-2-(thiophen-3-yl)-1,3,2-dioxaborolane (3.21) Conditions: 3-iodothiophene (42 mg, 0.2 mmol), bis(pinacolato)diboron (0.6 mmol, 152 mg), sodium hydride (7 mg, 1.5 eq), DMF (23 μ L, 1.5 eq), CH₃CN (1.0 ml), 24h. The product was isolated by flash chromatography (ethyl acetate/hexane= 1/100) as a white solid (51%). ¹H NMR (400 MHz, CDCl₃) δ 7.92 (d, J = 1.9 Hz, 1H), 7.44 – 7.38 (m, 1H), 7.34 (dd, J = 4.8, 2.7 Hz, 1H), 1.34 (s, 12H). ¹³C NMR (101 MHz, CDCl₃) δ 136.4 (s), 132.0 (s), 125.3 (s), 83.7 (s), 24.8 (s).

2-(benzo[d][1,3]dioxol-5-yl)-4,4,5,5-tetramethyl-1,3,2-dioxaborolane (3.22) Conditions: 5-iodobenzo[d][1,3]dioxole (50 mg, 0.2 mmol), bis(pinacolato)diboron (0.6 mmol, 152 mg), sodium hydride (7 mg, 1.5 eq), DMF (23 μ L, 1.5 eq), CH₃CN (1.0 ml), 24h. The product was isolated by flash chromatography (ethyl acetate/hexane= 1/50) as a colorless oil (73%). ¹H NMR (400 MHz, CDCl₃) δ 7.36 (dd, J = 7.7, 0.8 Hz, 1H), 7.24 (s, 1H), 6.83 (d, J = 7.7 Hz, 1H), 5.95 (s, 2H), 1.33 (s, 12H). ¹³C NMR (101 MHz, CDCl₃) δ 150.2 (s), 147.2 (s), 129.7 (s), 114.0 (s), 108.3 (s), 100.7 (s), 83.7 (s), 24.9 (s).

2-(2,3-dihydrobenzofuran-5-yl)-4,4,5,5-tetramethyl-1,3,2-dioxaborolane (3.23) Conditions: 5-iodo-2,3-dihydrobenzofuran (49 mg, 0.2 mmol), bis(pinacolato)diboron (0.6 mmol, 152 mg), sodium hydride (7 mg, 1.5 eq), DMF (23 μ L, 1.5 eq), CH₃CN (1.0 ml), 24h. The product was isolated by flash chromatography (ethyl acetate/hexane= 1/50) as a colorless oil (72%). ¹H NMR (400 MHz, CDCl₃) δ 7.66 (s, 1H), 7.61 (d, J = 8.0 Hz, 1H), 6.79 (d, J = 8.0 Hz, 1H), 4.57 (t, J = 8.7 Hz, 2H), 3.19 (t, J = 8.7 Hz, 2H), 1.33 (s, 12H). ¹³C NMR (101 MHz, CDCl₃) δ 162.9 (s), 135.6 (s), 131.5 (s), 126.5 (s), 109.0 (s), 83.5 (s), 71.4 (s), 29.2 (s), 24.9 (s).

2-isopropyl-5-methylcyclohexyl 4-(4,4,5,5-tetramethyl-1,3,2-dioxaborolan-2-yl)benzoate (3.24) Conditions: 2-isopropyl-5-methylcyclohexyl 4-iodobenzoate (77 mg, 0.2 mmol), bis(pinacolato)diboron (0.6 mmol, 152 mg), sodium hydride (7 mg, 1.5 eq), DMF (23 μ L, 1.5 eq), CH₃CN (1.0 ml), 24h. The product was isolated by flash chromatography (ethyl

acetate/hexane= 1/50) as a white solid (47%). ¹H NMR (400 MHz, CDCl₃) δ 8.01 (d, *J* = 8.2 Hz, 2H), 7.86 (d, *J* = 8.2 Hz, 2H), 4.94 (td, *J* = 10.9, 4.4 Hz, 1H), 2.13 (d, *J* = 11.9 Hz, 1H), 1.94 (dtd, *J* = 13.9, 7.0, 2.7 Hz, 1H), 1.74 (dd, *J* = 10.8, 7.8 Hz, 2H), 1.61 – 1.52 (m, 2H), 1.35 (s, 12H), 1.21 – 1.05 (m, 2H), 0.92 (t, *J* = 7.2 Hz, 7H), 0.79 (d, *J* = 6.9 Hz, 3H). ¹³C NMR (101 MHz, CDCl₃) δ 166.1 (s), 134.6 (s), 133.1 (s), 128.6 (s), 84.1 (s), 75.0 (s), 47.3 (s), 41.0 (s), 34.36 (s), 31.5 (s), 26.6 (s), 24.9 (s), 24.8 (s), 23.7 (s), 22.0 (s), 20.7 (s), 16.6 (s).

diethyl (4-methoxyphenyl)phosphonate (3.25) Conditions: 1-iodo-4-methoxybenzene (47 mg, 0.2 mmol), triethyl phosphite (100 mg, 0.6 mmol), sodium hydride (10 mg, 2 eq), DMF (1.0 ml), 24h. The product was isolated by flash chromatography (ethyl acetate/hexane= 2/1) as a light yellow oil (35.2 mg, 72%). ¹H NMR (400 MHz, CDCl₃) δ 7.73 (dd, *J* = 12.7, 8.7 Hz, 2H), 6.95 (dd, *J* = 8.7, 3.3 Hz, 2H), 4.16 – 3.99 (m, 4H), 3.84 (s, 3H), 1.30 (t, *J* = 7.1 Hz, 6H). ³¹P NMR (162 MHz, CDCl₃) δ 20.47 – 19.03 (m). ¹³C NMR (101 MHz, CDCl₃) δ 162.9 (d, *J* = 3.4 Hz), 133.8 (d, *J* = 11.3 Hz), 119.6 (d, *J* = 195.0 Hz), 114.0 (d, *J* = 16.0 Hz), 61.9 (d, *J* = 5.3 Hz), 55.3 (s), 16.3 (d, *J* = 6.6 Hz).

diethyl p-tolylphosphonate (3.26) Conditions: 1-iodo-4-methylbenzene (44 mg, 0.2 mmol), triethyl phosphite (100 mg, 0.6 mmol), sodium hydride (10 mg, 2 eq), DMF (1.0 ml), 24h. The product was isolated by flash chromatography (ethyl acetate/hexane= 2/1) as a light yellow oil (31.5 mg, 69%). ¹H NMR (400 MHz, CDCl₃) δ 7.63 (dd, *J* = 13.1, 8.0 Hz, 2H), 7.20 (dd, *J* = 7.0, 4.8 Hz, 2H), 4.10 – 3.94 (m, 4H), 2.33 (s, 3H), 1.24 (t, *J* = 7.1 Hz, 6H). ³¹P NMR (162 MHz, CDCl₃) δ 19.55 (d, *J* = 4.0 Hz). ¹³C NMR (101 MHz, CDCl₃) δ 142.9 (d, *J* = 3.1 Hz), 131.8 (d, *J* = 10.3 Hz), 129.2 (d, *J* = 15.4 Hz), 125.1 (d, *J* = 190.2 Hz), 62.0 (d, *J* = 5.3 Hz), 21.6 (d, *J* = 1.3 Hz), 16.3 (d, *J* = 6.5 Hz).

diethyl (4-(tert-butyl)phenyl)phosphonate (3.27) Conditions: 1-(tert-butyl)-4-iodobenzene (52 mg, 0.2 mmol), triethyl phosphite (100 mg, 0.6 mmol), sodium hydride (10 mg, 2 eq), DMF (1.0 ml), 24h. The product was isolated by flash chromatography (ethyl acetate/hexane= 2/1) as a light yellow oil (40.5 mg, 75%). ¹H NMR (400 MHz, CDCl₃) δ 7.72 (dd, *J* = 13.0, 8.4 Hz, 2H), 7.52 – 7.38 (m, 2H), 4.17 – 3.99 (m, 4H), δ 1.31 (s, 9H), 1.30 (t, *J* = 7.0 Hz, 6H). ³¹P NMR (162 MHz, CDCl₃) δ 19.49 (dddd, *J* = 16.3, 12.3, 8.2, 4.0 Hz). ¹³C NMR (101 MHz, CDCl₃) δ 155.9 (d, *J* = 3.2 Hz), 131.7 (d, *J* = 10.3 Hz), 125.5 (d, *J* = 15.2 Hz), 125.0 (d, *J* = 190.3 Hz), 62.0 (d, *J* = 5.4 Hz), 35.0 (s), 31.1 (s), 16.3 (d, *J* = 6.6 Hz).

diethyl (4-(dimethylcarbamoyl)phenyl)phosphonate (3.28) Conditions: 4-iodo-*N,N*-dimethylbenzamide (55 mg, 0.2 mmol), triethyl phosphite (100 mg, 0.6 mmol), sodium hydride (10 mg, 2 eq), DMF (1.0 ml), 24h. The product was isolated by flash chromatography (ethyl acetate /methanol= 100/1) as a yellow oil (33.1 mg, 58%). ¹H NMR (400 MHz, CDCl₃) δ 7.83 (dd, *J* = 13.1, 8.1 Hz, 2H), 7.62 – 7.35 (m, 2H), 4.27 – 3.92 (m, 4H), 3.10 (s, 3H), 2.93 (s, 3H), 1.30 (t, *J* = 7.1 Hz, 6H). ³¹P NMR (162 MHz, CDCl₃) δ 17.48 (ddd, *J* = 12.5, 8.3, 4.2 Hz).

¹³C NMR (101 MHz, CDCl₃) δ 170.5 (s), 140.2 (d, *J* = 3.2 Hz), 131.9 (d, *J* = 10.1 Hz), 129.8 (d, *J* = 188.6 Hz), 127.0 (d, *J* = 15.1 Hz), 62.3 (d, *J* = 5.5 Hz), 39.4 (s), 35.3 (s), 16.3 (d, *J* = 6.5 Hz).

diethyl (4-(trifluoromethyl)phenyl)phosphonate (3.29) Conditions: 1-iodo-4-(trifluoromethyl)benzene (54 mg, 0.2 mmol), triethyl phosphite (100 mg, 0.6 mmol), sodium hydride (10 mg, 2 eq), DMF (1.0 ml), 24h. The product was isolated by flash chromatography (ethyl acetate/hexane= 1/1) as a light yellow oil (26.5 mg, 47%). ¹H NMR (400 MHz, CDCl₃) δ 7.94 (dd, *J* = 13.0, 8.1 Hz, 2H), 7.73 (dd, *J* = 8.1, 3.4 Hz, 2H), 4.23 – 4.05 (m, 4H), 1.33 (t, *J* = 7.1 Hz, 6H). ³¹P NMR (162 MHz, CDCl₃) δ 16.25 (s). ¹⁹F NMR (377 MHz, CDCl₃) δ -63.30 (s).

¹³C NMR (101 MHz, CDCl₃) δ 134.1 (dd, *J* = 32.7, 3.3 Hz), 132.9 (d, *J* = 187.9 Hz), 132.2 (d, *J* = 10.1 Hz), 125.3 (dq, *J* = 15.1, 3.7 Hz), 123.6 (d, *J* = 272.9 Hz), 62.5 (d, *J* = 5.6 Hz), 16.3 (d, *J* = 6.4 Hz). HRMS (ESI): [M+K]⁺ calcd for C₁₂H₁₇KO₄P⁺, 295.0496 m/z; found, 295.0489 m/z.

diethyl (4-fluorophenyl)phosphonate (3.30) Conditions: 1-fluoro-4-iodobenzene (44 mg, 0.2 mmol), triethyl phosphite (100 mg, 0.6 mmol), sodium hydride (10 mg, 2 eq), DMF (1.0 ml), 24h. The product was isolated by flash chromatography (ethyl acetate/hexane= 2/1) as a light yellow oil (26.0 mg, 56%). ¹H NMR (400 MHz, CDCl₃) δ 7.87 – 7.72 (m, 2H), 7.14 (ddd, *J* = 11.9, 5.3, 3.2 Hz, 2H), 4.20 – 4.01 (m, 4H), 1.31 (t, *J* = 7.1 Hz, 6H). ¹⁹F NMR (377 MHz, CDCl₃) δ -105.97 – -106.12 (m). ³¹P NMR (162 MHz, CDCl₃) δ 17.81 (s). ¹³C NMR (101 MHz, CDCl₃) δ 165.4 (dd, *J* = 253.5, 3.9 Hz), 134.4 (dd, *J* = 11.3, 8.9 Hz), 124.5 (dd, *J* = 192.8, 3.5 Hz), 115.8 (dd, *J* = 21.4, 16.3 Hz), 62.2 (d, *J* = 5.4 Hz), 16.3 (d, *J* = 6.4 Hz).

diethyl pyridin-3-ylphosphonate (3.31) Conditions: 3-iodopyridine (41 mg, 0.2 mmol), triethyl phosphite (100 mg, 0.6 mmol), sodium hydride (10 mg, 2 eq), DMF (1.0 ml), 24h. The product was isolated by flash chromatography (ethyl acetate/hexane= 2/1) as a light yellow oil (18.9 mg, 44%). ¹H NMR (400 MHz, CDCl₃) δ 8.96 (d, *J* = 5.7 Hz, 1H), 8.79 – 8.71 (m, 1H),

8.09 (ddt, $J = 13.3, 7.8, 1.8$ Hz, 1H), 7.39 (dt, $J = 8.2, 4.2$ Hz, 1H), 4.24 – 4.07 (m, 4H), 1.33 (t, $J = 7.1$ Hz, 6H). ^{31}P NMR (162 MHz, CDCl_3) δ 15.76 (s). ^{13}C NMR (101 MHz, CDCl_3) δ 153.0 (d, $J = 1.7$ Hz), 152. (d, $J = 12.2$ Hz), 139.5 (d, $J = 8.3$ Hz), 125.0 (d, $J = 189.1$ Hz), 123.4 (d, $J = 11.6$ Hz), 62.6 (d, $J = 5.6$ Hz), 16.3 (d, $J = 6.3$ Hz).

diethyl pyridin-2-ylphosphonate (3.32) Conditions: 2-iodopyridine (41 mg, 0.2 mmol), triethyl phosphite (100 mg, 0.6 mmol), sodium hydride (10 mg, 2 eq), DMF (1.0 ml), 24h. The product was isolated by flash chromatography (ethyl acetate/hexane= 2/1) as a light yellow oil (15.1 mg, 35%). ^1H NMR (400 MHz, CDCl_3) δ 8.80 (d, $J = 4.6$ Hz, 1H), 7.97 (t, $J = 7.2$ Hz, 1H), 7.80 (qd, $J = 7.6, 1.6$ Hz, 1H), 7.42 (ddd, $J = 6.5, 2.4, 1.1$ Hz, 1H), 4.31 – 4.16 (m, 4H), 1.35 (t, $J = 7.1$ Hz, 6H). ^{31}P NMR (162 MHz, CDCl_3) δ 11.37 – 10.22 (m). ^{13}C NMR (101 MHz, CDCl_3) δ 152.0 (d, $J = 227.1$ Hz), 150.5 (d, $J = 22.9$ Hz), 136.1 (d, $J = 12.3$ Hz), 128.2 (d, $J = 25.2$ Hz), 126.0 (d, $J = 4.0$ Hz), 63.0 (d, $J = 6.0$ Hz), 16.4 (d, $J = 6.1$ Hz).

diethyl pyridin-4-ylphosphonate (3.33) Conditions: 4-iodopyridine (41 mg, 0.2 mmol), triethyl phosphite (100 mg, 0.6 mmol), sodium hydride (10 mg, 2 eq), DMF (1.0 ml), 24h. The product was isolated by flash chromatography (ethyl acetate/hexane= 2/1) as a light yellow oil (4.7 mg, 11%). ^1H NMR (400 MHz, CDCl_3) δ 8.77 (t, $J = 5.4$ Hz, 2H), 7.65 (dd, $J = 13.4, 5.7$ Hz, 2H), 4.16 (dt, $J = 15.2, 7.6$ Hz, 4H), 1.34 (t, $J = 7.1$ Hz, 6H). ^{31}P NMR (162 MHz, CDCl_3) δ 14.59 (d, $J = 13.4$ Hz). ^{13}C NMR (101 MHz, CDCl_3) δ 150.1 (d, $J = 12.4$ Hz), 137.5 (d, $J = 185.8$ Hz), 125.3 (d, $J = 8.1$ Hz), 62.8 (d, $J = 5.7$ Hz), 16.3 (d, $J = 6.3$ Hz).

3.5 References

1. (a) Suzuki, A. Organoborates in New Synthetic Reactions. *Acc. Chem. Res.* **1982**, *15*, 178–184. (b) Miyaura, N.; Suzuki, A. Palladium-catalyzed cross-coupling reactions of organoboron compounds. *Chem. Rev.* **1995**, *95*, 2457–2483. (c) Boronic Acids, Preparation and Applications in Organic Synthesis and Medicine; Hall, D. G., Ed.; *Wiley-VCH: Weinheim*, **2005**. (d) Wang, M.; Shi, Z. Methodologies and Strategies for Selective Borylation of C–Het and C–C Bonds. *Chem. Rev.* **2020**, *120*, 7348–7398.
2. (a) Moonen, K.; Laureyn, I.; Stevens, C. V. Synthetic Methods for Azaheterocyclic Phosphonates and Their Biological Activity. *Chem. Rev.* **2004**, *104*, 6177–6215. (b) (e) Montchamp, J.-L. Phosphinate Chemistry in the 21st Century: A Viable Alternative to the Use of Phosphorus Trichloride in Organophosphorus Synthesis. *Acc. Chem. Res.* **2014**, *47*, 77–87. (c) Van derJeught, S.; Stevens, C. V. Direct Phosphonylation of Aromatic Azaheterocycles. *Chem. Rev.* **2009**, *109*, 2672–2702.

3. (a) Khotinsky, E.; Melamed, M. Die Wirkung der Magnesiumorganischen Verbindungen auf die Borsäureester. *Ber. Dtsch. Chem. Ges.* **1909**, *42*, 3090–3096. (b) Letsinger, R. L.; Skoog, I. H. The Preparation and Some Properties of 2-Methyl-1-propene-1-Boronic Acid. *J. Org. Chem.* **1953**, *18*, 895–897.
4. Eymery, F.; Iorga, B.; Savignac, P. Synthesis of Phosphonates by Nucleophilic Substitution at Phosphorus: The SNP(V) Reaction. *Tetrahedron* **1999**, *55*, 13109–13150.
5. (a) Chow, W. K.; Yuen, O. Y.; Choy, P. Y.; So, C. M.; Lau, C. P.; Wong, W. T.; Kwong, F. Y. A Decade Advancement of Transition Metal-Catalyzed Borylation of Aryl Halides and Sulfonates. *RSC Adv.* **2013**, *3*, 12518–12539. (b) Ishiyama, T.; Murata, M.; Miyaura, N. Palladium(0)-Catalyzed Cross-Coupling Reaction of Alkoxydiboron with Haloarenes: A Direct Procedure for Arylboronic Esters. *J. Org. Chem.* **1995**, *60*, 7508–7510. (c) Verma, P. K.; Mandal, S.; Geetharani, K. Efficient Synthesis of Aryl Boronates via Cobalt-Catalyzed Borylation of Chloroarenes and Bromides. *ACS Catal.* **2018**, *8*, 4049–4054. (d) Kawamorita, S.; Ohmiya, H.; Iwai, T.; Sawamura, M. Palladium-Catalyzed Borylation of Sterically Demanding Aryl Halides with a Silica-Supported Compact Phosphane Ligand. *Angew. Chem., Int. Ed.* **2011**, *50*, 8363–8366. (e) Rosen, B. M.; Huang, C.; Percec, V. Sequential Ni-Catalyzed Borylation and Cross-Coupling of Aryl Halides via in situ Prepared Neopentylglycolborane. *Org. Lett.* **2008**, *10*, 2597–2600. (f) Bedford, R. B. How Low Does Iron Go? Chasing the Active Species in Fe-Catalyzed Cross-Coupling Reactions. *Acc. Chem. Res.* **2015**, *48*, 1485–1493. (g) Kleeberg, C.; Dang, L.; Lin, Z.; Marder, T. B. A Facile Route to Aryl Boronates: Room-Temperature, Copper-Catalyzed Borylation of Aryl Halides with Alkoxy Diboron Reagents. *Angew. Chem., Int. Ed.* **2009**, *48*, 5350–5354. (h) Bose, S. K.; Deisenberger, A.; Eichhorn, A.; Steel, P. G.; Lin, Z. Y.; Marder, T. B. Zinc-Catalyzed Dual C-X and C-H Borylation of Aryl Halides. *Angew. Chem., Int. Ed.* **2015**, *54*, 11843–11847.
6. Garrett, C.; Prasad, K. The Art of Meeting Palladium Specifications in Active Pharmaceutical Ingredients Produced by Pd-Catalyzed Reactions. *Adv. Synth. Catal.* **2004**, *346*, 889–900.
7. (a) Yamamoto, E.; Izumi, K.; Horita, Y.; Ito, H. Anomalous Reactivity of Silylborane: Transition-Metal-Free Boryl Substitution of Aryl, Alkenyl, and Alkyl Halides with Silylborane/Alkoxy Base Systems. *J. Am. Chem. Soc.* **2012**, *134*, 19997–20000. (b) Uematsu, R.; Yamamoto, E.; Maeda, S.; Ito, H.; Taketsugu, T. Reaction Mechanism of the Anomalous Formal Nucleophilic Borylation of Organic Halides with Silylborane: Combined Theoretical and Experimental Studies. *J. Am. Chem. Soc.* **2015**, *137*, 4090–4099. (c) Yamamoto, E.; Ukigai, S.; Ito, H. Boryl Substitution of Functionalized Aryl-, Heteroaryl- and Alkenyl Halides with Silylborane and an Alkoxy Base: Expanded Scope and Mechanistic Studies. *Chem. Sci.* **2015**, *6*, 2943–2951. (d) Zhang, J. M.; Wu, H. H.; Zhang, J. L. Cesium Carbonate Mediated Borylation of Aryl Iodides with Diboron in Methanol. *Eur. J. Org. Chem.* **2013**, *2013*, 6263–6266. (e) Zhang, L.; Jiao, L. Pyridine-Catalyzed Radical Borylation of Aryl Halides. *J. Am. Chem. Soc.* **2017**, *139*, 607–610.

8. (a) Jin, S.; Dang, H. T.; Haug, G. C.; He, R.; Nguyen, V. D.; Nguyen, V. T.; Arman, H. D.; Schanze, K. S.; Larionov, O. V. Visible Light Induced Borylation of C-O, C-N, and C-X Bonds. *J. Am. Chem. Soc.* **2020**, *142*, 1603–1613. (b) Nitelet, A.; Thevenet, D.; Schiavi, B.; Hardouin, C.; Fournier, J.; Tamion, R.; Pannecoucke, X.; Jubault, P.; Poisson, T. Copper-Photocatalyzed Borylation of Organic Halides under Batch and Continuous-Flow Conditions. *Chem.- Eur. J.* **2019**, *25*, 3262–3266. (c) Jiang, M.; Yang, H. J.; Fu, H. Visible-Light Photoredox Borylation of Aryl Halides and Subsequent Aerobic Oxidative Hydroxylation. *Org. Lett.* **2016**, *18*, 5248–5251.
9. (a) Cowper, N. G. W.; Chernowsky, C. P.; Williams, O. P.; Wickens, Z. K. Potent Reductants via Electron-Primed Photoredox Catalysis: Unlocking Aryl Chlorides for Radical Coupling. *J. Am. Chem. Soc.* **2020**, *142*, 2093–2099. (b) He, Y.; Wu, H.; Toste, F. D. A Dual Catalytic Strategy for Carbon-Phosphorus Cross-Coupling via Gold and Photoredox Catalysis. *Chem. Sci.* **2015**, *6*, 1194–1198. (c) Shaikh, R. S.; Düsel, S. J. S.; König, B. Visible-Light Photo-Arbusov Reaction of Aryl Bromides and Trialkyl Phosphites Yielding Aryl Phosphonates. *ACS Catal.* **2016**, *6*, 8410–8414. (d) Neumeier, M.; Sampedro, D.; Majek, M.; de la Pena O' Shea, V. A.; Jacobi von Wangelin, A.; Perez-Ruiz, R. Dichromatic Photocatalytic Substitutions of Aryl Halides with a Small Organic Dye. *Chem. Eur. J.* **2018**, *24*, 105–108. (e) Ghosh, I.; Shaikh, R. S.; König, B. Sensitization-Initiated Electron Transfer for Photoredox Catalysis. *Angew. Chem. Int. Ed.* **2017**, *56*, 8544–8549.
10. (a) Chen, K.; Zhang, S.; He, P.; Li, P. Efficient Metal-Free Photochemical Borylation of Aryl Halides under Batch and Continuous-Flow Conditions. *Chem. Sci.* **2016**, *7*, 3676–3680. (b) Mfuh, A. M.; Doyle, J. D.; Chhetri, B.; Arman, H. D.; Larionov, O. V. Scalable, Metal- and Additive-Free, Photoinduced Borylation of Haloarenes and Quaternary Arylammonium Salts. *J. Am. Chem. Soc.* **2016**, *138*, 2985–2988. (c) Tian, Y.-M.; Guo, X.-N.; Braunschweig, H.; Radius, U.; Marder, T. B. Photo induced Borylation for the Synthesis of Organoboron Compounds. *Chem. Rev.* **2021**, *121* (7), 3561–3597.
11. (a) Zeng, H.; Dou, Q.; Li, C.-J. Photoinduced Transition-Metal-Free Cross-Coupling of Aryl Halides with H-Phosphonates. *Org. Lett.* **2019**, *21*, 1301–1305.
12. (a) Pan, L.; Elmasry, J.; O'Connor, T.; Cooke, M. V.; Lauthé, S. Photochemical Regioselective C(sp³)-H Amination of Amides Using *N*-haloimides. *Org. Lett.* **2021**, *23*, 3389–3393. (b) Pan L.; Cooke MV.; Spencer A.; Lauthé S. Dimsyl Anion Enables Visible-Light-Promoted Charge Transfer in Cross-Coupling Reactions of Aryl Halides. *Adv. Synth. Catal.*, **2021** (DOI: 10.1002/adsc.202101052)

CHAPTER 4. MILD PHOTO-INDUCED PHOSPHONATION OF ARYL IODIDES USING DIPEA AND TRIALKYL PHOSPHITES

4.1 Introduction

Aromatic phosphonates are common moieties found in pharmaceuticals, agrochemicals, material sciences, and ligands in transition-metal catalysis (Figure 4.1).¹

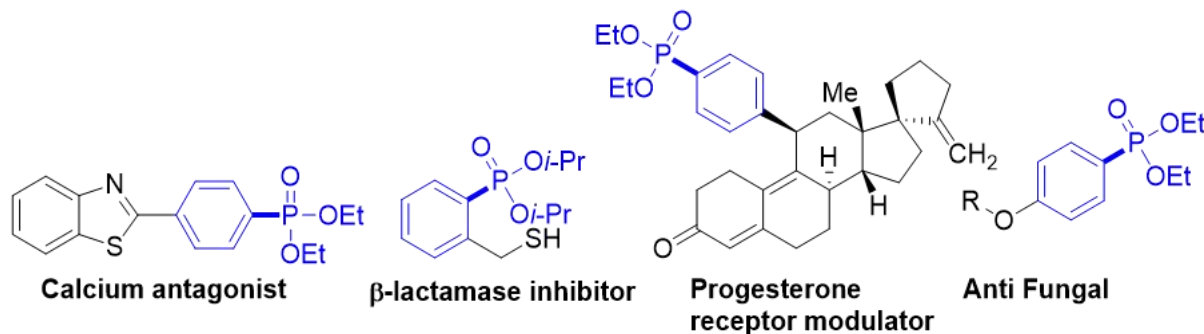
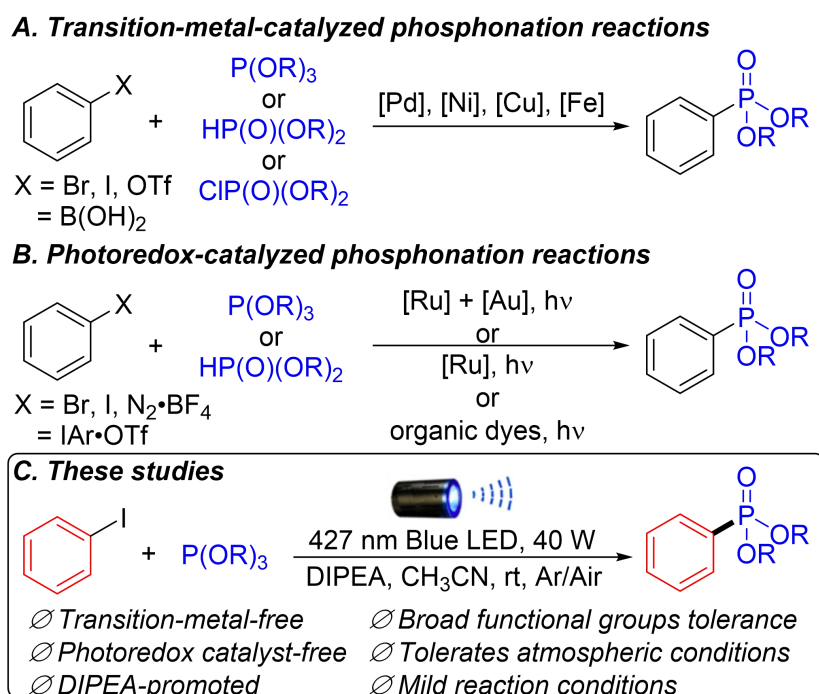


Figure 4.1. Examples of Aromatic Phosphonates in Pharmaceutical Agents.

Many reviews comprehensively summarize C–P formation because phosphorus compounds are an integral part of many biochemical processes.² The classical synthesis of aryl phosphonates involves transition-metal-catalyzed cross-coupling of various aryl precursors with phosphorus sources. These processes have explored the reactivity of a wide range of metal catalysts such as Pd, Ni, Cu, and Fe. However, the potentially toxic nature of metals, their cost, as well as the cost of the associated ligands, substrate scope limitations, and harsh reaction conditions have encouraged the development of new routes for the synthesis of aryl phosphonates (Scheme 4.1-A).³

In the last decade, visible-light photoredox catalysis or dual catalytic strategies have been reliable alternatives in aryl phosphonate synthesis under mild reaction conditions (Scheme 4.1-B).⁴ Some methods still rely on transition-metal catalysts, which require costly purification for industrial applications. Examples of organic photocatalysts and catalyst-free methods exist, but remain rare and limited in scope and relative narrow functional group compatibility.^{4a, c,d,f} And they are often air sensitive. Our interest in transformations that are transition-metal-free has recently led us to develop photo-induced reactions that activate aryl halides and C–H bonds under mild reaction conditions.⁵ Our work showed that KO^{*t*}Bu in presence of light could be used

to activate aryl halides and *N*-haloimides via the formation of electron-donor-acceptor (EDA) complexes.^{5a,5b} However, expanding on these mechanistic discoveries require the development of methods that use milder bases that do not promote side reactions and decompose the desired product. Here, we report a simple DIPEA-mediated photo-induced cross coupling reaction of aryl iodide with trialkyl phosphites. The reaction proceeds under mild reaction conditions under both inert atmosphere or in air. This method avoids the use of photocatalysts and can tolerate diverse functional groups as well as natural products and pharmaceutical frameworks (Scheme 4.1-C).



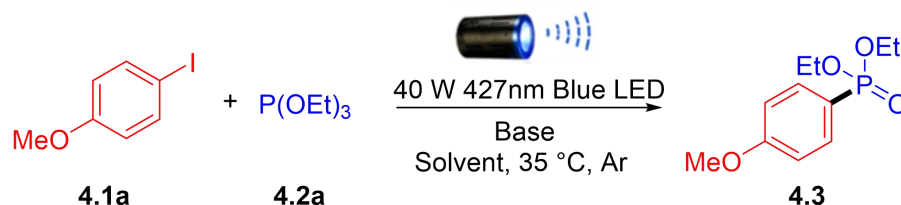
Scheme 4.1. Approaches for C-P Bond Formation.

4.2 Results and Discussion

We selected 1-iodo-4-methoxybenzene (**4.1a**) and triethyl phosphite (**4.2a**) as model reagents for this transformation. We initiated our screens by looking at eight possible bases that promote the desired transformation in *N,N*-dimethylformamide (DMF) under blue-light irradiation (entries 1–8). The use of *tert*-butoxide bases (entries 1–3) showed the formation of the desired product, albeit in low to moderate yields (11–45%). Using a weaker carbonate base (Cs₂CO₃) only formed the phosphonate product in trace amounts (entry 4). Organic bases such as DABCO, DBU, and Et₃N were also ineffective in generating the desired product in meaningful

yields (entries 5–7). Excitingly, diisopropylethylamine (DIPEA) in DMF generated the desired product in 72% yield (entry 8). This was quite unexpected given that Et₃N, which is structurally similar, only generated the product in trace amounts. A control experiment in the absence of base (entry 9) or light (entry 10) confirmed the necessity of both those elements to form the desired product. Using acetonitrile (CH₃CN) as solvent further improved the yield (92%) in spite of reducing the amount of DIPEA to only 2 equivalents (entry 11). The use of CH₃CN also simplified work-up and purification procedures as it is easier to remove than DMF. Interestingly, addition of 2 equivalents of DMF in acetonitrile (entry 12), increased the yield to 95%. However, addition of water (50 μ l) to the solvent system had a major deleterious effect reducing the yield to 27% (entry 13). On the other hand, atmospheric conditions (entry 14) did not affect product formation when compared to reactions under argon. Finally, a time study showed that the reaction can be completed in as little as 8h (entry 15).

Table 4.1. Optimization of reaction conditions.^a



entry	base (<i>equiv.</i>)	4.2a (<i>equiv.</i>)	solvent (<i>mL</i>)	yield (%) ^[b]
1	KOtBu (3.0)	3.0	DMF (1.0)	12
2	NaOtBu (3.0)	3.0	DMF (1.0))	45
3	LiOtBu (3.0)	3.0	DMF (1.0)	11
4	Cs ₂ CO ₃ (3.0)	3.0	DMF (1.0)	trace
5	DABCO (3.0)	3.0	DMF (1.0)	trace
6	DBU (3.0)	3.0	DMF (1.0)	4
7	Et ₃ N (3.0)	3.0	DMF (1.0)	trace
8	DIPEA (3.0)	3.0	DMF (1.0)	72
9	-	3.0	DMF (1.0)	-
10 ^[c]	DIPEA (3.0)	3.0	DMF (1.0)	-
11	DIPEA (2.0)	3.0	CH ₃ CN	92

Table 4.1. Continued.

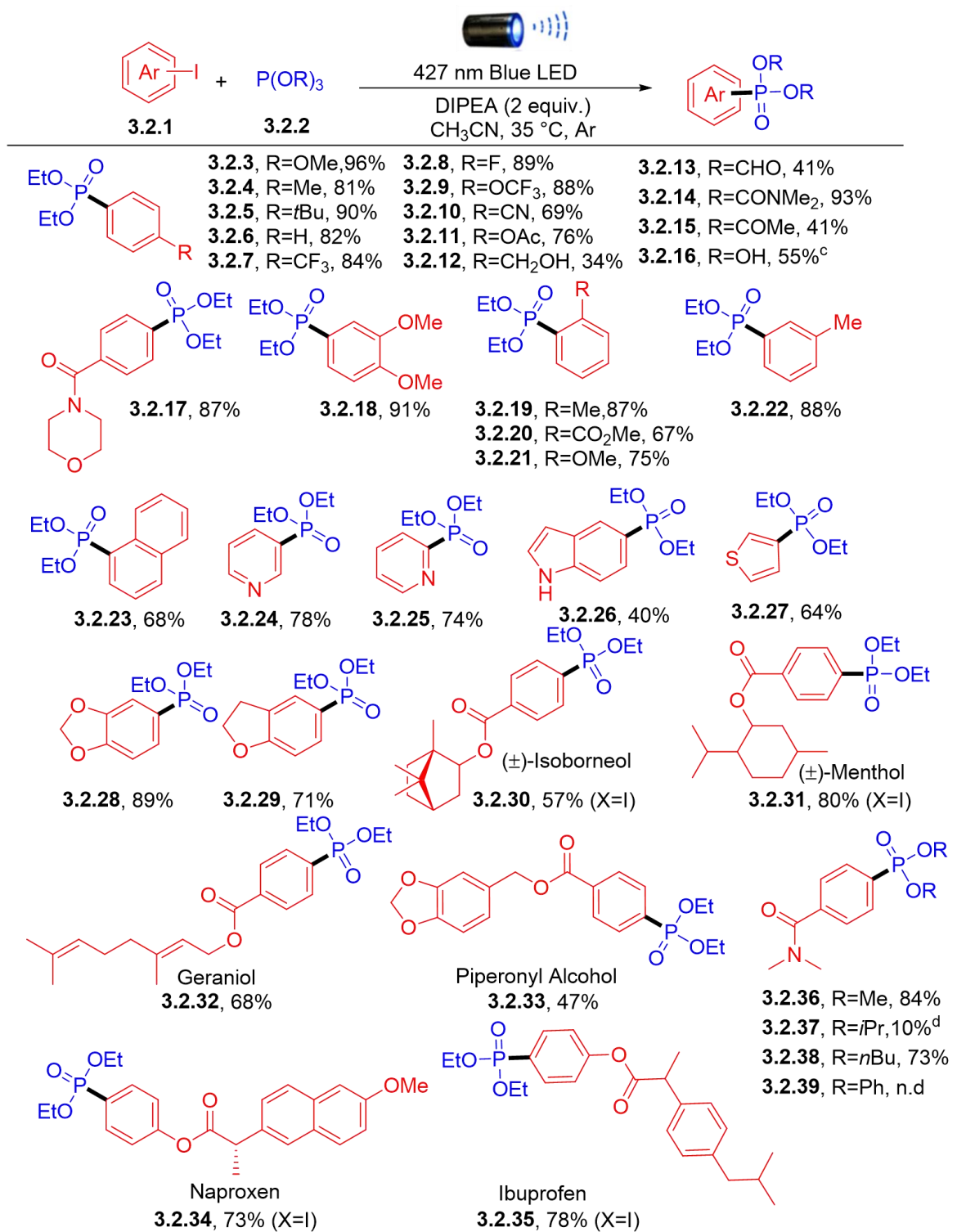
12	DIPEA (2.0)	3.0	DMF/CH ₃ CN (2eq/1.0)	95(96) ^[d]
13	DIPEA (2.0)	3.0	DMF/CH ₃ CN (2eq/1.0) + 50 μ l H ₂ O	27
14 ^[c]	DIPEA (2.0)	3.0	CH ₃ CN	90
15 ^[f]	DIPEA (2.0)	3.0	CH ₃ CN	90

a. Reaction conditions: **4.1a** (0.2 mmol), **4.2a** (0.6 mmol), DIPEA (0.4 mmol), Solvent (1 ml), 35 °C (Heating caused by the LED lamp.), under Ar, 24h. b. Yields are based on **4.1a**, determined by ¹HNMR using dibromomethane as internal standard. c. The reaction was performed in the dark covered by aluminum foil, and heated to 40 °C. d. Isolated yield. e. The reaction was performed in air. f. 8h.

On the basis of the optimized reaction conditions, the substrate scope was investigated using a variety of aryl iodides (Scheme 4.2). A wide variety of electron-rich and electron-poor arenes were investigated as well as the presence of functional groups. Using triethyl phosphite (**4.2a**) as the coupling partner, the reaction afforded products **4.3–4.5** in excellent yields (81–96%) in the presence of electron-donating groups (Me, OMe, *t*Bu). Electron-neutral iodobenzene gave product **4.6** in good 82% yield. Electron-withdrawing groups (F, CF₃, OCF₃) also generated the desired products **4.7–4.9** in good yields (84–89%). The nitrile (CN) functionality afforded product **4.10** in good but lower yield (69%), presumably due to hydrolysis. The transformation tolerated functional groups sensitive to nucleophiles or nucleophilic bases. Labile aryl acetate **4.11** was formed in good yield (76%). However, unprotected alcohol (**4.12**) and aldehyde (**4.13**) moieties showed limited transformation. Tertiary amide **4.14** was obtained in excellent yield (93%) and 4-iodoacetophenone afforded product **4.15** in 41% yield. Trimethylsilyl (TMS) protected 4-iodophenol generated product **4.16** in moderate yield (55%), but was deprotected during column chromatography purification. Morpholine containing amide gave product **4.17** in good yield (87%). Highly electron-donating product **4.18** with *para* and *meta* substituents was obtained in excellent yield (91%). Steric bulk in the *ortho* position was also tolerated affording products **4.19–4.21** in good yields (67–87%), and *meta* substitution was also well-tolerated in product **4.22** (88%). Finally, 1-iodonaphthalene afforded product **4.23** in 68% yield.

Given the great performance of this transformation in this initial scope, we expanded our investigations to heteroarenes and natural product-containing substrates. Pyridine moieties afforded both *meta*- and *ortho*-substituted products **4.24** and **4.25** in good yields (78% and 74%).

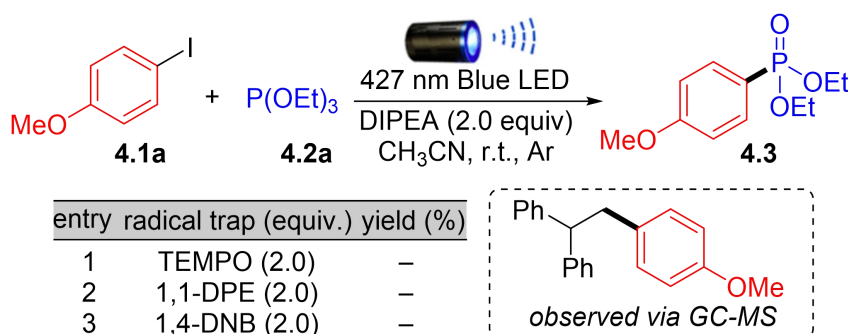
5-Iodoindole afforded product **4.26** in 40% yield, while the 3-iodothiophene gave product **4.27** in good yield (64%). Electron-rich substrates such as 1,3-benzodioxole and 2,3-dihydrobenzofuran afforded products **4.28** and **4.29** in good to excellent yields (71–89%). Furthermore, various esters containing natural product frameworks were investigated under standard conditions. Isoborneol and menthol derivatives afforded products **4.30** and **4.31** in 57% and 80% yields, respectively. Geraniol derivative, which contains potentially reactive alkene functionalities, gave product **4.32** in good yield (68%). Esterified piperonyl alcohol (**4.33**) was also tolerated albeit in lower yields (47%). Additionally, two pharmaceutical containing esters were investigated under standard conditions. Naproxen and ibuprofen derivatives gave products **4.34** and **4.35** in good yields (73–78%), which indicated it as a facile route for late-stage functionalization and modification that could benefit drug discovery and structure activity relationship studies. Finally, different trialkyl phosphite reagents were also investigated under the optimal conditions to assess their reactivity. While $\text{P}(\text{OEt})_3$ afforded desired product **4.14** in 93% yield, the use of $\text{P}(\text{OMe})_3$ gave product **4.36** in lower, but still good, 84% yield. Increasing steric hindrance around the phosphorous atom with $\text{P}(\text{O}i\text{Pr})_3$ had a negative effect on product formation giving product **37** in only 10% yield. $\text{P}(\text{OnBu})_3$ afforded product **4.38** in good yield (73%), but easily hydrolysable $\text{P}(\text{OPh})_3$ did not afford desired product **4.39**.



Scheme 4.2. Substrate scope.^a

a. Reaction conditions: Aryl iodides (0.2 mmol), DIPEA (2.0 eq), Trialkyl Phosphites (3.0 eq), MeCN (1.0 ml), under Ar, 24h. b. isolated yield. c. R = OTMS, deprotected after flash column chromatography. d. confirmed by GC-MS, ¹HNMR yield.

To interrogate the mechanism for this photo-induced transformation, we carried out a series of control experiments in Scheme 4. Initial mechanistic studies using three radical trapping agents showed a complete quenching of the reaction. The addition of 2,2,6,6-Tetramethylpiperidinyloxy (TEMPO), 1,1-diphenylethylene (1,1-DPE), and 1,4-dinitrobenzene (1,4-DNB) to the reaction mixture prevented the formation of the desired product, indicating that this reaction proceeds through a radical pathway. It is worth noting that an aryl radical intermediate was trapped as a 1,1-DPE adduct and observed via GC-MS (Scheme 4.3).



Scheme 4.3. Control experiments.

On the basis of the above obtained mechanistic experiment results and previous literature,^{4c,6} a plausible reaction mechanism is proposed (Figure 4.2). The aryl halide is reduced to an aryl radical anion with the assistance of DIPEA. Following the fragmentation, an aryl radical and iodide anion are formed. Next, the aryl radical reacts with triethyl phosphite to yield the product with the help of DIPEA radical cation.

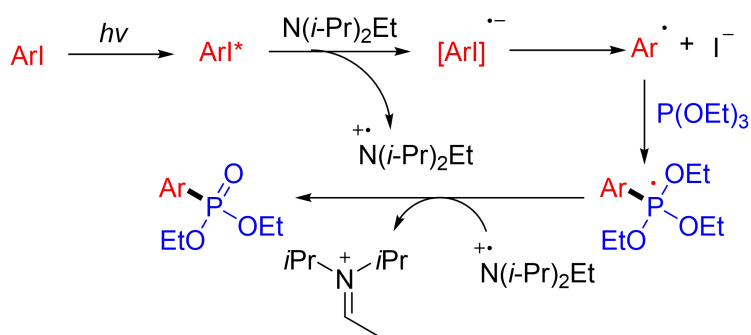


Figure 4.2. Proposed reaction mechanism.

4.3 Summary

In summary, we have developed a simple and efficient visible-light photoredox cross-coupling reaction between aryl iodides with trialkyl phosphites under mild conditions in Ar or air

without transition-metal catalysts, photocatalyst and ligands. The method exhibits broad tolerance of functional groups. Natural products and pharmaceutical molecules are tolerated in these conditions. The mechanism of the visible-light photoredox reaction was investigated and corresponding aryl radical were trapped and detected. We believe that the present results will be helpful for the development of industry. Further studies to determine the mechanistic details of this process and to expand the applications of this synthetic strategy are ongoing in our laboratory.

4.4 Experimental

General Information: All the solvents and commercially available reagents were purchased from commercial sources (Acros Organics, TCI, Alfa Aesar, Sigma-Aldrich, Oakwood) and used directly. Thin layer chromatography (TLC) was performed on EMD precoated plates (silica gel 60 F254, Art 5715) and visualized by fluorescence quenching under UV light or stains for TLC Plates. Column chromatography was performed on EMD Silica Gel 60 (200–300 Mesh) using a forced flow of 0.5–1.0 bar. The ^1H and ^{13}C NMR spectra were obtained on a Bruker AVANCE III-400 or 500 spectrometer. ^1H NMR data was reported as: chemical shift (δ ppm), multiplicity, coupling constant (Hz), and integration. ^{13}C NMR data was reported in terms of chemical shift (δ ppm), multiplicity, and coupling constant (Hz). High Resolution Mass Spectrometry (HRMS) analysis was obtained using Agilent Technologies 6520 Accurate-Mass Q-TOF LC/MS system. UV-Vis was obtained using GENESYSTM 10S UV-Vis Spectrophotometer and fisherbrand macro quartz cuvettes (cat. No. 14-958-112). Two Kessil (427 nm, 40W) Blue LED lamps were used for this light-promoted reaction. The vial was placed approximately 3 cm away from the Blue LEDs, with the LEDs shining directly at the side of the vial as shown in following picture. Six reactions could be set up at the same time. A fan above the reaction vials can keep the temperature around 35°C. 10ml microwave reaction vial secured by 20mm aluminum seals with 0.125-inch thick, blue PTFE/ white silicone septa were used for the reaction.

General procedure for the preparation of starting materials: A 25 mL round bottom flask equipped with a stir bar was charged with acid (3 mmol), alcohol (2 mmol), DCC (0.6 g, 3 mmol) and 12 mL of CH_2Cl_2 . Then 4-DMAP (0.4 mmol) was added in one portion. The reaction was stirred for 4 h at room temperature. After filtration, the solution was concentrated under

reduced pressure. The residue was purified by flash column chromatography to give product.

General procedure for the synthesis of Aromatic Phosphonates: Put a 10 mL microwave vial into the glove box. The vial was charged with the solid aryl halides (0.2 mmol) and capped with 20 mm microwave crimp caps with septa. Go out of the glove box. The vial was charged with trialkyl phosphites (0.6 mmol), DIPEA (0.4 mmol), CH₃CN 1.0 ml). And then put the vial approximately 3 cm away from the Blue LED and stirred. After 24h, the product was determined by GC-MS. The reaction mixture was diluted and transferred to a scintillation vial with EtOAc. The reaction mixture was concentrated in vacuo. Then the residue was purified by flash chromatography on silica gel to yield the desired products.

Analytical Data of Compounds:

diethyl (4-methoxyphenyl)phosphonate (4.3) Conditions: 1-iodo-4-methoxybenzene (47 mg, 0.2 mmol), DIPEA (52 mg, 0.4 mmol), triethyl phosphite (100 mg, 0.6 mmol), CH₃CN (1.0 ml), 24h. The product was isolated by flash chromatography (ethyl acetate/hexane = 2/1) as a light yellow oil (46.8 mg, 96%). ¹H NMR (500 MHz, CDCl₃) δ 7.72 (dd, *J* = 12.6, 8.6 Hz, 2H), 6.94 (dd, *J* = 8.5, 2.9 Hz, 2H), 4.22 – 3.92 (m, 4H), 3.82 (s, 3H), 1.28 (t, *J* = 7.1 Hz, 6H). ¹³C NMR (126 MHz, CDCl₃) δ 162.8 (d, *J* = 3.4 Hz), 133.8 (d, *J* = 11.3 Hz), 119.5 (d, *J* = 194.9 Hz), 114.0 (d, *J* = 16.1 Hz), 61.9 (d, *J* = 5.3 Hz), 55.3 (s), 16.3 (d, *J* = 6.6 Hz). ³¹P NMR (162 MHz, CDCl₃) δ 19.70 (dtd, *J* = 16.2, 8.0, 4.1 Hz).

diethyl p-tolylphosphonate (4.4) Conditions: 1-iodo-4-methylbenzene (44 mg, 0.2 mmol), DIPEA (52 mg, 0.4 mmol), triethyl phosphite (100 mg, 0.6 mmol), CH₃CN (1.0 mL), 24h. The product was isolated by flash chromatography (ethyl acetate/hexane = 2/1) as a light yellow oil (36.9 mg, 81%). ¹H NMR (400 MHz, CDCl₃) δ 7.69 (dd, *J* = 13.1, 8.0 Hz, 2H), 7.26 (dd, *J* = 7.4, 4.3 Hz, 2H), 4.16 – 4.00 (m, 4H), 2.39 (s, 3H), 1.30 (t, *J* = 7.1 Hz, 6H). ³¹P NMR (162 MHz, CDCl₃) δ 19.54 (s). ¹³C NMR (101 MHz, CDCl₃) δ 142.9 (d, *J* = 3.1 Hz), 131.8 (d, *J* = 10.3 Hz), 129.2 (d, *J* = 15.4 Hz), 125.1 (d, *J* = 190.3 Hz), 62.0 (d, *J* = 5.3 Hz), 21.6 (s), 16.3 (d, *J* = 6.5 Hz).

diethyl (4-(tert-butyl)phenyl)phosphonate (4.5) Conditions: 1-(tert-butyl)-4-iodobenzene (52 mg, 0.2 mmol), DIPEA (52 mg, 0.4 mmol), triethyl phosphite (100 mg, 0.6 mmol), CH₃CN (1.0 mL), 24h. The product was isolated by flash chromatography (ethyl acetate/hexane = 2/1) as a light yellow oil (48.6 mg, 90%). ¹H NMR (400 MHz, CDCl₃) δ 7.80 – 7.64 (m, 2H), 7.52 – 7.40 (m, 2H), 4.18 – 3.97 (m, 4H), δ 1.31 (s, 9H), 1.30 (t, *J* = 7.0 Hz, 6H). ³¹P NMR (162 MHz, CDCl₃) δ 19.48 (dddd, *J* = 16.2, 12.3, 8.1, 3.9 Hz). ¹³C NMR (101 MHz, CDCl₃) δ 155.9 (d, *J* =

3.2 Hz), 131.7 (d, $J = 10.3$ Hz), 125.5 (d, $J = 15.2$ Hz), 125.0 (d, $J = 190.3$ Hz), 62.0 (d, $J = 5.4$ Hz), 35.0 (s), 31.1 (s), 16.3 (d, $J = 6.6$ Hz).

diethyl phenylphosphonate (4.6) Conditions: iodobenzene (41 mg, 0.2 mmol), DIPEA (52 mg, 0.4 mmol), triethyl phosphite (100 mg, 0.6 mmol), CH₃CN (1.0 mL), 24h. The product was isolated by flash chromatography (ethyl acetate/hexane = 2/1) as a light yellow oil (35.1 mg, 82%). ¹H NMR (400 MHz, CDCl₃) δ 7.85 – 7.76 (m, 2H), 7.54 (td, $J = 7.5, 1.4$ Hz, 1H), 7.49 – 7.41 (m, 2H), 4.20 – 4.02 (m, 4H), 1.31 (t, $J = 7.1$ Hz, 6H). ³¹P NMR (162 MHz, CDCl₃) δ 19.63 – 18.05 (m). ¹³C NMR (101 MHz, CDCl₃) δ 132.4 (d, $J = 3.1$ Hz), 131.8 (d, $J = 9.9$ Hz), 128.5 (d, $J = 15.0$ Hz), 128.4 (d, $J = 187.9$ Hz), 62.1 (d, $J = 5.4$ Hz), 16.3 (d, $J = 6.5$ Hz).

diethyl (4-(trifluoromethyl)phenyl)phosphonate (4.7) Conditions: 1-iodo-4-(trifluoromethyl)benzene (54 mg, 0.2 mmol), DIPEA (52 mg, 0.4 mmol), triethyl phosphite (100 mg, 0.6 mmol), CH₃CN (1.0 mL), 24h. The product was isolated by flash chromatography (ethyl acetate/hexane = 1/1) as a light yellow oil (47.4 mg, 84%). ¹H NMR (400 MHz, CDCl₃) δ 7.93 (dd, $J = 13.0, 8.1$ Hz, 2H), 7.71 (dd, $J = 8.1, 3.4$ Hz, 2H), 4.22 – 4.03 (m, 4H), 1.32 (t, $J = 7.1$ Hz, 6H). ³¹P NMR (162 MHz, CDCl₃) δ 16.24 (s). ¹⁹F NMR (377 MHz, CDCl₃) δ -63.32 (s). ¹³C NMR (101 MHz, CDCl₃) δ 134.1 (qd, $J = 33, 3$ Hz), 132.9 (dd, $J = 187.8, 0.9$ Hz), 132.2 (d, $J = 10.1$ Hz), 125.3 (dq, $J = 15.2, 3.7$ Hz), 123.6 (q, $J = 272.7$ Hz), 62.5 (d, $J = 5.6$ Hz), 16.3 (d, $J = 6.4$ Hz).

diethyl (4-fluorophenyl)phosphonate (4.8) Conditions: 1-fluoro-4-iodobenzene (44 mg, 0.2 mmol), DIPEA (52 mg, 0.4 mmol), triethyl phosphite (100 mg, 0.6 mmol), CH₃CN (1.0 mL), 24h. The product was isolated by flash chromatography (ethyl acetate/hexane = 2/1) as a light yellow oil (41.3 mg, 89%). ¹H NMR (400 MHz, CDCl₃) δ 7.81 (ddd, $J = 13.9, 8.5, 5.7$ Hz, 2H), 7.14 (td, $J = 8.7, 3.1$ Hz, 2H), 4.18 – 4.00 (m, 4H), 1.31 (t, $J = 7.1$ Hz, 6H). ¹⁹F NMR (377 MHz, CDCl₃) δ -105.85 – -106.29 (m). ³¹P NMR (162 MHz, CDCl₃) δ 18.46 – 17.09 (m). ¹³C NMR (101 MHz, CDCl₃) δ 165.4 (dd, $J = 253.4, 3.9$ Hz), 134.4 (dd, $J = 11.3, 8.9$ Hz), 124.6 (dd, $J = 192.7, 3.4$ Hz), 115.8 (dd, $J = 21.4, 16.3$ Hz), 62.2 (d, $J = 5.4$ Hz), 16.3 (d, $J = 6.4$ Hz).

diethyl (4-(trifluoromethoxy)phenyl)phosphonate (4.9) Conditions: 1-iodo-4-(trifluoromethoxy)benzene (58 mg, 0.2 mmol), DIPEA (52 mg, 0.4 mmol), triethyl phosphite (100 mg, 0.6 mmol), CH₃CN (1.0 mL), 24h. The product was isolated by flash chromatography (ethyl acetate/hexane = 1/1) as a light yellow oil (52.4 mg, 88%). ¹H NMR (400 MHz, CDCl₃) δ 7.79 (dd, $J = 12.9, 8.7$ Hz, 2H), 7.28 – 7.16 (m, 2H), 4.19 – 3.92 (m, 4H), 1.26 (t, $J = 7.1$ Hz, 6H).

^{19}F NMR (377 MHz, CDCl_3) δ -57.68 (s). ^{31}P NMR (162 MHz, CDCl_3) δ 17.69 – 16.31 (m). ^{13}C NMR (101 MHz, CDCl_3) δ 152.2 (s), 133.8 (d, J = 11.0 Hz), 127.2 (d, J = 191.6 Hz), 120.5 (d, J = 15.8 Hz), δ 120.3 (q, J = 258.7 Hz), 62.3 (d, J = 5.5 Hz), 16.3 (d, J = 6.4 Hz).

diethyl (4-cyanophenyl)phosphonate (4.10) Conditions: 4-iodobenzonitrile (46 mg, 0.2 mmol), DIPEA (52 mg, 0.4 mmol), triethyl phosphite (100 mg, 0.6 mmol), CH_3CN (1.0 mL), 24h. The product was isolated by flash chromatography (ethyl acetate/hexane = 1/1) as a light yellow oil (33.0 mg, 69%). ^1H NMR (400 MHz, CDCl_3) δ 7.91 (dd, J = 13.1, 8.3 Hz, 2H), 7.79 – 7.69 (m, 2H), 4.19 – 4.05 (m, 4H), 1.32 (t, J = 7.1 Hz, 6H). ^{31}P NMR (162 MHz, CDCl_3) δ 15.32 (dtd, J = 16.7, 8.4, 4.2 Hz). ^{13}C NMR (101 MHz, CDCl_3) δ 134.0 (d, J = 187.8 Hz), 132.3 (d, J = 9.8 Hz), 132.0 (d, J = 15.0 Hz), 117.8 (s), 116.0 (d, J = 3.5 Hz), 62.7 (d, J = 5.7 Hz), 16.3 (d, J = 6.3 Hz).

4-(diethoxyphosphoryl)phenyl acetate (4.11) Conditions: 4-iodophenyl acetate (52 mg, 0.2 mmol), DIPEA (52 mg, 0.4 mmol), triethyl phosphite (100 mg, 0.6 mmol), CH_3CN (1.0 mL), 24h. The product was isolated by flash chromatography (ethyl acetate/hexane = 2/1) as a light yellow oil (41.3 mg, 76%). ^1H NMR (400 MHz, CDCl_3) δ 7.90 – 7.77 (m, 2H), 7.23 – 7.16 (m, 2H), 4.19 – 4.02 (m, 4H), 2.31 (s, 3H), 1.32 (t, J = 7.1 Hz, 6H). ^{31}P NMR (162 MHz, CDCl_3) δ 18.38 – 17.77 (m). ^{13}C NMR (101 MHz, CDCl_3) δ 168.8 (s), 153.9 (d, J = 3.8 Hz), 133.4 (d, J = 10.9 Hz), 126.0 (d, J = 191.2 Hz), 121.8 (d, J = 15.9 Hz), 62.2 (d, J = 5.4 Hz), 21.1 (s), 16.3 (d, J = 6.5 Hz). HRMS (ESI): $[\text{M}+\text{H}]^+$ calcd for $\text{C}_{12}\text{H}_{18}\text{O}_5\text{P}^+$, 273.0886 m/z; found, 273.0874 m/z.

diethyl (4-(hydroxymethyl)phenyl)phosphonate (4.12) Conditions: (4-iodophenyl)methanol (47 mg, 0.2 mmol), DIPEA (52 mg, 0.4 mmol), triethyl phosphite (100 mg, 0.6 mmol), CH_3CN (1.0 mL), 24h. The product was isolated by flash chromatography (ethyl acetate /methanol = 100/1) as a light yellow oil (16.6 mg, 34%). ^1H NMR (400 MHz, CDCl_3) δ 7.78 (dd, J = 13.1, 8.1 Hz, 2H), 7.46 (dd, J = 8.1, 3.9 Hz, 2H), 4.76 (s, 2H), 4.19 – 3.99 (m, 4H), 2.19 (s, 1H), 1.31 (t, J = 7.1 Hz, 6H). ^{31}P NMR (162 MHz, CDCl_3) δ 18.79 (s). ^{13}C NMR (101 MHz, CDCl_3) δ 145.6 (d, J = 3.0 Hz), 132.0 (d, J = 10.3 Hz), 127.3 (d, J = 189.2 Hz), 126.6 (d, J = 15.3 Hz), 64.6 (s), 62.1 (d, J = 5.4 Hz), 16.3 (d, J = 6.5 Hz).

diethyl (4-formylphenyl)phosphonate (4.13) Conditions: 4-iodobenzaldehyde (46 mg, 0.2 mmol), DIPEA (52 mg, 0.4 mmol), triethyl phosphite (100 mg, 0.6 mmol), CH_3CN (1.0 mL), 24h. The product was isolated by flash chromatography (ethyl acetate/hexane = 2/1) as a light yellow oil (19.8 mg, 41%). ^1H NMR (400 MHz, CDCl_3) δ 10.07 (s, 1H), 7.97 (dd, J = 12.5, 6.8

Hz, 4H), 4.21 – 4.06 (m, 4H), 1.32 (t, $J = 7.1$ Hz, 6H). ^{31}P NMR (162 MHz, CDCl_3) δ 16.34 (s). ^{13}C NMR (101 MHz, CDCl_3) δ 191.6 (s), 138.8 (d, $J = 3.1$ Hz), 134.9 (d, $J = 186.0$ Hz), 132.4 (d, $J = 10.0$ Hz), 129.4 (d, $J = 15.2$ Hz), 62.6 (d, $J = 5.6$ Hz), 16.3 (d, $J = 6.3$ Hz).

diethyl (4-(dimethylcarbamoyl)phenyl)phosphonate (4.14) Conditions: 4-iodo-*N,N*-dimethylbenzamide (55 mg, 0.2 mmol), DIPEA (52 mg, 0.4 mmol), triethyl phosphite (100 mg, 0.6 mmol), CH_3CN (1.0 mL), 24h. The product was isolated by flash chromatography (ethyl acetate /methanol = 100/1) as a yellow oil (53.0 mg, 93%). ^1H NMR (400 MHz, CDCl_3) δ 7.82 (dd, $J = 13.1, 8.2$ Hz, 2H), 7.61 – 7.36 (m, 2H), 4.21 – 3.94 (m, 4H), 3.09 (s, 3H), 2.92 (s, 3H), 1.30 (t, $J = 7.1$ Hz, 6H). ^{31}P NMR (162 MHz, CDCl_3) δ 17.47 (dddd, $J = 16.5, 12.5, 8.2, 4.0$ Hz). ^{13}C NMR (101 MHz, CDCl_3) δ 170.5 (s), 140.2 (d, $J = 3.2$ Hz), 131.9 (d, $J = 10.1$ Hz), 129.7 (d, $J = 188.7$ Hz), 127.0 (d, $J = 15.2$ Hz), 62.3 (d, $J = 5.5$ Hz), 39.4 (s), 35.3 (s), 16.3 (d, $J = 6.4$ Hz).

diethyl (4-acetylphenyl)phosphonate (4.15) Conditions: 1-(4-iodophenyl)ethan-1-one (49 mg, 0.2 mmol), DIPEA (52 mg, 0.4 mmol), triethyl phosphite (100 mg, 0.6 mmol), CH_3CN (1.0 mL), 24h. The product was isolated by flash chromatography (ethyl acetate/hexane = 2/1) as a light yellow oil (21.0 mg, 41%). ^1H NMR (400 MHz, CDCl_3) δ 8.06 – 7.99 (m, 2H), 7.92 (dd, $J = 12.8, 8.4$ Hz, 2H), 4.23 – 4.05 (m, 4H), 2.64 (s, 3H), 1.33 (t, $J = 7.1$ Hz, 6H). ^{31}P NMR (162 MHz, CDCl_3) δ 16.96 – 16.71 (m). ^{13}C NMR (101 MHz, CDCl_3) δ 197.5 (s), 139.9 (d, $J = 3.3$ Hz), 133.5 (d, $J = 186.8$ Hz), 132.1 (d, $J = 10.0$ Hz), 128.1 (d, $J = 15.0$ Hz), 62.4 (d, $J = 5.5$ Hz), 26.8 (s), 16.3 (d, $J = 6.4$ Hz).

diethyl (4-hydroxyphenyl)phosphonate (4.16) Conditions: (4-iodophenoxy)trimethylsilane (58 mg, 0.2 mmol), DIPEA (52 mg, 0.4 mmol), triethyl phosphite (100 mg, 0.6 mmol), CH_3CN (1.0 mL), 24h. The product was isolated by flash chromatography (ethyl acetate /methanol = 100/1) as a light yellow oil (25.3 mg, 55%). ^1H NMR (400 MHz, CDCl_3) δ 7.63 (dd, $J = 12.9, 8.6$ Hz, 2H), 7.03 – 6.93 (m, 2H), 4.15 – 3.99 (m, 4H), 1.31 (t, $J = 7.1$ Hz, 6H). ^{31}P NMR (162 MHz, CDCl_3) δ 20.81 (ddd, $J = 12.0, 8.1, 4.1$ Hz). ^{13}C NMR (101 MHz, CDCl_3) δ 161.6 (d, $J = 3.4$ Hz), 133.8 (d, $J = 11.7$ Hz), 116.7 (d, $J = 197.2$ Hz), 116.0 (d, $J = 16.4$ Hz), 62.3 (d, $J = 5.5$ Hz), 16.3 (d, $J = 6.6$ Hz).

diethyl (4-(morpholine-4-carbonyl)phenyl)phosphonate (4.17) Conditions: (4-iodophenyl)(morpholino)methanone (63 mg, 0.2 mmol), DIPEA (52 mg, 0.4 mmol), triethyl phosphite (100 mg, 0.6 mmol), CH_3CN (1.0 mL), 24h. The product was isolated by flash chromatography (ethyl acetate /methanol = 100/1) as a yellow oil (56.9 mg, 87%). ^1H NMR (400

MHz, CDCl₃) δ 7.83 (dd, J = 13.1, 8.1 Hz, 2H), 7.46 (dd, J = 8.1, 3.8 Hz, 2H), 4.18 – 4.01 (m, 4H), 3.85 – 3.29 (m, 8H), 1.30 (t, J = 7.1 Hz, 6H). ³¹P NMR (162 MHz, CDCl₃) δ 17.88 – 16.42 (m). ¹³C NMR (101 MHz, CDCl₃) δ 169.3 (s), 139.2 (d, J = 3.2 Hz), 132.1 (d, J = 10.1 Hz), 130.3 (d, J = 188.6 Hz), 127.0 (d, J = 15.1 Hz), 66.8 (s), 62.4 (d, J = 5.6 Hz), 45.2 (d, J = 539.3 Hz), 16.3 (d, J = 6.4 Hz). HRMS (ESI): [M+K]⁺ calcd for C₁₅H₂₂NKO₅P⁺, 366.0867 m/z; found, 366.0835 m/z.

diethyl (3,4-dimethoxyphenyl)phosphonate (4.18) Conditions: 4-iodo-1,2-dimethoxybenzene (53 mg, 0.2 mmol), DIPEA (52 mg, 0.4 mmol), triethyl phosphite (100 mg, 0.6 mmol), CH₃CN (1.0 mL), 24h. The product was isolated by flash chromatography (ethyl acetate/hexane = 2/1) as a light yellow oil (49.9 mg, 91%). ¹H NMR (400 MHz, CDCl₃) δ 7.33 (ddd, J = 13.4, 8.2, 1.7 Hz, 1H), 7.21 (dd, J = 14.1, 1.4 Hz, 1H), 6.87 (dd, J = 8.2, 4.4 Hz, 1H), 4.11 – 3.93 (m, 4H), 3.85 (s, 6H), 1.25 (t, J = 7.1 Hz, 6H). ³¹P NMR (162 MHz, CDCl₃) δ 19.64 (qd, J = 13.2, 7.7 Hz). ¹³C NMR (101 MHz, CDCl₃) δ 152.5 (d, J = 3.5 Hz), 148.9 (d, J = 18.8 Hz), 125.7 (d, J = 10.0 Hz), 119.7 (d, J = 194.0 Hz), 114.0 (d, J = 12.7 Hz), 110.9 (d, J = 18.4 Hz), 62.0 (d, J = 5.3 Hz), 56.1 (s), 55.9 (s), 16.3 (d, J = 6.5 Hz).

diethyl o-tolylphosphonate (4.19) Conditions: 1-iodo-2-methylbenzene (44 mg, 0.2 mmol), DIPEA (52 mg, 0.4 mmol), triethyl phosphite (100 mg, 0.6 mmol), CH₃CN (1.0 mL), 24h. The product was isolated by flash chromatography (ethyl acetate/hexane = 2/1) as a light yellow oil (39.7 mg, 87%). ¹H NMR (400 MHz, CDCl₃) δ 8.01 – 7.86 (m, 1H), 7.45 (t, J = 7.5 Hz, 1H), 7.35 – 7.22 (m, 2H), 4.24 – 4.04 (m, 4H), 1.35 (t, J = 7.1 Hz, 6H). ¹³C NMR (101 MHz, CDCl₃) δ 141.8 (d, J = 10.2 Hz), 133.9 (d, J = 10.3 Hz), 132.4 (d, J = 3.0 Hz), 131.2 (d, J = 14.9 Hz), 126.8 (d, J = 184.1 Hz), 125.4 (d, J = 14.9 Hz), 61.9 (d, J = 5.5 Hz), 21.2 (d, J = 3.6 Hz), 16.3 (d, J = 6.5 Hz). ³¹P NMR (162 MHz, CDCl₃) δ 19.45 (s).

methyl 2-(diethoxyphosphoryl)benzoate (4.20) Conditions: methyl 2-iodobenzoate (52 mg, 0.2 mmol), DIPEA (52 mg, 0.4 mmol), triethyl phosphite (100 mg, 0.6 mmol), CH₃CN (1.0 mL), 24h. The product was isolated by flash chromatography (ethyl acetate/hexane = 2/1) as a light yellow oil (36.4 mg, 67%). ¹H NMR (400 MHz, CDCl₃) δ 8.02 – 7.91 (m, 1H), 7.70 (ddd, J = 5.1, 4.2, 1.6 Hz, 1H), 7.62 – 7.52 (m, 2H), 4.25 – 4.05 (m, 4H), 3.93 (s, 3H), 1.33 (t, J = 7.1 Hz, 6H). ³¹P NMR (162 MHz, CDCl₃) δ 16.12 (d, J = 7.0 Hz). ¹³C NMR (101 MHz, CDCl₃) δ 168.4 (d, J = 4.9 Hz), 136.2 (d, J = 8.7 Hz), 133.9 (d, J = 8.2 Hz), 132.1 (d, J = 2.9 Hz), 130.6 (d, J =

13.9 Hz), 129.2 (d, $J = 12.5$ Hz), 127.5 (d, $J = 187.4$ Hz), 62.5 (d, $J = 5.7$ Hz), 52.7 (s), 16.3 (d, $J = 6.6$ Hz).

diethyl (2-methoxyphenyl)phosphonate (4.21) Conditions: 1-iodo-2-methoxybenzene (47 mg, 0.2 mmol), DIPEA (52 mg, 0.4 mmol), triethyl phosphite (100 mg, 0.6 mmol), CH₃CN (1.0 mL), 24h. The product was isolated by flash chromatography (ethyl acetate/hexane = 2/1) as a light yellow oil (36.6 mg, 75%). ¹H NMR (400 MHz, CDCl₃) δ 7.80 (ddd, $J = 14.8, 7.5, 1.7$ Hz, 1H), 7.53 – 7.45 (m, 1H), 7.00 (tdd, $J = 7.5, 3.4, 0.6$ Hz, 1H), 6.96 – 6.90 (m, 1H), 4.22 – 4.04 (m, 4H), 3.89 (s, 3H), 1.32 (t, $J = 7.1$ Hz, 6H). ³¹P NMR (162 MHz, CDCl₃) δ 17.18 (dd, $J = 12.3, 7.4$ Hz). ¹³C NMR (101 MHz, CDCl₃) δ 161.3 (d, $J = 2.7$ Hz), 135.0 (d, $J = 7.0$ Hz), 134.3 (d, $J = 2.1$ Hz), 120.4 (d, $J = 14.5$ Hz), 116.6 (d, $J = 187.7$ Hz), 111.2 (d, $J = 9.4$ Hz), 62.1 (d, $J = 5.5$ Hz), 55.8 (s), 16.4 (d, $J = 6.5$ Hz).

diethyl m-tolylphosphonate (4.22) Conditions: 1-iodo-3-methylbenzene (44 mg, 0.2 mmol), DIPEA (52 mg, 0.4 mmol), triethyl phosphite (100 mg, 0.6 mmol), CH₃CN (1.0 mL), 24h. The product was isolated by flash chromatography (ethyl acetate/hexane = 2/1) as a light yellow oil (40.1 mg, 88%). ¹H NMR (400 MHz, CDCl₃) δ 7.70 – 7.51 (m, 2H), 7.34 (t, $J = 4.4$ Hz, 2H), 4.19 – 3.99 (m, 4H), 2.38 (s, 3H), 1.31 (t, $J = 7.1$ Hz, 6H). ¹³C NMR (101 MHz, CDCl₃) δ 138.3 (d, $J = 15.0$ Hz), 133.2 (d, $J = 3.2$ Hz), 132.3 (d, $J = 10.0$ Hz), 128.8 (d, $J = 9.7$ Hz), 128.4 (d, $J = 15.8$ Hz), 128.1 (d, $J = 186.9$ Hz), 62.1 (d, $J = 5.4$ Hz), 21.3 (s), 16.3 (d, $J = 6.5$ Hz). ³¹P NMR (162 MHz, CDCl₃) δ 19.28 (s).

diethyl naphthalen-1-ylphosphonate (4.23) Conditions: 1-iodonaphthalene (51 mg, 0.2 mmol), DIPEA (52 mg, 0.4 mmol), triethyl phosphite (100 mg, 0.6 mmol), CH₃CN (1.0 mL), 24h. The product was isolated by flash chromatography (ethyl acetate/hexane = 2/1) as a light yellow oil (35.9 mg, 68 %). ¹H NMR (400 MHz, CDCl₃) δ 8.52 (d, $J = 8.5$ Hz, 1H), 8.24 (ddd, $J = 16.3, 7.0, 0.9$ Hz, 1H), 8.03 (d, $J = 8.2$ Hz, 1H), 7.89 (d, $J = 8.1$ Hz, 1H), 7.64 – 7.57 (m, 1H), 7.57 – 7.49 (m, 2H), 4.26 – 4.02 (m, 4H), 1.30 (t, $J = 7.1$ Hz, 6H). ³¹P NMR (162 MHz, CDCl₃) δ 19.64 – 18.76 (m). ¹³C NMR (101 MHz, CDCl₃) δ 134.6 (d, $J = 9.1$ Hz), 133.6 (d, $J = 12.7$ Hz), 133.6 (d, $J = 3.4$ Hz), 132.7 (d, $J = 11.0$ Hz), 128.8 (d, $J = 1.8$ Hz), 127.4 (s), 126.7 (d, $J = 4.2$ Hz), 126.4 (s), 124.7 (d, $J = 182.7$ Hz), 124.5 (d, $J = 16.6$ Hz), 62.2 (d, $J = 5.3$ Hz), 16.3 (d, $J = 6.5$ Hz).

diethyl pyridin-3-ylphosphonate (4.24) Conditions: 3-iodopyridine (41 mg, 0.2 mmol), DIPEA (52 mg, 0.4 mmol), triethyl phosphite (100 mg, 0.6 mmol), CH₃CN (1.0 mL), 24h. The

product was isolated by flash chromatography (ethyl acetate /methanol = 200/1) as a light yellow oil (33.5 mg, 78%). ^1H NMR (400 MHz, CDCl_3) δ 8.94 (dd, J = 6.4, 1.1 Hz, 1H), 8.74 (dt, J = 4.4, 2.0 Hz, 1H), 8.08 (ddt, J = 13.3, 7.8, 1.9 Hz, 1H), 7.42 – 7.32 (m, 1H), 4.22 – 4.04 (m, 4H), 1.32 (t, J = 7.1 Hz, 6H). ^{31}P NMR (162 MHz, CDCl_3) δ 15.74 (s). ^{13}C NMR (101 MHz, CDCl_3) δ 152.9 (d, J = 1.7 Hz), 152.2 (d, J = 12.2 Hz), 139.5 (d, J = 8.3 Hz), 125.0 (d, J = 189.1 Hz), 123.4 (d, J = 11.5 Hz), 62.6 (d, J = 5.6 Hz), 16.3 (d, J = 6.4 Hz).

diethyl pyridin-2-ylphosphonate (4.25) Conditions: 2-iodopyridine (41 mg, 0.2 mmol), DIPEA (52 mg, 0.4 mmol), triethyl phosphite (100 mg, 0.6 mmol), CH_3CN (1.0 mL), 24h. The product was isolated by flash chromatography (ethyl acetate /methanol = 200/1) as a light yellow oil (31.8 mg, 74%). ^1H NMR (400 MHz, CDCl_3) δ 8.79 (d, J = 4.5 Hz, 1H), 7.97 (t, J = 7.2 Hz, 1H), 7.79 (qd, J = 7.6, 1.6 Hz, 1H), 7.47 – 7.37 (m, 1H), 4.31 – 4.15 (m, 4H), 1.34 (t, J = 7.1 Hz, 6H). ^{31}P NMR (162 MHz, CDCl_3) δ 11.36 – 10.19 (m). ^{13}C NMR (101 MHz, CDCl_3) δ 152.0 (d, J = 227.2 Hz), 150.5 (d, J = 22.8 Hz), 136.1 (d, J = 12.3 Hz), 128.2 (d, J = 25.2 Hz), 126.0 (d, J = 4.0 Hz), 63.0 (d, J = 6.0 Hz), 16.4 (d, J = 6.1 Hz).

diethyl (1H-indol-5-yl)phosphonate (4.26) Conditions: 5-iodo-1H-indole (49 mg, 0.2 mmol), DIPEA (52 mg, 0.4 mmol), triethyl phosphite (100 mg, 0.6 mmol), CH_3CN (1.0 mL), 24h. The product was isolated by flash chromatography (ethyl acetate/hexane = 2/1) as a light yellow oil (20.2 mg, 40%). ^1H NMR (400 MHz, CDCl_3) δ 9.21 (s, 1H), 8.18 (d, J = 14.4 Hz, 1H), 7.58 (ddd, J = 12.0, 8.4, 1.2 Hz, 1H), 7.47 (dd, J = 8.4, 3.4 Hz, 1H), 7.33 – 7.27 (m, 1H), 6.64 – 6.58 (m, 1H), 4.19 – 4.01 (m, 4H), 1.31 (t, J = 7.1 Hz, 6H). ^{31}P NMR (162 MHz, CDCl_3) δ 22.51 – 22.20 (m). ^{13}C NMR (101 MHz, CDCl_3) δ 138.1 (d, J = 2.9 Hz), 127.6 (d, J = 18.0 Hz), 126.1 (d, J = 11.3 Hz), 125.8 (s), 124.5 (d, J = 12.1 Hz), 117.8 (d, J = 190.8 Hz), 111.5 (d, J = 16.7 Hz), 103.3 (s), 61.9 (d, J = 5.2 Hz), 16.4 (d, J = 6.7 Hz).

diethyl thiophen-3-ylphosphonate (4.27) Conditions: 3-iodothiophene (42 mg, 0.2 mmol), DIPEA (52 mg, 0.4 mmol), triethyl phosphite (100 mg, 0.6 mmol), CH_3CN (1.0 mL), 24h. The product was isolated by flash chromatography (ethyl acetate/hexane = 1/1) as a light yellow oil (28.2 mg, 64%). ^1H NMR (400 MHz, CDCl_3) δ 7.99 (ddd, J = 8.2, 2.8, 1.1 Hz, 1H), 7.42 (dt, J = 5.0, 3.1 Hz, 1H), 7.37 – 7.30 (m, 1H), 4.17 – 4.07 (m, 4H), 1.32 (t, J = 7.0 Hz, 6H). ^{31}P NMR (162 MHz, CDCl_3) δ 13.21 (ddd, J = 11.9, 8.0, 4.1 Hz). ^{13}C NMR (101 MHz, CDCl_3) δ 135.4 (d, J = 18.0 Hz), 129.6 (d, J = 197.0 Hz), 129.0 (d, J = 16.7 Hz), 127.2 (d, J = 19.5 Hz), 62.2 (d, J = 5.4 Hz), 16.3 (d, J = 6.5 Hz).

diethyl benzo[d][1,3]dioxol-5-ylphosphonate (4.28) Conditions: 5-iodobenzo[d][1,3]dioxole (50 mg, 0.2 mmol), DIPEA (52 mg, 0.4 mmol), triethyl phosphite (100 mg, 0.6 mmol), CH₃CN (1.0 mL), 24h. The product was isolated by flash chromatography (ethyl acetate/hexane = 2/1) as a light yellow oil (45.9 mg, 89%). ¹H NMR (400 MHz, CDCl₃) δ 7.37 (ddd, *J* = 14.0, 7.9, 1.3 Hz, 1H), 7.19 (dd, *J* = 12.9, 1.1 Hz, 1H), 6.88 (dd, *J* = 7.9, 3.6 Hz, 1H), 6.02 (s, 2H), 4.19 – 3.96 (m, 4H), 1.31 (t, *J* = 7.1 Hz, 6H). ³¹P NMR (162 MHz, CDCl₃) δ 19.11 – 18.27 (m). ¹³C NMR (101 MHz, CDCl₃) δ 151.2 (d, *J* = 3.5 Hz), 147.9 (d, *J* = 22.6 Hz), 127.5 (d, *J* = 11.1 Hz), 121.3 (d, *J* = 193.6 Hz), 111.3 (d, *J* = 12.3 Hz), 108.6 (d, *J* = 18.7 Hz), 101.6 (s), 62.1 (d, *J* = 5.3 Hz), 16.3 (d, *J* = 6.5 Hz).

diethyl (2,3-dihydrobenzofuran-5-yl)phosphonate (4.29) Conditions: 5-iodo-2,3-dihydrobenzofuran (49 mg, 0.2 mmol), DIPEA (52 mg, 0.4 mmol), triethyl phosphite (100 mg, 0.6 mmol), CH₃CN (1.0 mL), 24h. The product was isolated by flash chromatography (dichloromethane/ethyl acetate = 2/1) as a light yellow oil (36.4 mg, 71%). ¹H NMR (400 MHz, CDCl₃) δ 7.62 (dd, *J* = 12.5, 0.8 Hz, 1H), 7.56 (dd, *J* = 13.2, 8.2 Hz, 1H), 6.81 (dd, *J* = 8.2, 3.2 Hz, 1H), 4.61 (t, *J* = 8.8 Hz, 2H), 4.14 – 3.97 (m, 4H), 3.22 (t, *J* = 8.8 Hz, 2H), 1.29 (t, *J* = 7.1 Hz, 6H). ³¹P NMR (162 MHz, CDCl₃) δ 20.30 (ddd, *J* = 15.9, 7.9, 4.4 Hz). ¹³C NMR (101 MHz, CDCl₃) δ 163.7 (d, *J* = 3.3 Hz), 133.0 (d, *J* = 11.8 Hz), 128.8 (d, *J* = 11.6 Hz), 127.7 (d, *J* = 17.4 Hz), 119.3 (d, *J* = 194.1 Hz), 109.5 (d, *J* = 17.1 Hz), 71.8 (s), 61.9 (d, *J* = 5.3 Hz), 29.1 (d, *J* = 1.2 Hz), 16.3 (d, *J* = 6.6 Hz).

(1S,4S)-1,7,7-trimethylbicyclo[2.2.1]heptan-2-yl 4-(diethoxyphosphoryl)benzoate (4.30) Conditions: 1,7,7-trimethylbicyclo[2.2.1]heptan-2-yl 4-iodobenzoate (77 mg, 0.2 mmol), DIPEA (52 mg, 0.4 mmol), triethyl phosphite (100 mg, 0.6 mmol), CH₃CN (1.0 mL), 24h. The product was isolated by flash chromatography (ethyl acetate/hexane = 2/1) as a light yellow oil (45.0 mg, 57%). ¹H NMR (400 MHz, CDCl₃) δ 8.06 (dd, *J* = 8.3, 3.9 Hz, 2H), 7.87 (dd, *J* = 12.9, 8.3 Hz, 2H), 4.92 (dd, *J* = 7.2, 4.3 Hz, 1H), 4.21 – 4.02 (m, 4H), 1.96 – 1.87 (m, 2H), 1.79 (t, *J* = 3.7 Hz, 1H), 1.75 – 1.68 (m, 1H), 1.64 – 1.55 (m, 1H), 1.31 (t, *J* = 7.1 Hz, 6H), 1.23 (dt, *J* = 6.9, 3.5 Hz, 1H), 1.20 – 1.12 (m, 1H), 1.10 (s, 3H), 0.89 (d, *J* = 13.9 Hz, 6H). ³¹P NMR (162 MHz, CDCl₃) δ 17.06 (ddtd, *J* = 16.4, 12.3, 8.1, 4.0 Hz). ¹³C NMR (101 MHz, CDCl₃) δ 165.2 (s), 134.3 (d, *J* = 3.2 Hz), 133.1 (d, *J* = 186.5 Hz), 131.8 (d, *J* = 10.1 Hz), 129.3 (d, *J* = 15.0 Hz), 82.2 (s), 62.4 (d, *J* = 5.5 Hz), 49.1 (s), 47.01 (s), 45.1 (s), 38.9 (s), 33.7 (s), 27.0 (s), 20.1 (d, *J* = 3.8 Hz), 16.3 (d, *J* = 6.4 Hz), 11.6 (s).

2-isopropyl-5-methylcyclohexyl 4-(diethoxyphosphoryl)benzoate (4.31) Conditions: 2-isopropyl-5-methylcyclohexyl 4-iodobenzoate (77 mg, 0.2 mmol), DIPEA (52 mg, 0.4 mmol), triethyl phosphite (100 mg, 0.6 mmol), CH₃CN (1.0 mL), 24h. The product was isolated by flash chromatography (ethyl acetate/hexane = 2/1) as a light yellow oil (63.4 mg, 80%). ¹H NMR (400 MHz, CDCl₃) δ 8.09 (dd, *J* = 8.1, 3.8 Hz, 2H), 7.86 (dd, *J* = 12.9, 8.2 Hz, 2H), 4.93 (td, *J* = 10.9, 4.4 Hz, 1H), 4.22 – 3.99 (m, 4H), 2.09 (d, *J* = 11.8 Hz, 1H), 1.91 (dtd, *J* = 13.8, 6.9, 2.5 Hz, 1H), 1.71 (d, *J* = 12.0 Hz, 2H), 1.58 – 1.49 (m, 2H), 1.30 (td, *J* = 7.0, 1.1 Hz, 6H), 1.17 – 1.03 (m, 2H), 0.94 – 0.87 (m, 7H), 0.77 (d, *J* = 6.9 Hz, 3H). ³¹P NMR (162 MHz, CDCl₃) δ 17.14 (dtd, *J* = 16.4, 8.2, 4.0 Hz). ¹³C NMR (101 MHz, CDCl₃) δ 165.2 (s), 134.3 (d, *J* = 3.2 Hz), 133.0 (d, *J* = 186.4 Hz), 131.8 (d, *J* = 10.0 Hz), 129.4 (d, *J* = 15.0 Hz), 75.5 (s), 62.4 (d, *J* = 5.5 Hz), 47.2 (s), 40.9 (s), 34.3 (s), 31.4 (s), 26.5 (s), 23.6 (s), 22.0 (s), 20.7 (s), 16.5 (s), 16.3 (d, *J* = 6.4 Hz).

(E)-3,7-dimethylocta-2,6-dien-1-yl 4-(diethoxyphosphoryl)benzoate (4.32) Conditions: (E)-3,7-dimethylocta-2,6-dien-1-yl 4-iodobenzoate (77 mg, 0.2 mmol), DIPEA (52 mg, 0.4 mmol), triethyl phosphite (100 mg, 0.6 mmol), CH₃CN (1.0 mL), 24h. The product was isolated by flash chromatography (ethyl acetate/hexane = 2/1) as a light yellow oil (53.6 mg, 68%). ¹H NMR (400 MHz, CDCl₃) δ 8.10 (dd, *J* = 8.2, 3.9 Hz, 2H), 7.86 (dd, *J* = 12.9, 8.2 Hz, 2H), 5.44 (t, *J* = 6.7 Hz, 1H), 5.07 (t, *J* = 6.0 Hz, 1H), 4.84 (d, *J* = 7.1 Hz, 2H), 4.20 – 4.00 (m, 4H), 2.08 (td, *J* = 12.2, 6.7 Hz, 4H), 1.75 (s, 3H), 1.65 (s, 3H), 1.58 (s, 3H), 1.30 (t, *J* = 7.1 Hz, 6H). ³¹P NMR (162 MHz, CDCl₃) δ 17.09 (dddd, *J* = 16.5, 12.4, 8.2, 4.0 Hz). ¹³C NMR (101 MHz, CDCl₃) δ 165.8 (s), 142.9 (s), 134.0 (d, *J* = 3.2 Hz), 133.1 (d, *J* = 186.4 Hz), 131.9 (s), 131.7 (d, *J* = 10.0 Hz), 129.4 (d, *J* = 15.0 Hz), 123.7 (s), 118.1 (s), 62.4 (s), 62.3 (d, *J* = 5.8 Hz), 39.5 (s), 26.3 (s), 25.6 (s), 17.67 (s), 16.6 (s), 16.3 (d, *J* = 6.3 Hz).

benzo[d][1,3]dioxol-5-ylmethyl 4-(diethoxyphosphoryl)benzoate (4.33) Conditions: benzo[d][1,3]dioxol-5-ylmethyl 4-iodobenzoate (76 mg, 0.2 mmol), DIPEA (52 mg, 0.4 mmol), triethyl phosphite (100 mg, 0.6 mmol), CH₃CN (1.0 mL), 24h. The product was isolated by flash chromatography (ethyl acetate/hexane = 2/1) as a light yellow oil (36.9 mg, 47%). ¹H NMR (400 MHz, CDCl₃) δ 8.18 – 8.05 (m, 2H), 7.87 (dd, *J* = 12.9, 8.3 Hz, 2H), 6.98 – 6.88 (m, 2H), 6.80 (d, *J* = 7.7 Hz, 1H), 5.97 (s, 2H), 5.27 (s, 2H), 4.19 – 4.03 (m, 4H), 1.31 (t, *J* = 7.1 Hz, 6H). ³¹P NMR (162 MHz, CDCl₃) δ 17.08 – 16.47 (m). ¹³C NMR (101 MHz, CDCl₃) δ 165.6 (d, *J* = 0.8 Hz), 147.9 (d, *J* = 8.0 Hz), 134.0 (d, *J* = 77.8 Hz), 133.0 (d, *J* = 105.2 Hz), 131.8 (d, *J* = 10.0 Hz), 129.5 (d, *J* = 15.0 Hz), 129.4 (s), 122.4 (s), 108.7 (d, *J* = 77.2 Hz), 101.2 (s), 67.2 (s), 62.4 (d, *J* =

5.5 Hz), 16.3 (d, $J = 6.3$ Hz). HRMS (ESI): $[M+H]^+$ calcd for $C_{19}H_{22}O_7P^+$, 393.1098 m/z; found, 393.1068 m/z.

4-(diethoxyphosphoryl)phenyl (S)-2-(6-methoxynaphthalen-2-yl)propanoate (4.34)

Conditions: 4-iodophenyl (S)-2-(6-methoxynaphthalen-2-yl)propanoate (86 mg, 0.2 mmol), DIPEA (52 mg, 0.4 mmol), triethyl phosphite (100 mg, 0.6 mmol), CH_3CN (1.0 mL), 24h. The product was isolated by flash chromatography (ethyl acetate/hexane = 1/1) as a light yellow oil (64.5 mg, 73%). 1H NMR (400 MHz, $CDCl_3$) δ 7.76 (ddd, $J = 13.9, 12.7, 8.9$ Hz, 5H), 7.48 (dd, $J = 8.5, 1.7$ Hz, 1H), 7.20 – 7.05 (m, 4H), 4.16 – 4.00 (m, 5H), 3.92 (s, 3H), 1.70 (d, $J = 7.1$ Hz, 3H), 1.29 (td, $J = 7.1, 0.9$ Hz, 6H). ^{31}P NMR (162 MHz, $CDCl_3$) δ 18.52 – 17.21 (m). ^{13}C NMR (101 MHz, $CDCl_3$) δ 172.7 (s), 157.9 (s), 154.1 (d, $J = 3.9$ Hz), 134.8 (s), 133.9 (s), 133.3 (d, $J = 11.0$ Hz), 129.3 (s), 129.0 (s), 127.5 (s), 126.1 (d, $J = 20.7$ Hz), 125.9 (d, $J = 190.9$ Hz), 121.7 (d, $J = 15.9$ Hz), 119.2 (s), 105.7 (s), 62.2 (d, $J = 5.3$ Hz), 55.4 (s), 45.6 (s), 18.4 (s), 16.3 (d, $J = 6.5$ Hz). HRMS (ESI): $[M+H]^+$ calcd for $C_{24}H_{28}O_6P^+$, 443.1618 m/z; found, 443.1638 m/z.

4-(diethoxyphosphoryl)phenyl 2-(4-isobutylphenyl)propanoate (4.35)

Conditions: 4-iodophenyl 2-(4-isobutylphenyl)propanoate (82 mg, 0.2 mmol), DIPEA (52 mg, 0.4 mmol), triethyl phosphite (100 mg, 0.6 mmol), CH_3CN (1.0 mL), 24h. The product was isolated by flash chromatography (ethyl acetate/hexane = 1/1) as a light yellow oil (65.3 mg, 78%). 1H NMR (400 MHz, $CDCl_3$) δ 7.78 (dd, $J = 12.9, 8.6$ Hz, 2H), 7.27 (t, $J = 5.5$ Hz, 2H), 7.17 – 7.07 (m, 4H), 4.17 – 3.98 (m, 4H), 3.93 (q, $J = 7.1$ Hz, 1H), 2.46 (d, $J = 7.2$ Hz, 2H), 1.86 (dp, $J = 13.5, 6.8$ Hz, 1H), 1.60 (d, $J = 7.1$ Hz, 3H), 1.29 (t, $J = 7.1$ Hz, 6H), 0.90 (d, $J = 6.6$ Hz, 6H). ^{31}P NMR (162 MHz, $CDCl_3$) δ 17.94 (dtd, $J = 12.2, 8.0, 4.1$ Hz). ^{13}C NMR (101 MHz, $CDCl_3$) δ 172.7 (s), 154.1 (d, $J = 3.8$ Hz), 141.0 (s), 136.9 (s), 133.3 (d, $J = 11.0$ Hz), 129.6 (s), 127.2 (s), 125.8 (d, $J = 191.0$ Hz), 121.7 (d, $J = 15.9$ Hz), 62.2 (d, $J = 5.4$ Hz), 45.3 (s), 45.0 (s), 30.2 (s), 22.4 (s), 18.4 (s), 16.3 (d, $J = 6.5$ Hz). HRMS (ESI): $[M+Na]^+$ calcd for $C_{23}H_{31}NaO_5P^+$, 441.1801 m/z; found, 441.1802 m/z.

dimethyl (4-(dimethylcarbamoyl)phenyl)phosphonate (4.36)

Conditions: 4-iodo-*N,N*-dimethylbenzamide (55 mg, 0.2 mmol), DIPEA (52 mg, 0.4 mmol), trimethyl phosphite (74 mg, 0.6 mmol), CH_3CN (1.0 mL), 24h. The product was isolated by flash chromatography (ethyl acetate /methanol = 80/1) as a yellow oil (43.2 mg, 84%). 1H NMR (400 MHz, $CDCl_3$) δ 7.81 (dd, $J = 13.1, 8.1$ Hz, 2H), 7.48 (dd, $J = 8.0, 3.8$ Hz, 2H), 3.74 (d, $J = 11.1$ Hz, 6H), 3.09 (s, 3H), 2.92 (s, 3H). ^{31}P NMR (162 MHz, $CDCl_3$) δ 20.50 – 19.53 (m). ^{13}C NMR (101 MHz, $CDCl_3$) δ

170.4 (s), 140.5 (d, $J = 3.2$ Hz), 132.1 (d, $J = 10.1$ Hz), 128.3 (d, $J = 189.3$ Hz), 127.0 (d, $J = 15.2$ Hz), 52.8 (d, $J = 5.6$ Hz), 39.4 (s), 35.3 (s). HRMS (ESI): $[M+H]^+$ calcd for $C_{11}H_{17}NO_4P^+$, 258.0890 m/z; found, 258.0905 m/z.

dibutyl (4-(dimethylcarbamoyl)phenyl)phosphonate (4.38) Conditions: 4-iodo-*N,N*-dimethylbenzamide (55 mg, 0.2 mmol), DIPEA (52 mg, 0.4 mmol), tributyl phosphite (150 mg, 0.6 mmol), CH_3CN (1.0 mL), 24h. The product was isolated by flash chromatography (ethyl acetate) as a yellow oil (49.8 mg, 73%). 1H NMR (400 MHz, $CDCl_3$) δ 7.81 (dd, $J = 13.1, 8.1$ Hz, 2H), 7.47 (dd, $J = 8.0, 3.8$ Hz, 2H), 4.13 – 3.88 (m, 4H), 3.09 (s, 3H), 2.93 (s, 3H), 1.68 – 1.57 (m, 4H), 1.43 – 1.30 (m, 4H), 0.88 (t, $J = 7.4$ Hz, 6H). ^{31}P NMR (162 MHz, $CDCl_3$) δ 18.14 – 17.35 (m). ^{13}C NMR (101 MHz, $CDCl_3$) δ 170.5 (s), 140.2 (d, $J = 3.2$ Hz), 131.9 (d, $J = 10.0$ Hz), 129.7 (d, $J = 188.8$ Hz), 126.9 (d, $J = 15.1$ Hz), 66.0 (d, $J = 5.8$ Hz), 39.4 (s), 35.3 (s), 32.4 (d, $J = 6.5$ Hz), 18.7 (s), 13.5 (s). HRMS (ESI): $[M+H]^+$ calcd for $C_{17}H_{29}NO_4P^+$, 342.1829 m/z; found, 342.1800 m/z.

4.5 References

1. (a) Moonen, K.; Laureyn, I.; Stevens, C. V. Synthetic Methods for Azaheterocyclic Phosphonates and Their Biological Activity. *Chem. Rev.* **2004**, *104*, 6177–6215. (b) Jiang, W.; Allan, G.; Fiordeliso, J. J.; Linton, O.; Tannenbaum, P.; Xu, J.; Zhu, P.; Gunnet, J.; Demarest, K.; Lundeen, S.; et al. New Progesterone Receptor Antagonists: Phosphorus-Containing 11 β -Aryl-Substituted Steroids. *Bioorg. Med. Chem.* **2006**, *14*, 6726–6732. (c) Lassaux, P.; Hamel, M.; Gulea, M.; Delbruck, H.; Mercuri, P. S.; Horsfall, L.; Dehareng, D.; Kupper, M.; Frere, J. M.; Hoffmann, K.; Galleni, M.; Bebrone, C. MercaptoPhosphonate Compounds as Broad-Spectrum Inhibitors of the Metallo-Beta-Lactamases. *J. Med. Chem.* **2010**, *53*, 4862–4876. (d) Van derJeught, S.; Stevens, C. V. Direct Phosphonylation of Aromatic Azaheterocycles. *Chem. Rev.* **2009**, *109*, 2672–2702. (e) Erion, M. D.; van Poelje, P. D.; Dang, Q.; Kasibhatla, S. R.; Potter, S. C.; Reddy, M. R.; Reddy, K. R.; Jiang, T.; Lipscomb, W. N. MB06322 (CS-917): A Potent and Selective Inhibitor of Fructose 1,6-Bisphosphatase for Controlling Gluconeogenesis in Type 2 Diabetes. *Proc. Natl. Acad. Sci. U. S. A.* **2005**, *102*(22), 7970–7975.
2. (a) Baillie, C.; Xiao, J. Catalytic Synthesis of Phosphines and Related Compounds. *Curr. Org. Chem.* **2003**, *7*, 477–514. (b) Tappe, F. M. J.; Trepohl, V. T.; Oestreich, M. Transition-Metal-Catalyzed C-P Cross-Coupling Reactions. *Synthesis*. **2010**, 3037–3061. (c) Demmer, C. S.; Krosgaard-Larsen, N.; Bunch, L. Review on Modern Advances of Chemical Methods for the Introduction of a Phosphonic Acid Group. *Chem. Rev.* **2011**, *111*, 7981–8006. (d) Queffelec, C.; Petit, M.; Janvier, P.; Knight, D. A.; Bujoli, B. Surface Modification Using Phosphonic Acids and Esters. *Chem. Rev.* **2012**, *112*, 3777–3807. (e) Montchamp, J.-L. Phosphinate Chemistry in the 21st Century: A Viable Alternative to the Use of Phosphorus Trichloride in Organophosphorus Synthesis. *Acc. Chem. Res.* **2014**, *47*, 77–87.

3. (a) Liu, C.; Szostak, M. Decarbonylative Phosphorylation of Amides by Palladium and Nickel Catalysis: The Hirao Cross-Coupling of Amide Derivatives. *Angew. Chem. Int. Ed.* **2017**, *56*, 12718–12722. (b) Zhuang, R.; Xu, J.; Cai, Z.; Tang, G.; Fang, M.; Zhao, Y. Copper-Catalyzed C-P Bond Construction via Direct Coupling of Phenylboronic Acids with H-Phosphonate Diesters. *Org. Lett.* **2011**, *13*, 2110–2113. (c) Bai, Y.; Liu, N.; Wang, S.; Wang, S.; Ning, S.; Shi, L.; Cui, L.; Zhang, Z.; Xiang, J. Nickel-Catalyzed Electrochemical Phosphorylation of Aryl Bromides. *Org. Lett.* **2019**, *21*, 6835–6838. (d) Kalek, M.; Jezowska, M.; Stawinski, J. Preparation of Arylphosphonates by Palladium (0)-Catalyzed Cross-Coupling in the Presence of Acetate Additives: Synthetic and Mechanistic Studies. *Adv. Synth. Catal.* **2009**, *351*, 3207–3216.
4. (a) Cowper, N. G. W.; Chernowsky, C. P.; Williams, O. P.; Wickens, Z. K. Potent Reductants via Electron-Primed Photoredox Catalysis: Unlocking Aryl Chlorides for Radical Coupling. *J. Am. Chem. Soc.* **2020**, *142*, 2093–2099. (b) He, Y.; Wu, H.; Toste, F. D. A Dual Catalytic Strategy for Carbon-Phosphorus Cross-Coupling via Gold and Photoredox Catalysis. *Chem. Sci.* **2015**, *6*, 1194–1198. (c) Shaikh, R. S.; Düsel, S. J. S.; König, B. Visible-Light Photo-Arbusov Reaction of Aryl Bromides and Trialkyl Phosphites Yielding Aryl Phosphonates. *ACS Catal.* **2016**, *6*, 8410–8414. (d) Neumeier, M.; Sampedro, D.; Majek, M.; de la Pena O'Shea, V. A.; Jacobi von Wangelin, A.; Perez-Ruiz, R. Dichromatic Photocatalytic Substitutions of Aryl Halides with a Small Organic Dye. *Chem. Eur. J.* **2018**, *24*, 105–108. (e) Ghosh, I.; Shaikh, R. S.; König, B. Sensitization-Initiated Electron Transfer for Photoredox Catalysis. *Angew. Chem. Int. Ed.* **2017**, *56*, 8544–8549. (f) Zeng, H.; Dou, Q.; Li, C.-J. Photoinduced Transition-Metal-Free Cross-Coupling of Aryl Halides with H-Phosphonates. *Org. Lett.* **2019**, *21*, 1301–1305.
5. (a) Pan, L.; Elmasry, J.; Osccorima, T.; Cooke, M. V.; Laulhé, S. Photochemical Regioselective C(sp³)-H Amination of Amides Using N-Haloimides. *Org. Lett.* **2021**, *23*, 3398–3393. (b) Pan, L.; Cooke, M. V.; Spencer, A.; Laulhé, S. Dimsyl Anion Enables Visible-Light-Promoted Charge Transfer in Cross-Coupling Reactions of Aryl Halides. *Adv. Synth. Catal.* **2021**, doi : 10.1002/adsc.202101052. (c) Gasonoo, M.; Thom, Z. W.; Laulhé, S. Regioselective α -Amination of Ethers Using Stable N-Chloroimides and Lithium tert-Butoxide. *J. Org. Chem.* **2019**, *84*, 8710–8716.
6. (a) Liu, W.; Li, J.; Huang, C.-Y.; Li, C.-J. Aromatic Chemistry in the Excited State: Facilitating Metal-Free Substitutions and CrossCouplings. *Angew. Chem. Int. Ed.* **2020**, *59*, 1786–1796. (b) Chen, K.; He, P.; Zhang, S.; Li, P. Synthesis of aryl trimethylstannanes from aryl halides: an efficient photochemical method. *Chem. Commun.* **2016**, *52*, 9125–9128. (c) Miao, R.; Wang, D.; Xiao, J.; Ma, J.; Xue, D.; Lie, F.; Fang, Y. Halogen bonding matters: visible light-induced photoredox catalyst-free aryl radical formation and its applications. *Phys. Chem. Chem. Phys.*, **2020**, *22*, 10212–10218.

CHAPTER 5. PHOTOCHEMICAL REGIOSELECTIVE C(SP³)-H AMINATION OF AMIDES USING *N*-HALOIMIDES

(Reproduced in part with permission from Pan, L.; Elmasry, J.; Osscorma, T.; Cooke, M. V.; Laulhé, S. “Photochemical Regioselective C(sp³)-H Amination of Amides Using *N*-haloimides”, *Org. Lett.* **2021**, 23, 3389–3393. Copyright 2021 American Chemical Society)

5.1 Introduction

Amines and amides are key intermediates in chemical synthesis and they are also present in biologically active natural products, synthetic intermediates, and pharmaceutical agents.¹ In particular, the amido amination functional group is found in various bioactive compounds such as metolazone, fluspirilene, lymecycline, and primidone (Figure 5.1).

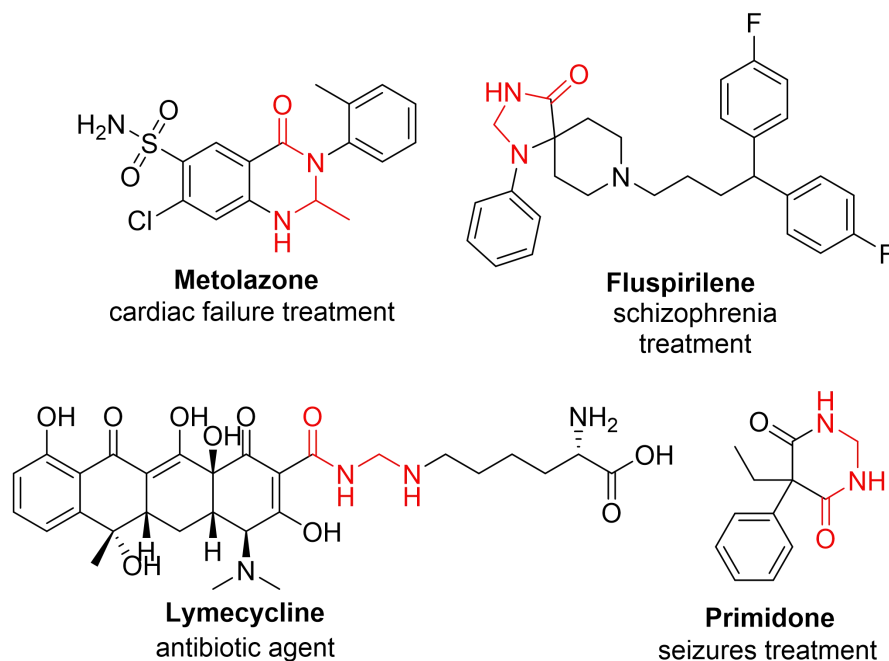
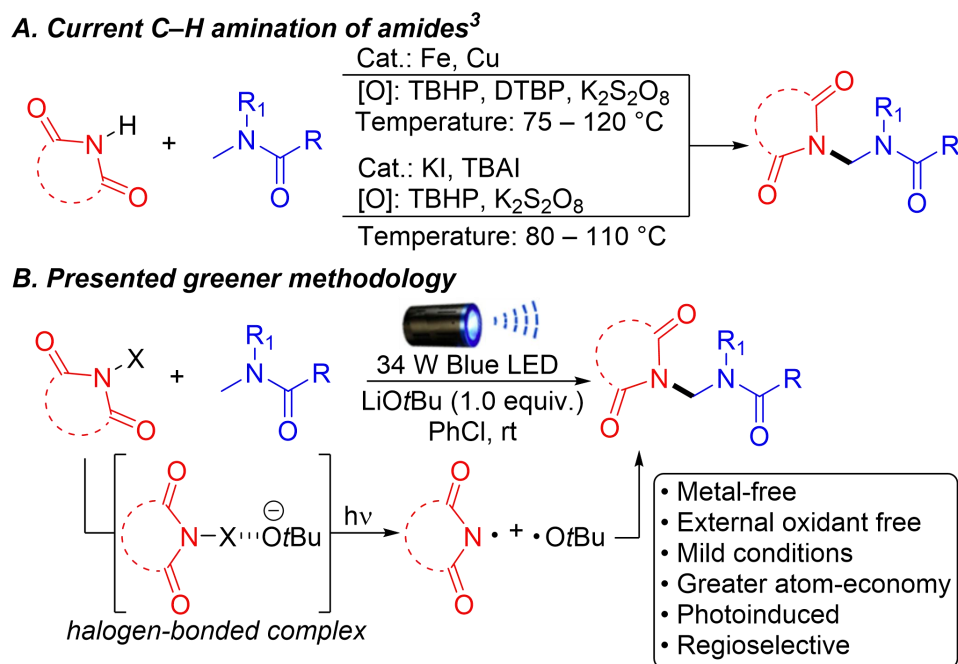


Figure 5.1. Representative biologically active compounds containing amido amination functional group.

Traditionally, these difficult to access compounds have been generated through condensation reactions with formaldehyde.² Due to the importance of this amido amination framework, the development of C–H amination methodologies that selectively targets the amino

carbon of amides has attracted some attention in the organic community.³ Currently, two general approaches have been employed to achieve this (Scheme 5.1-A): i) Transition metal-catalyzed C–H aminations,^{3a–d} and ii) metal-free C–H aminations.^{3e–h} Unfortunately, both of these approaches require the use of stoichiometric strong oxidants or peroxides at high temperatures, increasing accident risks and waste footprint. Consequently, the development of metal-free and atom-economical strategies is of particular importance.

Visible light photoredox processes have recently found many applications in organic synthesis due to the advantages of being readily available, sustainability, mild reaction conditions among others.⁴ Inspired by our previous C–H amination strategies using *N*-haloimides,⁵ herein we report a metal-free C(sp³)–H amination of amides in the presence of lithium *tert*-butoxide using visible light photoexcitation. Our approach does not require a photocatalyst or a peroxide initiator, significantly increasing the atom-economy of the reaction, and proceeds under mild reaction conditions, making this methodology among the greenest approaches to selectively generate the amido aminal functional group (Scheme 5.1-B). Mechanistic work proposes that a halogen-bonded electron-donor-acceptor complex between *tert*-butoxide and the *N*-haloimide is responsible for the observed reactivity.



Scheme 5.1. A. Current methods to access the amido aminal functional group require the use of catalysts and strong oxidants at high temperatures. B. Presented photoexcited C–H activation under mild reaction conditions.

5.2 Results and Discussion

We started our investigation using *N*-bromophthalimide (**5.1a**) and dimethylacetamide (**5.2a**) in the presence of stoichiometric amounts of LiOtBu under blue light (Table 5.1). Initial solvent screening showed that the desired amination product **5.3aa** could be obtained using PhCF₃, PhCl, CH₃CN or benzene (entries 1-4), but chlorobenzene provided the best yields (entry 2). Screening of bases showed that the nature of the counter ion seems to play a major role in this chemistry. Indeed, while lithium *tert*-butoxide generated the product in 67% yield, switching to sodium or potassium *tert*-butoxide has a major deleterious effect giving the desired product in only 24% and 2% yields, respectively (entries 5 & 6). The use of bases other than *tert*-butoxides did not generate the product in synthetically useful yields (entry 7). The stoichiometry of the base was also evaluated (entries 8–11). The absence of LiOtBu as a control reaction did not generate the desired product, and deviating base equivalency from the optimal 1 equivalent had a deleterious effect on yield. Thermal activation of the reaction in the absence of light showed a sharp decline in the yield (entry 12), further demonstrating that it is light, and not the heat generated by the lamps, that activate the reaction. Also, reducing the equivalency of **5.2a** (entries 13 & 14) leads to a reduction in yields of the desired product. Finally, performing the reaction open to the atmosphere leads to a decline in yields (entry 15).

Table 5.1. Optimization of reaction conditions.^a



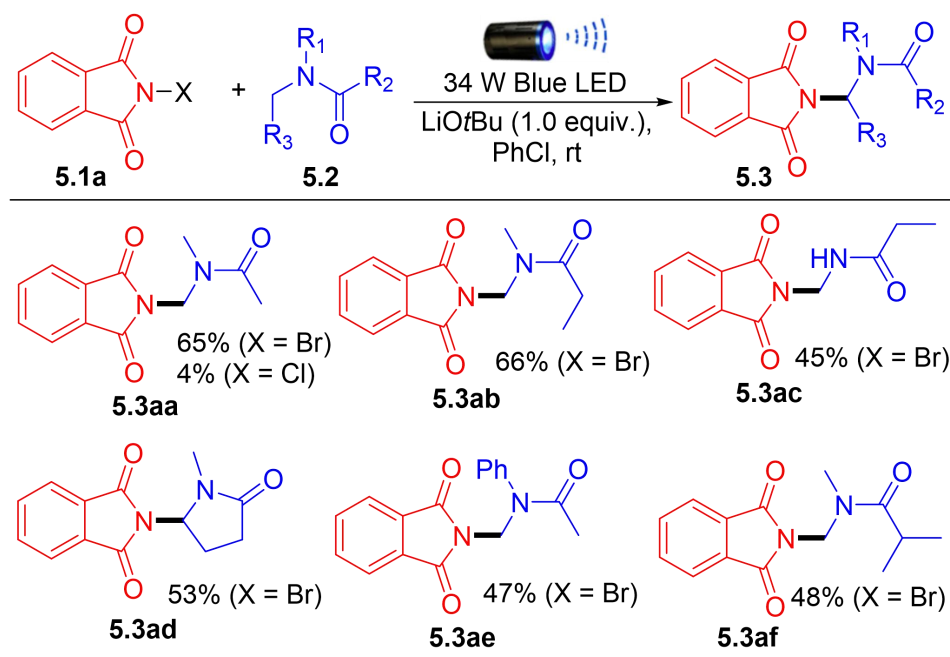
Entry	Base (equiv.)	Solvent (mL)	Yield (%) ^b
1	LiOtBu (1.0)	PhCF ₃ (1.0)	42
2	LiOtBu (1.0)	PhCl (1.0)	67 (65) ^c
3	LiOtBu (1.0)	CH ₃ CN (1.0)	10
4	LiOtBu (1.0)	PhH (1.0)	49
5	NaOtBu (1.0)	PhCl (1.0)	24
6	KOtBu (1.0)	PhCl (1.0)	2
7	DBU (1.0)	PhCl (1.0)	8

Table 5.1. continued.

8	-	PhCl (1.0)	-
9	LiOtBu (0.75)	PhCl (1.0)	45
10	LiOtBu (1.25)	PhCl (1.0)	63
11	LiOtBu (1.5)	PhCl (1.0)	35
12 ^d	LiOtBu(1.0)	PhCl (1.0)	7
13 ^e	LiOtBu(1.0)	PhCl (1.0)	44
14 ^f	LiOtBu(1.0)	PhCl (1.0)	60
15 ^g	LiOtBu(1.0)	PhCl (1.0)	16

a. Reaction conditions: **5.1a** (0.2 mmol, 1 eq.), **5.2a** (1.0 mmol, 5 eq.), base (1 eq.), solvent (1 mL), room temperature around reaction flask was 35 °C (heating caused by the LED lamp), reaction flask capped, overnight. b. ¹H-NMR yields using dibromomethane as internal standard. c. Isolated yield. d. The reaction performed at 60 °C without light. e. **5.2a** (2.5 eq.) was used instead of 5 eq. f. **5.2a** (4 eq.) was used instead of 5 eq. g. The reaction was performed by adding 20 µL of H₂O.

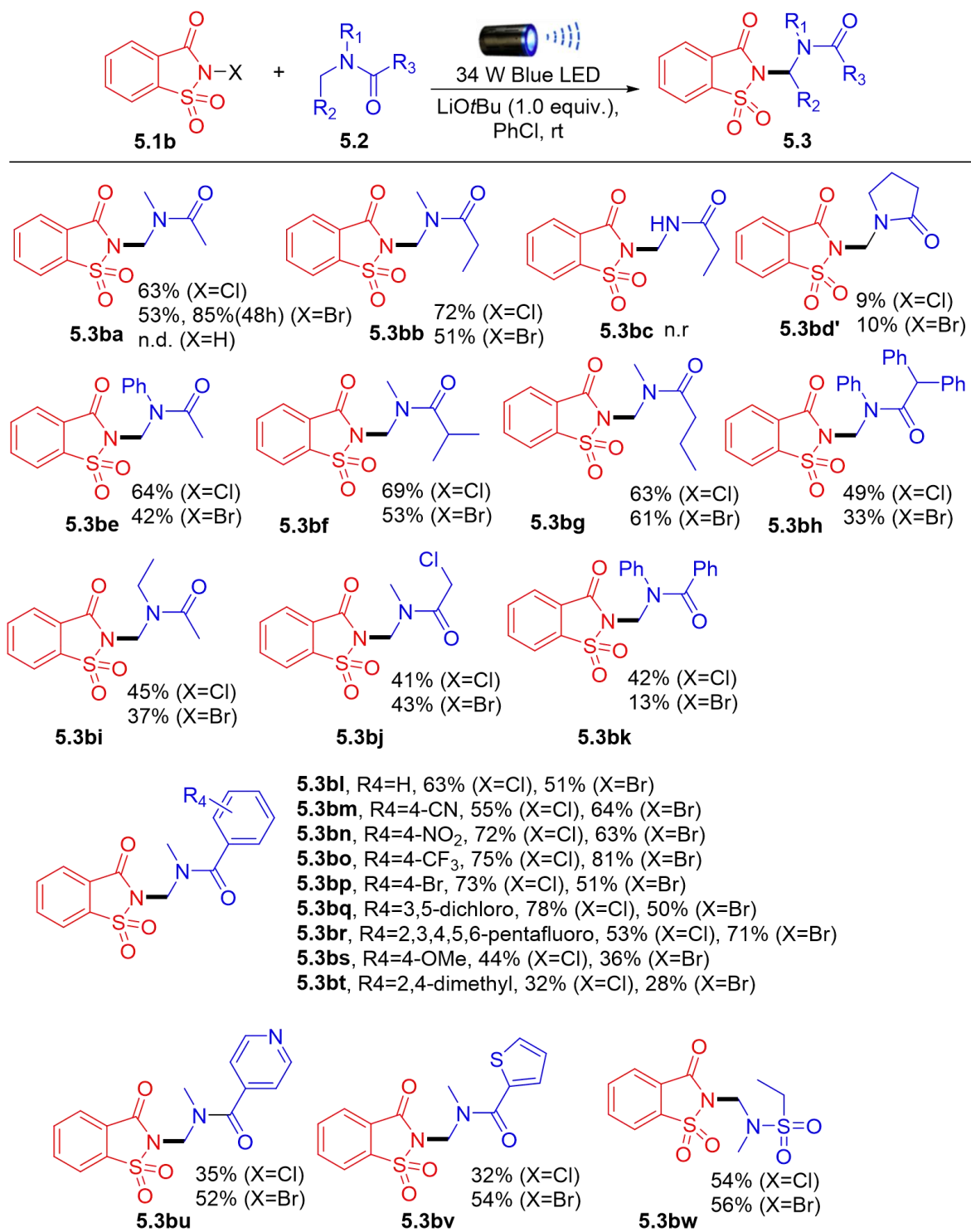
With the optimized conditions in hand, we initiated an amide substrate scope study using **5.1a** as our amine source (Scheme 5.2). As expected, moderate to good yields were obtained. Both secondary and tertiary aliphatic amides generated the desired products **5.3aa**, **5.3ab**, **5.3ac**, and **5.3af**. Interestingly, the use of *N*-chlorophthalimide leads to an almost complete shut down of the reaction provide product **5.3aa** in only 4% yield as opposed to 65% yield when **5.1a** is used. *N*-methyl-2-pyrrolidone also generated the desired product **5.3ad** in 53% yield with a selective amination of the methylene position over the methyl group. Finally, the presence of an aromatic moiety is well tolerated, and amination of the methyl group is observed predominantly (**5.3ae**).



Scheme 5.2. Amination of amides with *N*-Bromophthalimide.^{a,b}

a. Reaction conditions: **5.1a** (0.2 mmol), **5.2** (1.0 mmol), LiOtBu (0.2 mmol), 1.0 mL PhCl, room temperature around reaction flask was 35 °C (heating caused by the LED lamp.), overnight. b. Isolated yields.

We then investigated other possible *N*-haloimide sources and we found that *N*-halosaccharin **5.1b** was significantly more efficient at performing the desired amination than **5.1a**. As shown in Scheme 5.3, a large variety of amides can be selectively aminated at the amino carbon in moderate to good yields. This is particularly important because literature precedent has shown that *N*-halosaccharin reacts effectively with aromatic compounds via Csp²–H activation.⁶ Despite our solvent being chlorobenzene, the major product of these reactions remain the formation of the amino aminal product, indicating that the addition of LiOtBu plays a role in inducing chemoselectivity. The main reactivity difference between **5.1a** and **5.1b** comes from the difference in pK_a between phthalimide (8.3) and saccharin (1.6). The stronger electron withdrawing groups in saccharin destabilizes the imidyl radical, further increasing its reactivity. Also, stronger electron withdrawing groups in saccharin will increase the sigma-hole of the halogen, thereby favoring stronger halogen-bonding interactions with the *tert*-butoxide base.

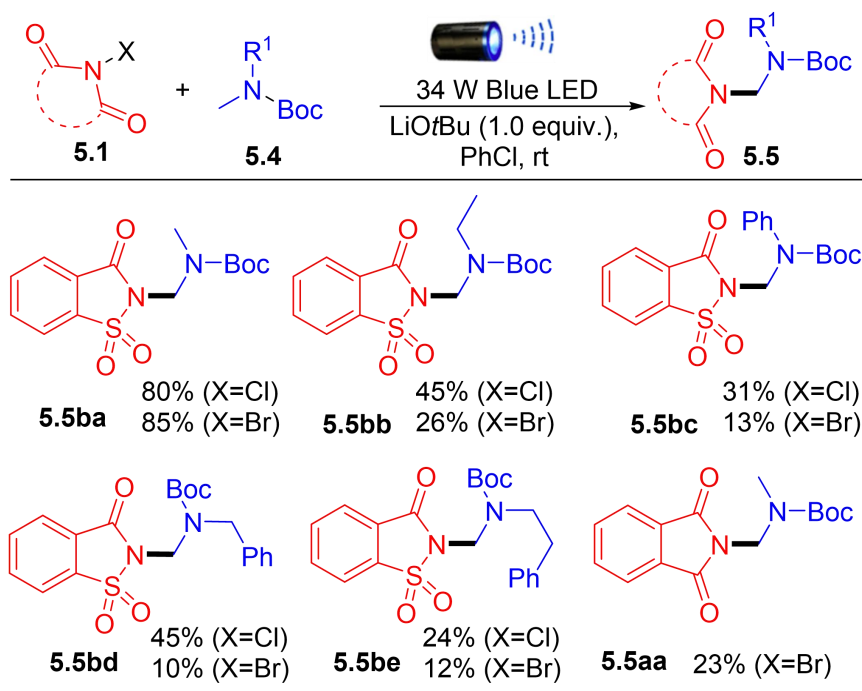


Scheme 5.3. Amination of amides by *N*-halosaccharins.^{a,b}

a. Reaction conditions: **5.1b** (0.2 mmol), **5.2** (1.0 mmol), LiOtBu (0.2 mmol), 1.0 mL PhCl, room temperature around reaction flask was 35 °C (heating caused by the LED lamp), overnight. b. Isolated yields.

Aliphatic amide derivatives could be aminated in good to excellent yields using both *N*-bromo and *N*-chlorosaccharin (**5.3ba** and **5.3bb**). As shown for product **5.3ba**, the reaction does not proceed when the halogen is replaced by hydrogen, indicating the necessity of using the *N*-haloimide motif. An important observation is the complementary reactivity between *N*-bromophthalimide **5.1a** and *N*-halosaccharin **5.1b**; while secondary amide **5.2c** and *N*-methyl-2-pyrrolidone provided the desired product when using **5.1a**, this was not the case with **5.1b** giving little to no products **5.3bc** and **5.3bd'**.

Further, *N*-methyl-2-pyrrolidone reactivity seemed to switch from the methylene position to the methyl position (**5.3bd'**). Highly acidic alpha-positions such as in product **5.3bh** still provided the desired product in moderate yield, and unsymmetrical *N*-ethyl-*N*-methyl amides showed regioselectivity towards the methyl group over the methylene carbon (**5.3bi**). Aromatic amides bearing electron-withdrawing groups (-CN, -NO₂, -CF₃) (**5.3bm–5.3bo**) presented better yields compared with electron-donating groups (-OMe, -Me) (**5.3bl–5.3bt**). It is also noteworthy that aromatic halogens (F, Cl, or Br) were well tolerated and provided the desired products in good yields (**5.3bp–5.3br**), enabling further manipulations of the products through cross-coupling transformations. Heteroaromatic amides were also aminated in moderate yields (**5.3bu** and **5.3bv**). Importantly, unlike in previously reported aminations using **5.1b**,⁸ our approach did not seem to react significantly with the aromatic moieties of the amides, and only small amounts of aminated chlorobenzene were observed. Finally, as expected, sulfonamides tolerated the reaction conditions well furnishing the desired product **5.3bw** in 56% yield.



Scheme 5.4. Amination of Boc-protected amines.^{a,b}

a. Reaction conditions: **5.1** (0.2 mmol), **5.4** (1.0 mmol), LiOtBu (0.2 mmol), 1.0 mL PhCl, room temperature around reaction flask was 35 °C (heating caused by the LED lamp), overnight. b. Isolated yields.

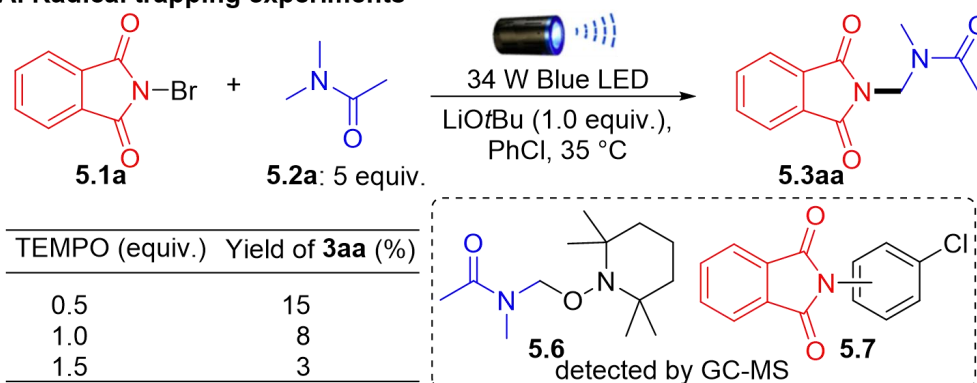
An additional screen important to the synthetic organic chemistry community is the possibility to selectively aminate protected amines in the form of carbamates (Scheme 5.4). Indeed, we hypothesized that carbamates and amides would react similarly under our reaction conditions, but would provide a facile deprotection strategy. Much to our delight, *tert*-butoxycarbonyl (Boc) protected amines tolerated our mild reaction conditions and provided the desired products in moderate to good yields (Scheme 5.4). Boc-protected dimethylamine and *N*-ethyl- *N*-methyl amine provided the desired products **5.5ba** and **5.5bb** in excellent and good yields, respectively, when using *N*-halosaccharin. Boc-protected *N*-methylaniline also generated the desired product **5.5bc**, albeit in lower yields. Of particular interest is the ability to selectively aminate Boc-protected methamphetamine derivatives in low to moderate yields, to give rise to potentially new bioactive compounds such as **5.5bd** and **5.5be**. As expected, the use of unsymmetrical amides favors the formation of the aminated product in the methyl position, even in presence of a more stable benzylic carbon (**5.5bb**, **5.5bd**, and **5.5be**). This further emphasizes the possible role of steric hindrance as the driving force for the regioselectivity of the reaction.

Finally, *N*-halophthalimide can also be used to aminate boc-protected amines in lower yields, as shown for product **5.5aa** (Scheme 5.4).

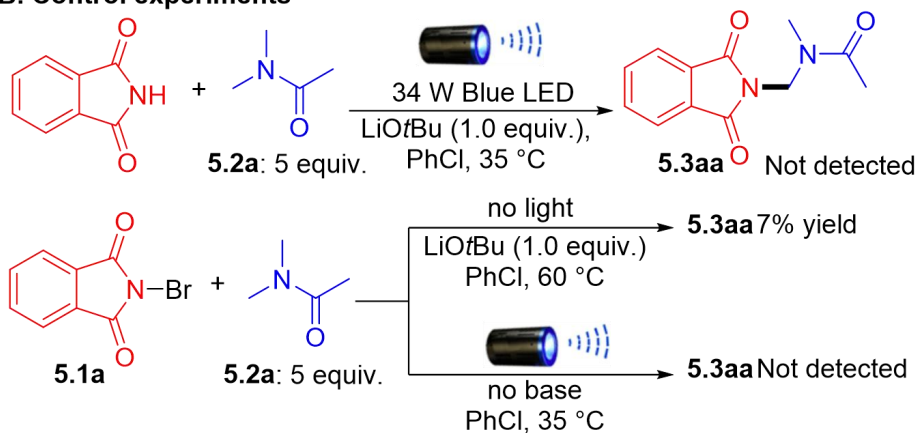
The reaction was further probed with other imide and amide derivatives, however the yields obtained were often low. The *N*-haloimide reagents require the presence of an aromatic moiety to avoid decomposition of the imidyl radical. Additionally, we presume that the aromatic moiety interacts with the solvent (chlorobenzene) via π -stacking, which stabilizes the reactive intermediate.

To provide some insights into the reaction mechanism, a series of control experiments were carried out as shown in Scheme 5.5. As expected, addition of a radical scavenger such as TEMPO (2,2,6,6-tetramethyl-1-piperidinyloxy) drastically hampered the reaction. Importantly, through this experiment, we observed the generation of compound **5.6** in GC-MS, which indicates the formation of the amide radical at the amino carbon (Scheme 5.5-A). Additionally, throughout our reactions, we can also observe the amination of solvent in the form of compound **5.7** through GC-MS, similar to previously published transformations,⁶ indicating the formation of the imidyl radical. We presume that homolytic cleavage of the *N*-haloimide prior to activation by LiOtBu is in part responsible for this side reactivity,⁸ which is observed as the primary product in the absence of LiOtBu. Also as previously mentioned in the table of optimization, in the absence of LiOtBu or light no product is generated, and replacing *N*-haloimides with the non-halogenated imide (such as phthalimide) does not generate any observable product (Scheme 5.5-B).

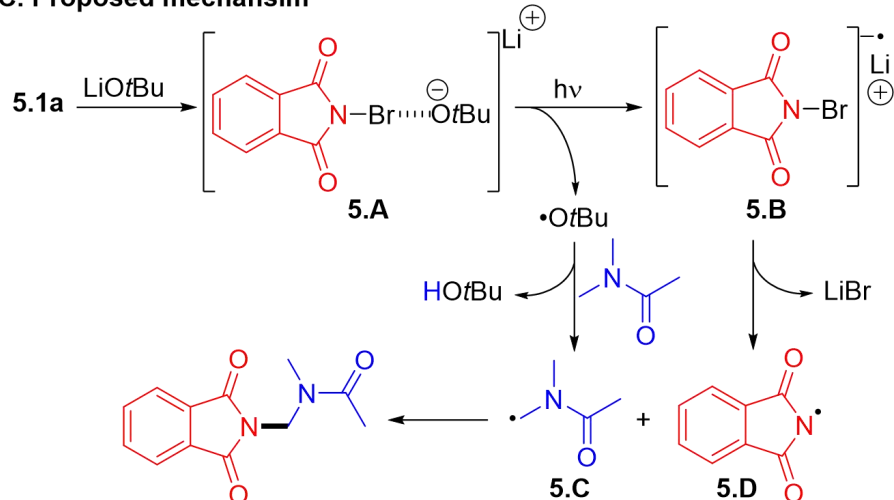
A. Radical trapping experiments



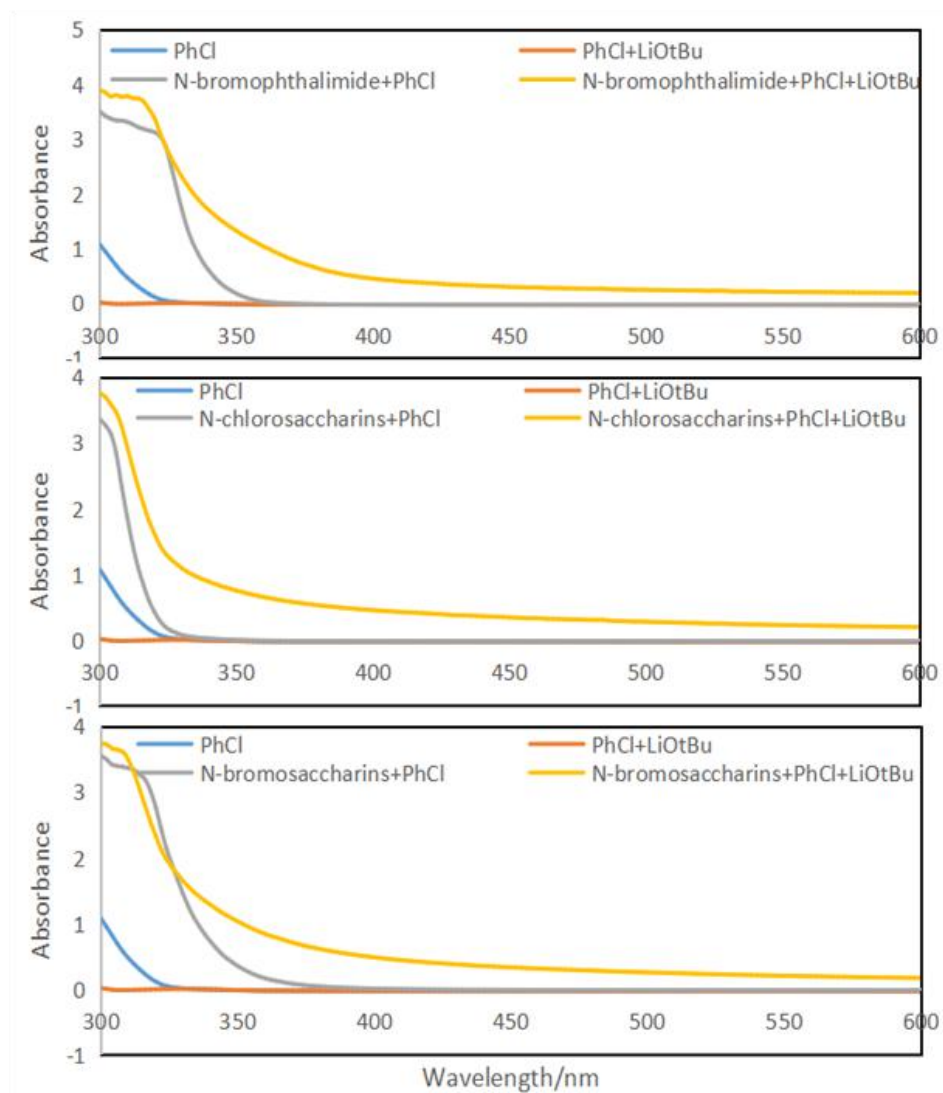
B. Control experiments



C. Proposed mechanism



Scheme 5.5. A. radical trapping experiments. B. Control experiments. C. Proposed mechanism.



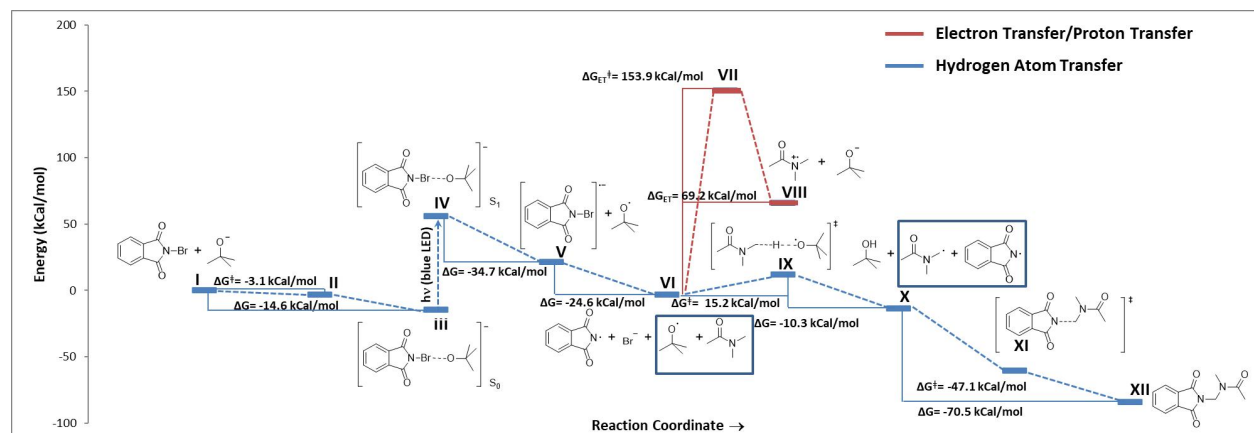
Scheme 5.6. UV-vis spectroscopic measurements.

UV-vis spectroscopic measurements on various combination of **5.1a**, **5.1b** and lithium *tert*-butoxide in PhCl. Spectra taken with 0.04mmol of substrate in 2mL of PhCl; concentration 0.02mmol/mL.

To further understand the role played by LiOtBu, we performed a series of UV-vis spectroscopic measurements on various combinations of **5.1a**, **5.1b** and lithium *tert*-butoxide in PhCl (Scheme 5.6). The combination of *N*-haloimides, LiOtBu and PhCl (yellow line) showed an increased in absorption throughout all waves lengths, but also shows that this combination can absorb blue light (380–500 nm) while the other combinations of reagents (blue, red, and grey lines) do not show significant light absorbing property in the blue light wavelength in this test. This indicates that LiOtBu is interacting with the *N*-haloimide, possibly via halogen bonding,⁷

and generates a halogen-bonded adduct capable of absorbing blue light to initiate the radical reaction.

To further understand the process in which the reaction takes place, the energetic profile of the mechanism was explored through quantum calculations (Scheme 5.7). The formation of an electron-donor-acceptor (EDA) complex presents an exergonic energy profile (-14.6 kCal/mol), denoting that its formation is favored (**I**→**III**). The decomposition of the EDA complex to yield the radical anion is an endergonic process (36.1 kCal/mol) through conventional synthetic processes. However, through electronic excitation of the EDA complex (**III**→**IV**) this pathway becomes accessible, yielding *t*-BuO• and the radical anion **5.B** (**IV**→**V**). The latter is not stable and further decomposes to give the imidyl radical **5.D** and Br⁻ (**V**→**VI**). On the other hand, the generation of *N,N*-dimethylacetamide radical (**5.C**) can follow two possible mechanistic pathways, hydrogen atom transfer (HAT) and electron transfer/proton transfer (ET/PT). The first one can be categorized as the synchronized abstraction of a proton and an electron in a one-step reaction, while the second one refers to a sequential process in which first occurs a single electron transfer to give a radical cation as intermediary followed by a posterior proton transfer.⁸ Exploration of both mechanistic pathways reveals that the reaction follows a classic HAT mechanism (**VI**→**X**) since the ET/PT pathway (**VI**→**VIII**) is energetically hindered. Lastly, the radical-radical coupling between **5.D** and **5.C** to yield the desired product (**5.3aa**) displays an exergonic outline (**X**→**XII**).



Scheme 5.7. Energy reaction pathways (kCal/mol) of *N*-bromophthalimide **5.1a** with *tert*-butoxide through computational simulations using B3LYP/6-311+G(d,p)/MWB28 (Br) level of theory.

On the basis of the above obtained results and previous reports,^{3e-h, 9} we propose a plausible reaction mechanism in Scheme 5.5-C. Reaction between the *N*-haloimide and LiOtBu form a halogen bond adduct **5.A** that can absorb visible blue light and leads to a single-electron-transfer yielding radical anion **5.B** and *tert*-butoxide radical. Regioselective hydrogen abstraction of the amino carbon of the amide by the tBuO• radical generates stable radical intermediate **5.C**. Simultaneously, radical anion **5.B** decomposes through N–Br bond cleavage to generate phthalimidyl radical **5.D**. Fast radical-radical coupling between **5.C** and **5.D** generate the final product (Scheme 5.5-C). Side reactions between **5.D** and the solvent generate the aminated byproduct **5.7** and trapping of intermediate **5.C** was shown using TEMPO to give **5.6**.

5.3 Summary

In summary, the amination of amides was developed via a photochemical sp³ C–H bond functionalization process. This reaction showed good functional group compatibility. As mentioned earlier, current methods suffer from external radical initiators, oxidants, heat source and relative limited substrate scope in many cases. Therefore, this reported process provides a complementary and advantageous approach to access amine-containing organic molecules.

5.4 Acknowledgements

This publication was made possible, in part, with support from the Indiana Clinical and Translational Sciences Institute funded, in part by Grant Number UL1TR002529 from the National Institutes of Health, National Center for Advancing Translational Sciences, Clinical and Translational Sciences Award. The content is solely the responsibility of the authors and does not necessarily represent the official views of the National Institutes of Health. Start-up funding from Indiana University–Purdue University Indianapolis (IUPUI) was also used to support this research. National Institute of Dental & Craniofacial Research grant number 1R21DE029156-01.

5.5 Experimental

General Information: All the solvents and commercially available reagents were purchased from commercial sources (Acros Organics, TCI, Alfa Aesar, Sigma-Aldrich,

Oakwood) and used directly. Thin layer chromatography (TLC) was performed on EMD precoated plates (silica gel 60 F254, Art 5715) and visualized by fluorescence quenching under UV light or stains for TLC Plates. Column chromatography was performed on EMD Silica Gel 60 (200–300 Mesh) using a forced flow of 0.5–1.0 bar. The ^1H and ^{13}C NMR spectra were obtained on a Bruker AVANCE III-400 spectrometer. ^1H NMR data was reported as: chemical shift (δ ppm), multiplicity, coupling constant (Hz), and integration. ^{13}C NMR data was reported in terms of chemical shift (δ ppm), multiplicity, and coupling constant (Hz). High Resolution Mass Spectrometry (HRMS) analysis was obtained using Agilent Technologies 6520 Accurate-Mass Q-TOF LC/MS system. UV-Vis was obtained using GENESYS™ 10S UV-Vis Spectrophotometer and fisherbrand macro quartz cuvettes (cat. No. 14-958-112). Melting point was obtained using MPA160 Melting Point Apparatus. A Kessil broadband Blue LED lamp 34W (No. BL-20,391) was used for this light-promoted reaction. The vial was placed approximately 4 cm away from the Blue LED, with the LED shining directly at the side of the vial. 10 mL microwave reaction vial secured by 20mm aluminum seals with 0.125-inch thick, blue PTFE / white silicone septa was used for the reaction.

General procedure for the preparation of amides 5.2:

Procedure A: To a stirred solution of amine (6 mmol) in dichloromethane (18 mL) were added triethylamine (6.6 mmol) and acyl chloride (1.0 mmol) dropwisely under 0 °C. Then the mixture was stirred at r.t. overnight. Then the reaction mixture was poured into a separatory funnel and washed with saturated NaHCO_3 (aq) and extracted with 3*40 mL CH_2Cl_2 . The combined organic phases were dried over anhydrous Na_2SO_4 , concentrated under reduced pressure and purified by column chromatography to afford products **5.2**.

Procedure B: To a solution of carboxylic acid (6 mmol, 1.0 equiv) and DMF (4 drops) in CH_2Cl_2 (18 mL) at 0 °C was added $(\text{COCl})_2$ (2 equiv) dropwise. After completion of addition, the solution was stirred for 5 minutes at 0 °C and then stirred at rt for 1 h. The solution was concentrated in vacuo to obtain the crude acyl chloride, which will be used without purification. To a mixture of amine (6 mmol) (1.0 equiv) and triethylamine (2.0 equiv) in CH_2Cl_2 (18 mL) at 0 °C was added the solution of crude acyl chloride in CH_2Cl_2 dropwise. After stirred for 5 minutes at 0 °C, the mixture was allowed to warm to room temperature and stirred overnight. The reaction was quenched with a saturated NaHCO_3 solution and extracted with CH_2Cl_2 . The

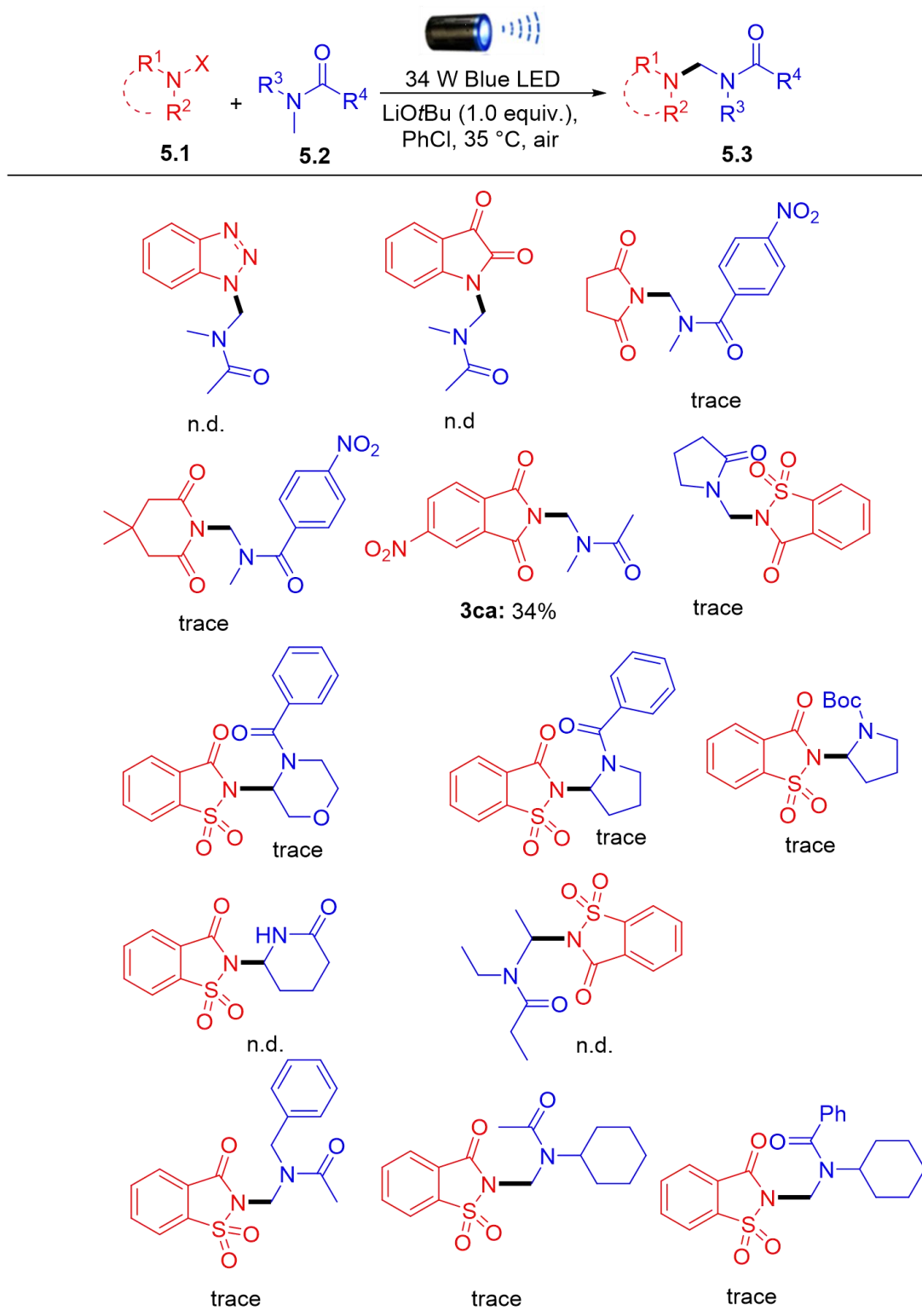
combined organic layers were washed with brine, dried over anhydrous Na₂SO₄ and concentrated in vacuo. The residue was purified by column to give compounds **5.2**.

General Procedure for the Preparation of *N*-Boc amines **5.4:**

According to literature, the *N*-Boc amines can be synthesized by the condensation of corresponding amines with di-*tert*-butyl dicarbonate. The corresponding amines (1.0 equiv.) and 4-dimethylaminopyridine (10 mol %) were mixed in a flask with a magnetic stirring bar. DCM was added as solvent. Then a solution of di-*tert*-butyl dicarbonate (1.1 equiv.) in DCM was added slowly under ice bath conditions. The mixture was stirred 10 min at 0 °C and then 24 h at rt. The solution was washed with water and brine, then dried over MgSO₄ and concentrated. The crude product was purified by flash column chromatography, and corresponding *N*-Boc amines **5.4** were obtained.

Synthesis of *N*-haloimides: To a mixture of imides (8 mmol), KBrO₃ (4 mmol) and sulphuric acid (97%, 0.33 mL, 7.58 g, 6 mmol) in aqueous acetic acid (70%, 5.6 mL), KBr (0.637g 5.4 mmol) was added portionwise at room temperature. The reaction mixture was stirred at room temperature overnight, the precipitate was filtered off, washed with water and dried to afford the crude product. The crude product was crystallized from acetic acid/water to get pure product which was thoroughly vacuum-dried at room temperature.

General Procedure for the Synthesis of C(sp³)-H Amination of Amides Product: A 10 mL microwave vial was charged with *N*-halo saccharins or *N*-halo phthalimides **5.1** or other nitrogen sources (0.2 mmol), LiOtBu (16 mg, 0.2 mmol), 1.0 ml PhCl. Then amides **5.2** or **5.4** (1 mmol) was added into the tube and capped with 20 mm microwave crimp caps with septa. The reaction mixture was stirred vigorously at room temperature for 3 mins and then put the vial approximately 4 cm away from the Blue LED lamp and then stirred overnight. After the completion of reaction, the product was determined by thin layer chromatography (TLC). The solvent was removed under vacuo, then the residue was purified by flash chromatography on silica gel to yield the desired product **5.3** or **5.5**.



Scheme 5.8. Additional substrate scope

a Reaction conditions: **5.1** (0.2 mmol), **5.2** (1.0 mmol), LiOtBu (0.2 mmol), 1.0 mL PhCl, 35 °C (Heating caused by the LED lamp.), overnight. b Isolated yields. n.d means no detected in TLC and NMR

1 mmol scale detailed method included for one-step transformations: A 10 mL microwave vial was charged with *N*-chlorosaccharin **5.1b** (218 mg, 1 mmol), LiOtBu (80 mg, 1 mmol), 3.0 mL PhCl. Then *N,N*-dimethylacetamide **5.2a** (435 mg, 5 mmol) was added into the tube and capped with 20 mm microwave crimp caps with septa. The reaction mixture was stirred vigorously at room temperature for 3 mins and then put the vial approximately 4 cm away from the Blue LED lamp and stirred 24h. After the completion of reaction, the product was determined by thin layer chromatography (TLC). The solvent was removed under vacuo, then the residue was purified by flash chromatography (ethyl acetate/dichloromethane=1/10 to 1/5) on silica gel to yield the desired product **5.3ba** (164 mg, 61 %).

Analytical Data of Compounds:

***N*-((1,3-dioxoisindolin-2-yl)methyl)-*N*-methylacetamide (5.3aa)** (mixture of rotamers) Conditions: *N*-bromophthalimide (45 mg, 0.2 mmol), LiOtBu (16 mg, 0.2 mmol), 1.0 mL PhCl, *N,N*-dimethylacetamide (87 mg, 1 mmol), overnight. The product was isolated by flash chromatography (ethyl acetate/hexane= 1/1 to 3/1) as a white solid (30.2 mg, 65%). ¹H NMR (400 MHz, CDCl₃) δ 7.87 – 7.57 (m, 4H), 5.19 (d, *J* = 36.1 Hz, 2H), 2.95 (d, *J* = 64.3 Hz, 3H), 2.18 (d, *J* = 147.2 Hz, 3H). ¹³C NMR (101 MHz, CDCl₃) δ 171.1 (s), 171.0(s), 167.8 (s), 167.6(s), 134.6 (s), 134.2 (s), 131.8 (s), 131.5 (s), 123.7 (s), 123.5 (s), 52.7 (s), 49.4 (s), 35.8 (s), 32.5 (s), 21.8 (s), 21.4 (s).

***N*-((1,3-dioxoisindolin-2-yl)methyl)-*N*-methylpropionamide (5.3ab)** (mixture of rotamers) Conditions: *N*-bromophthalimide (45 mg, 0.2 mmol), LiOtBu (16 mg, 0.2 mmol), 1.0 mL PhCl, *N,N*-dimethylpropionamide (101 mg, 1 mmol), overnight. The product was isolated by flash chromatography (ethyl acetate/hexane= 1/1 to 3/1) as a colorless oil (32.5 mg, 66%). ¹H NMR (400 MHz, CDCl₃) δ 7.91 – 7.81 (m, 2H), 7.80 – 7.67 (m, 2H), 5.27 (d, *J* = 34.7 Hz, 2H), 3.03 (d, *J* = 56.3 Hz, 3H), 2.55 (dq, *J* = 197.5, 7.3 Hz, 2H), 1.15 (dt, *J* = 28.9, 7.4 Hz, 3H). ¹³C NMR (101 MHz, CDCl₃) δ 174.4 (s), 174.2 (s), 167.9 (s), 167.7(s), 134.6 (s), 134.2 (s), 131.9 (s), 131.6 (s), 123.8 (s), 123.6 (s), 51.8 (s), 50.1 (s), 35.2 (s), 32.8 (s), 26.8 (s), 26.0 (s), 9.4 (s), 8.8 (s).

***N*-((1,3-dioxoisindolin-2-yl)methyl)propionamide (5.3ac)** (mixture of rotamers) Conditions: *N*-bromophthalimide (45 mg, 0.2 mmol), LiOtBu (16 mg, 0.2 mmol), 1.0 mL PhCl, *N*-methylpropionamide (87 mg, 1 mmol), overnight. The product was isolated by flash chromatography (ethyl acetate/hexane= 1/1 to 3/1) as a white solid (20.9 mg, 45%). ¹H NMR

(400 MHz, CDCl₃) δ 7.82 (dd, J = 5.4, 3.1 Hz, 2H), 7.70 (dd, J = 5.4, 3.1 Hz, 2H), 6.54 (s, 1H), 5.18 (d, J = 6.5 Hz, 2H), 2.20 (q, J = 7.6 Hz, 2H), 1.11 (t, J = 7.6 Hz, 3H). ¹³C NMR (101 MHz, CDCl₃) δ 173.4 (s), 167.5 (s), 134.3 (s), 131.9 (s), 123.6 (s), 42.5 (s), 29.3 (s), 9.3 (s).

2-(1-methyl-5-oxopyrrolidin-2-yl)isoindoline-1,3-dione (5.3ad) (mixture of rotamers) Conditions: *N*-bromophthalimide (45 mg, 0.2 mmol), LiOtBu (16 mg, 0.2 mmol), 1.0 mL PhCl, 1-methylpyrrolidin-2-one (99 mg, 1 mmol), overnight. The product was isolated by flash chromatography (ethyl acetate/hexane= 1/1 to 3/1) as a white solid (25.9 mg, 53%). ¹H NMR (400 MHz, CDCl₃) δ 7.89 – 7.67 (m, 4H), 5.78 (dd, J = 8.9, 1.5 Hz, 1H), 3.04 – 2.90 (m, 1H), 2.70 (s, 3H), 2.59 – 2.37 (m, 2H), 2.27 (ddd, J = 13.1, 7.7, 2.1 Hz, 1H). ¹³C NMR (101 MHz, CDCl₃) δ 175.3 (s), 167.4 (s), 134.6 (s), 131.5 (s), 123.7 (s), 65.7 (s), 29.6 (s), 27.1 (s), 23.2 (s).

***N*-((1,3-dioxoisoindolin-2-yl)methyl)-*N*-phenylacetamide (5.3ae)** (mixture of rotamers) Conditions: *N*-bromophthalimide (45 mg, 0.2 mmol), LiOtBu (16 mg, 0.2 mmol), 1.0 mL PhCl, *N*-methyl-*N*-phenylacetamide (149 mg, 1 mmol), overnight. The product was isolated by flash chromatography (ethyl acetate/hexane= 1/1 to 3/1) as a white solid (27.7 mg, 47%). m.p: 143-146 °C. ¹H NMR (400 MHz, CDCl₃) δ 7.77 (m, 2H), 7.73 – 7.64 (m, 2H), 7.37 – 7.28 (m, 3H), 7.15 (d, J = 6.6 Hz, 2H), 5.66 (s, 2H), 1.83 (d, J = 6.5 Hz, 3H). ¹³C NMR (101 MHz, CDCl₃) δ 170.5 (s), 167.1 (s), 140.4 (s), 134.2 (s), 131.6 (s), 129.8 (s), 128.6 (2C), 123.6 (s), 49.7 (s), 22.8 (s). HRMS (ESI) m/z : [M+H]⁺ calcd for C₁₇H₁₅N₂O₃ 295.1077 ; found 295.1077.

***N*-((1,3-dioxoisoindolin-2-yl)methyl)-*N*-methylisobutyramide (5.3af)** (mixture of rotamers) Conditions: *N*-bromophthalimide (45 mg, 0.2 mmol), LiOtBu (16 mg, 0.2 mmol), 1.0 mL PhCl, *N,N*-dimethylisobutyramide (115 mg, 1 mmol), overnight. The product was isolated by flash chromatography (ethyl acetate/hexane= 1/1 to 3/1) as a pale yellow solid (25.0 mg, 48%). ¹H NMR (400 MHz, CDCl₃) δ 7.90 – 7.65 (m, 4H), 5.27 (d, J = 14.6 Hz, 2H), 3.54 – 2.61 (dt, J = 13.1, 6.5 Hz, 1H), 3.04 (d, J = 79.8 Hz, 3H), 1.12 (dd, J = 33.6, 6.6 Hz, 6H). ¹³C NMR (101 MHz, CDCl₃) δ 178.0 (s), 177.4 (s), 167.9(s),167.6 (s), 134.6 (s), 134.2 (s), 131.9 (s), 131.6 (s), 123.8 (s), 123.6 (s), 51.7 (s), 50.47 (s), 35.2 (s), 33.1 (s), 30.7 (s), 29.9 (s), 19.9 (s), 19.0 (s). HRMS (ESI) m/z : [M+Na]⁺ calcd for C₁₄H₁₆N₂NaO₃ 283.1053; found 283.1041.

***N*-((1,1-dioxido-3-oxobenzo[d]isothiazol-2(3H)-yl)methyl)-*N*-methylacetamide (5.3ba)** (mixture of rotamers) Conditions: *N*-chlorosaccharin (44 mg, 0.2 mmol) or *N*-bromosaccharin(52 mg,0.2 mmol), LiOtBu (16mg, 0.2 mmol), 1.0 mL PhCl, *N,N*-dimethylacetamide (87 mg, 1 mmol), overnight. The product was isolated by flash chromatography (ethyl

acetate/dichloromethane=1/10 to 1/3) as a colorless oil (33.8 mg, 63% (X=Cl), 27.4 mg, 51%(X=Br)). ¹H NMR (400 MHz, CDCl₃) δ 8.07 – 7.99 (m, 1H), 7.96 – 7.76 (m, 3H), 5.40 (d, *J* = 51.6 Hz, 2H), 3.03 (d, *J* = 38.3 Hz, 3H), 2.23 (d, *J* = 108.9 Hz, 3H). ¹³C NMR (101 MHz, CDCl₃) δ 170.8 (s), 169.9 (s), 158.3 (s), 158.1 (s), 136.9 (s), 136.4 (s), 134.6 (s), 134.3 (s), 133.8 (s), 133.4 (s), 125.6 (s), 124.6 (s), 124.4 (s), 120.3 (s), 120.1 (s), 53.7 (s), 49.2 (s), 34.1 (s), 31.7 (s), 20.7 (s), 20.5 (s). HRMS (ESI) *m/z*: [M+K]⁺ calcd for C₁₁H₁₂KN₂O₄S 307.0149; found 307.0142.

***N*-((1,1-dioxido-3-oxobenzo[d]isothiazol-2(3H)-yl)methyl)-*N*-methylpropionamide (5.3bb)** (mixture of rotamers) Conditions: *N*-chlorosaccharin (44 mg, 0.2 mmol) or *N*-bromosaccharin(52 mg, 0.2 mmol), LiOtBu (16mg, 0.2 mmol), 1.0 mL PhCl, *N,N*-dimethylpropionamide (101 mg, 1 mmol), overnight. The product was isolated by flash chromatography (ethyl acetate/dichloromethane=1/10 to 1/3) as a pale yellow oil (40.66 mg, 72%(X=Cl), 28.8 mg, 51%(X=Br)). ¹H NMR (400 MHz, CDCl₃) δ 8.09 – 8.02 (m, 1H), 7.97 – 7.79 (m, 3H), 5.43 (d, *J* = 52.7 Hz, 2H), 3.06 (d, *J* = 29.9 Hz, 3H), 2.52 (dq, *J* = 136.3, 7.3 Hz, 2H), 1.23 – 1.04 (m, 3H). ¹³C NMR (101 MHz, CDCl₃) δ 173.8 (s), 173.1 (s), 158.2 (s), 158.1 (s), 136.9 (s), 136.5 (s), 134.5 (s), 134.2 (s), 133.8 (s), 133.4 (s), 125.7 (s), 124.6 (s), 124.4 (s), 120.2 (s), 120.0 (s), 52.8 (s), 49.7 (s), 33.4 (s), 32.0 (s), 25.65 (s), 25.2 (s), 8.4 (s), 7.8 (s). HRMS (ESI) *m/z*: [M+H]⁺ calcd for C₁₂H₁₅N₂O₄S 283.0747; found 283.0752.

2-((2-oxopyrrolidin-1-yl)methyl)benzo[d]isothiazol-3(2H)-one 1,1-dioxide (5.3bd') (mixture of rotamers) Conditions: *N*-chlorosaccharin (44 mg, 0.2 mmol) or *N*-bromosaccharin(52 mg, 0.2 mmol), LiOtBu (16mg, 0.2 mmol), 1.0 mL PhCl, 1-methylpyrrolidin-2-one (99 mg, 1 mmol), overnight. The product was isolated by flash chromatography (ethyl acetate/dichloromethane=1/10 to 1/3) as a yellow oil (5.0 mg, 9%(X=Cl), 5.6 mg, 10%(X=Br)). ¹H NMR (400 MHz, CDCl₃) δ 8.07 (d, *J* = 7.3 Hz, 1H), 7.96 – 7.81 (m, 3H), 5.36 (s, 2H), 3.50 (t, *J* = 7.0 Hz, 2H), 2.40 (t, *J* = 8.1 Hz, 2H), 2.09 – 1.97 (m, 2H). ¹³C NMR (101 MHz, CDCl₃) δ 175.8 (s), 158.2 (s), 137.8 (s), 135.4 (s), 134.5 (s), 126.7 (s), 125.5 (s), 121.2 (s), 46.0 (s), 45.9 (s), 30.4 (s), 17.9 (s). HRMS (ESI) *m/z*: [M+H]⁺ calcd for C₁₂H₁₃N₂O₄S 281.0591; found 281.0597.

***N*-((1,1-dioxido-3-oxobenzo[d]isothiazol-2(3H)-yl)methyl)-*N*-phenylacetamide (5.3be)** (mixture of rotamers) Conditions: *N*-chlorosaccharin (44 mg, 0.2 mmol) or *N*-bromosaccharin(52 mg, 0.2 mmol), LiOtBu (16mg, 0.2 mmol), 1.0 mL PhCl, *N*-methyl-*N*-phenylacetamide (149 mg,

1 mmol), overnight. The product was isolated by flash chromatography (ethyl acetate/dichloromethane=1/10 to 1/3) as a white solid (42.3 mg, 64%(X=Cl), 27.8 mg, 42%(X=Br)). m.p: 182-185 °C. ¹H NMR (400 MHz, CDCl₃) δ 7.91 – 7.68 (m, 4H), 7.36 – 7.16 (m, 5H), 5.76 (s, 2H), 1.83 (s, 3H). ¹³C NMR (101 MHz, CDCl₃) δ 171.1 (s), 158.4 (s), 140.5 (s), 138.0 (s), 135.2 (s), 134.3 (s), 129.9 (s), 128.8 (s), 128.5 (s), 126.4 (s), 125.5 (s), 121.1 (s), 50.3 (s), 22.5 (s). HRMS (ESI) m/z: [M+H]⁺ calcd for C₁₆H₁₅N₂O₄S 331.0747; found 331.0747.

***N*-((1,1-dioxido-3-oxobenzo[d]isothiazol-2(3H)-yl)methyl)-*N*-methylisobutyramide (5.3bf)** (mixture of rotamers) Conditions: *N*-chlorosaccharin (44 mg, 0.2 mmol) or *N*-bromosaccharin(52 mg, 0.2 mmol), LiOtBu (16mg, 0.2 mmol), 1.0 mL PhCl, *N,N*-dimethylisobutyramide (115 mg, 1 mmol), overnight. The product was isolated by flash chromatography (ethyl acetate/dichloromethane=1/10 to 1/3) as a pale yellow oil (40.9 mg, 69%(X=Cl), 31.4 mg, 53%(X=Br)). ¹H NMR (400 MHz, CDCl₃) δ 8.12 – 8.03 (m, 1H), 7.99 – 7.75 (m, 3H), 5.47 (d, *J* = 41.4 Hz, 2H), 3.30-2.80 (dt, *J* = 13.4, 6.7 Hz, 1H), 3.10 (d, *J* = 52.1 Hz, 3H), 1.18 (dd, *J* = 22.9, 6.5 Hz, 6H). ¹³C NMR (101 MHz, CDCl₃) δ 177.97 (s), 159.24 (s), 138.00 (s), 135.50 (s), 135.18 (s), 134.72 (s), 134.31 (s), 126.74 (s), 125.66 (s), 125.44 (s), 121.20 (s), 121.02 (s), 53.70 (s), 50.94 (s), 34.37 (s), 33.18 (s), 30.51 (s), 29.69 (s), 19.76 (s), 18.84 (s). HRMS (ESI) m/z: [M+H]⁺ calcd for C₁₃H₁₇N₂O₄S 297.0904; found 297.0889.

***N*-((1,1-dioxido-3-oxobenzo[d]isothiazol-2(3H)-yl)methyl)-*N*-methylbutyramide (5.3bg)** (mixture of rotamers) Conditions: *N*-chlorosaccharin (44 mg, 0.2 mmol) or *N*-bromosaccharin(52 mg, 0.2 mmol), LiOtBu (16mg, 0.2 mmol), 1.0 mL PhCl, *N,N*-dimethylbutyramide (1 mmol), overnight. The product was isolated by flash chromatography (ethyl acetate/dichloromethane=1/10 to 1/3) as a pale yellow solid (37.3 mg, 63%(X=Cl), 36.1 mg, 61%(X=Br)). ¹H NMR (400 MHz, CDCl₃) δ 8.11 – 8.03 (m, 1H), 7.97 – 7.79 (m, 3H), 5.45 (d, *J* = 51.7 Hz, 2H), 3.20 – 2.95 (m, 3H), 2.48 (dt, *J* = 134.7, 7.4 Hz, 2H), 1.70 (dp, *J* = 14.8, 7.5 Hz, 2H), 0.97 (dt, *J* = 14.9, 7.4 Hz, 3H). ¹³C NMR (101 MHz, CDCl₃) δ 173.0 (s), 172.3 (s), 158.3 (s), 158.1 (s), 137.0 (s), 136.5 (s), 134.5 (s), 134.2 (s), 133.7 (s), 133.3 (s), 130.5 (s), 128.2 (s), 125.7 (s), 124.6 (s), 124.4 (s), 120.2 (s), 120.0 (s), 34.2 (s), 33.7 (s), 33.5 (s), 31.9 (s), 17.6 (s), 17.0 (s), 12.9 (s), 128.8 (s). HRMS (ESI) m/z: [M+H]⁺ calcd for C₁₃H₁₇N₂O₄S 297.0904; found 297.0889.

***N*-((1,1-dioxido-3-oxobenzo[d]isothiazol-2(3H)-yl)methyl)-*N*,2,2-triphenylacetamide (5.3bh)** (mixture of rotamers) Conditions: *N*-chlorosaccharin (44 mg, 0.2 mmol) or *N*-

bromosaccharin(52 mg, 0.2 mmol), LiOtBu (16mg, 0.2 mmol), 1.0 mL PhCl, *N*-methyl-*N*,2,2-triphenylacetamide (301 mg, 1 mmol), overnight. The product was isolated by flash chromatography (ethyl acetate/dichloromethane=1/10 to 1/3) as a white solid (47.2 mg, 49%(X=Cl), 31.8 mg, 33%(X=Br)). m.p: 156-159 °C. ¹H NMR (400 MHz, CDCl₃) δ 7.85 – 7.62 (m, 4H), 7.32 – 7.20 (m, 3H), 7.19 – 7.01 (m, 12H), 5.77 (s, 2H), 4.83 (s, 1H). ¹³C NMR (101 MHz, CDCl₃) δ 172.4 (s), 158.5 (s), 139.7 (s), 139.1 (s), 138.0 (s), 135.2 (s), 134.3 (s), 129.8 (s), 129.1 (s), 129.0 (s), 129.0 (s), 128.4 (s), 127.0 (s), 126.4 (s), 125.5 (s), 121.1 (s), 54.7 (s), 50.9 (s). HRMS (ESI) m/z: [M+H]⁺ calcd for C₂₈H₂₃N₂O₄S 483.1373; found 483.1373.

***N*-((1,1-dioxido-3-oxobenzo[d]isothiazol-2(3H)-yl)methyl)-*N*-ethylacetamide (5.3bi)** (mixture of rotamers) Conditions: *N*-chlorosaccharin (44 mg, 0.2 mmol) or *N*-bromosaccharin(52 mg, 0.2 mmol), LiOtBu (16mg, 0.2 mmol), 1.0 mL PhCl, *N*-ethyl-*N*-methylacetamide (101 mg, 1 mmol), overnight. The product was isolated by flash chromatography (ethyl acetate/dichloromethane=1/10 to 1/3) as a pale yellow oil (25.4 mg, 45%(X=Cl), 20.9 mg, 37%(X=Br)). ¹H NMR (400 MHz, CDCl₃) δ 8.11 – 8.02 (m, 1H), 7.88 (m, 3H), 5.42 (d, *J* = 60.3 Hz, 2H), 3.50 (dq, *J* = 21.4, 7.1 Hz, 2H), 2.27 (d, *J* = 93.8 Hz, 3H), 1.20 (dt, *J* = 38.8, 7.1 Hz, 3H). ¹³C NMR (101 MHz, CDCl₃) δ 171.3 (s), 170.3 (s), 159.5 (s), 159.2 (s), 138.1 (s), 137.6 (s), 135.5 (s), 135.3 (s), 134.8 (s), 134.3 (s), 126.6 (s), 126.6 (s), 125.6 (s), 125.4 (s), 121.3 (s), 125.1 (s), 52.6 (s), 48.0 (s), 42.2 (s), 39.7 (s), 21.9 (s), 21.2 (s), 14.00 (s), 12.6 (s). HRMS (ESI) m/z: [M+H]⁺ calcd for C₁₂H₁₅N₂O₄S 283.0747; found 283.0752.

2-chloro-*N*-((1,1-dioxido-3-oxobenzo[d]isothiazol-2(3H)-yl)methyl)-*N*-methylacetamide (5.3bj) (mixture of rotamers) Conditions: *N*-chlorosaccharin (44 mg, 0.2 mmol) or *N*-bromosaccharin(52 mg, 0.2 mmol), LiOtBu (16mg, 0.2 mmol), 1.0 mL PhCl, 2-chloro-*N,N*-dimethylacetamide (122 mg, 1 mmol), overnight. The product was isolated by flash chromatography (ethyl acetate/dichloromethane=1/10 to 1/3) as a pale yellow solid (24.8 mg, 41%(X=Cl), 26.0 mg, 43%(X=Br)). ¹H NMR (400 MHz, CDCl₃) δ 8.13 – 8.06 (m, 1H), 8.02 – 7.81 (m, 3H), 5.47 (d, *J* = 38.8 Hz, 2H), 4.31 (d, *J* = 153.9 Hz, 2H), 3.15 (d, *J* = 49.2 Hz, 3H). ¹³C NMR (101 MHz, CDCl₃) δ 167.4 (s), 159.2 (s), 137.9 (s), 137.4 (s), 135.7 (s), 135.4 (s), 134.9 (s), 134.5 (s), 126.6 (s), 125.8 (s), 125.6 (s), 121.4 (s), 121.2 (s), 54.03.95 (s), 50.8 (s), 41.0 (s), 40.9 (s), 34.7 (s), 33.6 (s). HRMS (ESI) m/z: [M+K]⁺ calcd for C₁₁H₁₁ClKN₂O₄S 340.9760; found 340.9764.

***N*-((1,1-dioxido-3-oxobenzo[d]isothiazol-2(3H)-yl)methyl)-*N*-phenylbenzamide (5.3bk)** (mixture of rotamers) Conditions: *N*-chlorosaccharin (44 mg, 0.2 mmol) or *N*-bromosaccharin (52 mg, 0.2 mmol), LiOtBu (16mg, 0.2 mmol), 1.0 mL PhCl, *N*-methyl-*N*-phenylbenzamide (211mg, 1 mmol), overnight. The product was isolated by flash chromatography (ethyl acetate/dichloromethane=1/10 to 1/3) as a pale yellow solid (33.0 mg, 42%(X=Cl), 10.2 mg, 13%(X=Br)). m.p: 205-208 °C. ¹H NMR (400 MHz, CDCl₃) δ 7.94 (d, *J* = 7.8 Hz, 2H), 7.86 (t, *J* = 7.6 Hz, 1H), 7.78 (t, *J* = 7.5 Hz, 1H), 7.38 (d, *J* = 7.3 Hz, 2H), 7.19 (m, 8H), 6.04 (s, 2H). ¹³C NMR (101 MHz, CDCl₃) δ 171.0 (s), 158.5 (s), 141.0 (s), 138.0 (s), 135.2 (s), 134.8 (s), 134.2 (s), 130.1 (s), 129.3 (s), 128.9 (s), 128.3 (s), 127.7 (s), 127.6 (s), 126.4 (s), 125.5 (s), 121.0 (s), 52.0 (s). HRMS (ESI) *m/z*: [M+Na]⁺ calcd for C₂₁H₁₆N₂NaO₄S 415.0723; found 415.0726.

***N*-((1,1-dioxido-3-oxobenzo[d]isothiazol-2(3H)-yl)methyl)-*N*-methylbenzamide (5.3bl)** (mixture of rotamers) Conditions: *N*-chlorosaccharin (44 mg, 0.2 mmol) or *N*-bromosaccharin (52 mg, 0.2 mmol), LiOtBu (16mg, 0.2 mmol), 1.0 mL PhCl, *N,N*-dimethylbenzamide (149 mg, 1 mmol), overnight. The product was isolated by flash chromatography (ethyl acetate/dichloromethane=1/10 to 1/3) as a pale yellow oil (41.6 mg, 63%(X=Cl), 33.7 mg, 51%(X=Br)). ¹H NMR (400 MHz, CDCl₃) δ 8.05 (d, *J* = 7.0 Hz, 1H), 7.96 – 7.78 (m, 3H), 7.45 (d, *J* = 30.7 Hz, 5H), 5.55 (d, *J* = 101.1 Hz, 2H), 3.06 (s, 3H). ¹³C NMR (101 MHz, CDCl₃) δ 172.3 (s), 159.1 (s), 137.8 (s), 135.5 (s), 135.1 (s), 134.6 (s), 130.2 (s), 128.5 (s), 127.3 (s), 126.6 (s), 125.5 (s), 121.1 (s), 50.6 (s), 36.5 (s). HRMS (ESI) *m/z*: [M+H]⁺ calcd for C₁₆H₁₅N₂O₄S 331.0747; found 331.0747.

4-cyano-*N*-((1,1-dioxido-3-oxobenzo[d]isothiazol-2(3H)-yl)methyl)-*N*-methylbenzamide (5.3bm) (mixture of rotamers) Conditions: *N*-chlorosaccharin (44 mg, 0.2 mmol) or *N*-bromosaccharin (52 mg, 0.2 mmol), LiOtBu (16mg, 0.2 mmol), 1.0 mL PhCl, 4-cyano-*N,N*-dimethylbenzamide (174 mg, 1 mmol), overnight. The product was isolated by flash chromatography (ethyl acetate/dichloromethane=1/10 to 1/3) as a white solid (39.1 mg, 55%(X=Cl), 45.5 mg, 64%(X=Br)). m.p: 179-181 °C. ¹H NMR (400 MHz, CDCl₃) δ 8.22 – 7.39 (m, 8H), 5.44 (d, *J* = 157.9 Hz, 2H), 3.01 (d, *J* = 45.2 Hz, 3H). ¹³C NMR (101 MHz, CDCl₃) δ 170.3 (s), 159.0 (s), 139.4 (s), 137.8 (s), 135.5 (s), 134.7 (s), 132.4 (s), 127.8 (s), 126.5 (s), 125.7 (s), 121.2 (s), 118.1 (s), 114.0 (s), 50.2 (s), 36.3 (s). HRMS (ESI) *m/z*: [M+H]⁺ calcd for C₁₇H₁₄N₃O₄S 356.0700; found 356.0699.

***N*-((1,1-dioxido-3-oxobenzo[d]isothiazol-2(3H)-yl)methyl)-*N*-methyl-4-nitrobenzamide (5.3bn)** (mixture of rotamers) Conditions: *N*-chlorosaccharin (44 mg, 0.2 mmol) or *N*-bromosaccharin(52 mg, 0.2 mmol), LiOtBu (16mg, 0.2 mmol), 1.0 mL PhCl, *N,N*-dimethyl-4-nitrobenzamide (194 mg, 1 mmol), overnight. The product was isolated by flash chromatography (ethyl acetate/dichloromethane=1/10 to 1/3) as a white solid (54.1 mg, 72%(X=Cl), 47.3 mg, 63%(X=Br)). m.p: 127-129 °C. ¹H NMR (400 MHz, CDCl₃) δ 8.38 – 7.54 (m, 8H), 5.50 (d, *J* = 156.1 Hz, 2H), 3.07 (d, *J* = 49.9 Hz, 3H). ¹³C NMR (101 MHz, CDCl₃) δ 170.0 (s), 159.0 (s), 148.7 (s), 141.2 (s), 137.8 (s), 135.6 (s), 134.7 (s), 128.9 (s), 128.1 (s), 126.5 (s), 125.7 (s), 123.9 (s), 121.2 (s), 54.6 (s), 50.1 (s), 36.3 (s), 32.2 (s). HRMS (ESI) *m/z*: [M+H]⁺ calcd for C₁₆H₁₄N₃O₆S 376.0598; found 376.0585.

***N*-((1,1-dioxido-3-oxobenzo[d]isothiazol-2(3H)-yl)methyl)-*N*-methyl-4-(trifluoromethyl)benzamide (5.3bo)** (mixture of rotamers) Conditions: *N*-chlorosaccharin (44 mg, 0.2 mmol) or *N*-bromosaccharin(52 mg, 0.2 mmol), LiOtBu (16mg, 0.2 mmol), 1.0 mL PhCl, *N,N*-dimethyl-4-(trifluoromethyl)benzamide (217 mg, 1 mmol), overnight. The product was isolated by flash chromatography (ethyl acetate/dichloromethane=1/10 to 1/3) as a white solid (59.8 mg, 75%(X=Cl), 64.6 mg, 81%(X=Br)). ¹H NMR (400 MHz, CDCl₃) δ 8.07 (s, 1H), 7.99 – 7.81 (m, 3H), 7.64 (d, *J* = 27.8 Hz, 4H), 5.52 (d, *J* = 146.0 Hz, 2H), 3.02 (s, 3H). ¹³C NMR (101 MHz, CDCl₃) δ 170.84 (s), 159.03 (s), 138.66 (s), 137.75 (s), 135.50 (s), 134.61 (s), 132.00 (q, *J* = 32.7 Hz), 127.87 – 127.34 (m), 126.52 (s), 125.61 (s), 125.56 (s), 123.71 (q, *J* = 271 Hz), 121.15 (s), 54.76 (s), 50.22 (s), 36.32 (s), 31.89 (s). ¹⁹F NMR (377 MHz, CDCl₃) δ -62.91 (s). HRMS (ESI) *m/z*: [M+H]⁺ calcd for C₁₇H₁₄F₃N₂O₄S 399.0621; found 399.0609.

4-bromo-*N*-((1,1-dioxido-3-oxobenzo[d]isothiazol-2(3H)-yl)methyl)-*N*-methylbenzamide (5.3bp) (mixture of rotamers) Conditions: *N*-chlorosaccharin (44 mg, 0.2 mmol) or *N*-bromosaccharin(52 mg, 0.2 mmol), LiOtBu (16mg, 0.2 mmol), 1.0 mL PhCl, 4-bromo-*N,N*-dimethylbenzamide (228 mg, 1 mmol), overnight. The product was isolated by flash chromatography (ethyl acetate/dichloromethane=1/10 to 1/3) as a white solid (59.8 mg, 73%(X=Cl), 41.7 mg, 51%(X=Br)). ¹H NMR (400 MHz, CDCl₃) δ 8.07 (d, *J* = 7.2 Hz, 1H), 7.99 – 7.79 (m, 3H), 7.56 (d, *J* = 6.8 Hz, 2H), 7.39 (s, 2H), 5.66 (s, 2H), 3.06 (s, 3H). ¹³C NMR (101 MHz, CDCl₃) δ 171.3 (s), 159.0 (s), 137.8 (s), 135.4 (s), 134.6 (s), 133.9 (s), 131.7 (s), 129.1 (s), 126.6 (s), 125.6 (s), 124.6 (s), 121.1 (s), 50.4 (s), 36.5 (s). HRMS (ESI) *m/z*: [M+H]⁺ calcd for C₁₆H₁₄BrN₂O₄S 408.9852; found 408.9857.

3,5-dichloro-*N*-((1,1-dioxido-3-oxobenzo[d]isothiazol-2(3H)-yl)methyl)-*N*-methylbenzamide (5.3bq) (mixture of rotamers) Conditions: *N*-chlorosaccharin (44 mg, 0.2 mmol) or *N*-bromosaccharin(52 mg, 0.2 mmol), LiOtBu (16mg, 0.2 mmol), 1.0 mL PhCl, 3,5-dichloro-*N,N*-dimethylbenzamide (218 mg, 1 mmol), overnight. The product was isolated by flash chromatography (ethyl acetate/dichloromethane=1/10 to 1/3) as a white solid (62.3 mg, 78%(X=Cl), 39.9 mg, 50%(X=Br)). ¹H NMR (400 MHz, CDCl₃) δ 8.09 (d, *J* = 7.0 Hz, 1H), 8.00 – 7.83 (m, 3H), 7.39 (d, *J* = 26.1 Hz, 3H), 5.51 (d, *J* = 126.2 Hz, 2H), 3.05 (s, 3H). ¹³C NMR (101 MHz, CDCl₃) δ 169.3 (s), 159.0 (s), 137.8 (s), 135.5 (s), 135.4 (s), 134.6 (s), 130.2 (s), 126.5 (s), 125.7 (s), 121.2 (s), 54.7 (s), 50.1 (s), 36.3 (s), 31.6 (s). HRMS (ESI) *m/z*: [M+H]⁺ calcd for C₁₆H₁₃Cl₂N₂O₄S 398.9968; found 398.9979.

***N*-((1,1-dioxido-3-oxobenzo[d]isothiazol-2(3H)-yl)methyl)-2,3,4,5,6-pentafluoro-*N*-methylbenzamide (5.3br)** (mixture of rotamers) Conditions: *N*-chlorosaccharin (44 mg, 0.2 mmol) or *N*-bromosaccharin(52 mg, 0.2 mmol), LiOtBu (16mg, 0.2 mmol), 1.0 mL PhCl, 2,3,4,5,6-pentafluoro-*N,N*-dimethylbenzamide (239 mg, 1 mmol), overnight. The product was isolated by flash chromatography (ethyl acetate/dichloromethane=1/10 to 1/3) as a white solid (44.6 mg, 53%(X=Cl), 59.7 mg, 71%(X=Br)). m.p: 129-132 °C. ¹H NMR (400 MHz, CDCl₃) δ 8.08 (dd, *J* = 21.1, 7.5 Hz, 1H), 8.00 – 7.83 (m, 3H), 5.44 (d, *J* = 160.6 Hz, 2H), 3.16 (d, *J* = 80.2 Hz, 3H). ¹³C NMR (101 MHz, CDCl₃) δ 159.4 (d, *J* = 75 Hz), 159.2 (s), 159.0 (s), 144.8 (ddd, *J* = 12.8, 8.0, 3.9 Hz), 144.3 (ddd, *J* = 12.1, 8.2, 4.1 Hz), 142.5 – 142.1 (m), 141.8 (qd, *J* = 8.4, 3.9 Hz), 139.2 – 138.7 (m), 137.9 (s), 137.4 (s), 136.8 – 136.2 (m), 135.7 (s), 135.5(s), 134.9 (s), 134.6 (s), 126.5 (s), 126.3 (s), 125.8 (s), 125.6 (s), 121.3 (s), 121.3 (s), 110.3 (dd, *J* = 42.0, 20.2 Hz), 54.2 (s), 49.4 (s), 34.9 (s), 33.0 (s). ¹⁹F NMR (377 MHz, CDCl₃) δ -139.01 (tdd, *J* = 8.7, 5.8, 2.8 Hz), -139.94 (ddd, *J* = 11.6, 7.4, 3.4 Hz), -150.56 – -150.72 (m), -150.98 (tt, *J* = 20.6, 2.1 Hz), -159.62 (tt, *J* = 20.6, 5.8 Hz), -159.82 (ddd, *J* = 20.7, 16.1, 5.9 Hz). HRMS (ESI) *m/z*: [M+H]⁺ calcd for C₁₆H₁₀F₅N₂O₄S 421.0276; found 421.0282.

***N*-((1,1-dioxido-3-oxobenzo[d]isothiazol-2(3H)-yl)methyl)-4-methoxy-*N*-methylbenzamide (5.3bs)** (mixture of rotamers) Conditions: *N*-chlorosaccharin (44 mg, 0.2 mmol) or *N*-bromosaccharin(52 mg, 0.2 mmol), LiOtBu (16mg, 0.2 mmol), 1.0 mL PhCl, 4-methoxy-*N,N*-dimethylbenzamide (179 mg, 1 mmol), overnight. The product was isolated by flash chromatography (ethyl acetate/dichloromethane=1/10 to 1/3) as a white solid (31.7 mg, 44%(X=Cl), 25.9 mg, 36%(X=Br)). m.p: 223-227 °C. ¹H NMR (400 MHz, CDCl₃) δ 8.07 (d, *J*

= 7.4 Hz, 1H), 7.97 – 7.80 (m, 3H), 7.50 (d, J = 8.6 Hz, 2H), 6.92 (d, J = 8.5 Hz, 2H), 5.60 (s, 2H), 3.83 (s, 3H), 3.10 (s, 3H). ^{13}C NMR (101 MHz, CDCl_3) δ 172.2 (s), 161.2 (s), 159.1 (s), 137.9 (s), 135.3 (s), 134.5 (s), 129.6 (s), 127.2 (s), 126.7 (s), 125.5 (s), 121.1 (s), 113.7 (s), 55.4 (s), 53.4 (s), 31.6 (s). HRMS (ESI) m/z : $[\text{M}+\text{Na}]^+$ calcd for $\text{C}_{17}\text{H}_{16}\text{N}_2\text{NaO}_5\text{S}$ 383.0672; found, 383.0669.

***N*-((1,1-dioxido-3-oxobenzo[d]isothiazol-2(3H)-yl)methyl)-*N*,2,4-trimethylbenzamide (5.3bt)** (mixture of rotamers) Conditions: *N*-chlorosaccharin (44 mg, 0.2 mmol) or *N*-bromosaccharin (52 mg, 0.2 mmol), LiOtBu (16mg, 0.2 mmol), 1.0 mL PhCl , *N,N*,2,4-tetramethylbenzamide (177 mg, 1 mmol), overnight. The product was isolated by flash chromatography (ethyl acetate/dichloromethane=1/10 to 1/3) as a pale yellow solid (22.9 mg, 32%(X=Cl), 20.0 mg, 28%(X=Br)). ^1H NMR (400 MHz, CDCl_3) δ 8.06 (dd, J = 18.5, 7.3 Hz, 1H), 7.98 – 7.80 (m, 3H), 7.35 – 6.93 (m, 3H), 5.71 (s, 2H), 3.03 (d, J = 98.2 Hz, 3H), 2.42 – 2.24 (m, 6H). ^{13}C NMR (101 MHz, CDCl_3) δ 172.4 (s), 172.0 (s), 159.3 (s), 158.9 (s), 139.6 (s), 139.1 (s), 138.0 (s), 137.(s), 135.5 (s), 134.4 (s), 134.6 (s), 134.6 (s), 134.5 (s), 132.4 (s), 131.8 (s), 131.9 (s), 131.5 (s), 131.2 (s), 127.3 (s), 126.7 (s), 126.4 (s), 126.0 (s), 125.5 (s), 121.1 (s), 54.5 (s), 49.7 (s), 35.4 (s), 31.1 (s), 21.2 (s), 19.1 (s), 18.8 (s). HRMS (ESI) m/z : $[\text{M}+\text{K}]^+$ calcd for $\text{C}_{18}\text{H}_{18}\text{N}_2\text{KO}_4\text{S}$ 397.0619; found, 397.0609.

***N*-((1,1-dioxido-3-oxobenzo[d]isothiazol-2(3H)-yl)methyl)-*N*-methylisonicotinamide (5.3bu)** (mixture of rotamers) Conditions: *N*-chlorosaccharin (44 mg, 0.2 mmol) or *N*-bromosaccharin (52 mg, 0.2 mmol), LiOtBu (16mg, 0.2 mmol), 1.0 mL PhCl , *N,N*-dimethylisonicotinamide (150 mg, 1 mmol), overnight. The product was isolated by flash chromatography (ethyl acetate/dichloromethane=1/10 to 1/3) as a pale yellow oil (23.2 mg, 35%(X=Cl), 34.5 mg, 52%(X=Br)). ^1H NMR (400 MHz, CDCl_3) δ 8.73 (d, J = 18.7 Hz, 2H), 8.10 (s, 1H), 8.01 – 7.82 (m, 3H), 7.41 (d, J = 42.4 Hz, 2H), 5.50 (d, J = 156.8 Hz, 2H), 3.08 (d, J = 55.7 Hz, 3H). ^{13}C NMR (101 MHz, CDCl_3) δ 169.7 (s), 159.0 (s), 150.3 (s), 142.7 (s), 137.8 (s), 135.5 (s), 134.6 (s), 126.6 (s), 125.7 (s), 121.8 (s), 121.7 (s), 121.0 (s), 54.6 (s), 49.9 (s), 36.1 (s), 31.8 (s). HRMS (ESI) m/z : $[\text{M}+\text{Na}]^+$ calcd for $\text{C}_{15}\text{H}_{14}\text{N}_3\text{NaO}_4\text{S}$ 354.0519; found, 354.0515.

***N*-((1,1-dioxido-3-oxobenzo[d]isothiazol-2(3H)-yl)methyl)-*N*-methylthiophene-2-carboxamide (5.3bv)** (mixture of rotamers) Conditions: *N*-chlorosaccharin (44 mg, 0.2 mmol) or *N*-bromosaccharin (52 mg, 0.2 mmol), LiOtBu (16mg, 0.2 mmol), 1.0 mL PhCl , *N,N*-dimethylthiophene-2-carboxamide (155 mg, 1 mmol), overnight. The product was isolated by

flash chromatography (ethyl acetate/dichloromethane=1/10 to 1/3) as a white solid (21.5 mg, 32%(X=Cl), 36.3 mg, 54%(X=Br)). m.p: 124-127 °C. ¹H NMR (400 MHz, CDCl₃) δ 8.09 (d, *J* = 7.3 Hz, 1H), 7.97 – 7.80 (m, 3H), 7.50 (dd, *J* = 6.5, 4.4 Hz, 2H), 7.07 (dd, *J* = 4.8, 3.9 Hz, 1H), 5.67 (s, 2H), 3.31 (s, 3H). ¹³C NMR (101 MHz, CDCl₃) δ 165.2 (s), 159.2 (s), 137.9 (s), 136.5 (s), 135.4 (s), 134.5 (s), 130.4 (s), 130.0 (s), 126.9 (s), 126.6 (s), 125.6 (s), 121.1 (s), 52.7 (s), 35.9 (s). HRMS (ESI) *m/z*: [M+H]⁺ calcd for C₁₄H₁₃N₂O₄S₂ 337.0311; found 337.0319.

***N*-((1,1-dioxido-3-oxobenzo[d]isothiazol-2(3H)-yl)methyl)-*N*-methylethanesulfonamide (5.3bw)** (mixture of rotamers) Conditions: *N*-chlorosaccharin (44 mg, 0.2 mmol) or *N*-bromosaccharin(52 mg, 0.2 mmol), LiOtBu (16mg, 0.2 mmol), 1.0 mL PhCl, *N,N*-dimethylethanesulfonamide (137 mg, 1 mmol), overnight. The product was isolated by flash chromatography (ethyl acetate/dichloromethane=1/10 to 1/3) as a white solid (34.4 mg, 54%(X=Cl),35.7 mg, 56%(X=Br)). m.p: 144-147 °C. ¹H NMR (400 MHz, CDCl₃) δ 8.07 (d, *J* = 7.5 Hz, 1H), 8.00 – 7.79 (m, 3H), 5.32 (s, 2H), 3.16 (q, *J* = 7.4 Hz, 2H), 3.07 (s, 3H), 1.34 (t, *J* = 7.4 Hz, 3H). ¹³C NMR (101 MHz, CDCl₃) δ 159.6 (s), 137.6 (s), 135.7 (s), 134.8 (s), 126.5 (s), 125.7 (s), 121.3 (s), 53.8 (s), 46.9 (s), 34.8 (s), 7.9 (s). HRMS (ESI) *m/z*: [M+Na]⁺ calcd for C₁₁H₁₄N₂NaO₅S₂ 341.0236; found 341.0240.

***tert*-butyl ((1,1-dioxido-3-oxobenzo[d]isothiazol-2(3H)-yl)methyl)(methyl)carbamate (5.5ba)** (mixture of rotamers) Conditions: *N*-chlorosaccharin (44 mg, 0.2 mmol) or *N*-bromosaccharin(52 mg, 0.2 mmol), LiOtBu (16mg, 0.2 mmol), 1.0 mL PhCl, *tert*-butyl dimethylcarbamate (145 mg, 1 mmol), overnight. The product was isolated by flash chromatography (ethyl acetate/dichloromethane=1/10 to 1/3) as a pale yellow oil (52.2 mg, 80%(X=Cl), 55.5 mg, 85%(X=Br)). ¹H NMR (400 MHz, CDCl₃) δ 7.99 (d, *J* = 7.4 Hz, 1H), 7.81 (m, 3H), 5.32 (d, *J* = 18.4 Hz, 2H), 2.90 (s, 3H), 1.45 (d, *J* = 25.2 Hz, 9H). ¹³C NMR (101 MHz, CDCl₃) δ 159.3 (s), 154.4 (s), 138.1 (s), 135.3 (s), 134.3 (s), 126.7 (s), 125.4 (s), 121.0 (s), 81.6 (s), 81.0 (s), 53.0 (s), 52.8 (s), 33.7 (s), 33.3 (s), 28.1 (s). HRMS (ESI) *m/z*: [M+Na]⁺ calcd for C₁₄H₁₈N₂NaO₅S 349.0829; found 349.0840.

***tert*-butyl ((1,1-dioxido-3-oxobenzo[d]isothiazol-2(3H)-yl)methyl)(ethyl)carbamate (5.5bb)** (mixture of rotamers) Conditions: *N*-chlorosaccharin (44 mg, 0.2 mmol) or *N*-bromosaccharin(52 mg, 0.2 mmol), LiOtBu (16mg, 0.2 mmol), 1.0 mL PhCl, *tert*-butyl ethyl(methyl)carbamate (159 mg, 1 mmol), overnight. The product was isolated by flash chromatography (ethyl acetate/dichloromethane=1/10 to 1/3) as a pale yellow oil (30.6 mg,

45%(X=Cl), 17.7 mg, 26%(X=Br)). ¹H NMR (400 MHz, CDCl₃) δ 8.05 (d, *J* = 7.4 Hz, 1H), 7.94 – 7.78 (m, 3H), 5.37 (s, 2H), 3.41 (d, *J* = 6.7 Hz, 2H), 1.52 (d, *J* = 22.5 Hz, 9H), 1.17 (t, *J* = 7.0 Hz, 3H). ¹³C NMR (101 MHz, CDCl₃) δ 159.4 (s), 153.9 (s), 138.2 (s), 135.2 (s), 134.3 (s), 126.6 (s), 125.4 (s), 120.9 (s), 81.6 (s), 51.1 (s), 41.6 (s), 40.8 (s), 28.2 (s), 13.8 (s), 13.2 (s). HRMS (ESI) *m/z*: [M+Na]⁺ calcd for C₁₅H₂₀N₂NaO₅S 363.0985; found 363.0977.

***tert*-butyl ((1,1-dioxido-3-oxobenzo[d]isothiazol-2(3H)-yl)methyl)(phenyl)carbamate (5.5bc)** (mixture of rotamers) Conditions: *N*-chlorosaccharin (44 mg, 0.2 mmol) or *N*-bromosaccharin(52 mg, 0.2 mmol), LiOtBu (16mg, 0.2 mmol), 1.0 mL PhCl, *tert*-butyl methyl(phenyl)carbamate (207 mg, 1 mmol), overnight. The product was isolated by flash chromatography (ethyl acetate/dichloromethane=1/10 to 1/3) as a pale yellow oil (24.1 mg, 31%(X=Cl), 10.1 mg, 13%(X=Br)). ¹H NMR (400 MHz, CDCl₃) δ 7.95 – 7.74 (m, 4H), 7.37 – 7.23 (m, 5H), 5.76 (d, *J* = 10.1 Hz, 2H), 1.53 (s, 9H). ¹³C NMR (101 MHz, CDCl₃) δ 158.3 (s), 154.0 (s), 139.8 (s), 138.1 (s), 135.1 (s), 134.2 (s), 129.1 (s), 127.9 (s), 127.4 (s), 126.5 (s), 125.5 (s), 120.9 (s), 82.2 (s), 53.2 (s), 28.2 (s). HRMS (ESI) *m/z*: [M+H]⁺ calcd for C₁₉H₂₁N₂O₅S 389.1166; found 389.1167.

***tert*-butyl benzyl((1,1-dioxido-3-oxobenzo[d]isothiazol-2(3H)-yl)methyl)carbamate (5.5bd)** (mixture of rotamers) Conditions: *N*-chlorosaccharin (44 mg, 0.2 mmol) or *N*-bromosaccharin(52 mg, 0.2 mmol), LiOtBu (16mg, 0.2 mmol), 1.0 mL PhCl, *tert*-butyl benzyl(methyl)carbamate (221 mg, 1 mmol), overnight. The product was isolated by flash chromatography (ethyl acetate/dichloromethane=1/10 to 1/3) as a white solid (36.2 mg, 45%(X=Cl), 8.0 mg, 10%(X=Br)). ¹H NMR (400 MHz, CDCl₃) δ 7.97 (d, *J* = 7.4 Hz, 1H), 7.87 – 7.72 (m, 3H), 7.37 – 7.15 (m, 5H), 5.29 (d, *J* = 39.7 Hz, 2H), 4.49 (d, *J* = 9.5 Hz, 2H), 1.48 (d, *J* = 43.8 Hz, 9H). ¹³C NMR (101 MHz, CDCl₃) δ 159.5 (s), 154.5 (s), 138.2 (s), 137.5 (s), 135.2 (s), 134.3 (s), 128.5 (s), 128.4 (s), 127.5 (s), 125.4 (s), 120.9 (s), 82.0 (s), 50.6 (s), 48.6 (s), 28.2 (s). HRMS (ESI) *m/z*: [M+H]⁺ calcd for C₂₀H₂₃N₂O₅S 403.1322; found 403.1322.

***tert*-butyl ((1,1-dioxido-3-oxobenzo[d]isothiazol-2(3H)-yl)methyl)(phenethyl)carbamate (5.5be)** (mixture of rotamers) Conditions: *N*-chlorosaccharin (44 mg, 0.2 mmol) or *N*-bromosaccharin(52 mg, 0.2 mmol), LiOtBu (16mg, 0.2 mmol), 1.0 mL PhCl, *tert*-butyl methyl(phenethyl)carbamate (235 mg, 1 mmol), overnight. The product was isolated by flash chromatography (ethyl acetate/dichloromethane=1/10 to 1/3) as a pale-yellow oil (20.0 mg, 24%(X=Cl), 10.0 mg, 12%(X=Br)). ¹H NMR (400 MHz, CDCl₃) δ 8.06 (d, *J* = 7.3

Hz, 1H), 7.93 – 7.79 (m, 3H), 7.32 – 7.13 (m, 5H), 5.27 (d, J = 29.0 Hz, 2H), 3.58 (dt, J = 14.7, 7.4 Hz, 2H), 2.91 (dd, J = 14.5, 7.2 Hz, 2H), 1.54 (d, J = 30.6 Hz, 9H). ^{13}C NMR (101 MHz, CDCl_3) δ 159.546 (s), 154.0 (s), 138.9 (s), 138.2 (s), 135.2(s), 134.3 (s), 132.0 (s), 130.2 (s), 129.9 (s), 129.1 (s), 128.5 (s), 128.4 (s), 126.6 (s), 126.4 (s), 126.3 (s), 125.4 (s), 81.8 (s), 81.1 (s), 51.8 (s), 51.5 (s), 48.656 (s), 48.2 (s), 35.2 (s), 34.4 (s), 28.2 (s). HRMS (ESI) m/z : $[\text{M}+\text{H}]^+$ calcd for $\text{C}_{21}\text{H}_{25}\text{N}_2\text{O}_5\text{S}$ 417.1479; found 417.1467.

***tert*-butyl ((1,3-dioxoisindolin-2-yl)methyl)(methyl)carbamate (5.5aa) (mixture of rotamers)** Conditions: *N*-bromophthalimide (45 mg, 0.2 mmol), LiOtBu (16mg, 0.2 mmol), 1.0 mL PhCl, *tert*-butyl dimethylcarbamate (145 mg, 1 mmol), overnight. The product was isolated by flash chromatography (ethyl acetate/dichloromethane=1/10 to 1/3) as a white solid (13.4 mg, 23%). ^1H NMR (400 MHz, CDCl_3) δ 7.88 (dd, J = 5.4, 3.1 Hz, 2H), 7.74 (dd, J = 5.4, 3.1 Hz, 2H), 5.22 (s, 2H), 2.96 (s, 3H), 1.51 (s, 9H). ^{13}C NMR (101 MHz, CDCl_3) δ 167.8 (s), 155.0 (s), 134.2 (s), 131.9 (s), 123.6 (s), 80.7 (s), 51.4 (s), 33.9 (s), 28.3 (s). HRMS (ESI) m/z : $[\text{M}+\text{Na}]^+$ calcd for $\text{C}_{15}\text{H}_{18}\text{N}_2\text{NaO}_4$ 313.1159; found 313.1165.

***N*-methyl-*N*-((5-nitro-1,3-dioxoisindolin-2-yl)methyl)acetamide (5.3ca) (mixture of rotamers)** Conditions: 2-bromo-5-nitroisindoline-1,3-dione (54 mg, 0.2 mmol), LiOtBu (16mg, 0.2 mmol), 1.0 mL PhCl, *N,N*-dimethylacetamide (87 mg, 1 mmol), overnight. The product was isolated by flash chromatography (ethyl acetate/dichloromethane=1/10 to 1/3) as a yellow solid (18.9 mg, 34%). m.p.: 175-178 °C. ^1H NMR (400 MHz, CDCl_3) δ 8.74 – 8.54 (m, 2H), 8.08 (dd, J = 17.2, 8.1 Hz, 1H), 5.30 (d, J = 18.7 Hz, 2H), 3.06 (d, J = 82.5 Hz, 3H), 2.26 (d, J = 145.0 Hz, 3H). ^{13}C NMR (101 MHz, CDCl_3) δ 171.3 (s), 171.1 (s), 165.8 (s), 165.5 (s), 165.5 (s), 165.4 (s), 152.1 (s), 151.9 (s), 136.2 (s), 135.9 (s), 133.2 (s), 133.0 (s), 129.8 (s), 129.5 (s), 125.2 (s), 124.9 (s), 119.3 (s), 119.0 (s), 53.3 (s), 50.7 (s), 36.6 (s), 32.8 (s), 21.8 (s), 21.4 (s).

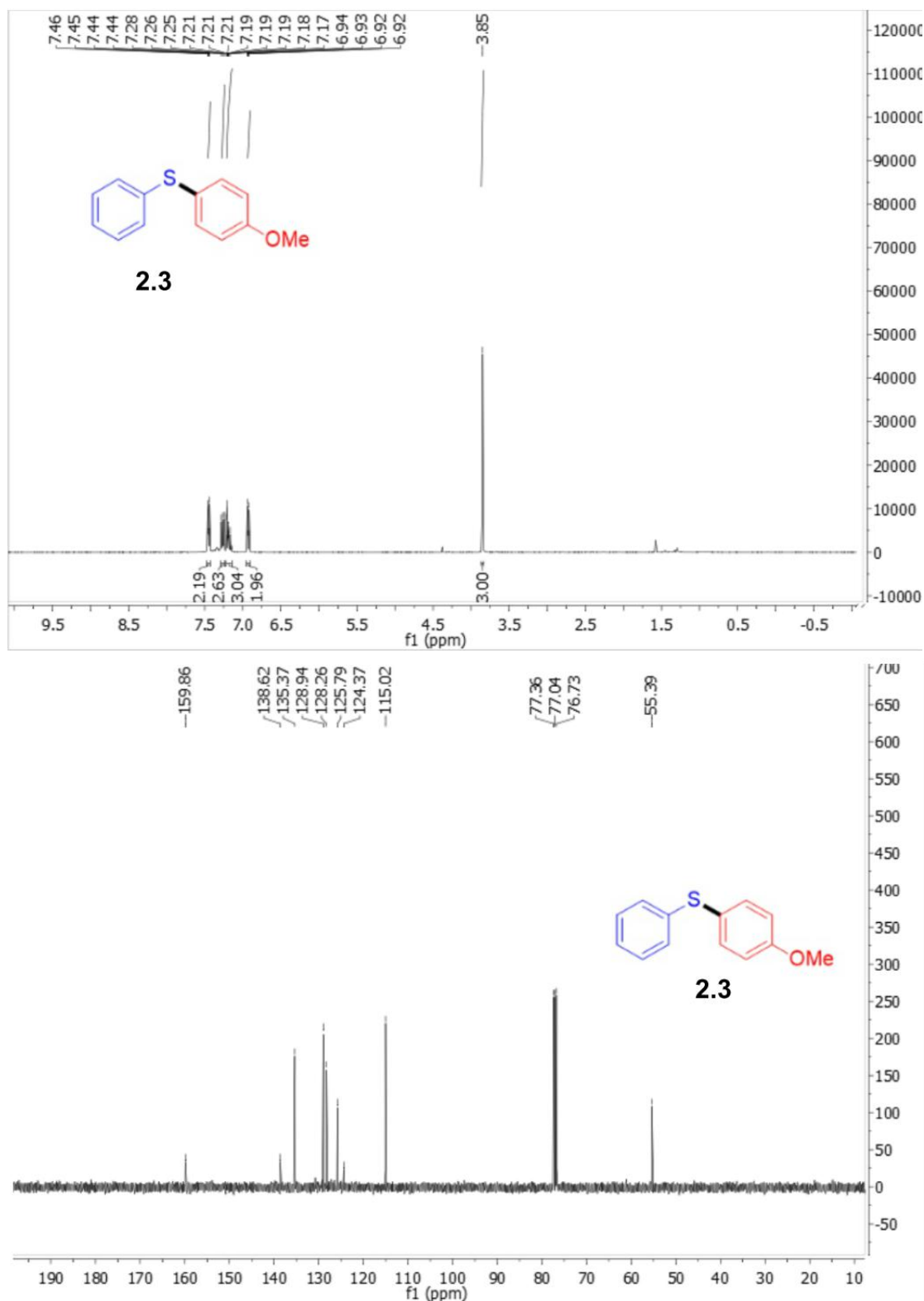
5.6 References

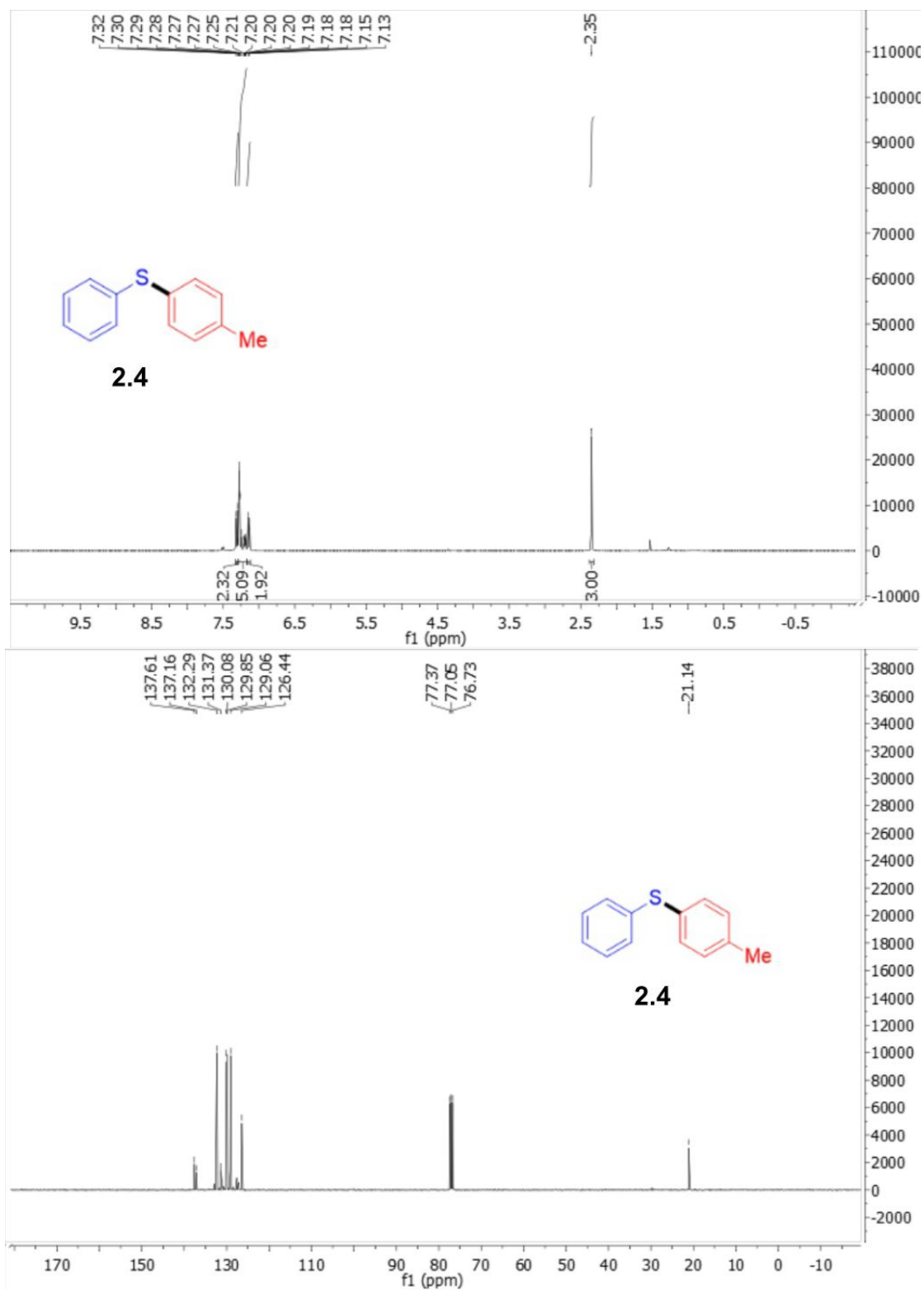
1. (a) Fischer J.; Ganellin C. R. Analogue-based Drug Discovery; WILEY-VCH Verlag GmbH & Co.KGaA: Weinheim, **2006**; p 457. (b) Van Epen, J. H. Experience with Fluspirilene (R 6218), a Long Acting Neuroleptic. *Psychiatr. Neurol. Neurochir.* **1970**, *73*, 277–284. (c) Taylor-Robinson, D.; Furr, P.M. Observations on the Antibiotic Treatment of Experimentally Induced Mycoplasmal Infections in Mice. *J. Antimicrob. Chemother.* **2000**, *45*, 903–907. (d) Pellock, J.M. Treatment of Epilepsy in the New Millennium. *Pharmacotherapy: The Journal of Human Pharmacology and Drug Therapy*, **2000**, *20*, 129S–138S.

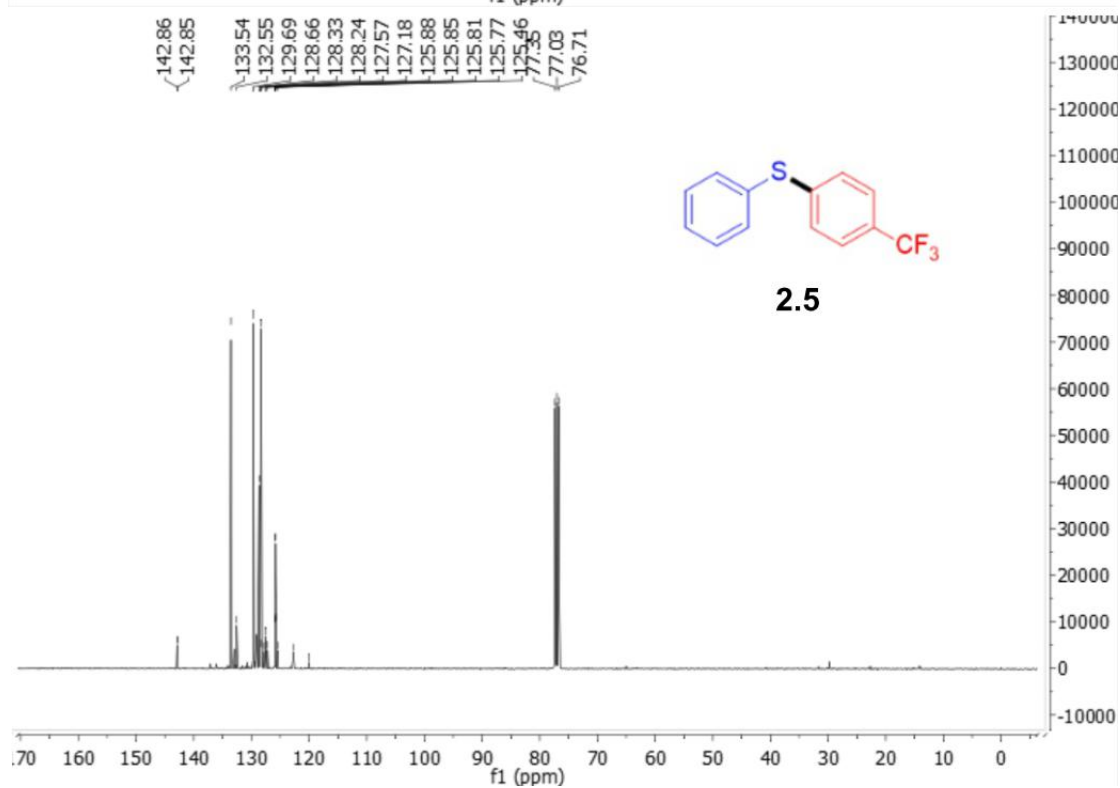
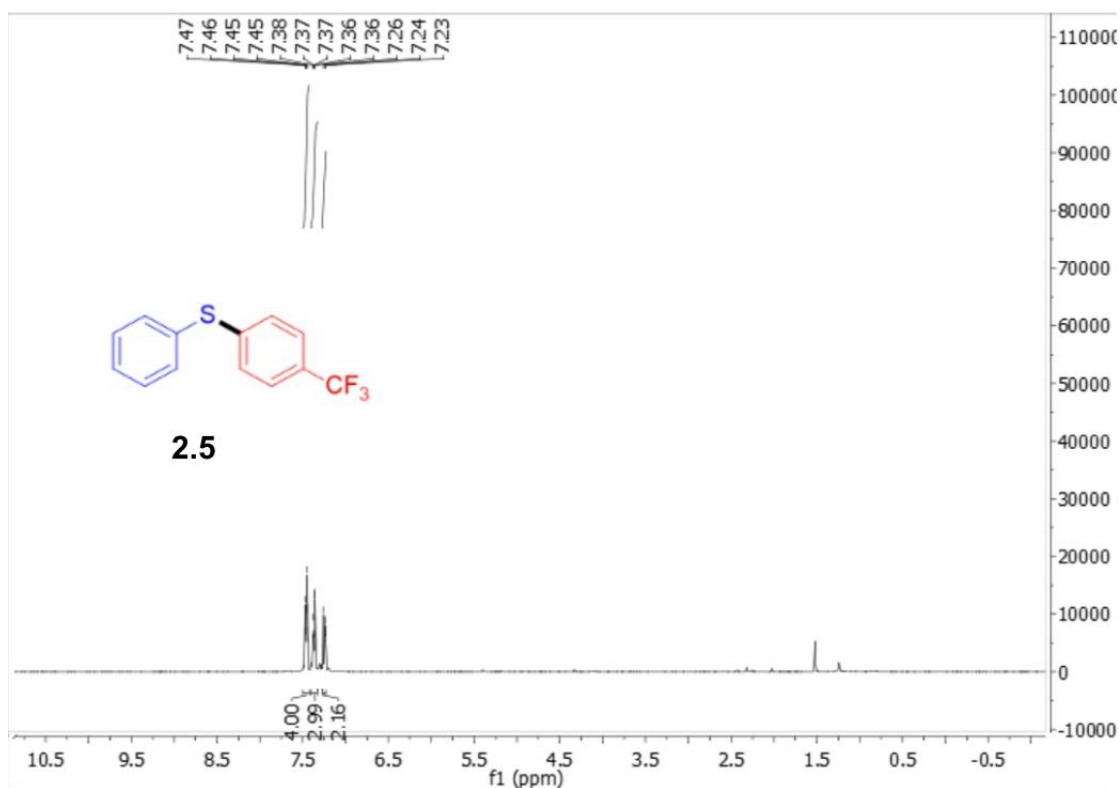
2. (a) Anisimova, N. A.; Belavin, I. Y.; Orlova, N. A.; Sergeev, V. N.; Shipov, A. G.; Baukov, Y. I. Silyl Variation of *N*-Amidoalkylation. *Zhurnal Obshchei Khimii*, **1983**, *53*, 1198–1199. (b) Hellmann, H.; Lösehm, I.; Lingens, F. Über *N*-Mannich-Basen, II. Mitteil.: Synthesen mit Dialkylamino-methyl-phthalimiden und deren quartären Salzen. *Chemische Berichte*, **1954**, *87*, 1690–1699.
3. (a) Only known examples of C–H amination to generate amido amins: (a) Sun, M.; Zhang, T.; Bao, W. FeCl₃ Catalyzed sp³ C–H Amination: Synthesis of Amins with Arylamines and Amides. *Tetrahedron Lett.* **2014**, *55*, 893–896. (b) Xia, Q.; Chen, W. Iron-Catalyzed *N*-Alkylation of Azoles via Cleavage of an sp³ C–H Bond Adjacent to a Nitrogen Atom. *J. Org. Chem.* **2012**, *77*, 9366–9373. (c) Saidulu, G.; Kumar, R. A.; Reddy, K. R. Iron-Catalyzed C–N Bond Formation via Oxidative Csp³–H Bond Functionalization Adjacent to Nitrogen in Amides and Anilines: Synthesis of *N*-Alkyl and *N*-Benzyl Azoles. *Tetrahedron Lett.* **2015**, *56*, 4200–4203. (d) Deng, X.; Lei, X.; Nie, G.; Jia, L.; Li, Y.; Chen, Y. Copper Catalyzed Cross-Dehydrogenative N²-Coupling of NH-1,2,3-Triazoles with *N,N*-Dialkylamides: *N*-Amidoalkylation of NH-1,2,3-Triazoles. *J. Org. Chem.* **2017**, *82*, 6163–6171. (e) Xu, S.; Luo, Z.; Jiang, Z.; Lin, D. Transition-Metal-Free *N*-Amidoalkylation of Purines with *N,N*-Dialkylamides. *Synlett* **2017**, *28*, 868–872. (f) Aruri, H.; Singh, U.; Kumar, M.; Sharma, S.; Aithagani, S. K.; Gupta, V. K.; Mignani, S.; Vishwakarma, R. A.; Singh, P. P. Metal-free Cross-Dehydrogenative Coupling of HN-Azoles with α -C(sp³)-H Amides via C–H Activation and Its Mechanistic and Application Studies. *J. Org. Chem.* **2017**, *82*, 1000–1012. (g) Zhu, Z.; Wang, Y.; Yang, M.; Huang, L.; Gong, J.; Guo, S.; Cai, H. A Metal-Free Cross-Dehydrogenative Coupling Reaction of Amides to Access *N*-Alkylazoles. *Synlett* **2016**, *27*, 2705–2708. (h) Lao, Z.-Q.; Zhong, W.-H.; Lou, Q.-H.; Li, Z.-J.; Meng, X.-B. KI-Catalyzed Imidation of sp³ C–H Bond Adjacent to Amide Nitrogen Atom. *Org. Biomol. Chem.* **2012**, *10*, 7869–7871. (i) Wan, Z.; Wang, D.; Yang, Z.; Zhang, H.; Wang, S.; Lei, A. Electrochemical Oxidative C(sp³)-H Azolation of Lactams Under Mild Conditions. *Green Chem.* **2020**, *22*, 3742–3747.
4. For selected reviews on photochemistry: (a) Ghosh, I.; Marzo, L.; Das, A.; Shaikh, R.; König, B. Visible Light Mediated Photoredox Catalytic Arylation Reactions. *Acc. Chem. Res.* **2016**, *49*, 1566–1577. (b) Tucker, J. W.; Stephenson, C. R. J. Shining Light on Photoredox Catalysis: Theory and Synthetic Applications. *J. Org. Chem.* **2012**, *77*, 1617–1622. (c) Prier, C. K.; Rankic, D. A.; MacMillan, D. W. C. Visible Light Photoredox Catalysis with Transition Metal Complexes: Applications in Organic Synthesis. *Chem. Rev.* **2013**, *113*, 5322–5363. (d) Skubi, K. L.; Blum, T. R.; Yoon, T. P. Dual Catalysis Strategies in Photochemical Synthesis. *Chem. Rev.* **2016**, *116*, 10035–10074.
5. Gasonoo, M.; Thom, Z. W.; Laulhe, S. Regioselective α -Amination of Ethers Using Stable *N*-Chloroimides and Lithium *tert*-Butoxide. *J. Org. Chem.* **2019**, *84*, 8710–8716.
6. Song, L.; Zhang, L.; Luo, S.; Cheng, J. Visible-Light Promoted Catalyst-Free Imidation of Arenes and Heteroarenes. *Chem.-Eur. J.* **2014**, *20*, 14231–14234.
7. Weinberger, C.; Hines, R.; Zeller, M.; Rosokha, S. V. Continuum of Covalent to Intermolecular Bonding in the Halogen Bonded Complexes of 1,4-Diazabicyclo [2.2.2] octane with Bromine Containing Electrophiles. *Chem. Commun.* **2018**, *54*, 8060–8063.

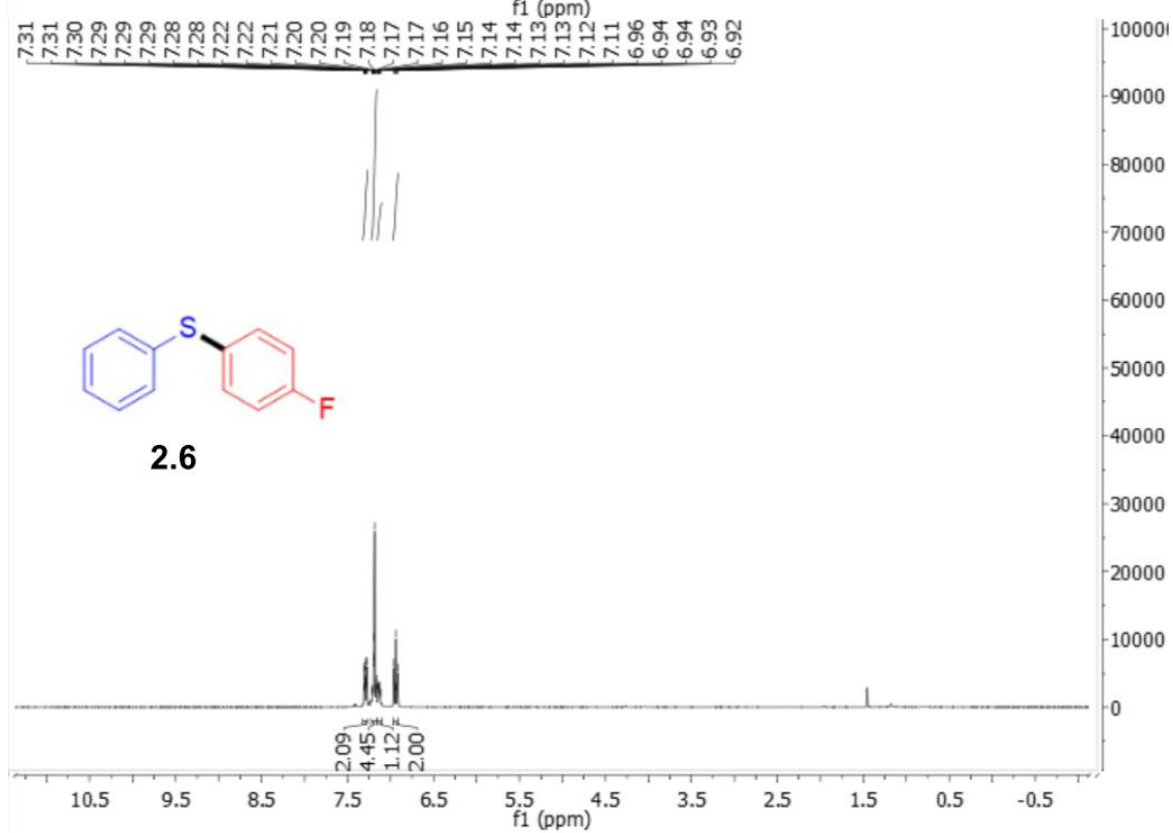
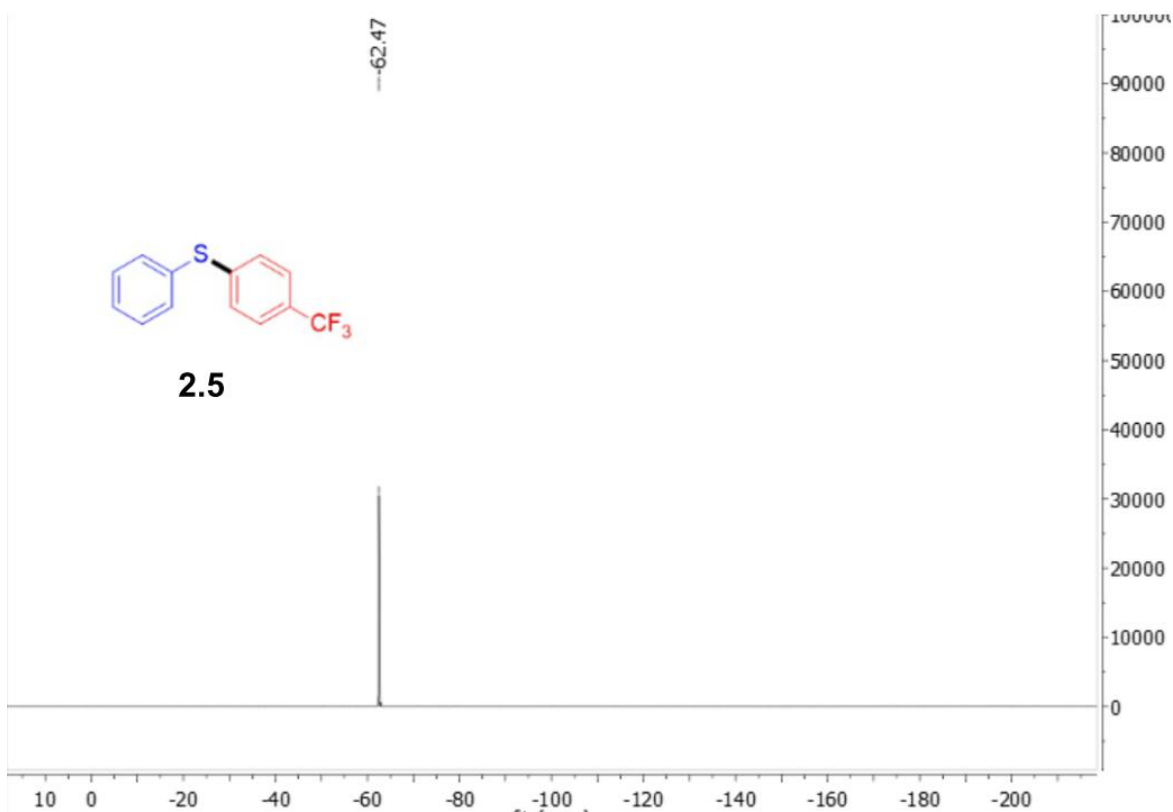
8. Hancock, A.N.; Tanko, J.M. Radical cation/anion and neutral radicals: a comparison. In *Encyclopedia of Radicals in Chemistry, Biology and Materials*, John Wiley & Sons, Chinchester, UK **2012**.
9. (a) Barham, J. P.; Coulthard, G.; Emery, K. J.; Doni, E.; Cumine, F.; Nocera, G.; John, M. P.; Berlouis, L. E. A.; McGuire, T.; Tuttle, T.; et al. KOTBu: A Privileged Reagent for Electron Transfer Reactions? *J. Am. Chem. Soc.* **2016**, *138*, 7402–7410. (b) Liu, X.; Zhao, X.; Liang, F.; Ren, B. *T*-BuONa-Mediated Direct C–H Halogenation of Electron-Deficient (Hetero)Arenes. *Org. Biomol. Chem.* **2018**, *16*, 886–889.

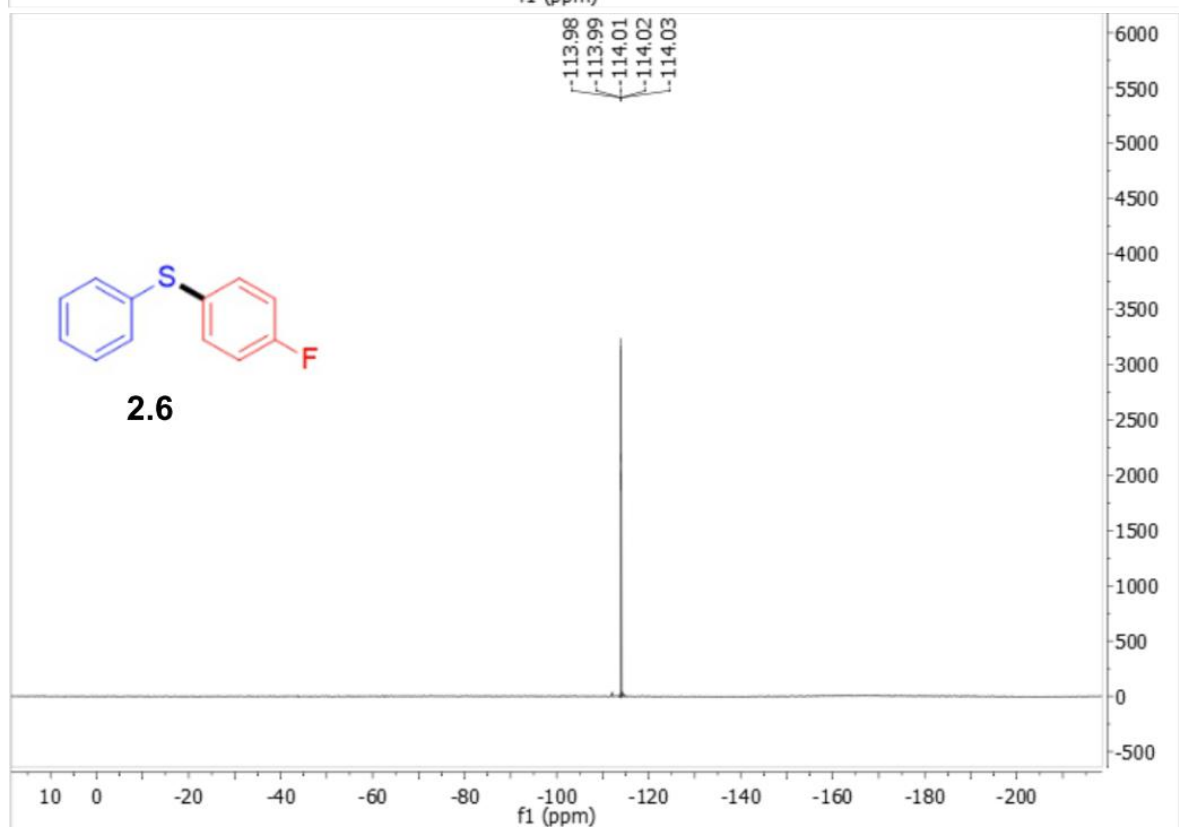
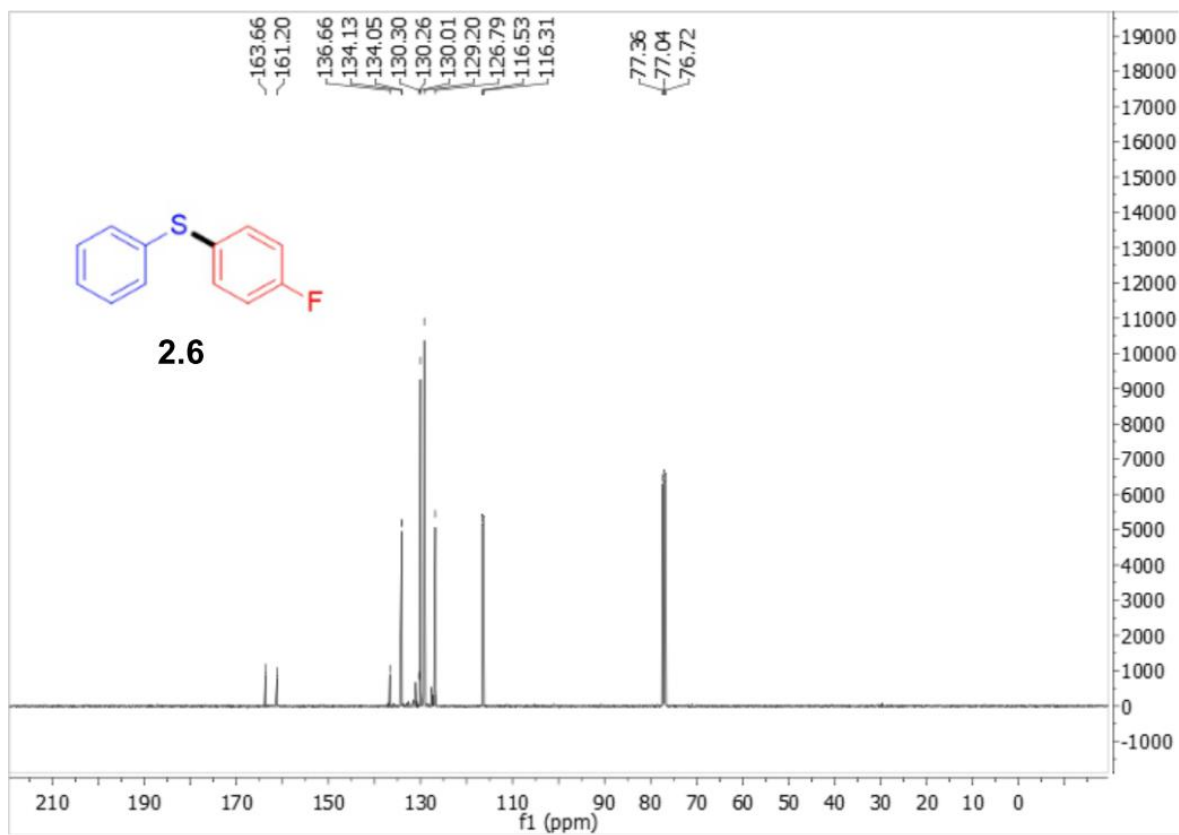
APPENDIX A. NMR SPECTRA

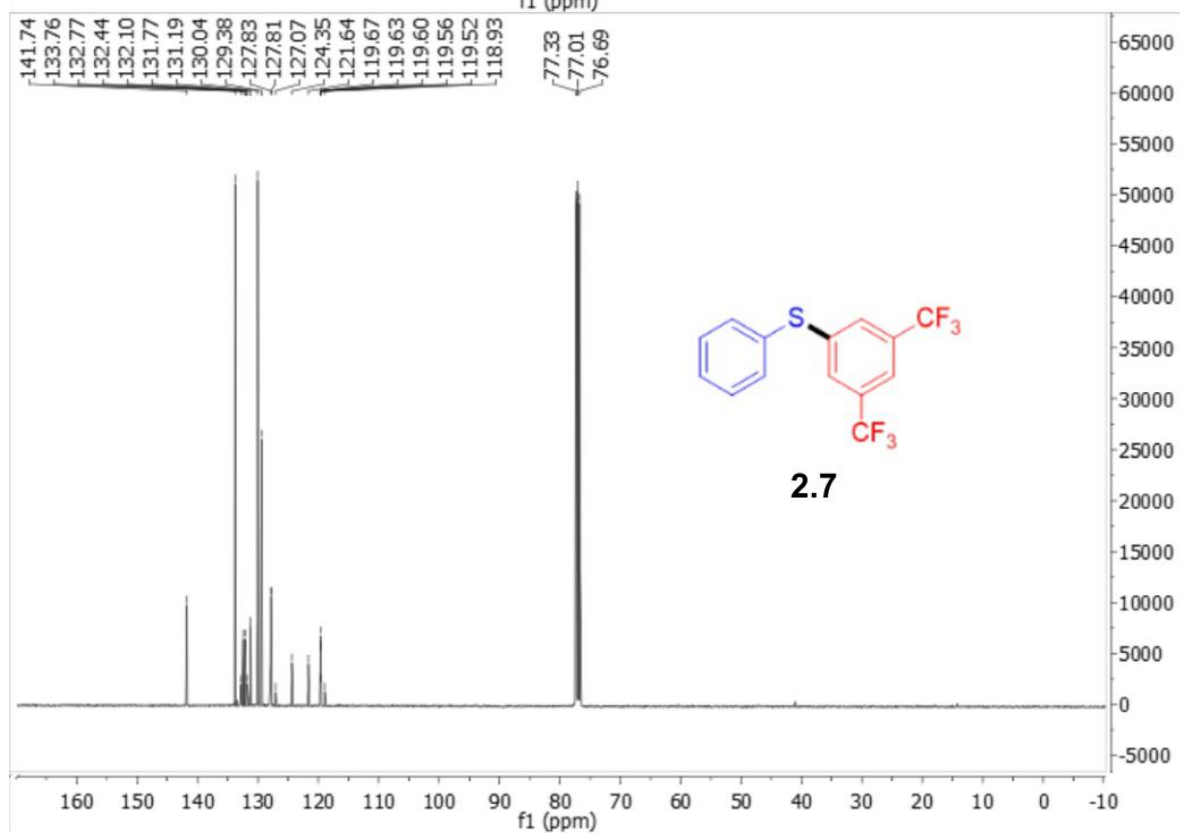
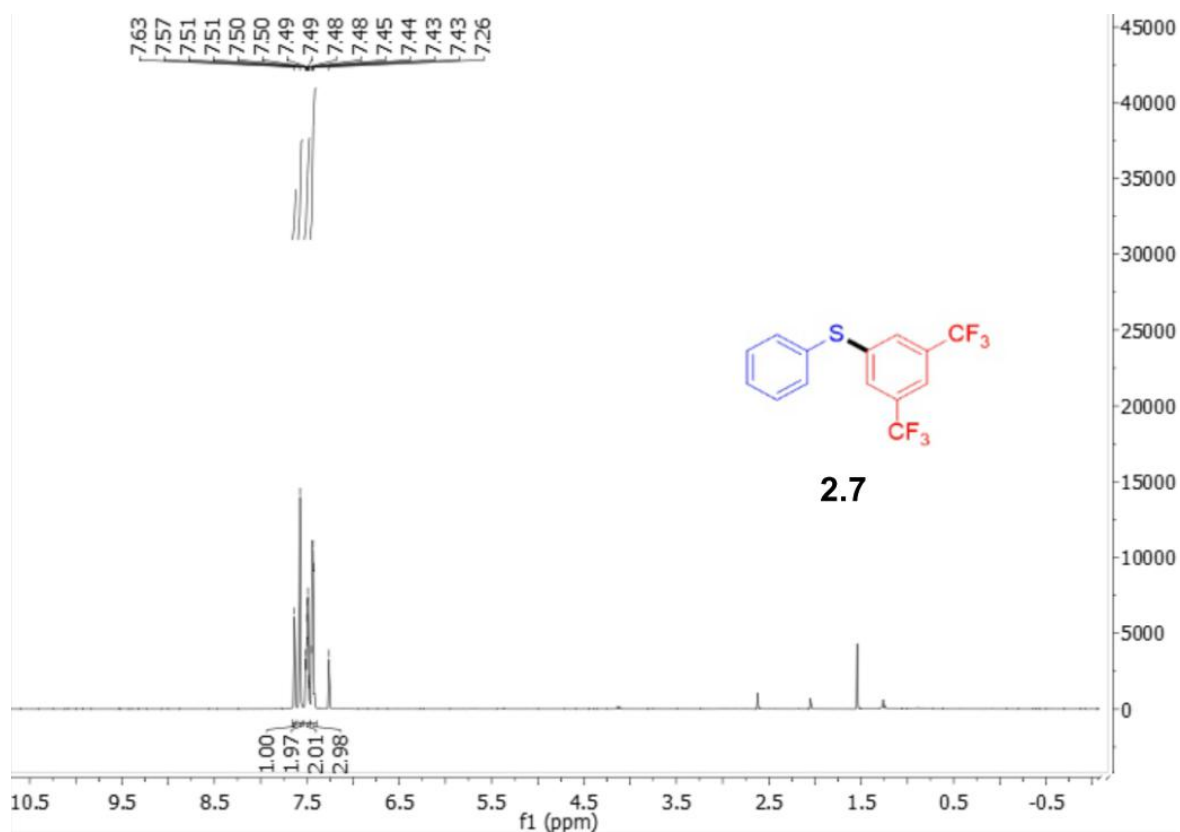


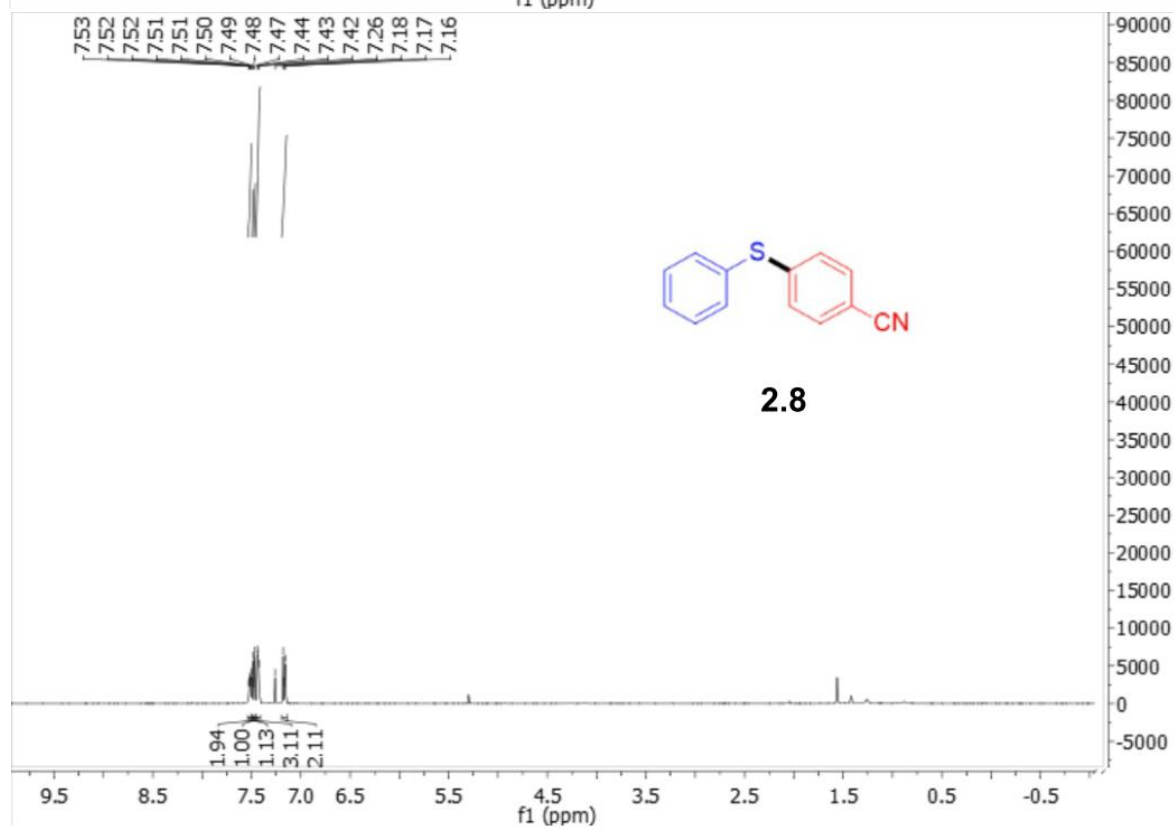
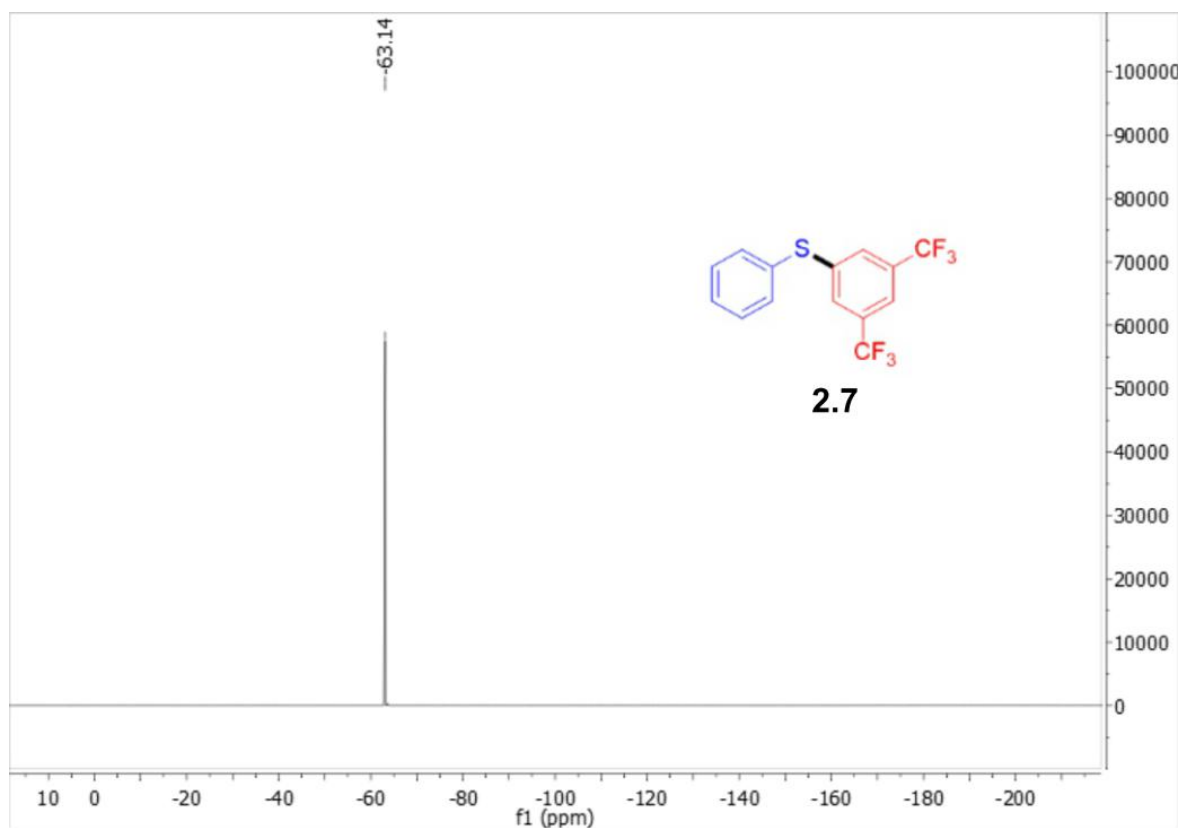


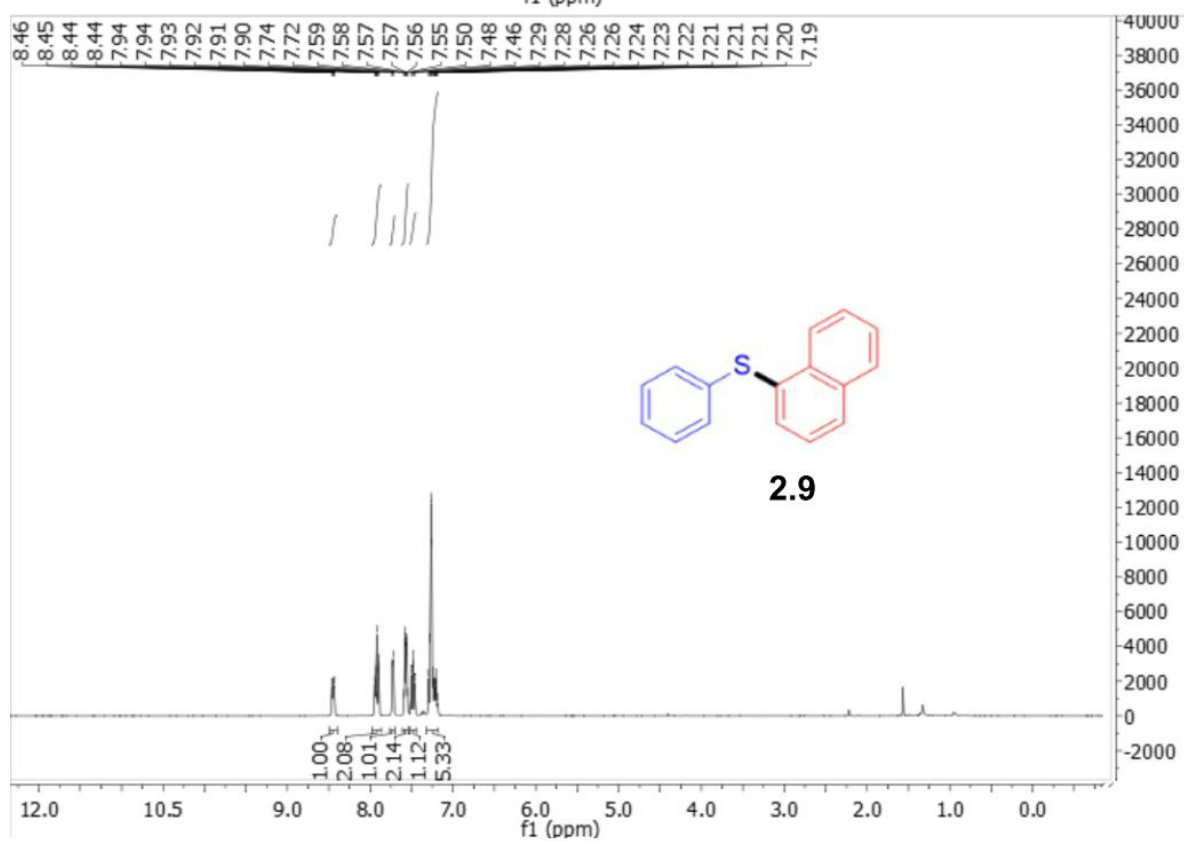
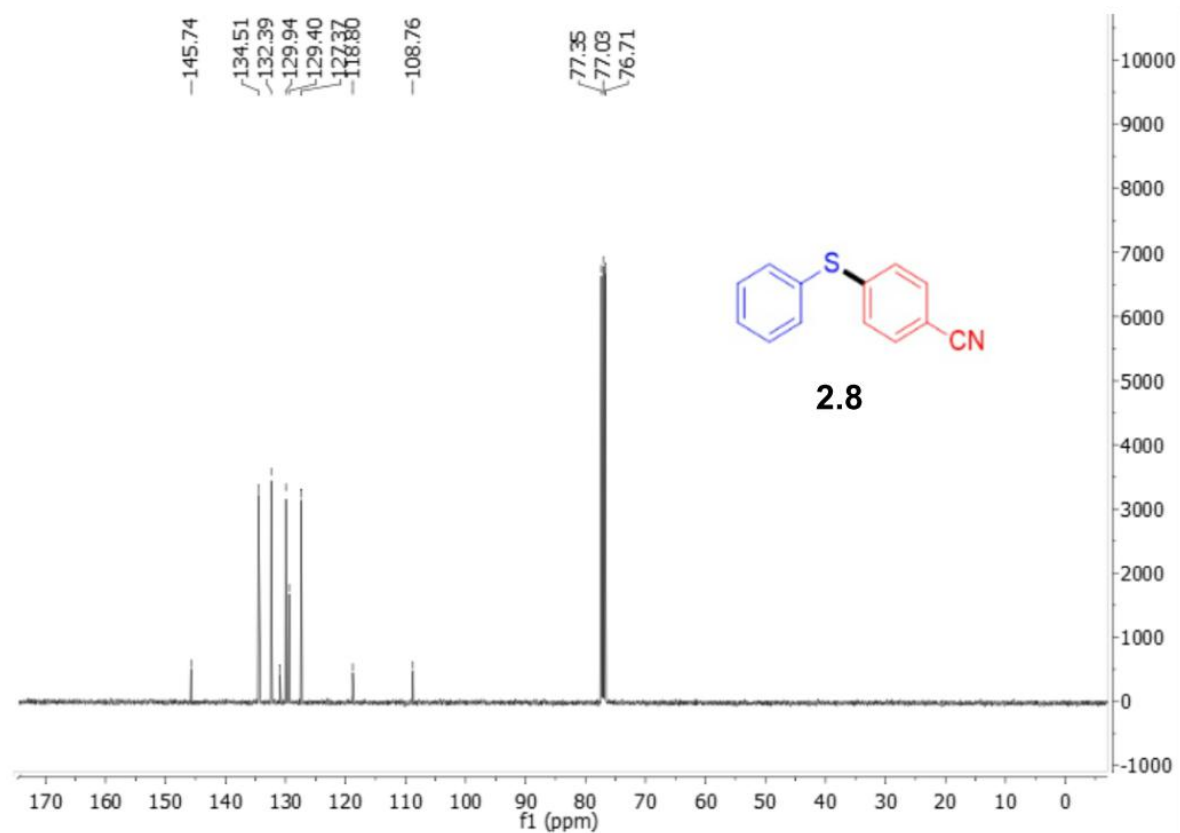


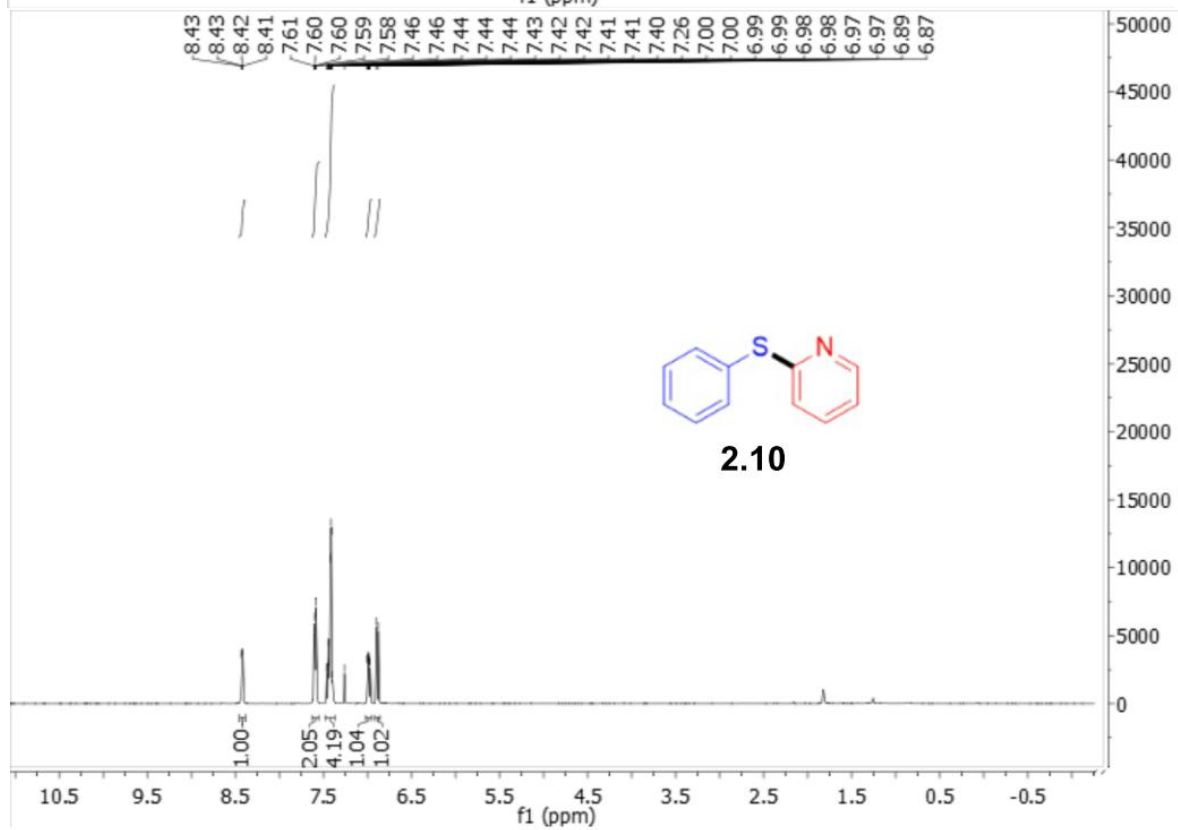
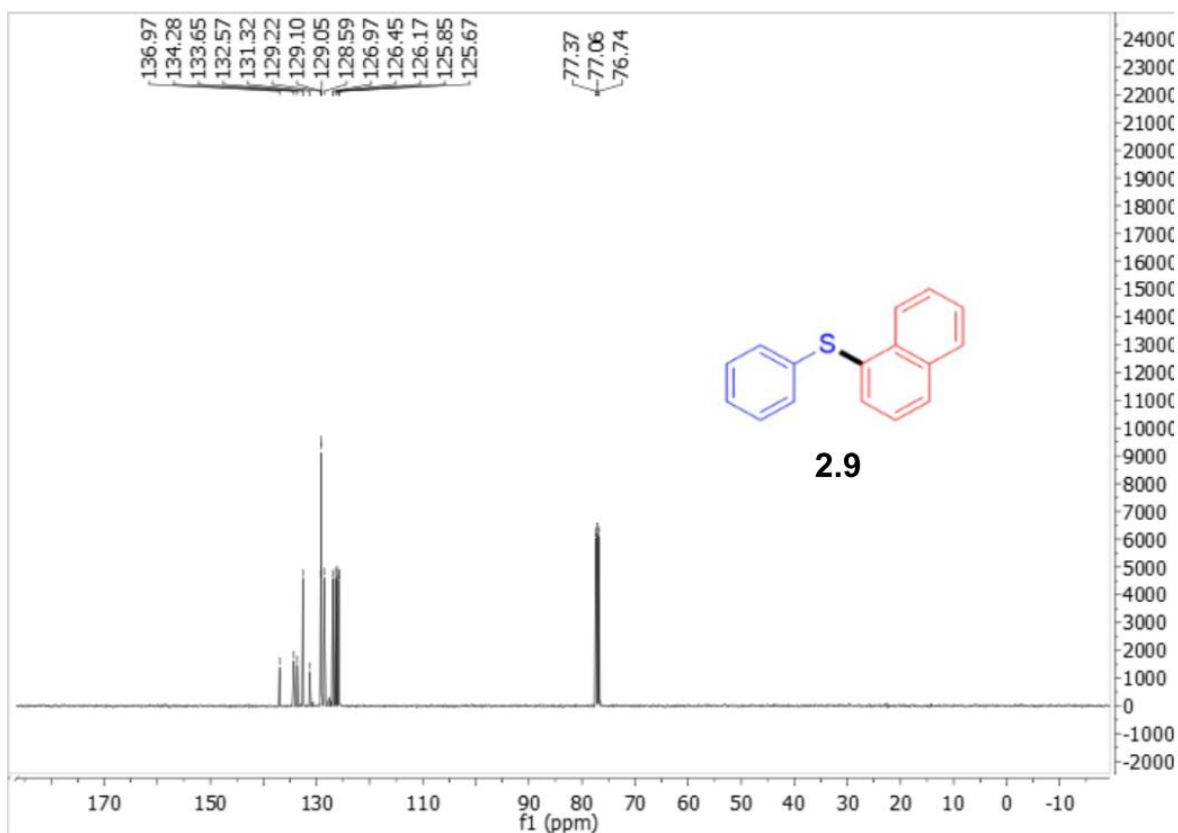


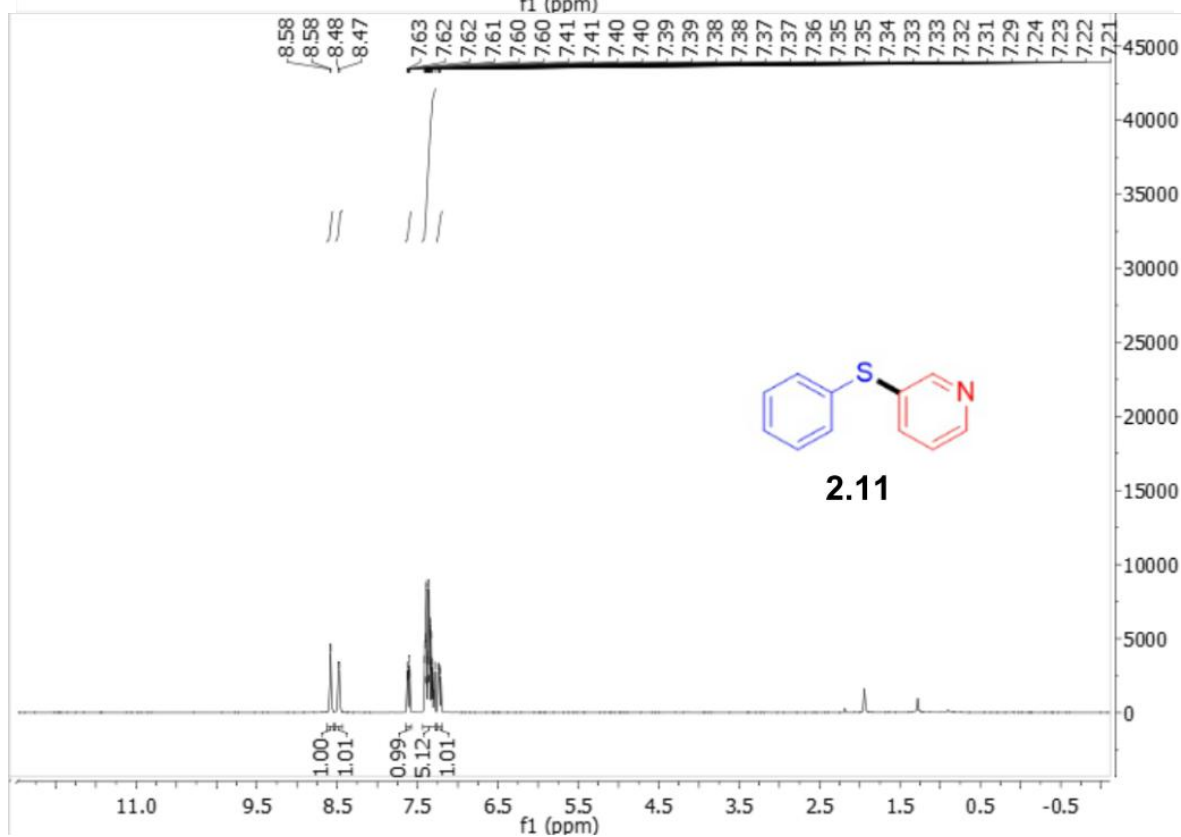
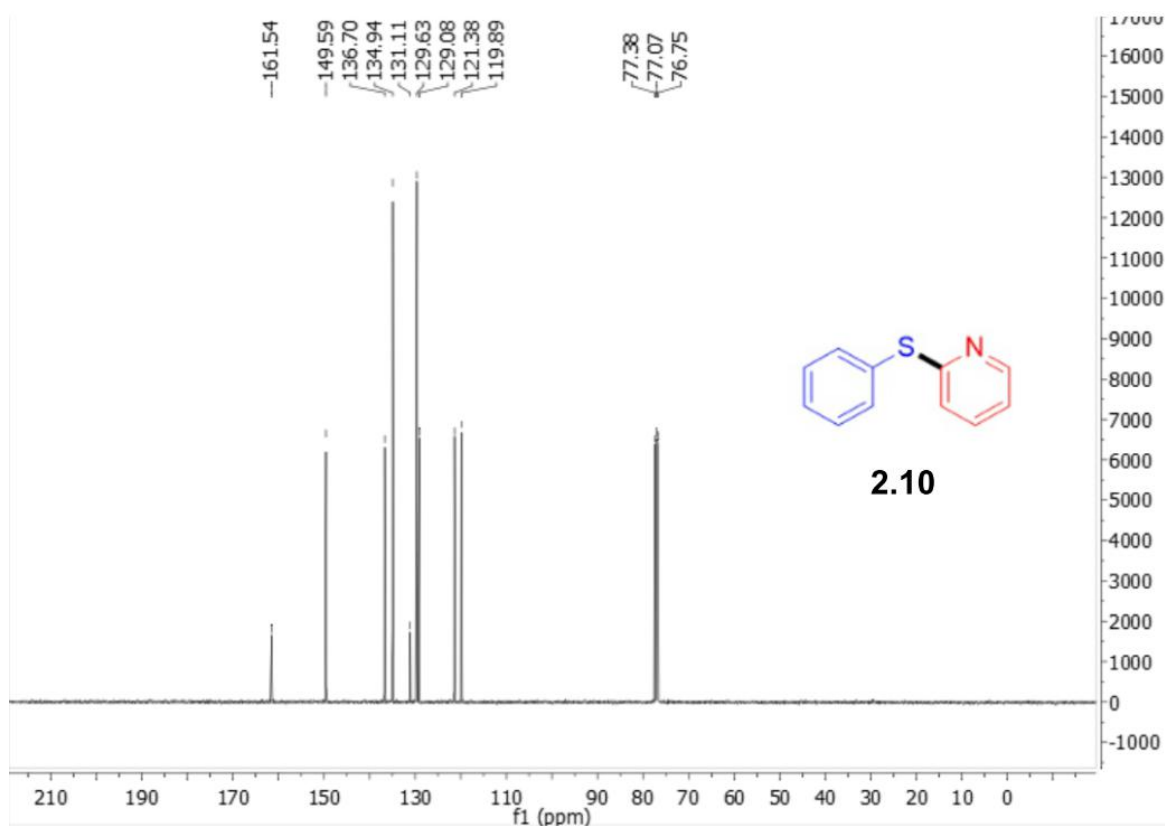


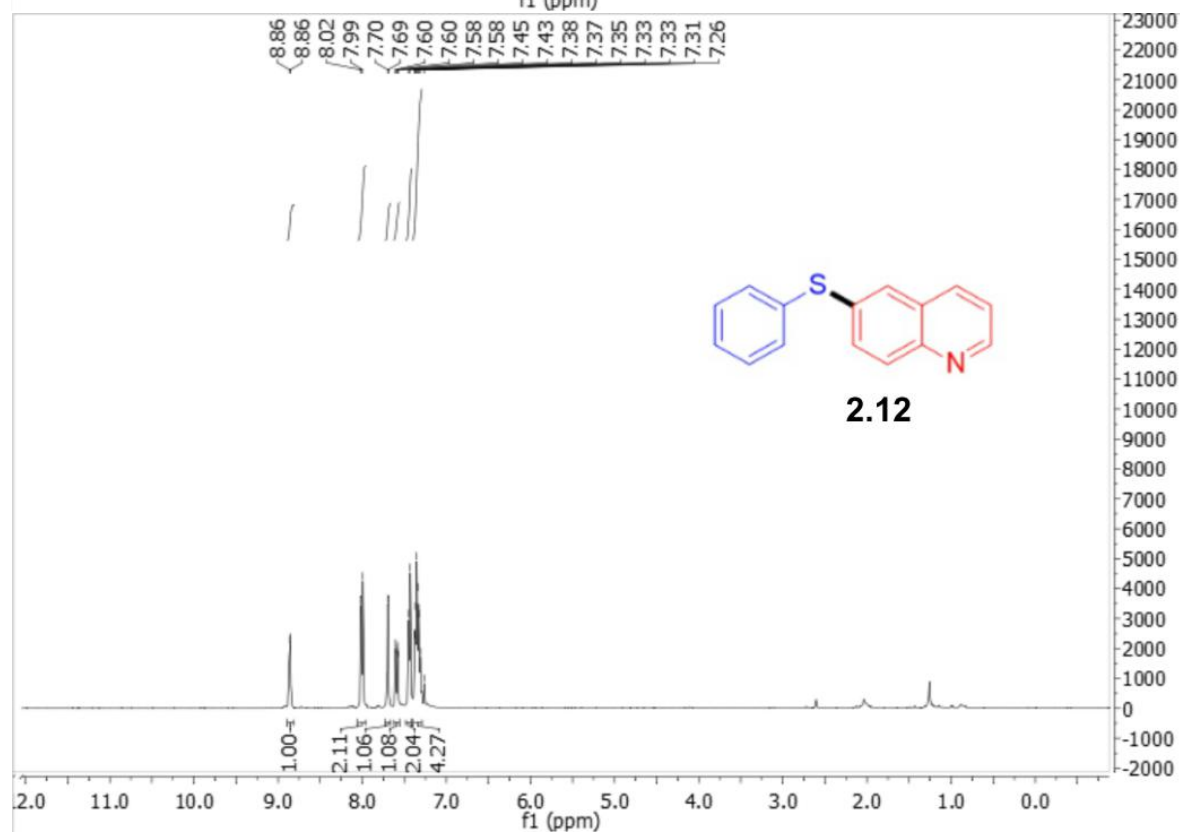
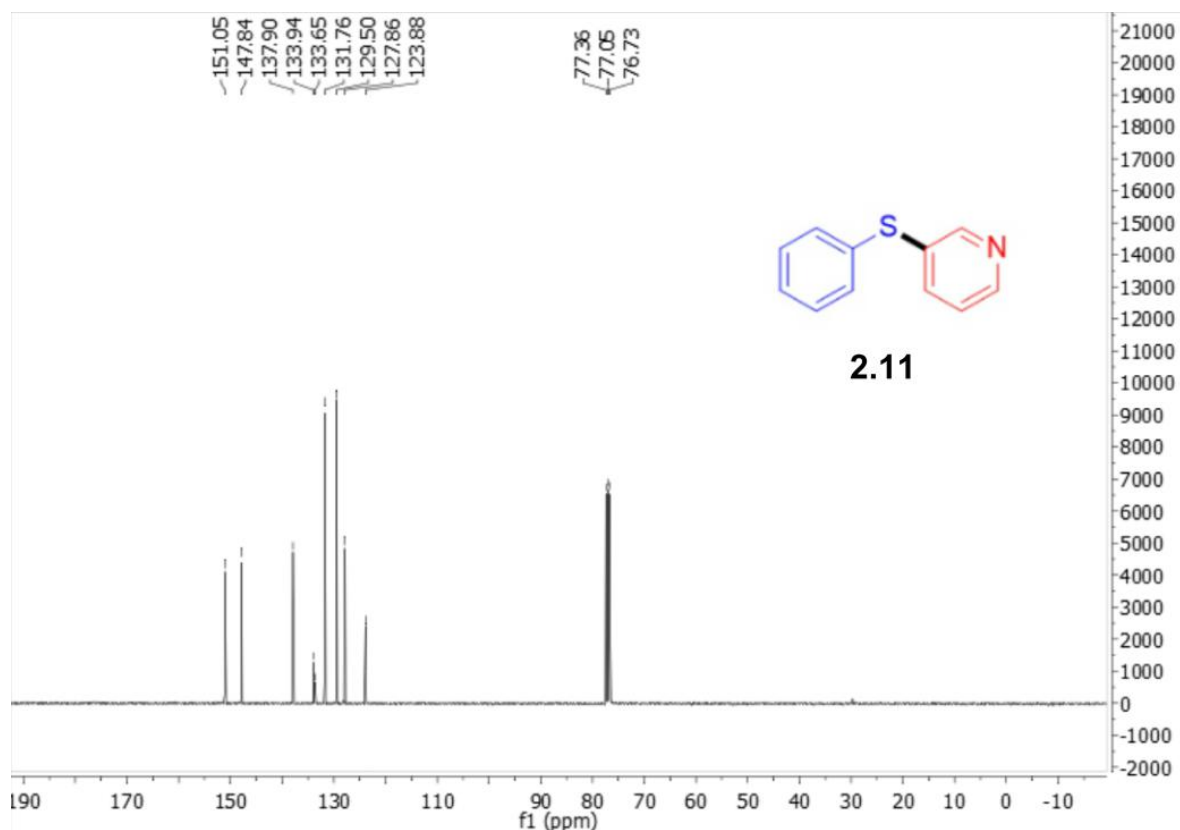


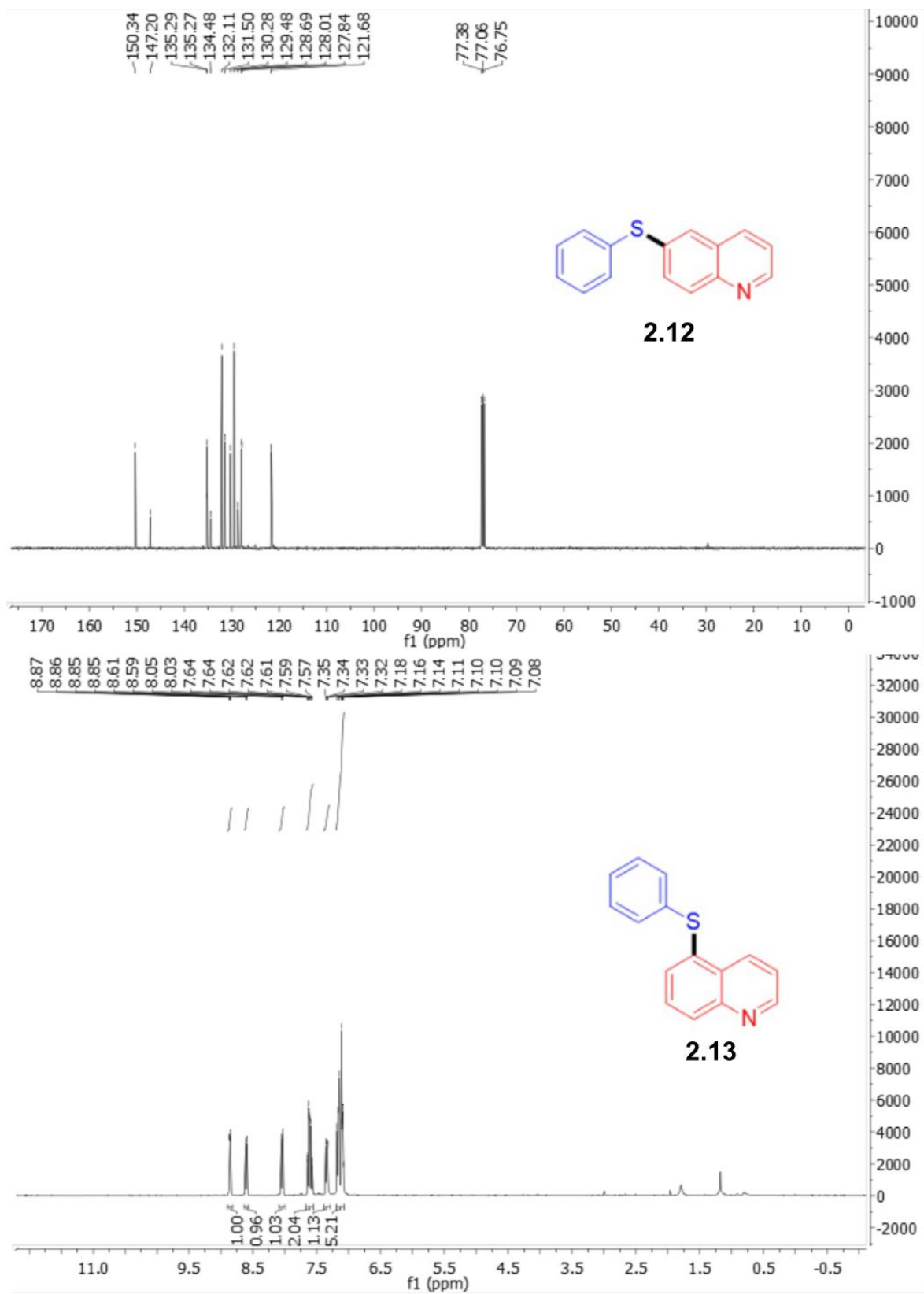


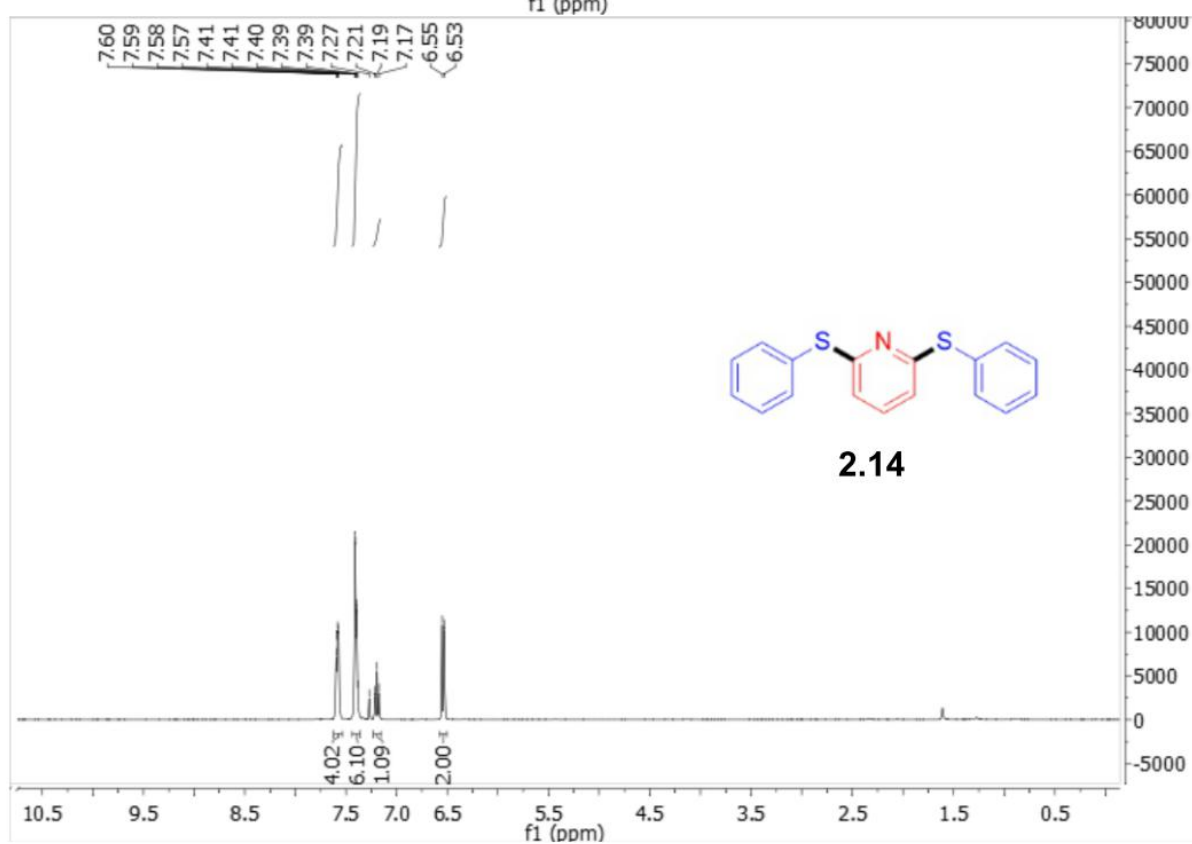
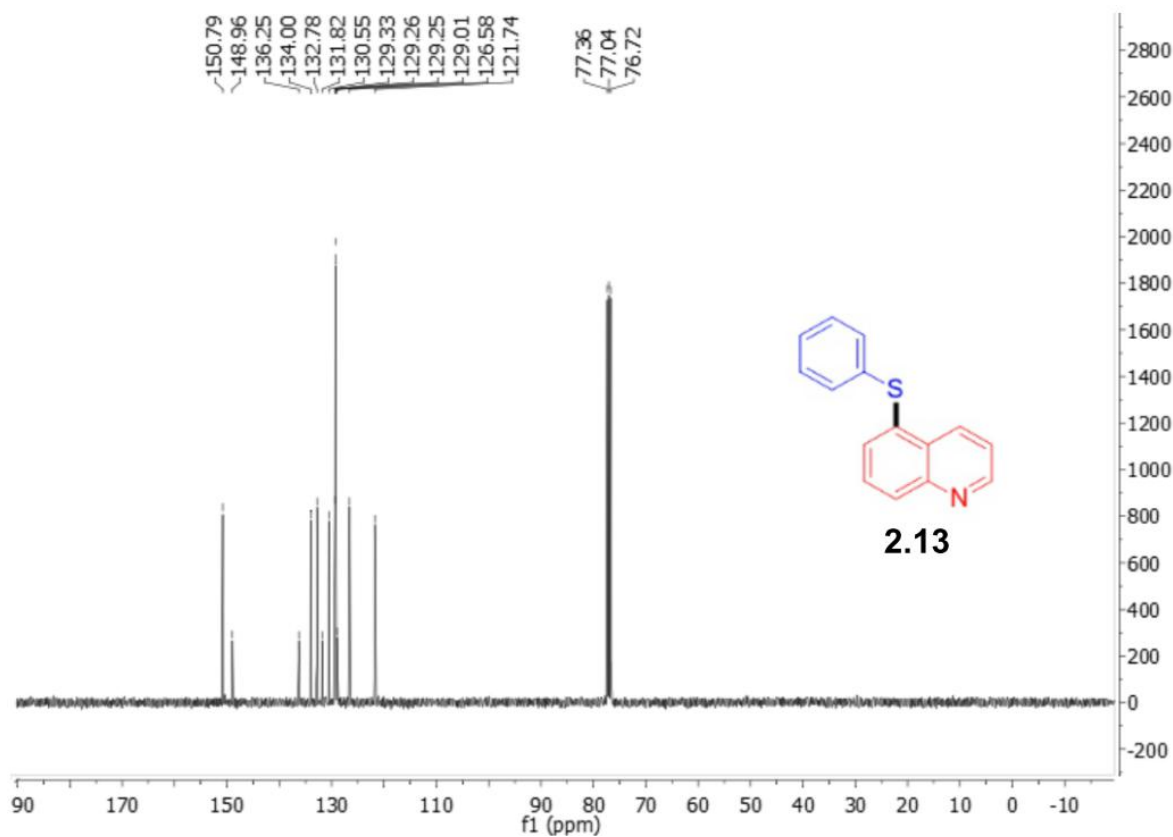


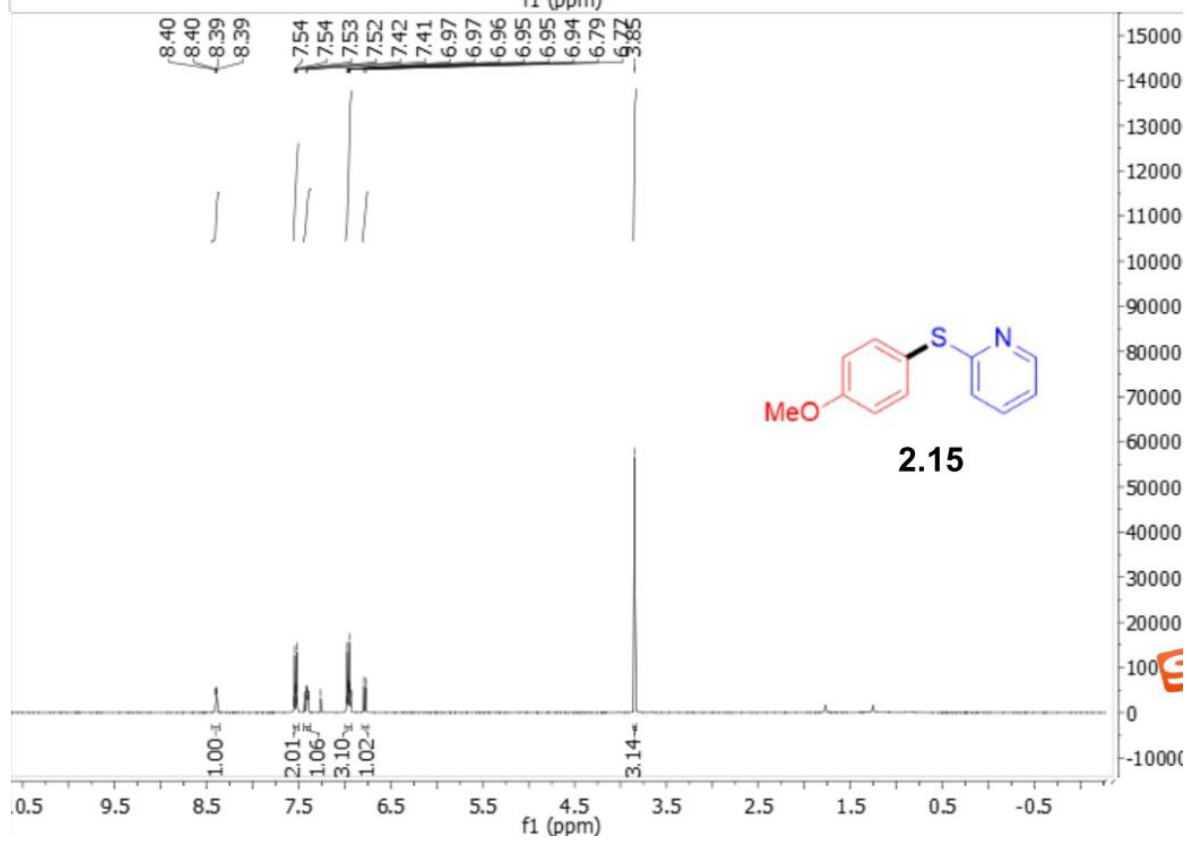
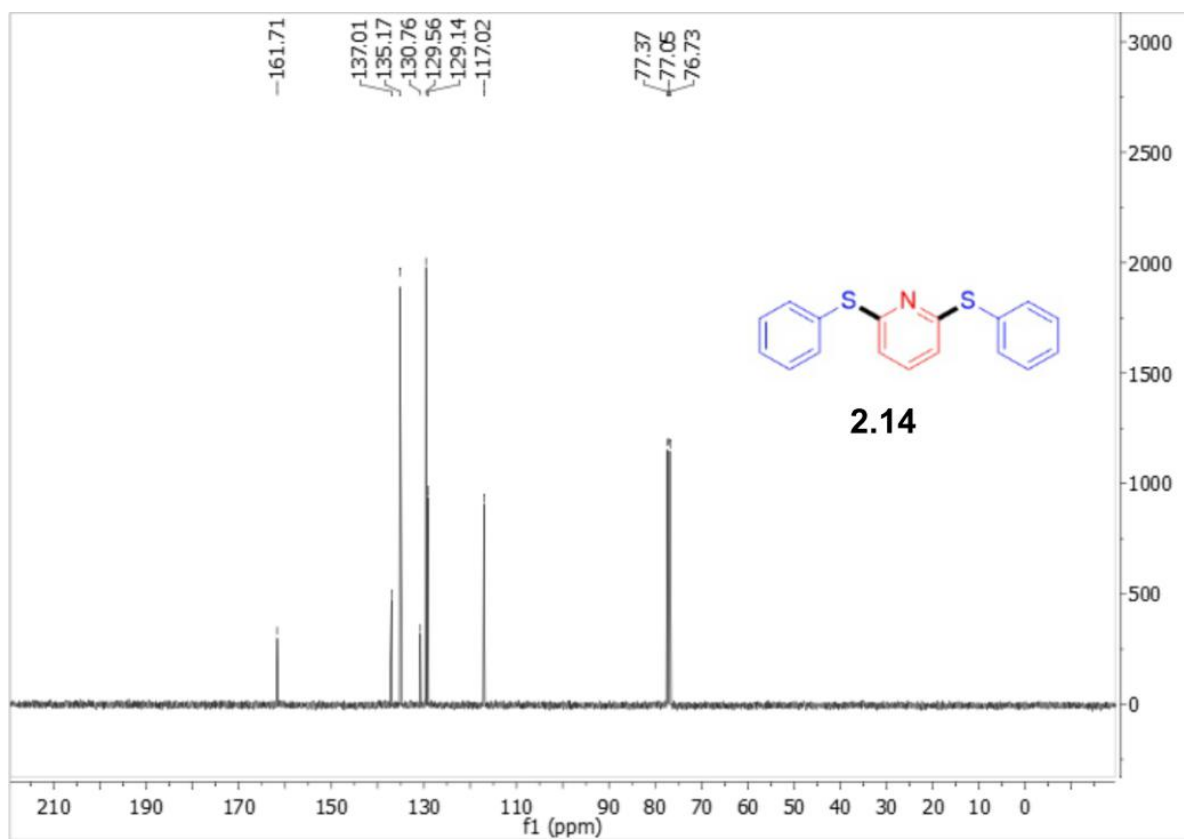


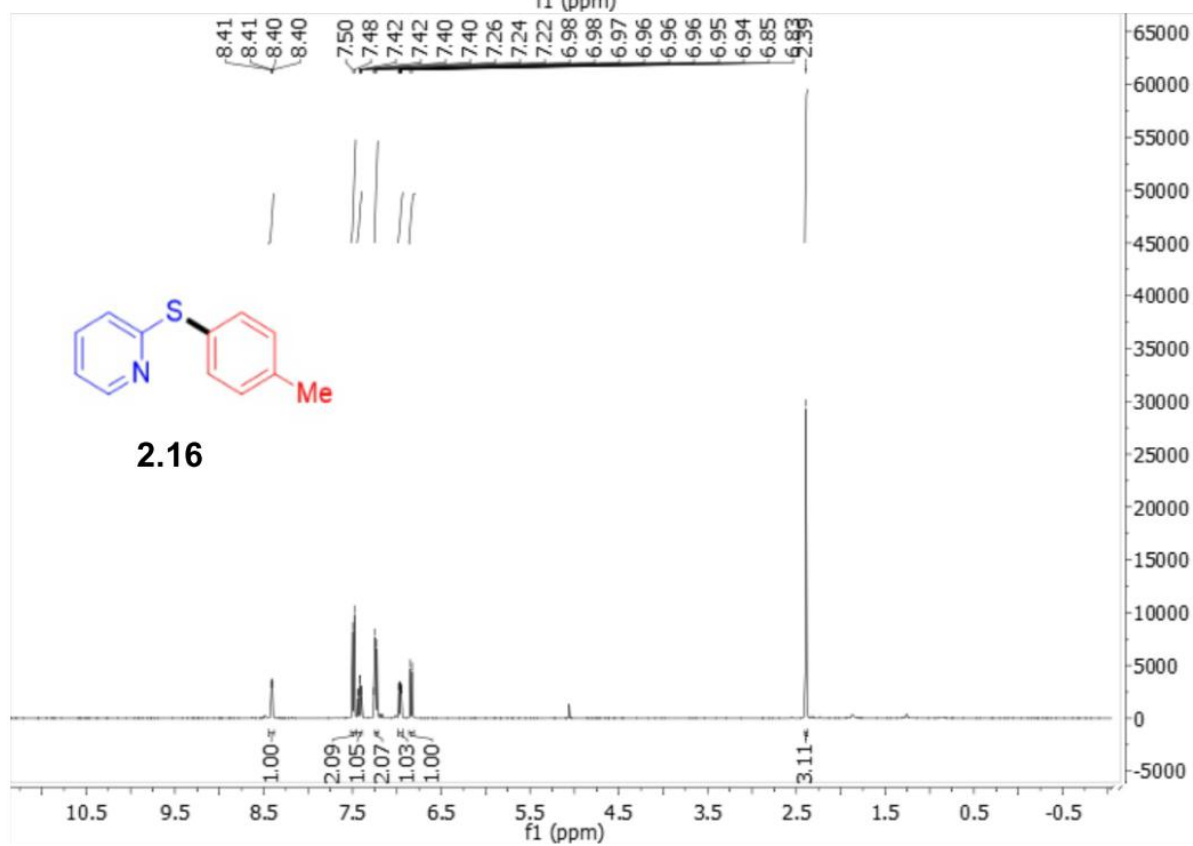
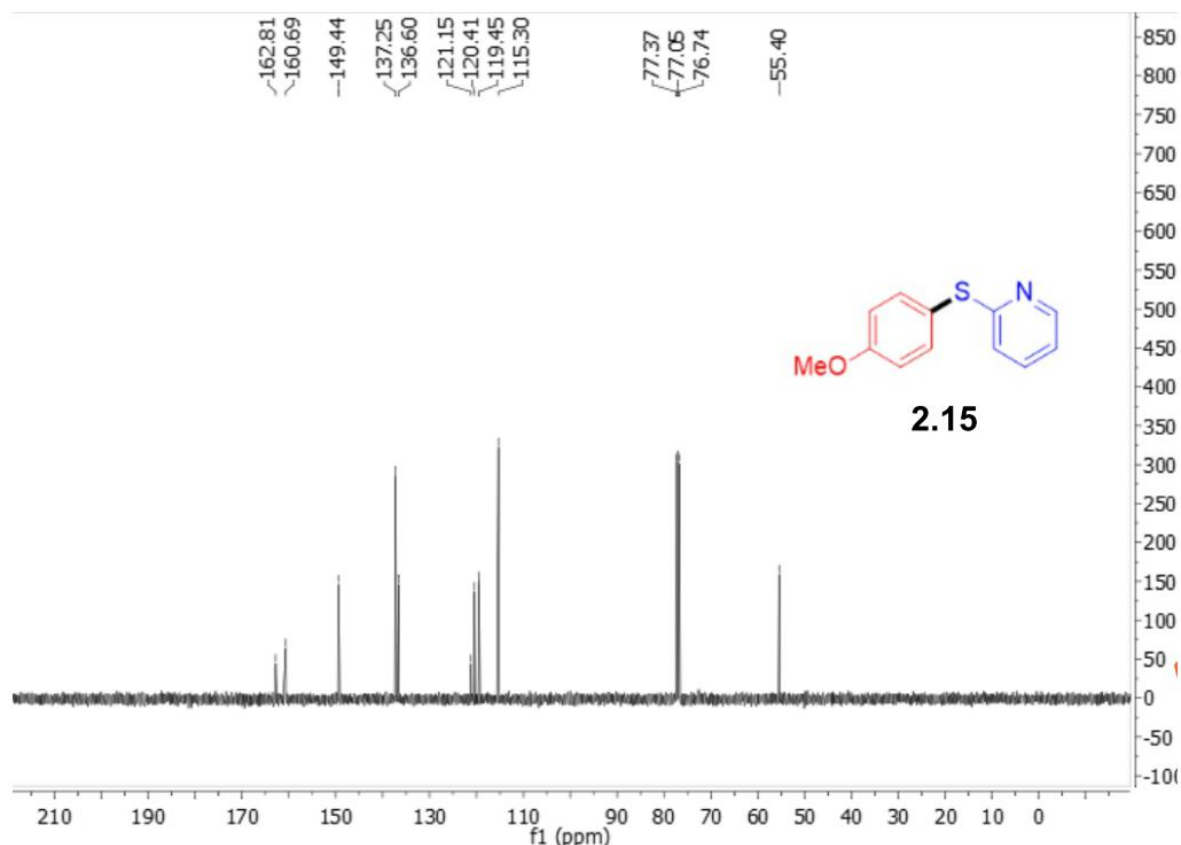


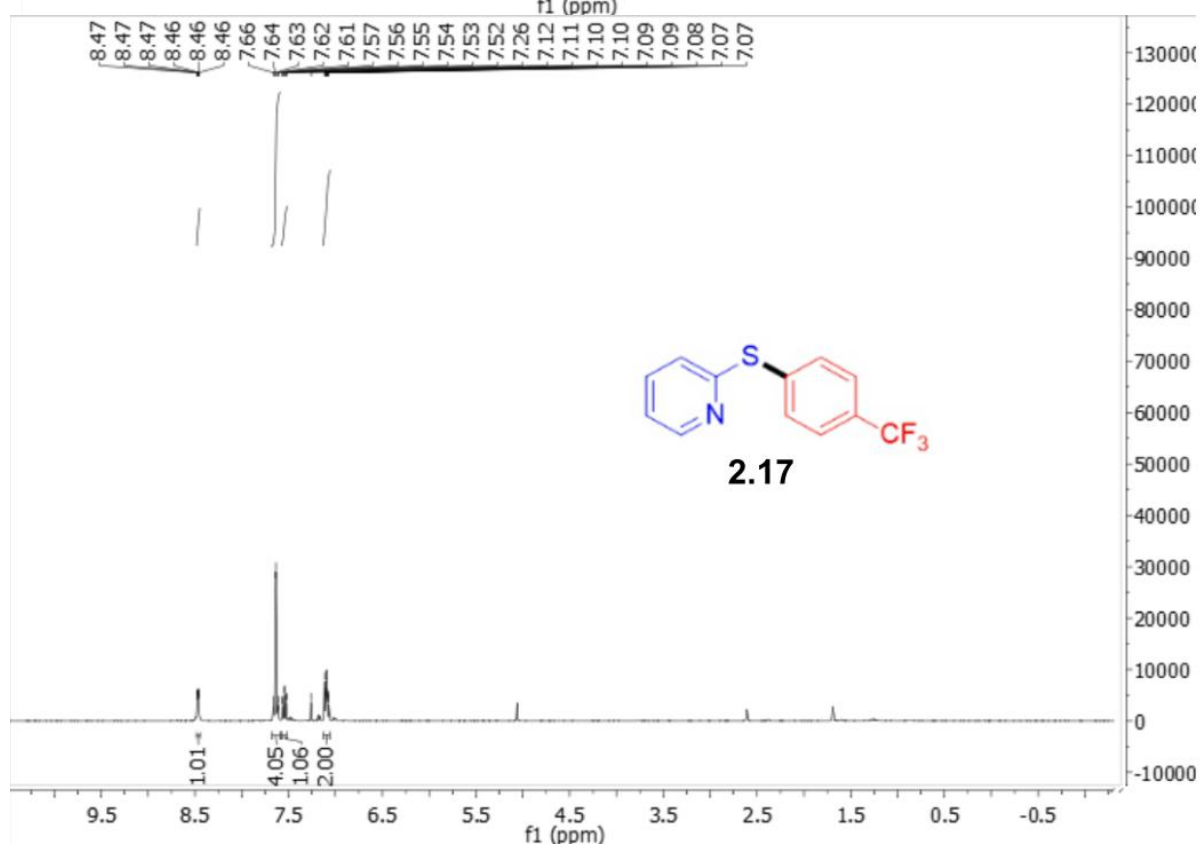
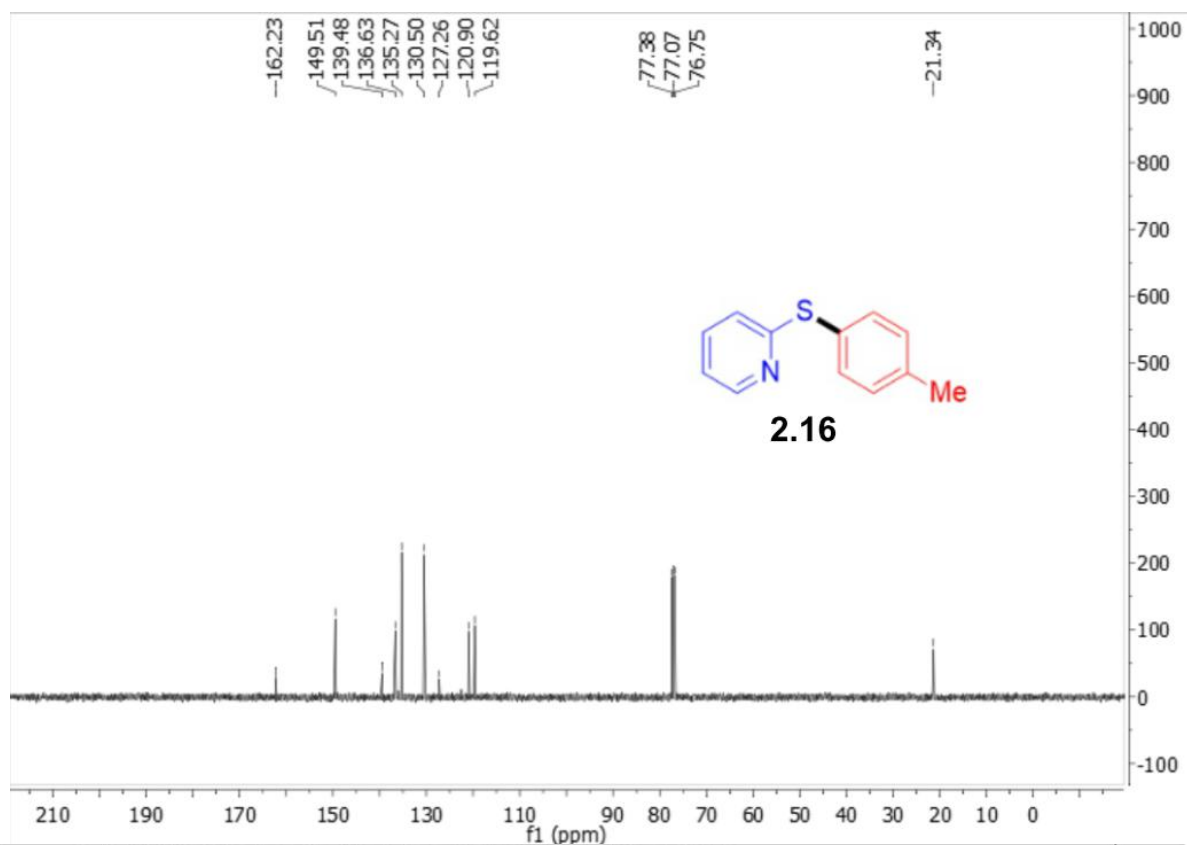


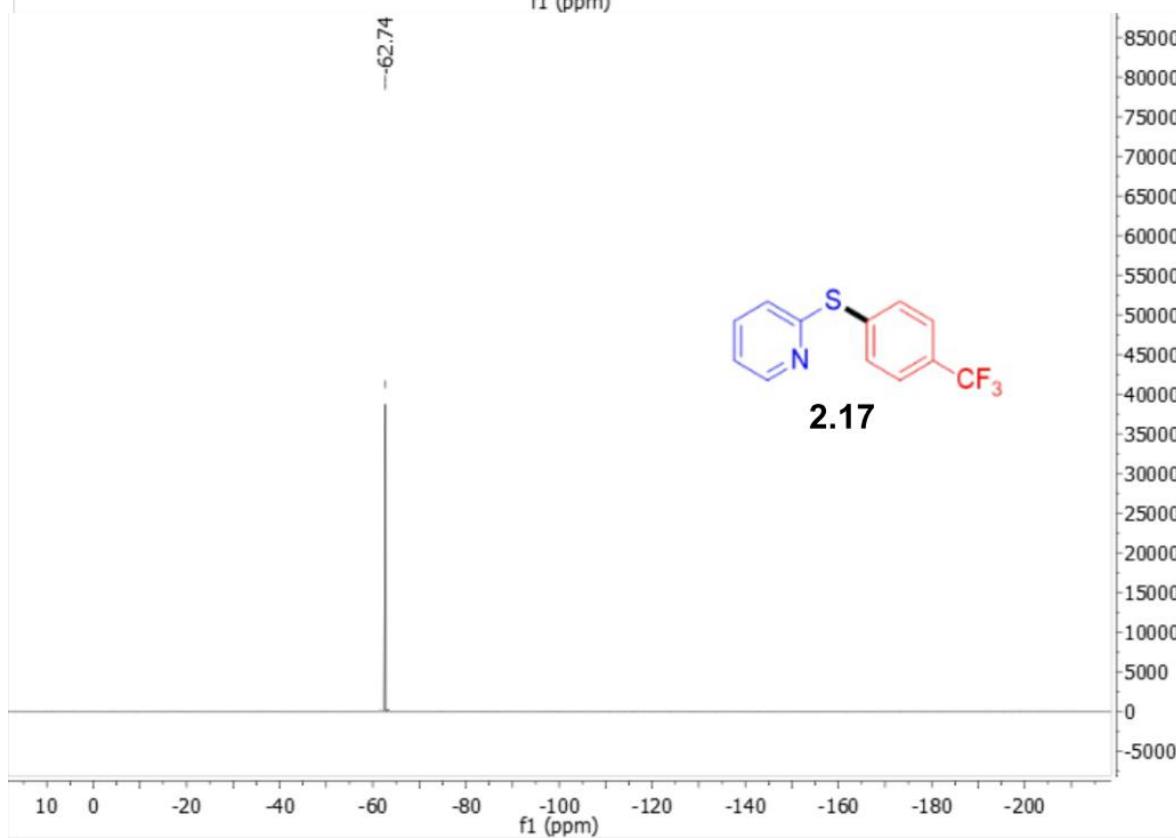
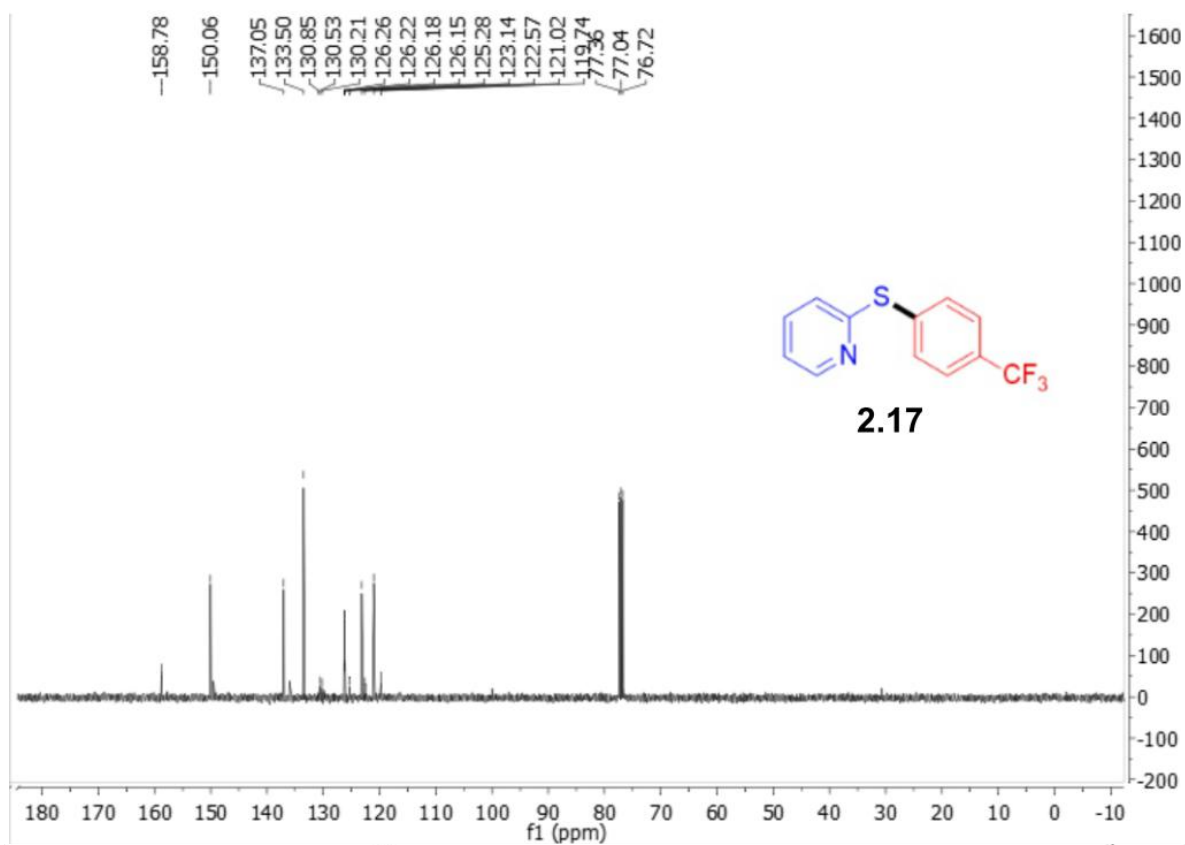


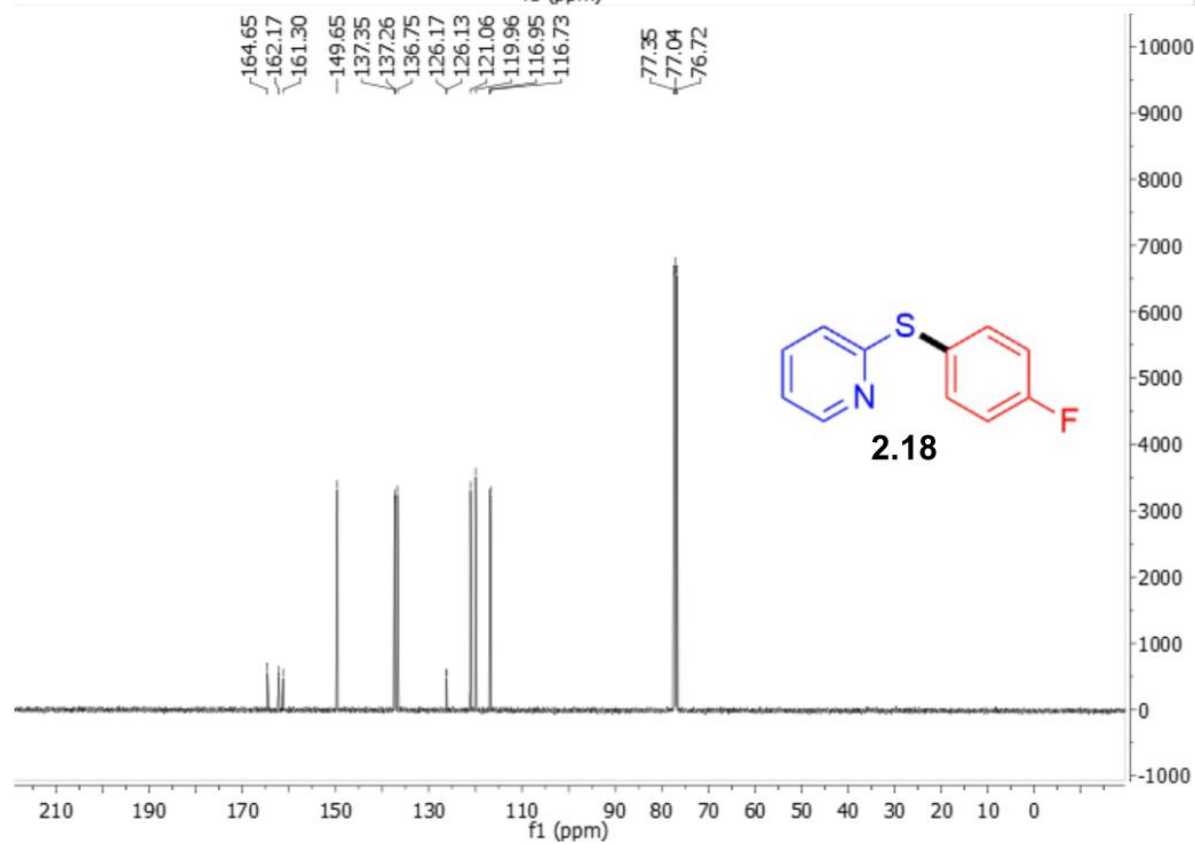
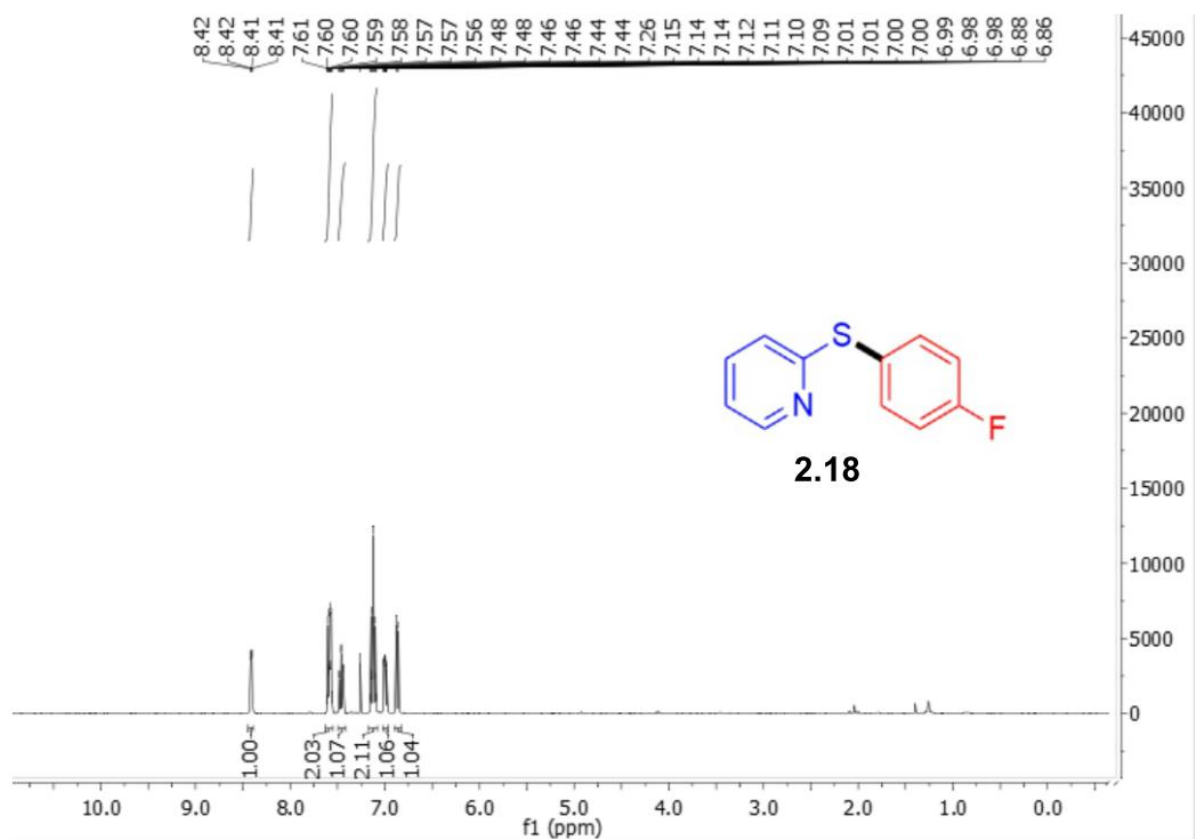


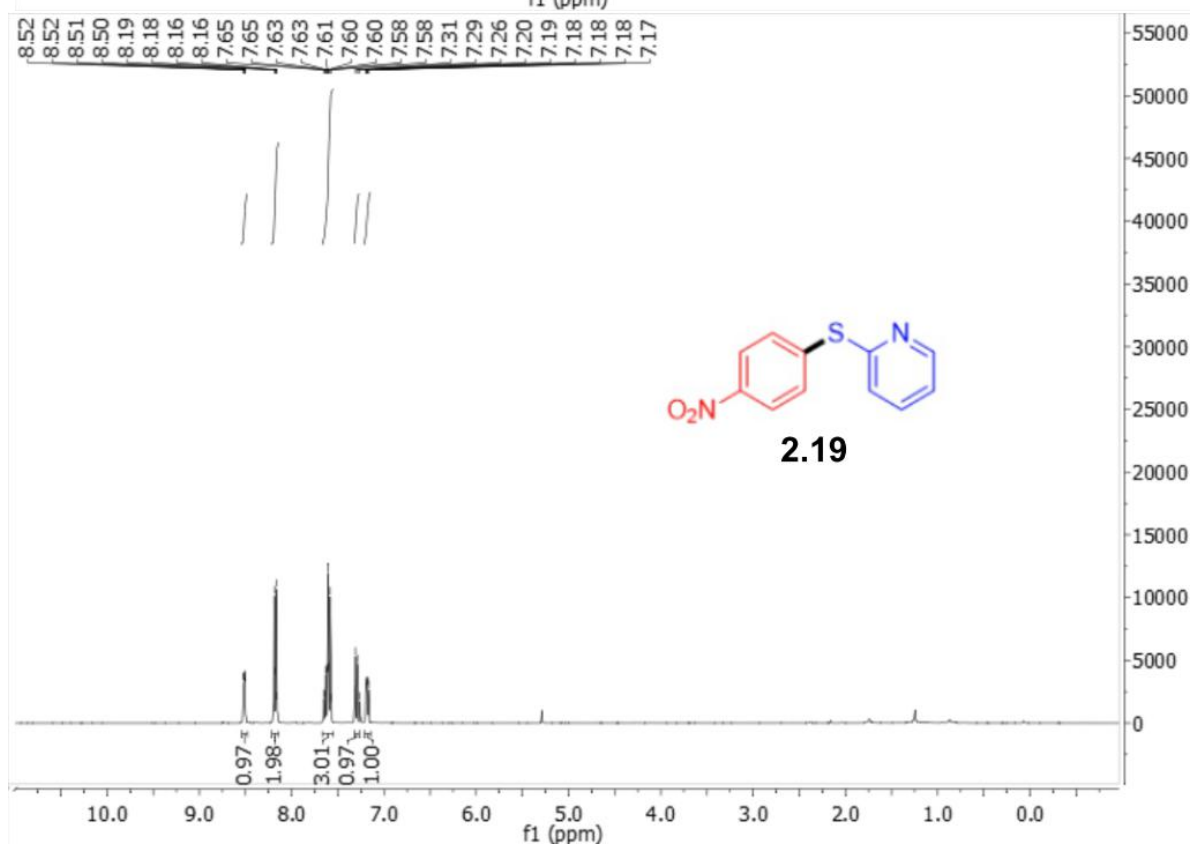
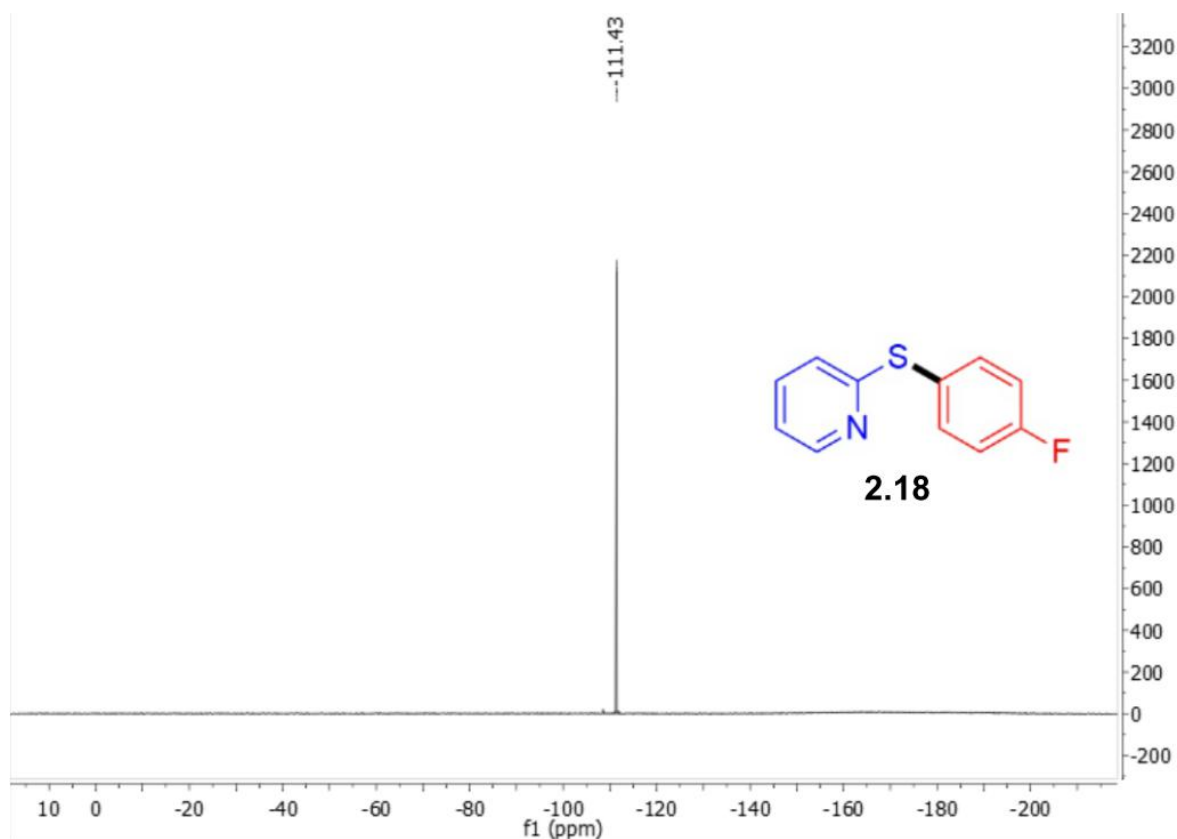


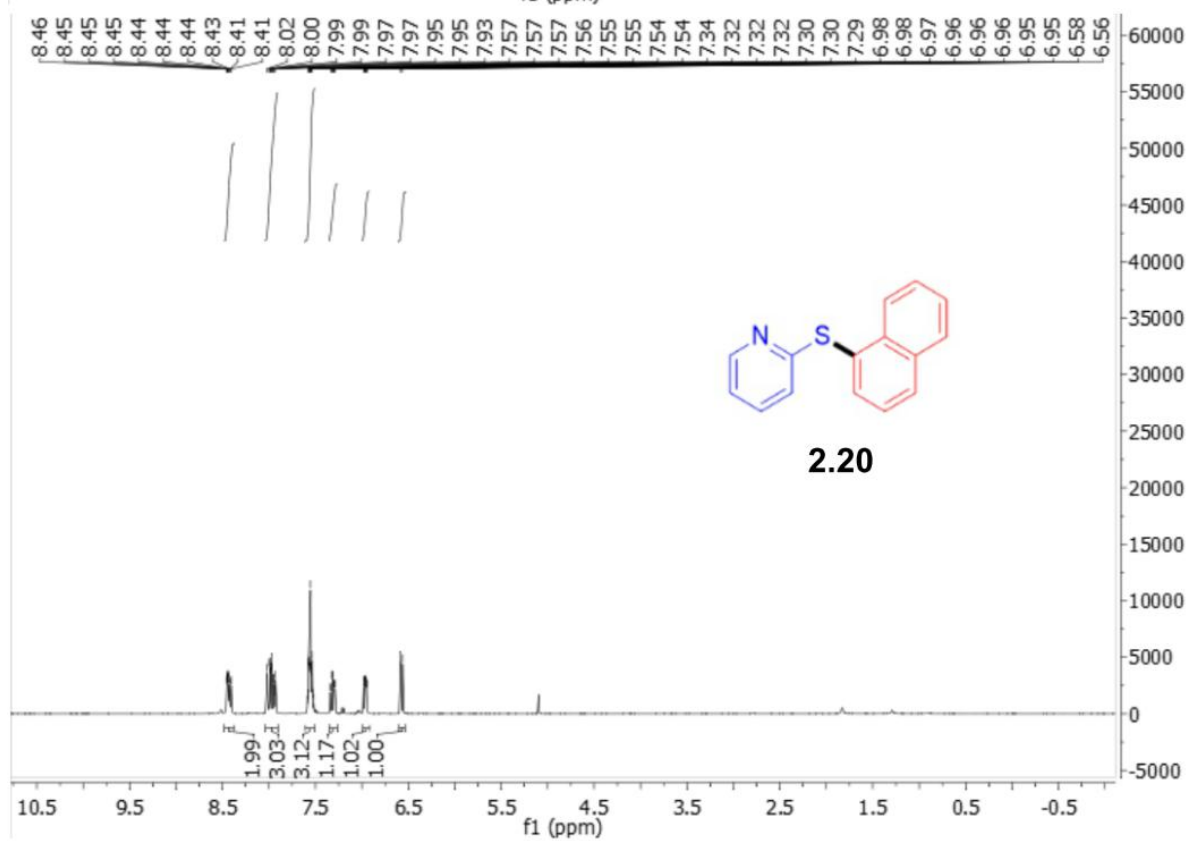
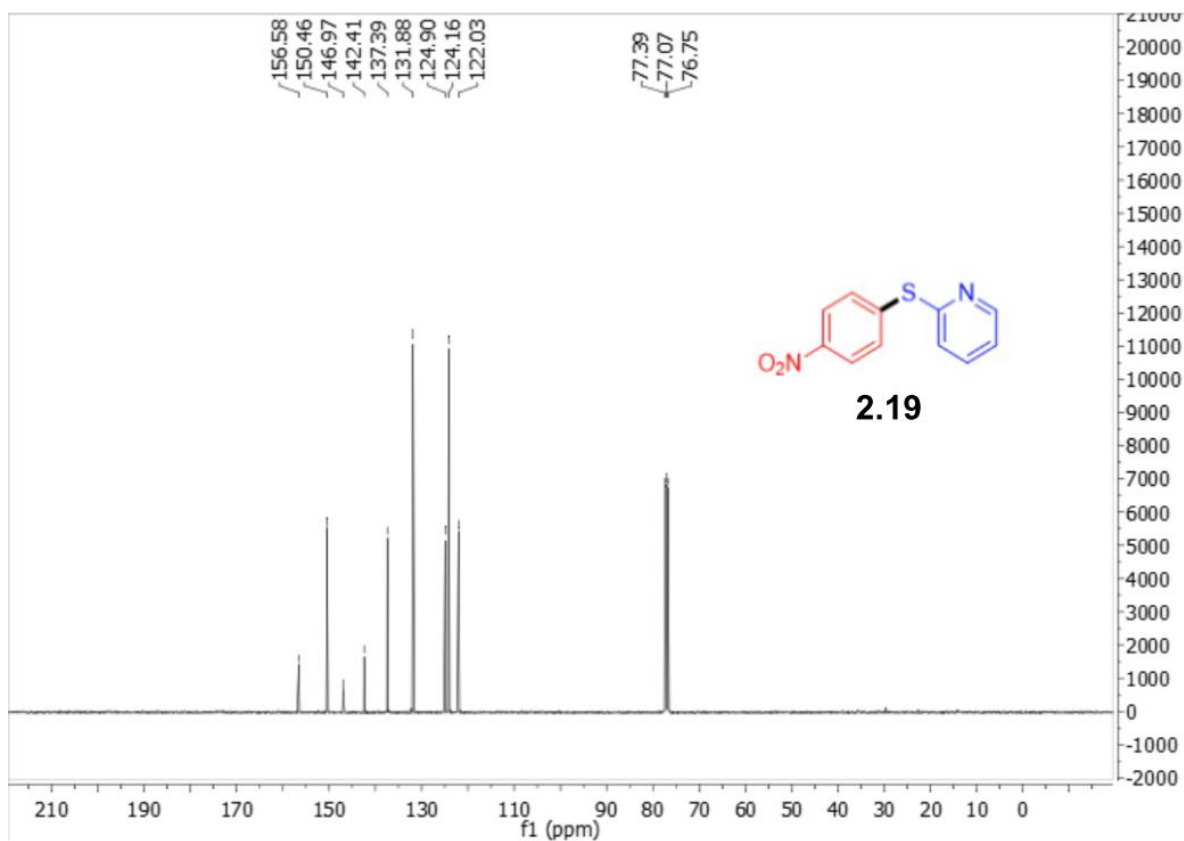


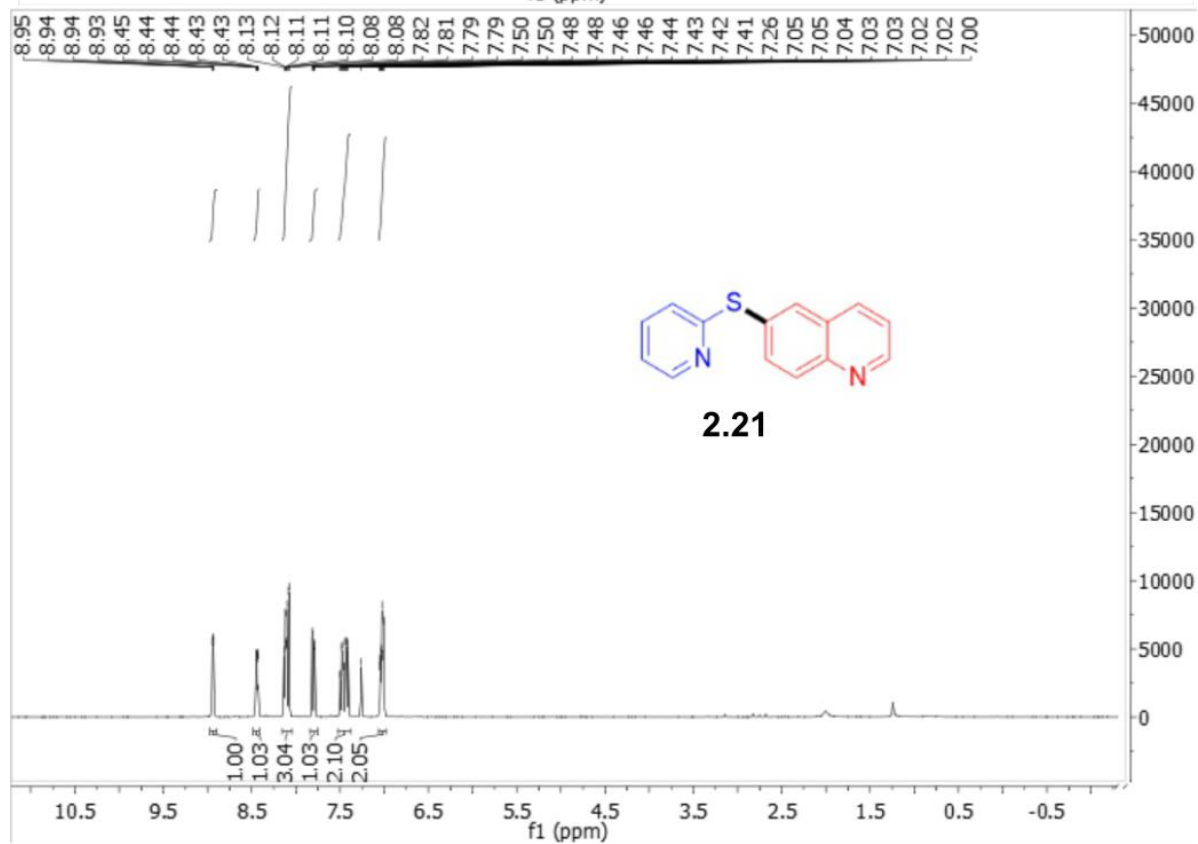
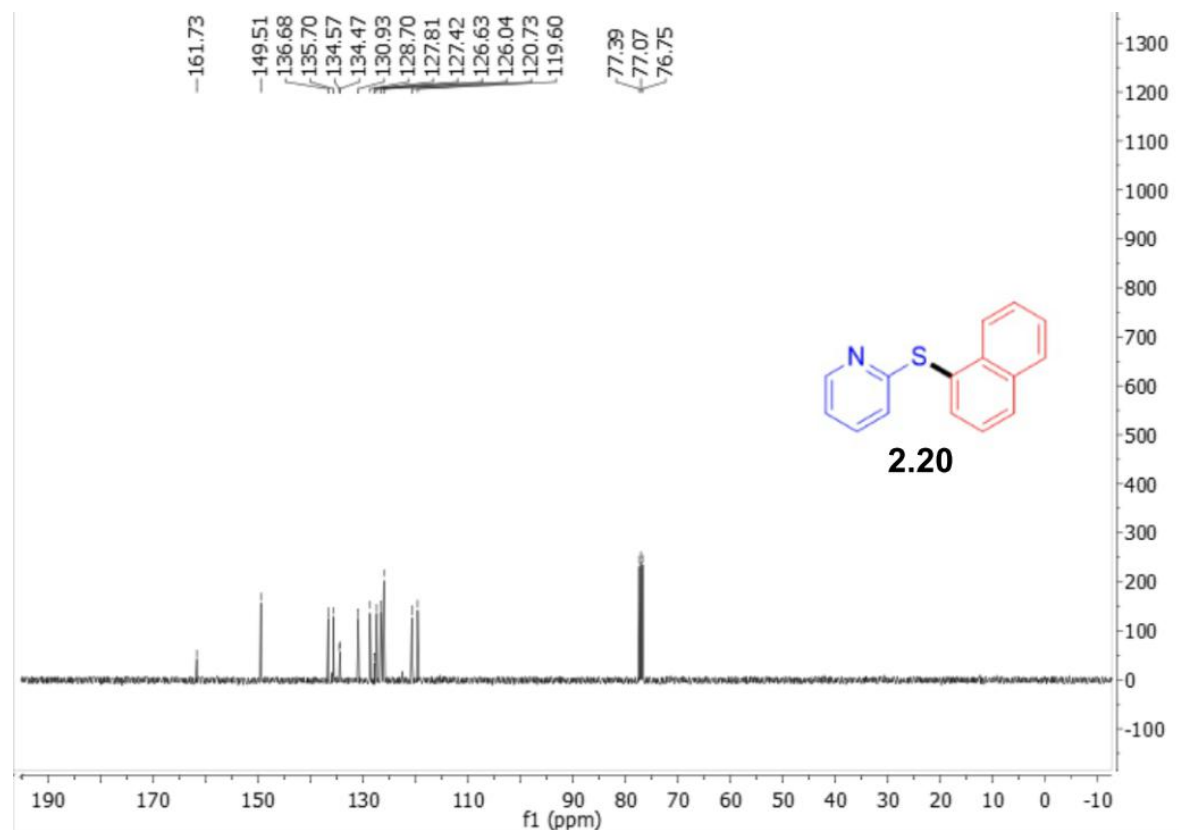


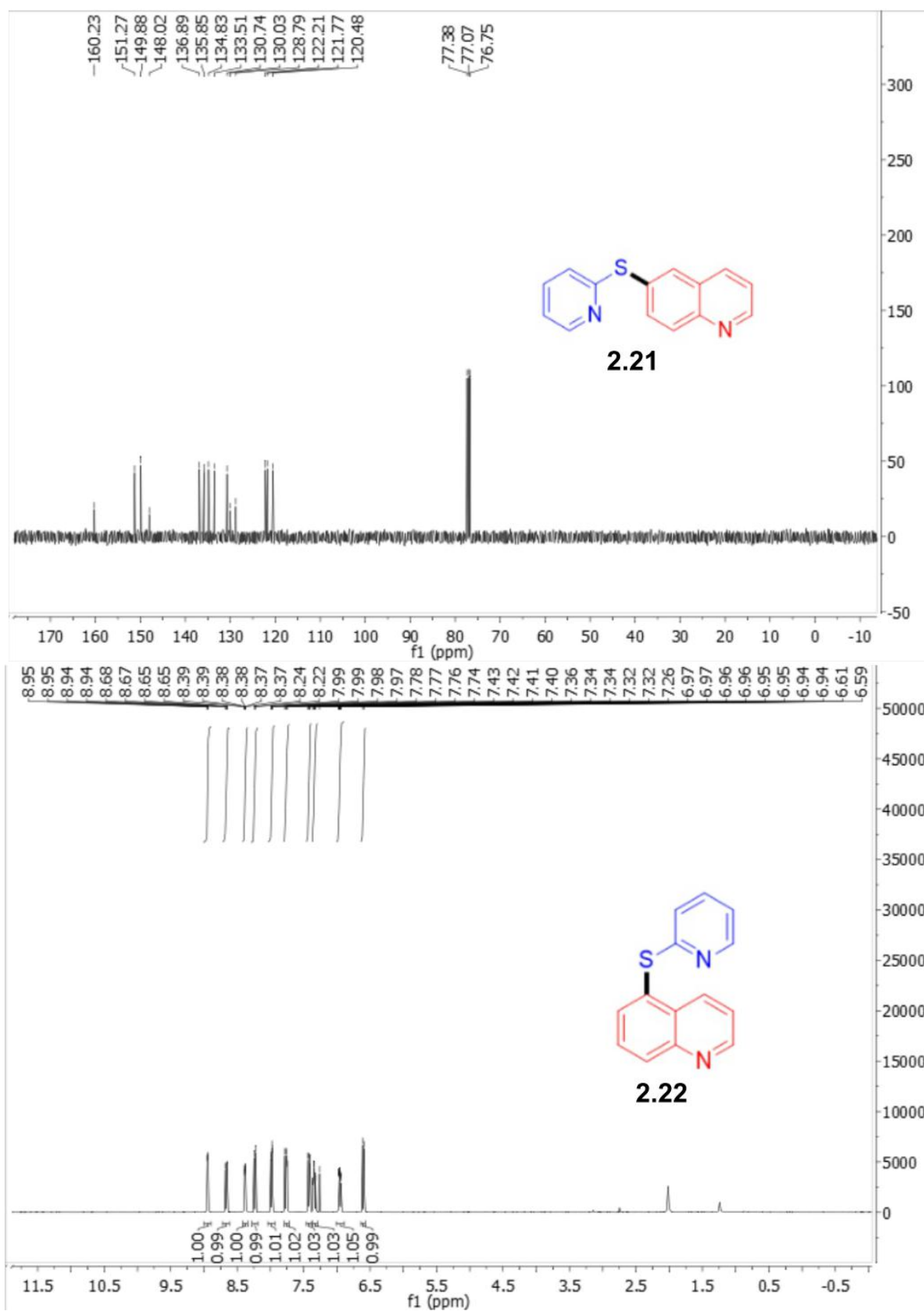


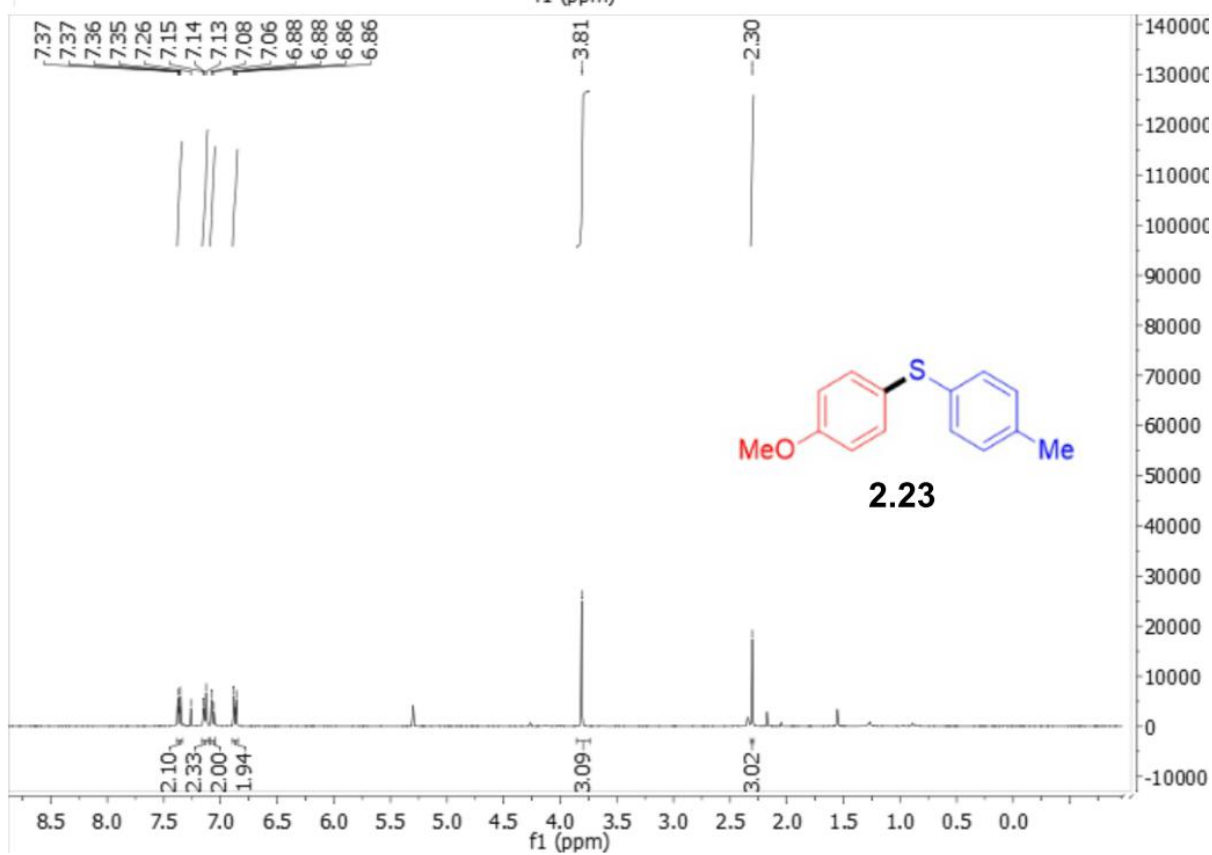
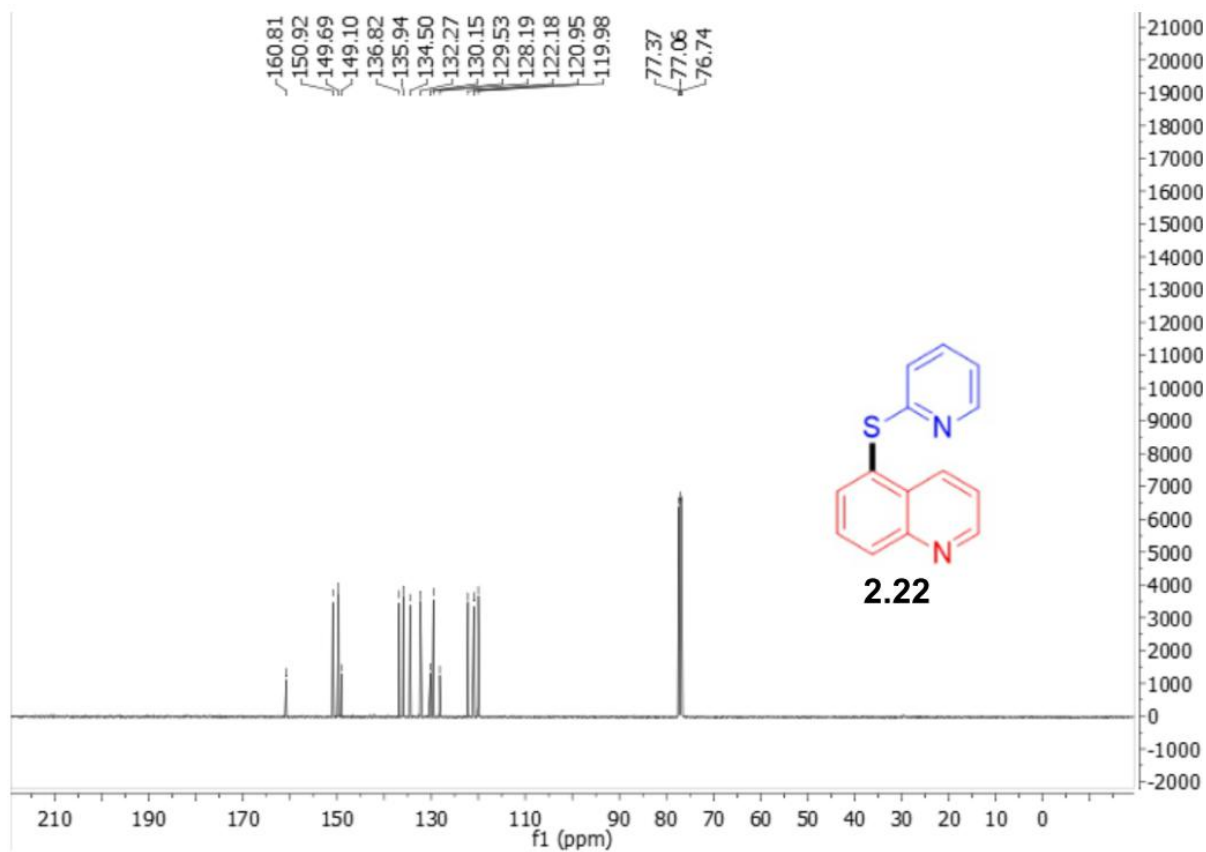


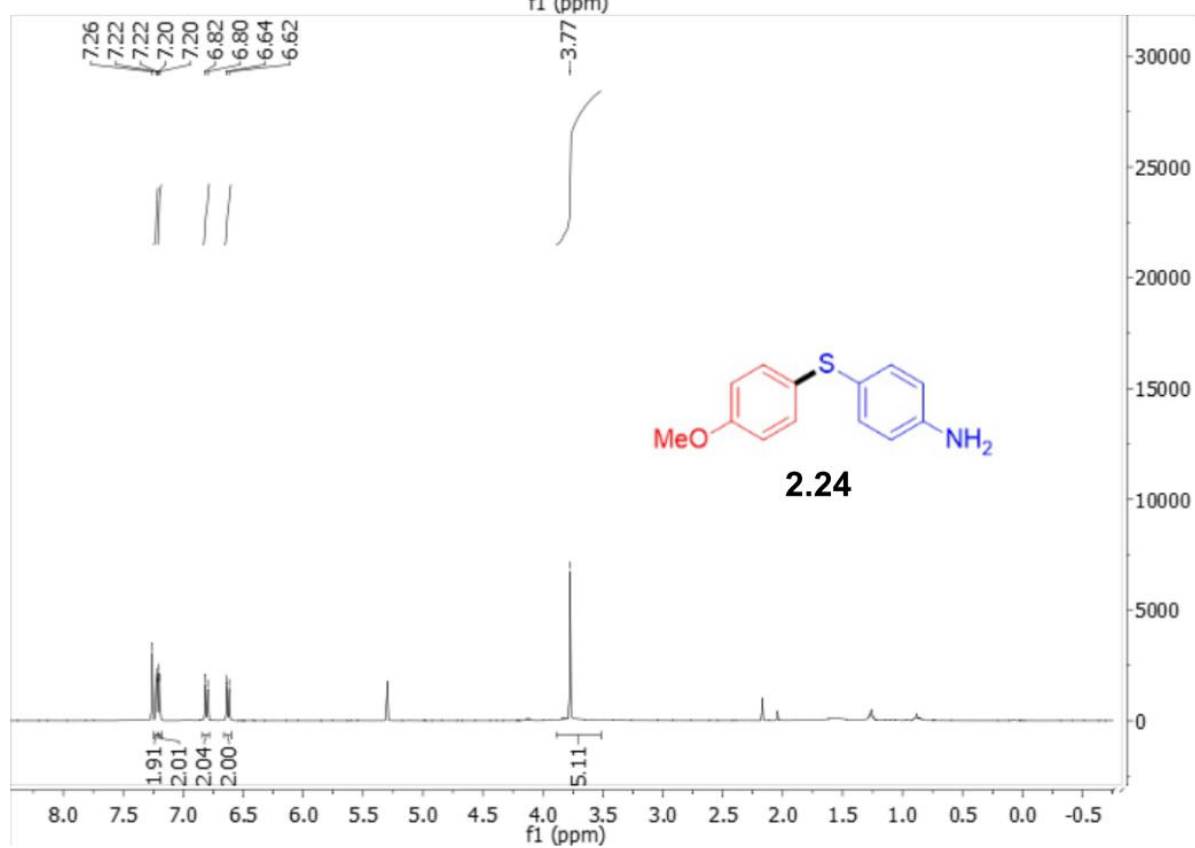
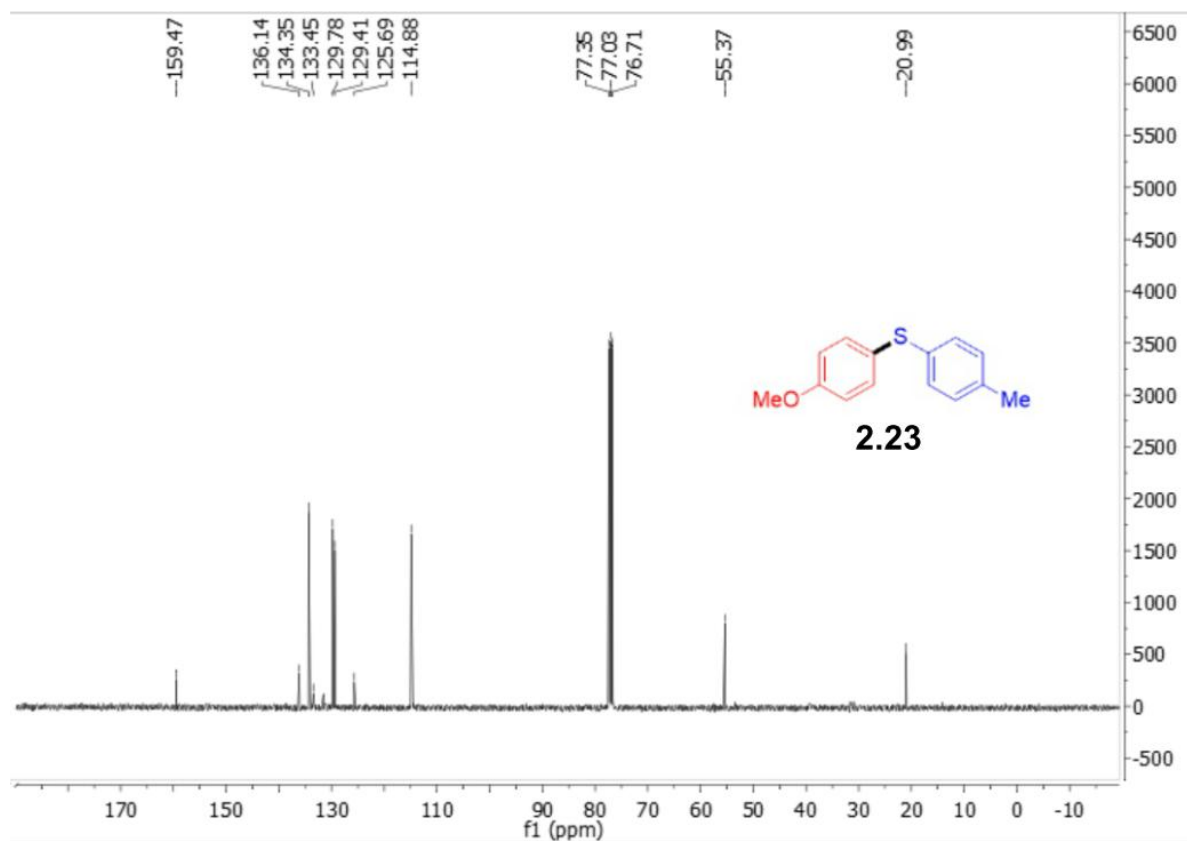


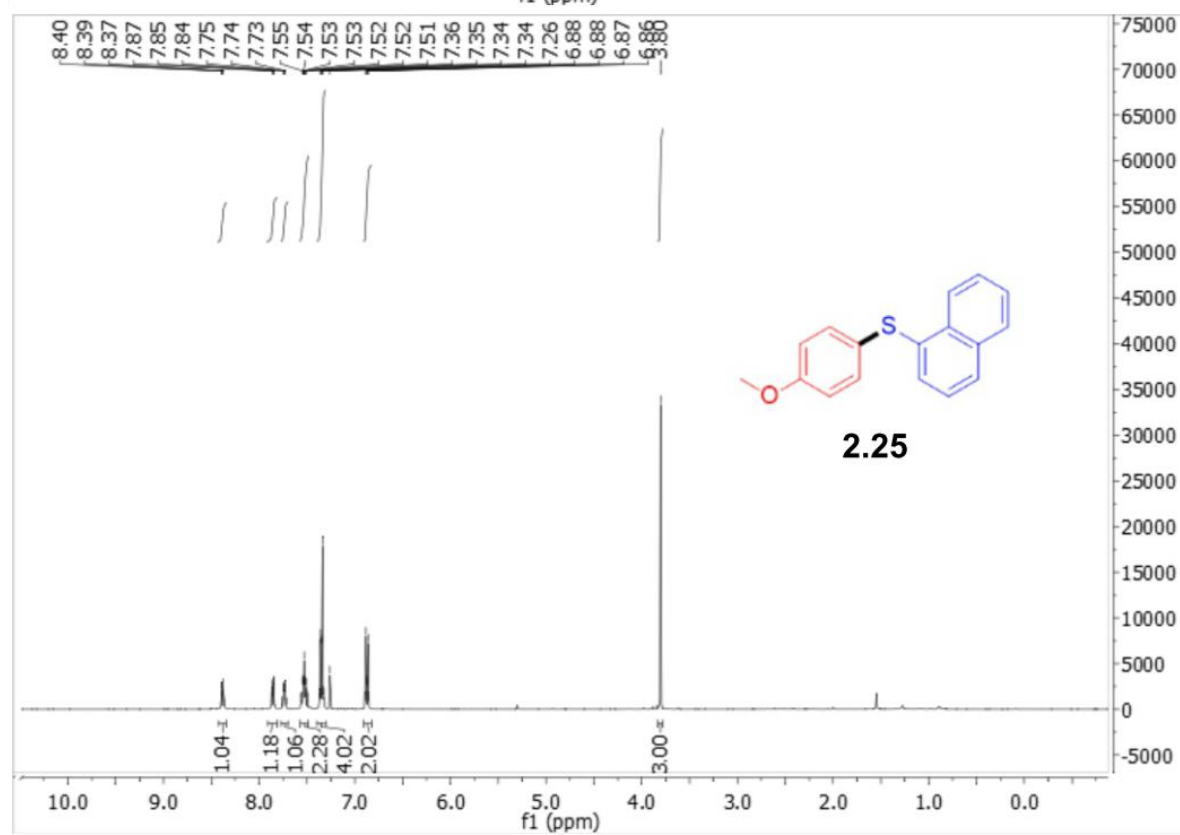
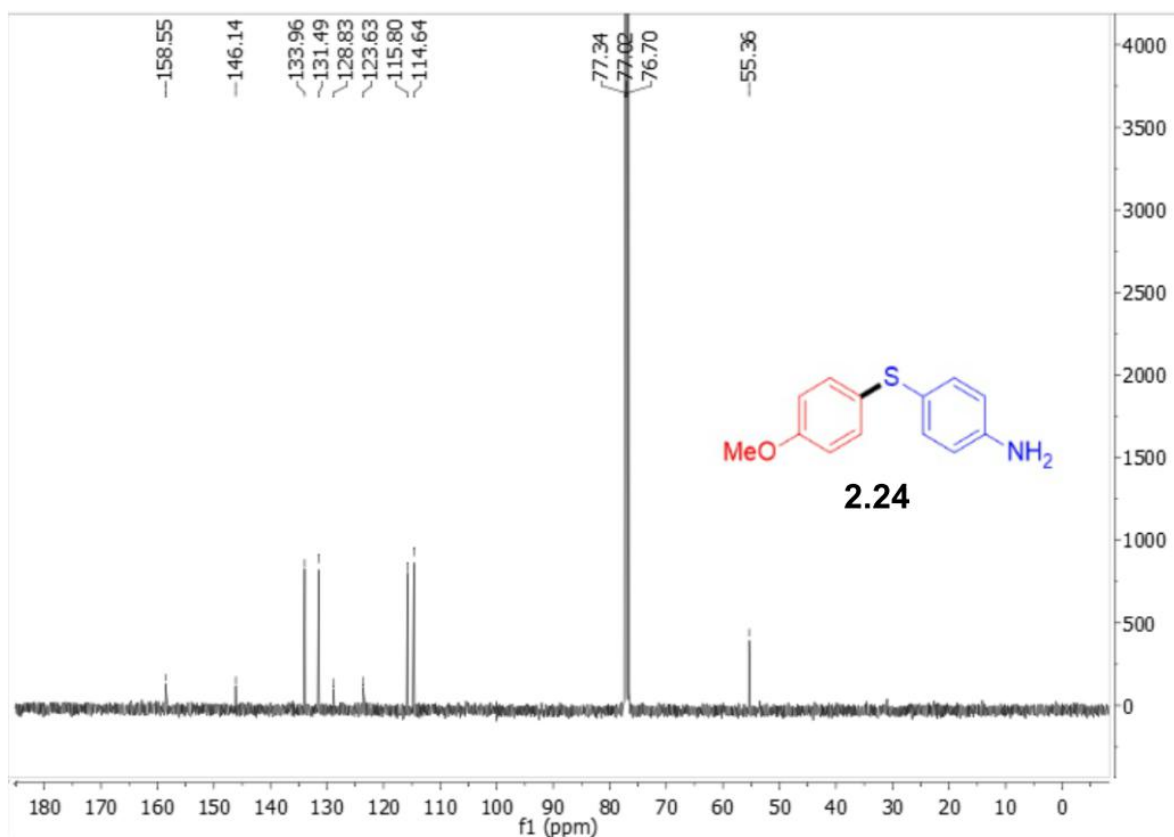


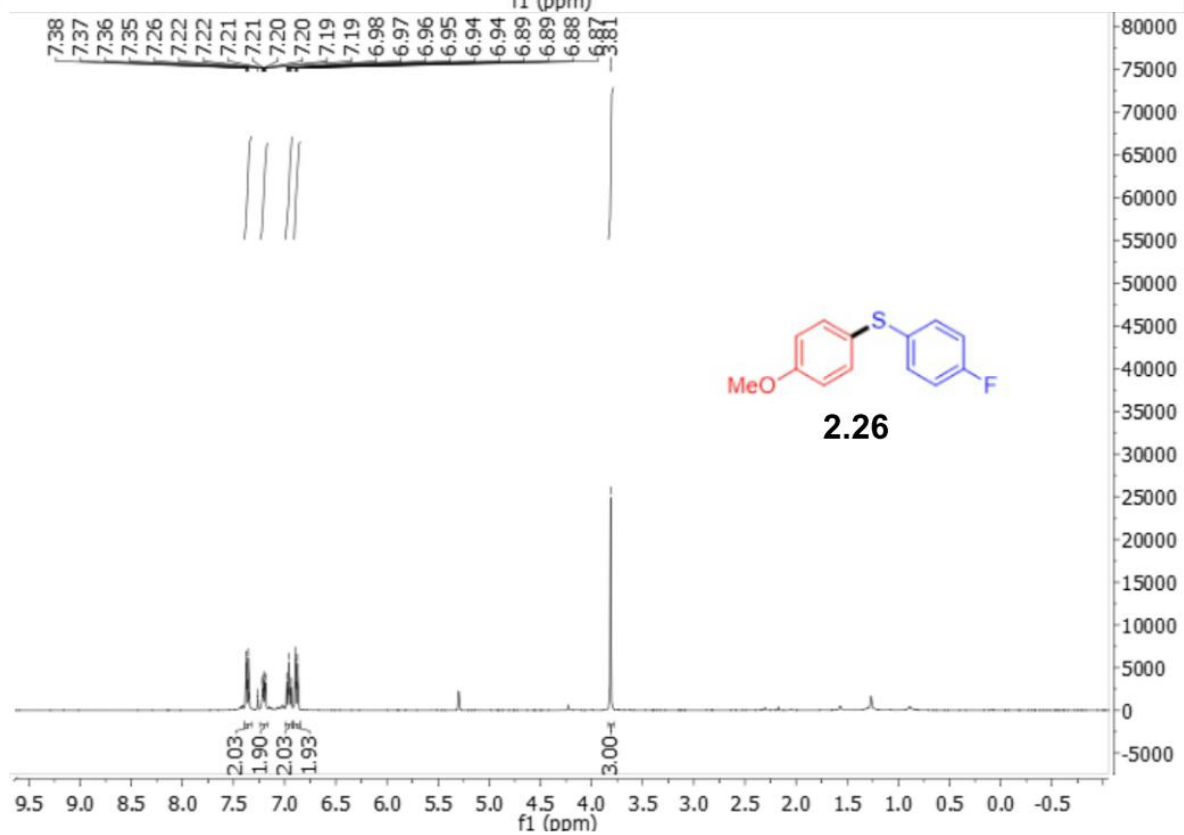
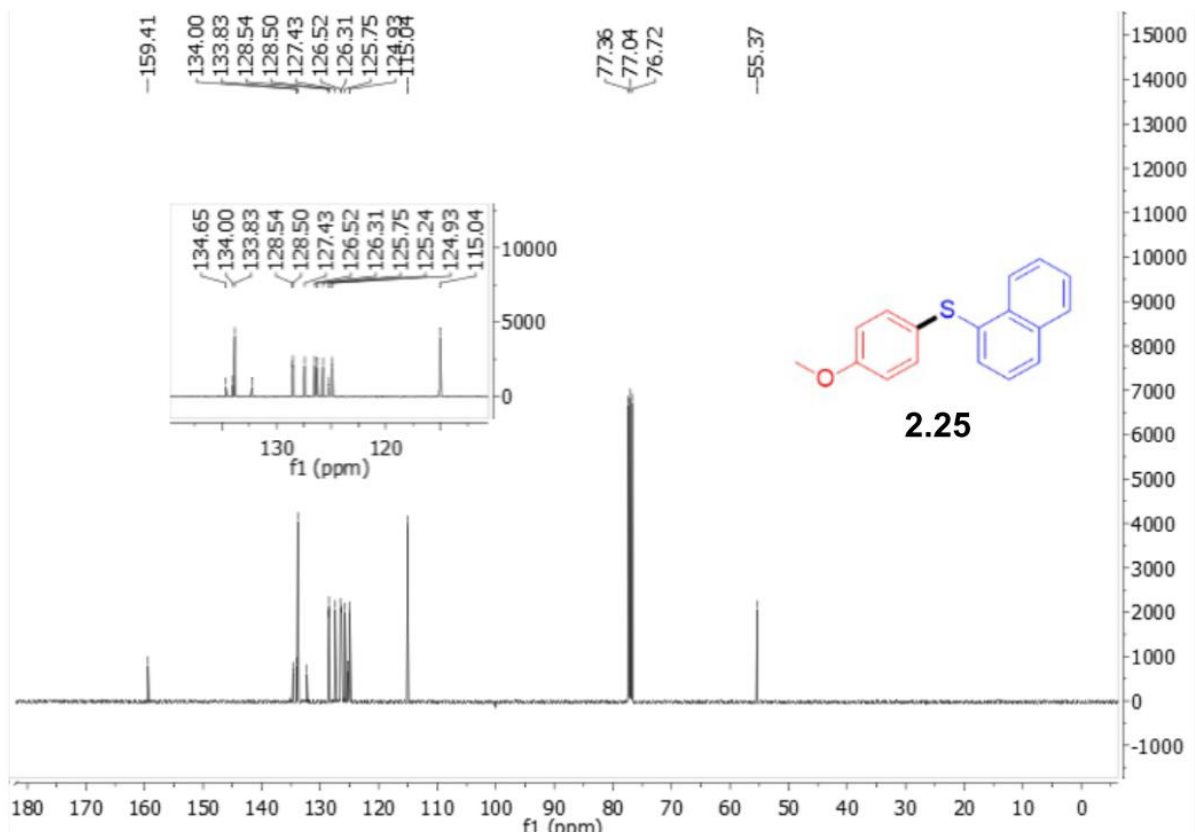


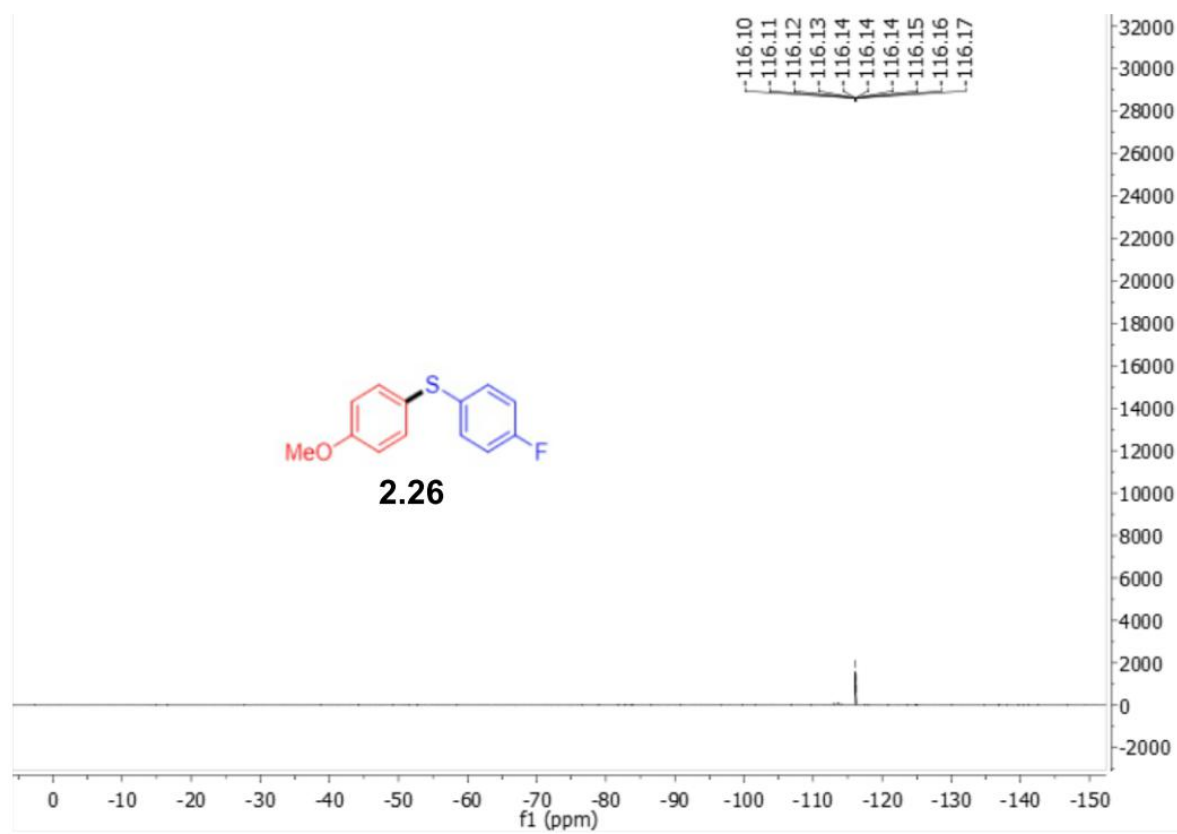
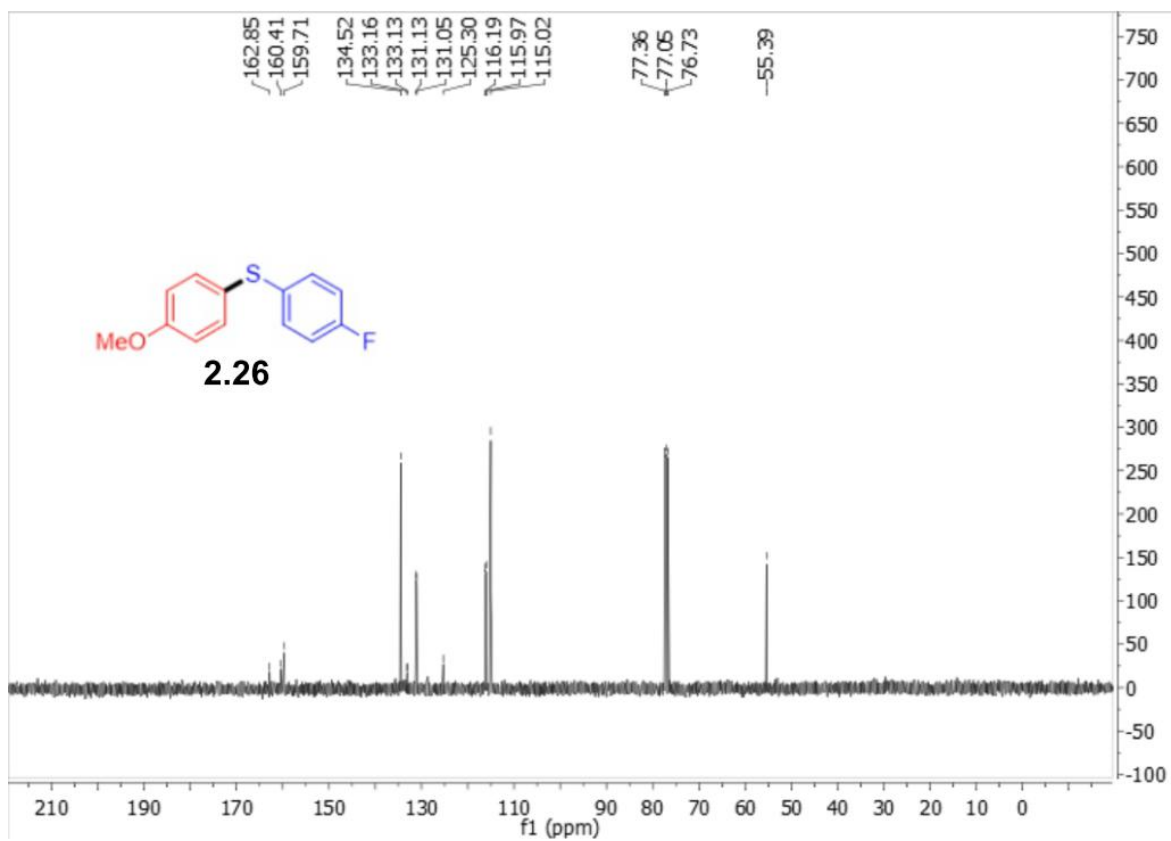


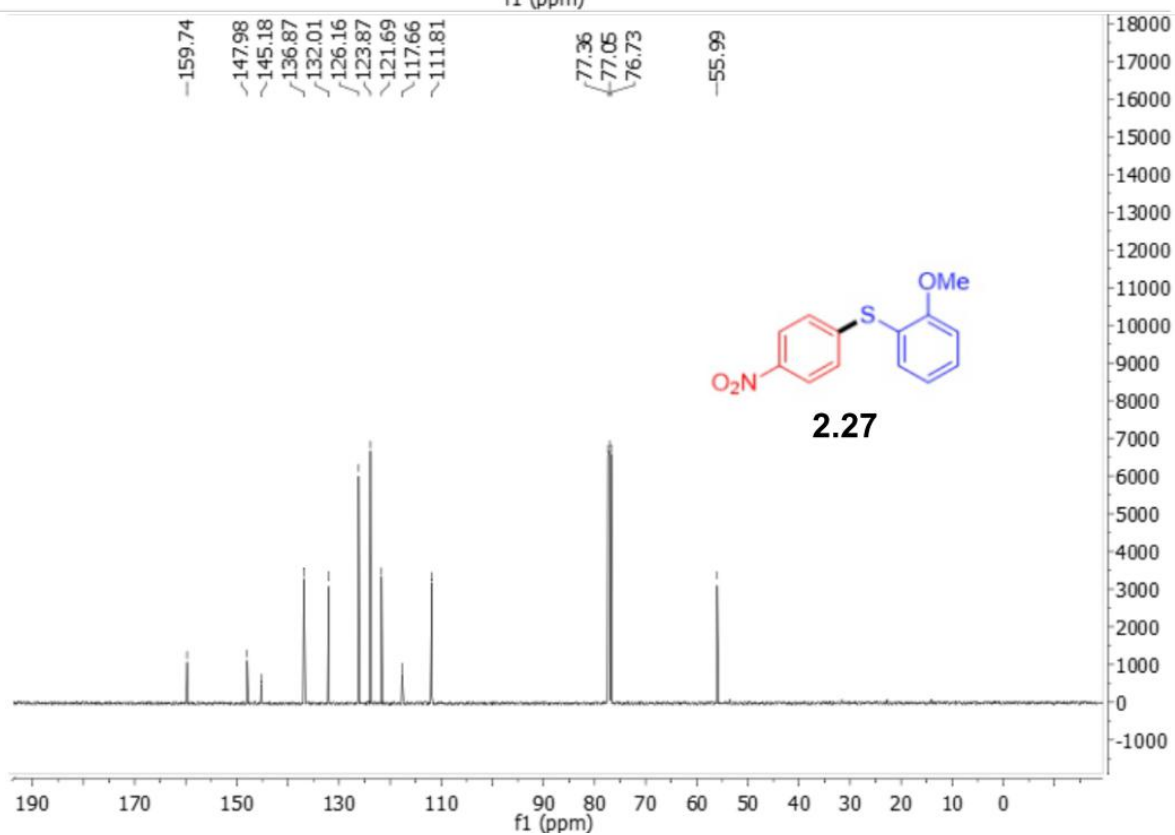
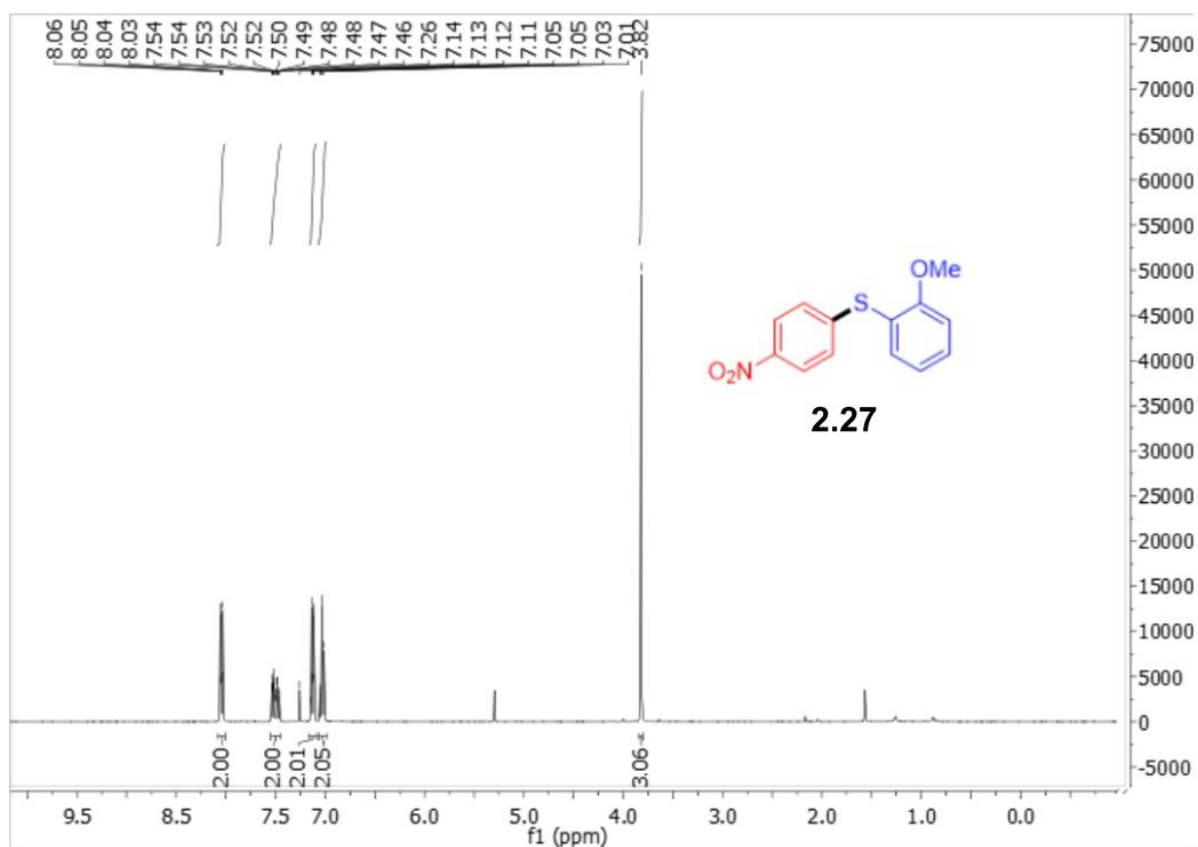


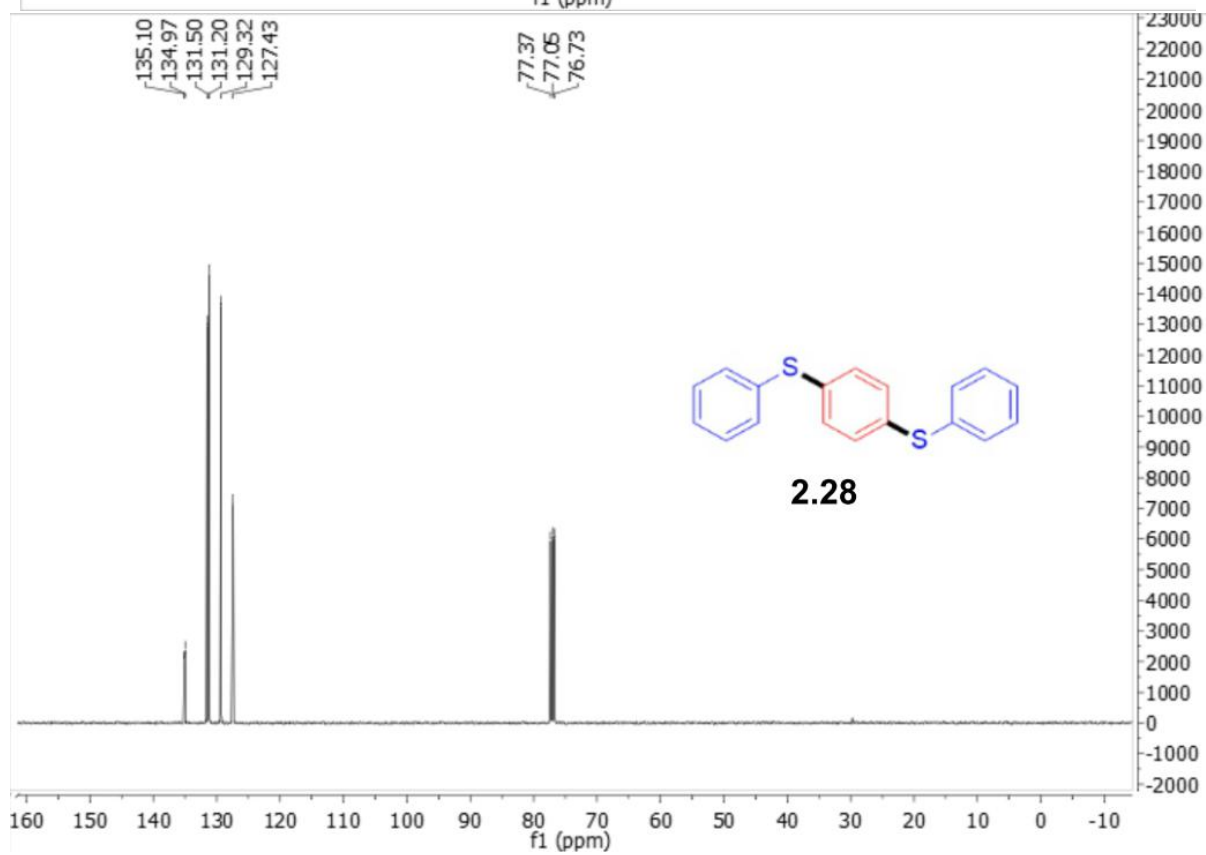
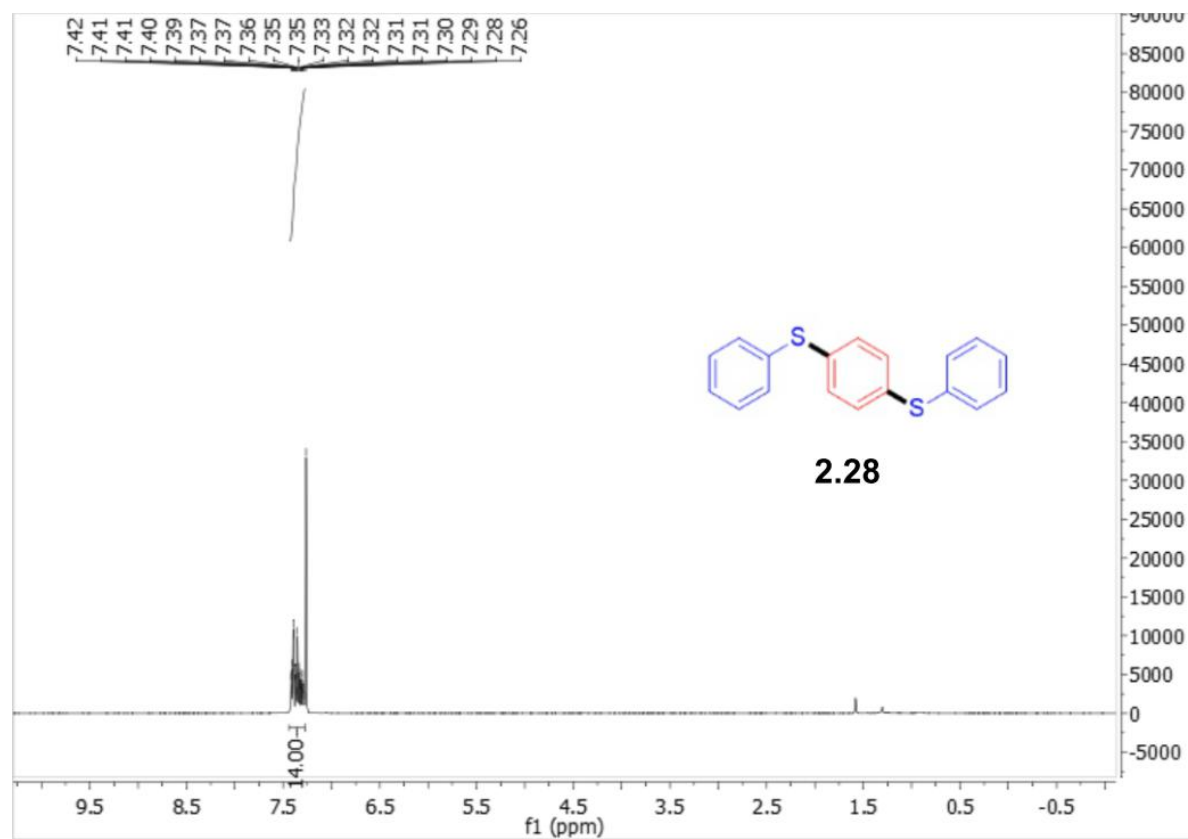


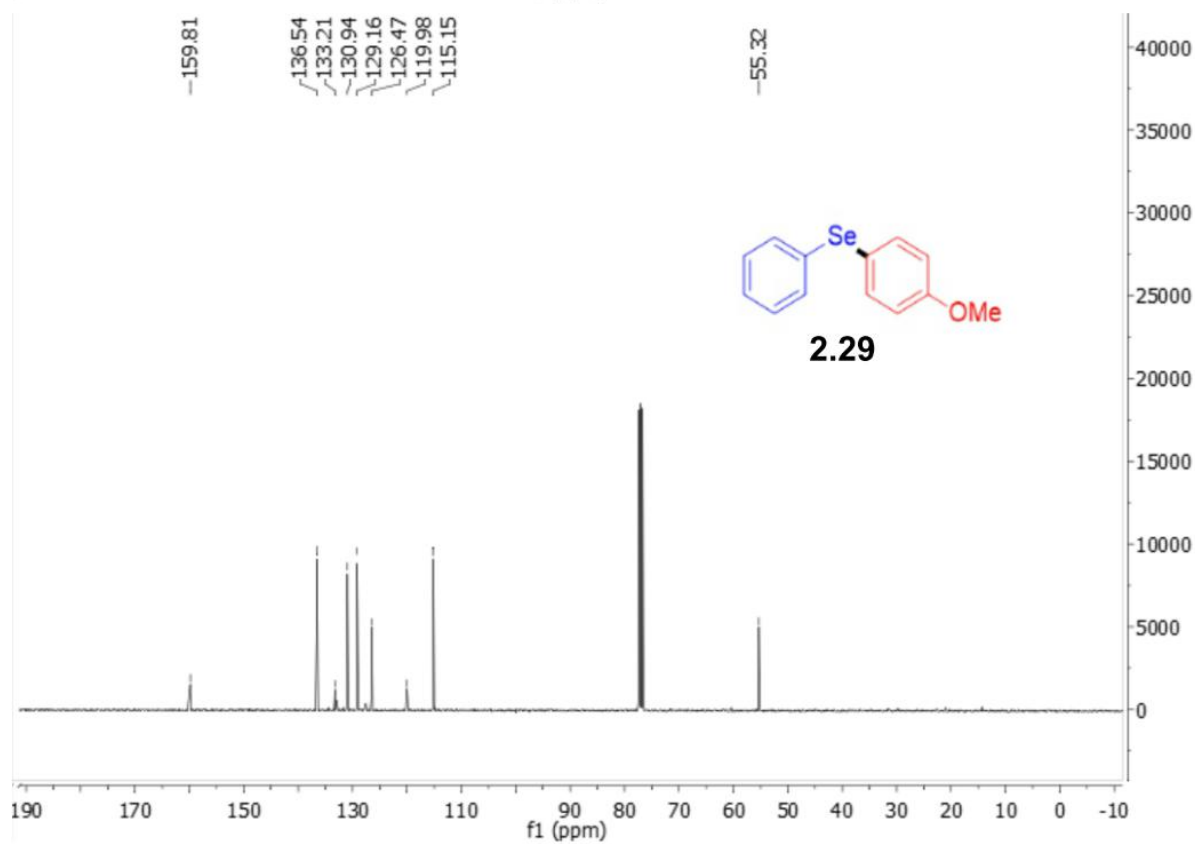
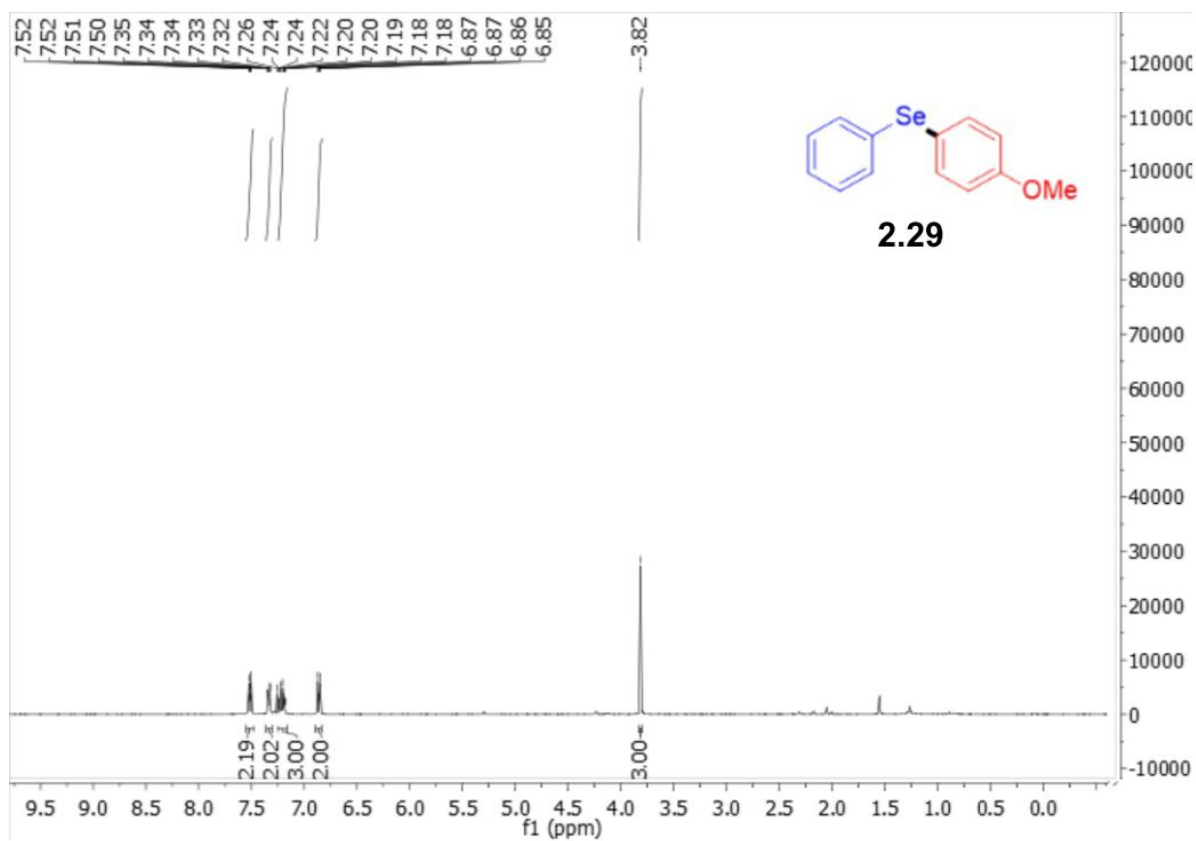


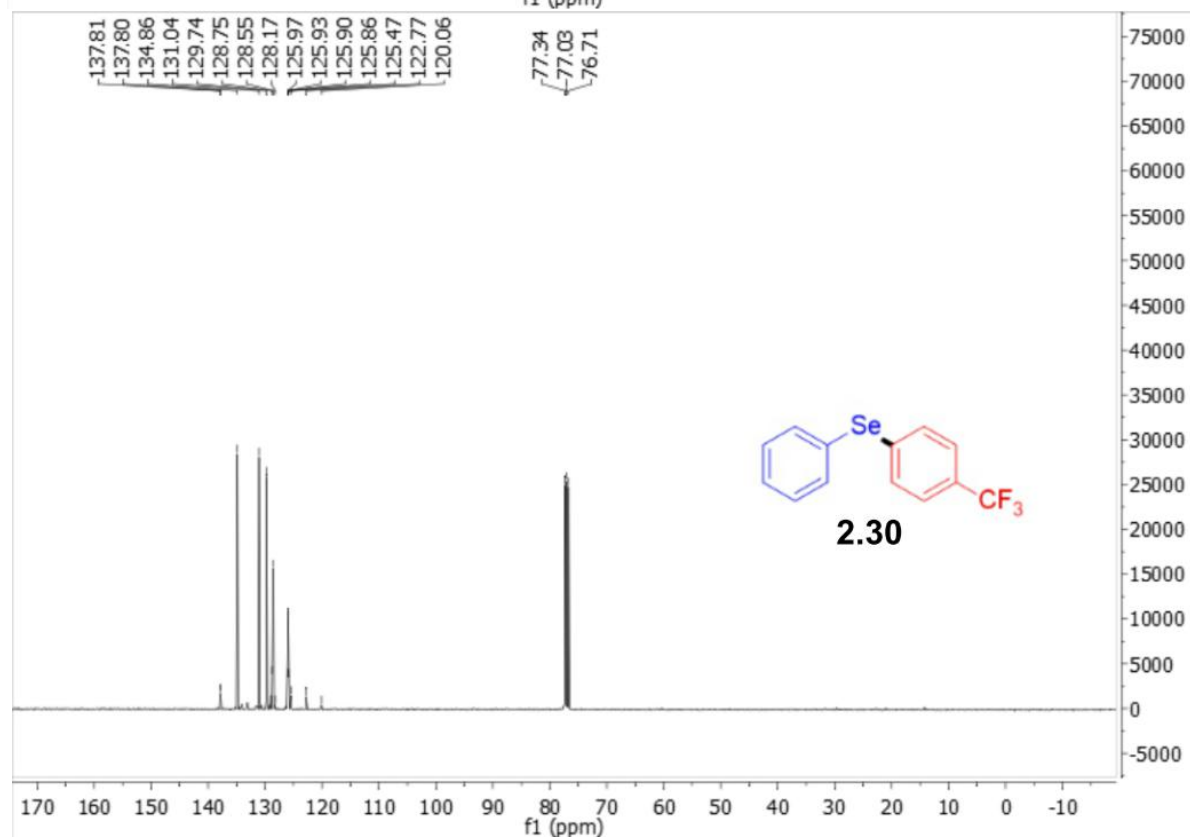
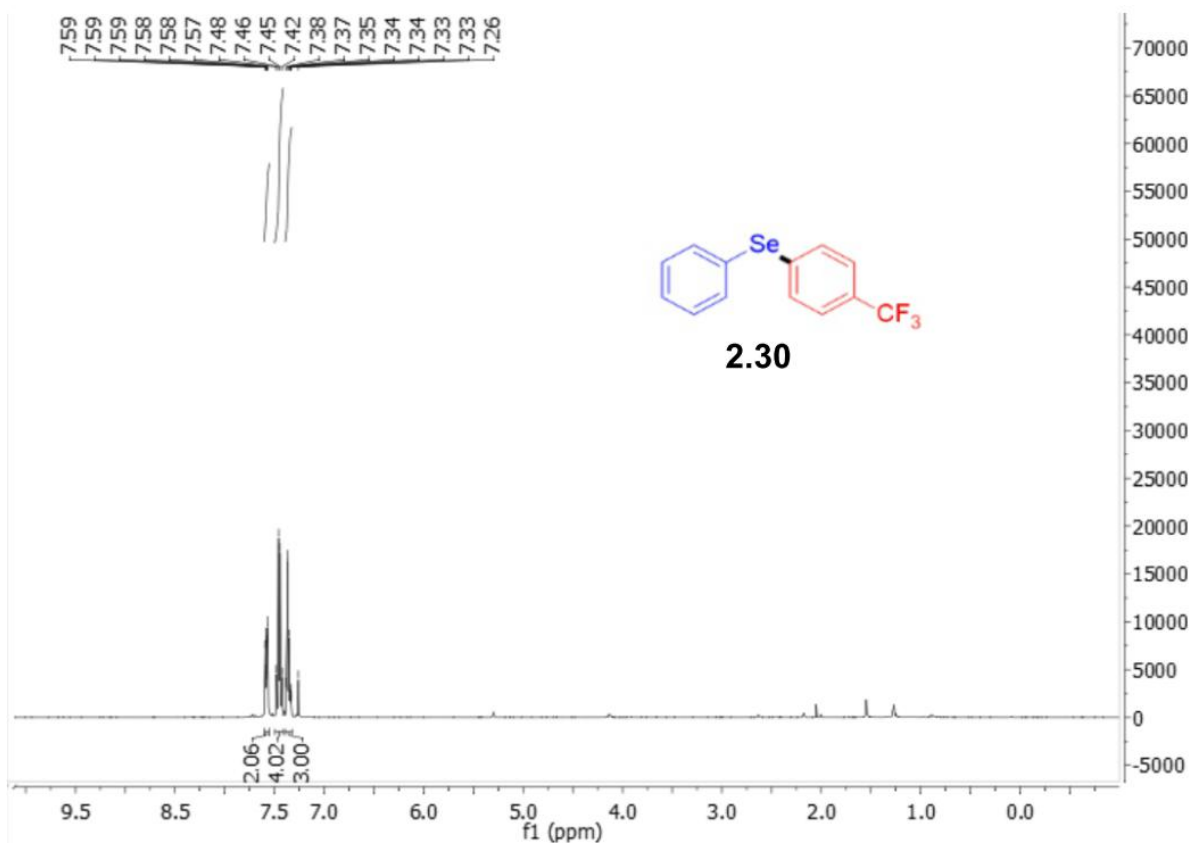


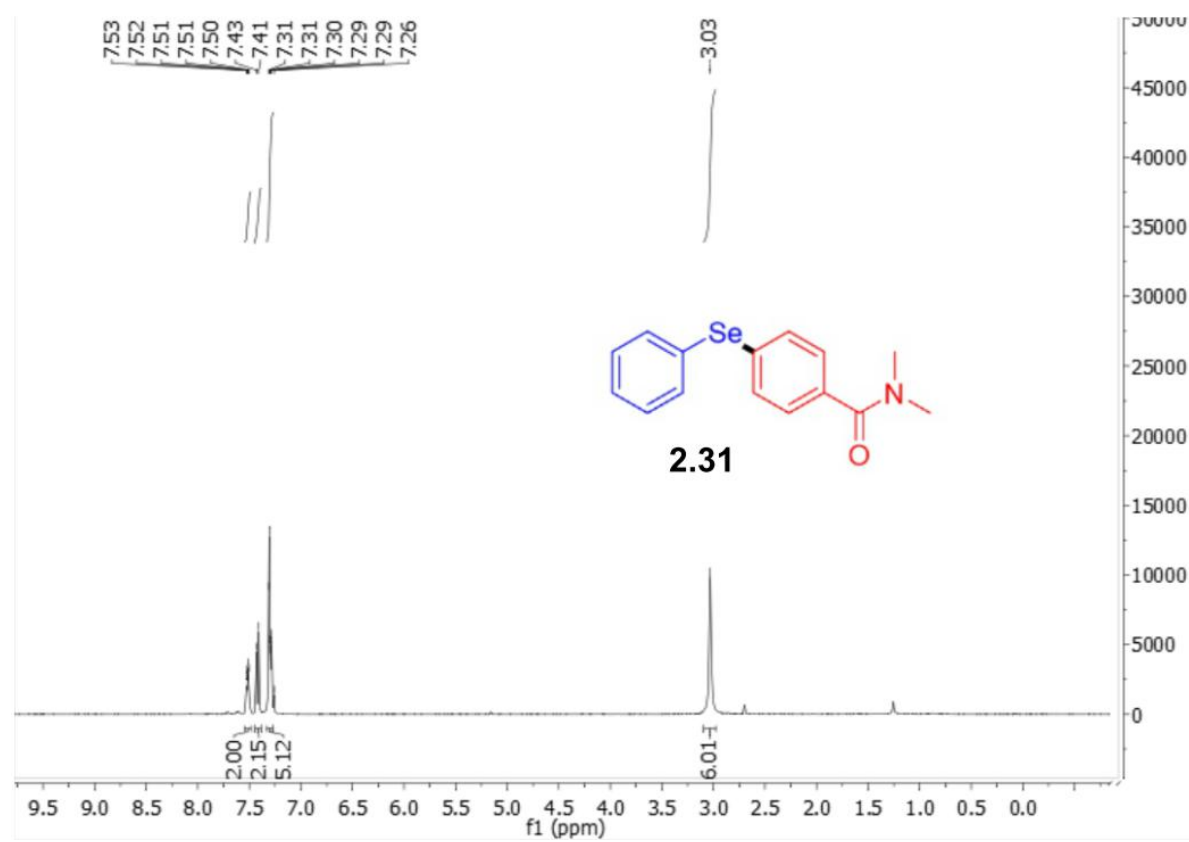
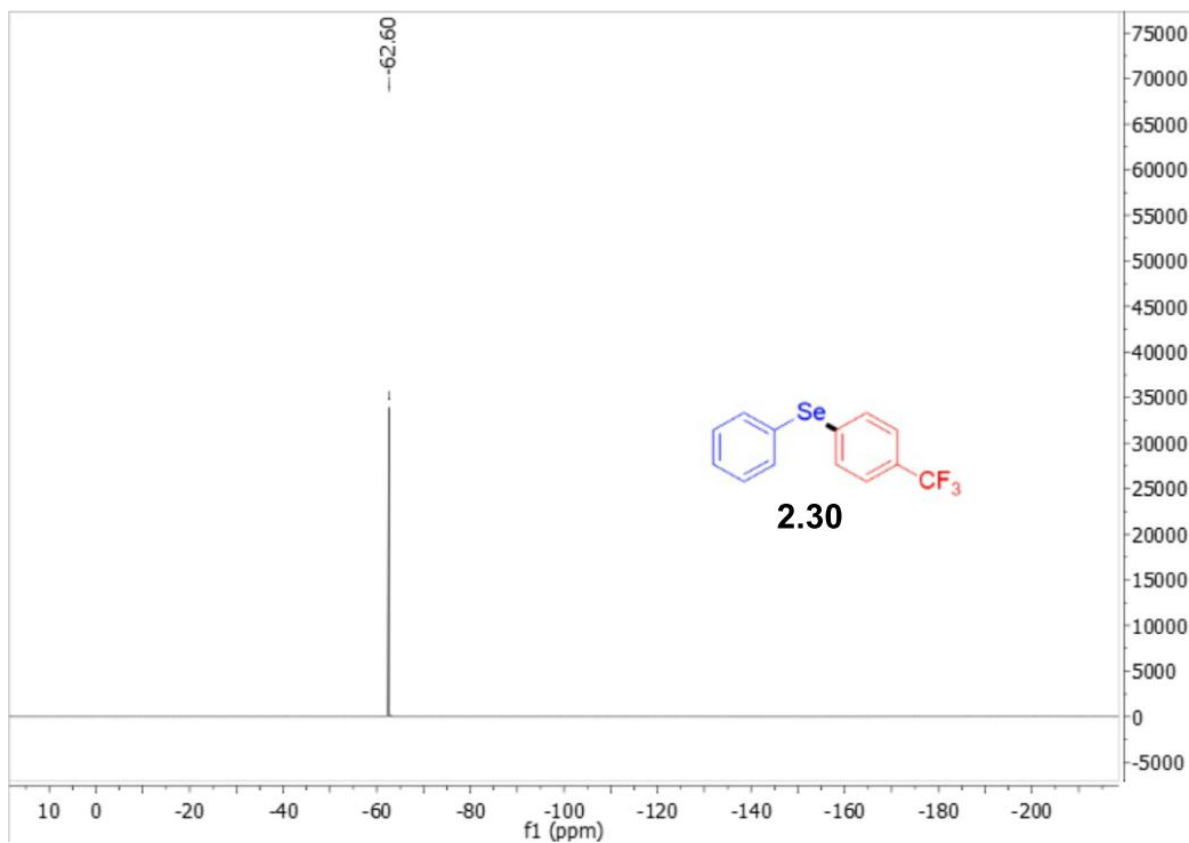


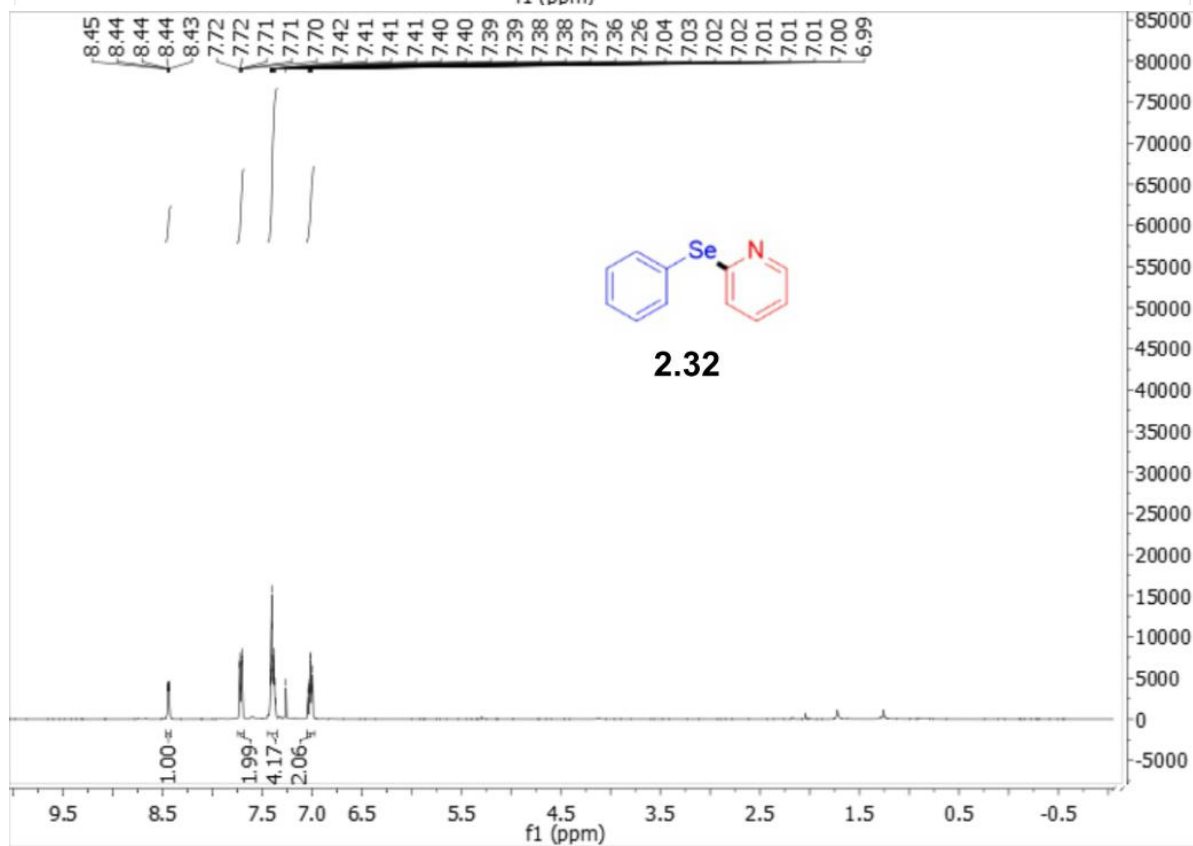
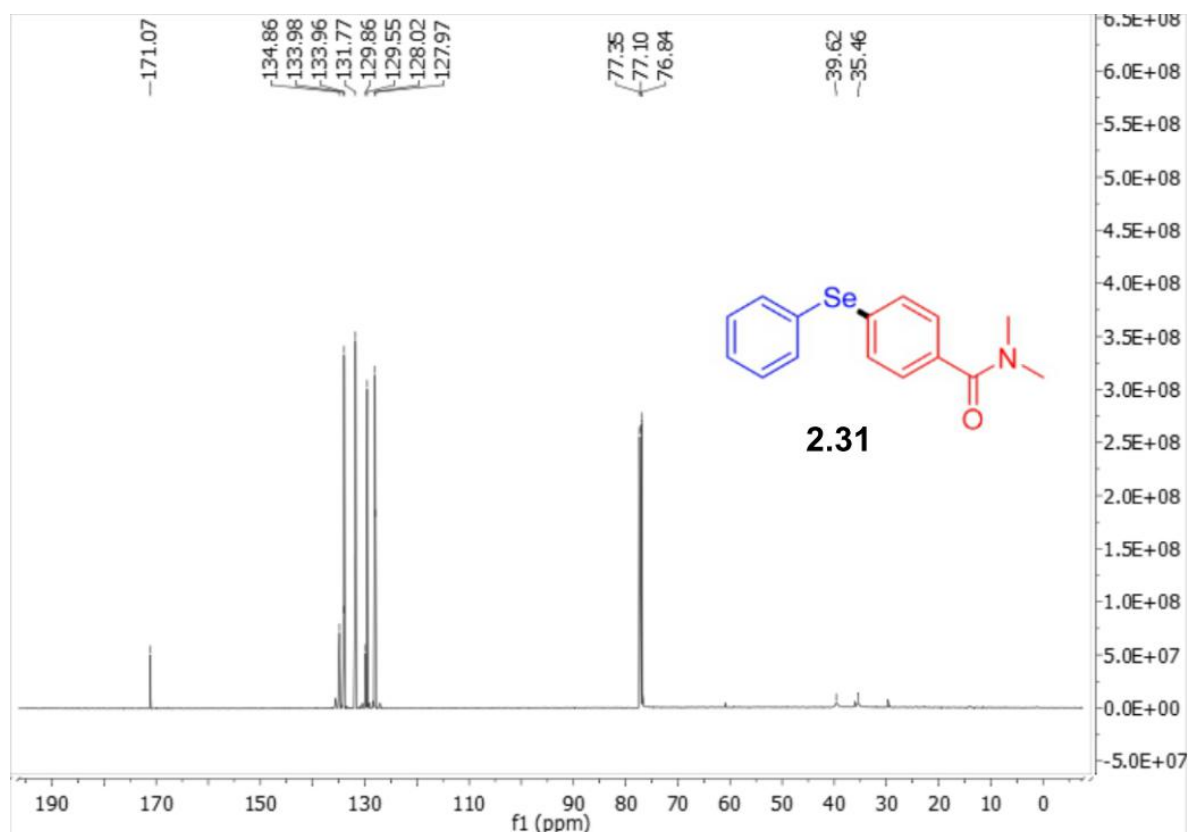


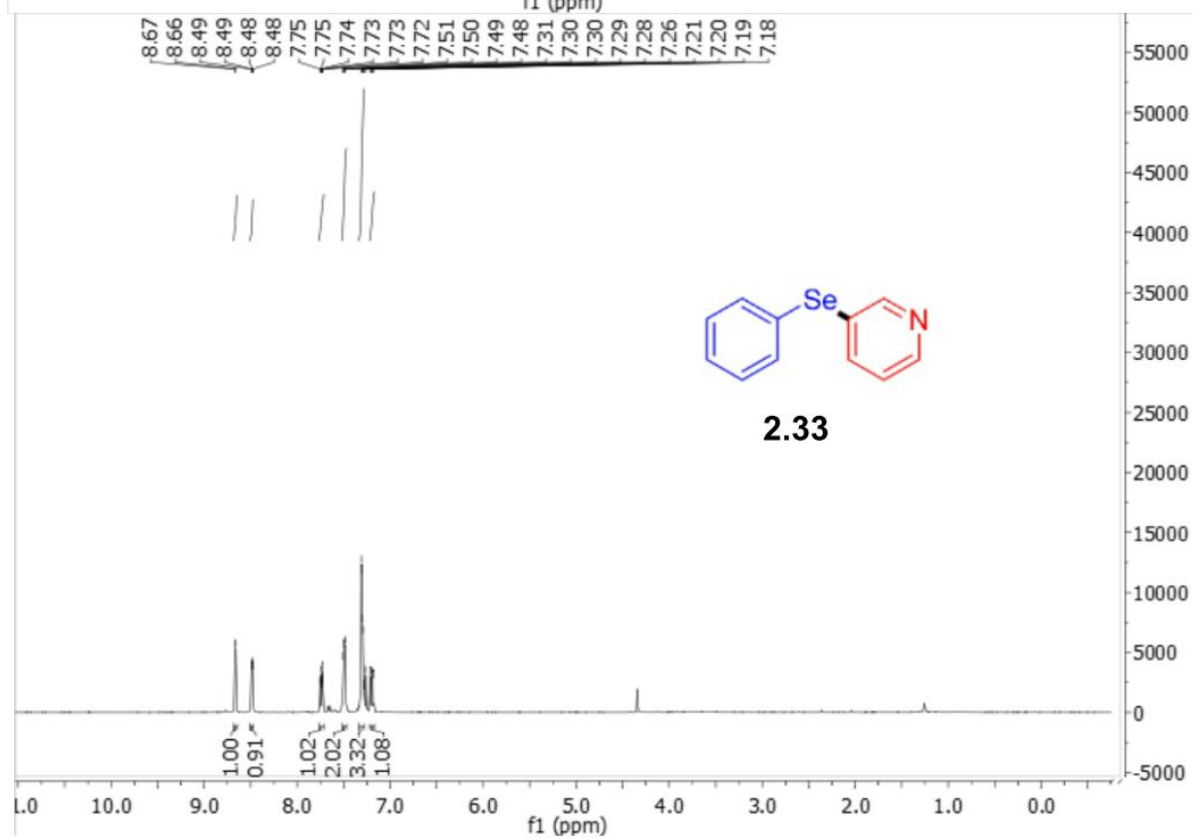
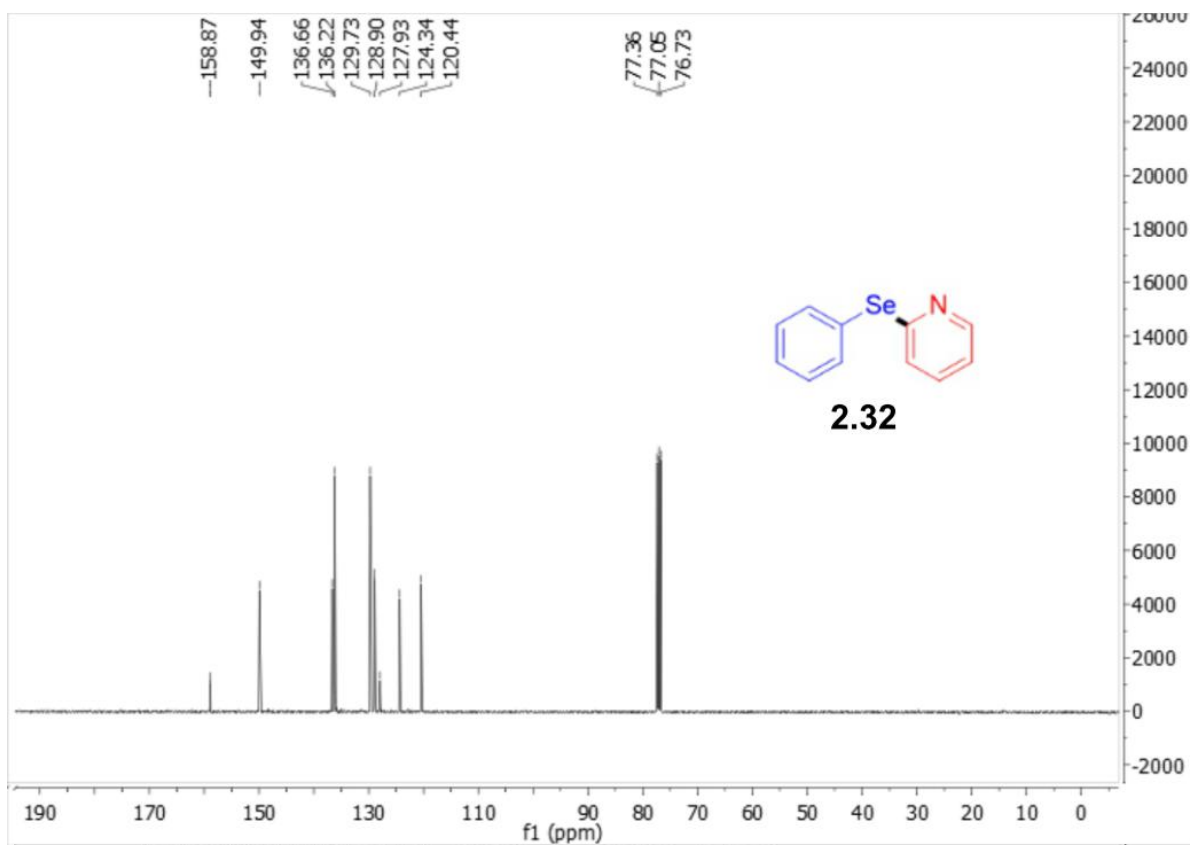


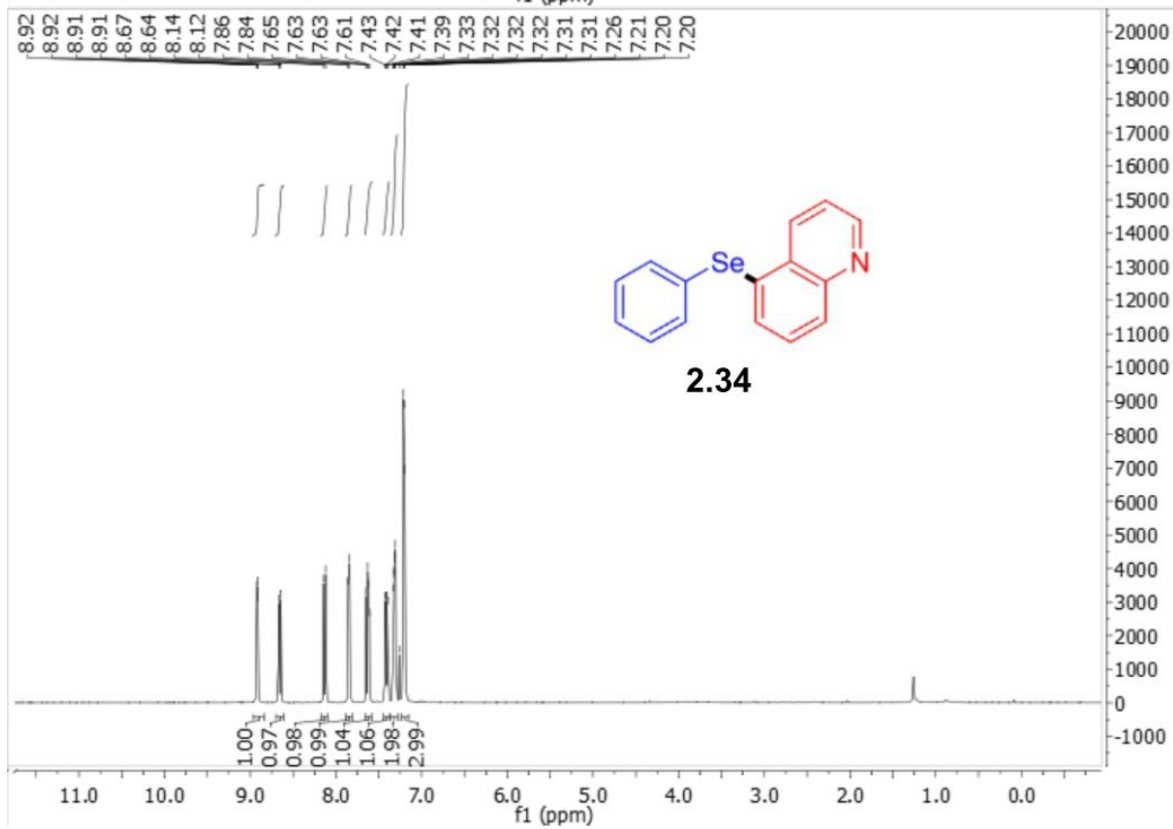
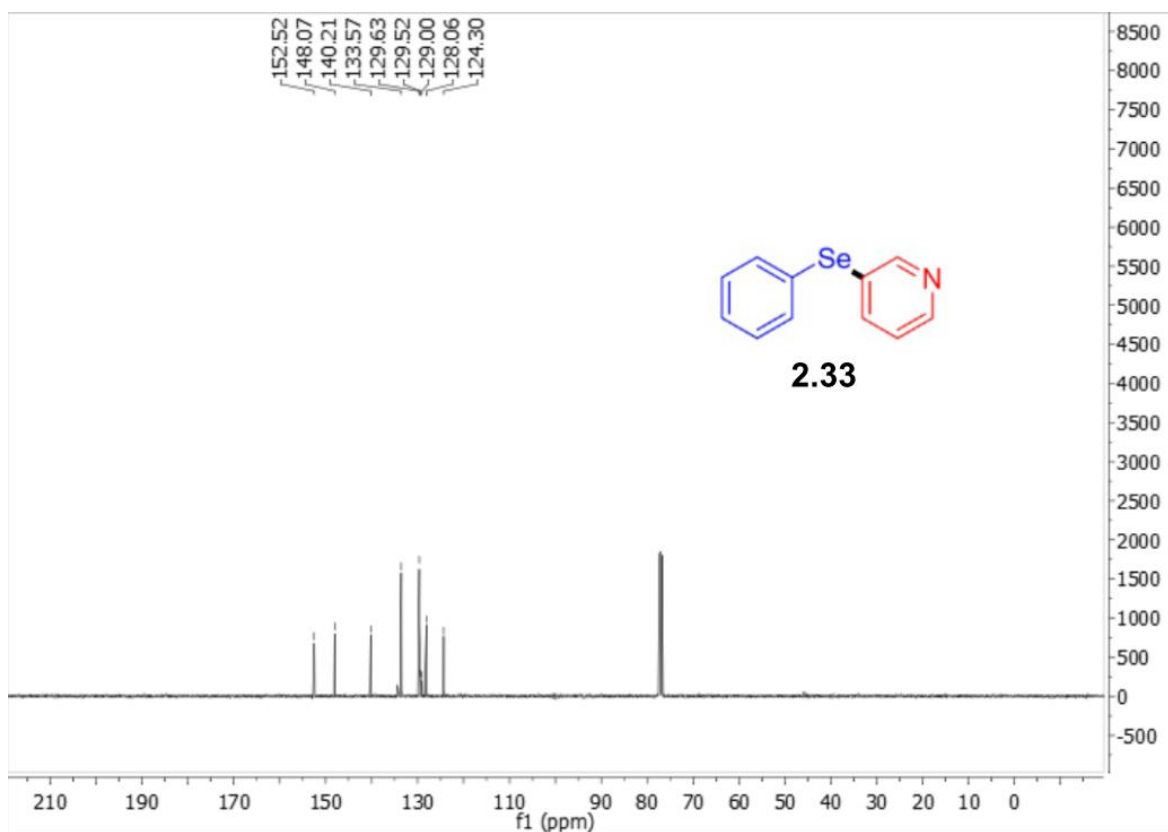


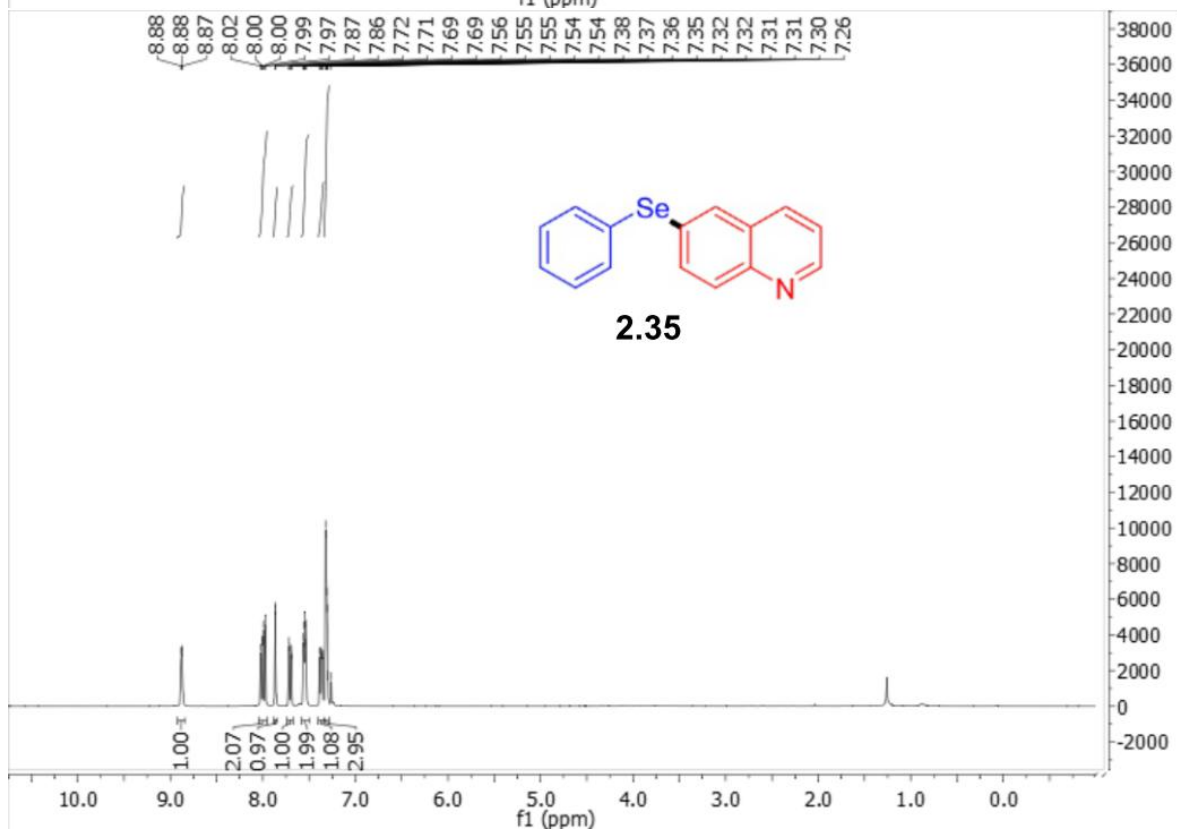
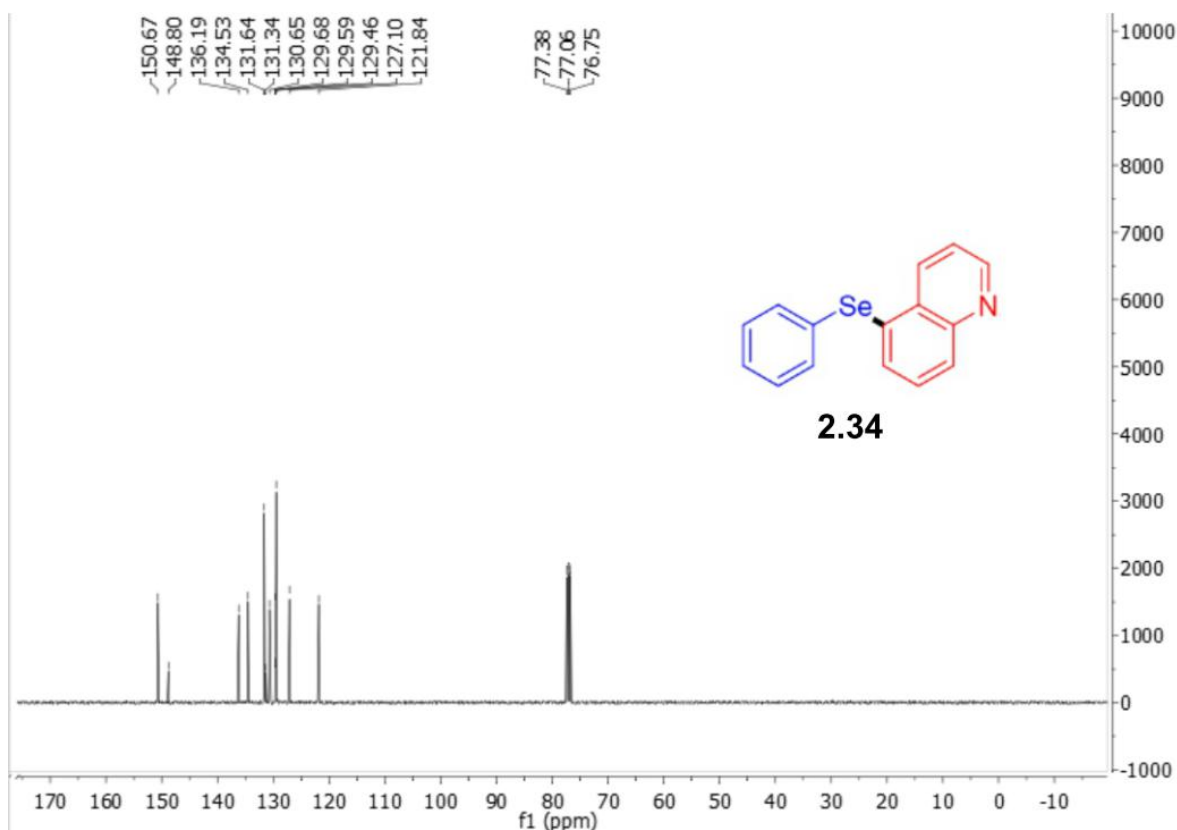


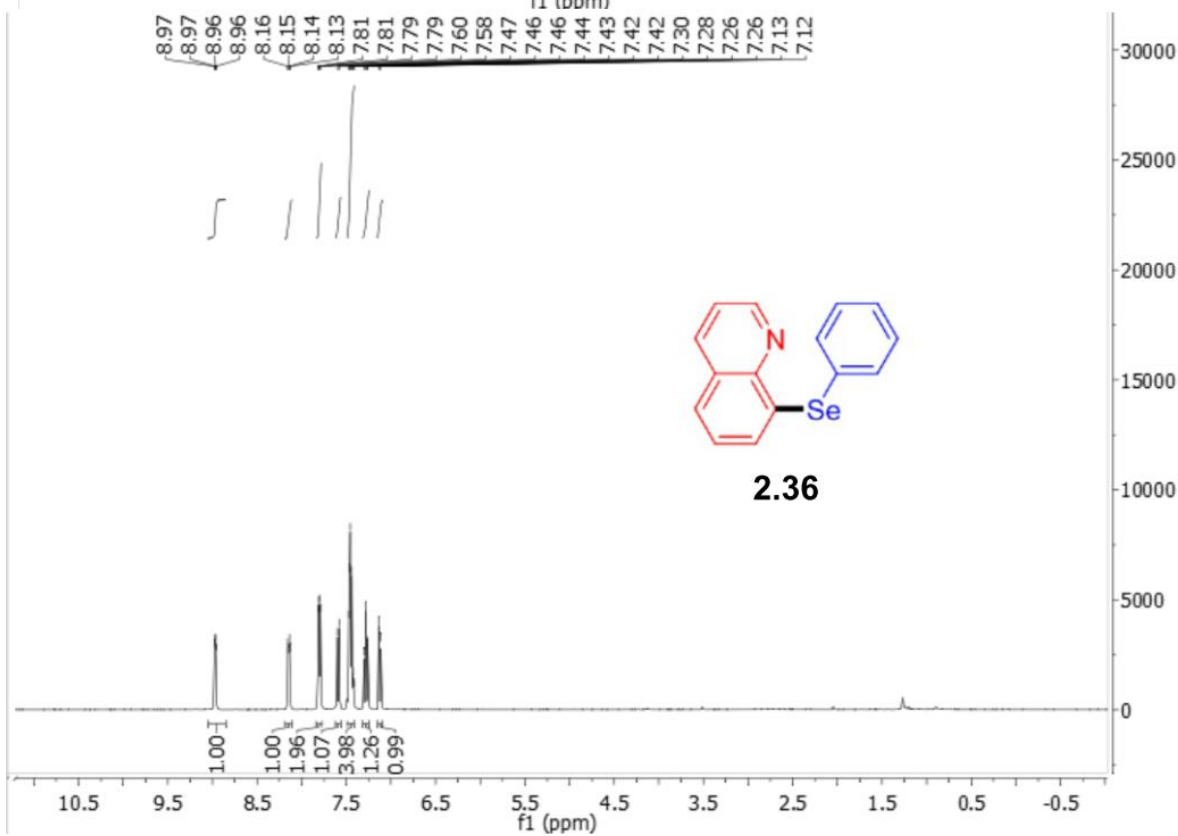
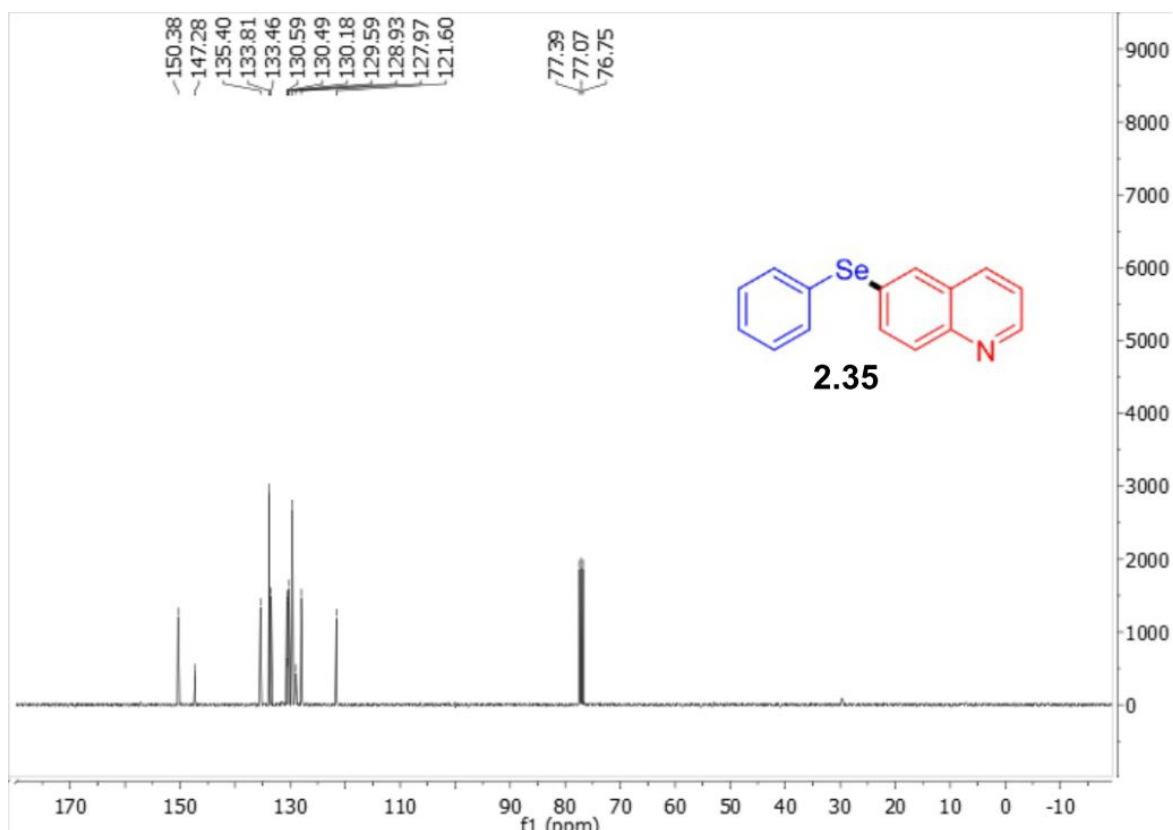


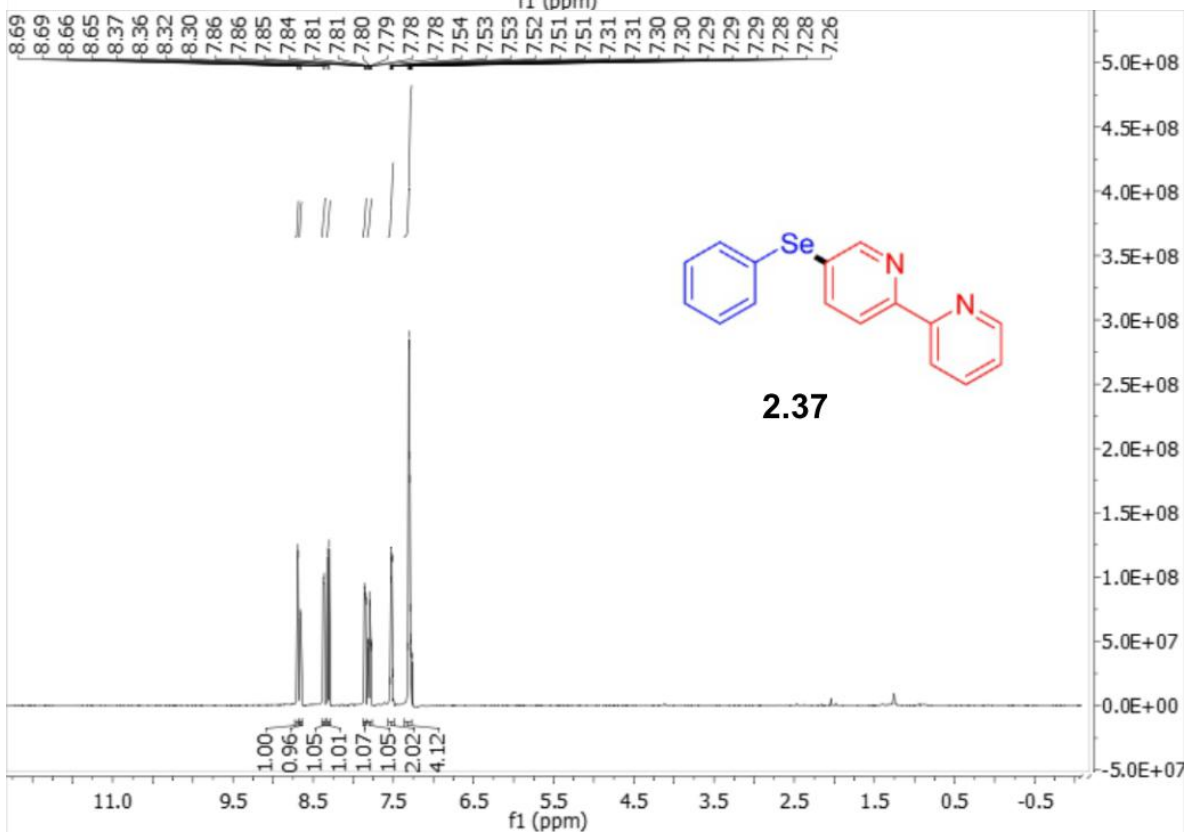
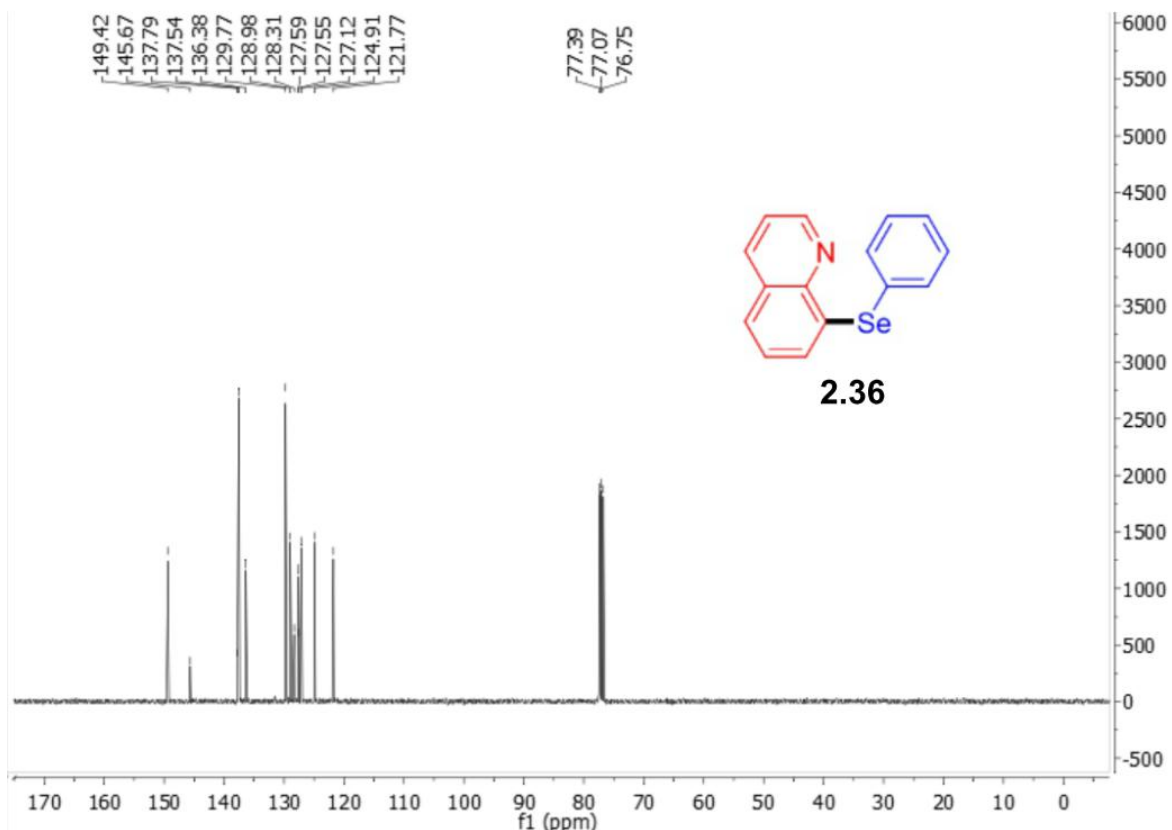


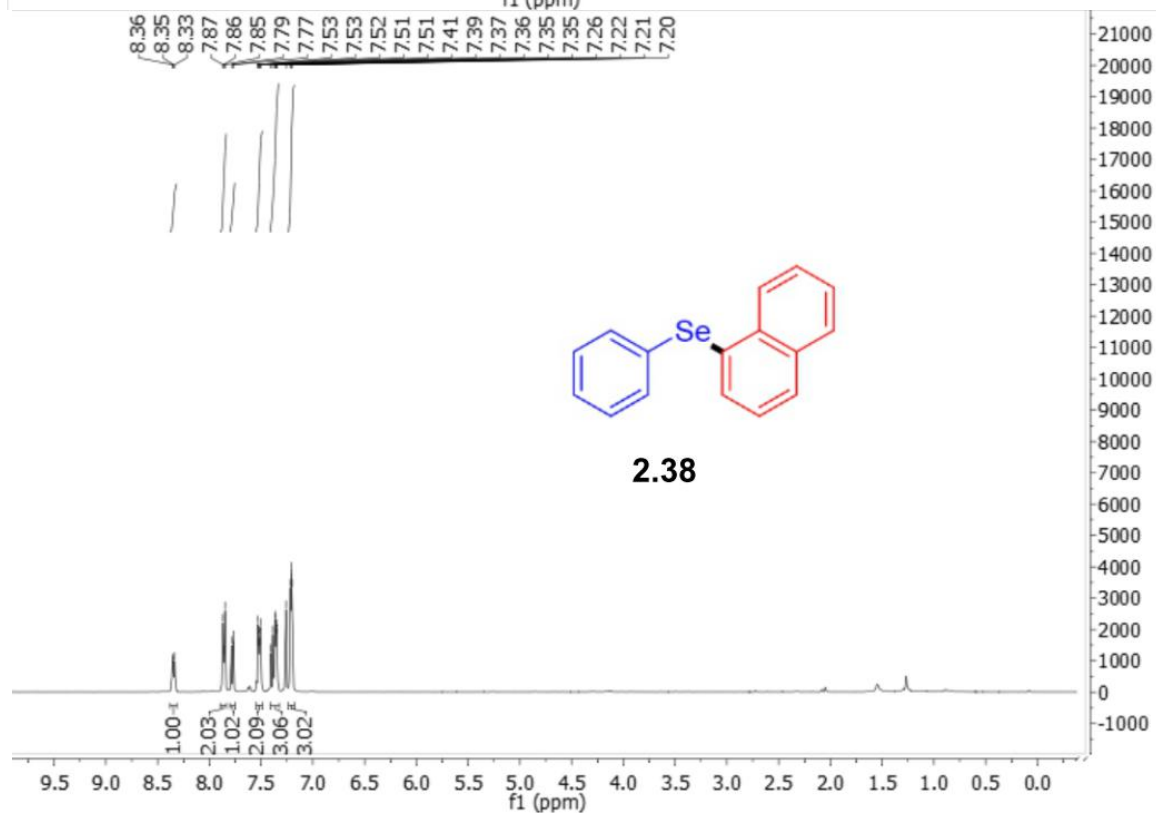
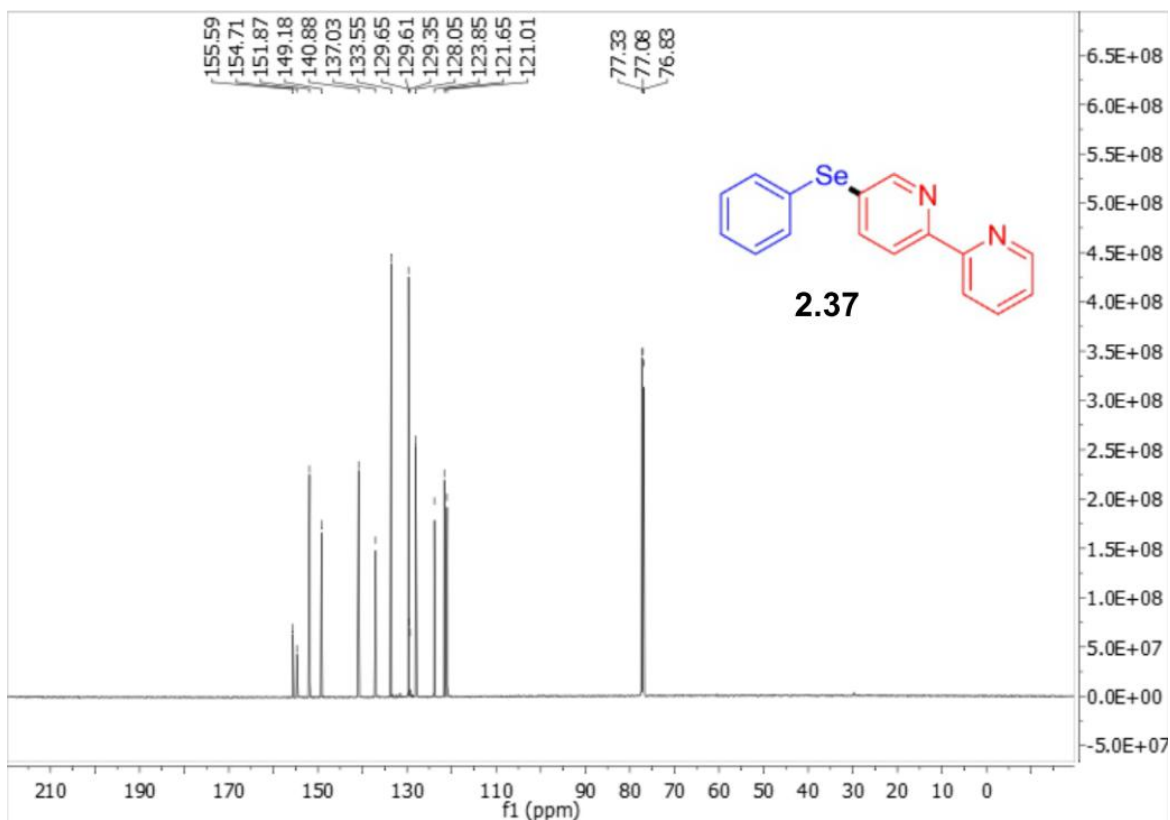


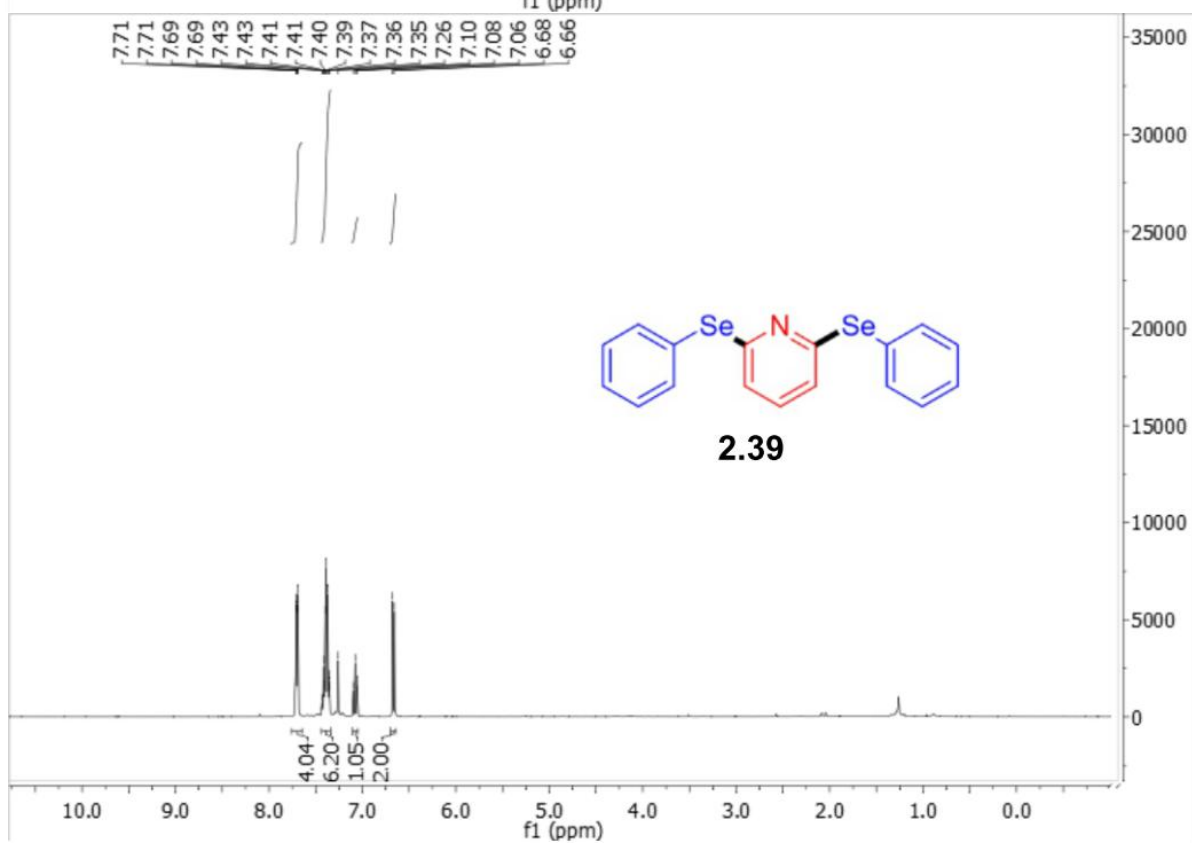
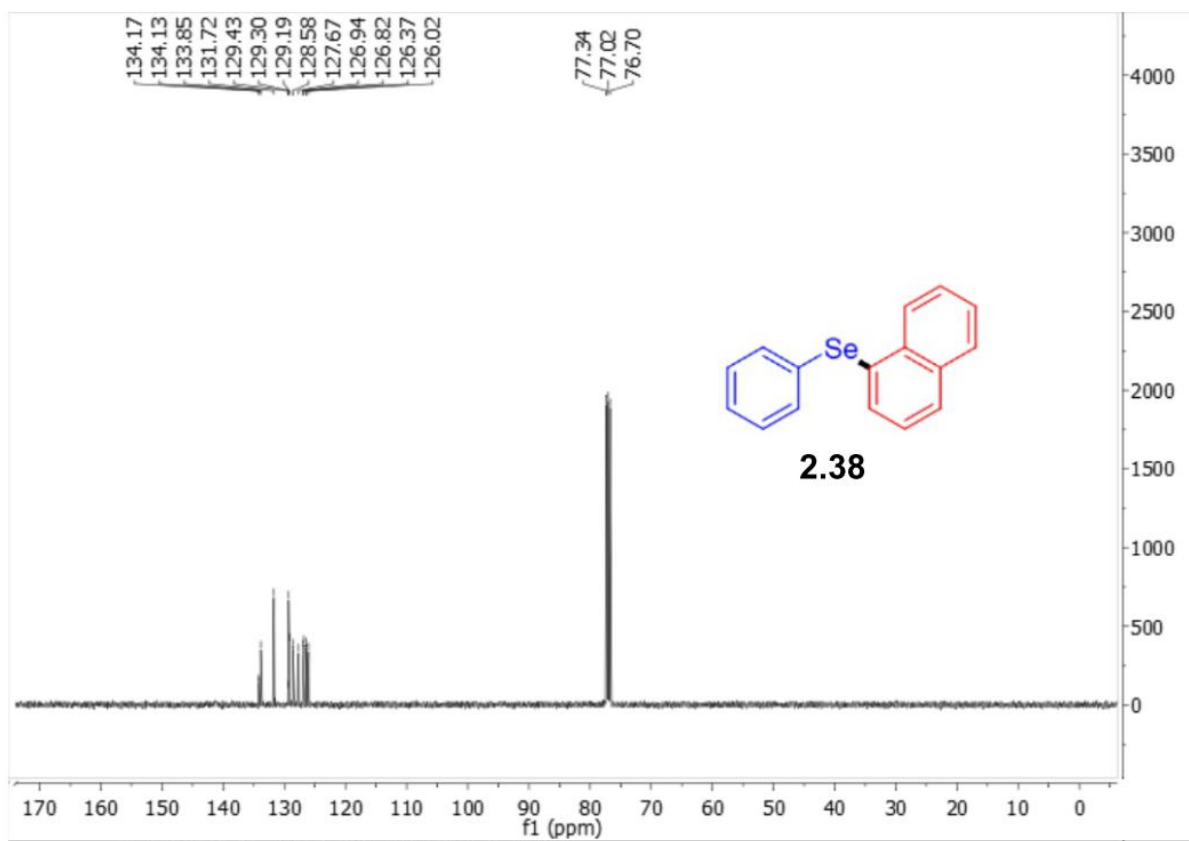


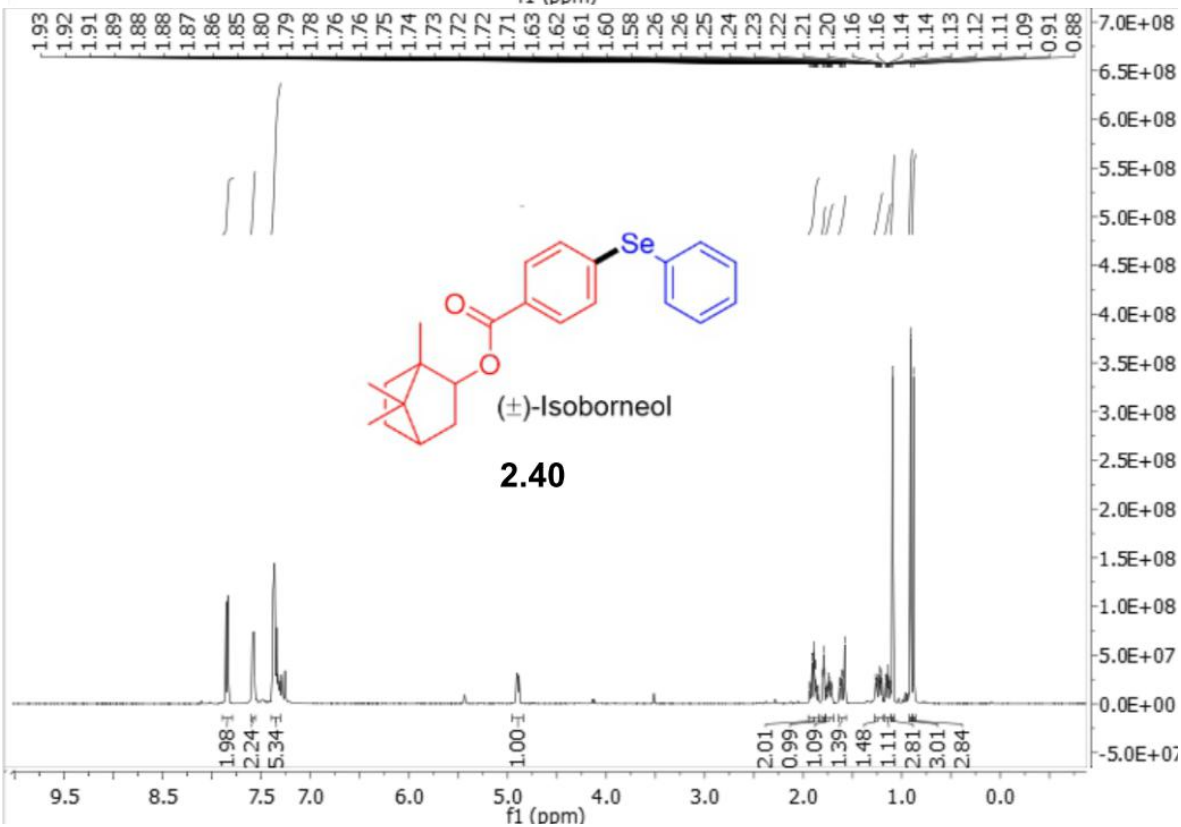
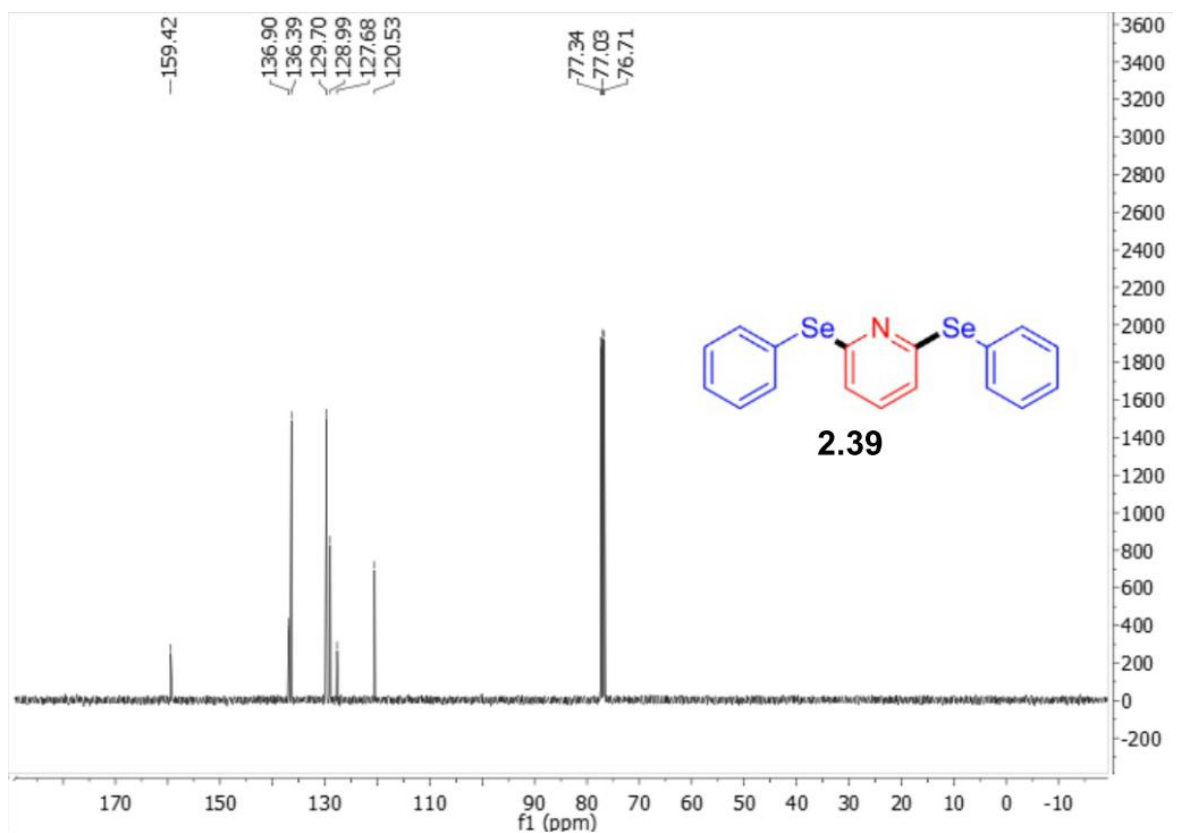


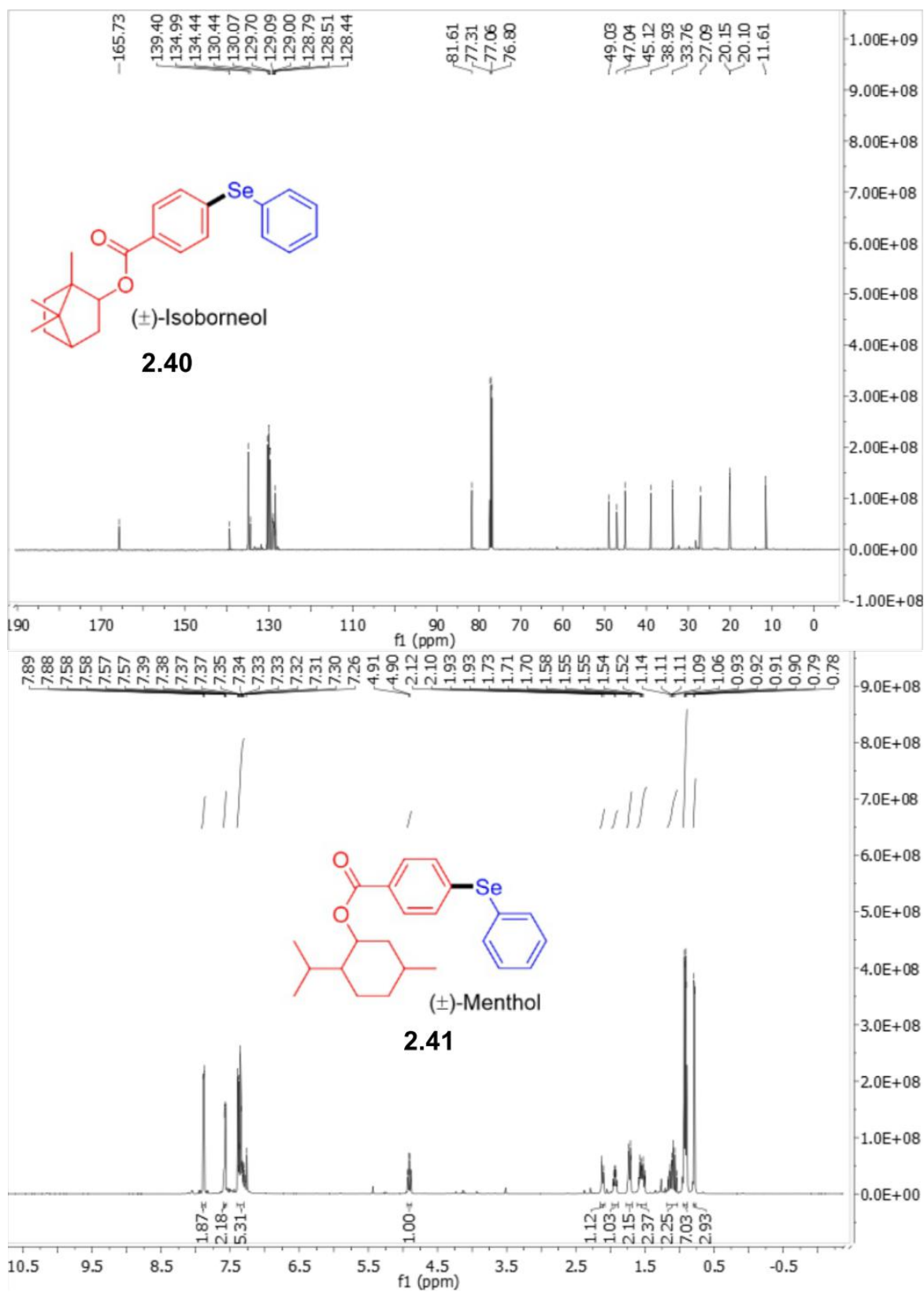


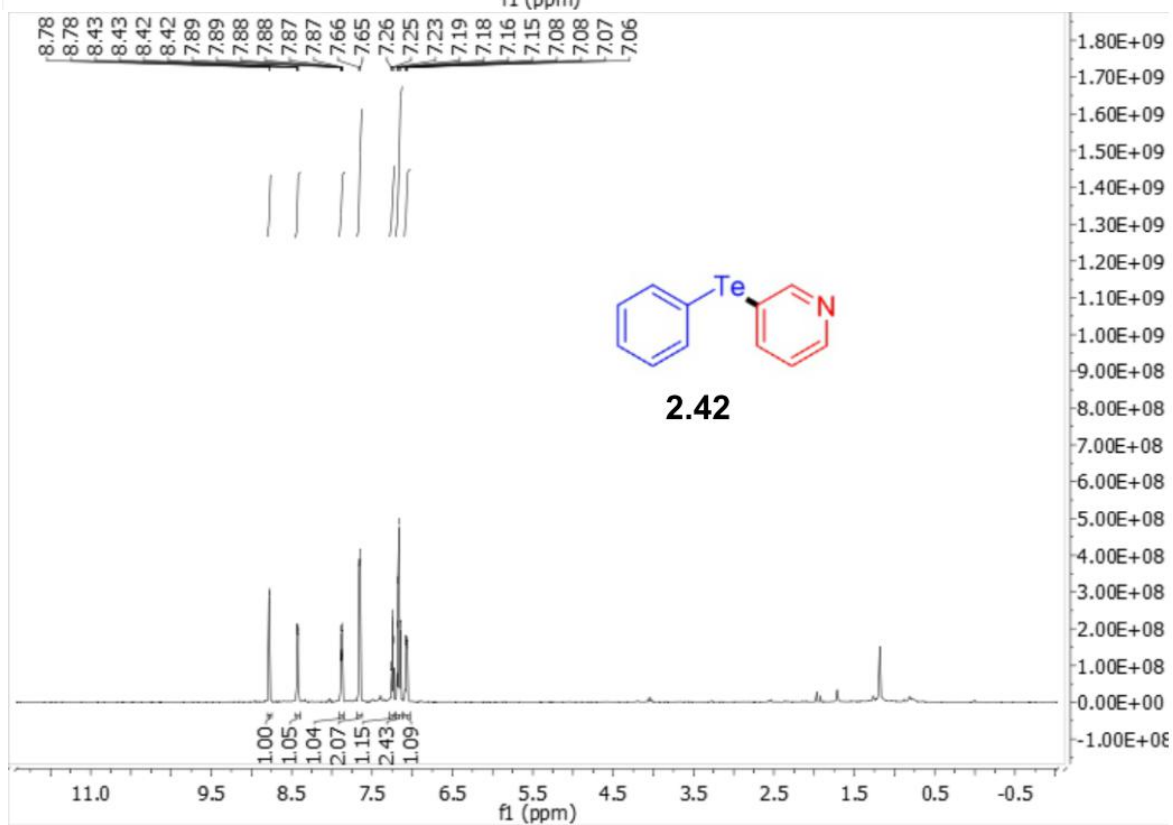
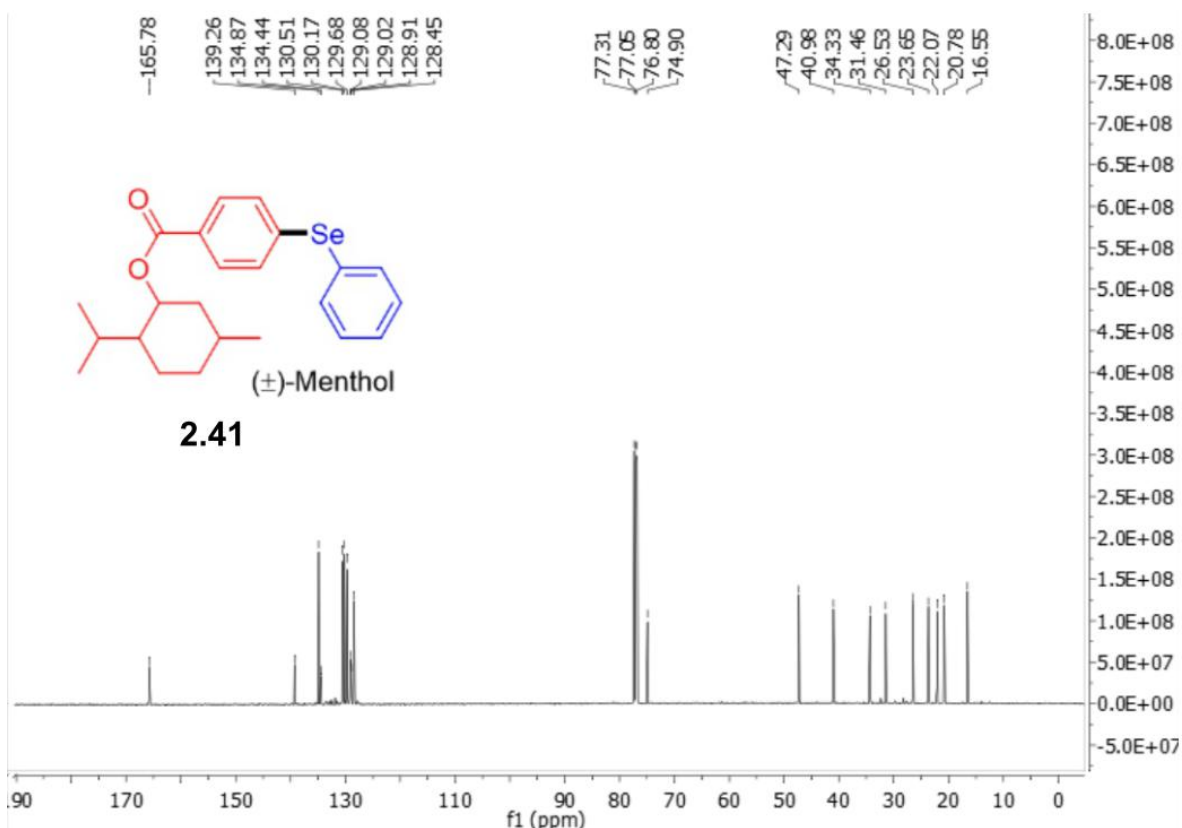


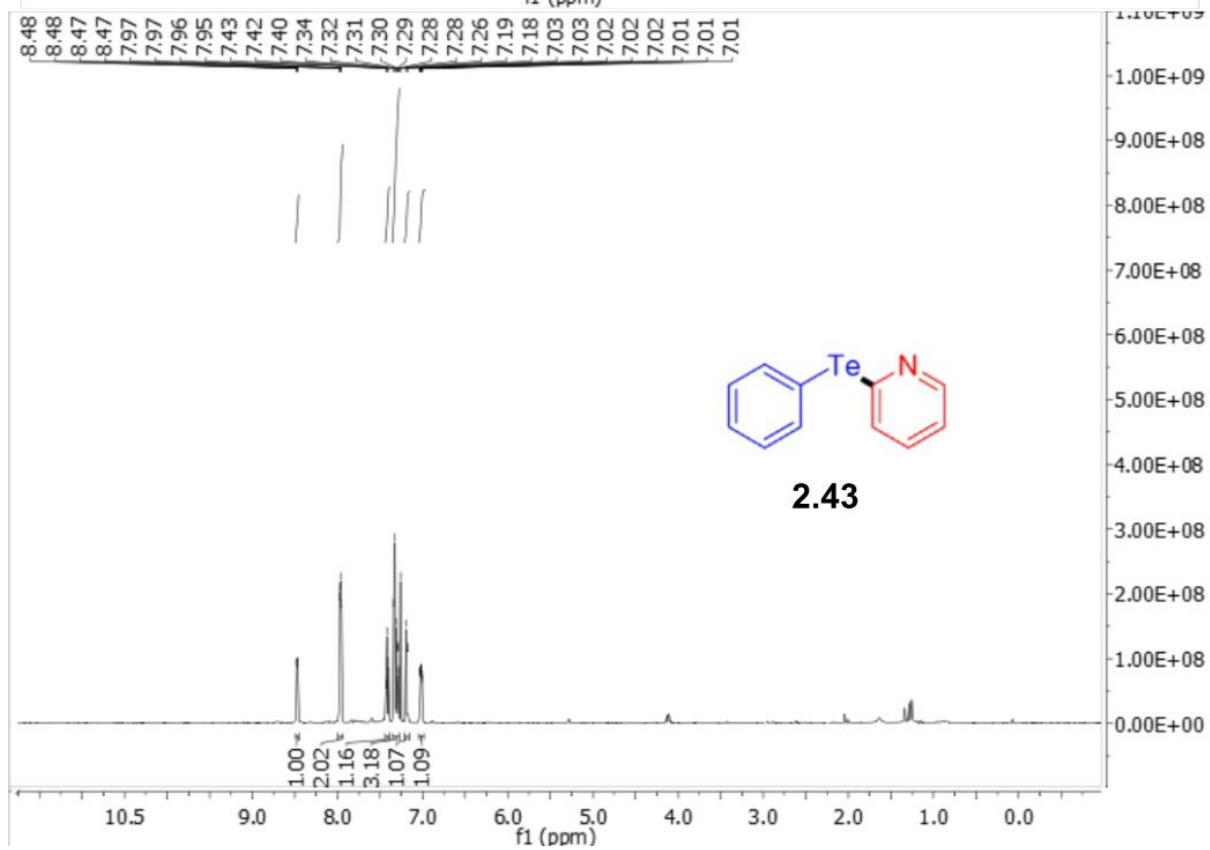
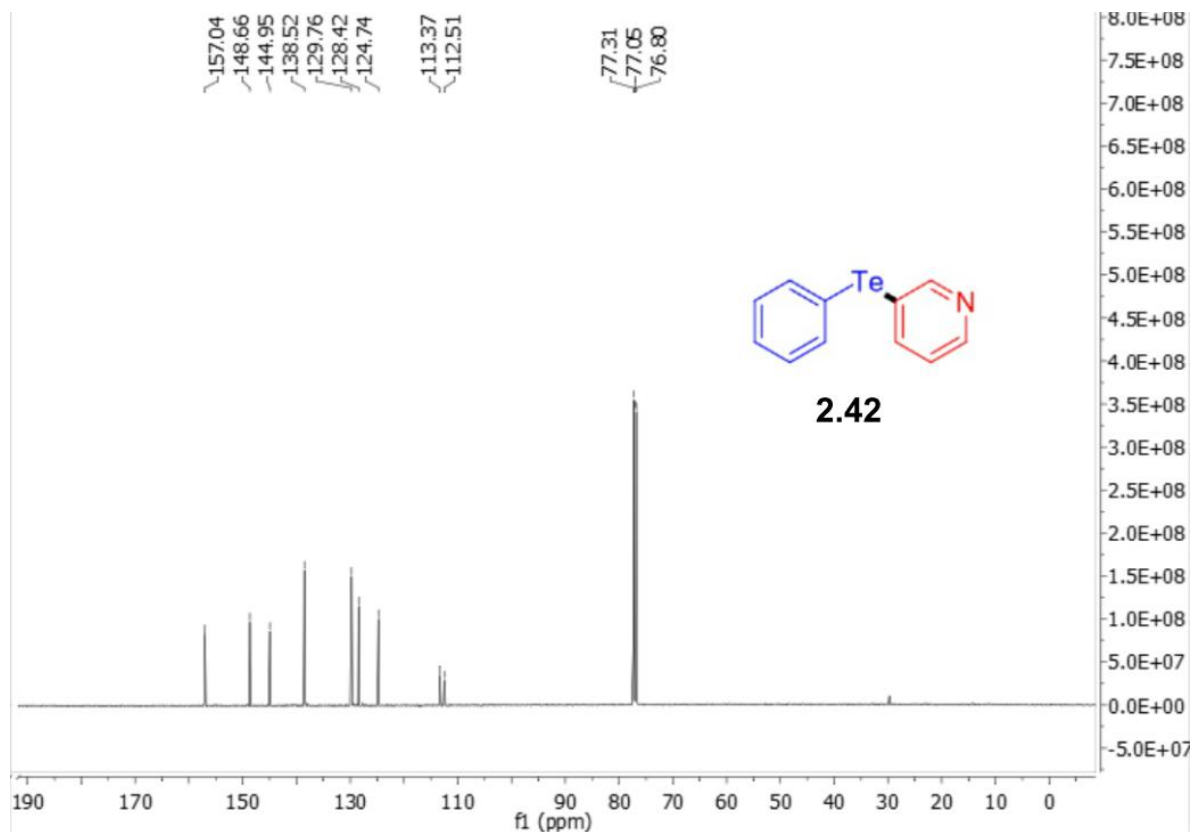


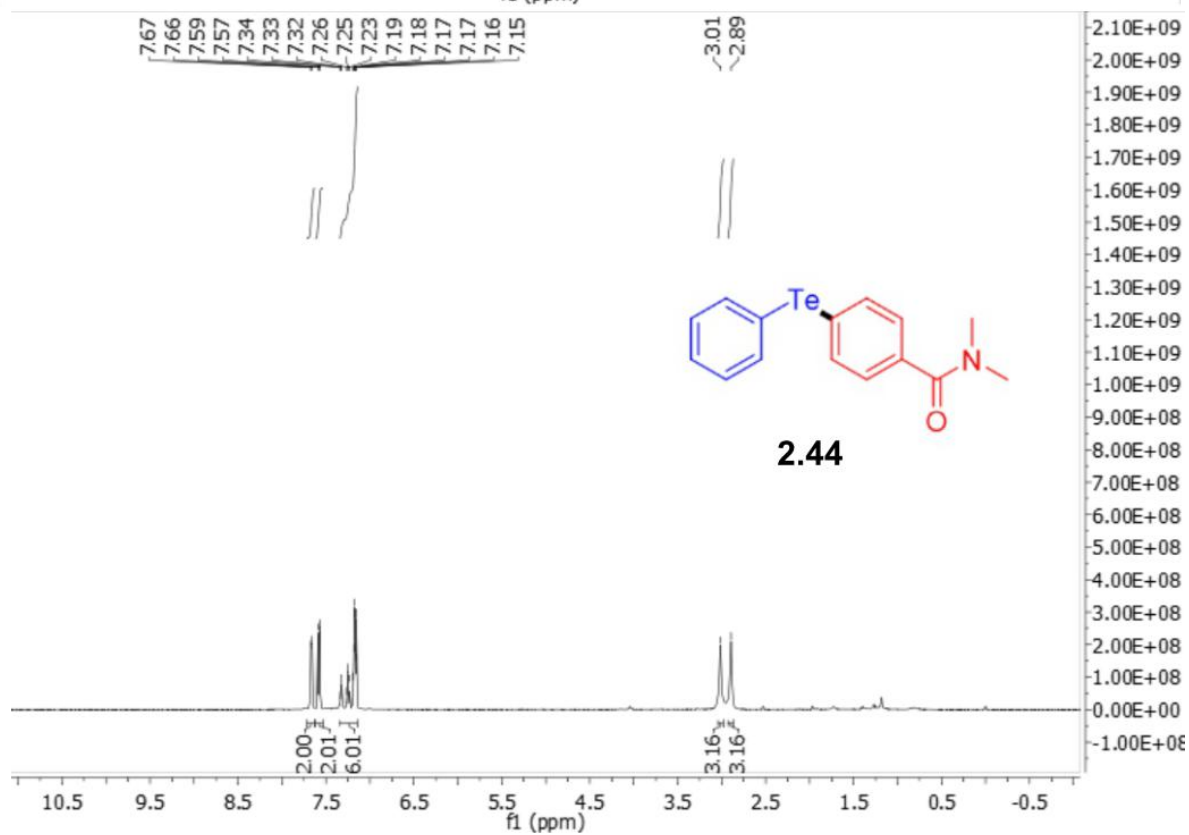
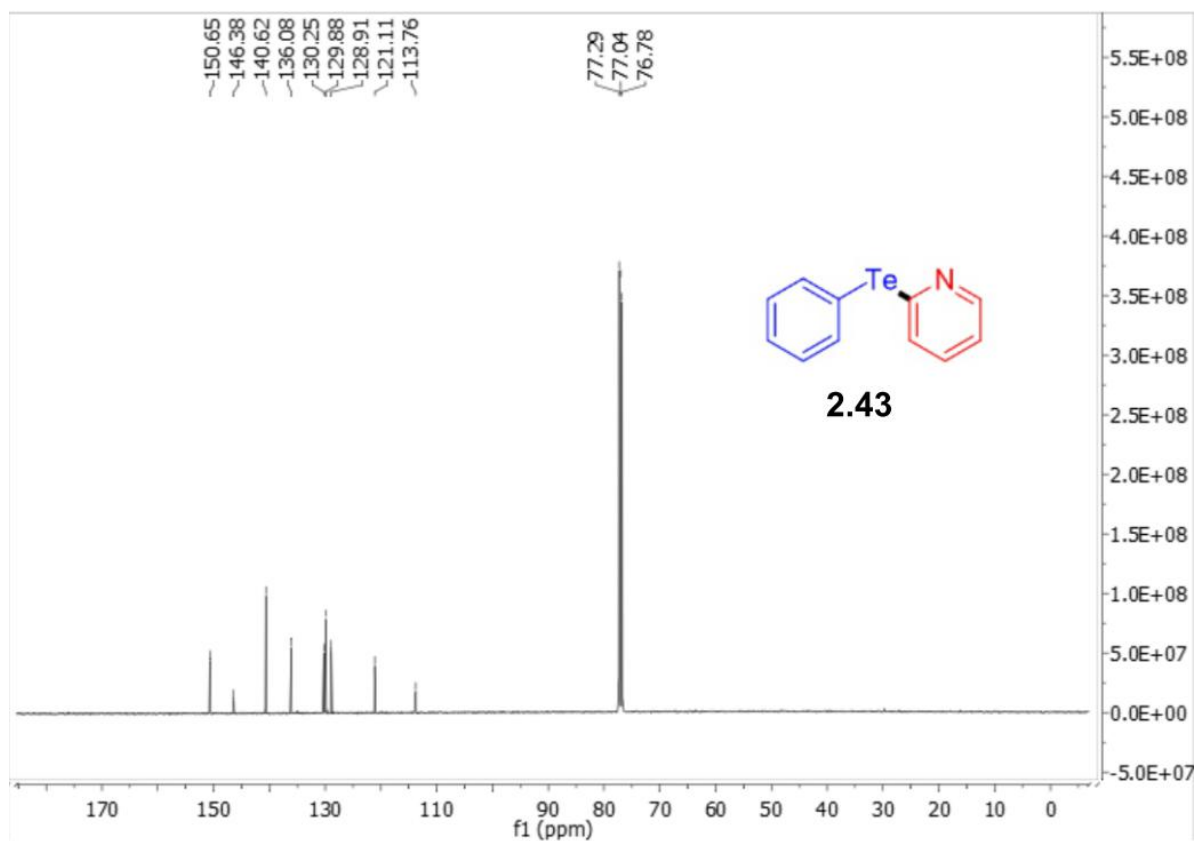


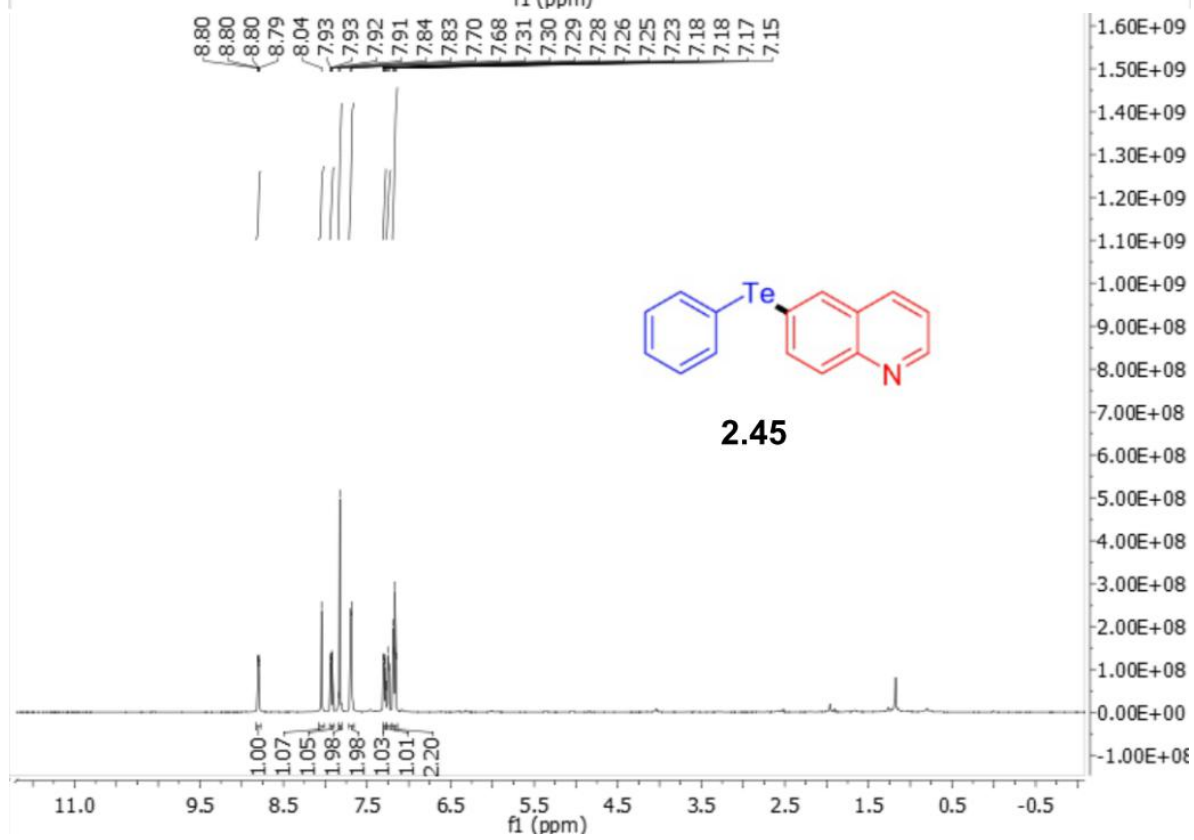
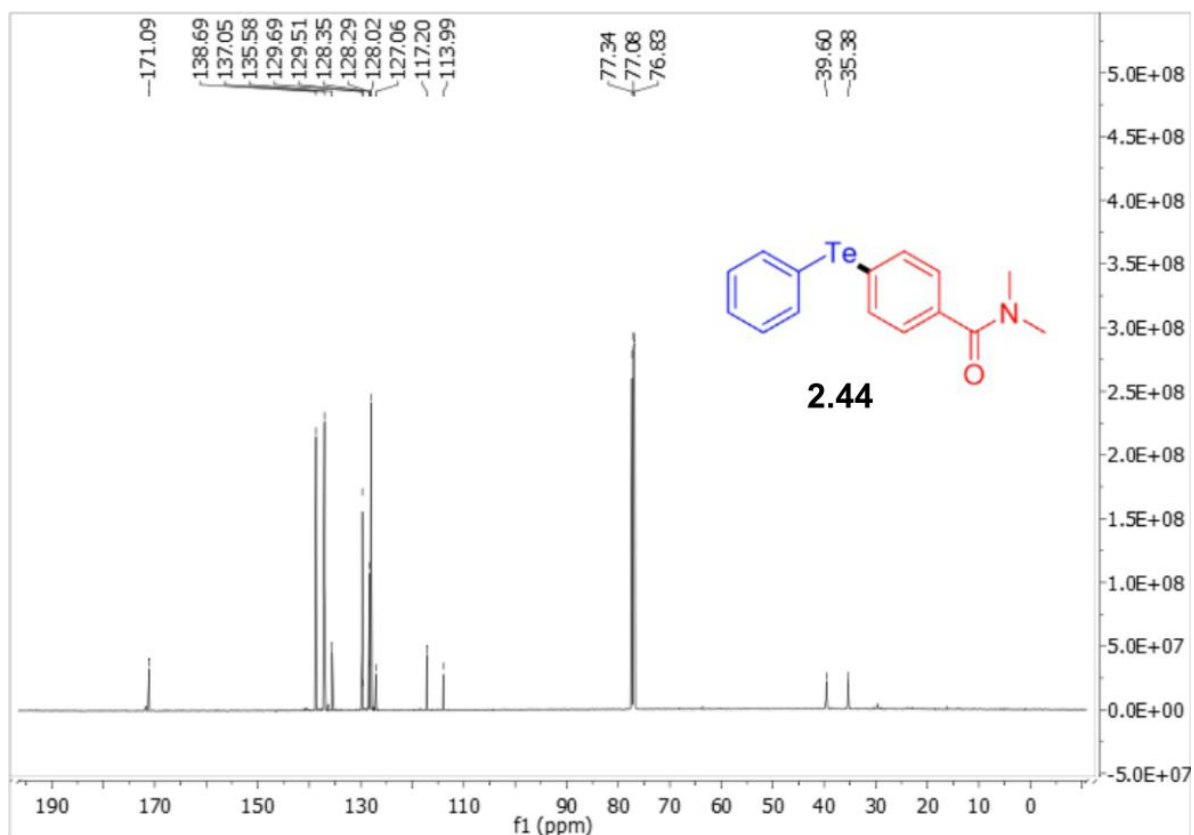


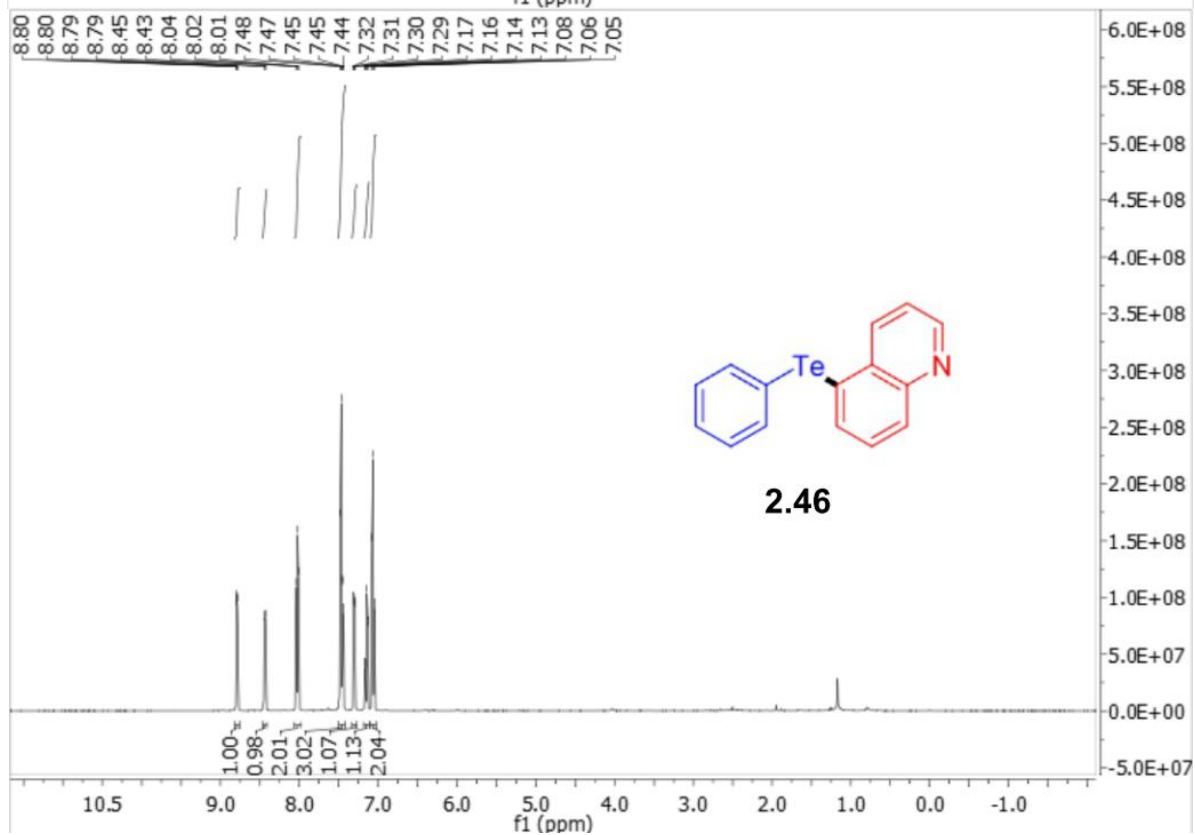
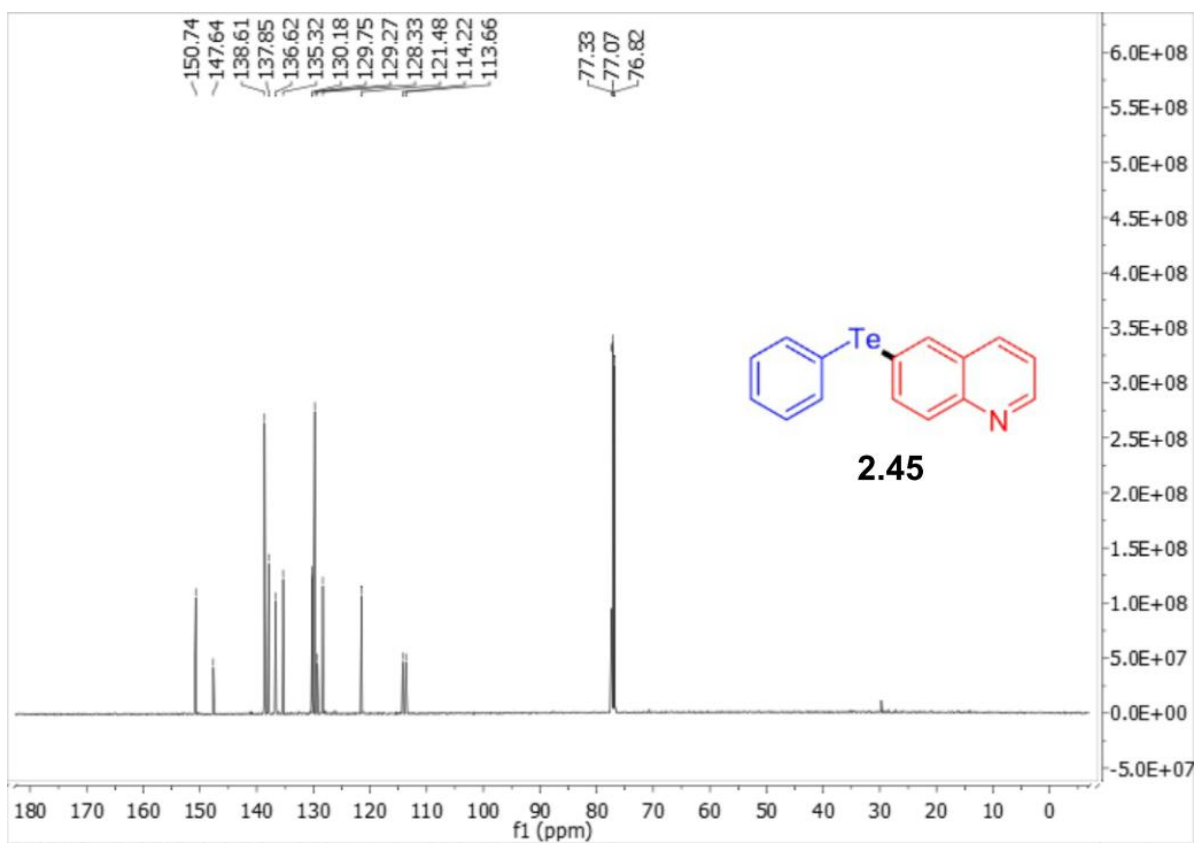


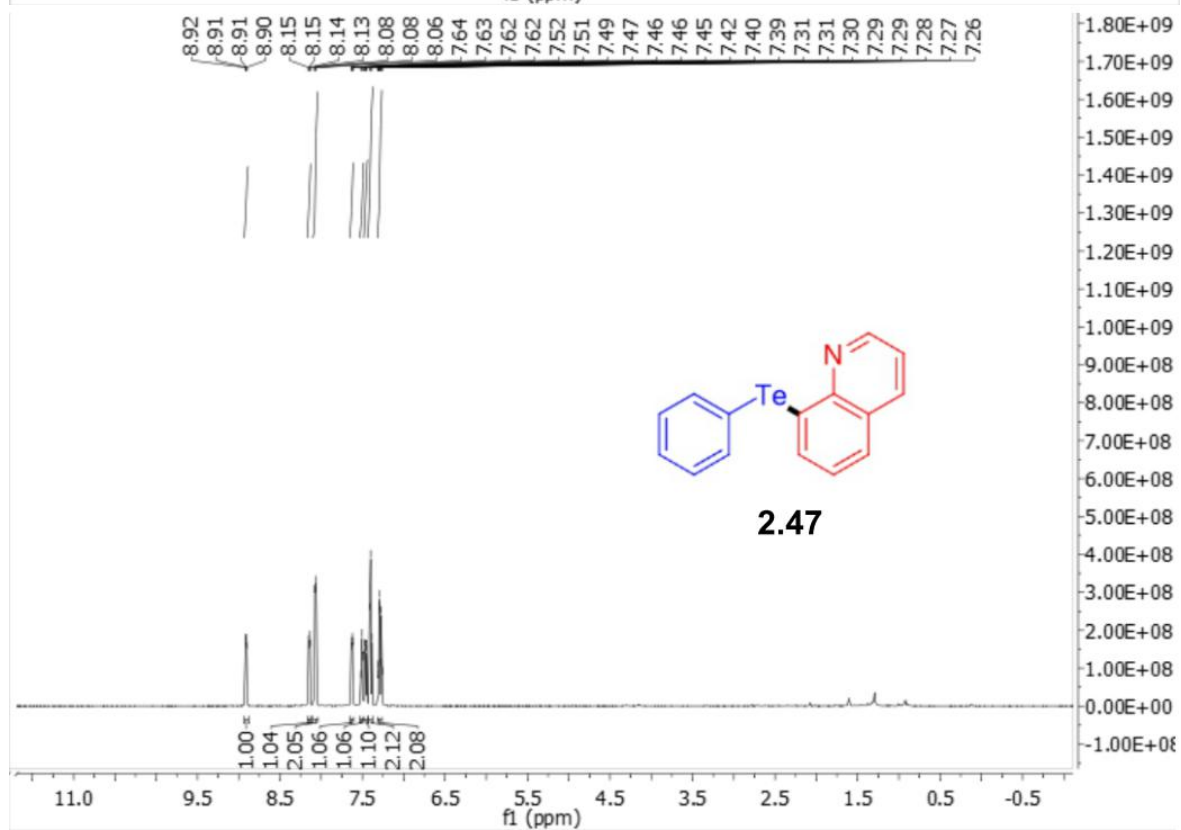
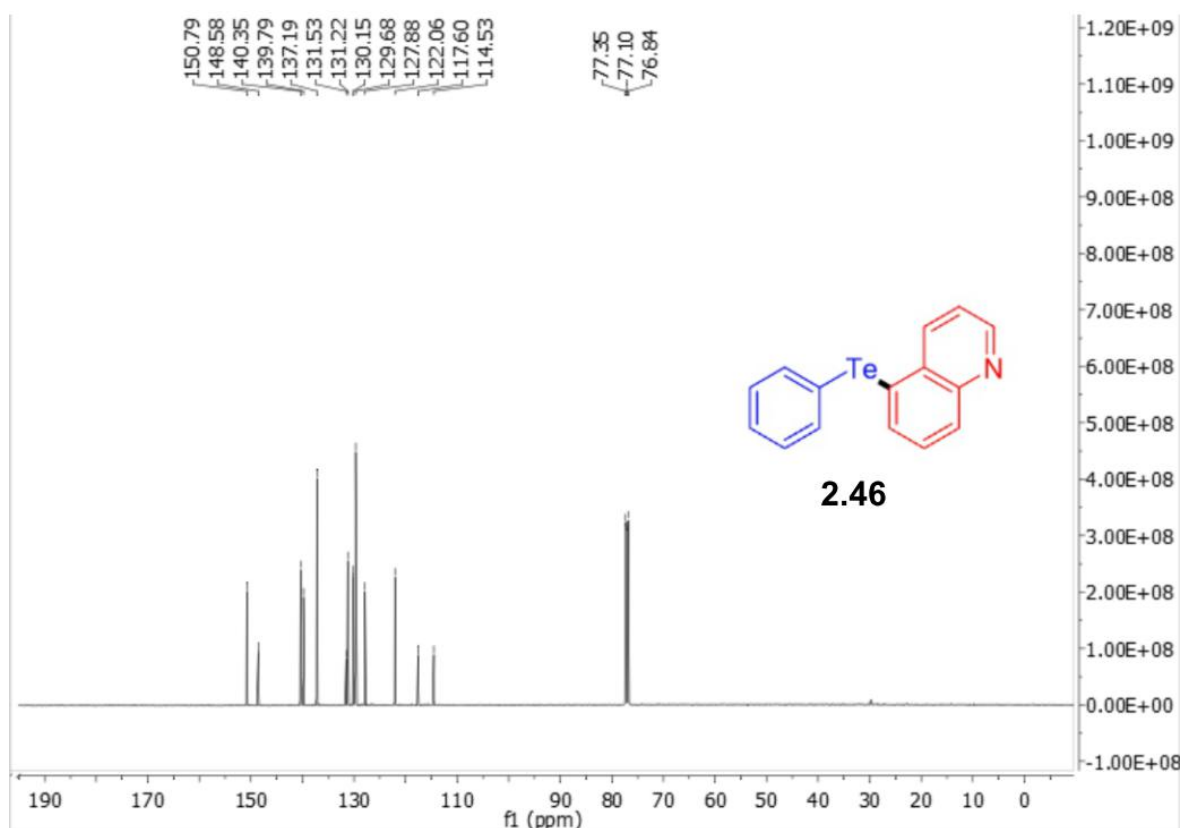


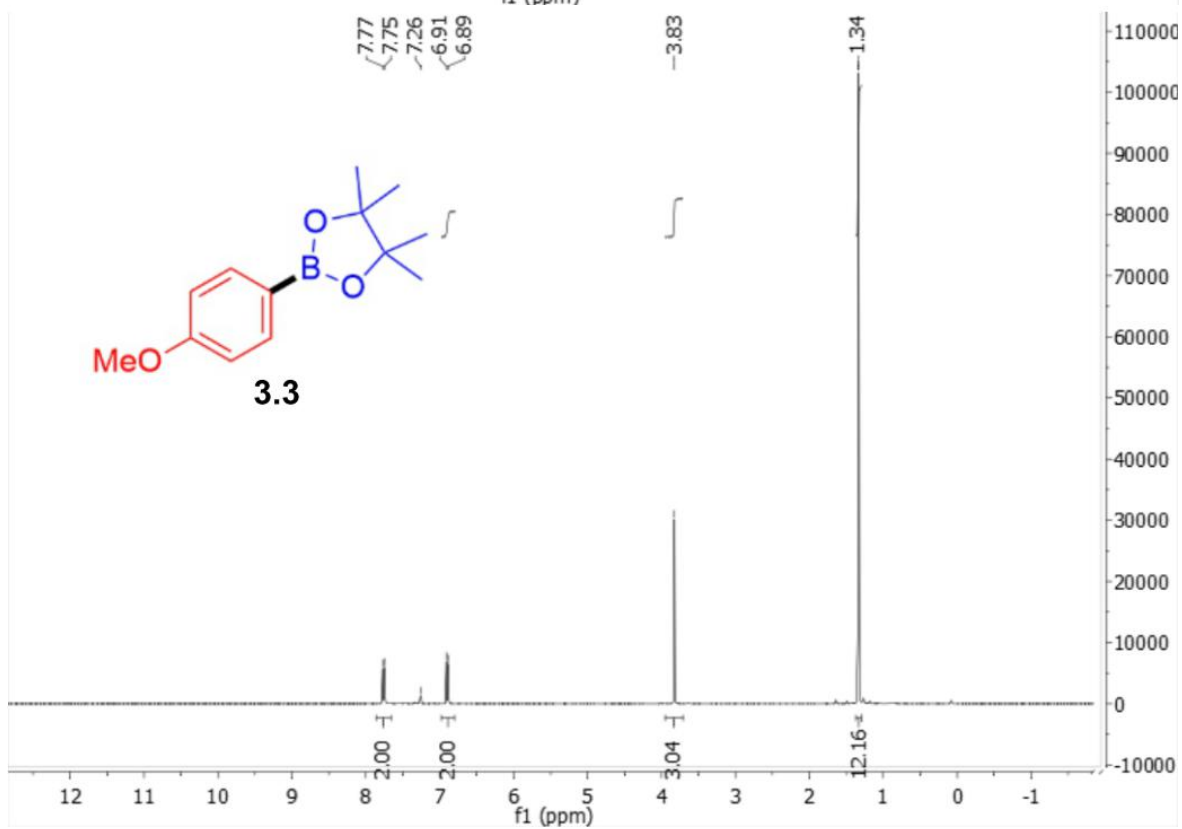
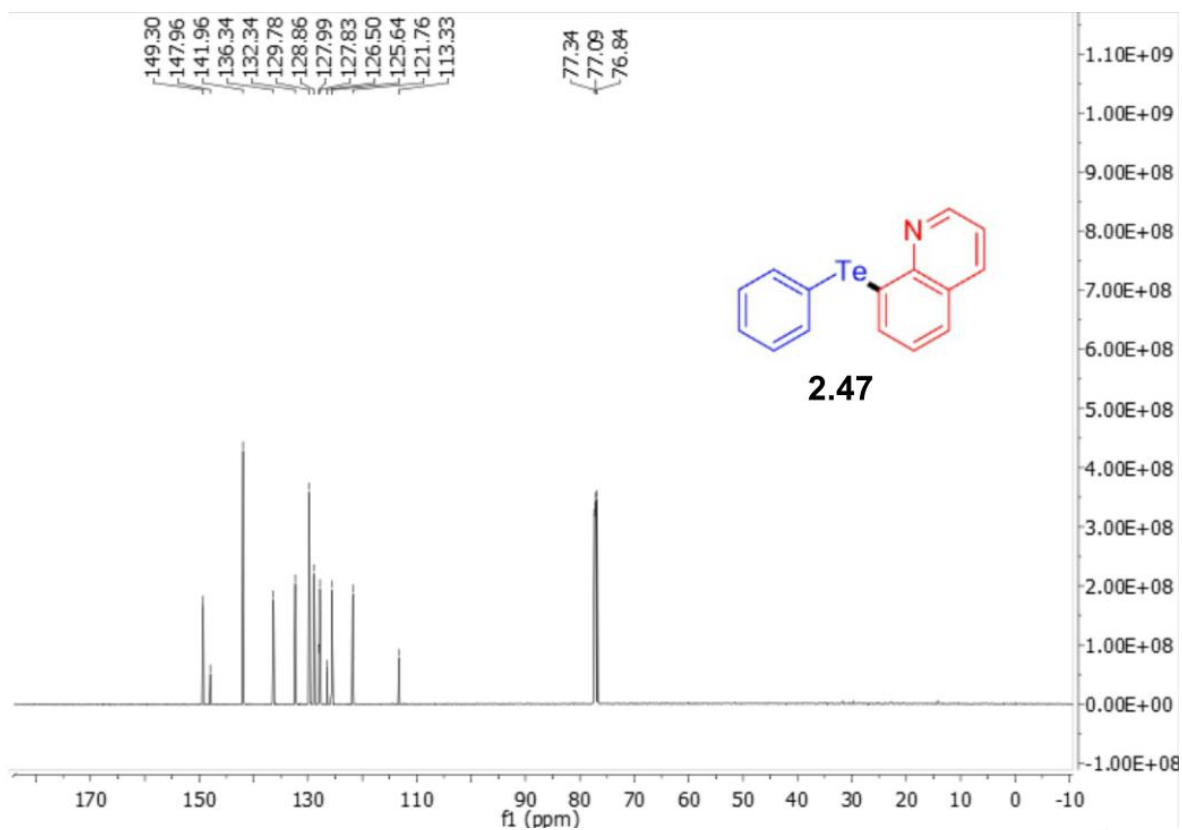


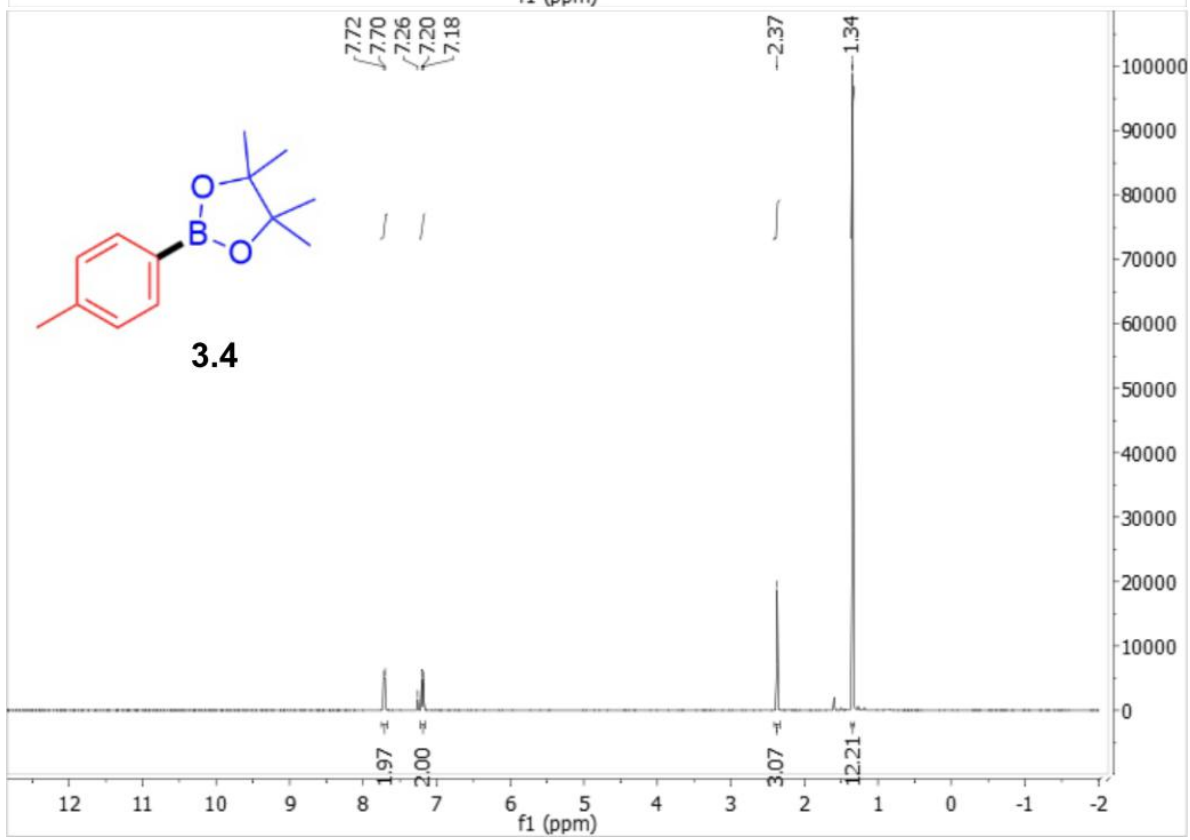
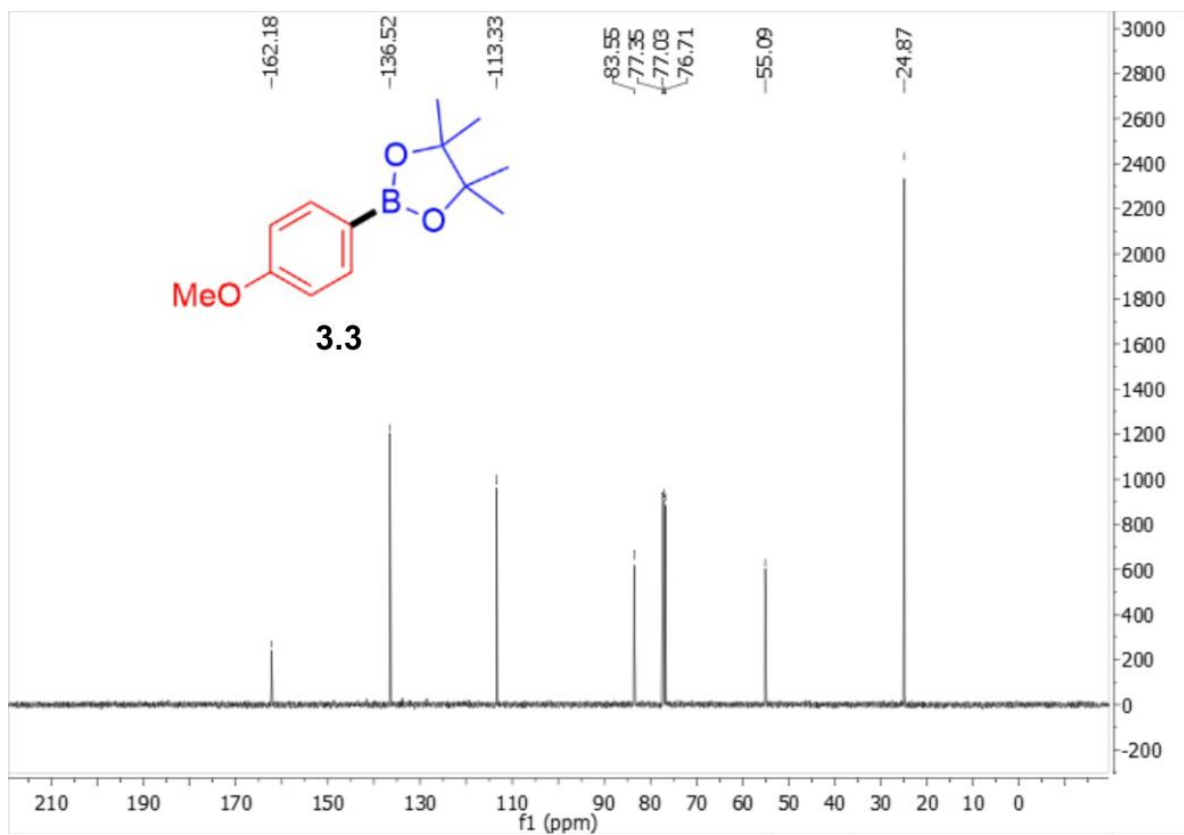


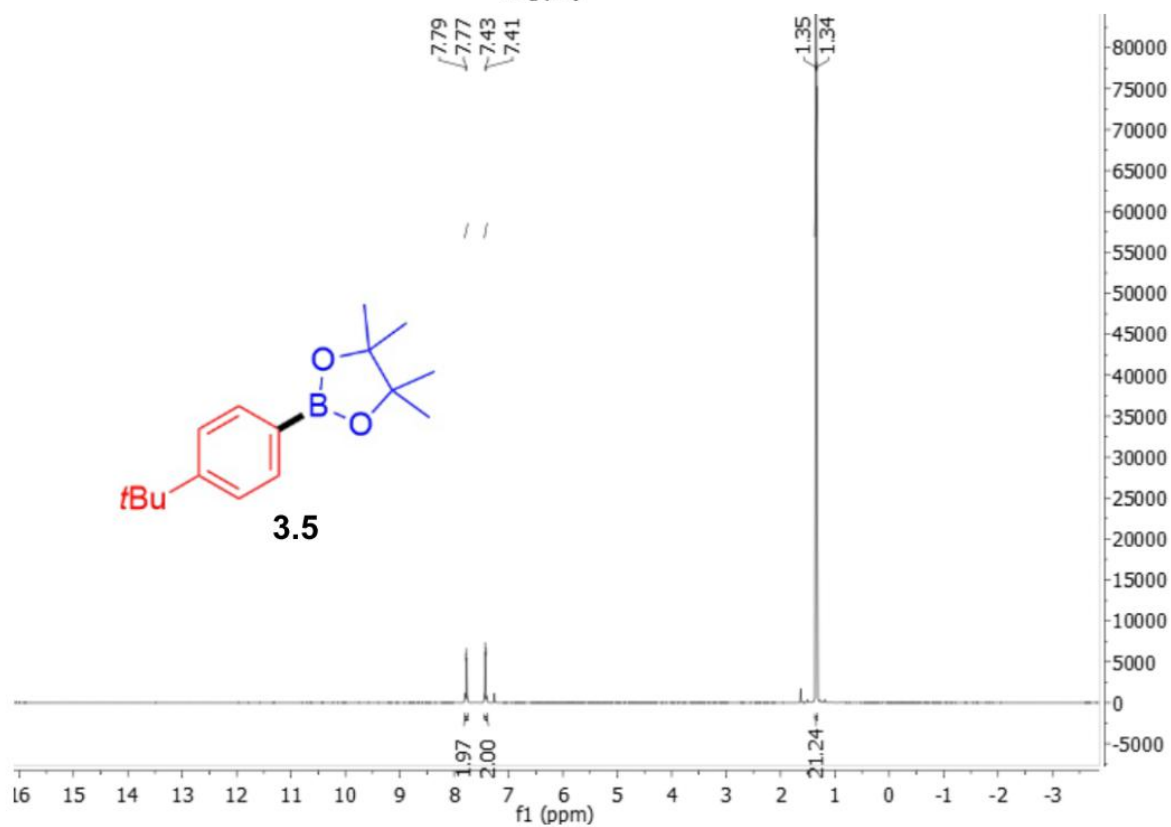
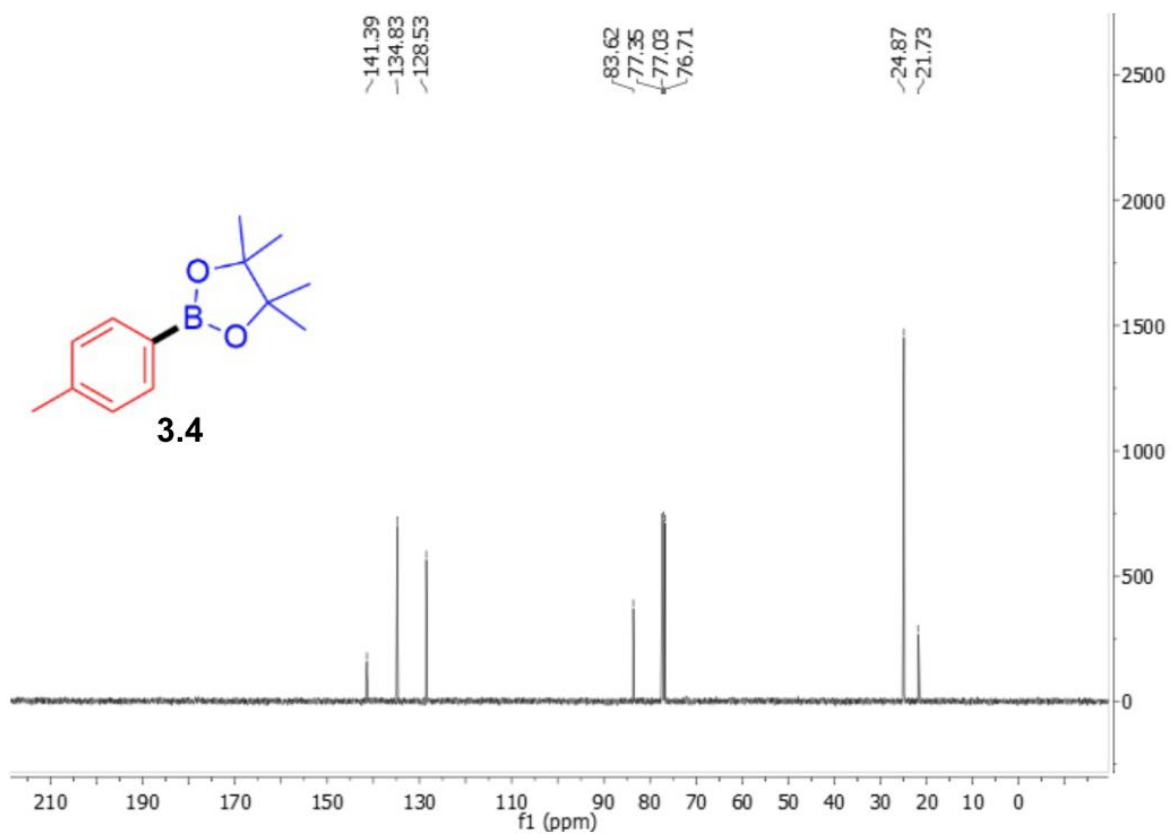


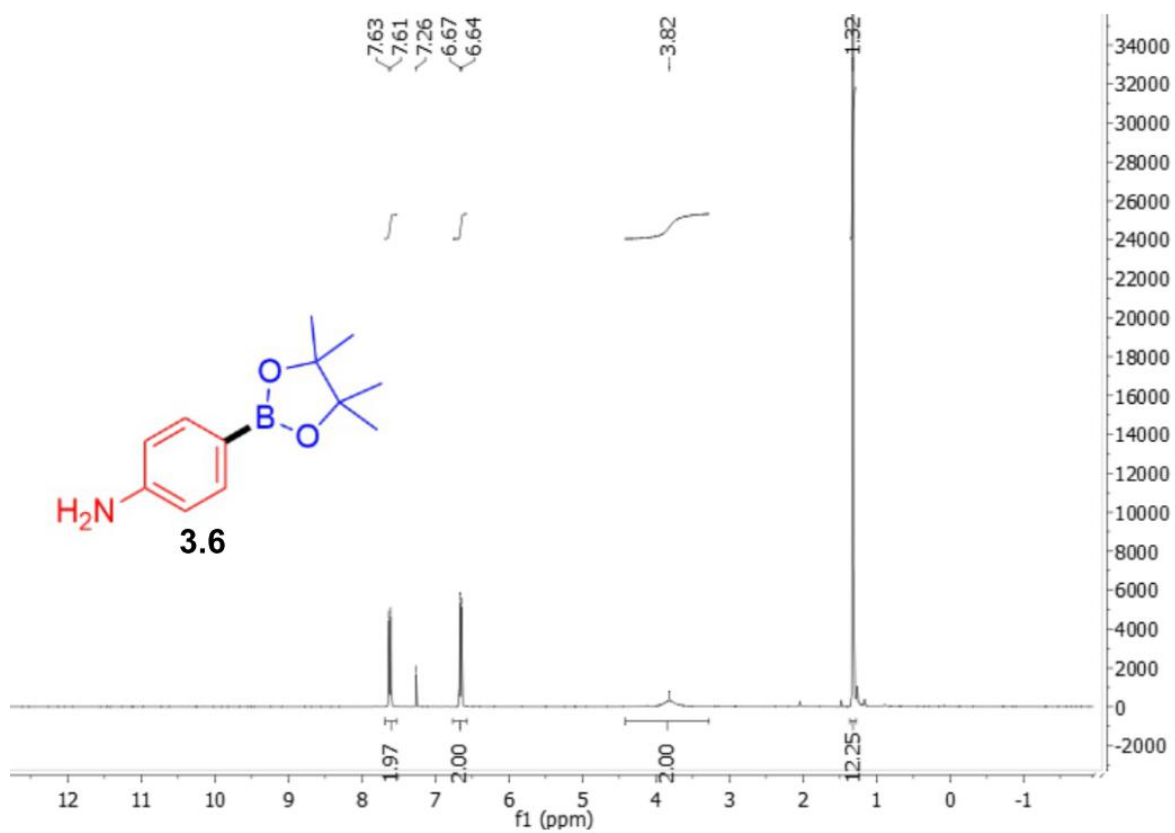
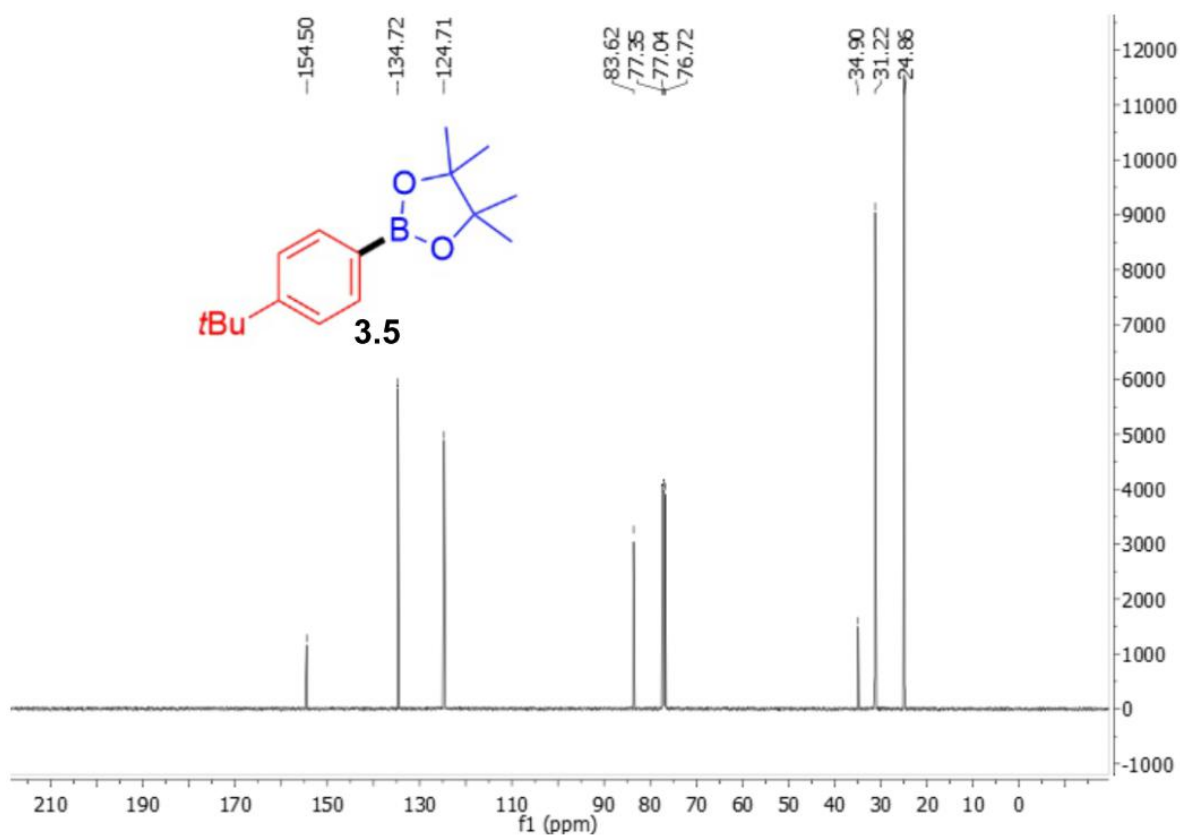


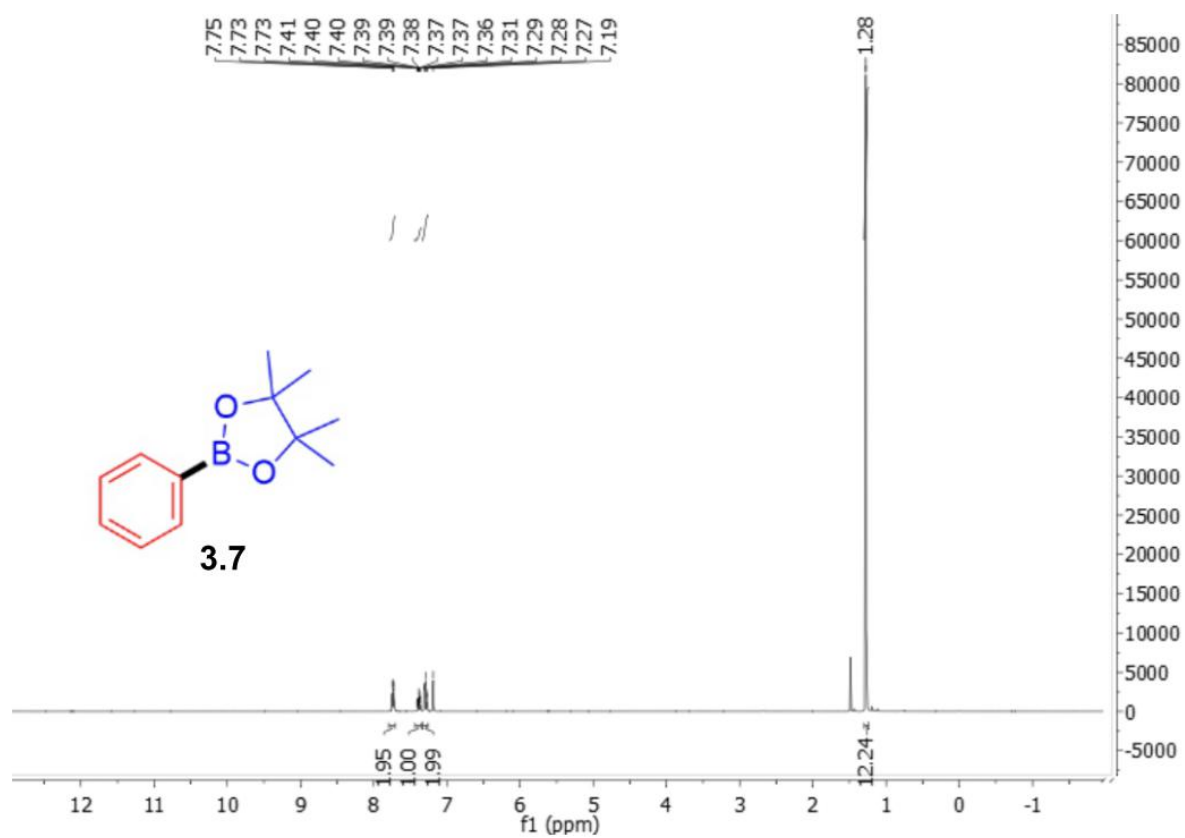
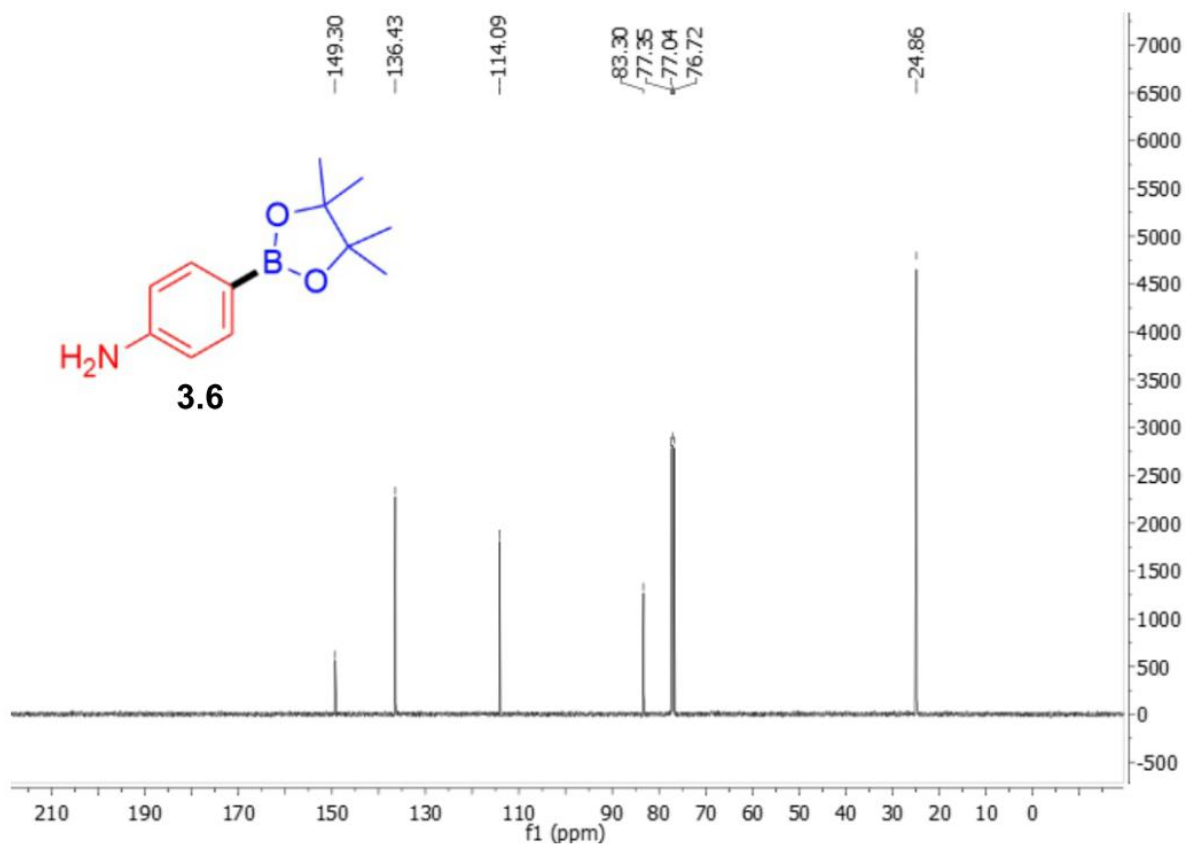


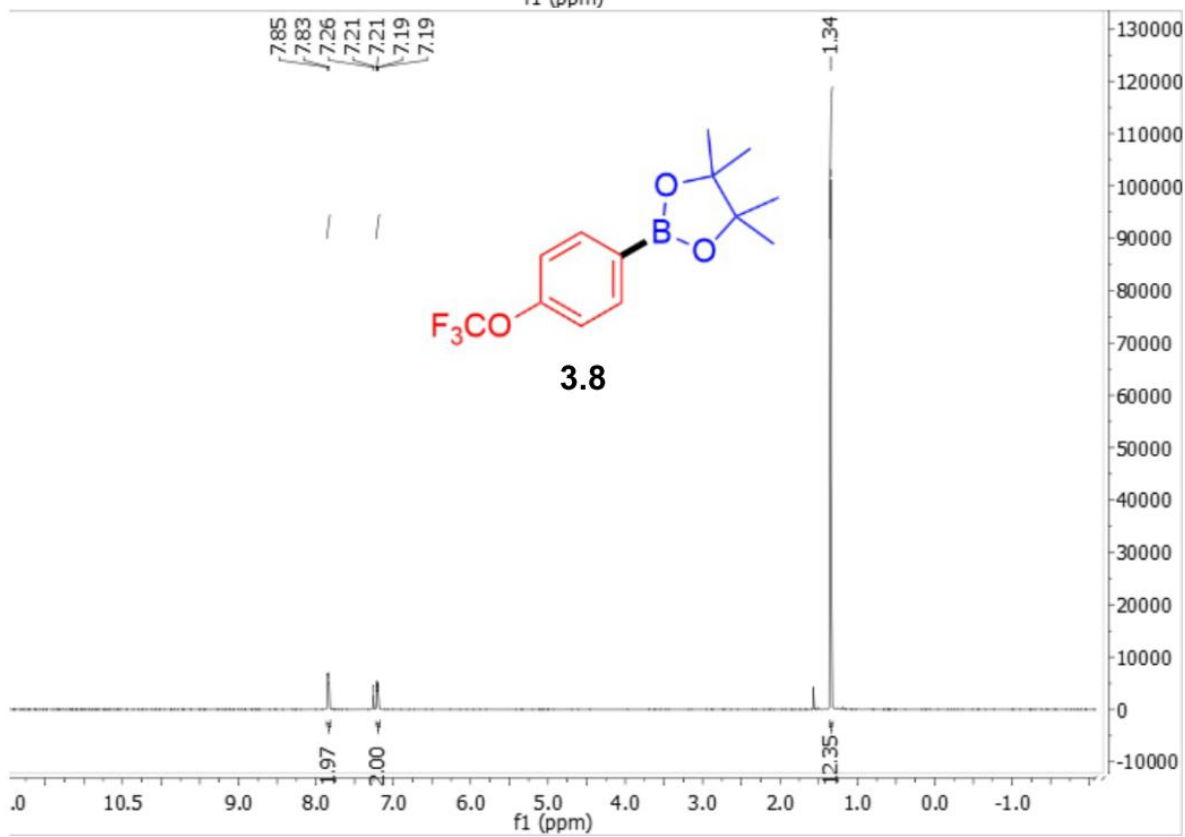
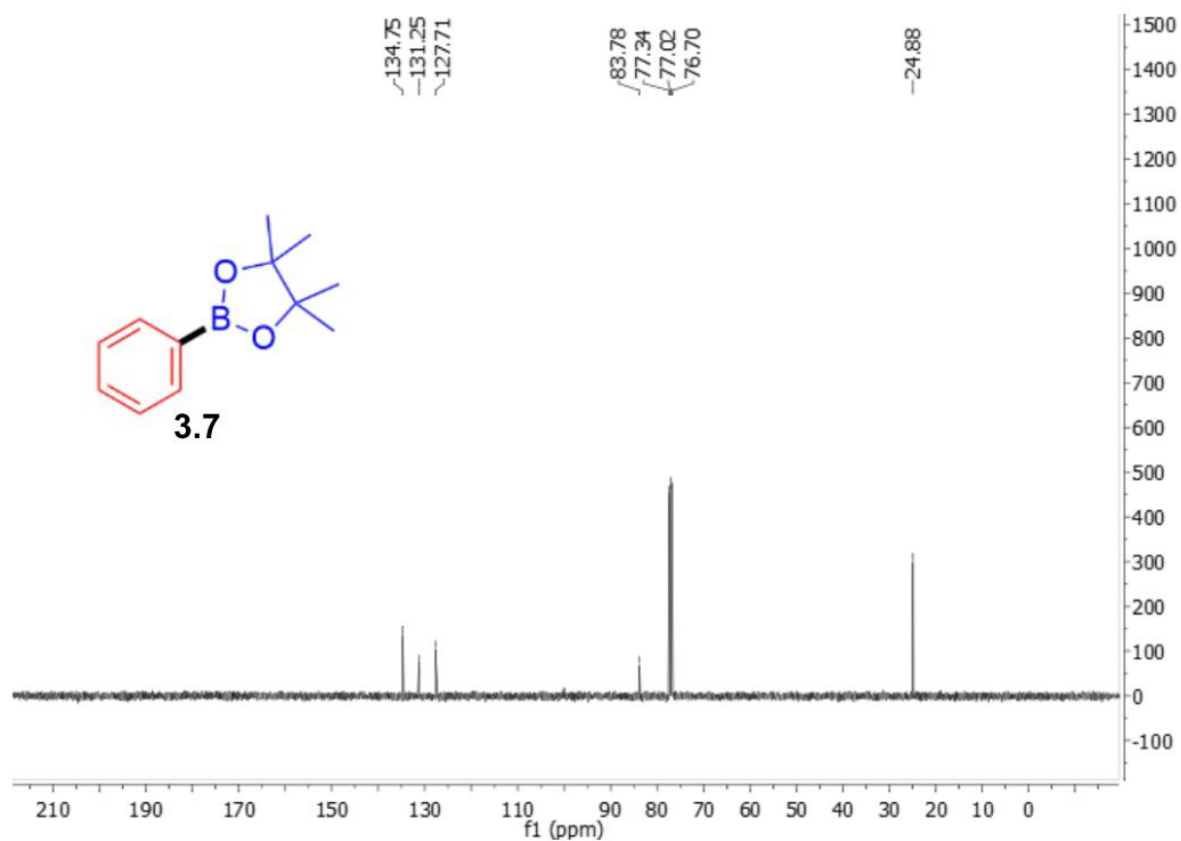


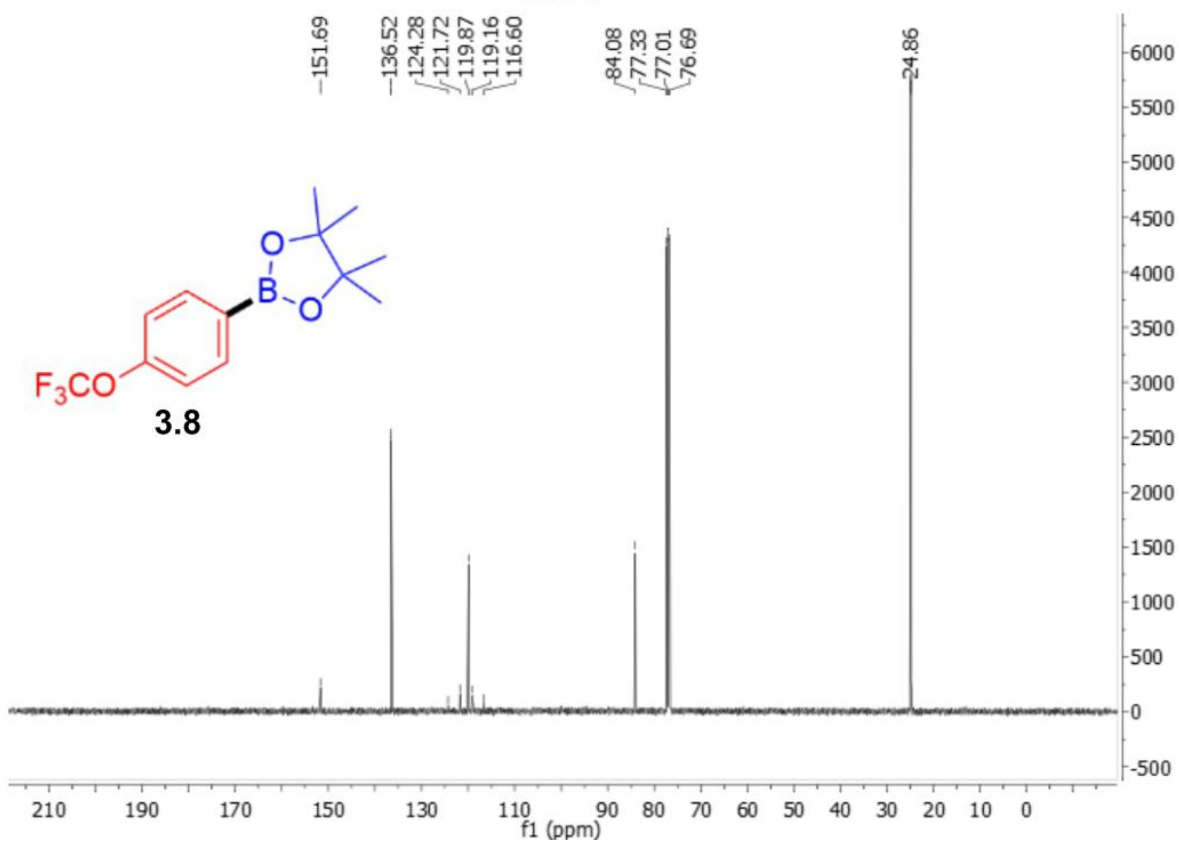
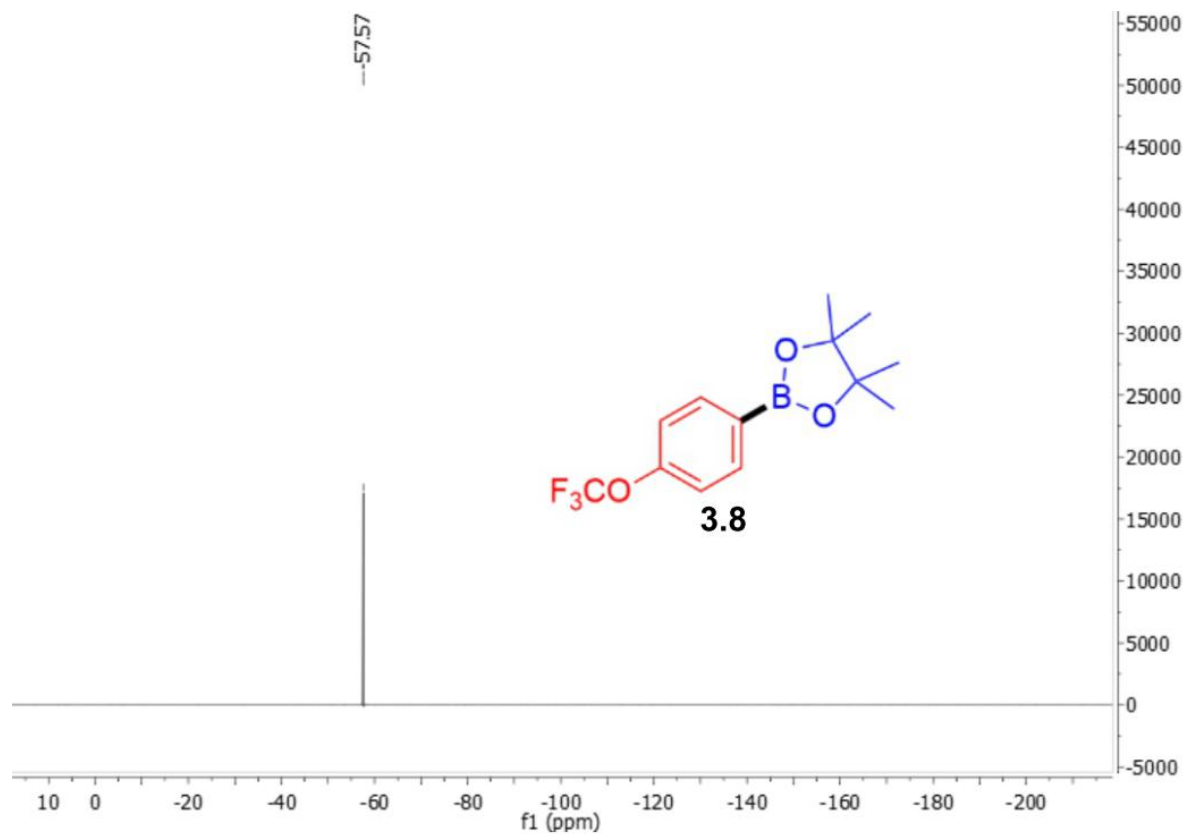


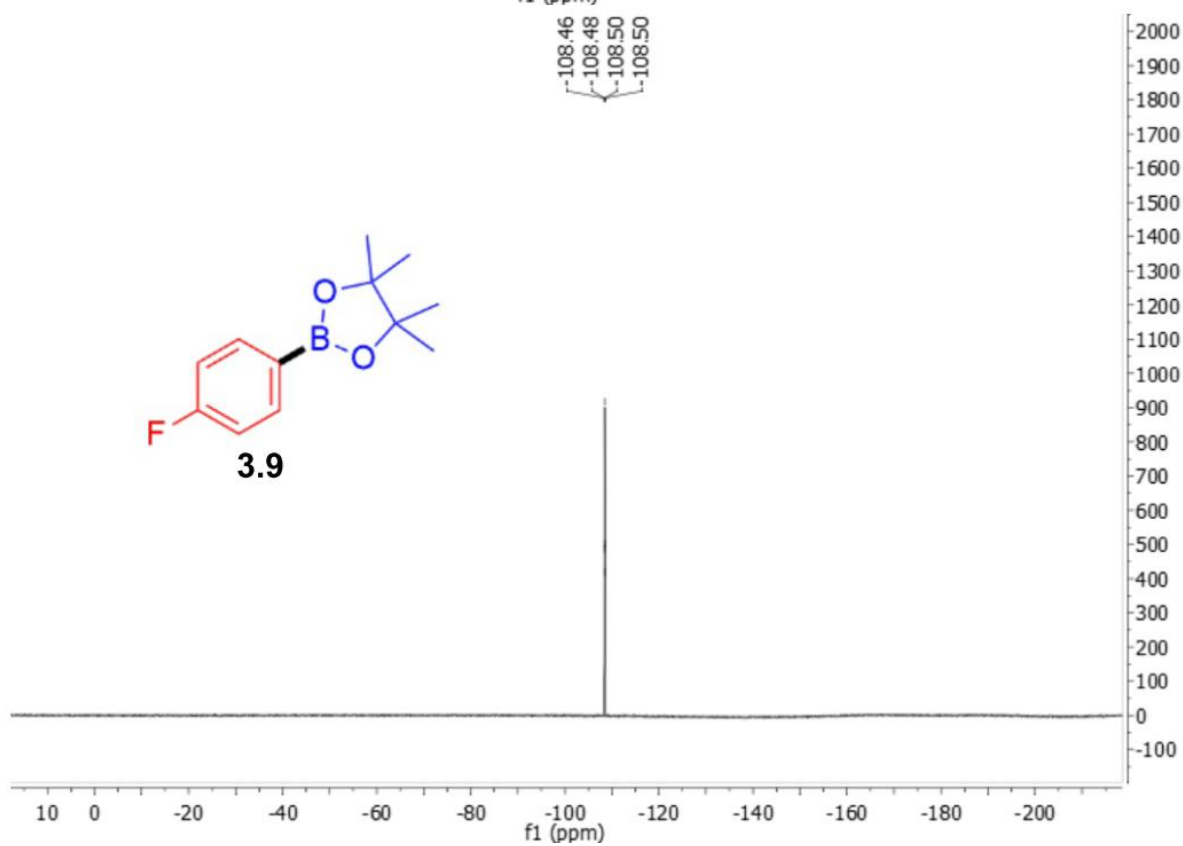
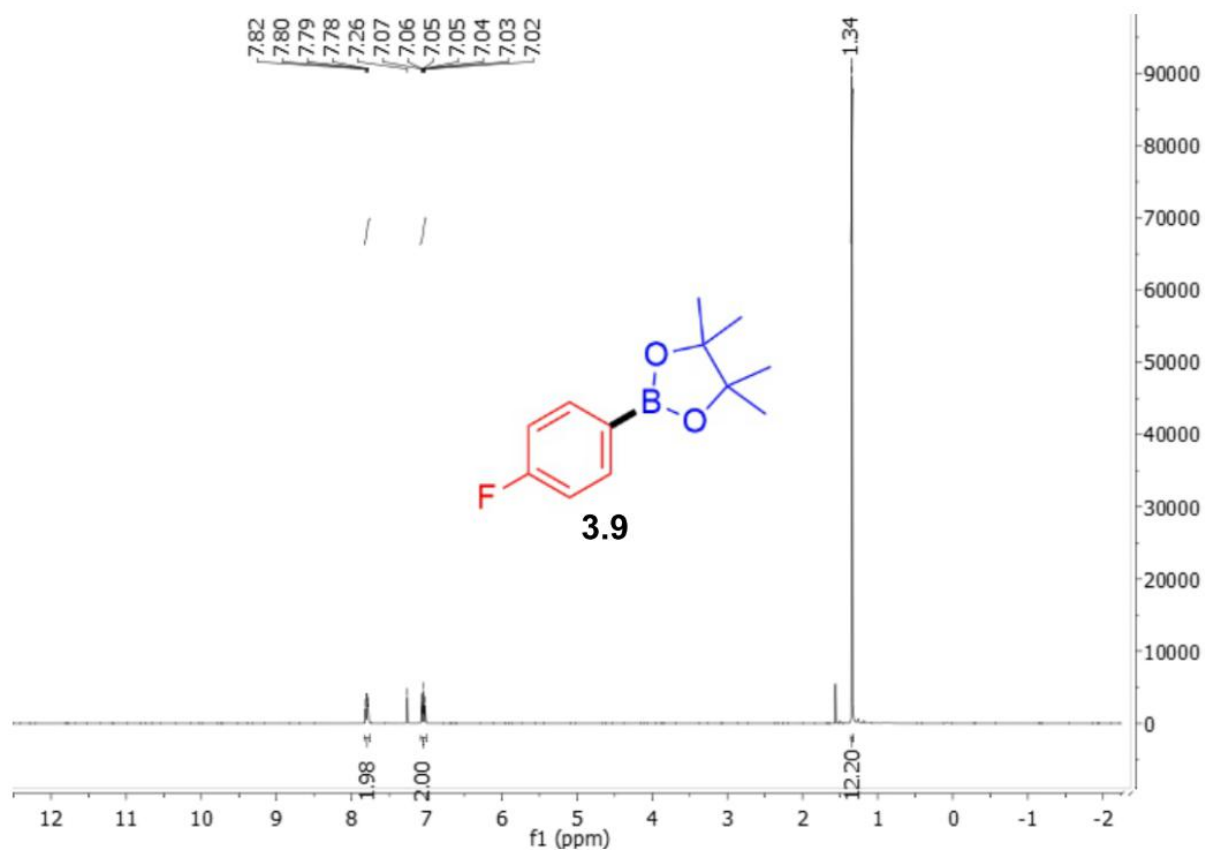


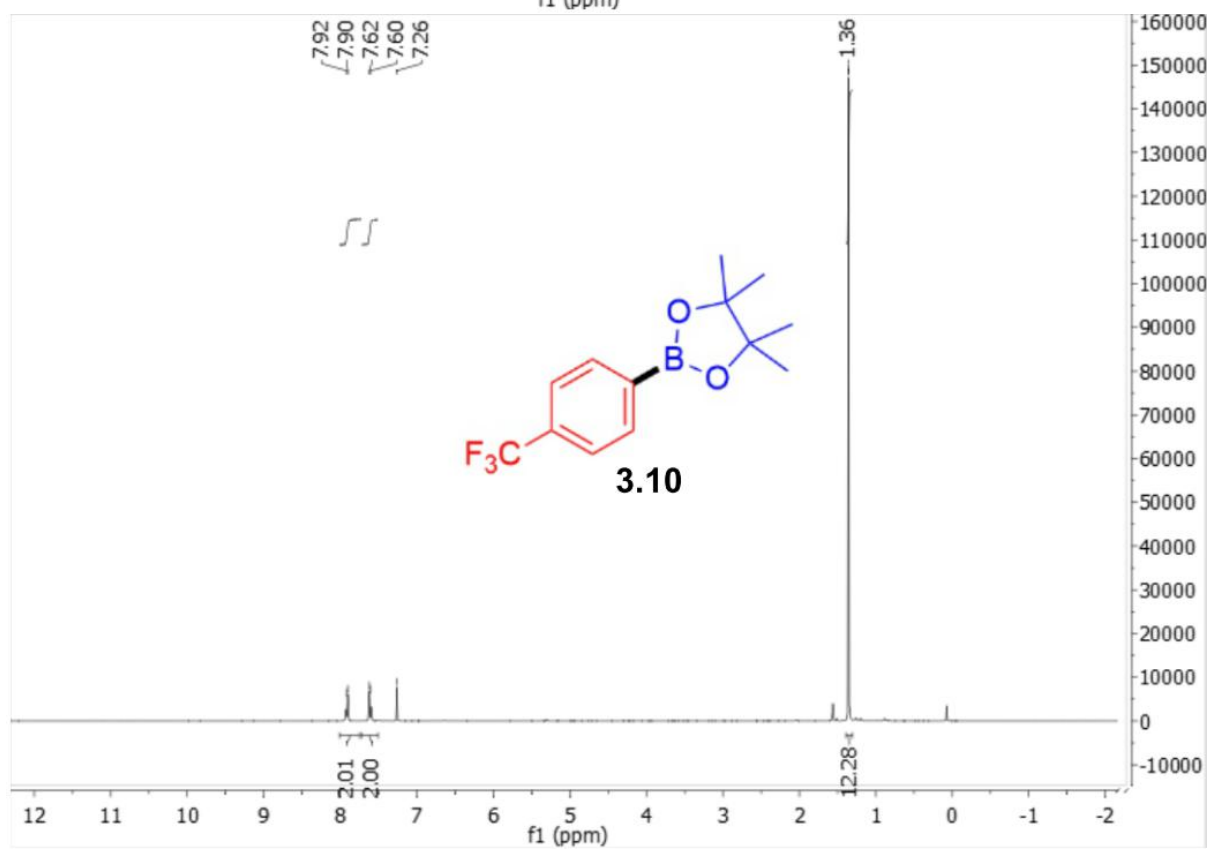
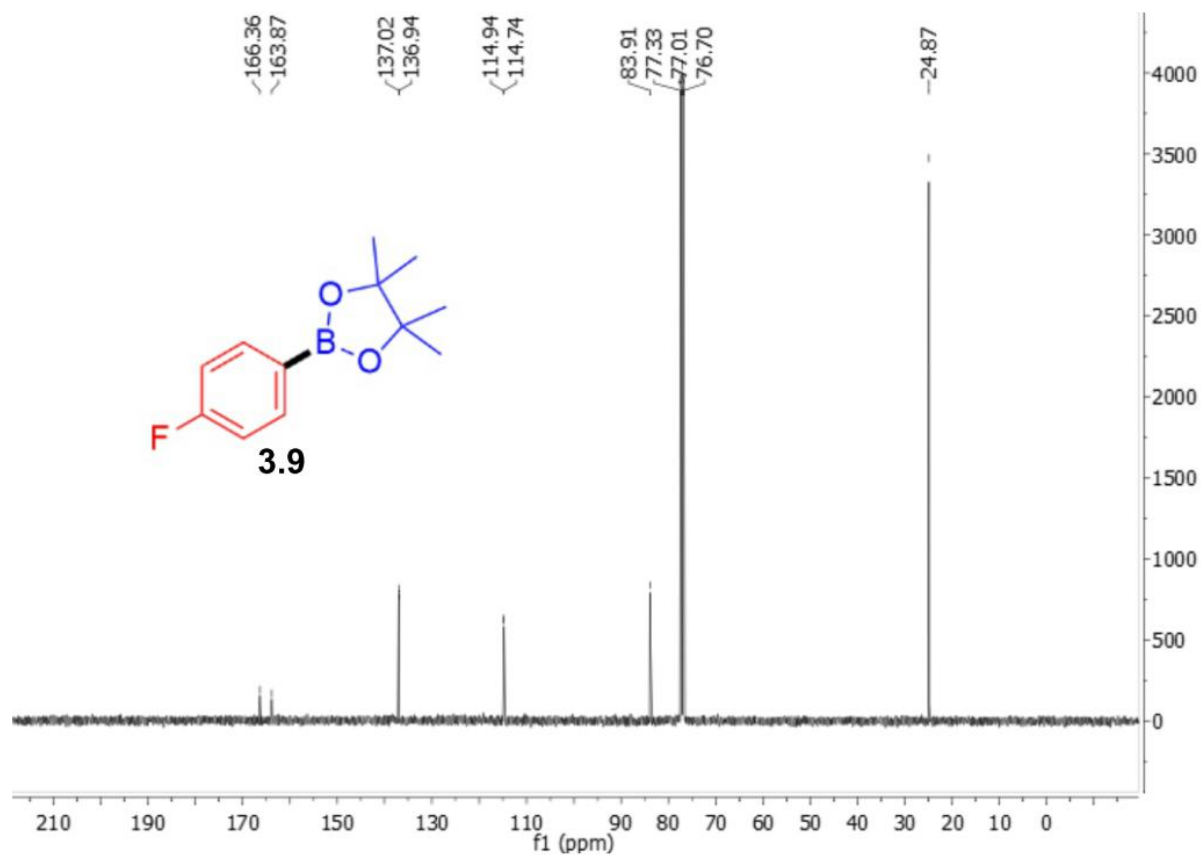


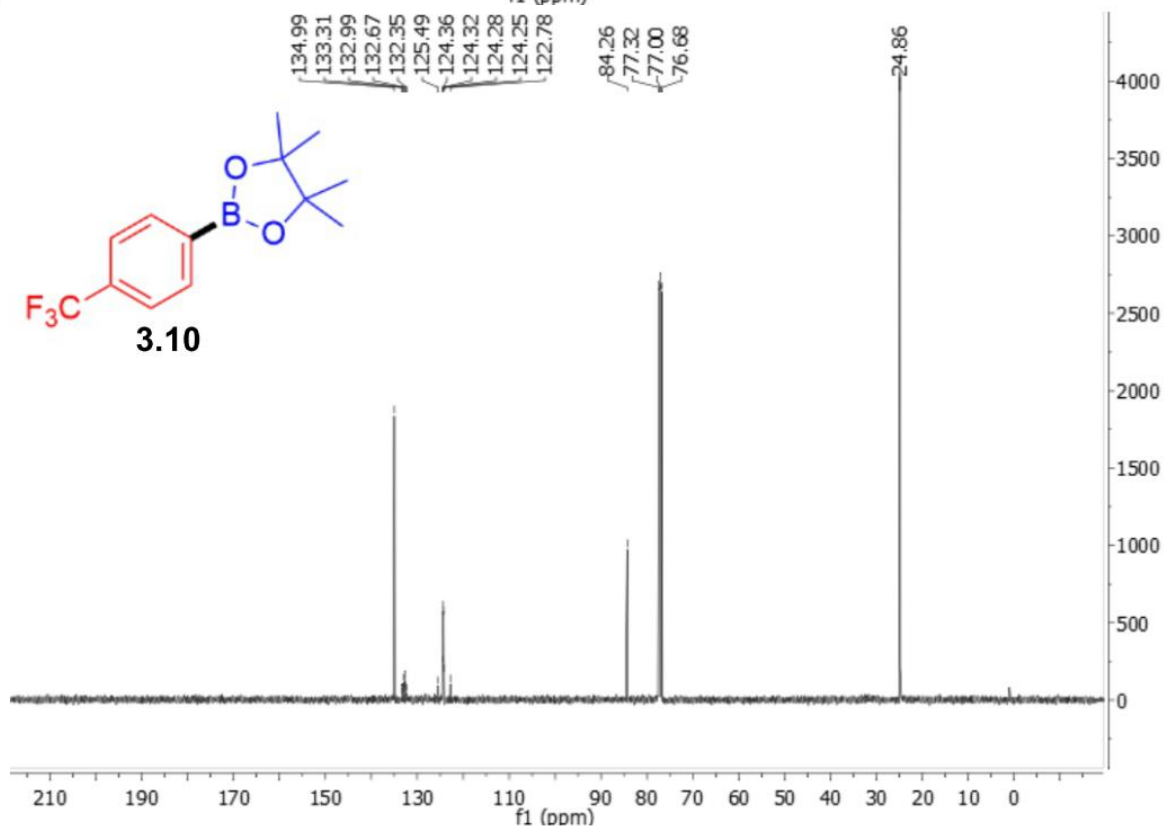
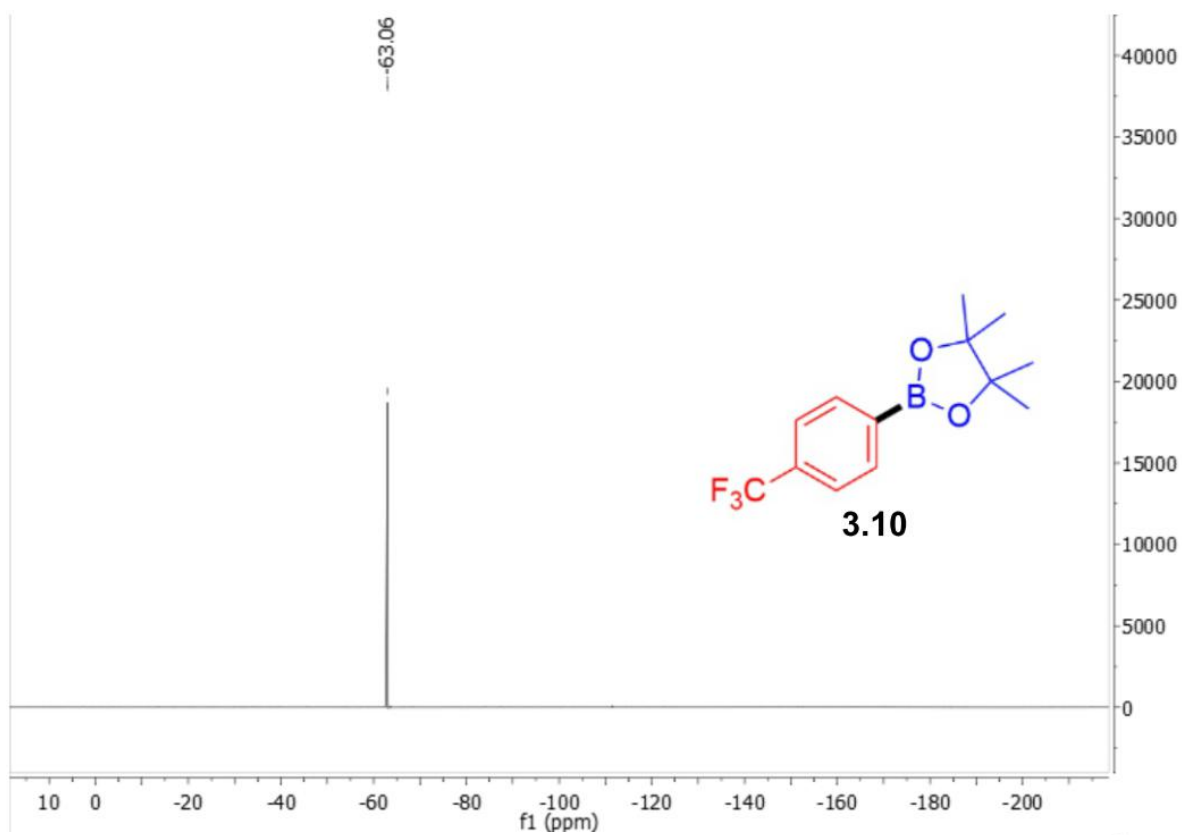


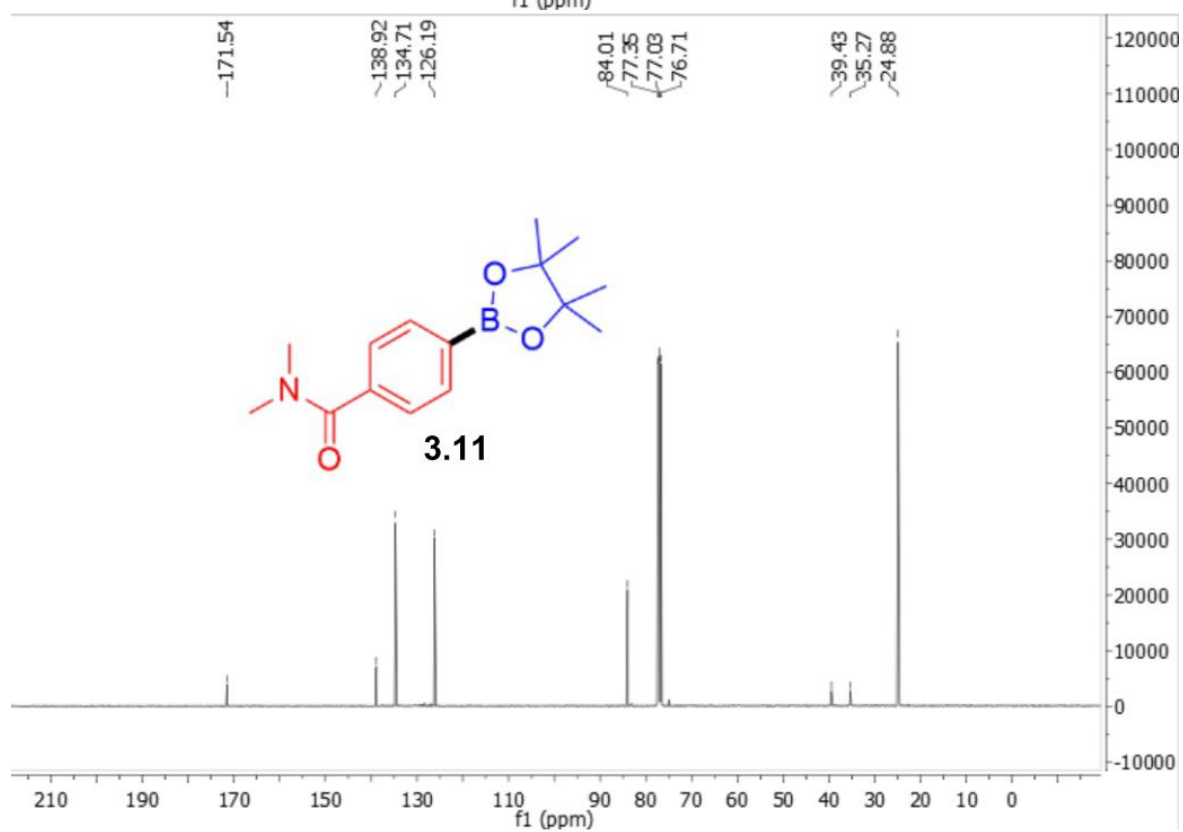
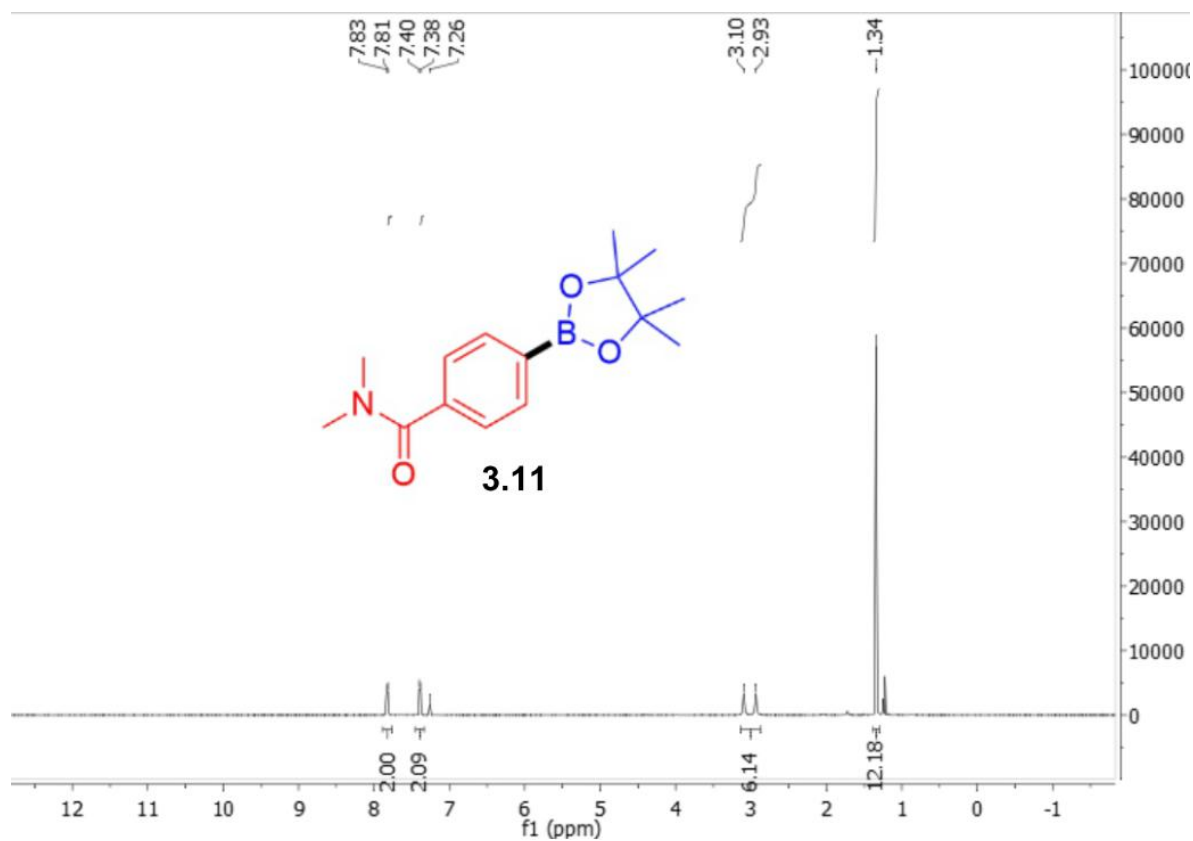


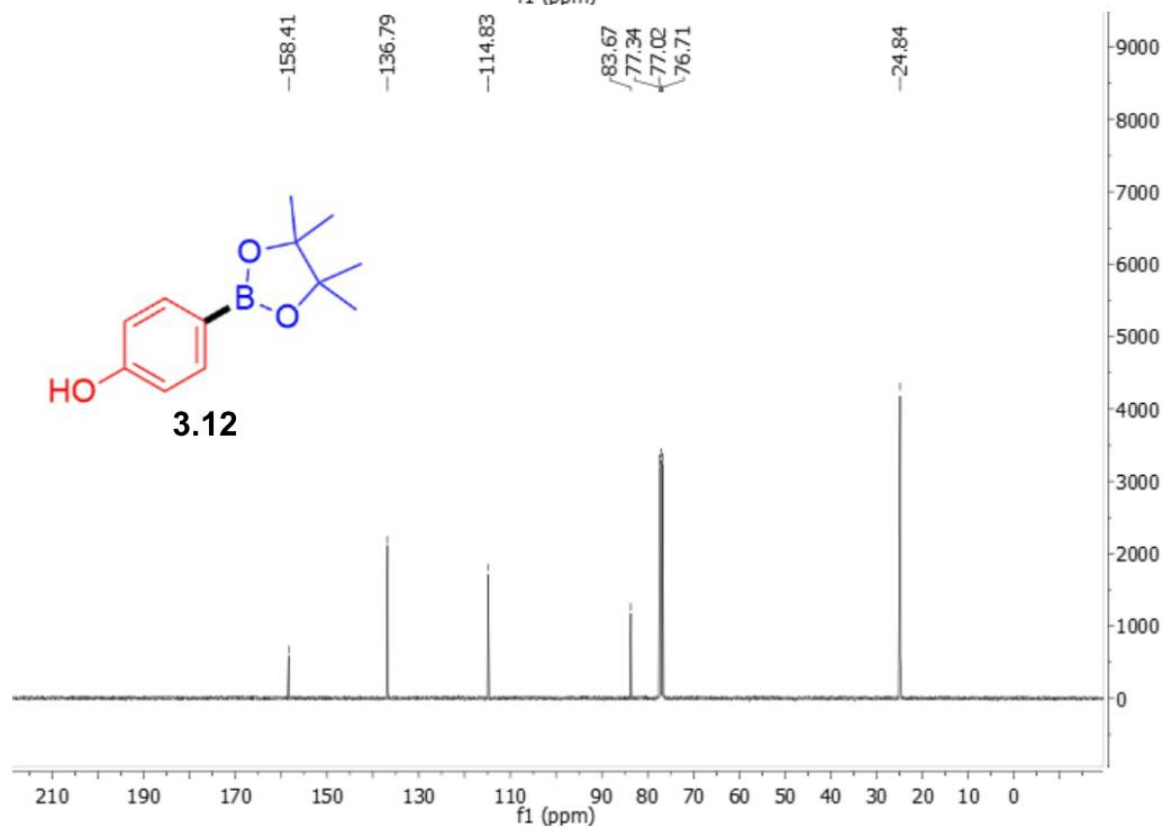
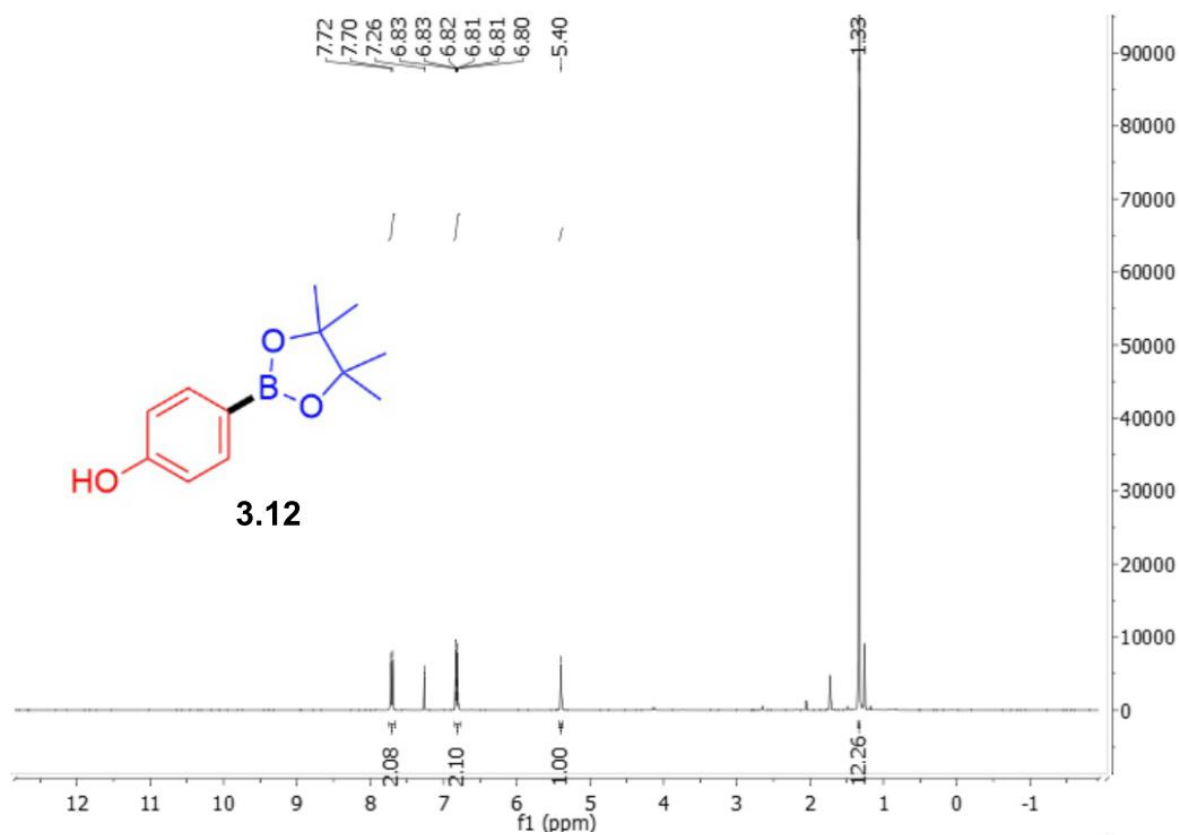


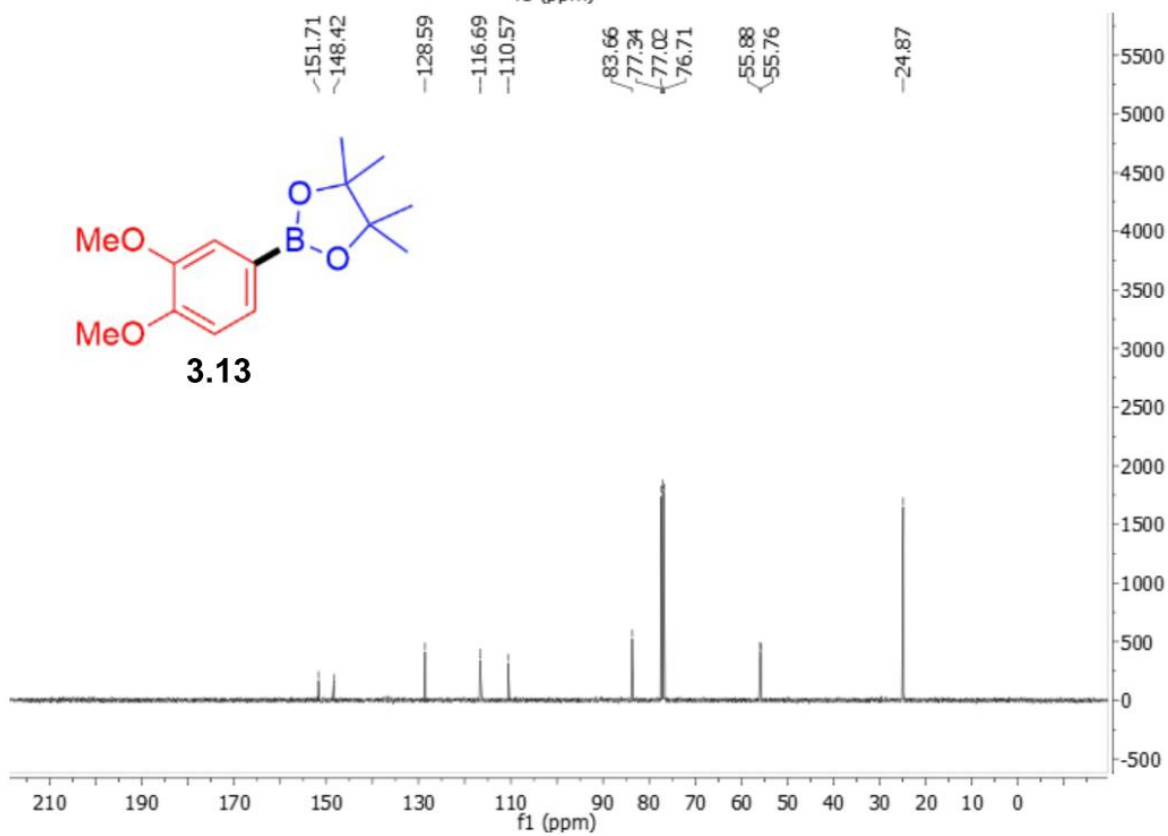
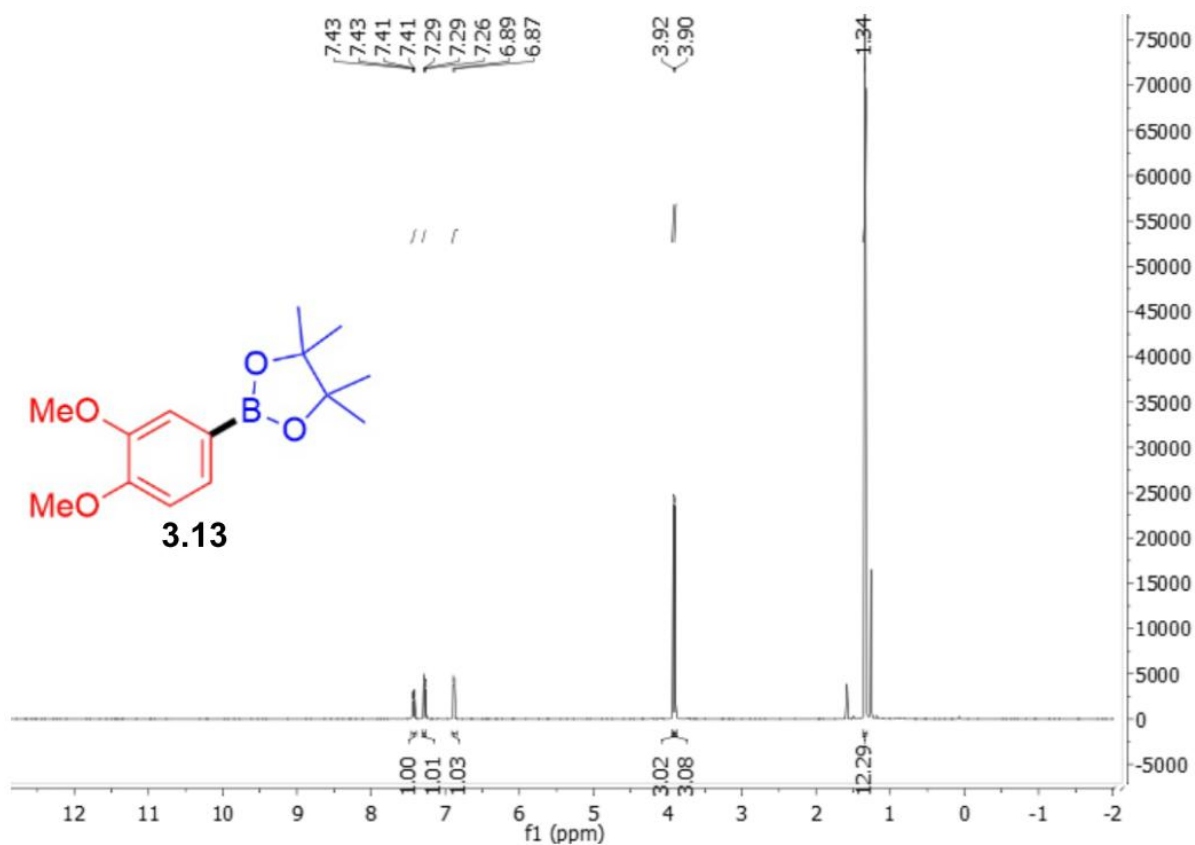


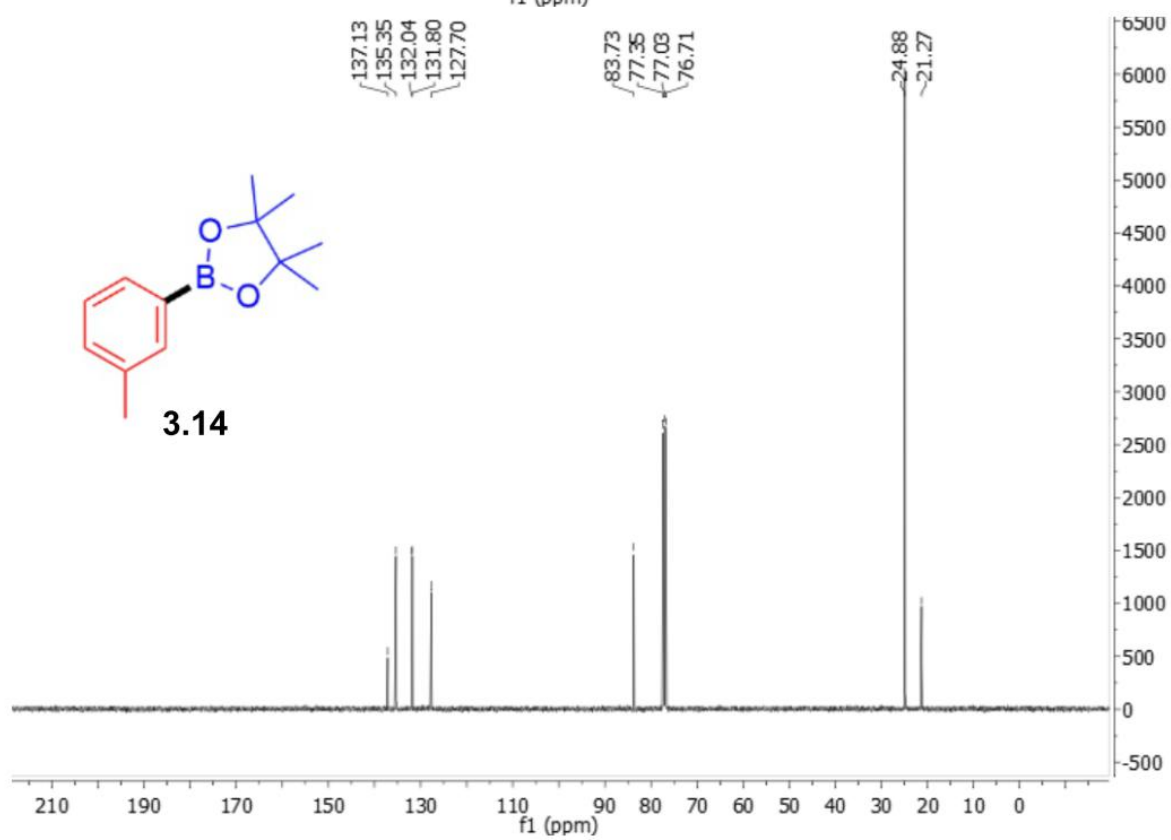
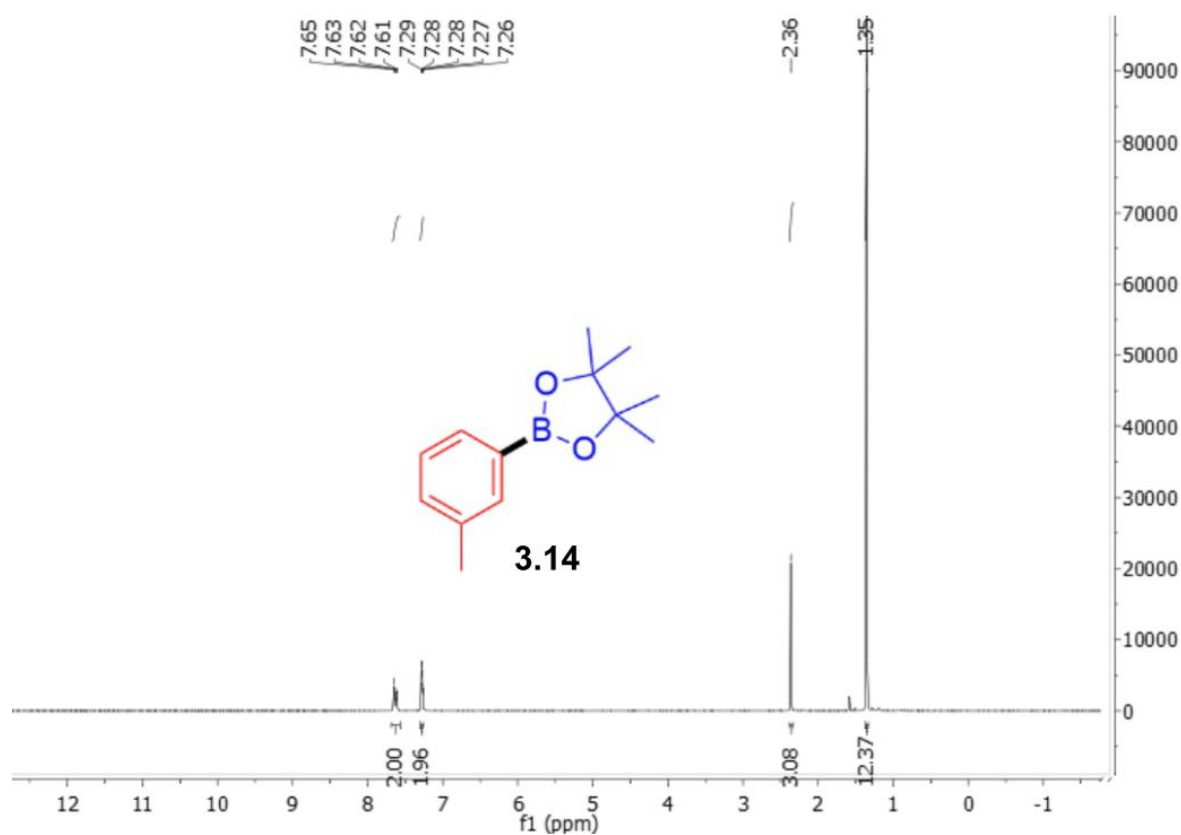


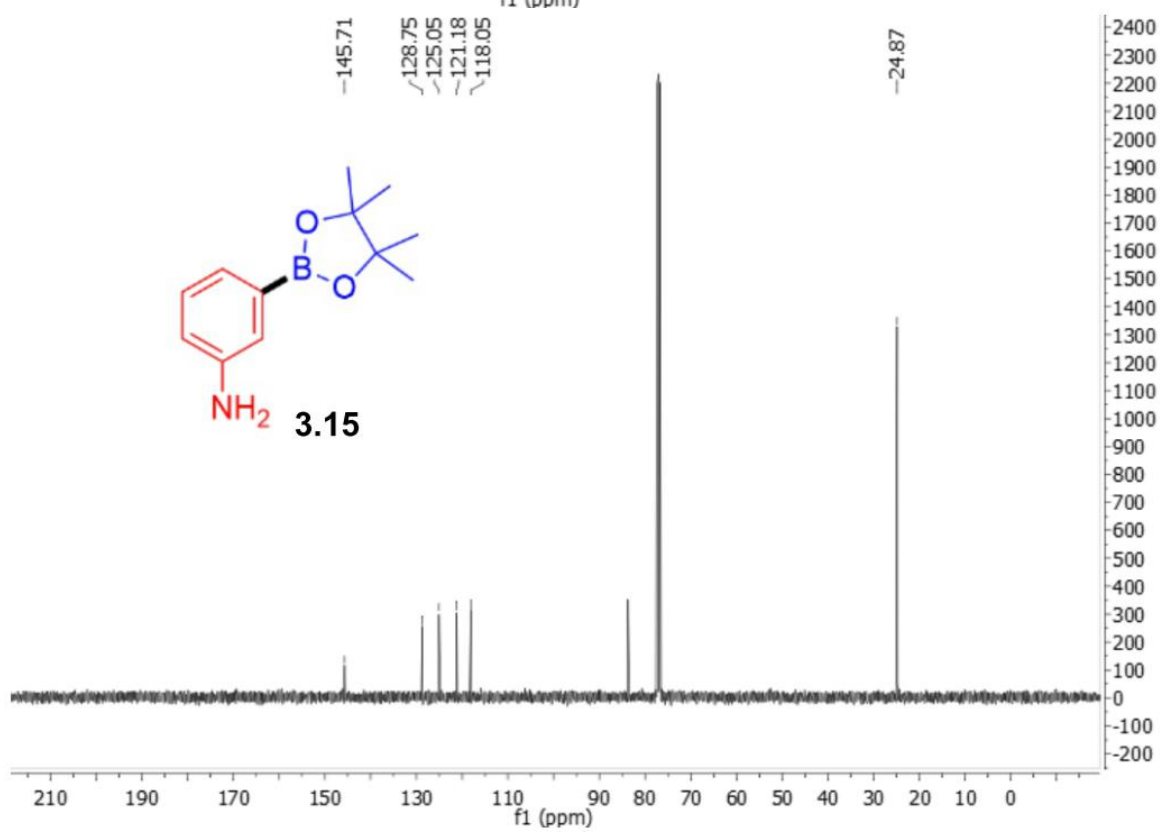
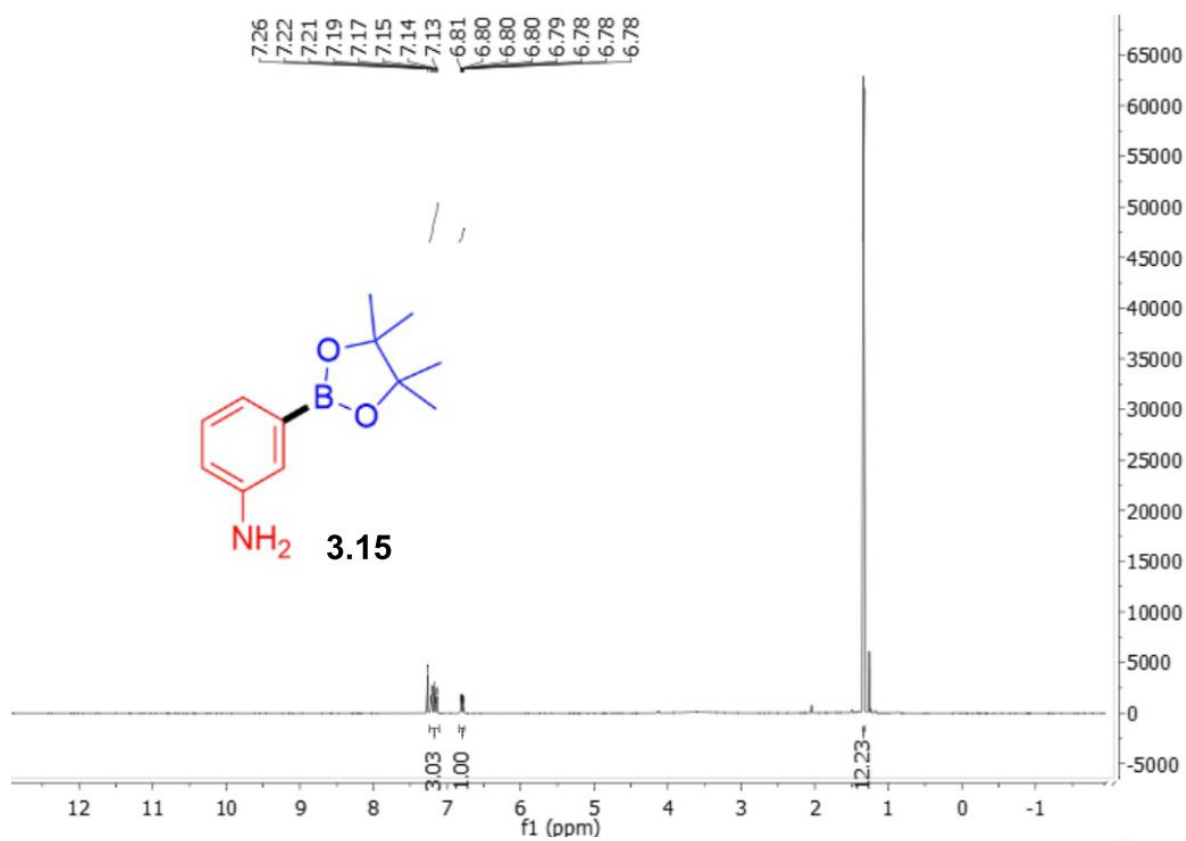


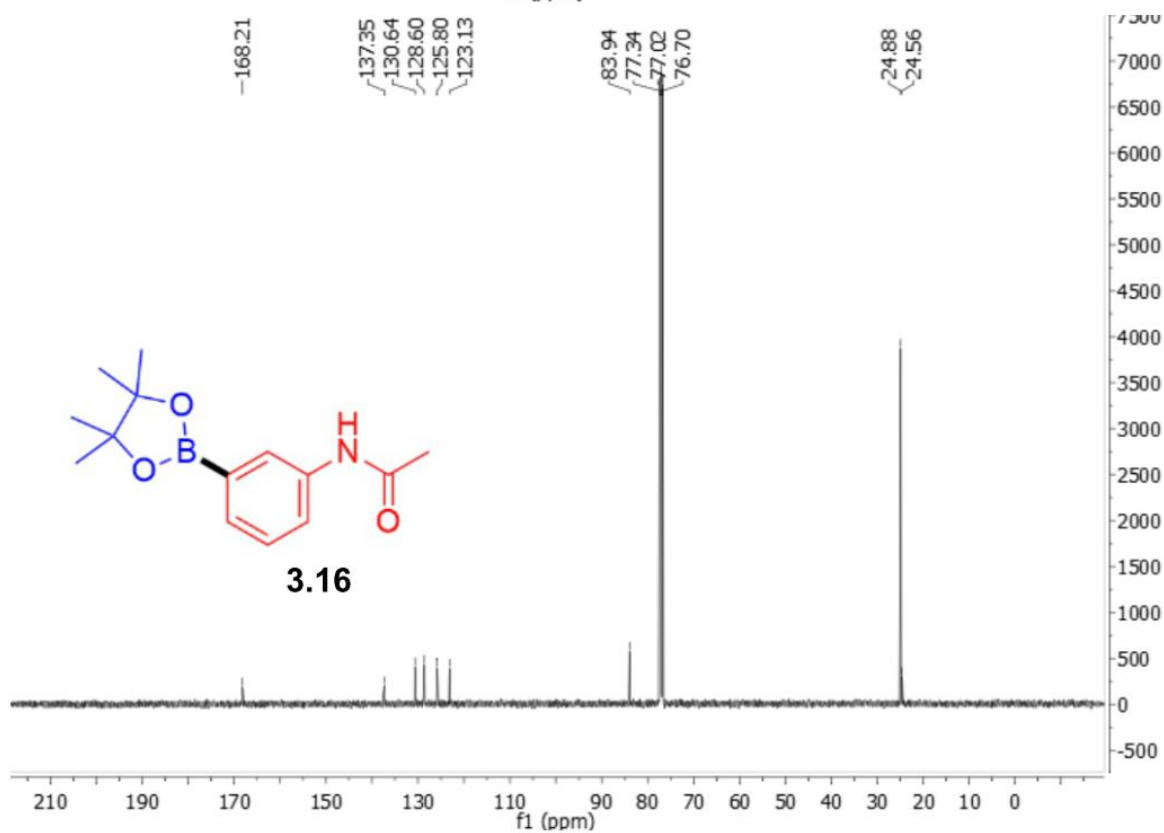
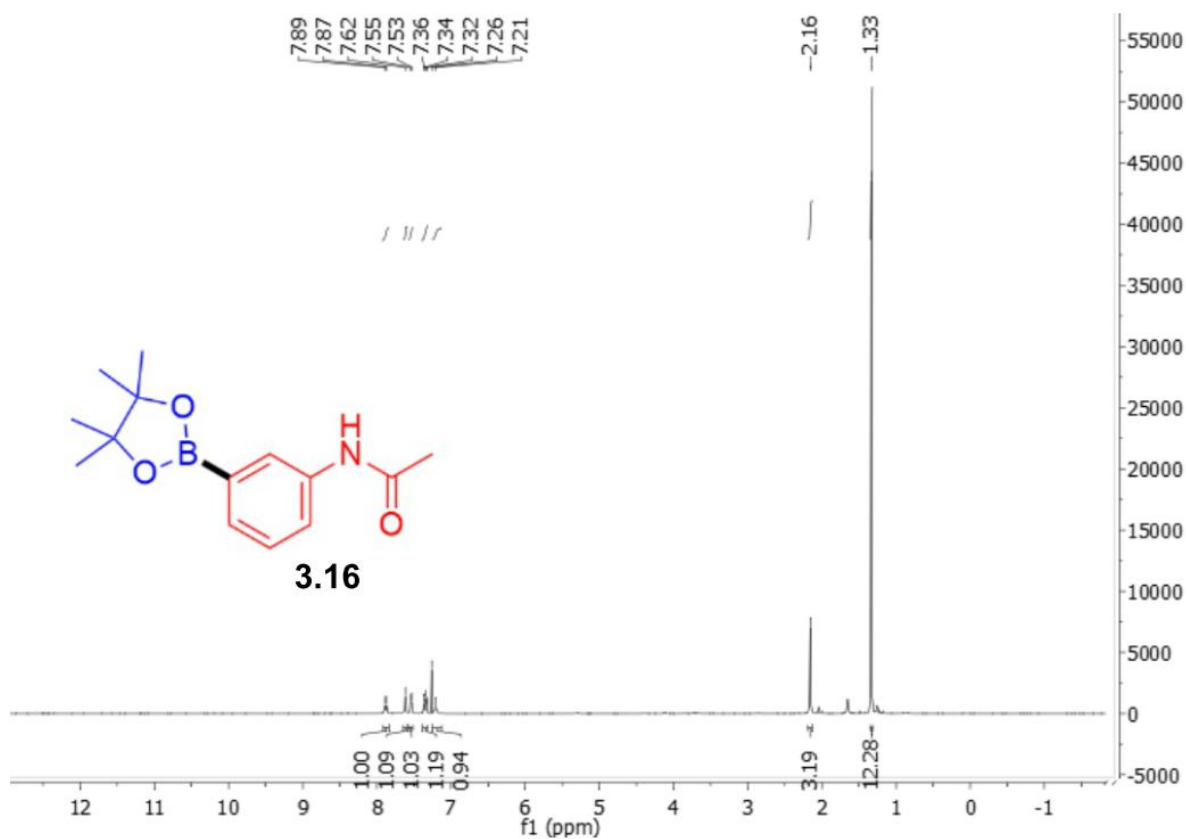


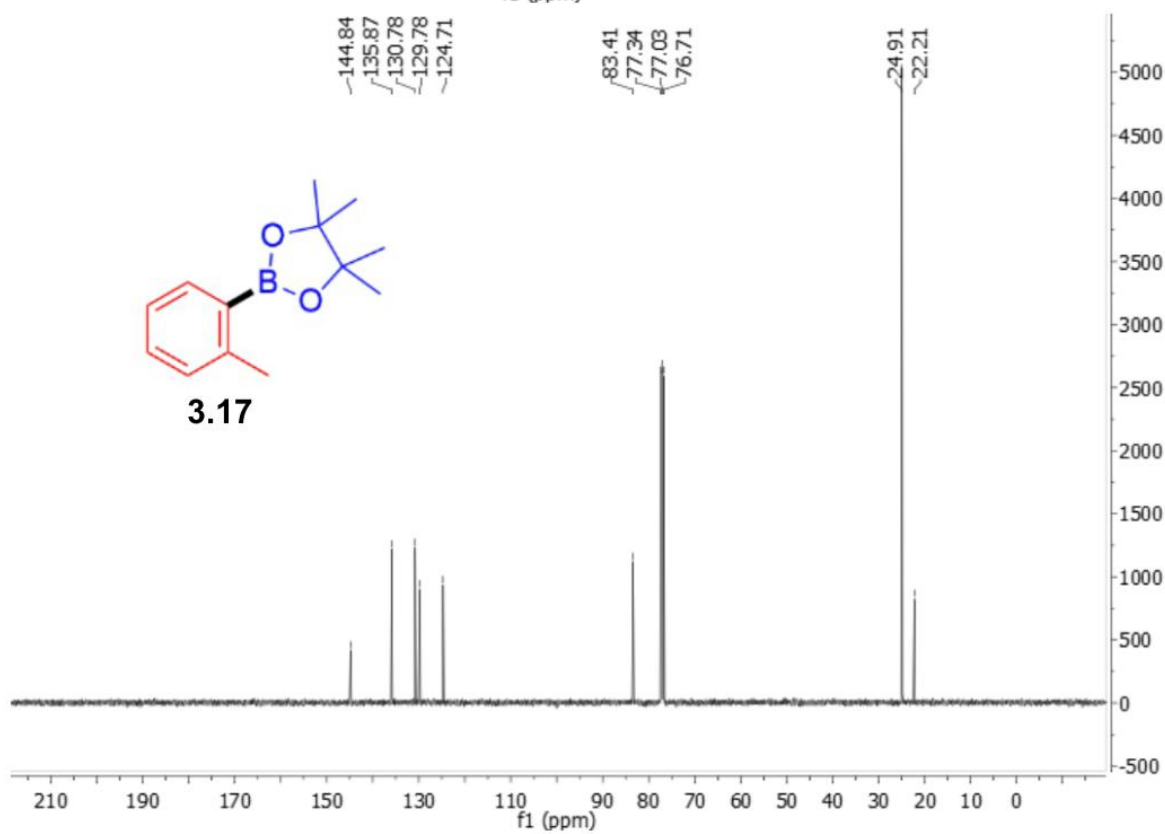
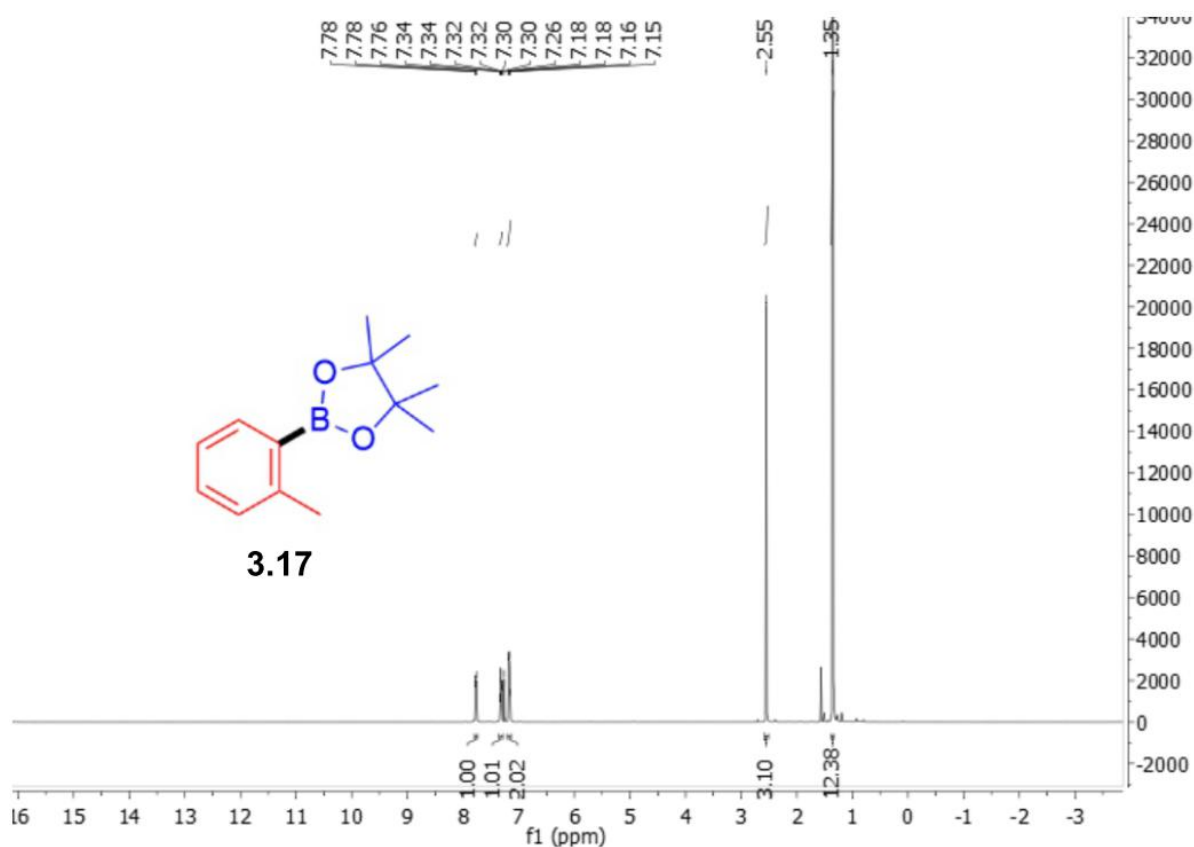


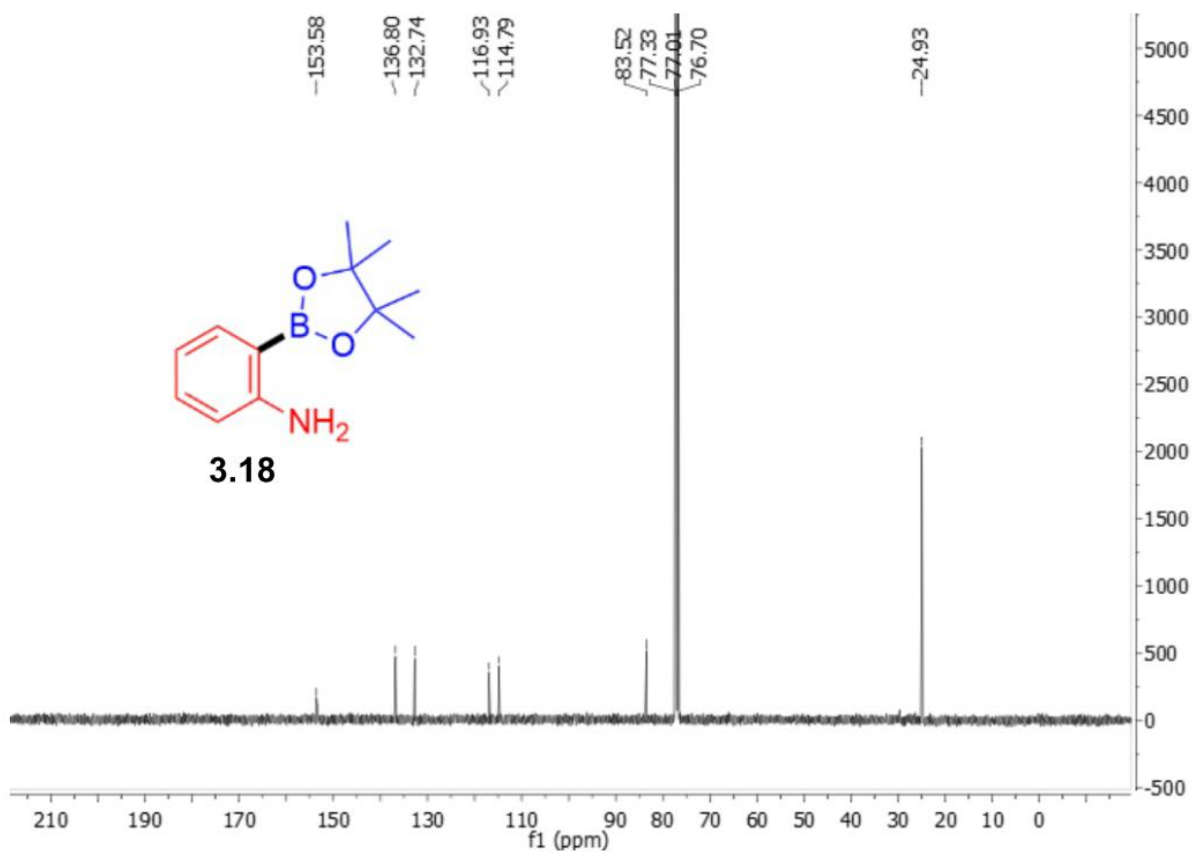
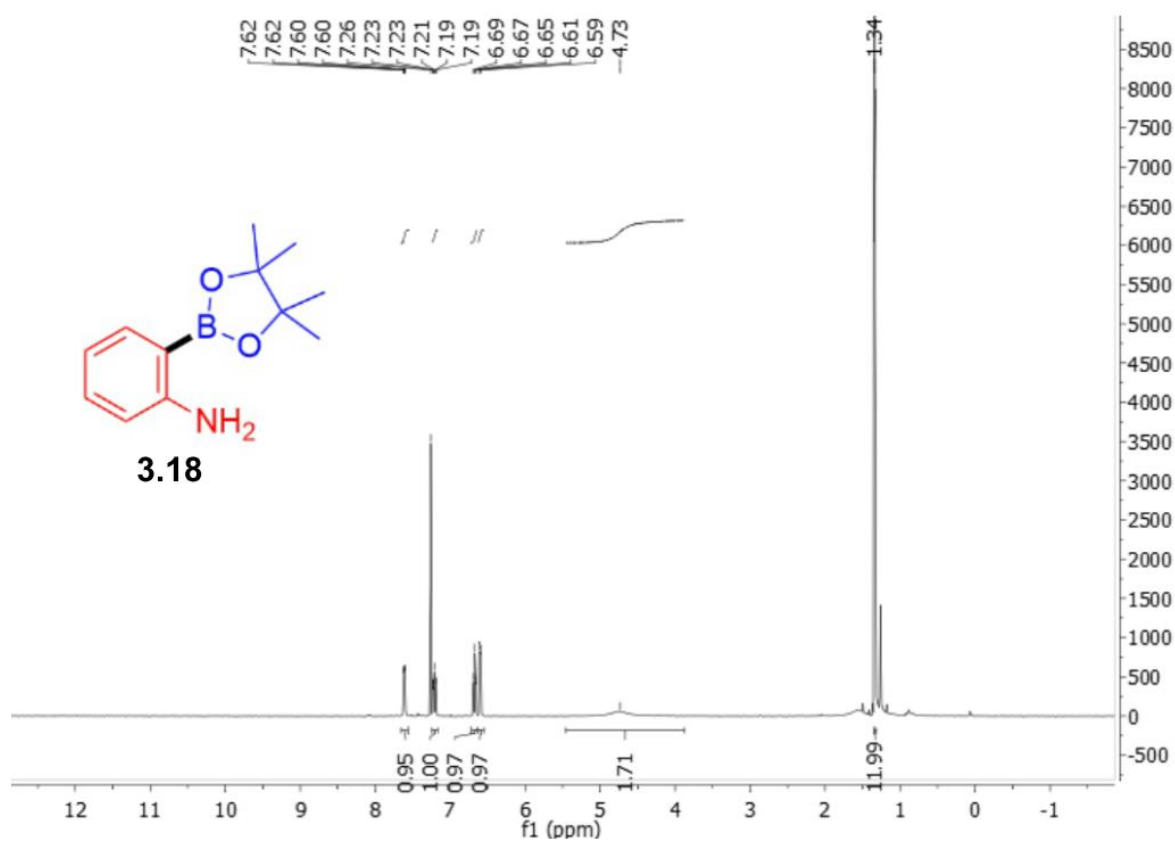


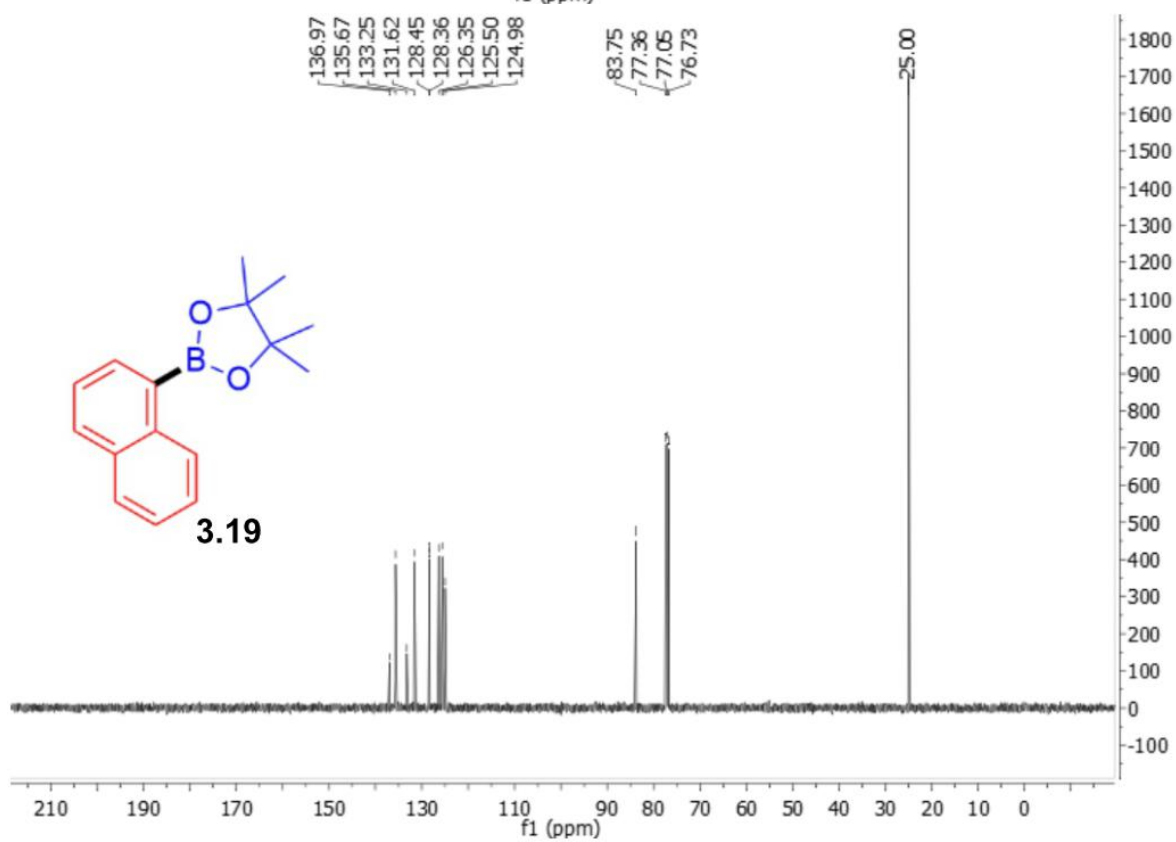
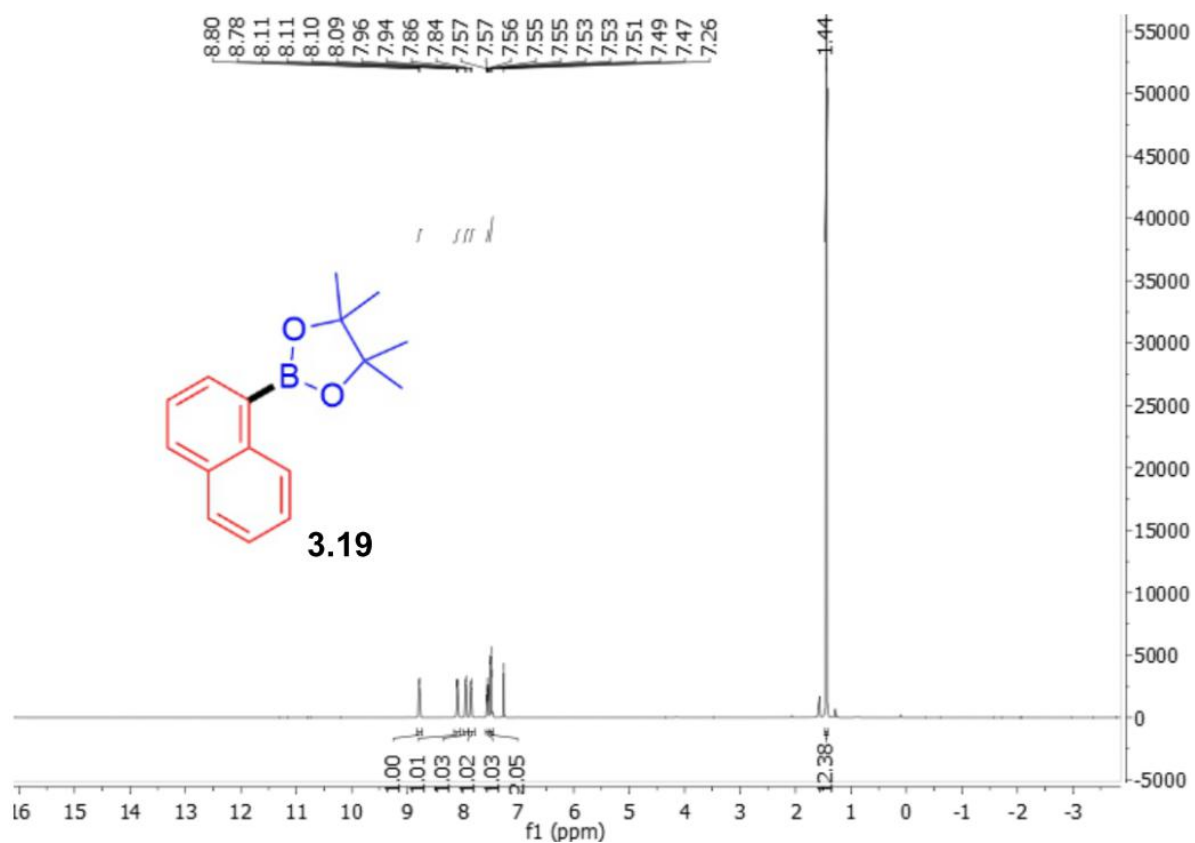


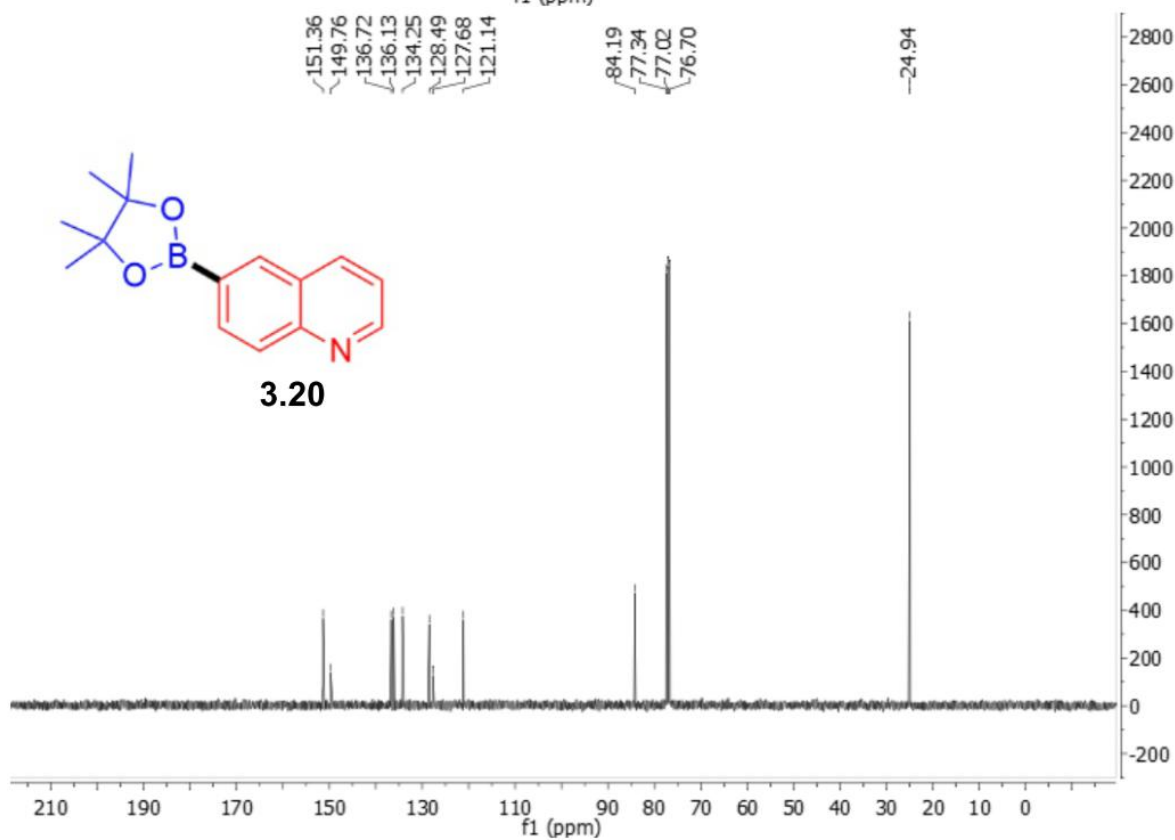
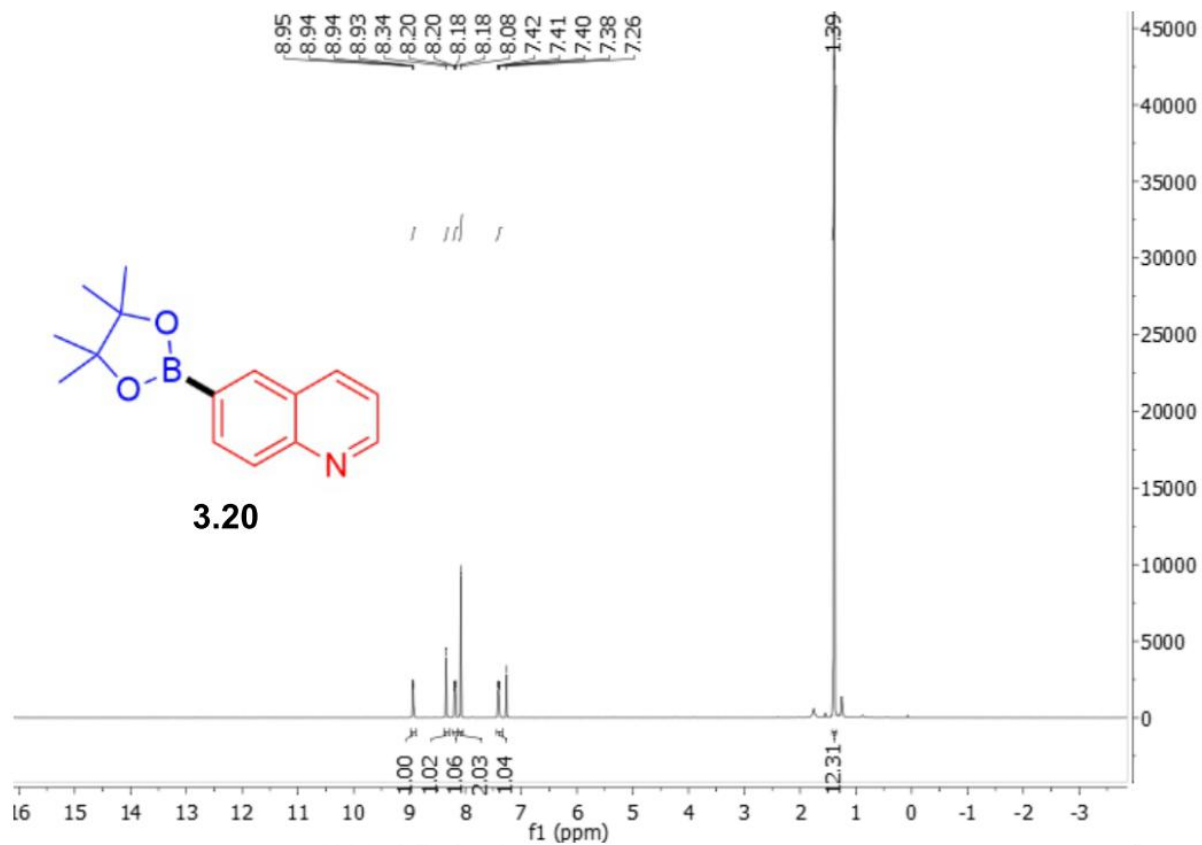


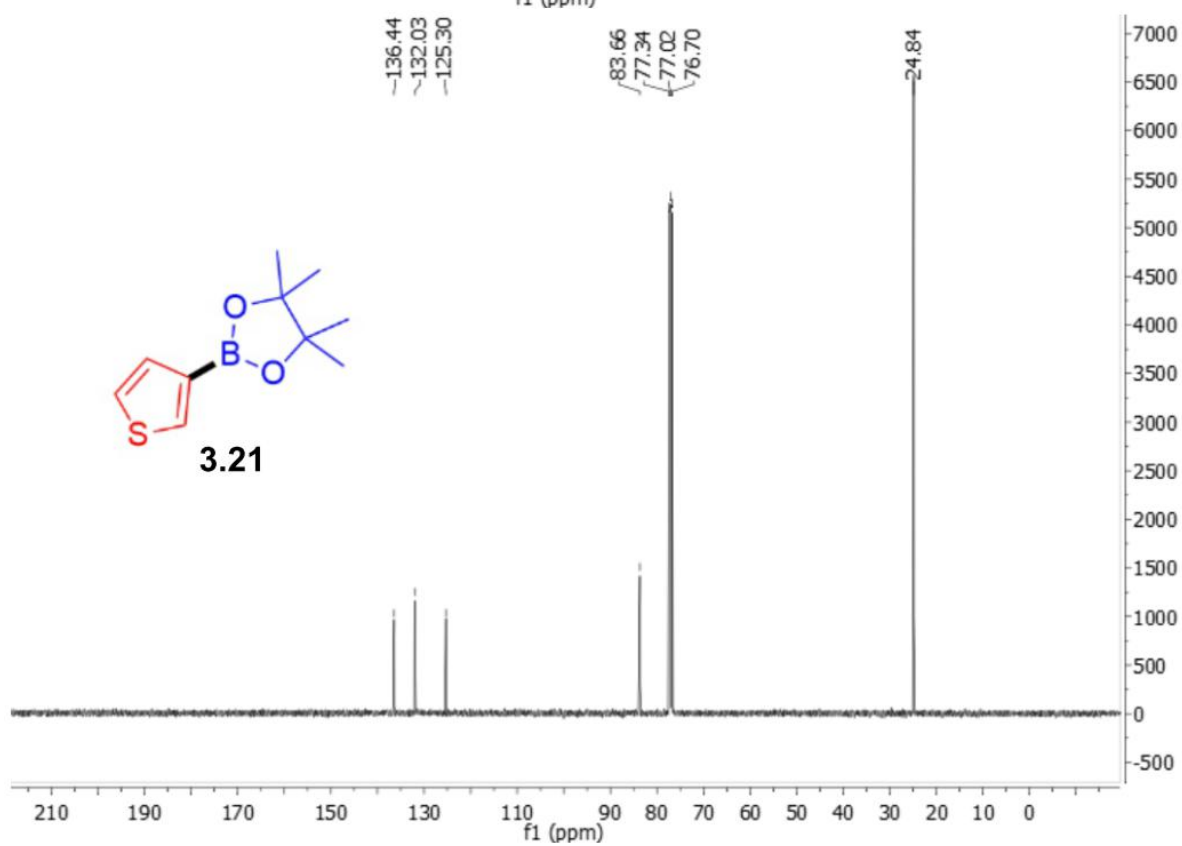
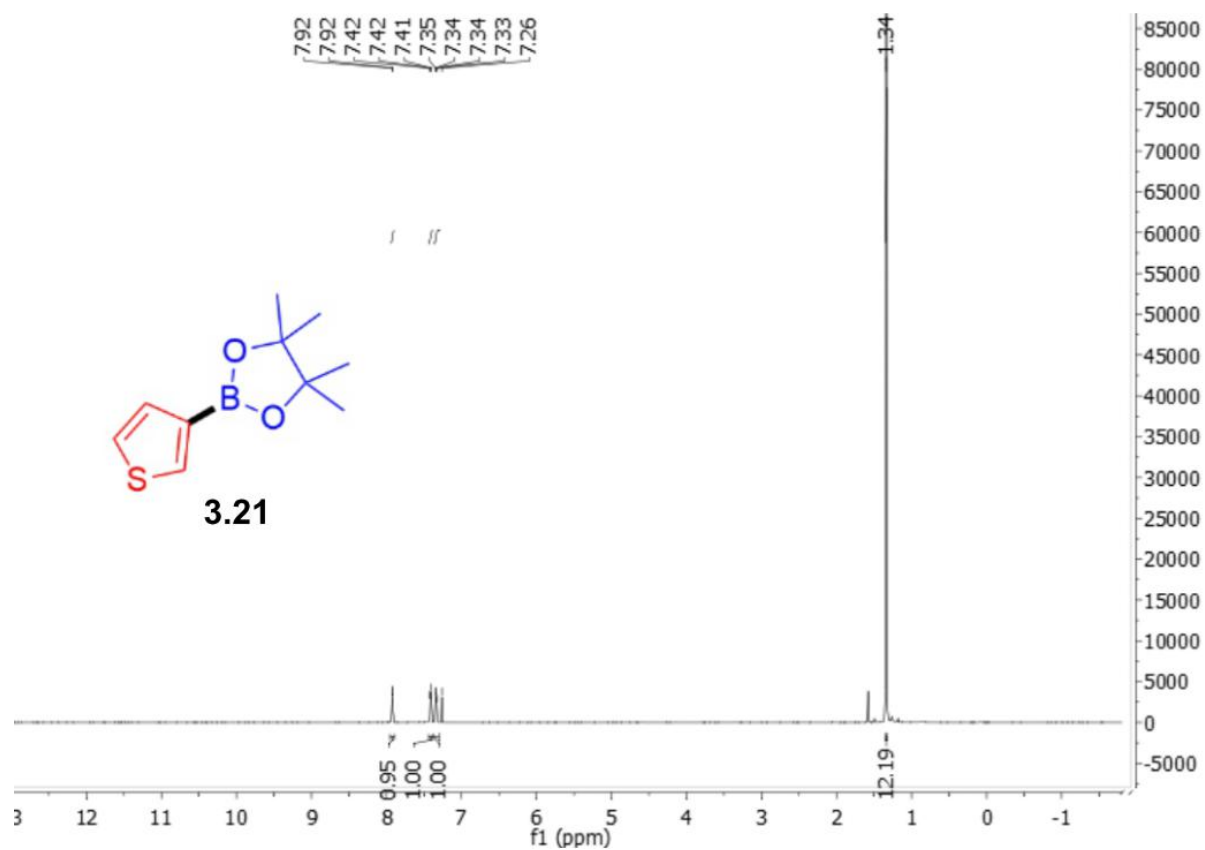


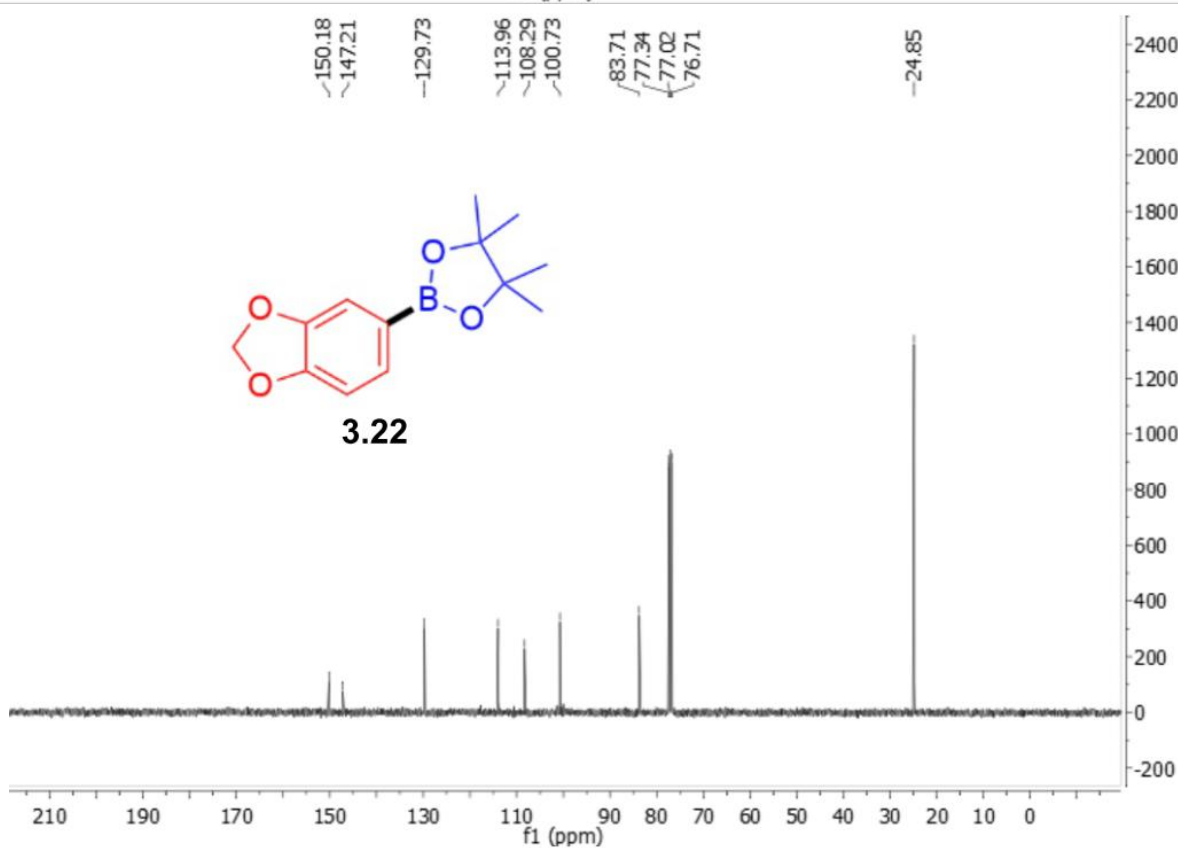
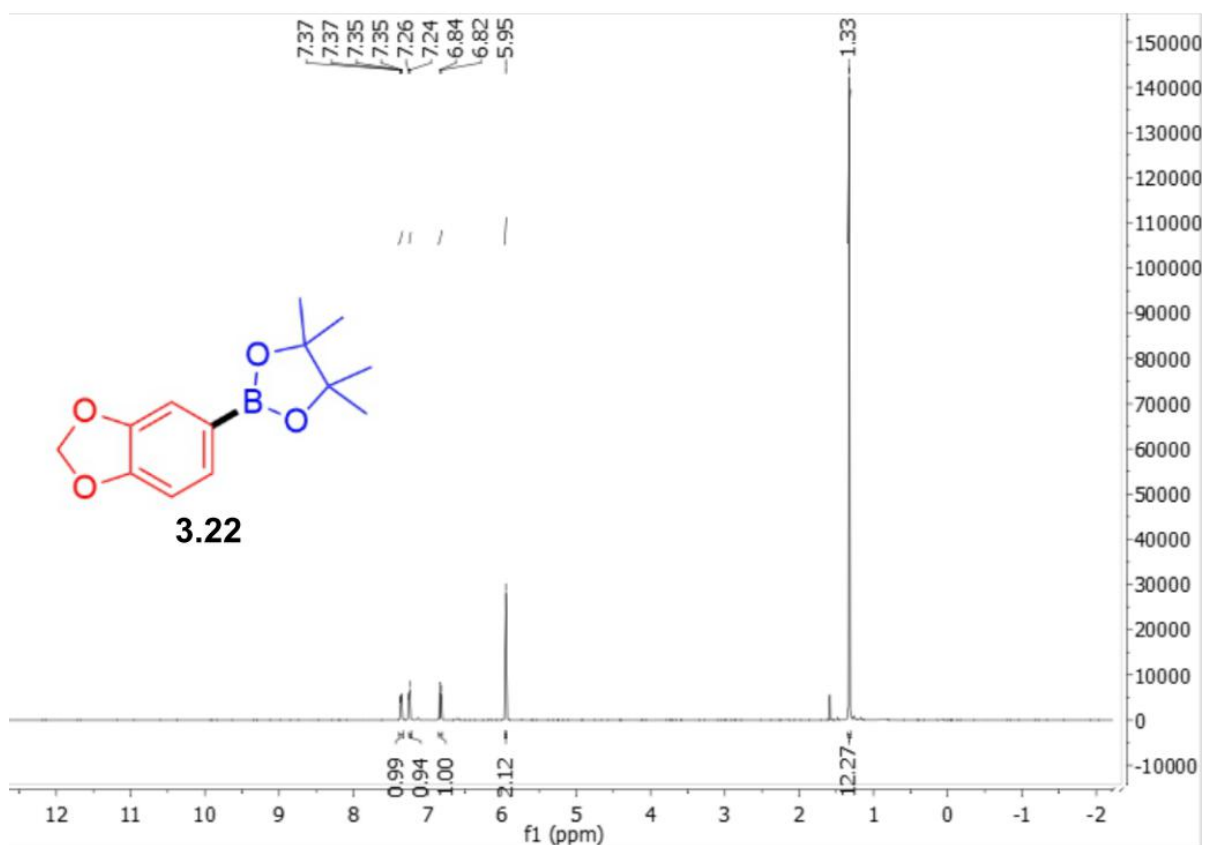


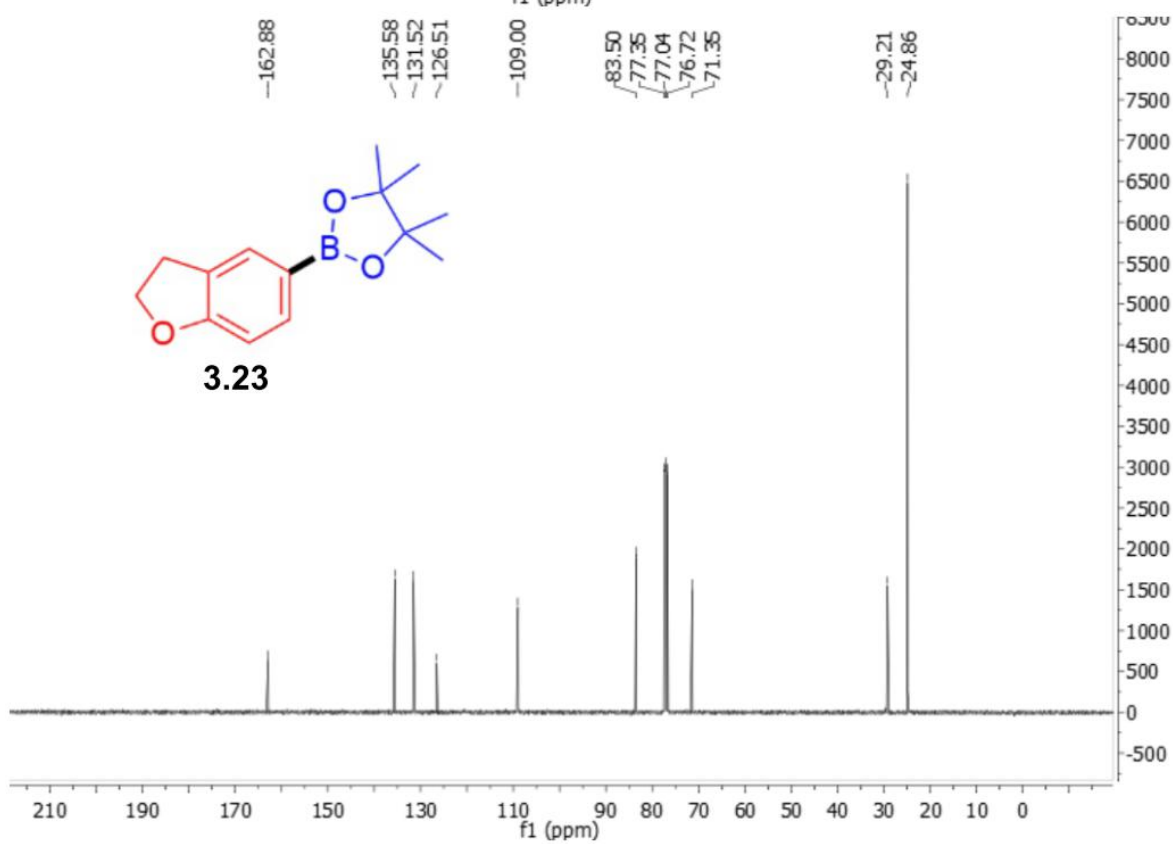
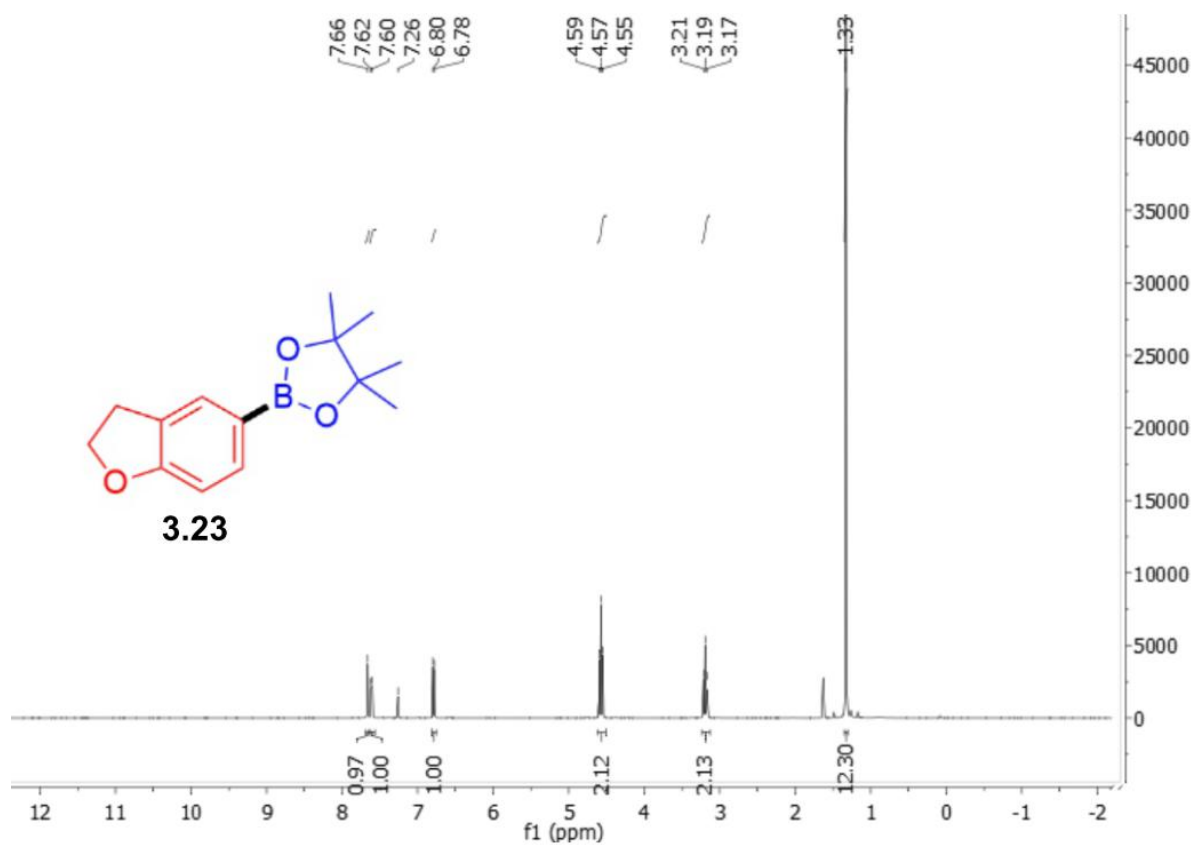


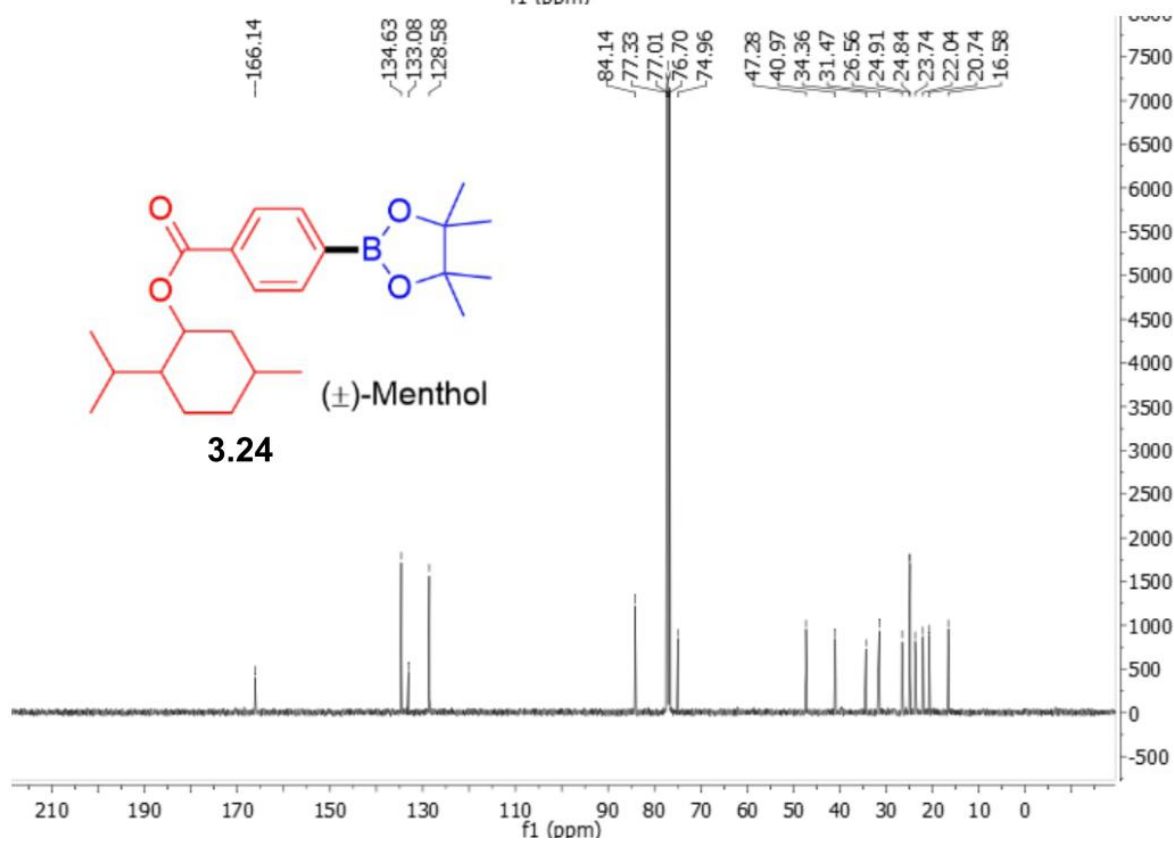
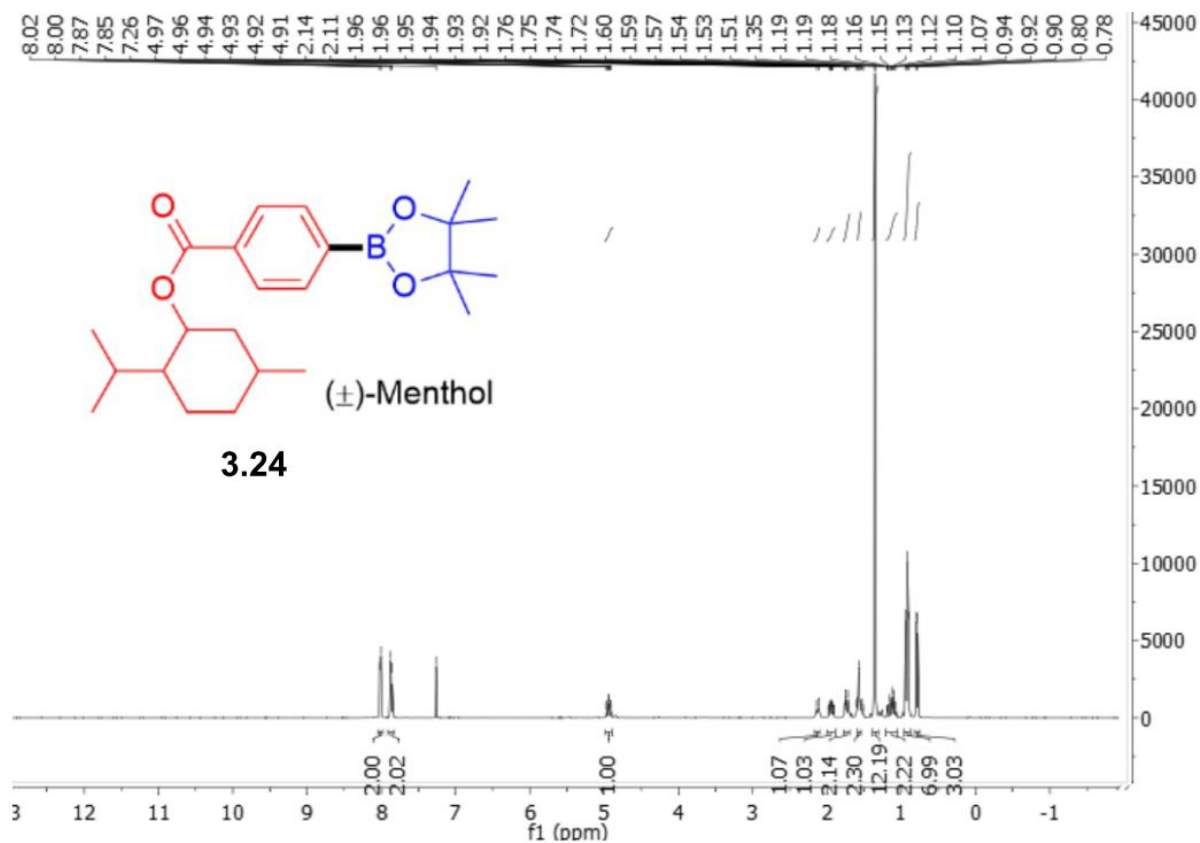


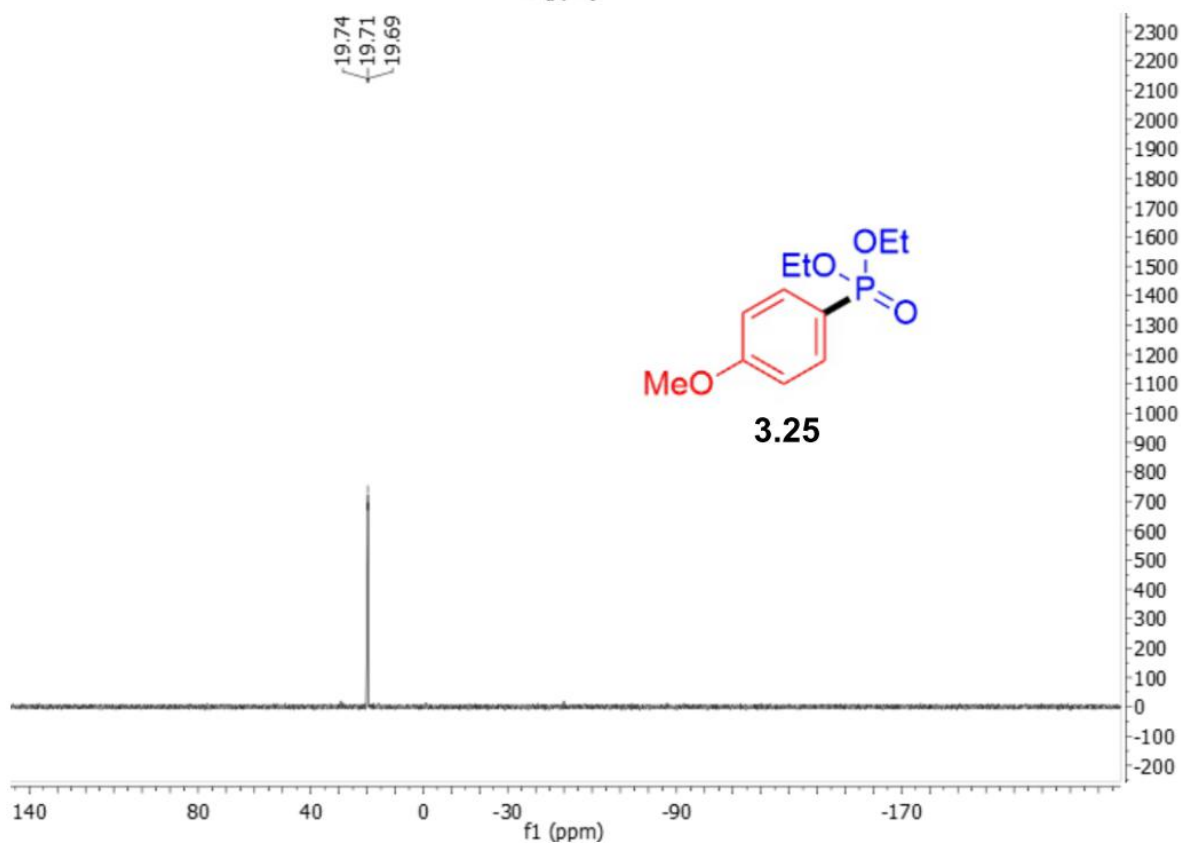
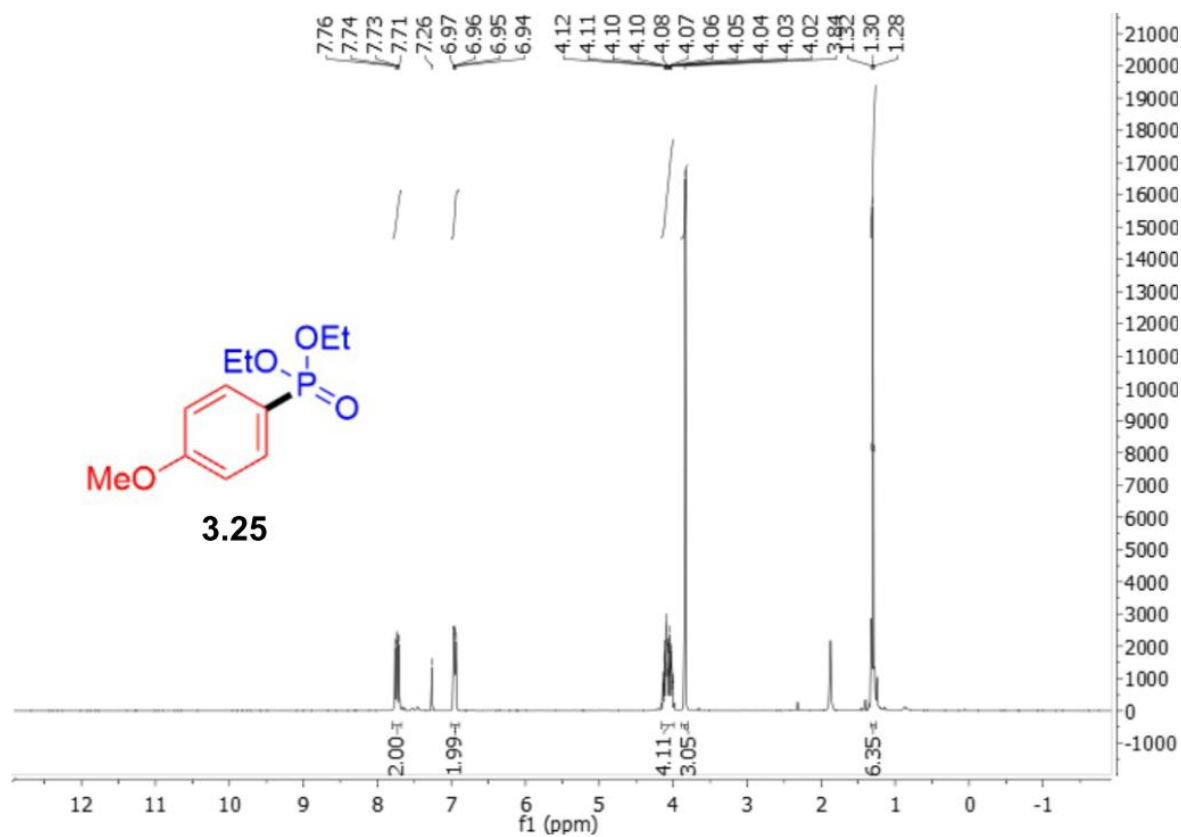


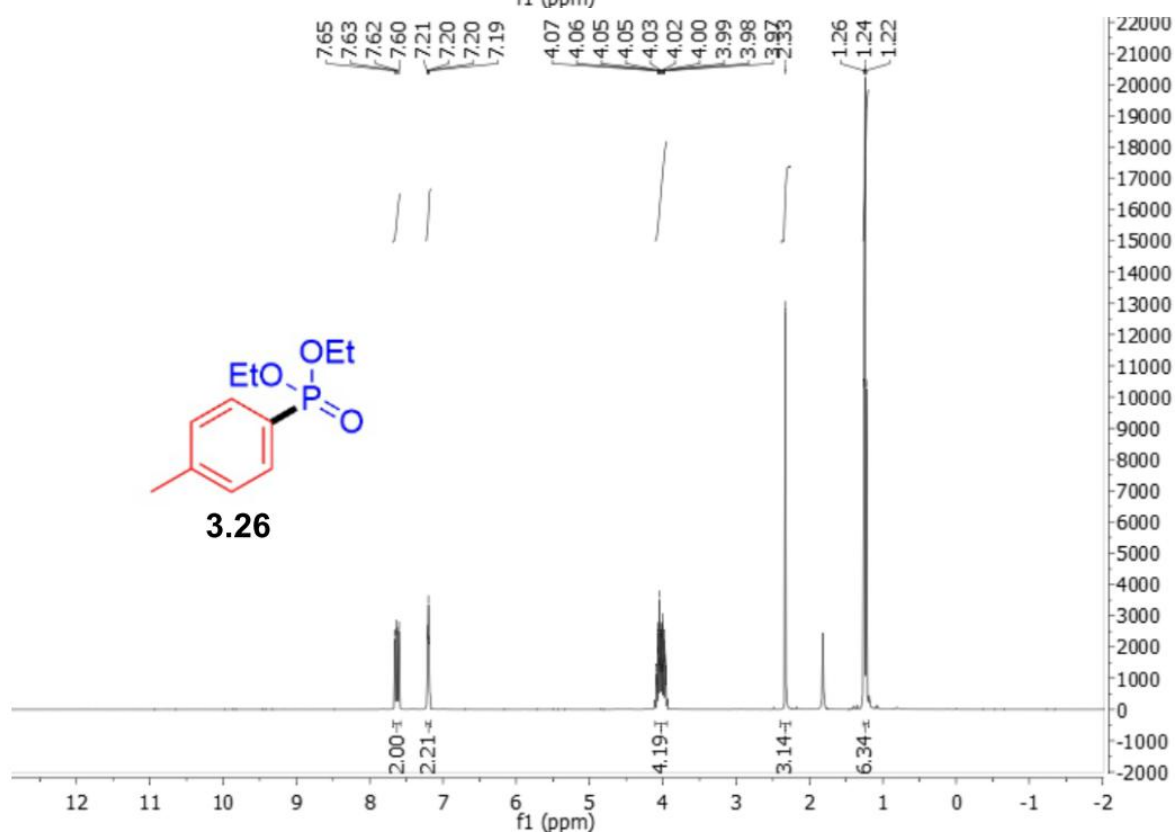
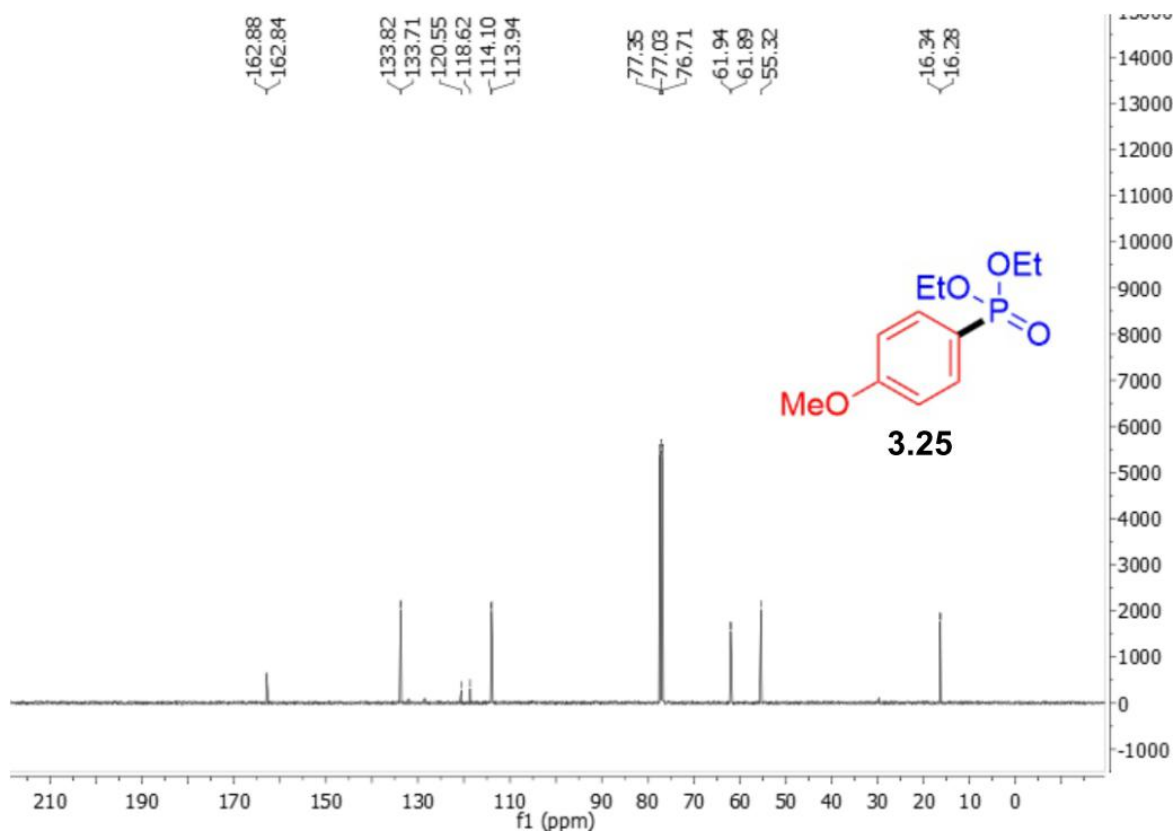


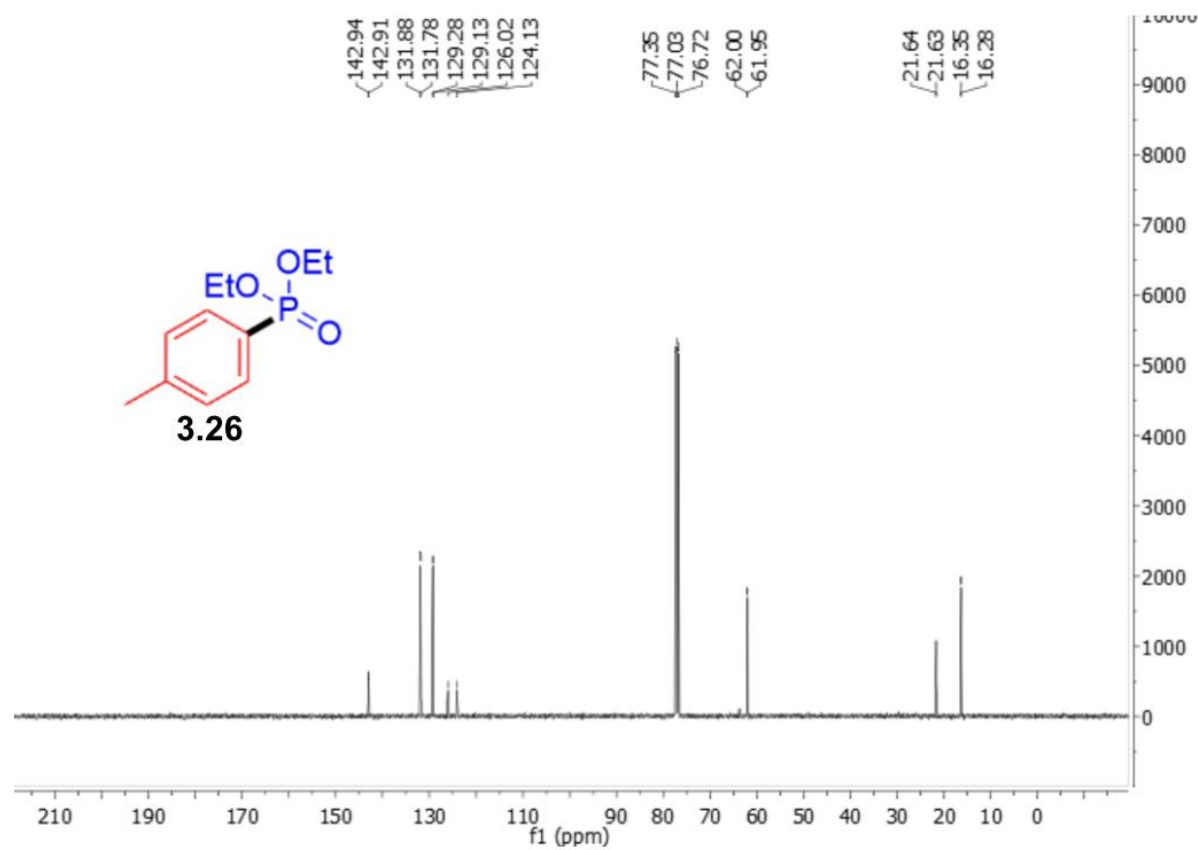
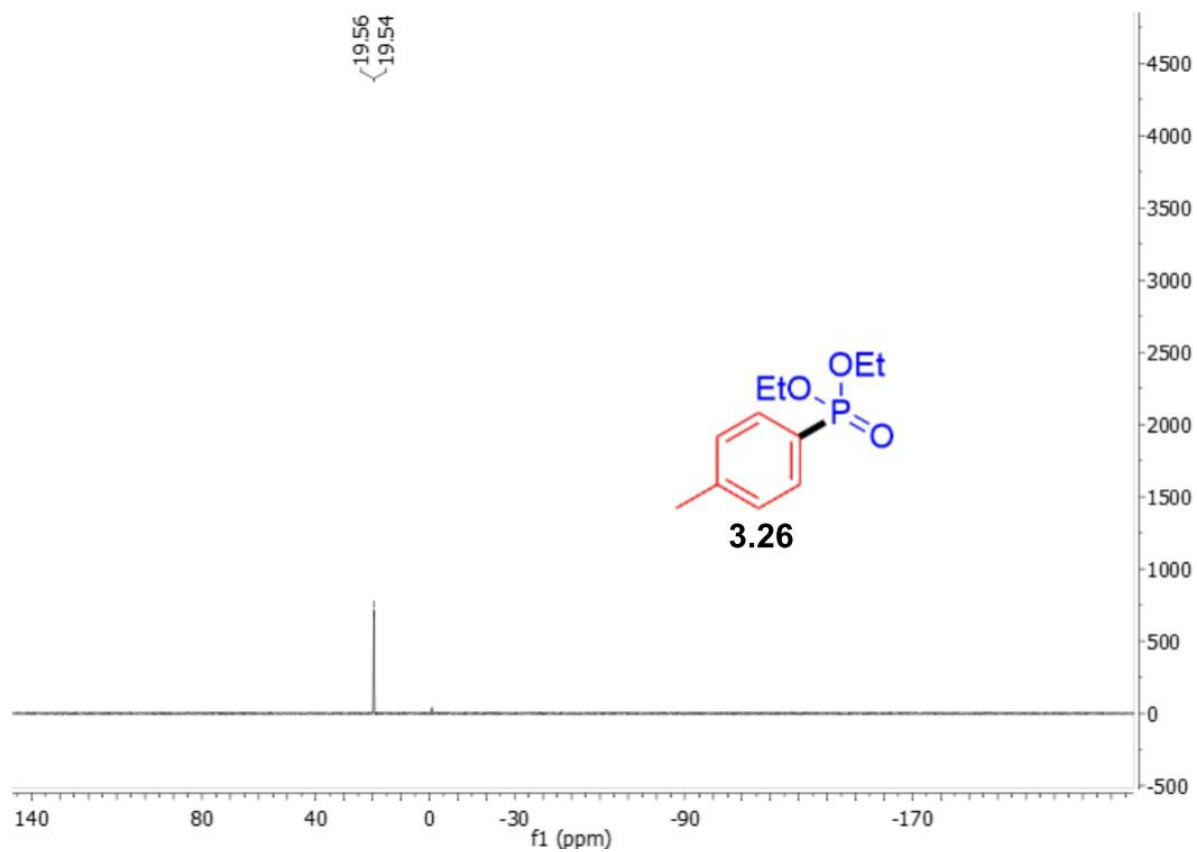


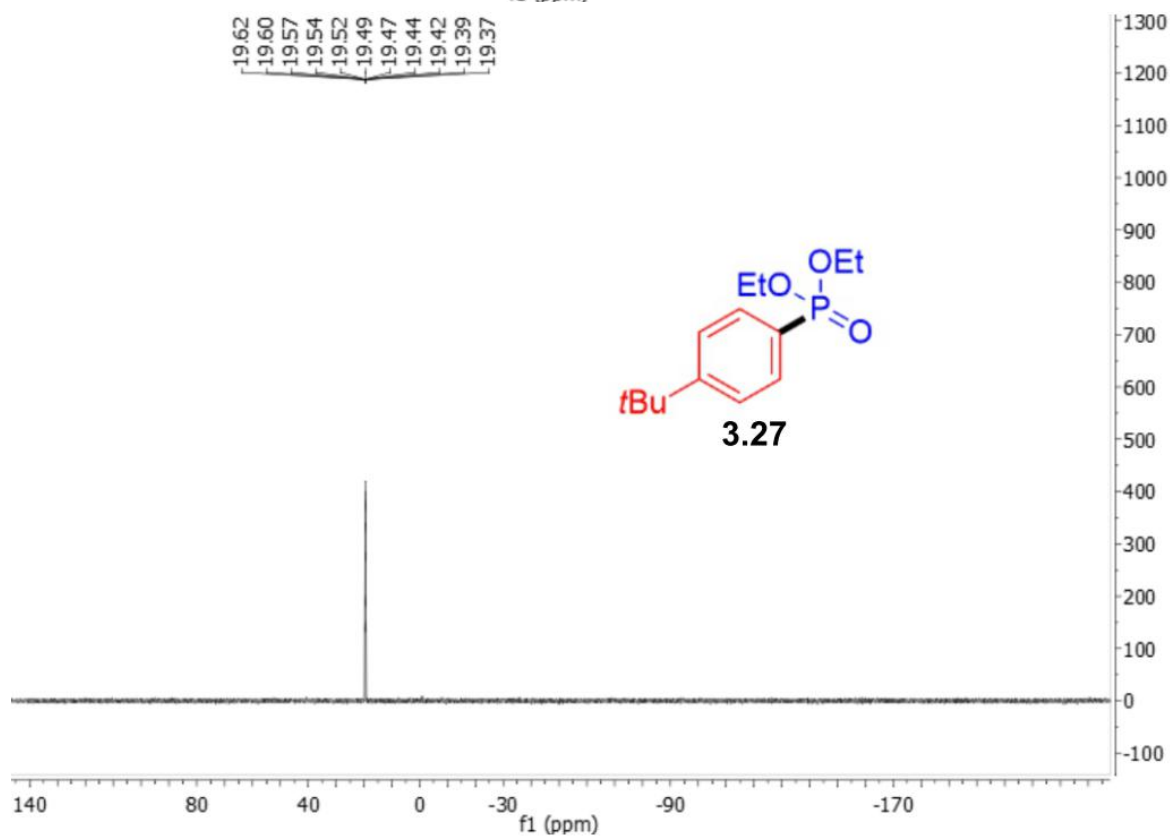
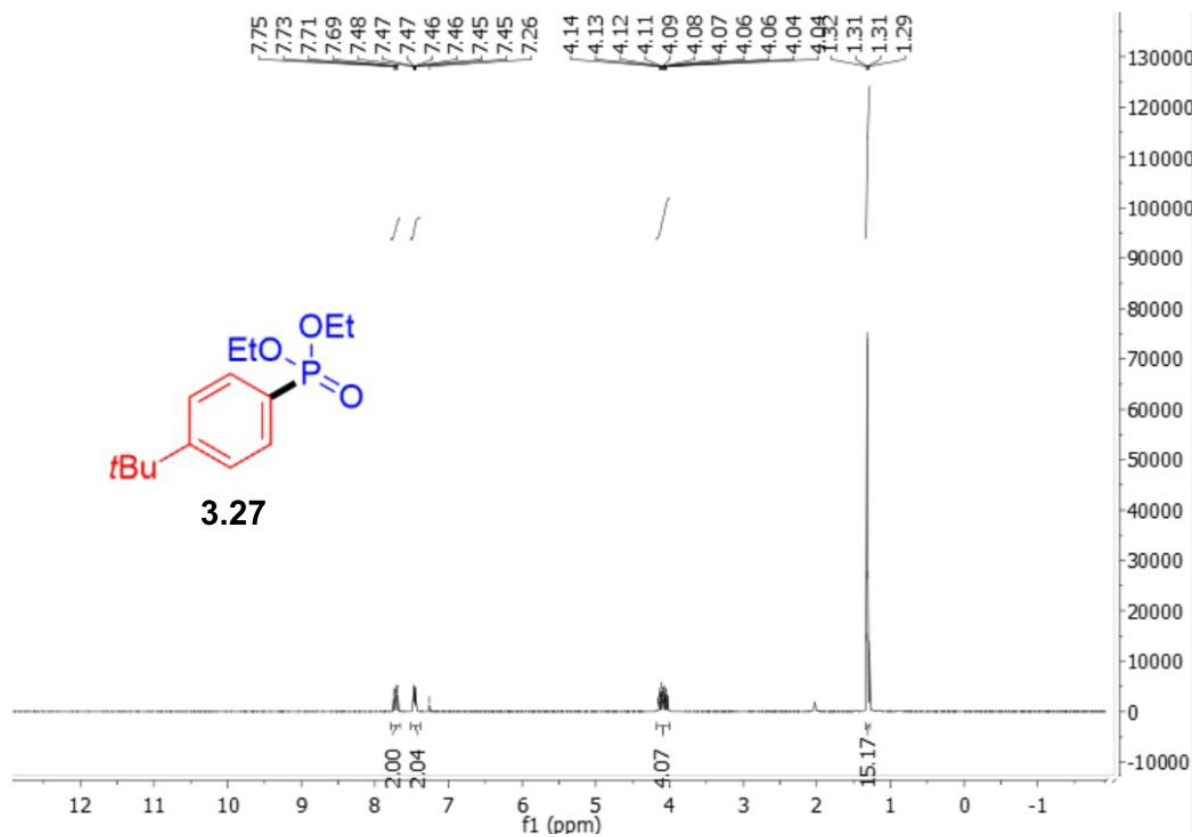


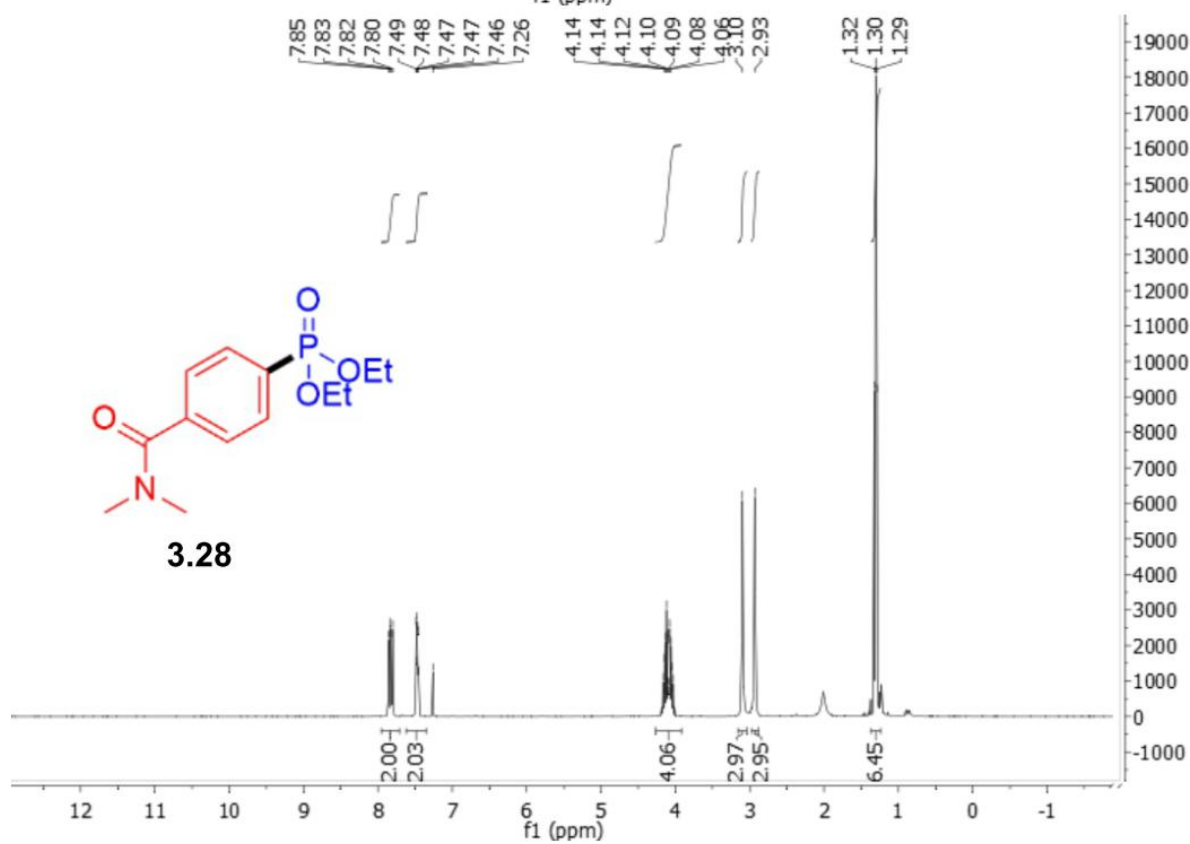
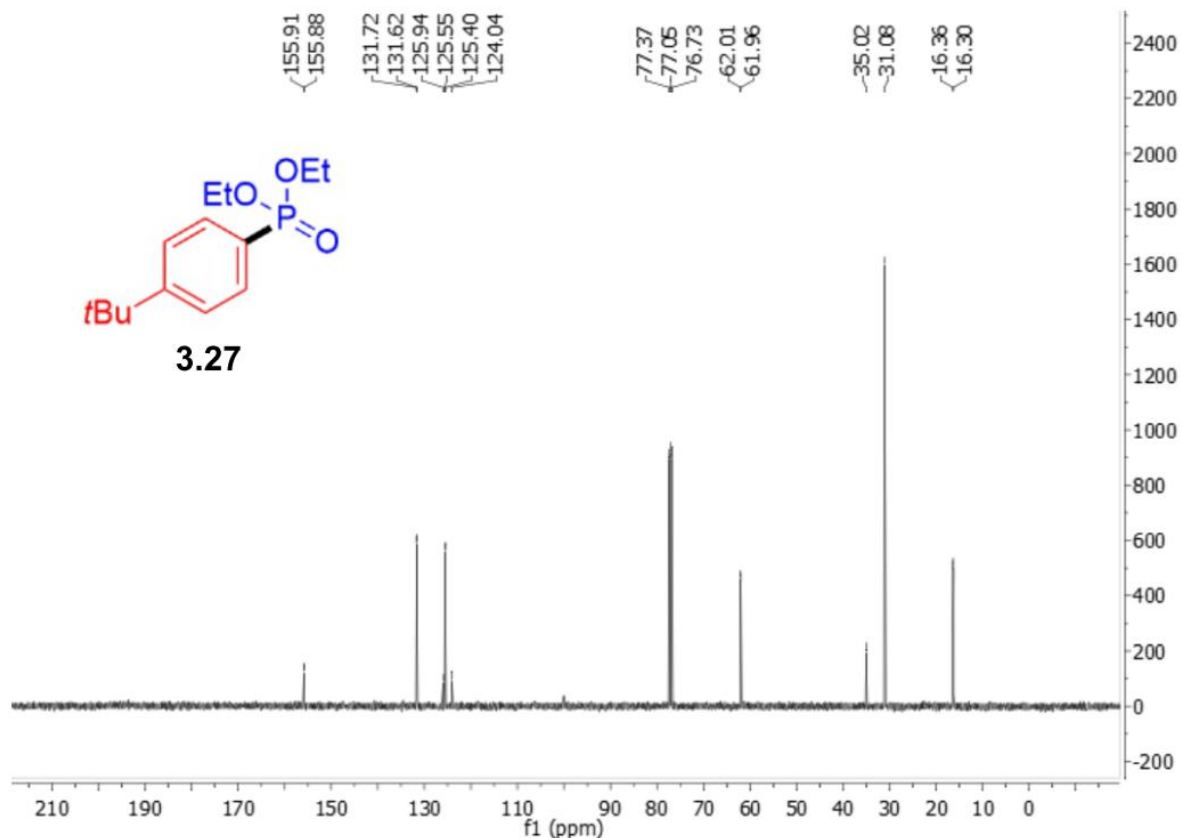


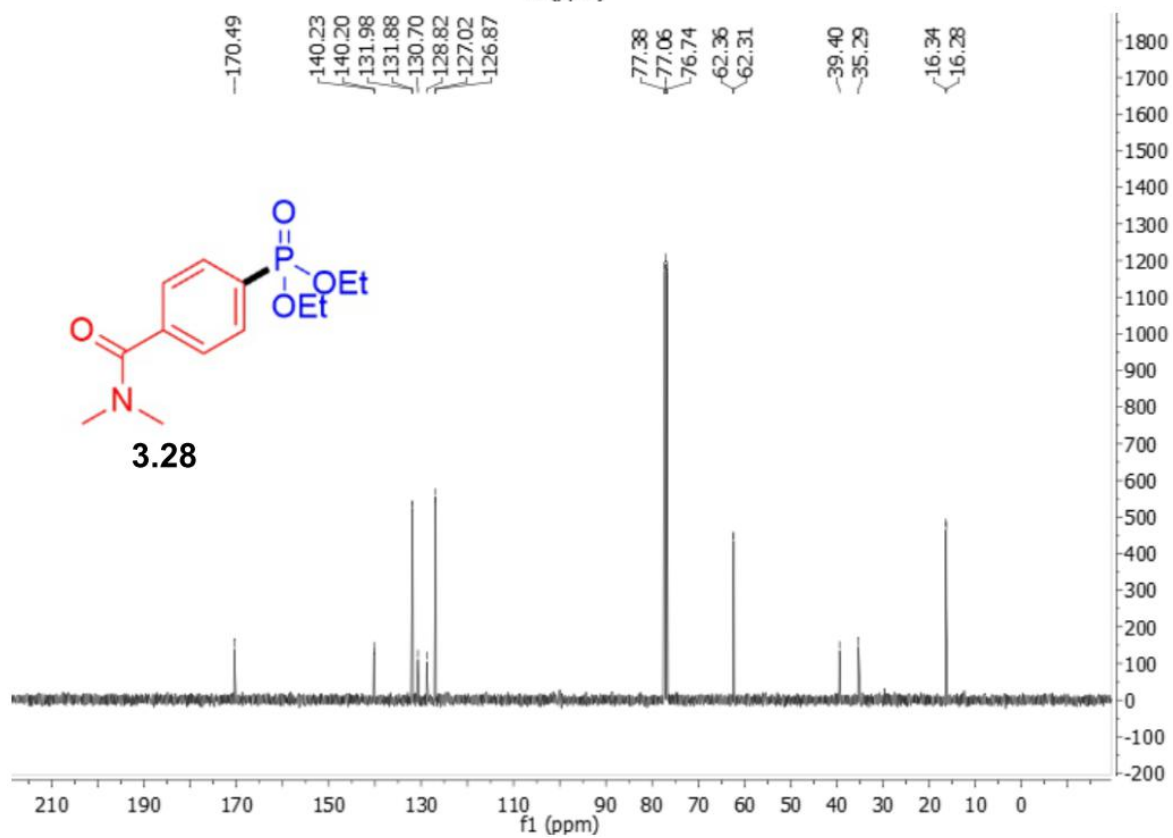
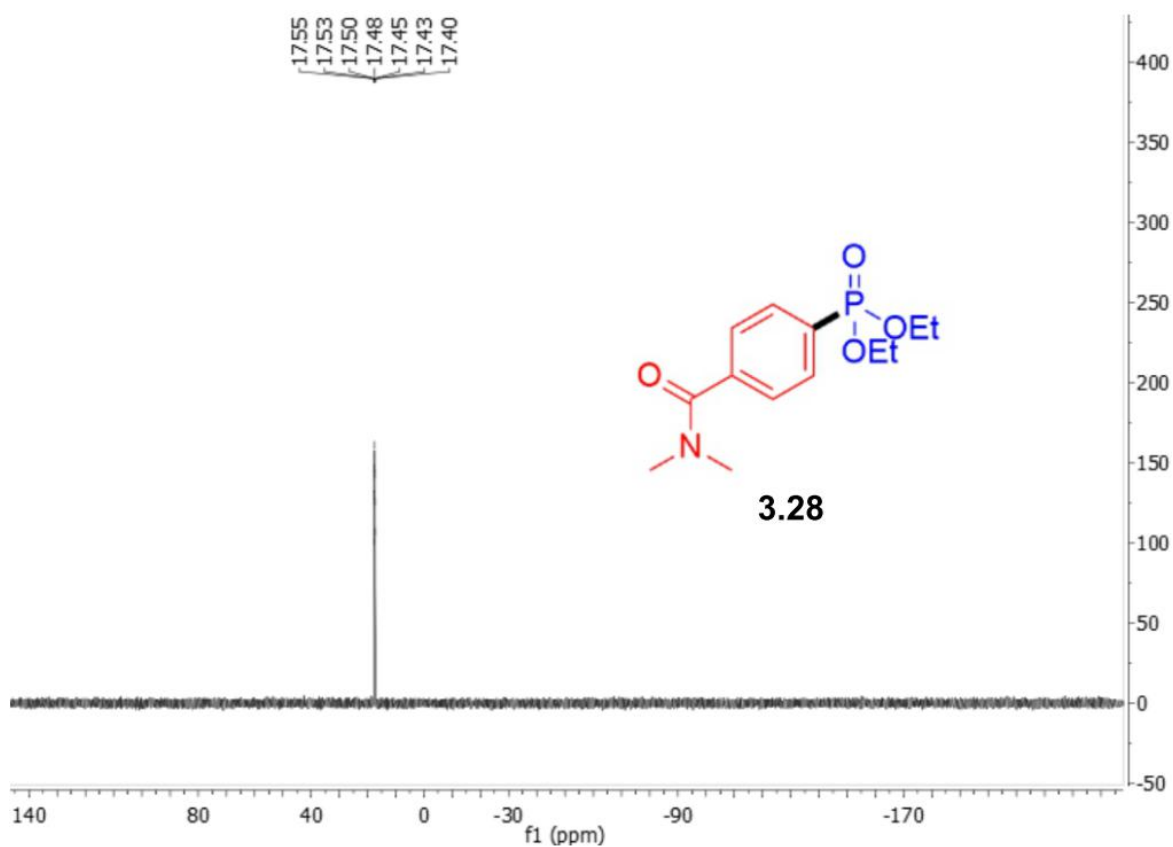


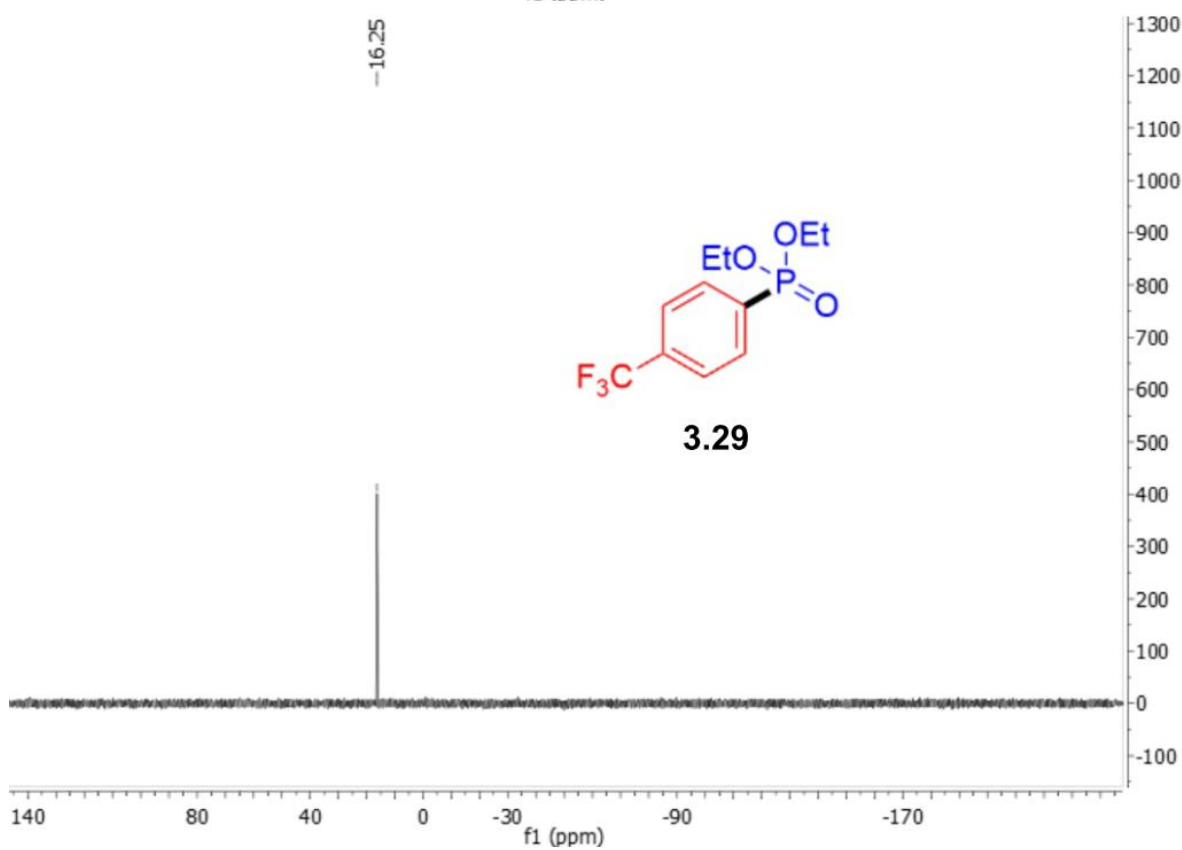
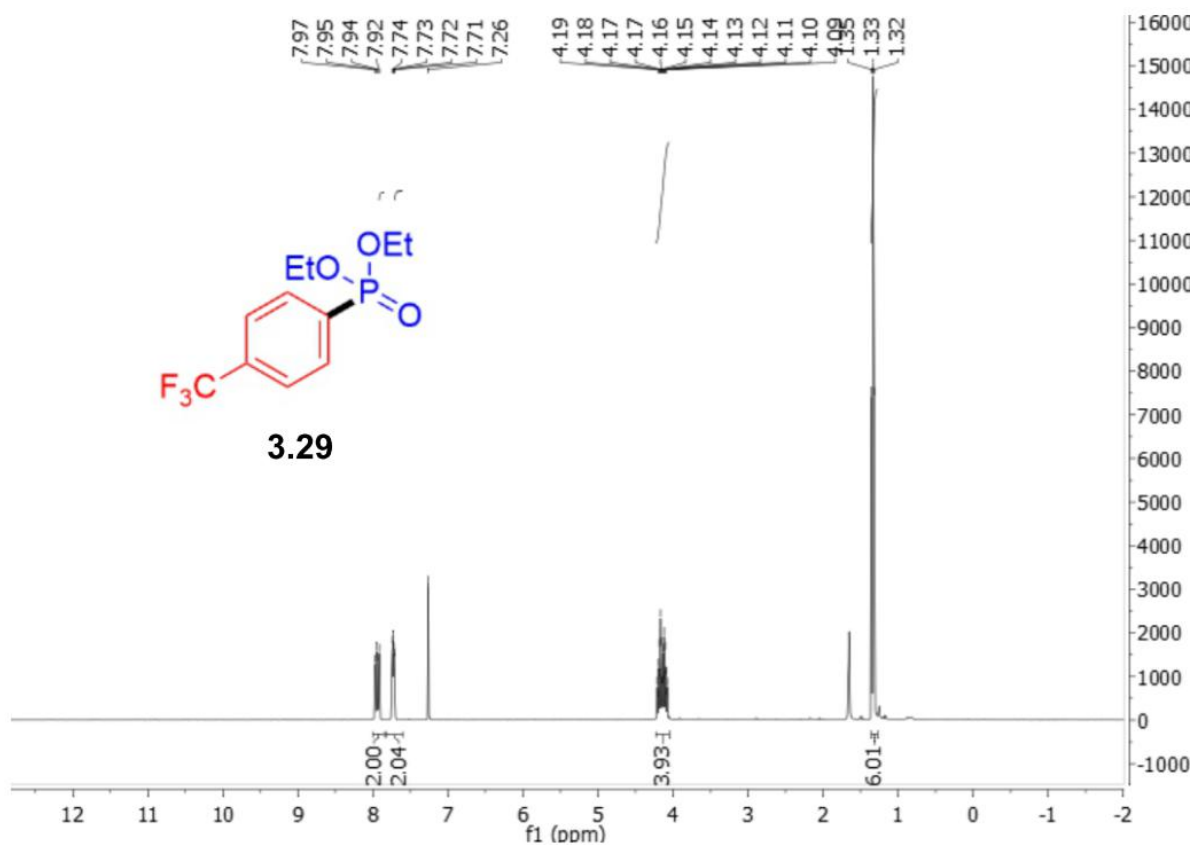


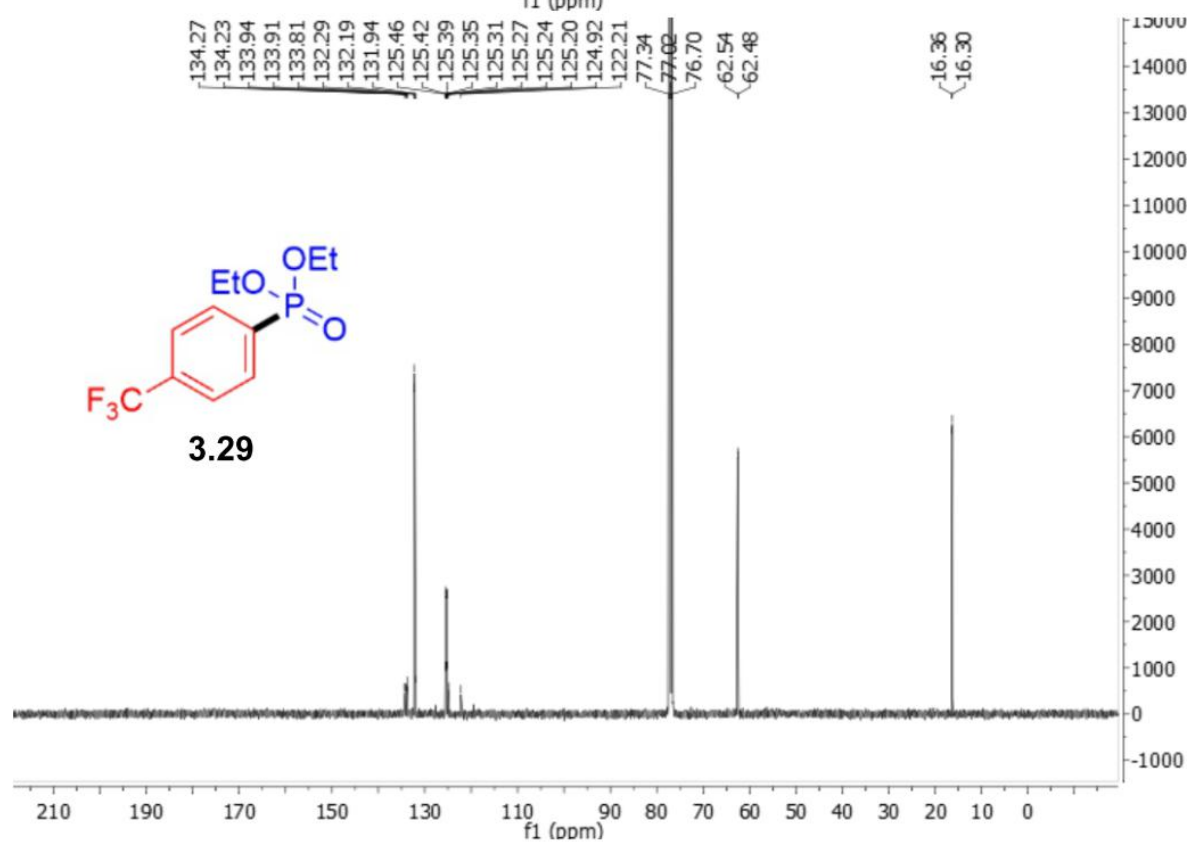
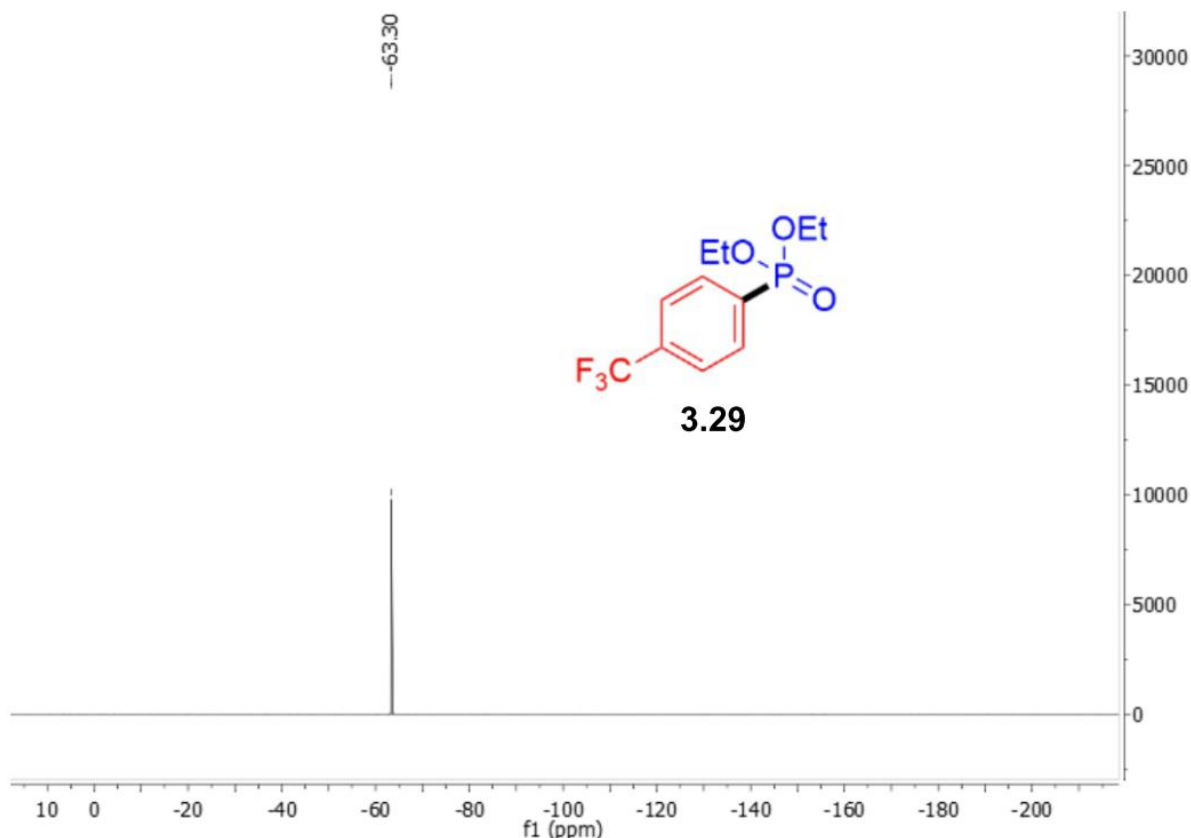


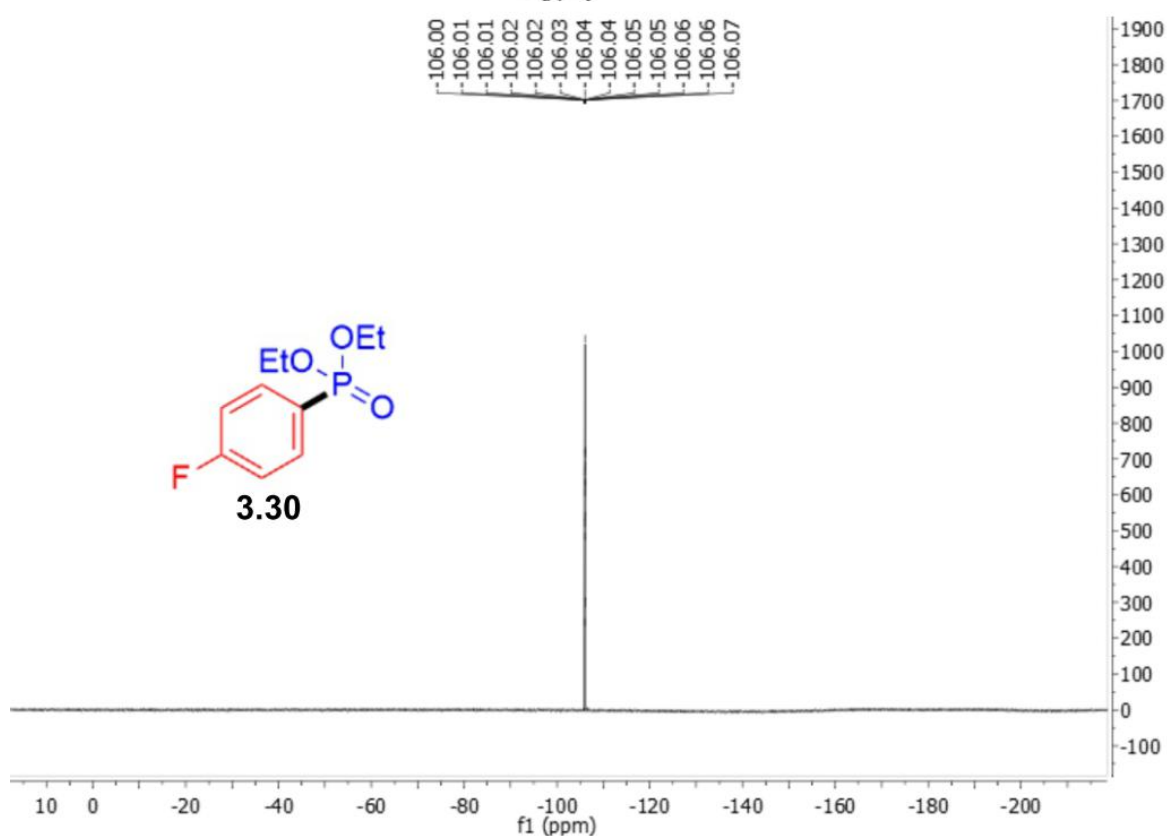
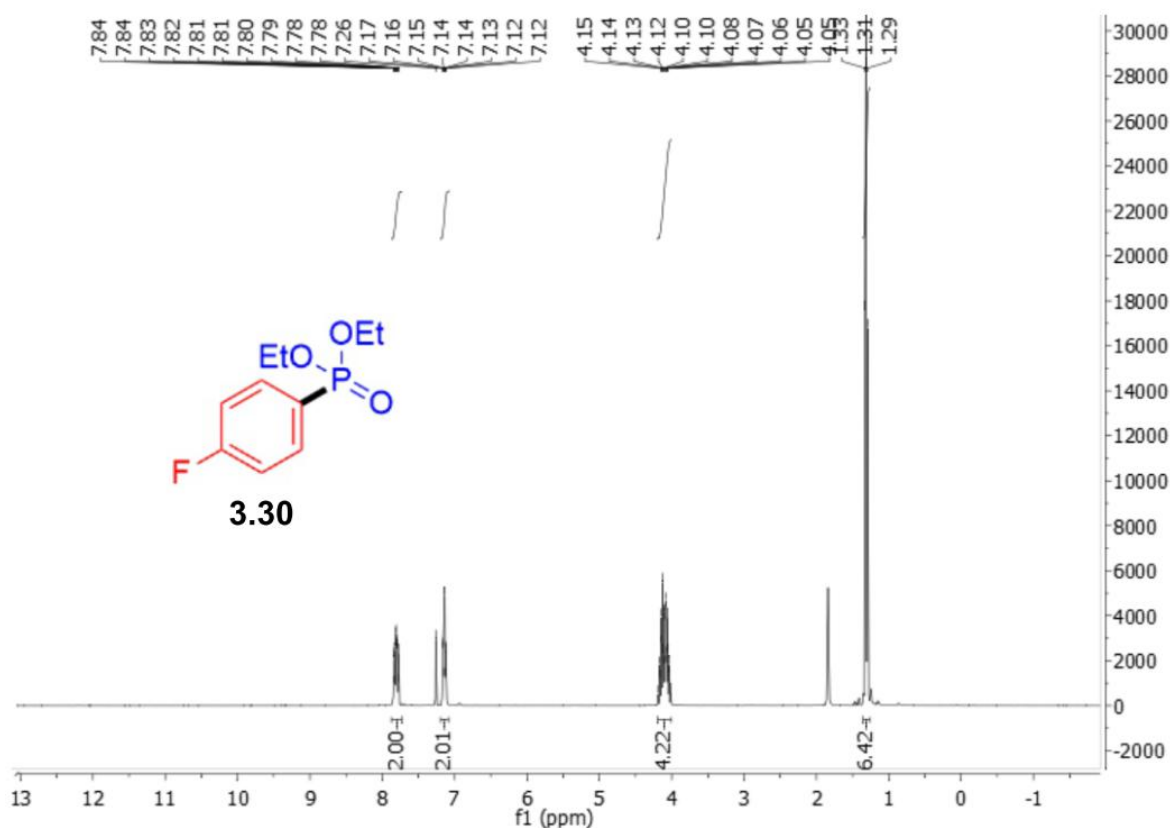


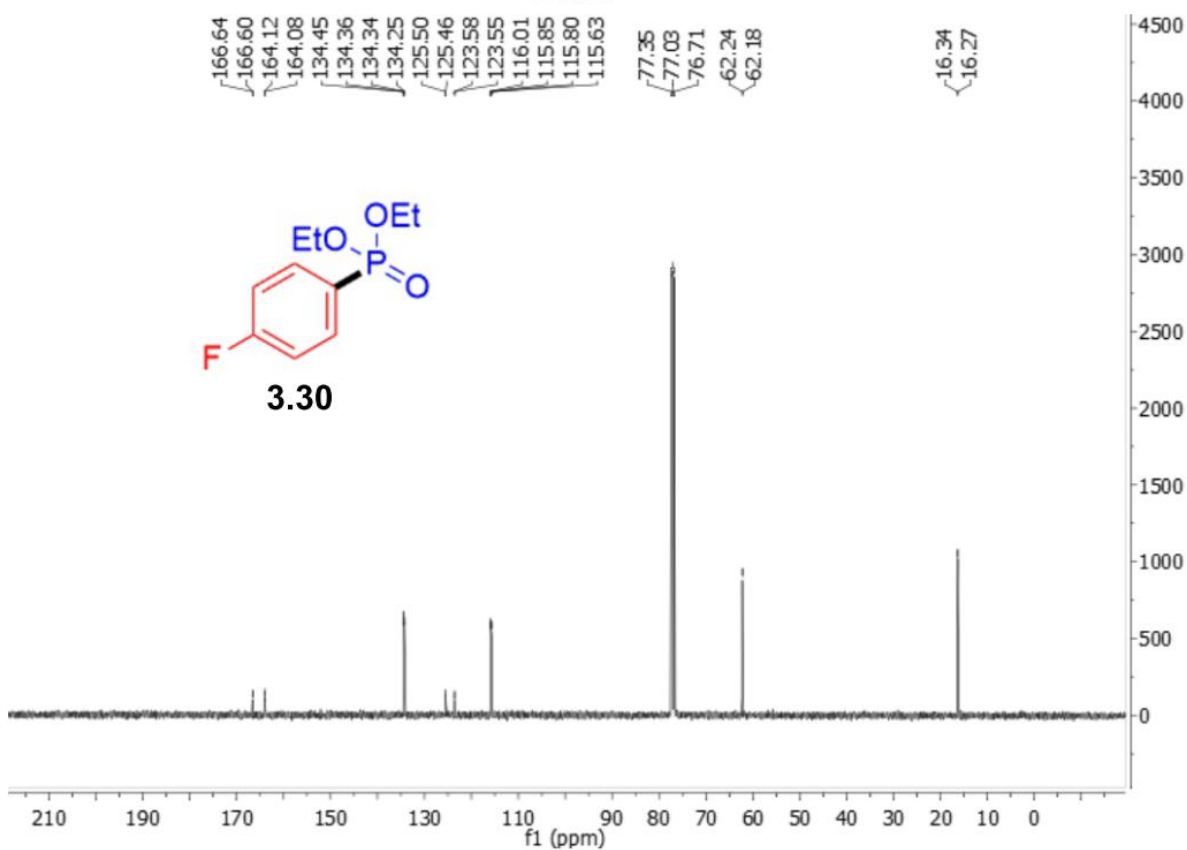
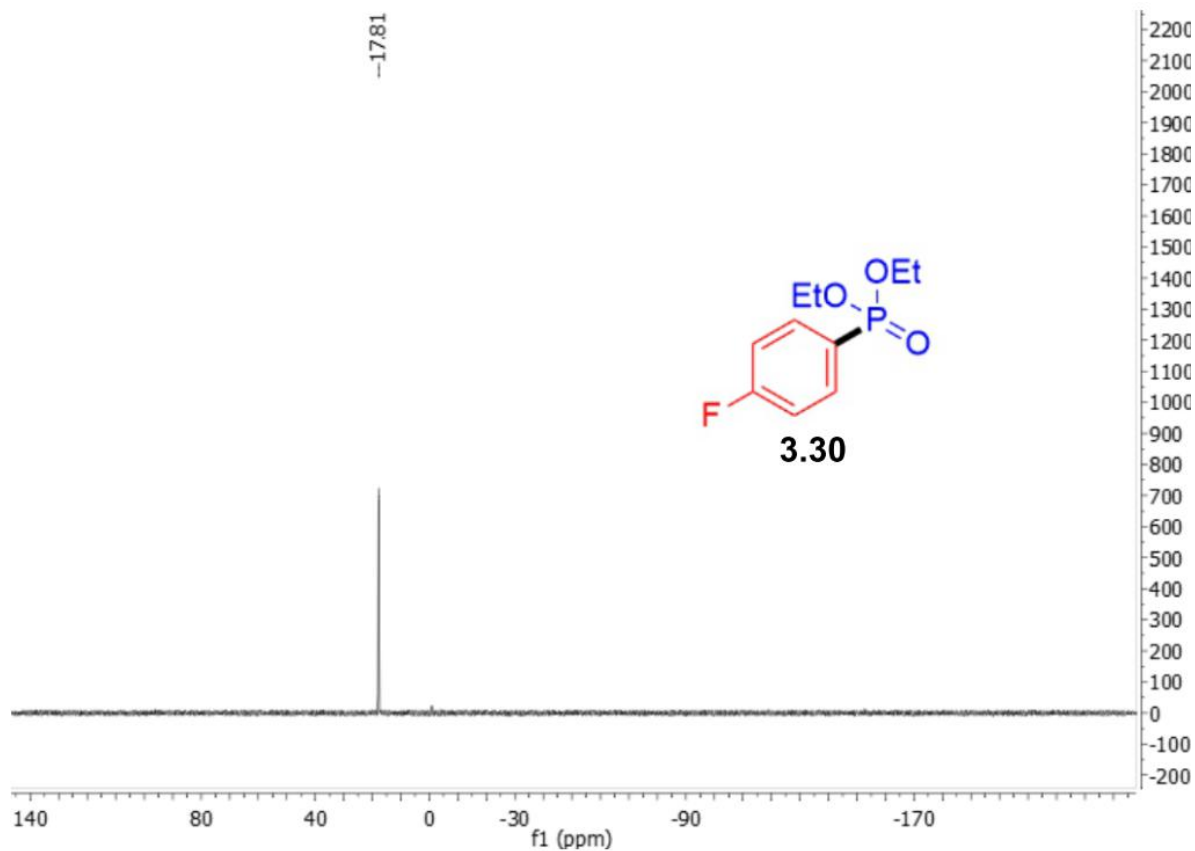


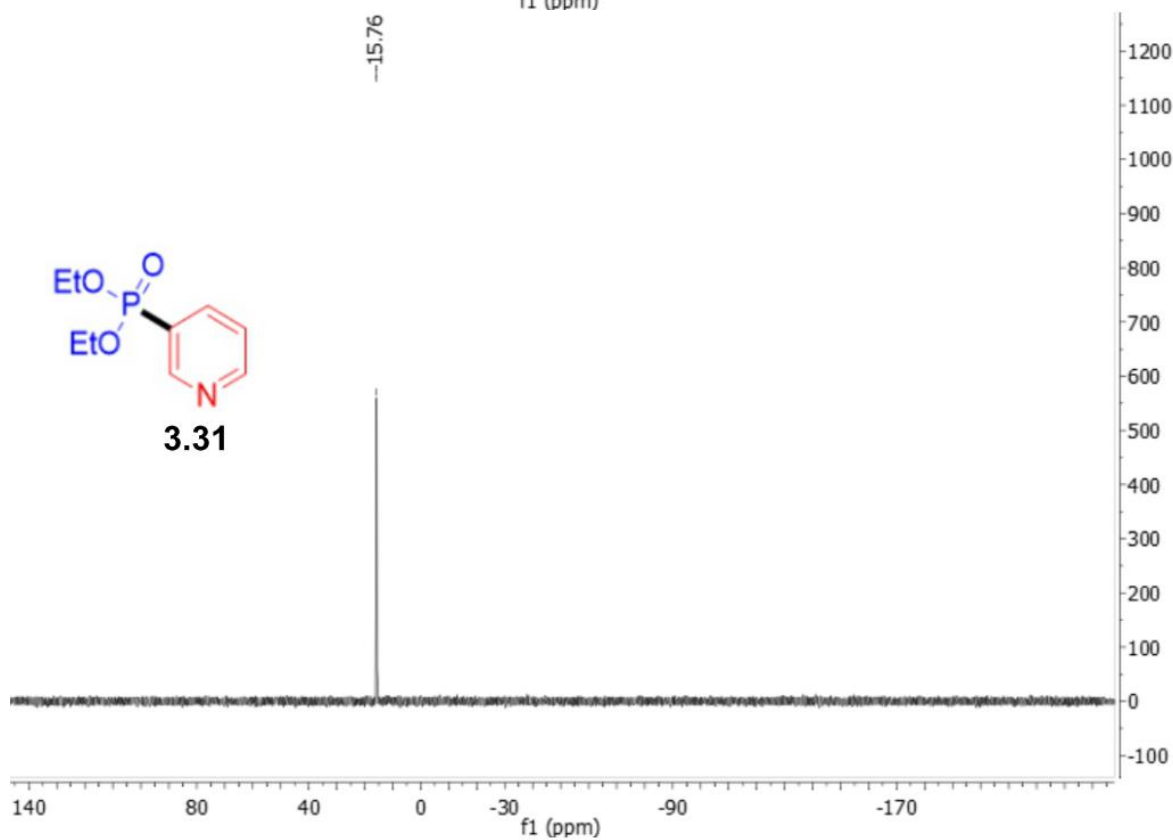
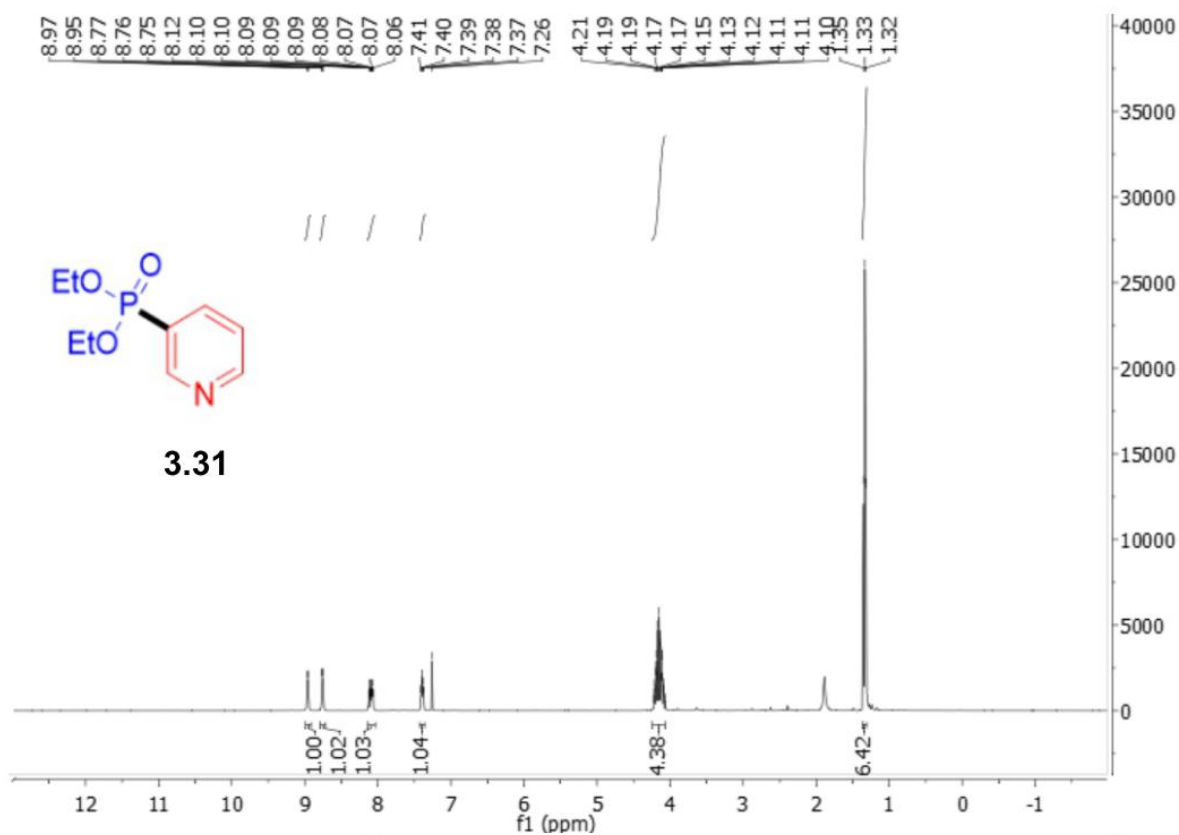


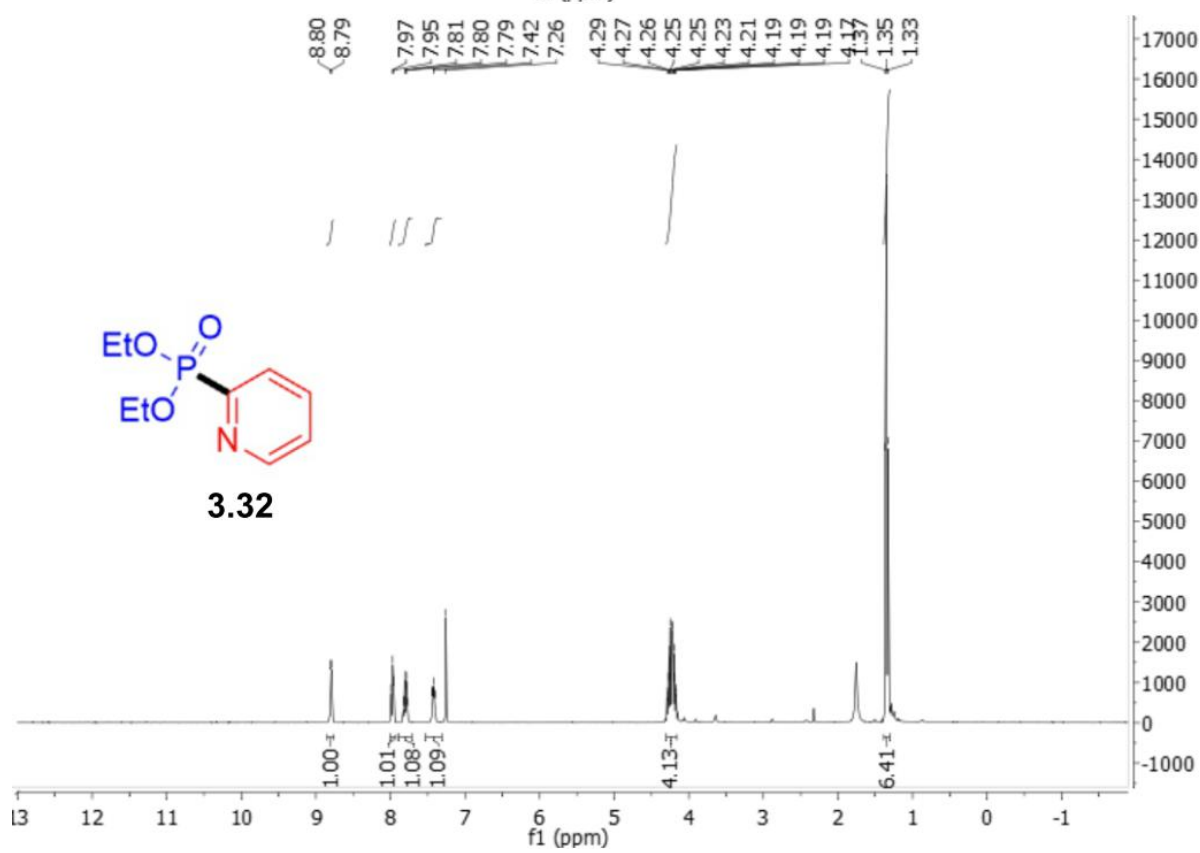
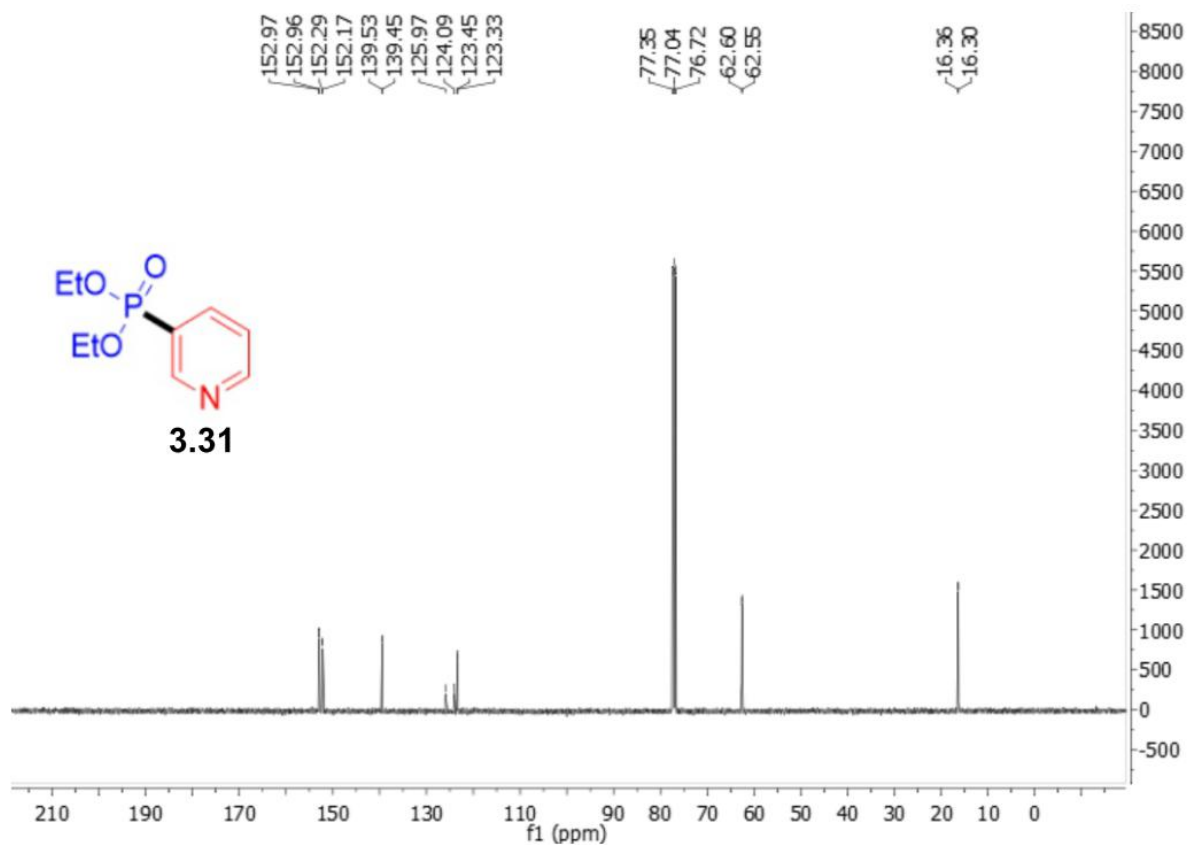


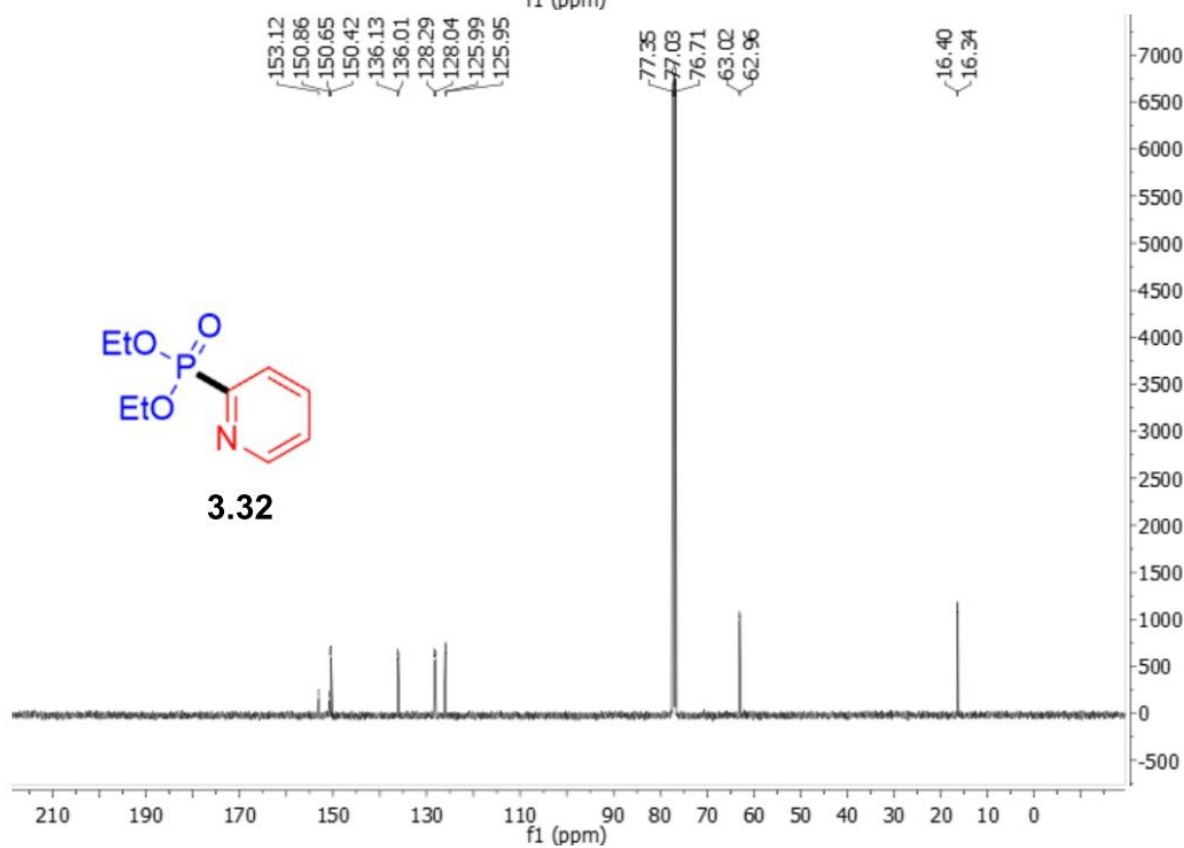
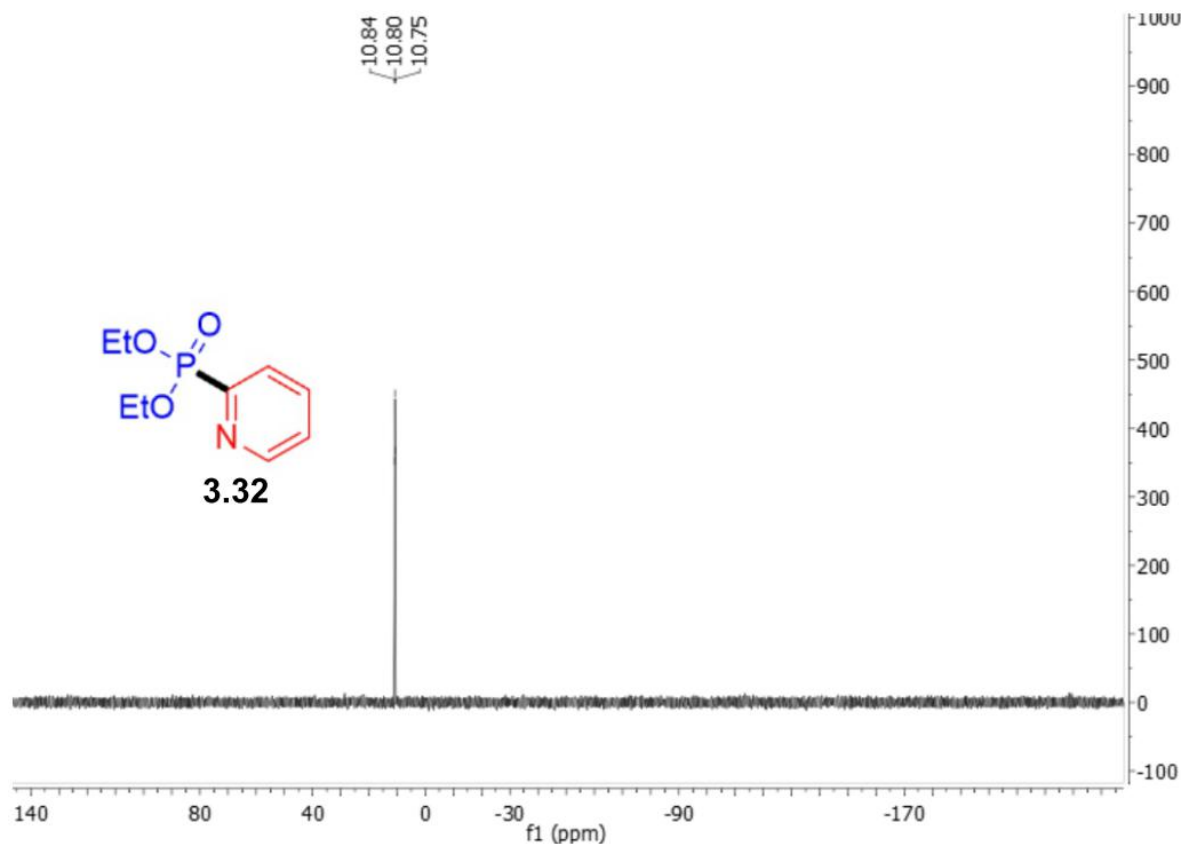


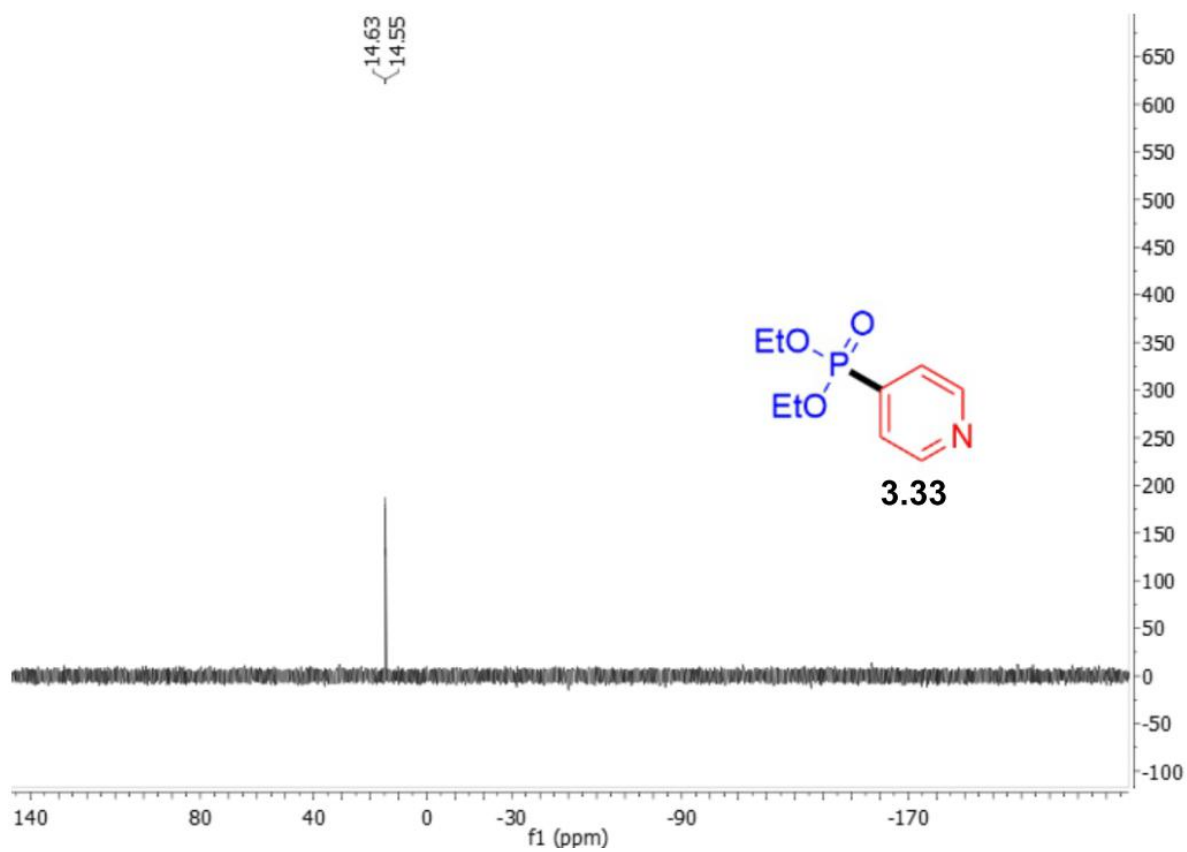
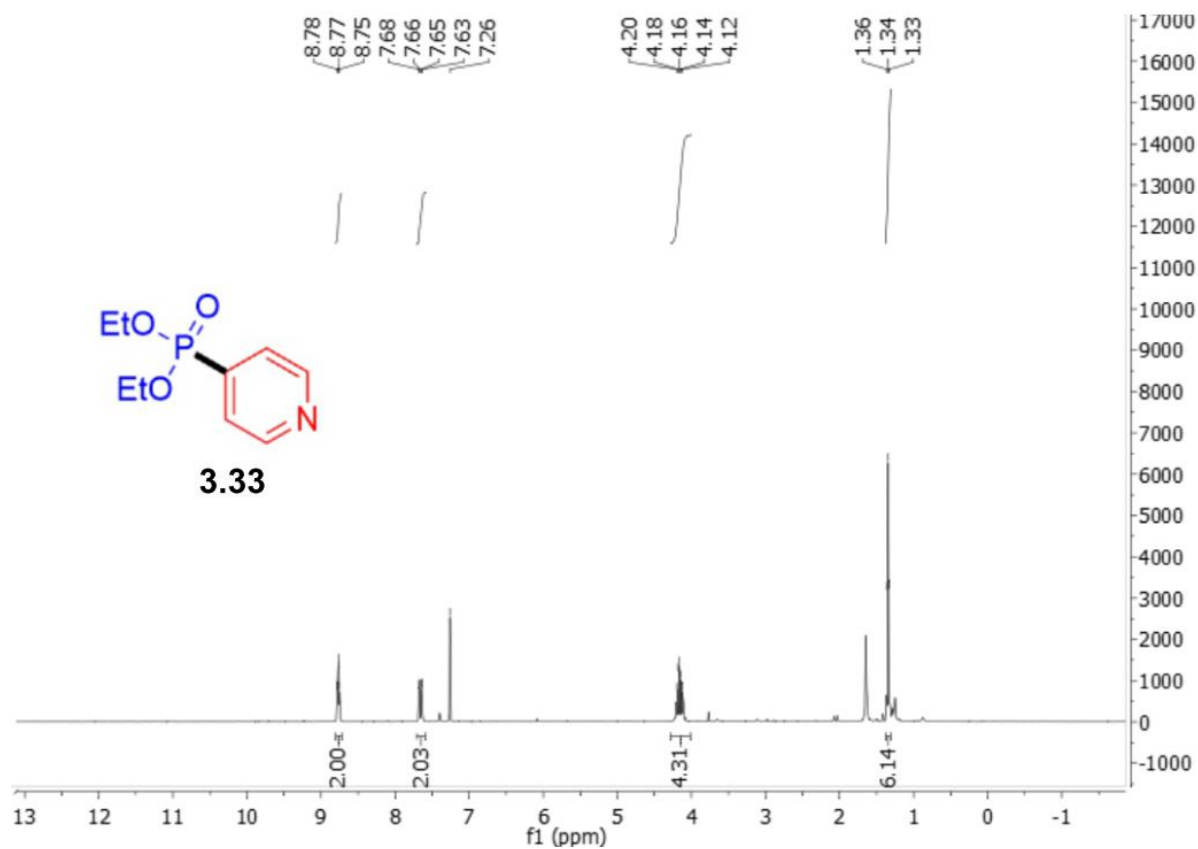


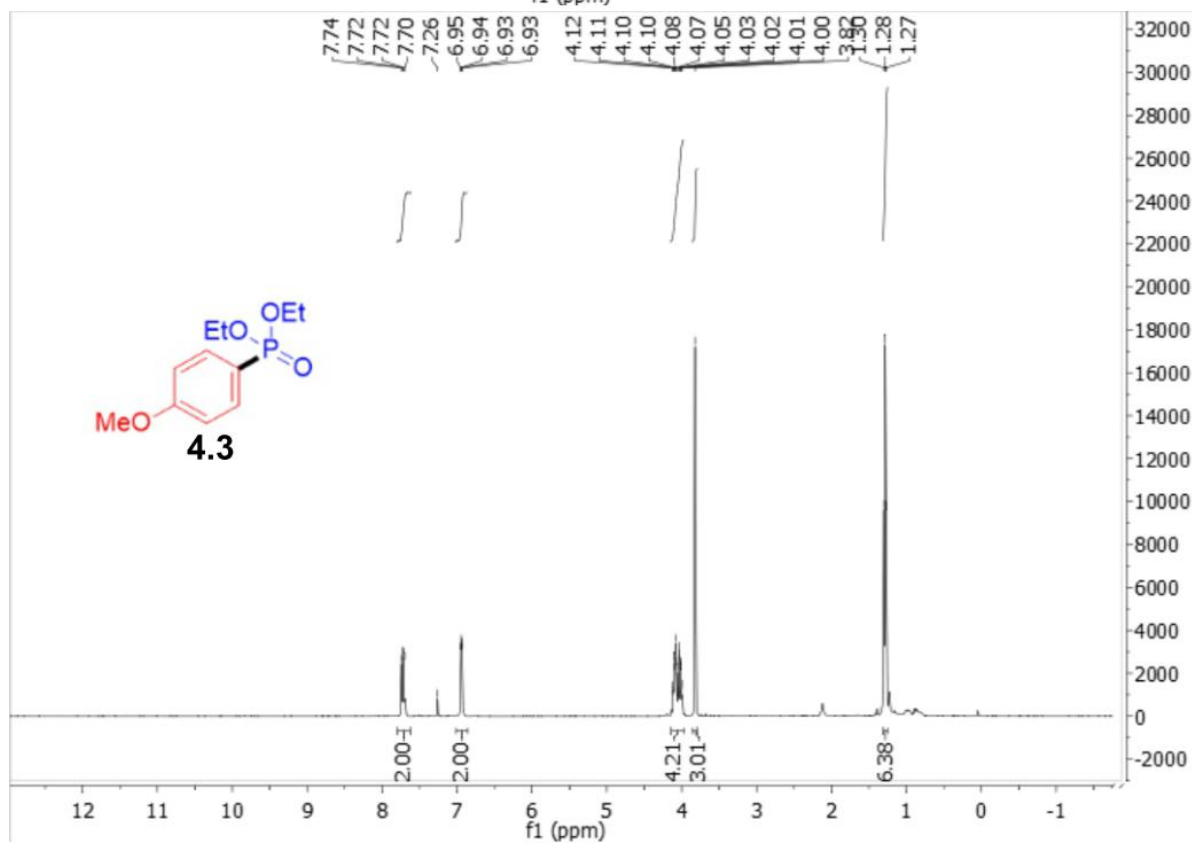
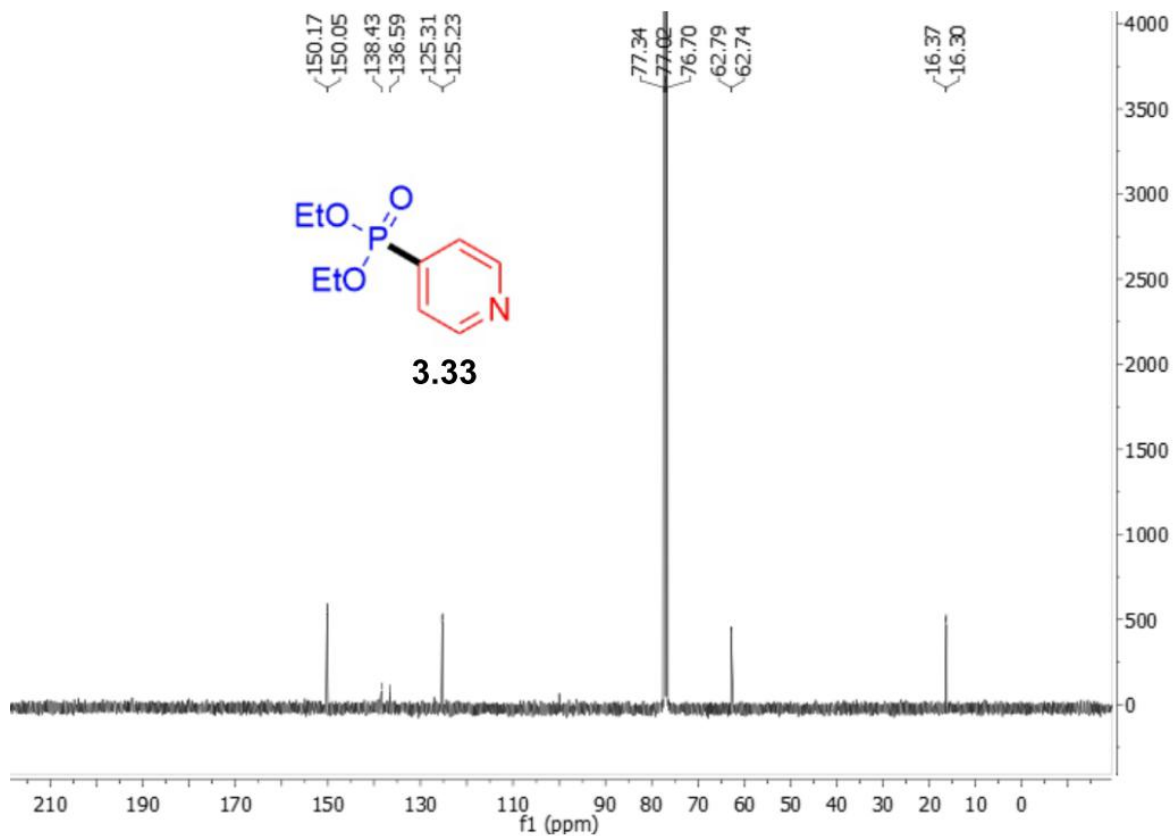


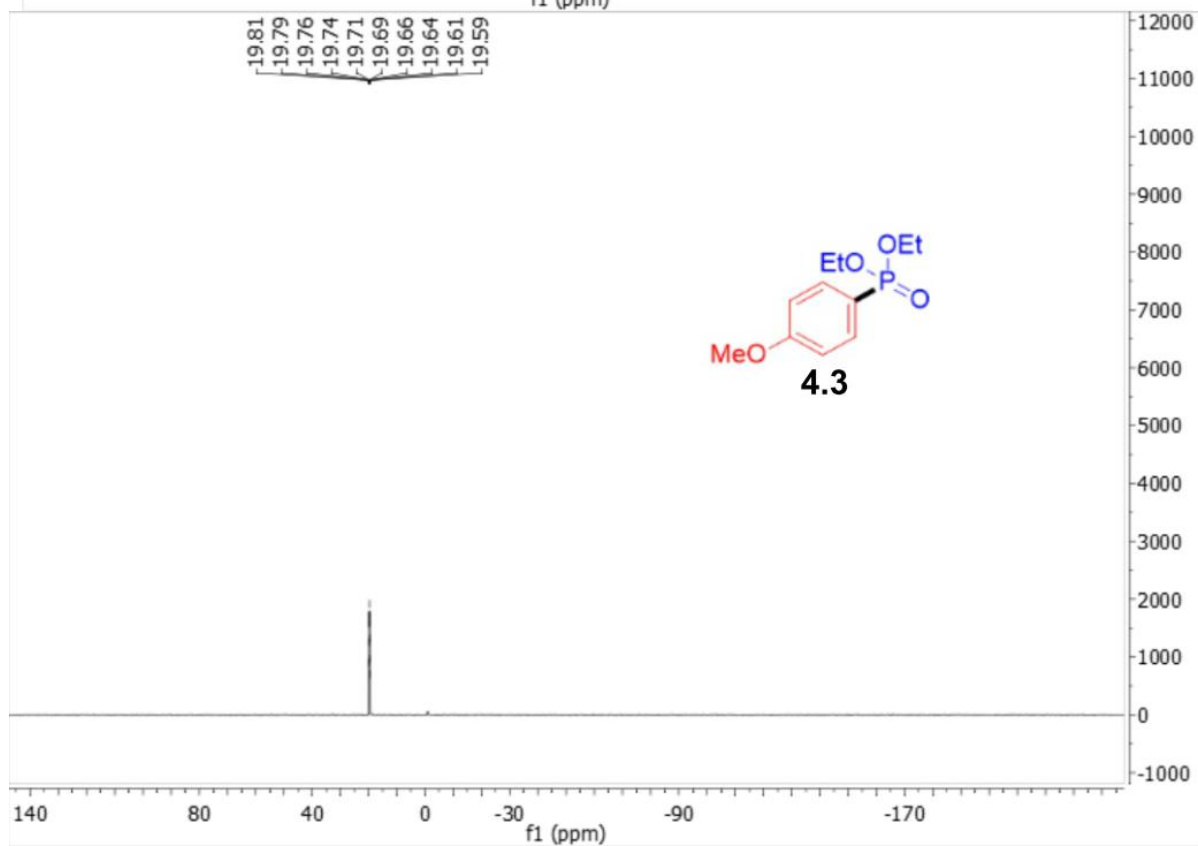
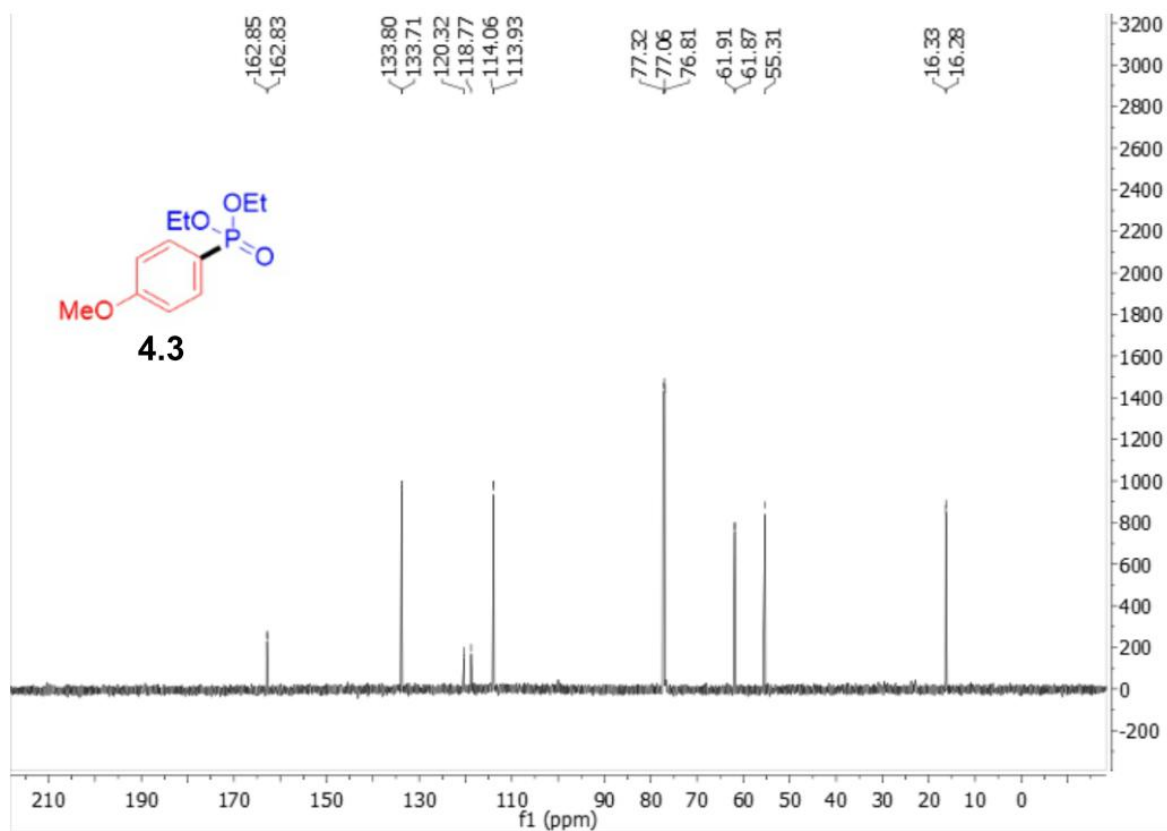


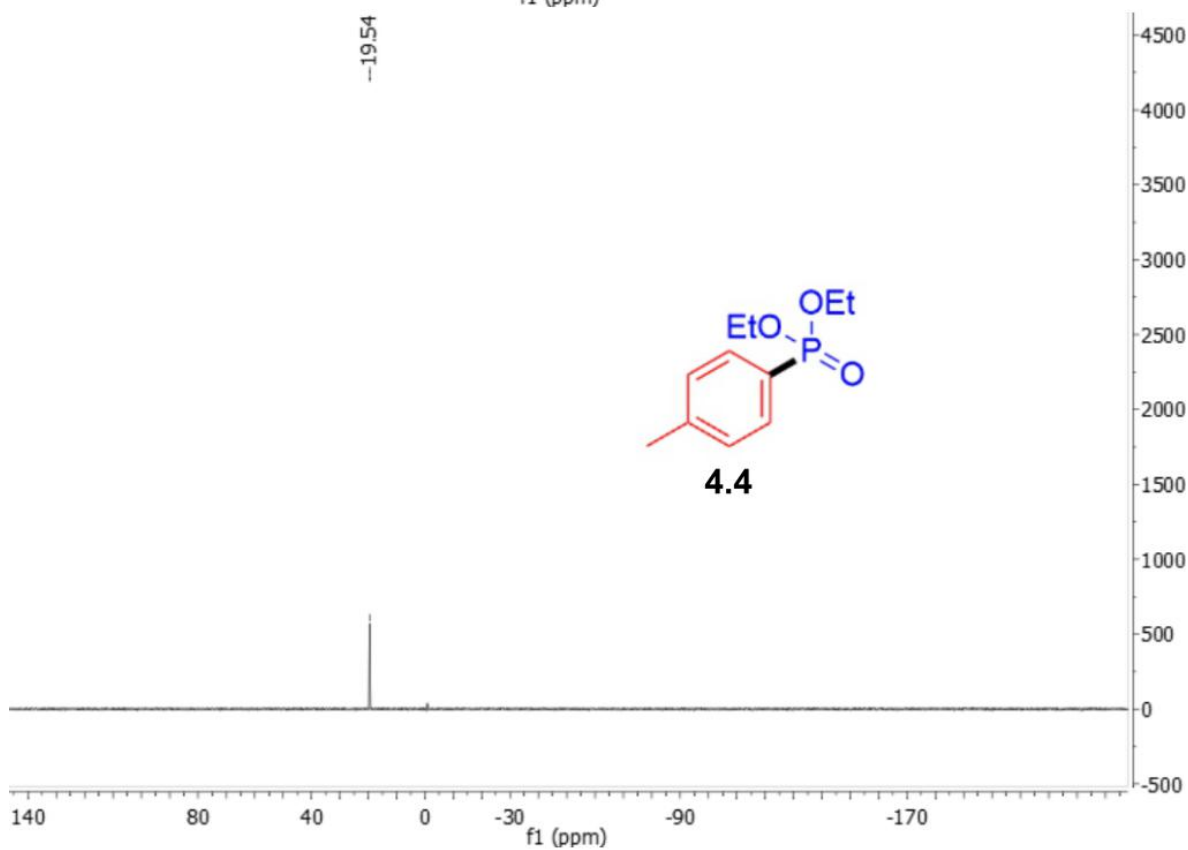
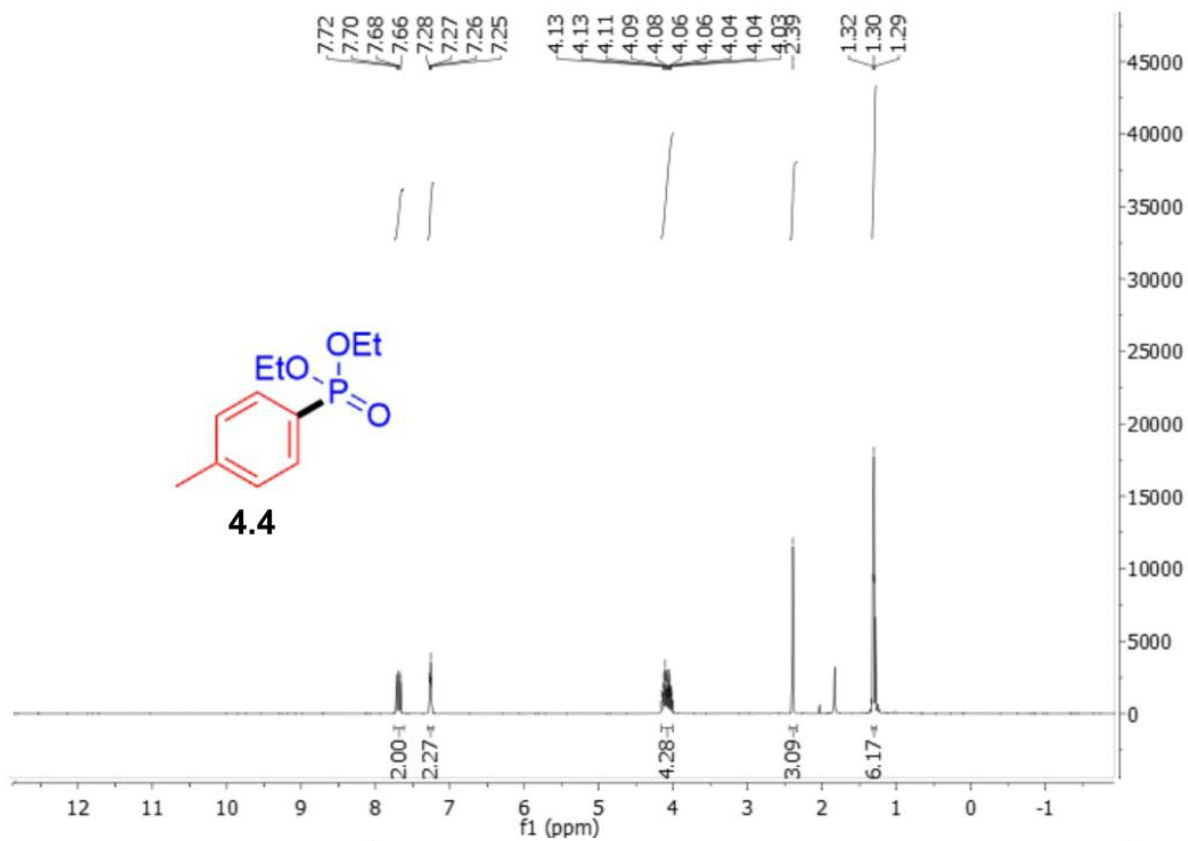


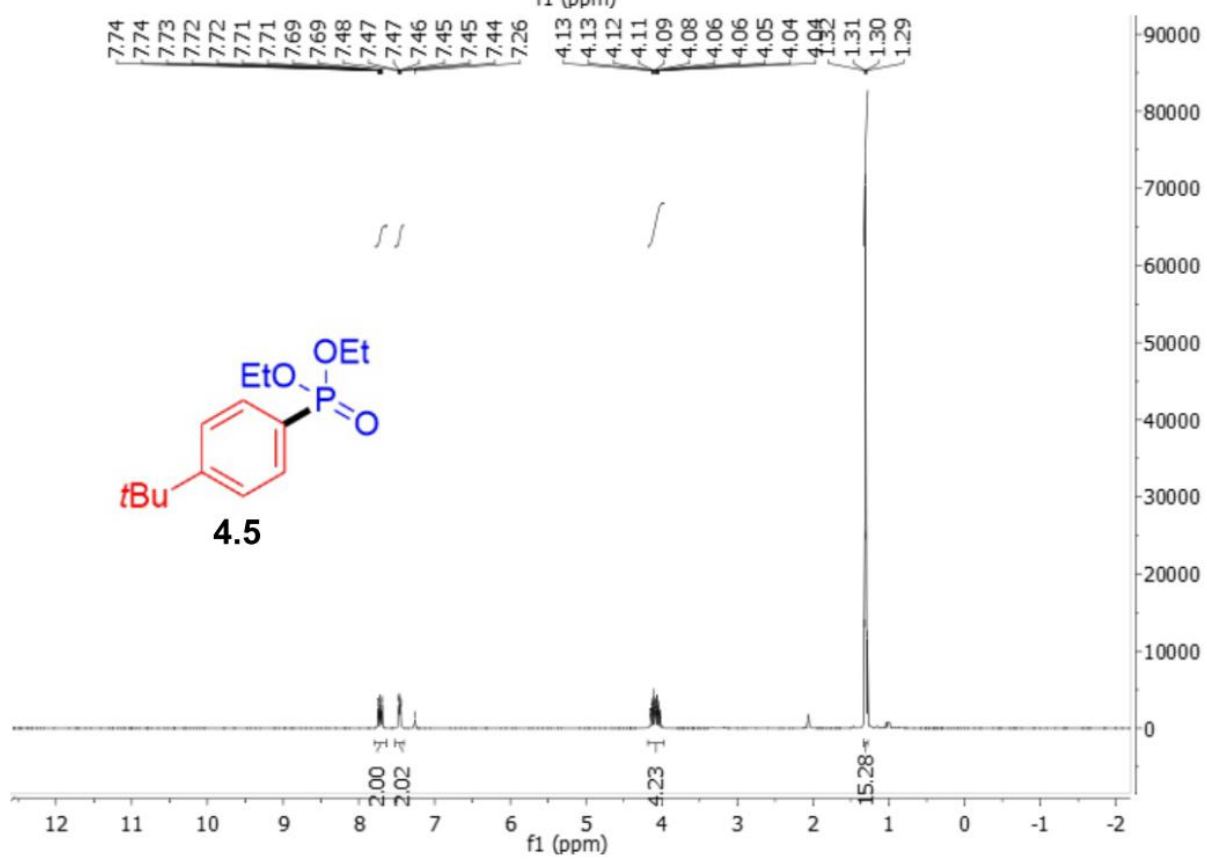
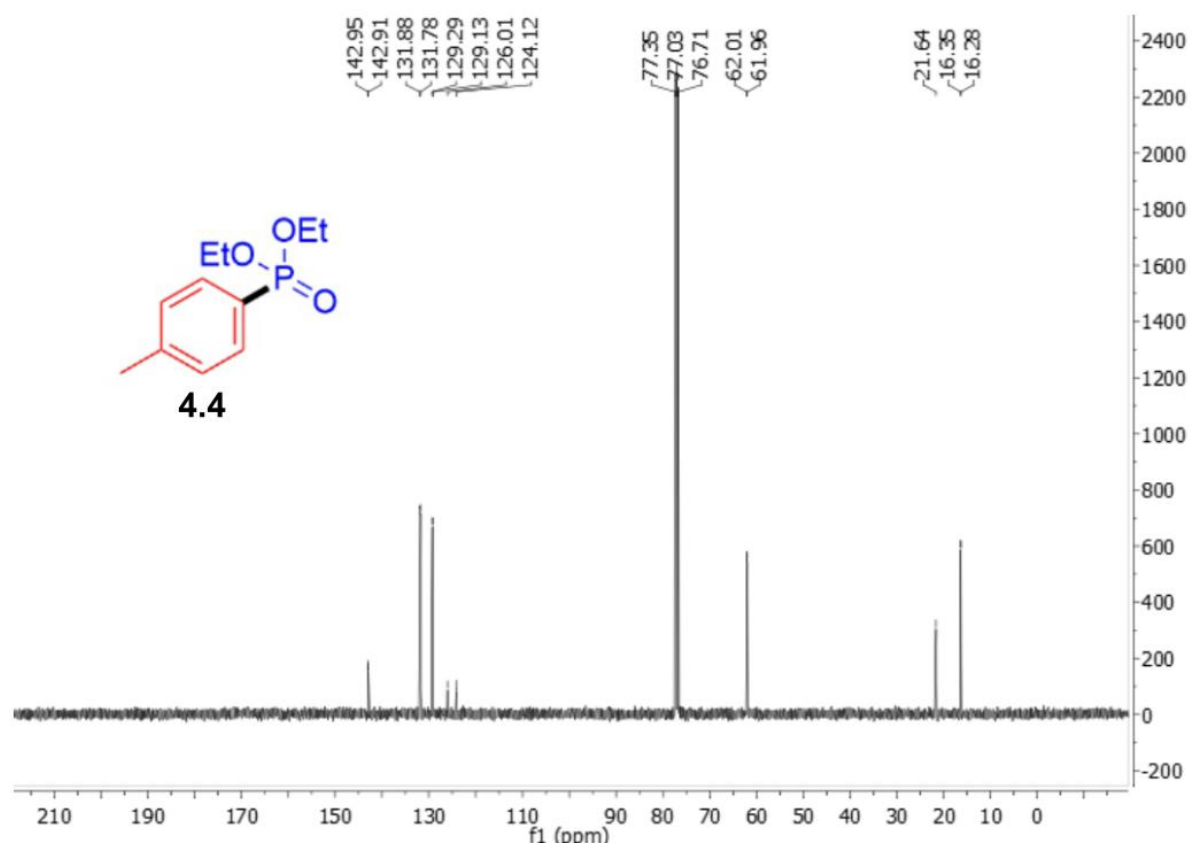


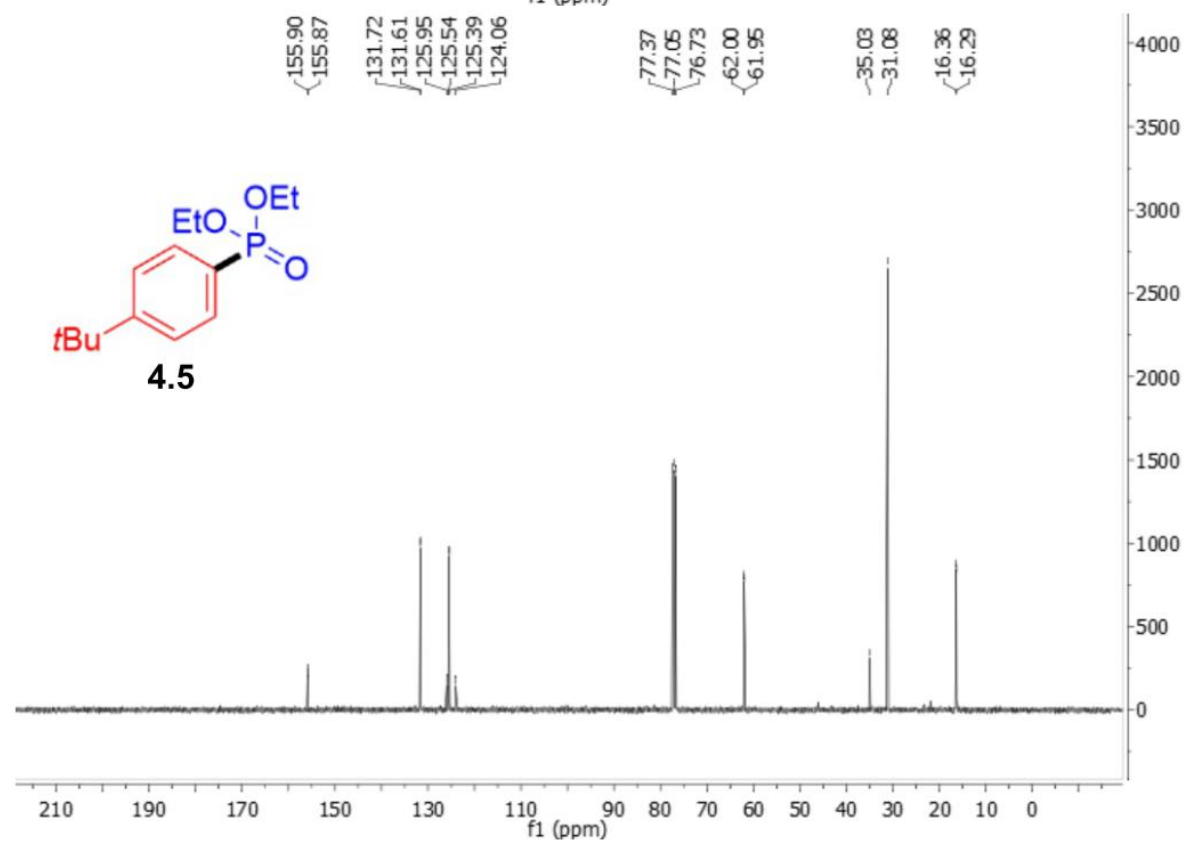
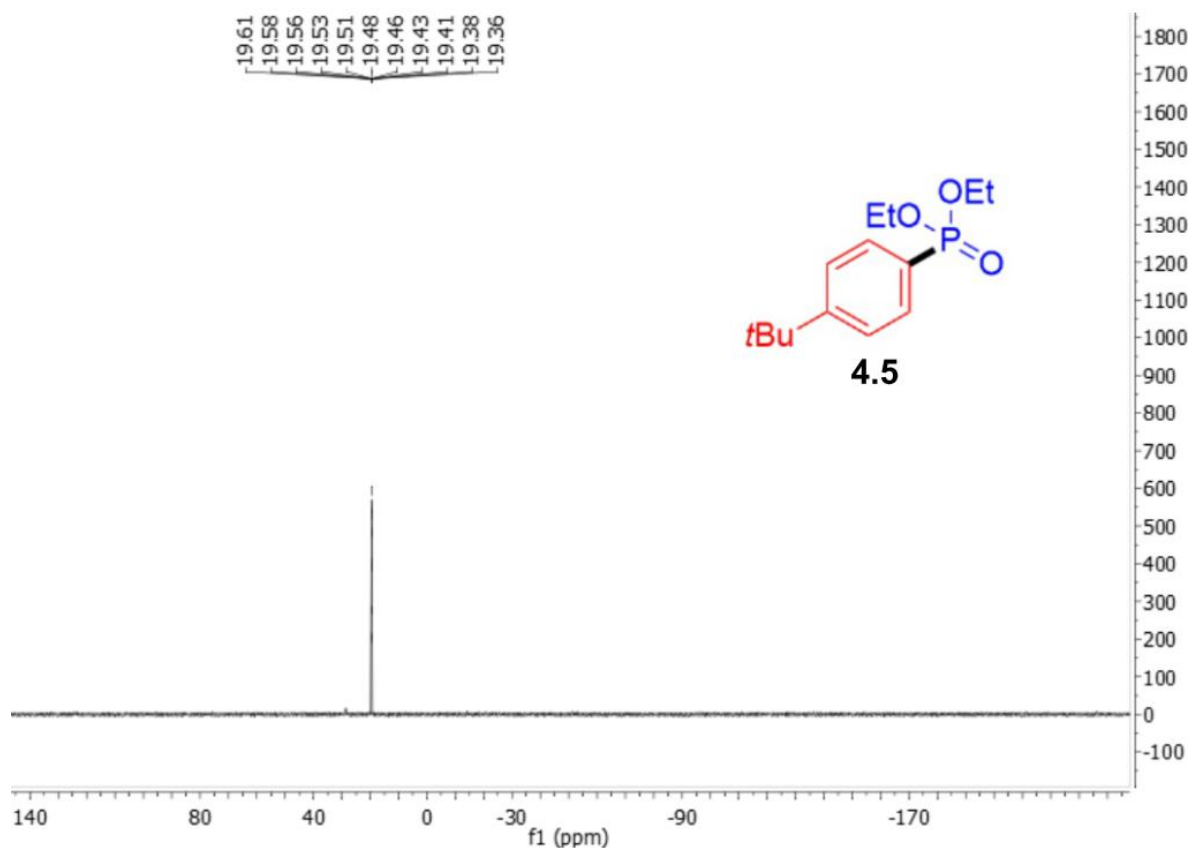


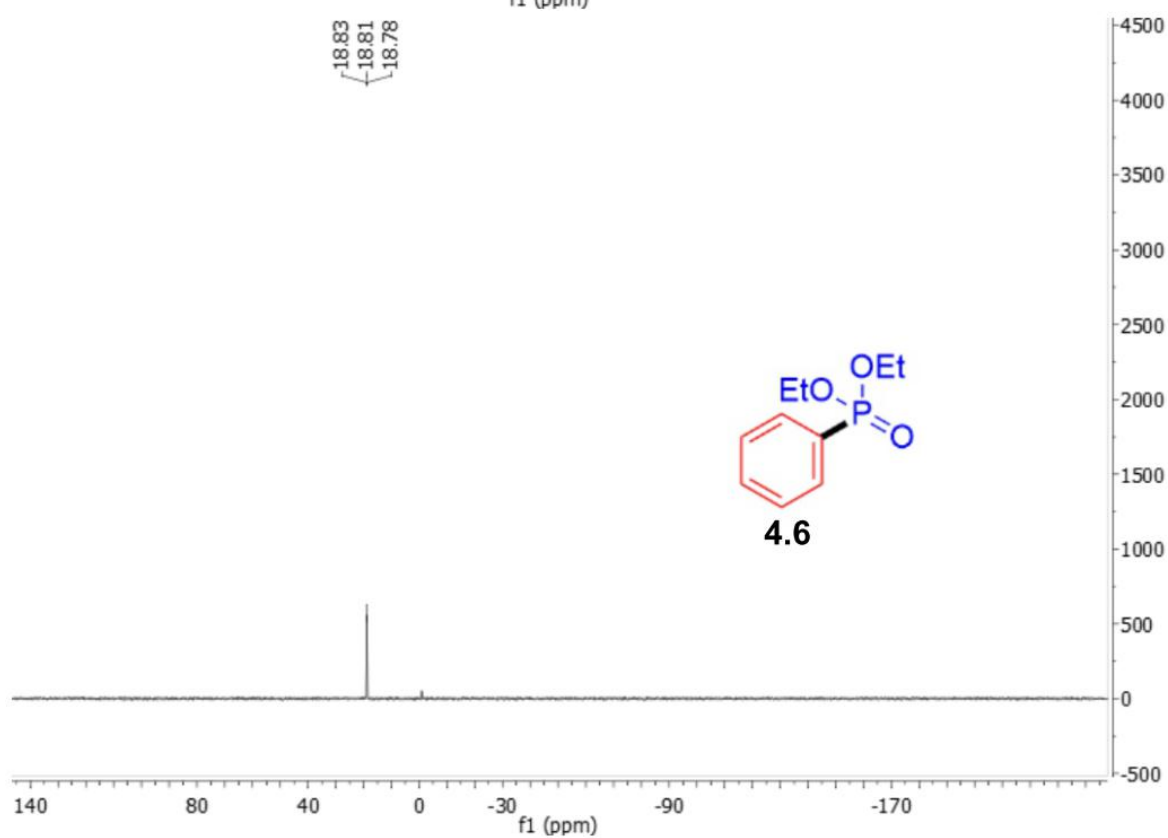
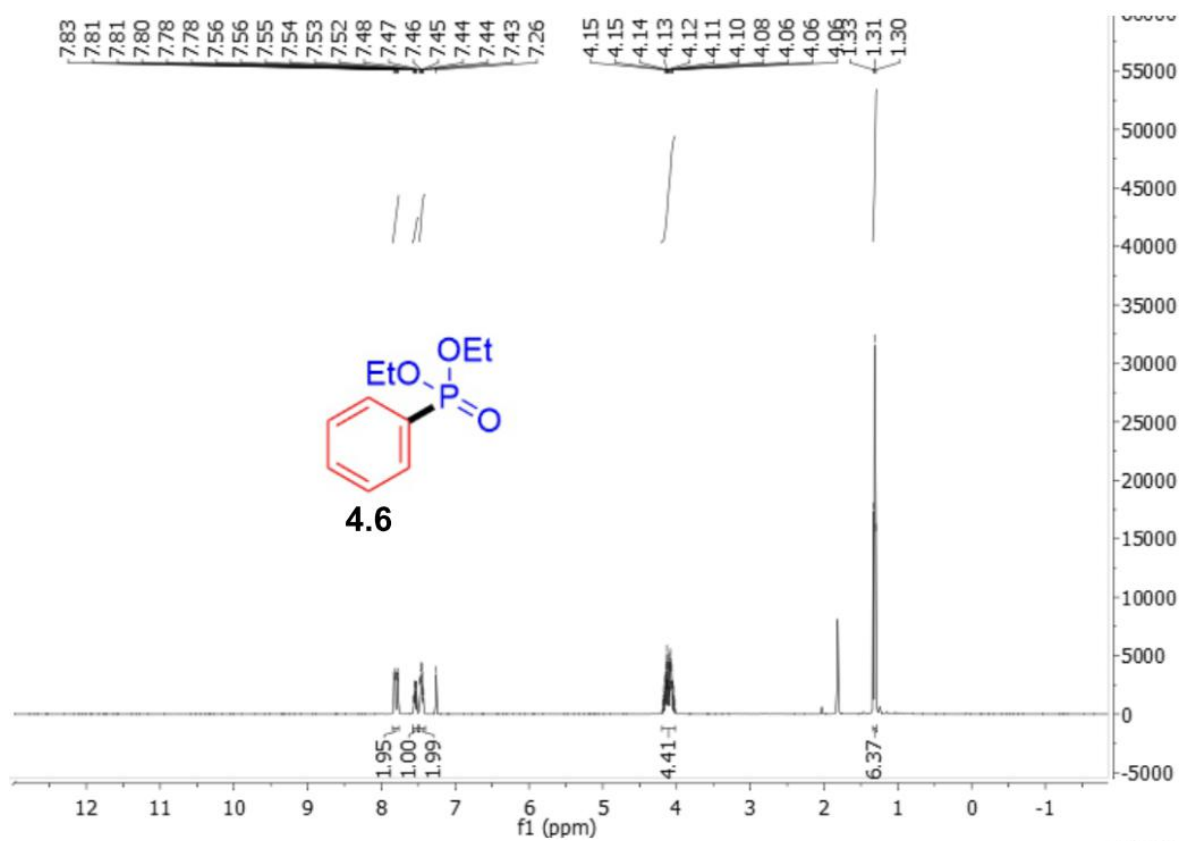


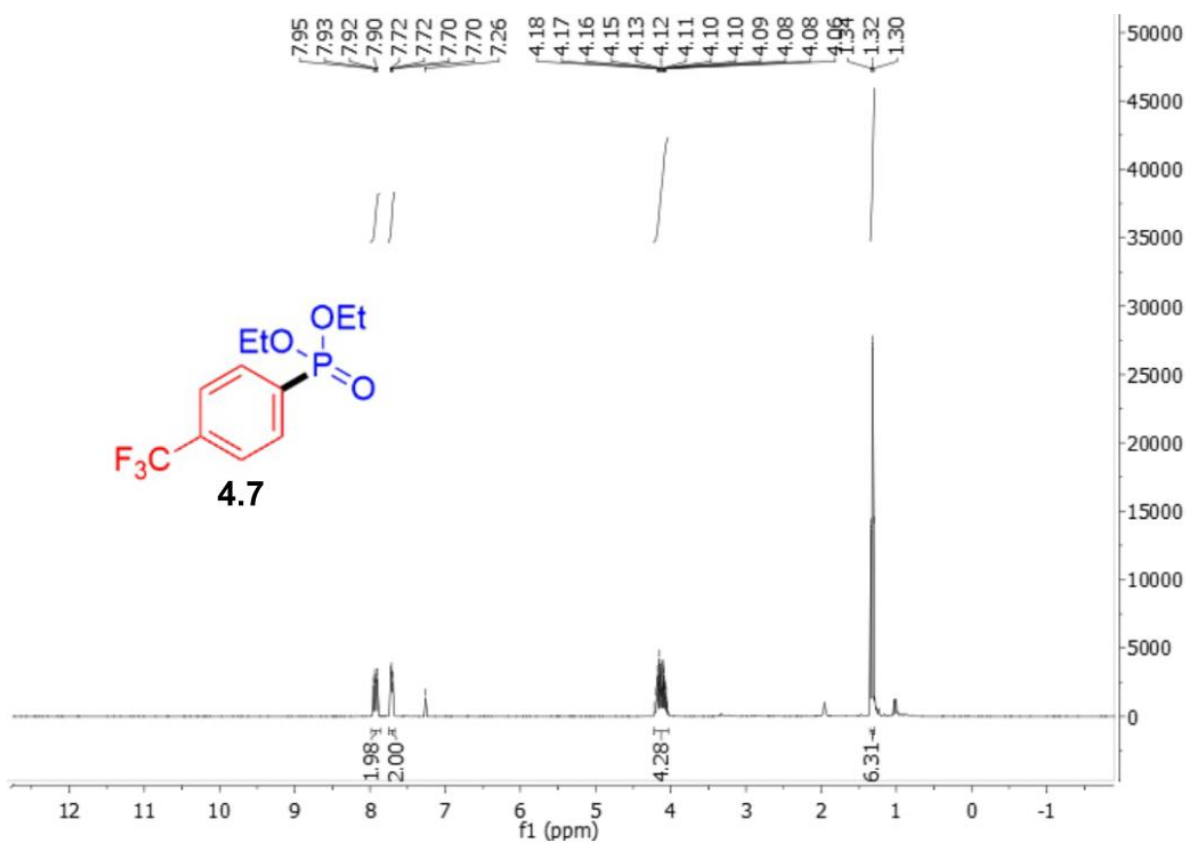
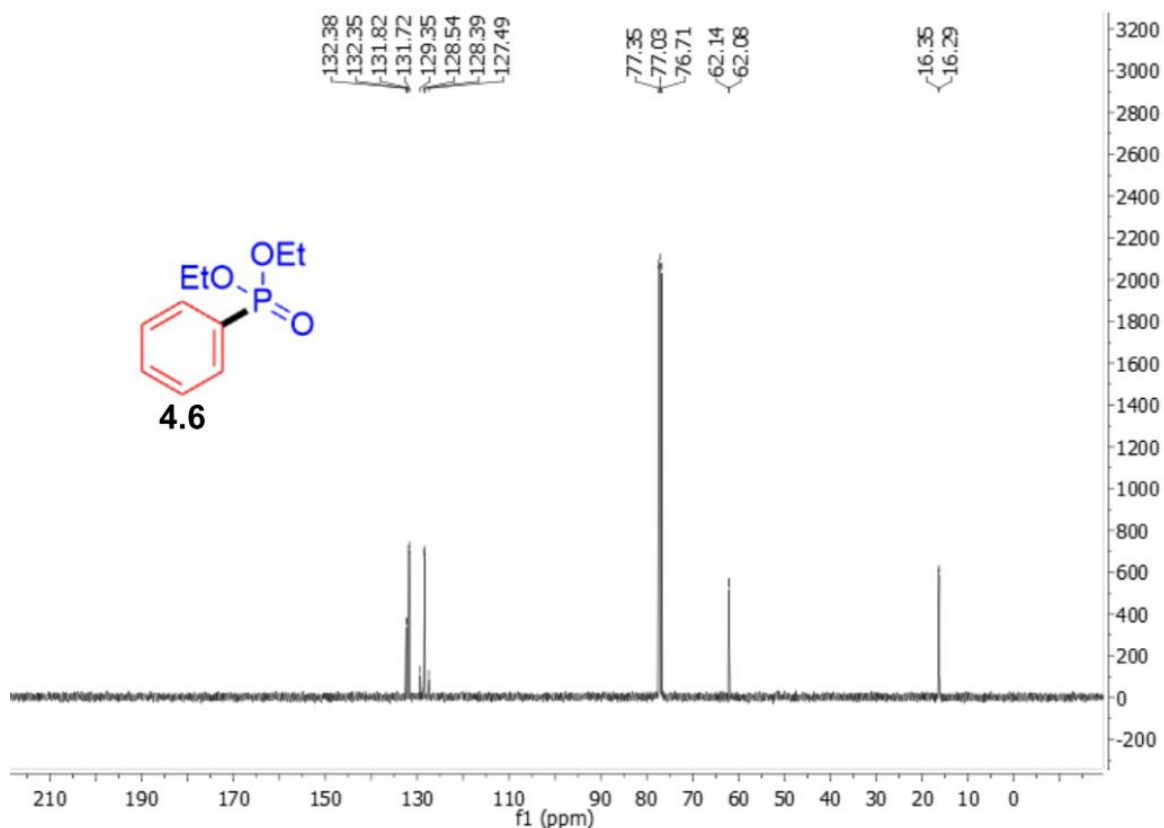


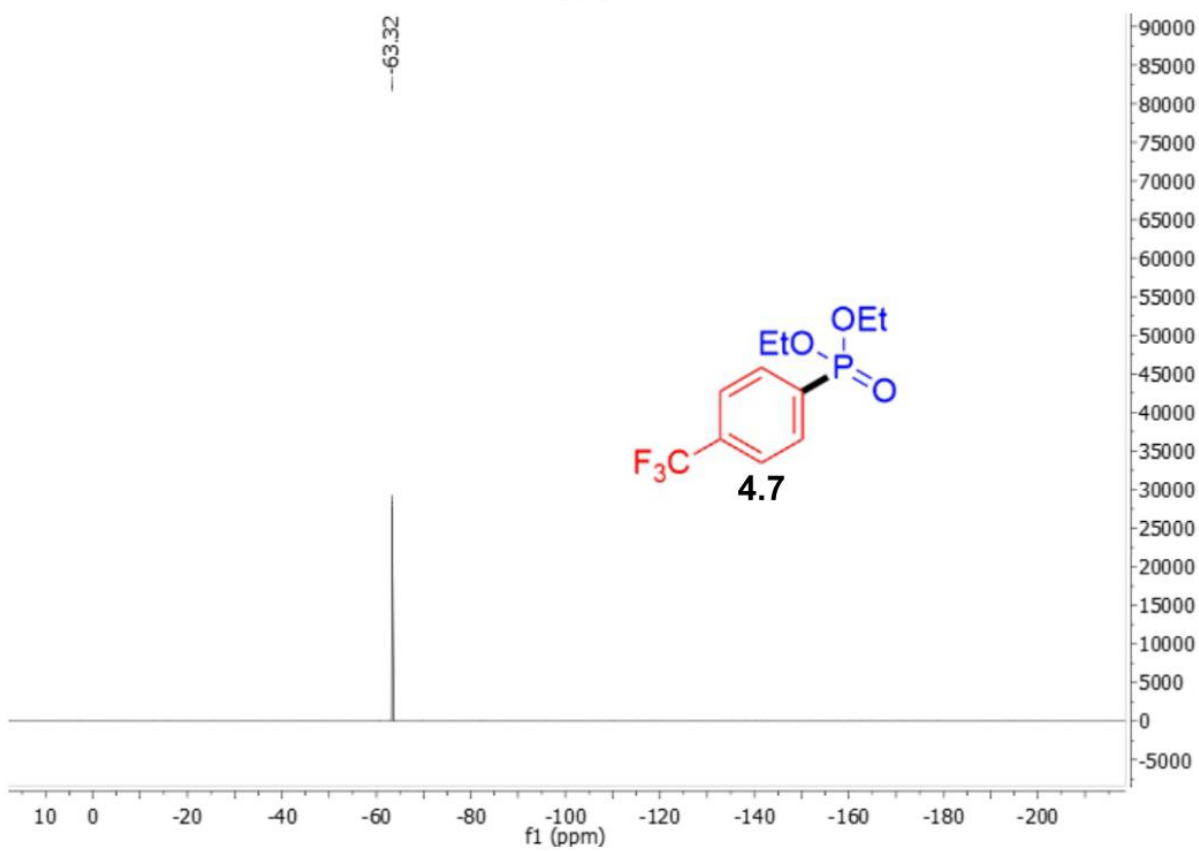
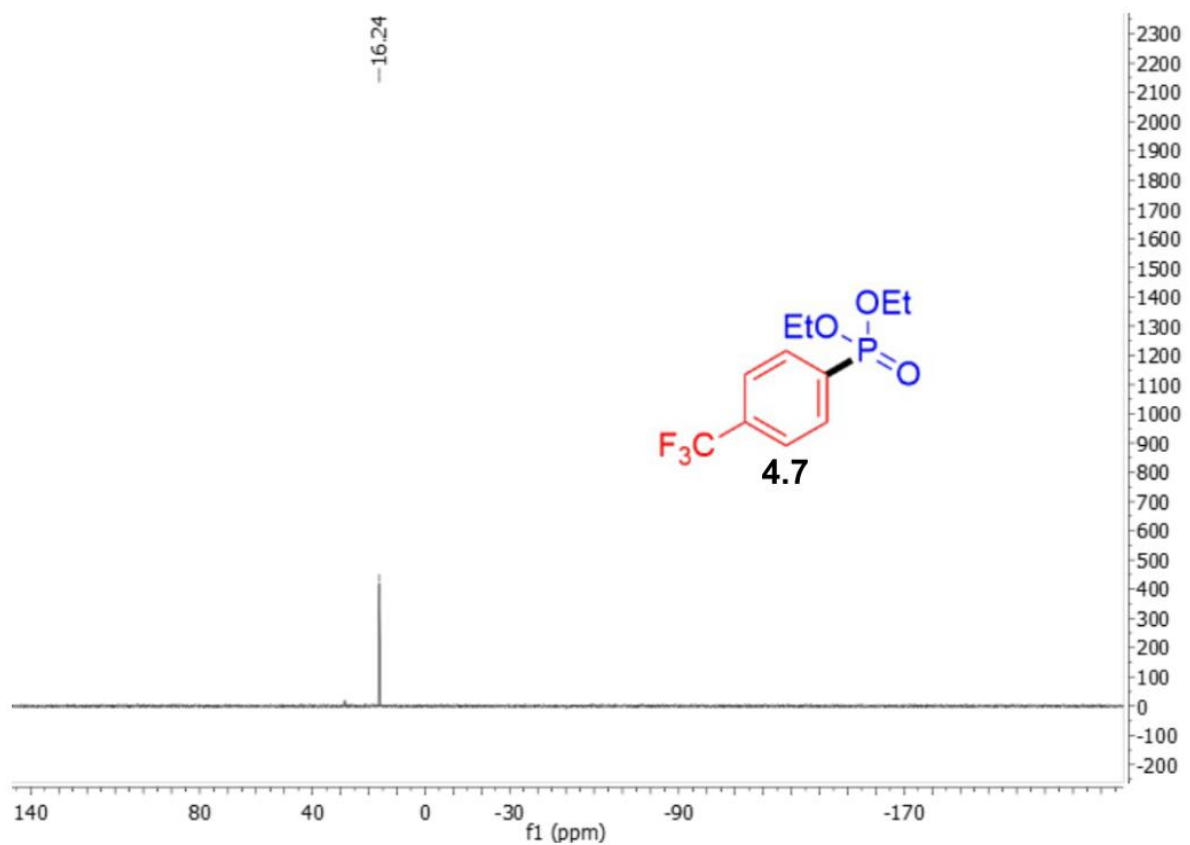


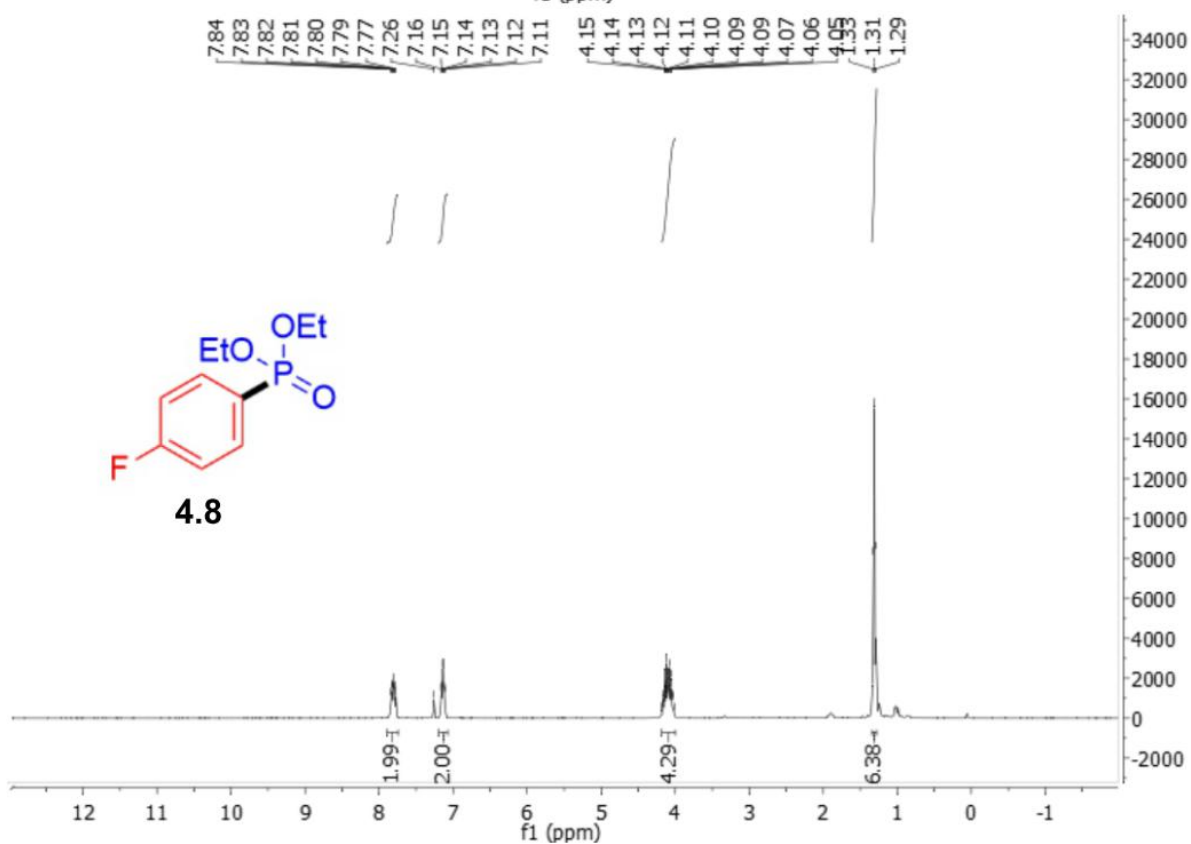
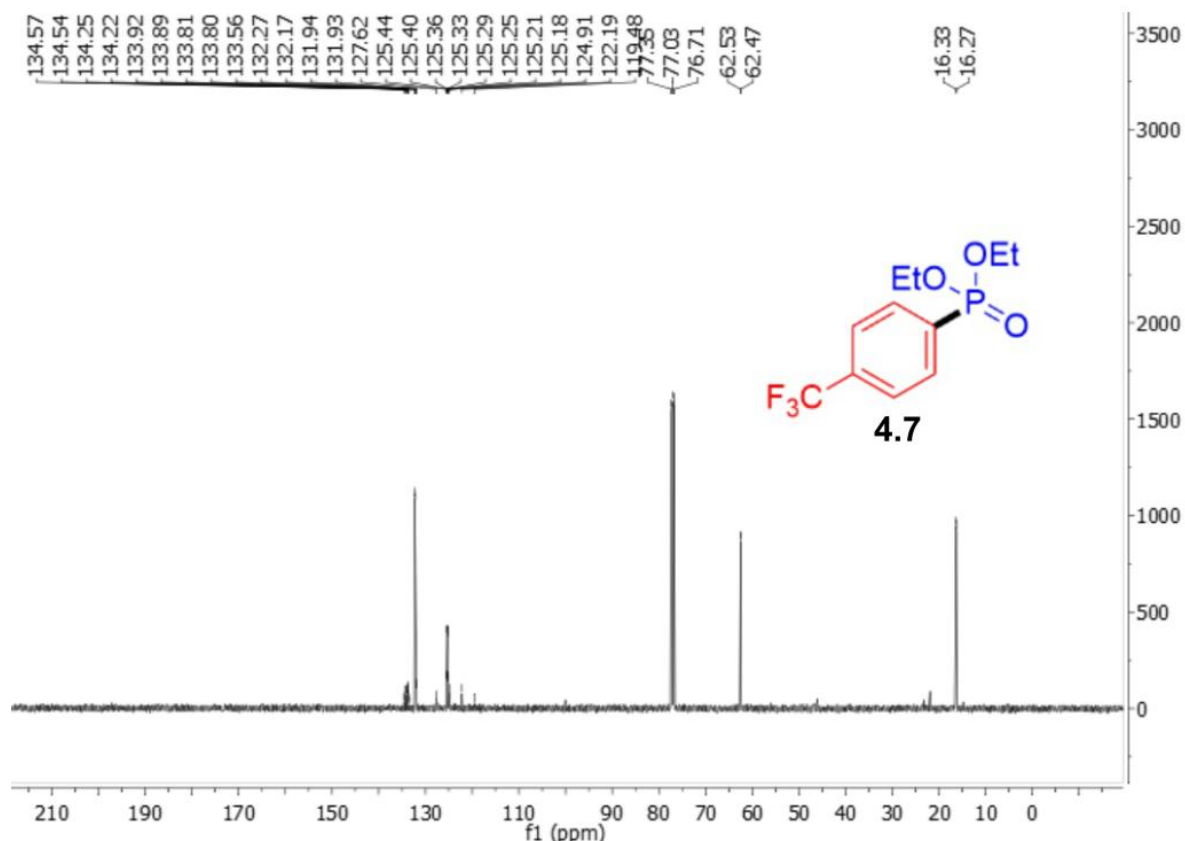


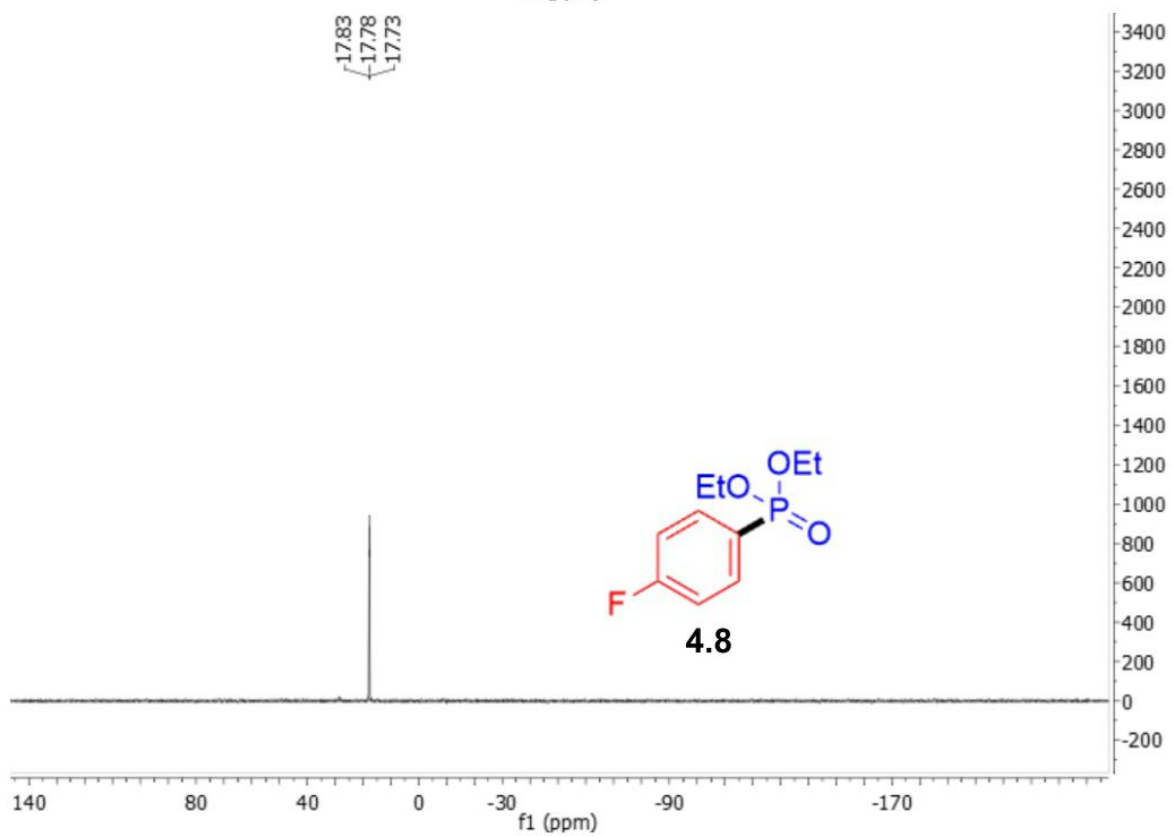
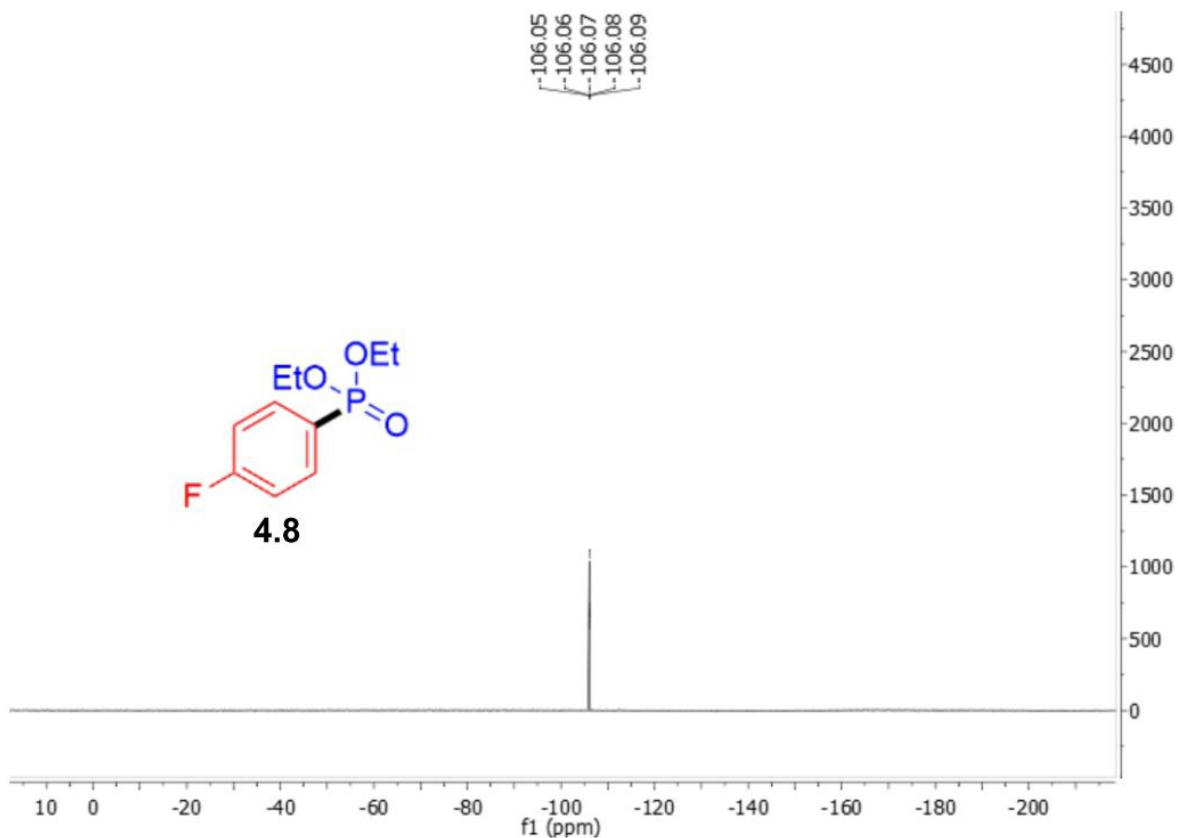


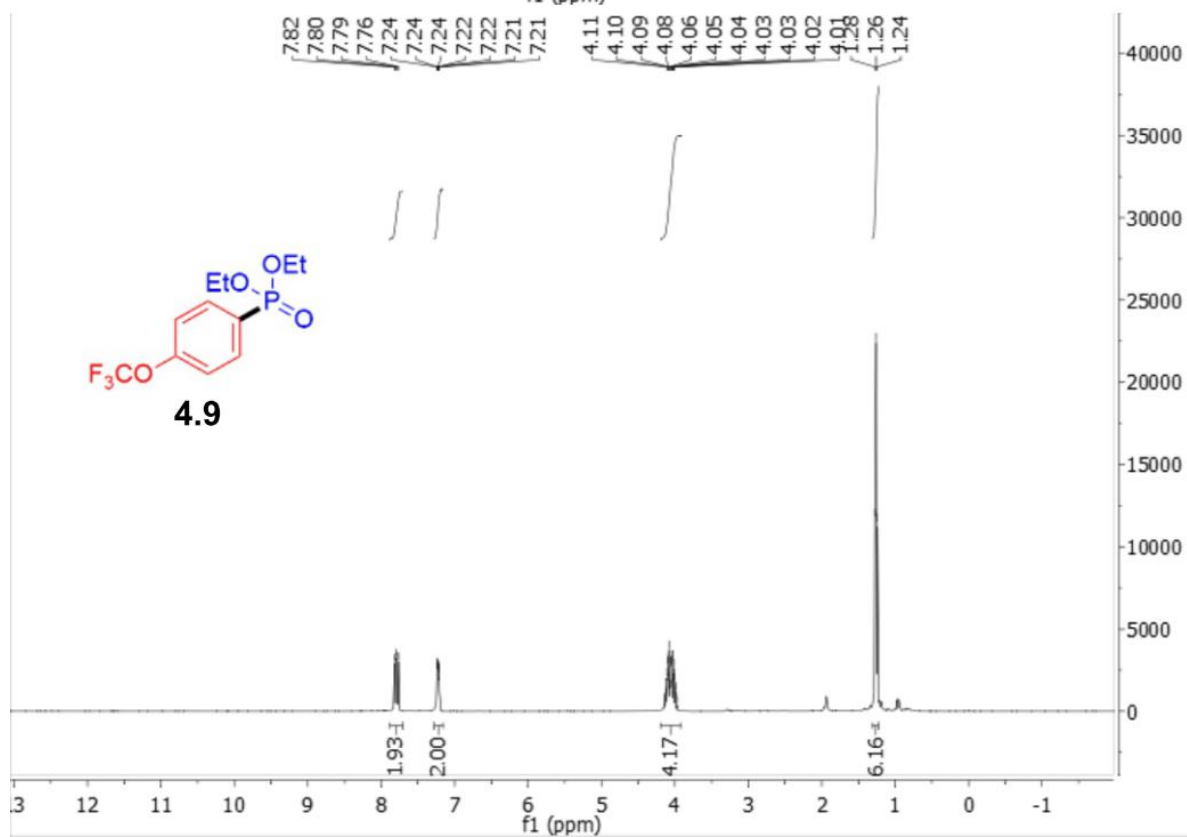
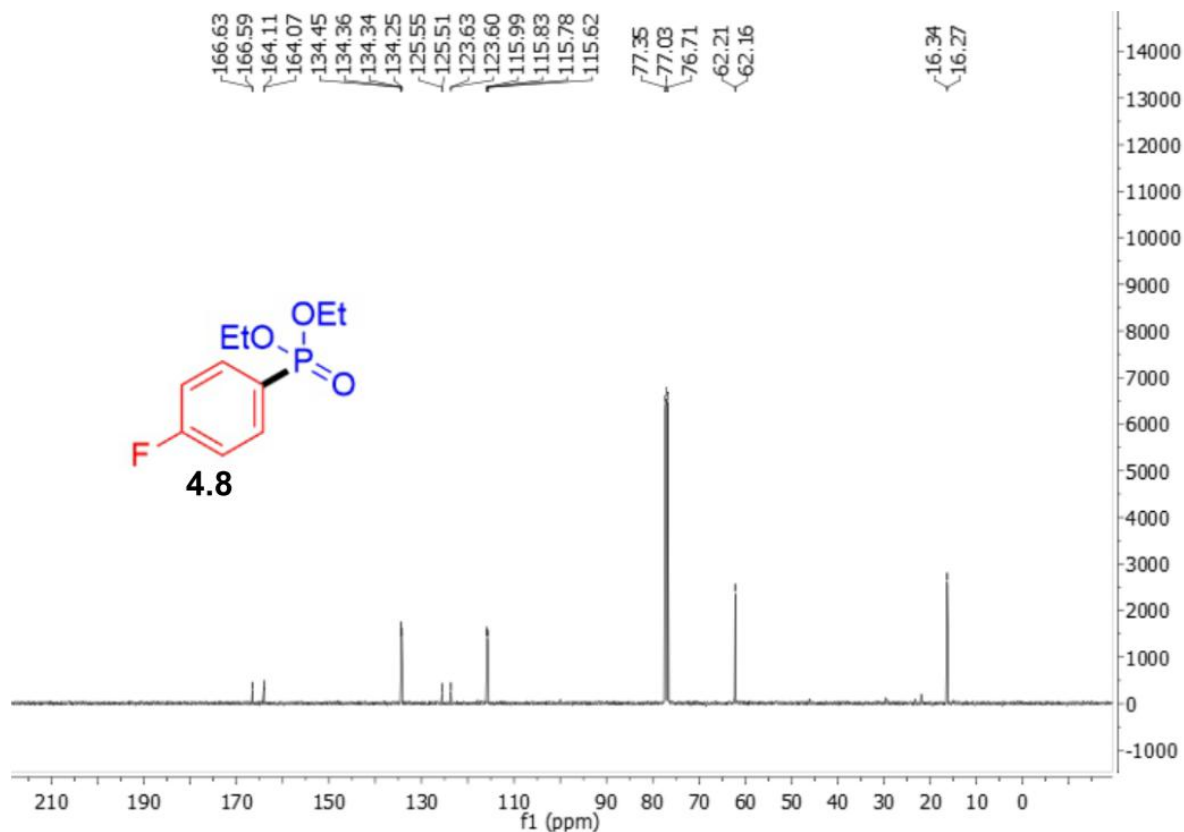


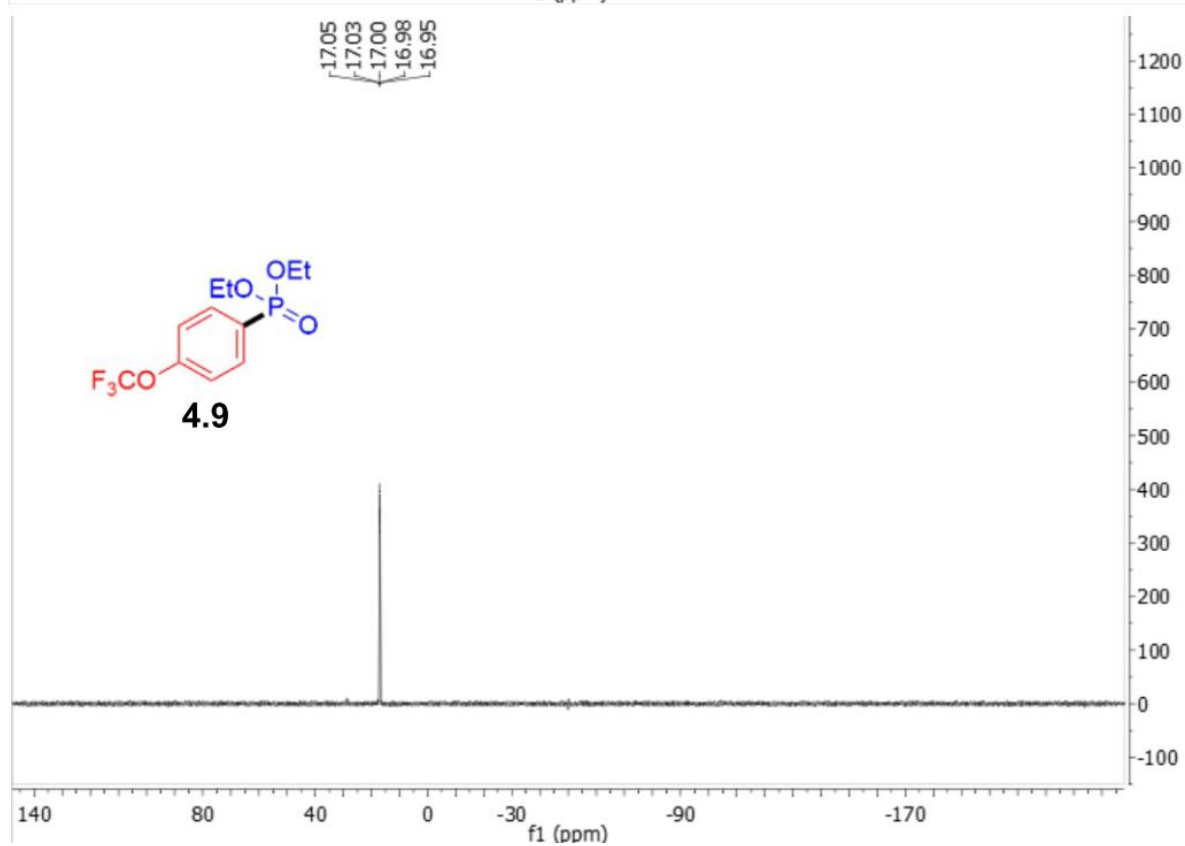
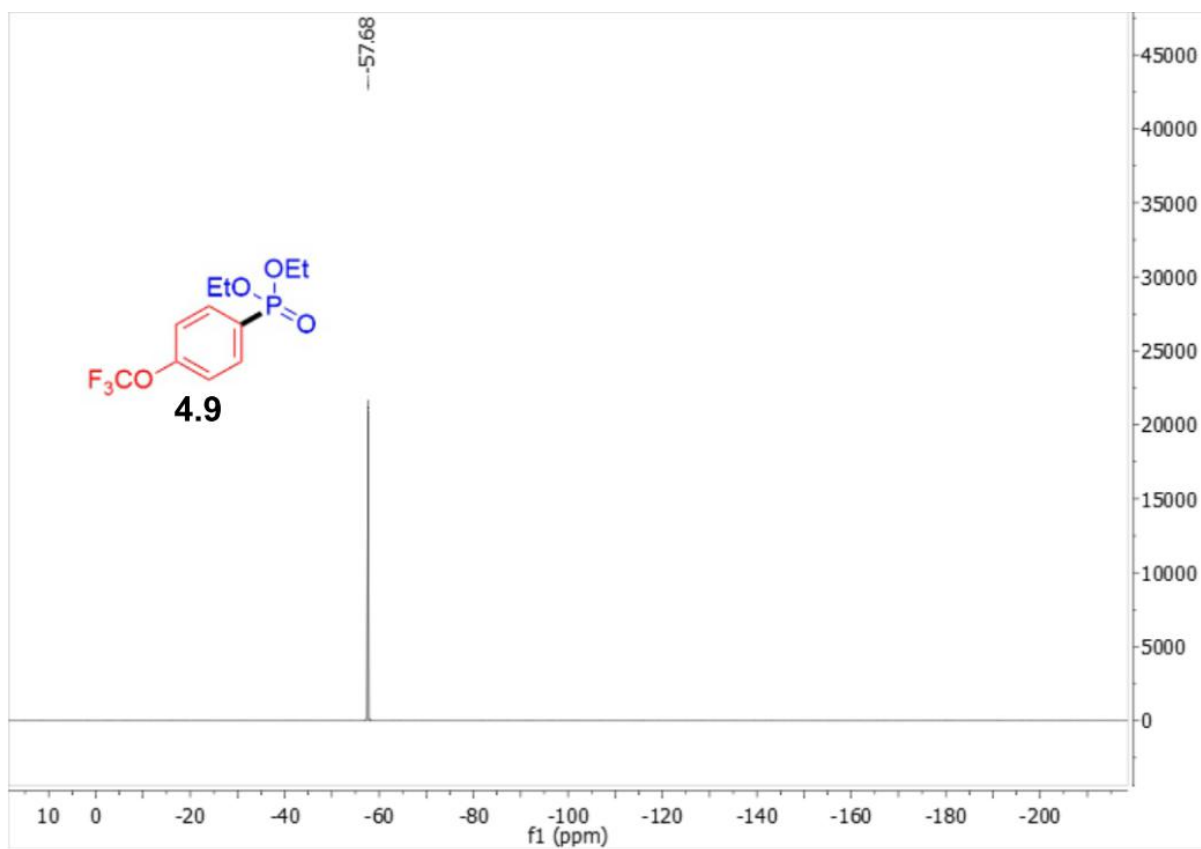


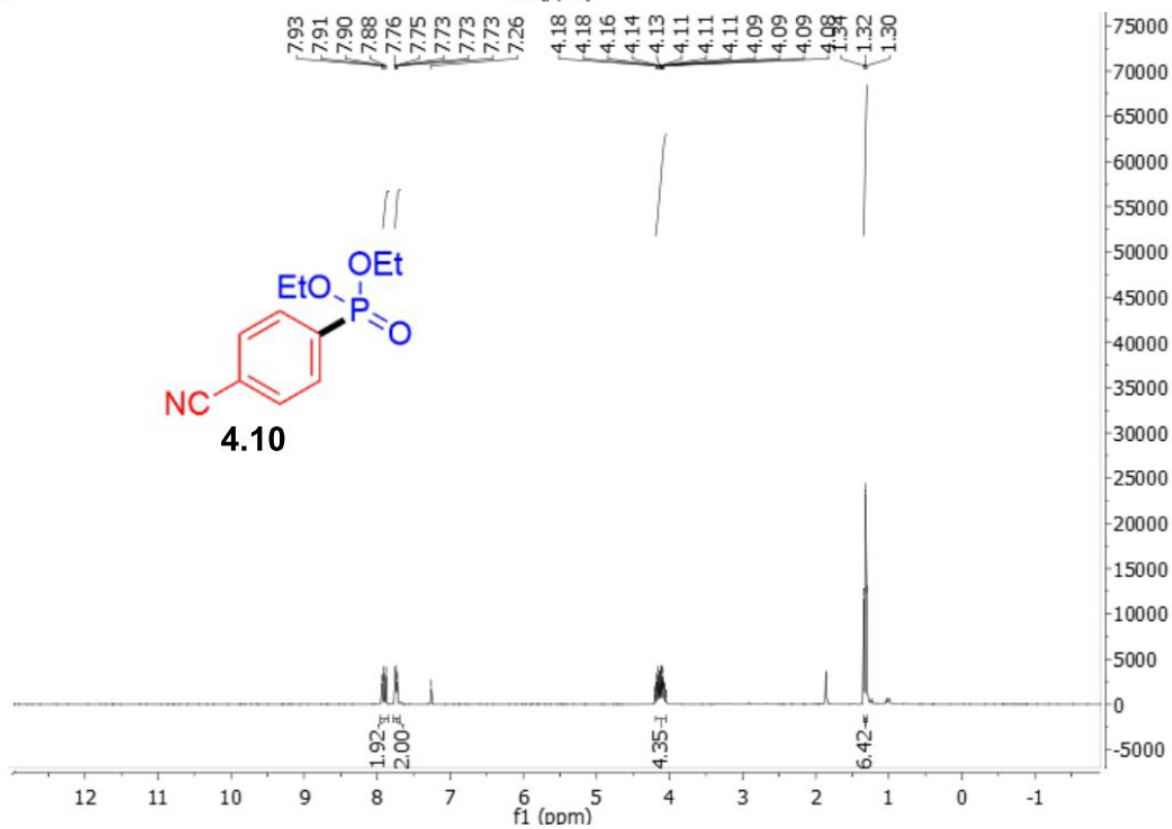
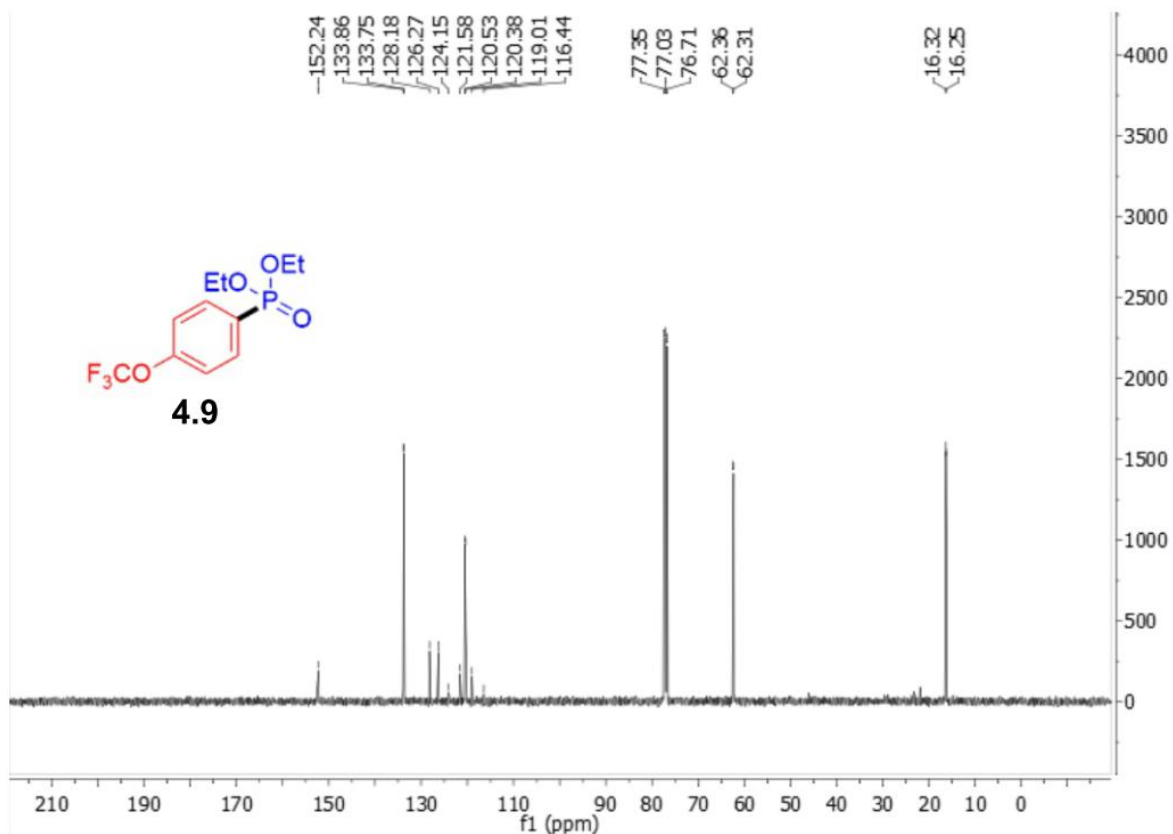


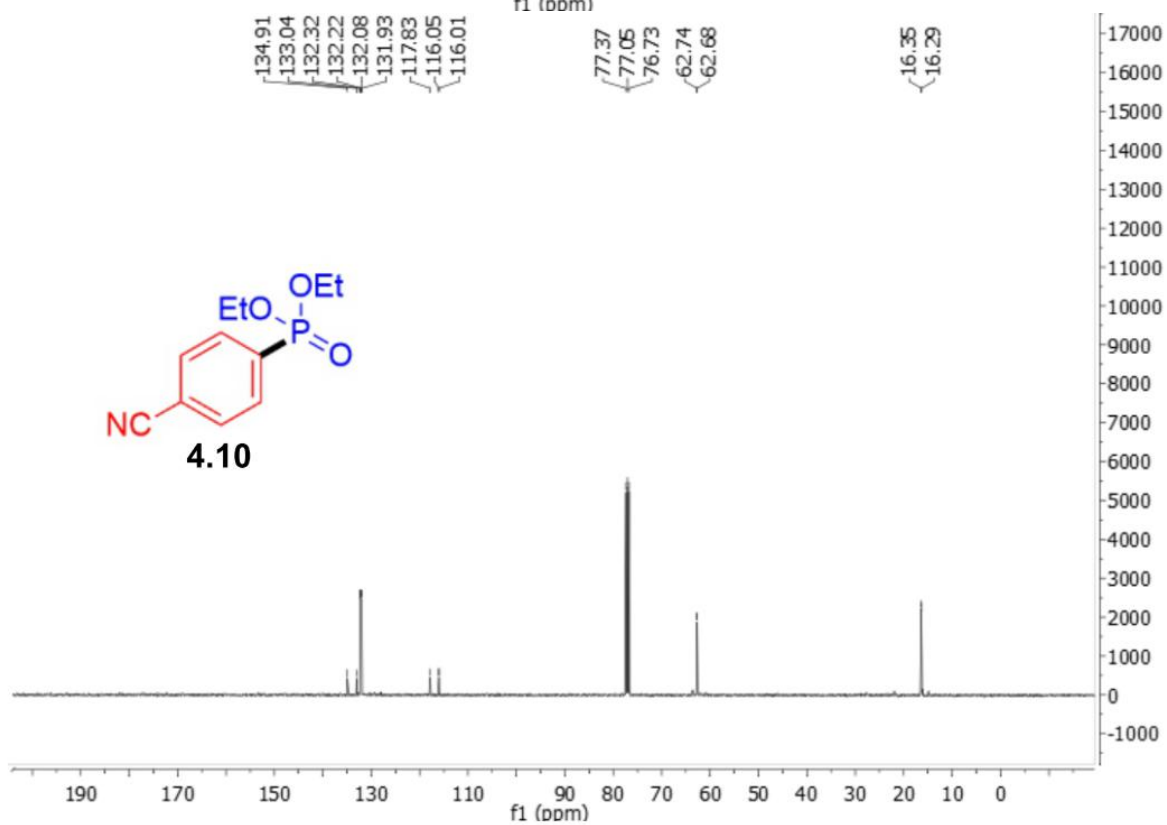
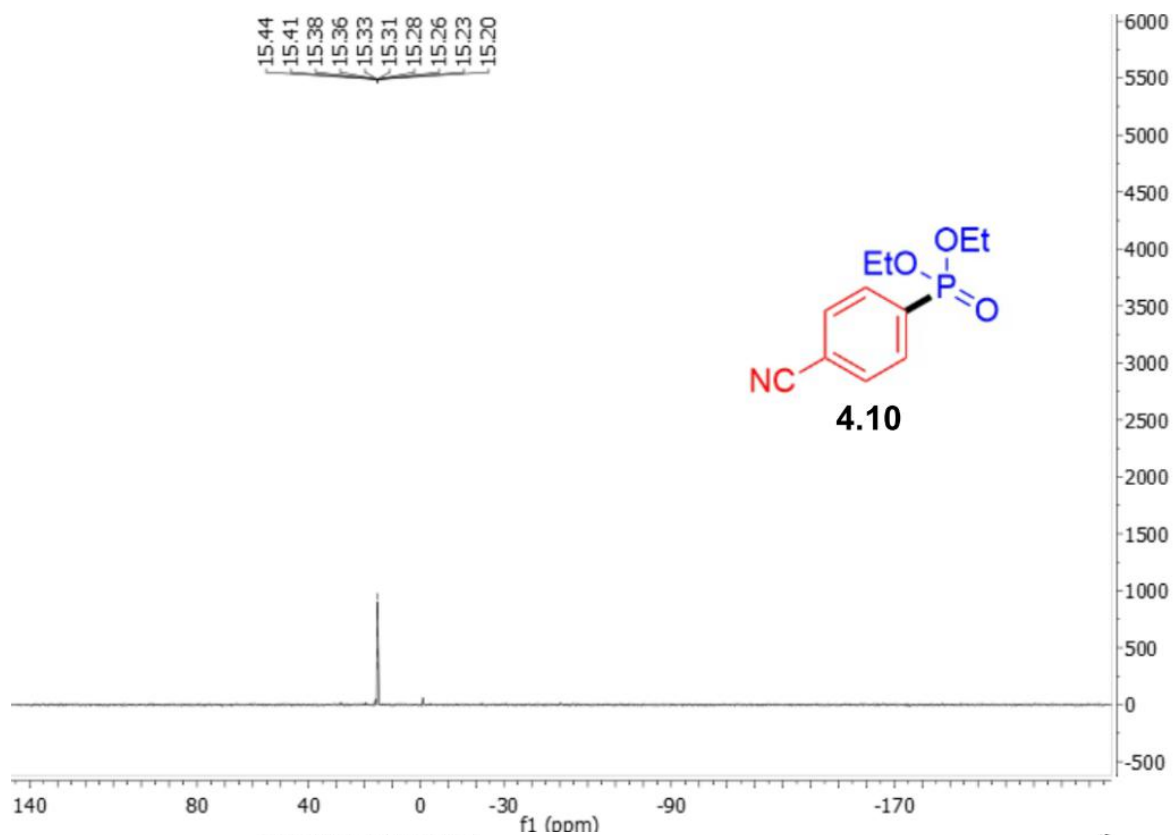


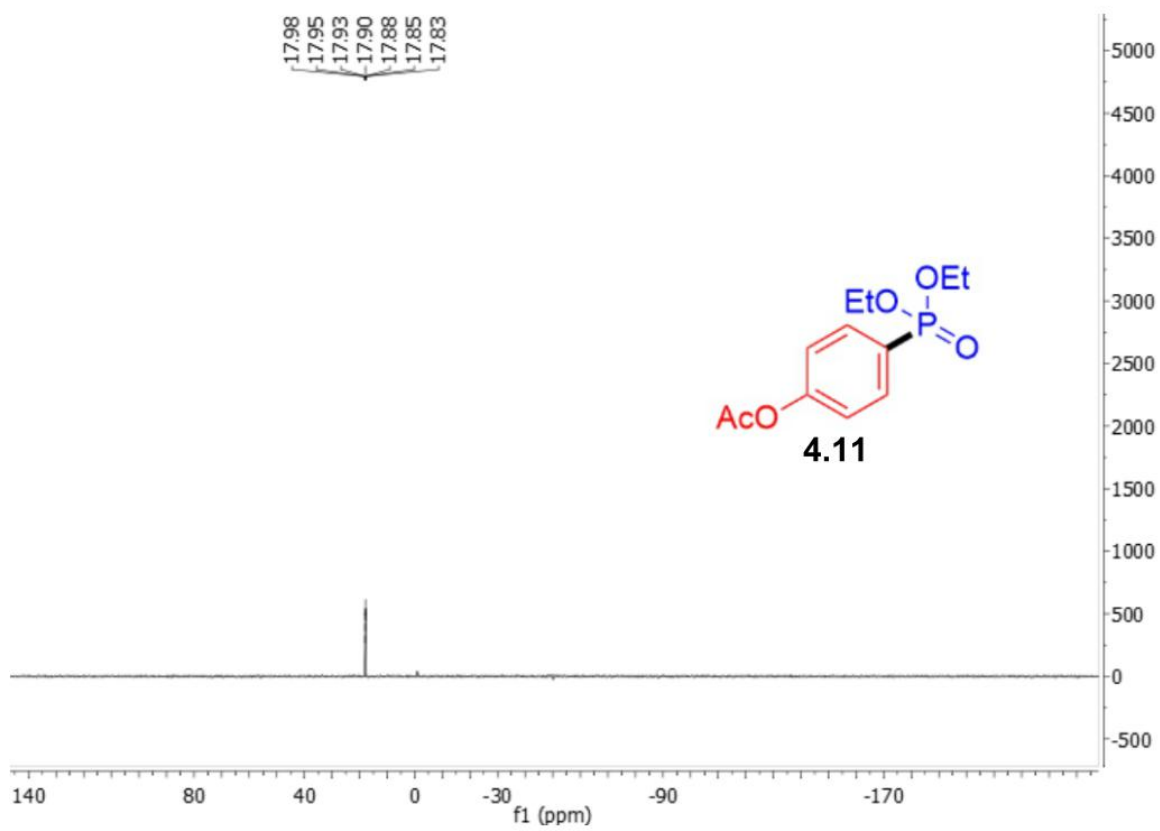
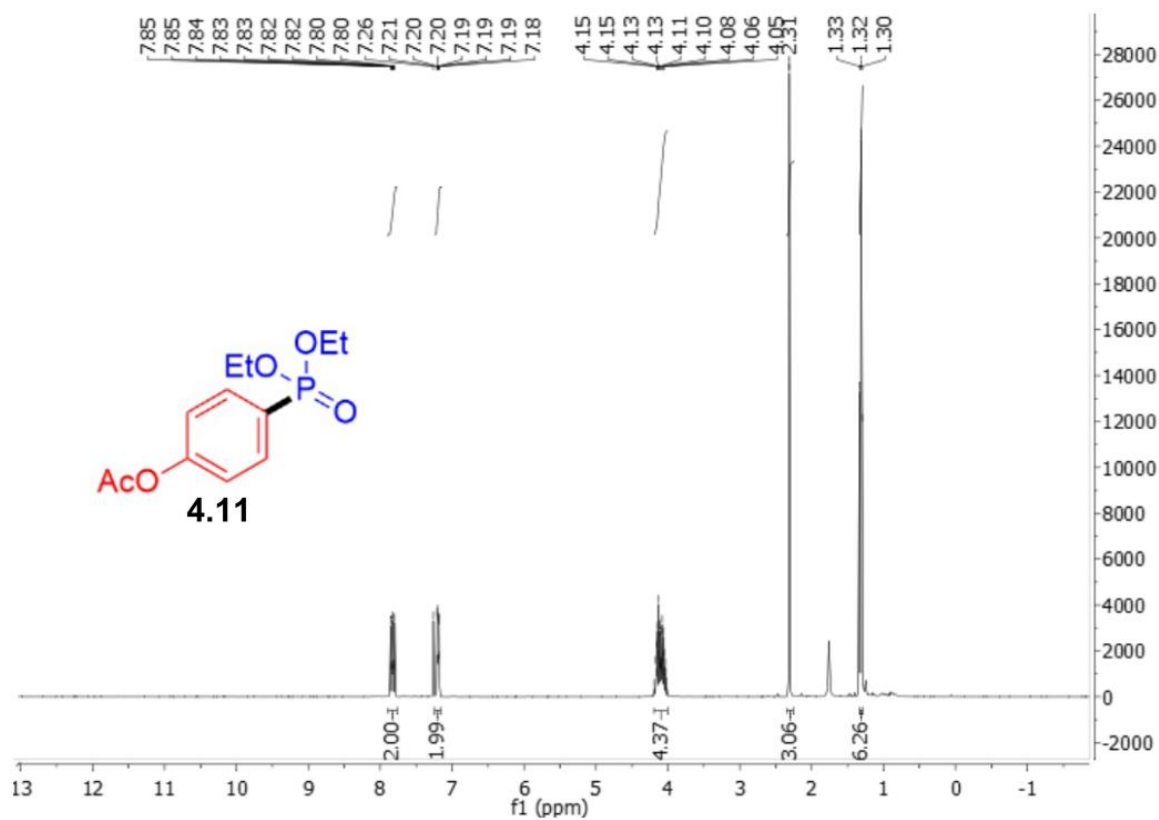


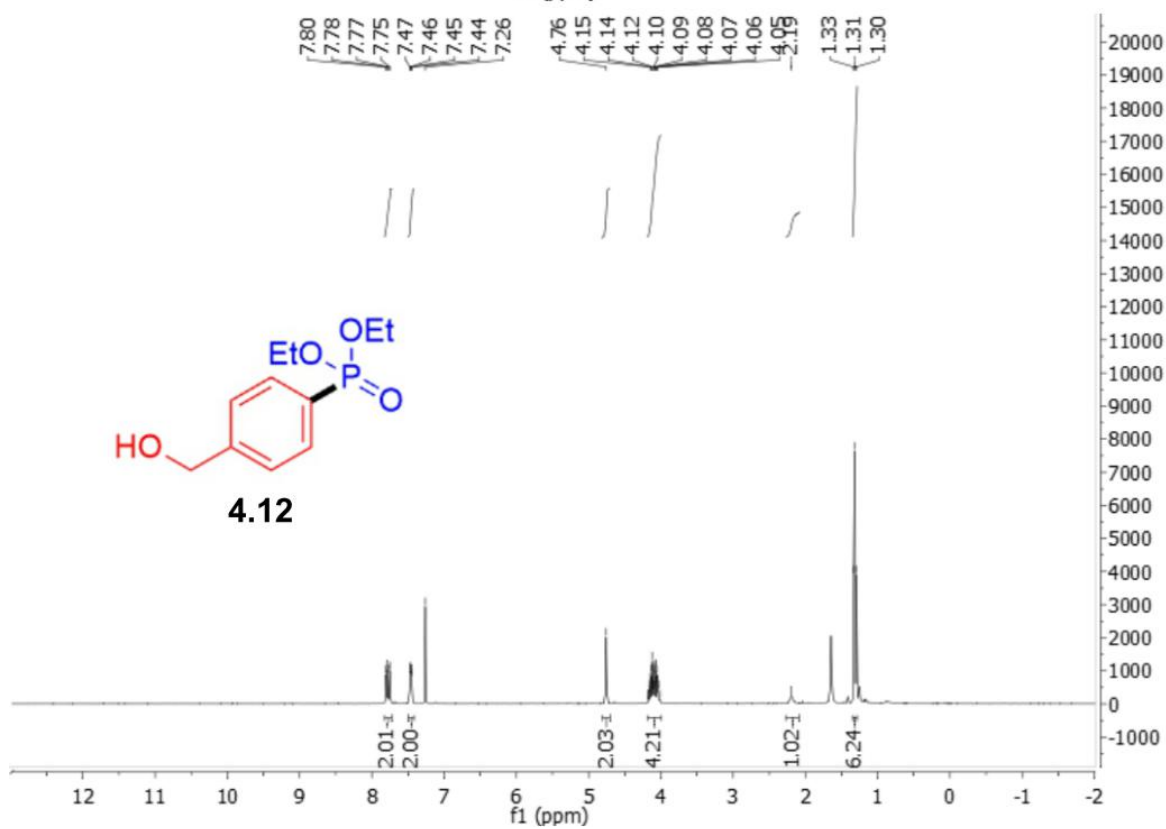
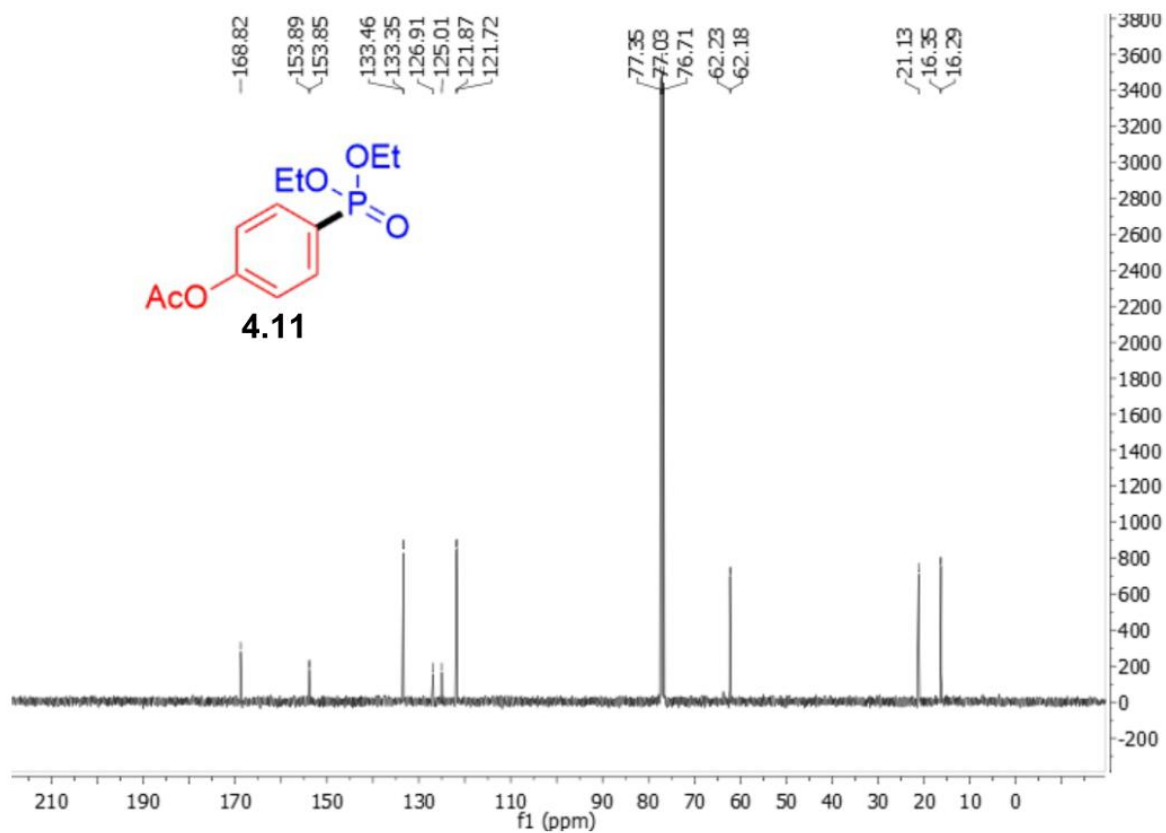


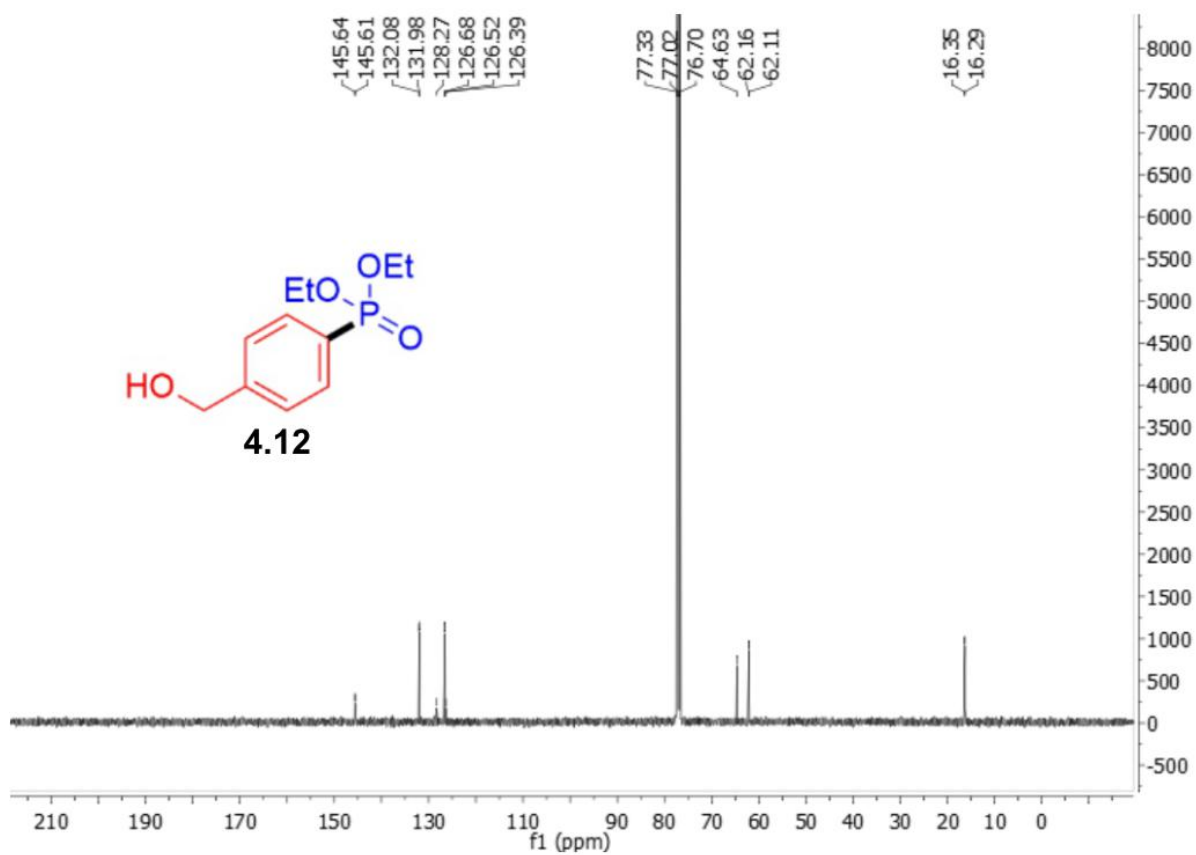
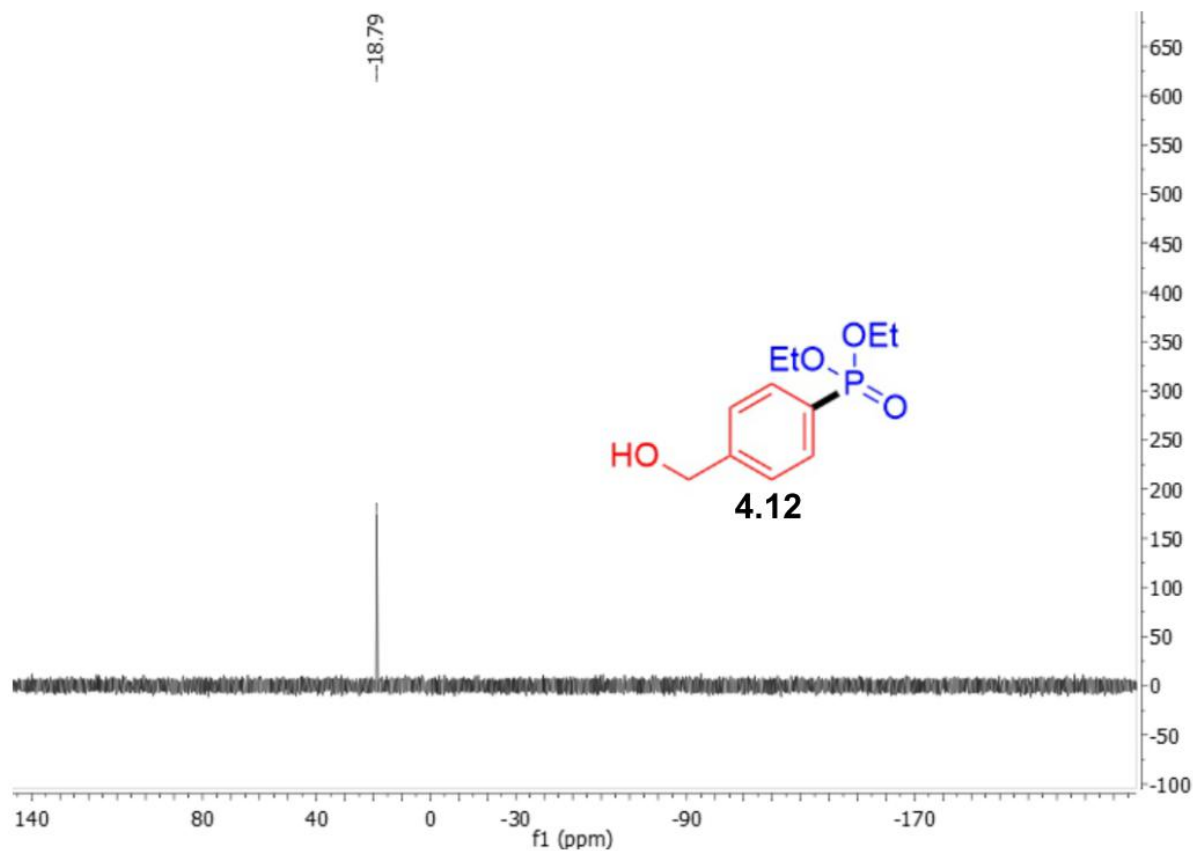


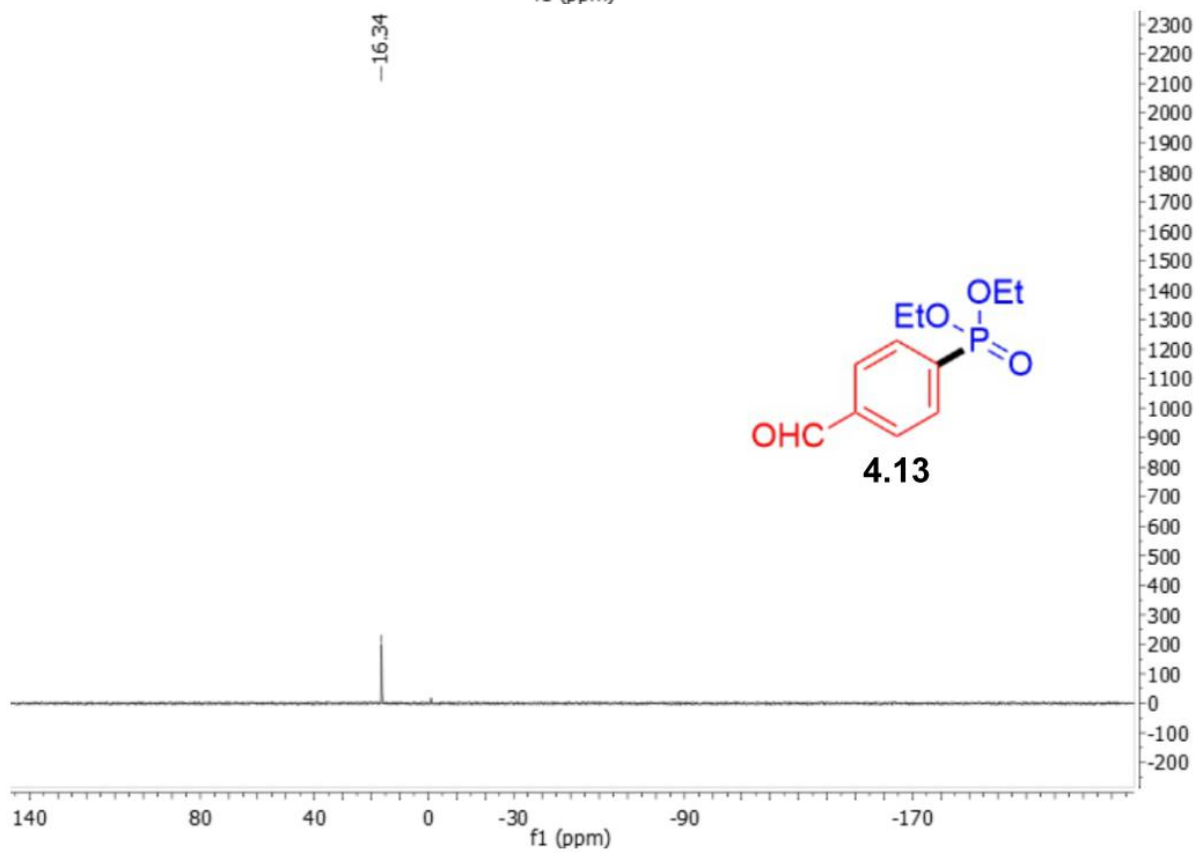
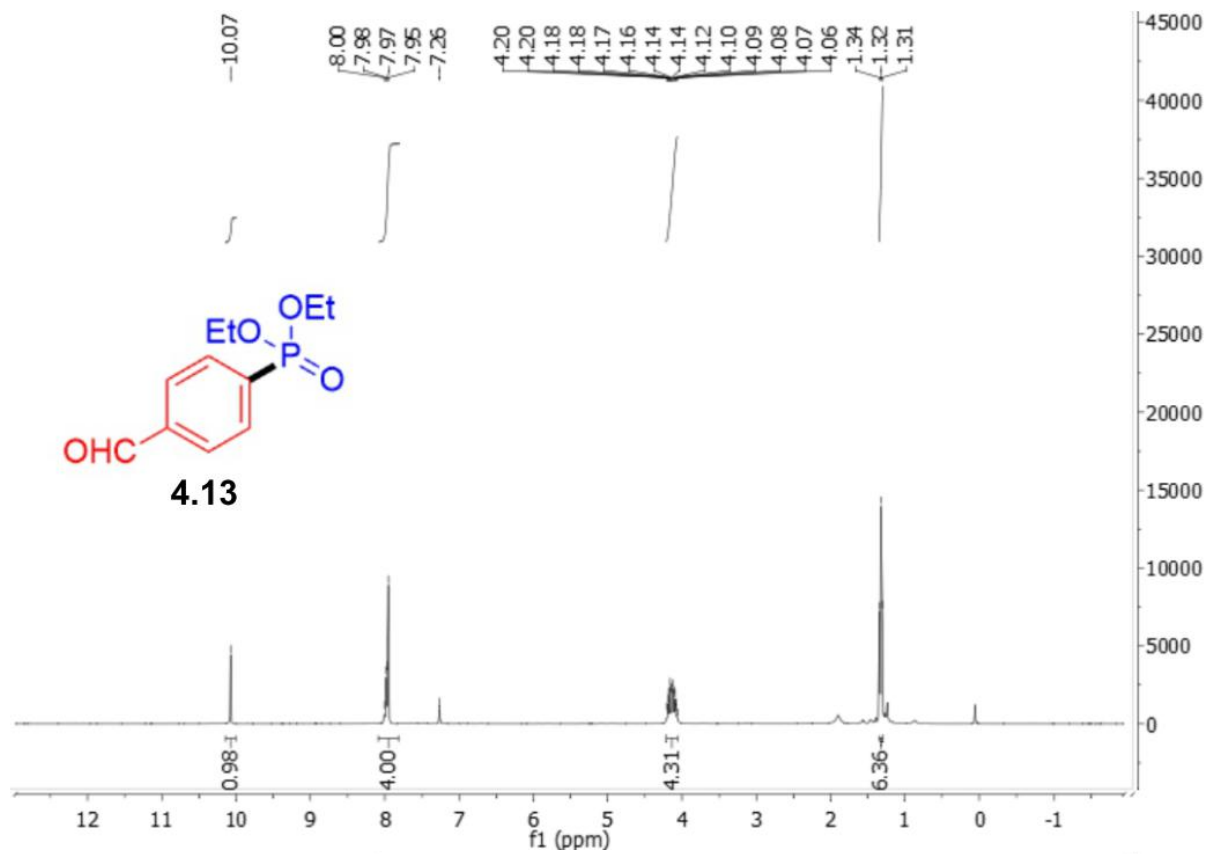


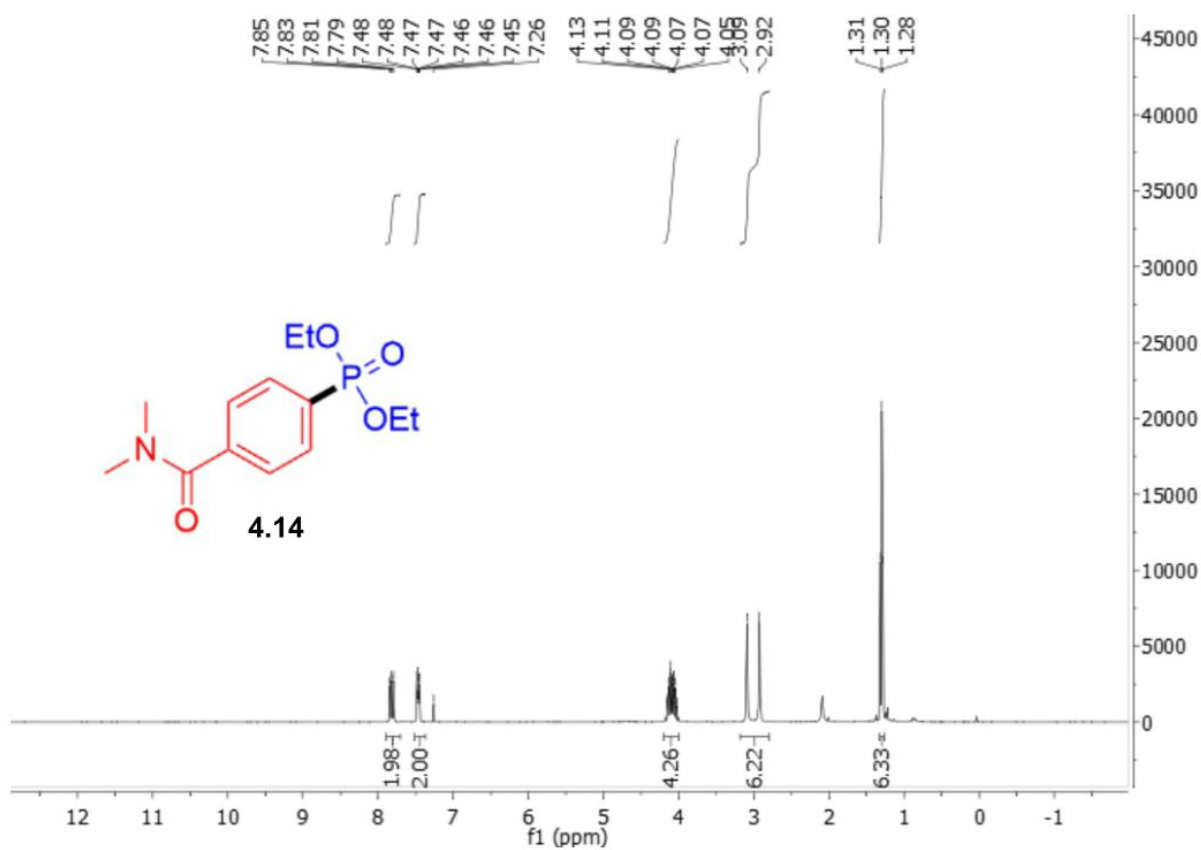
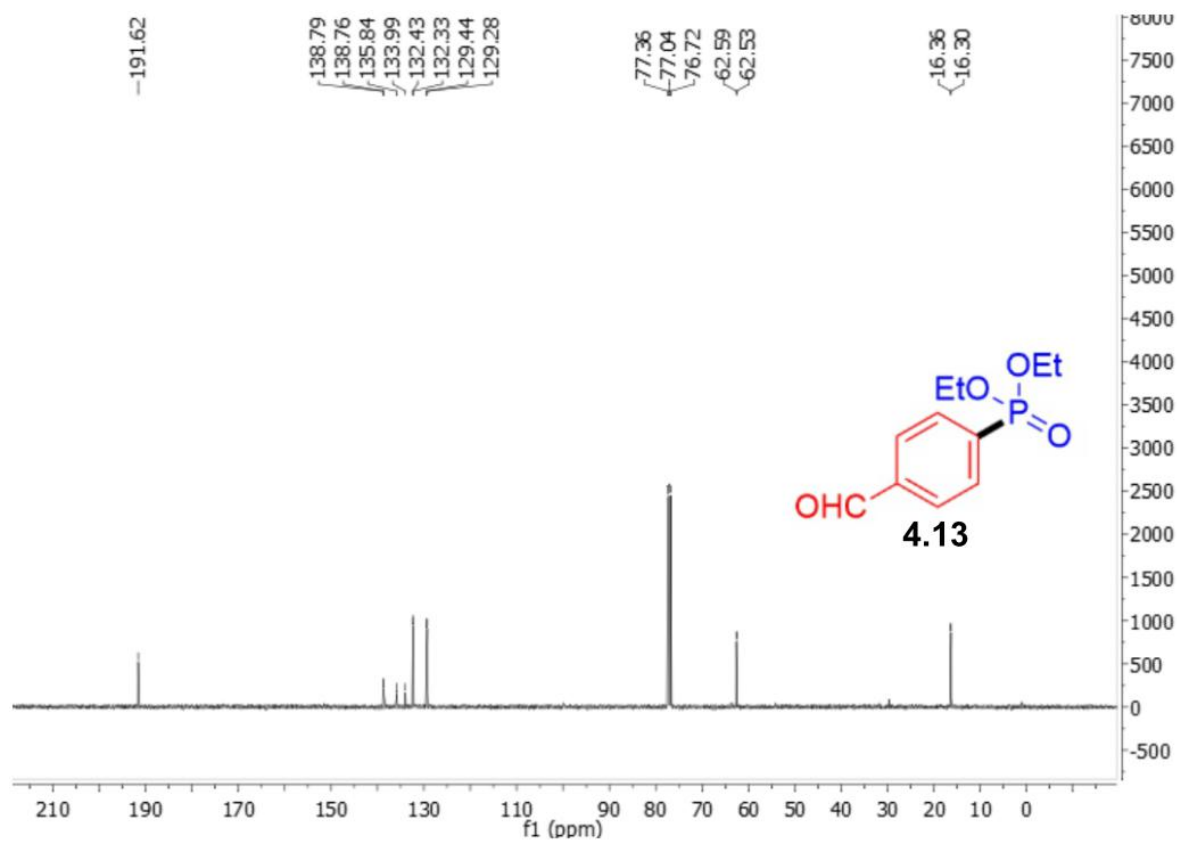


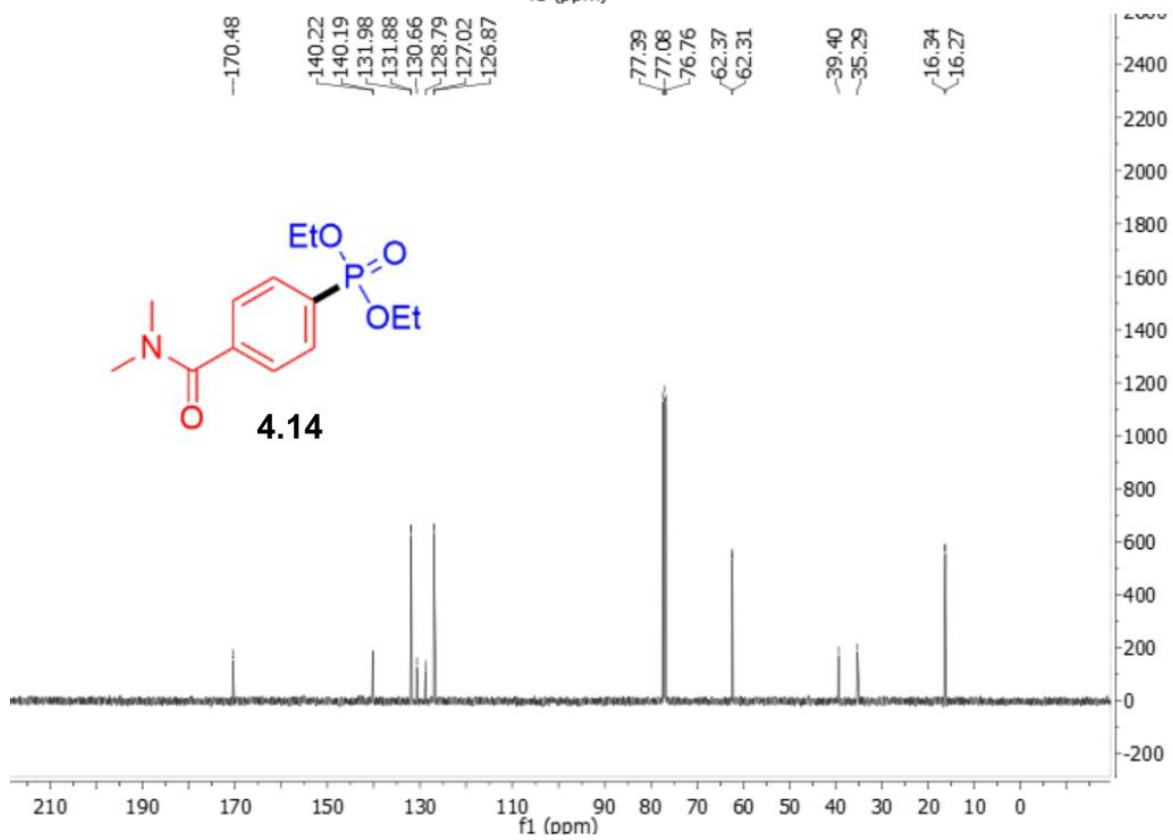
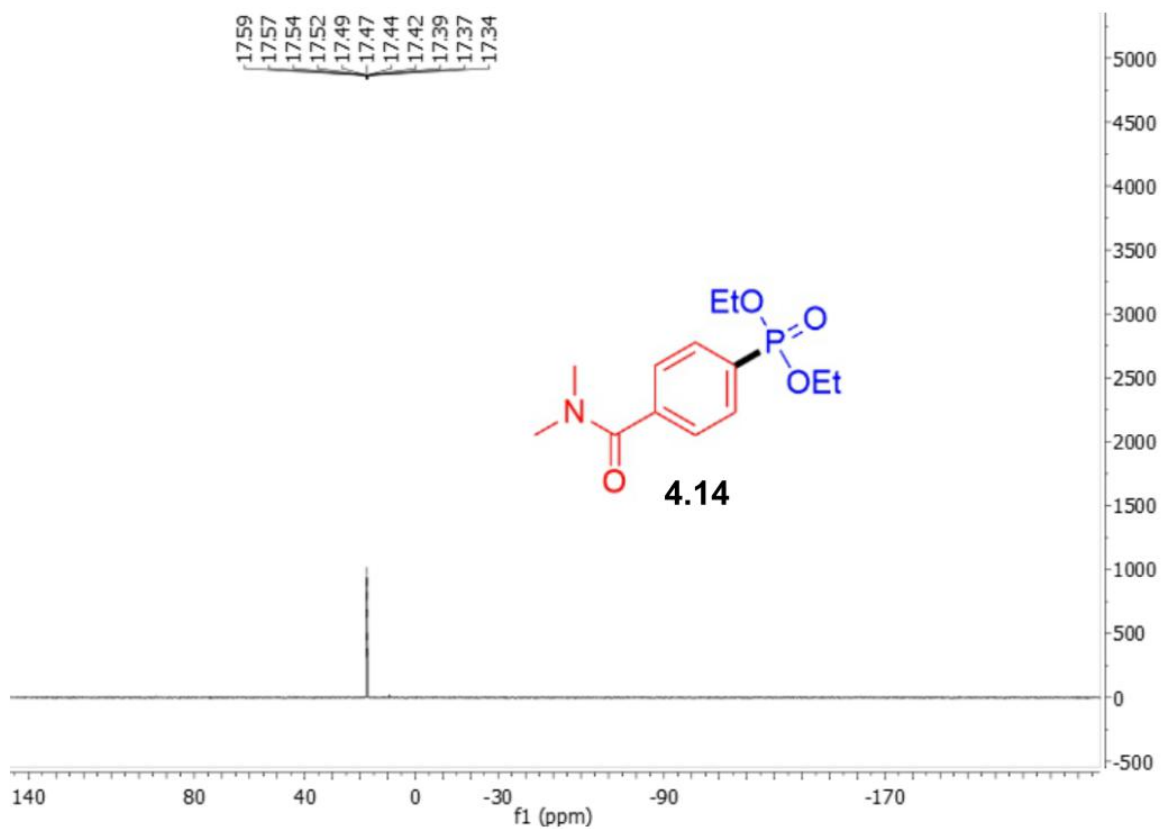


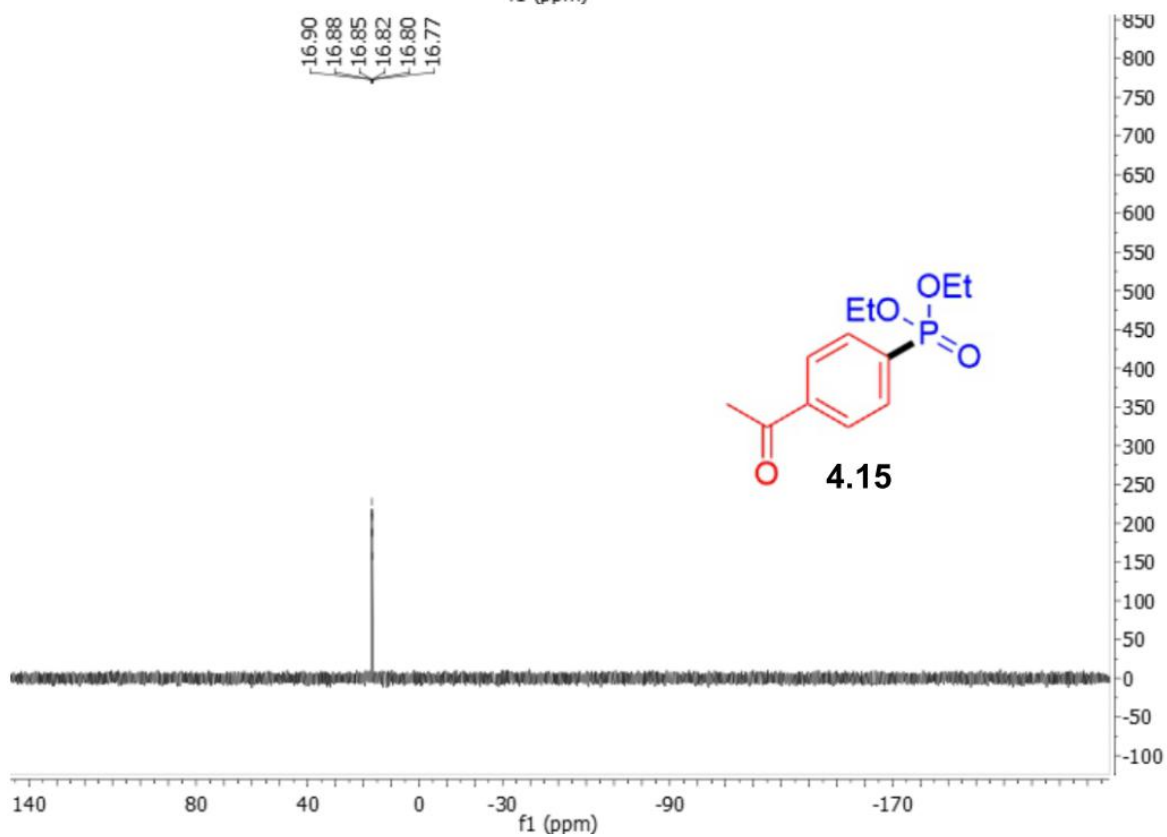
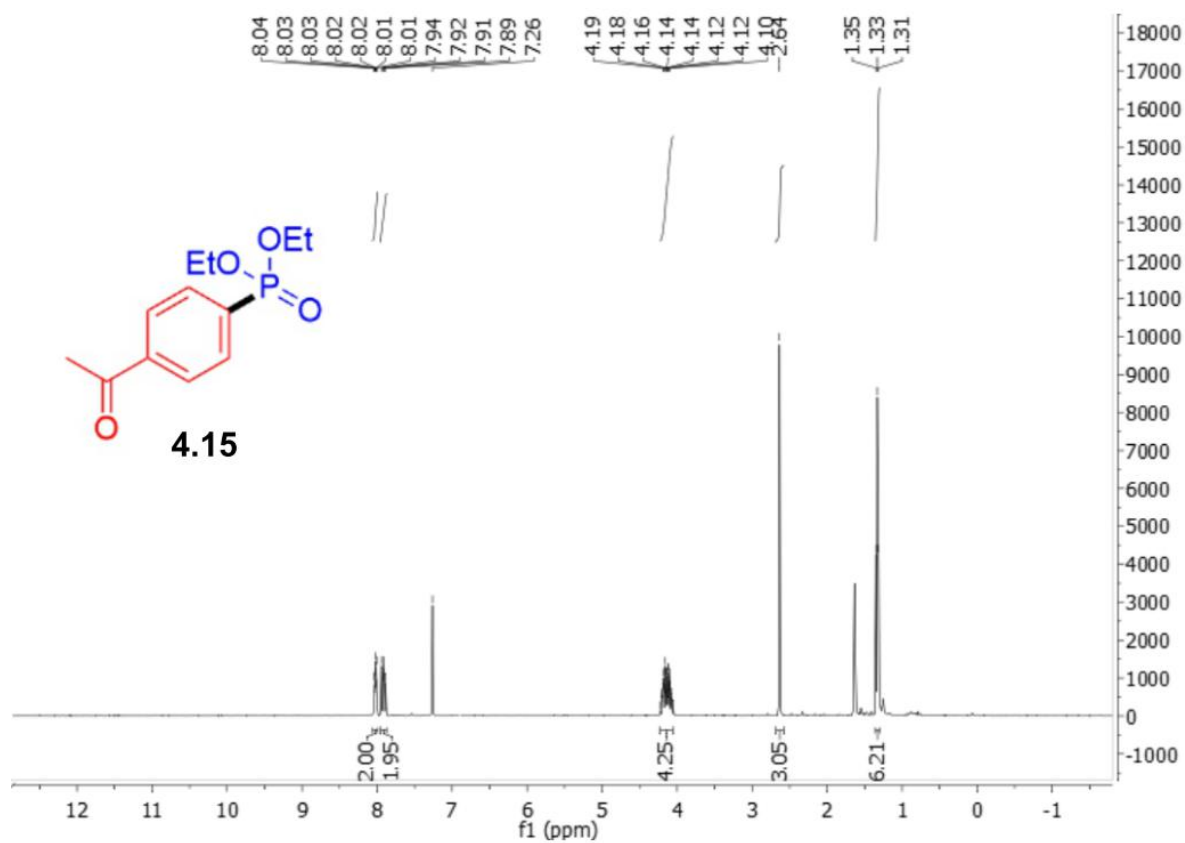


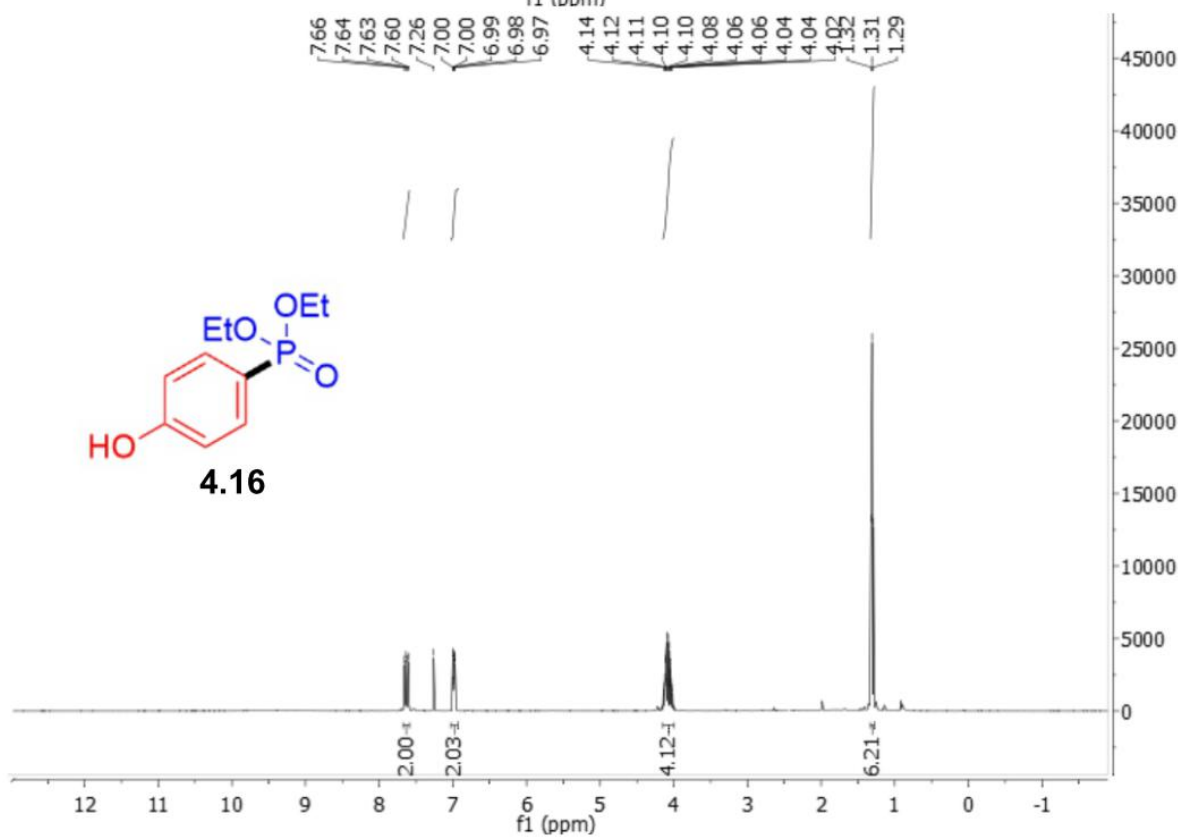
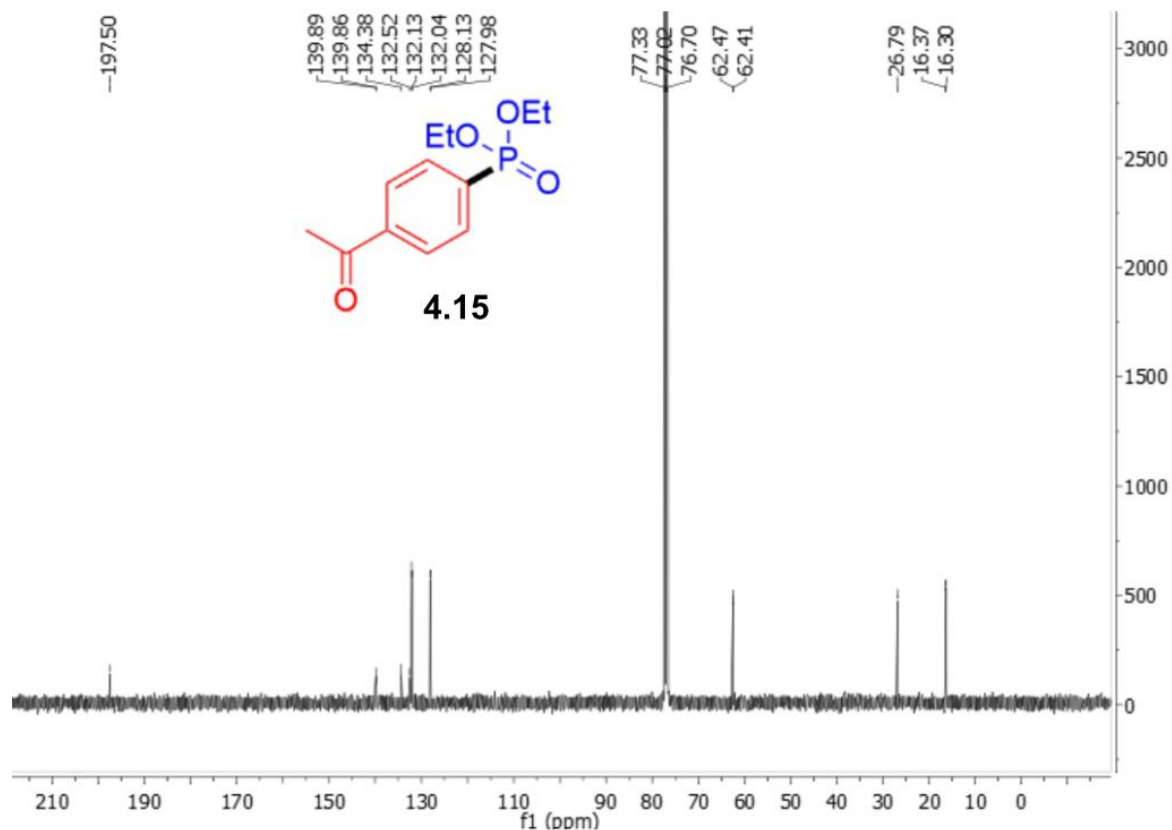


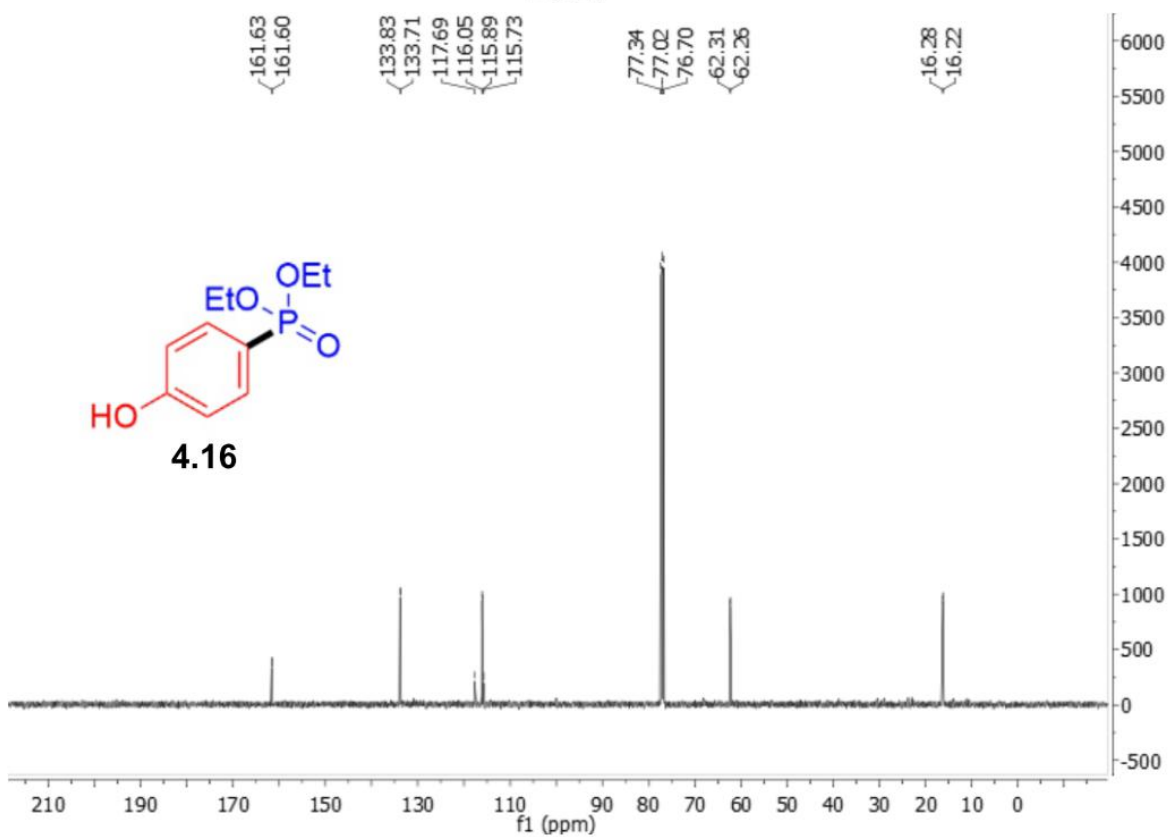
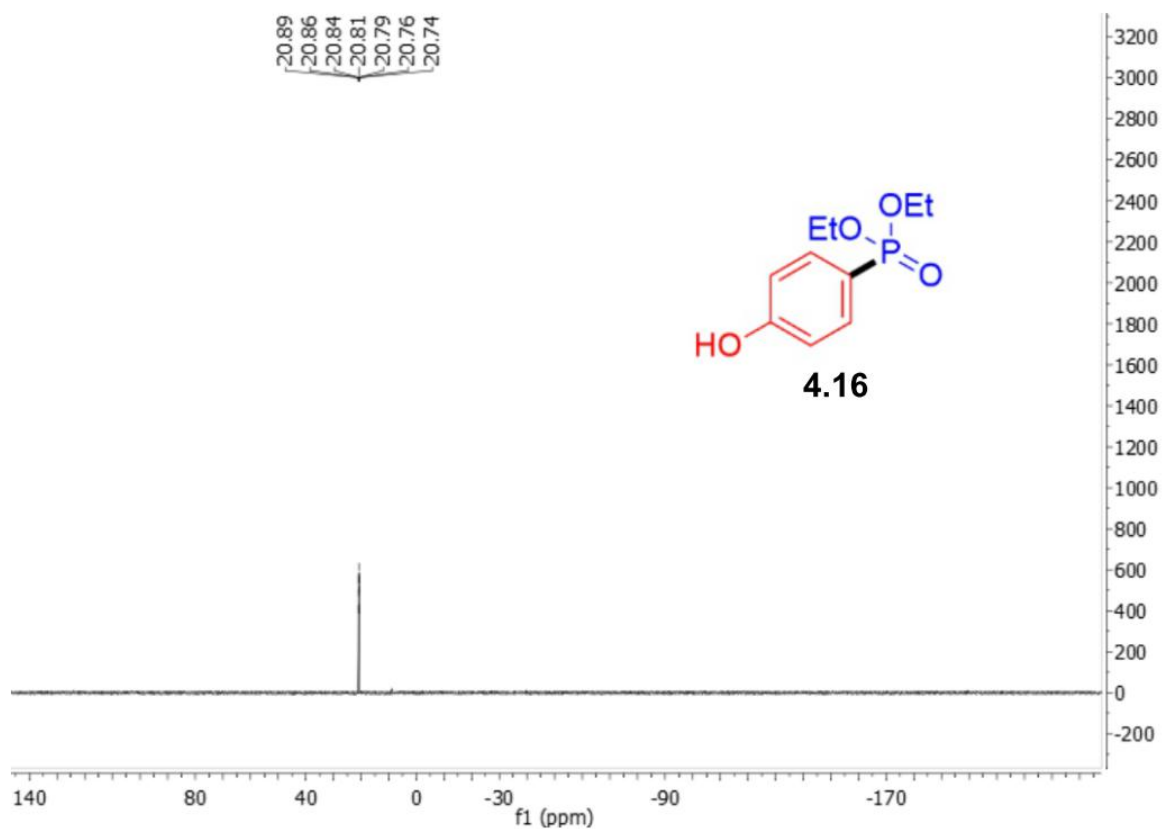


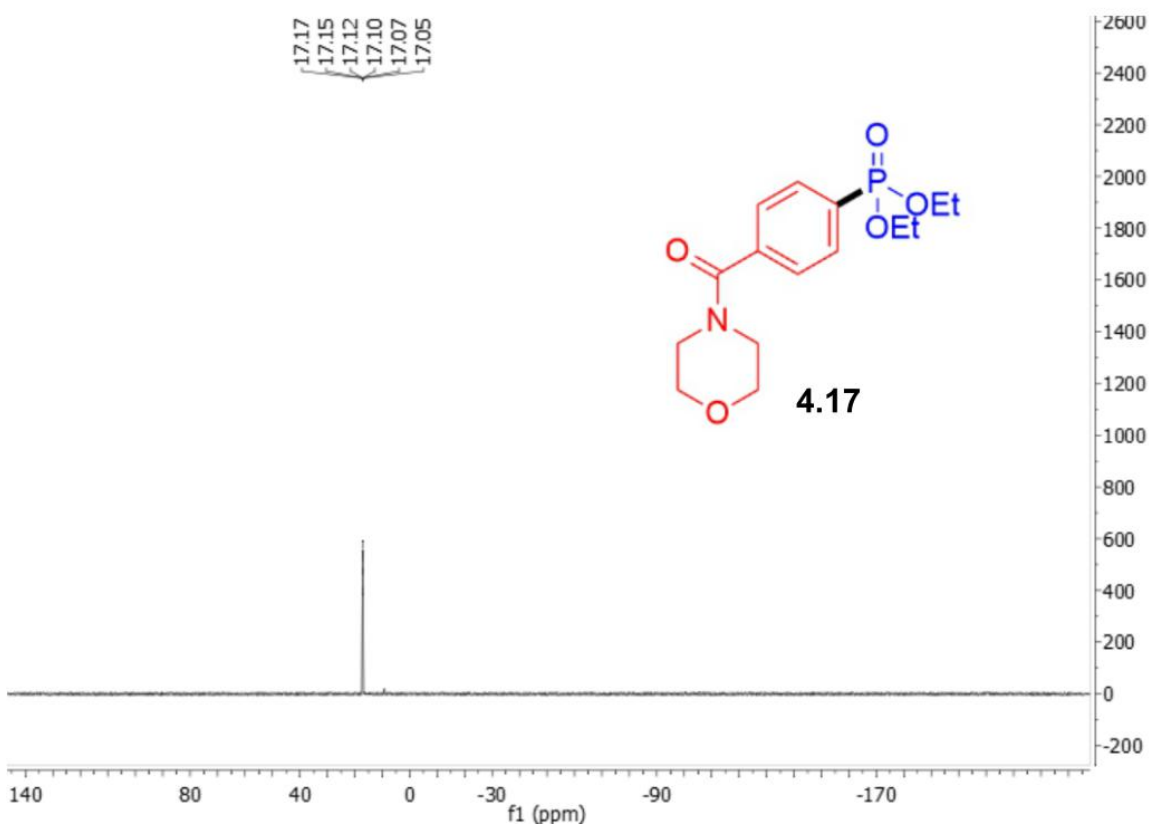
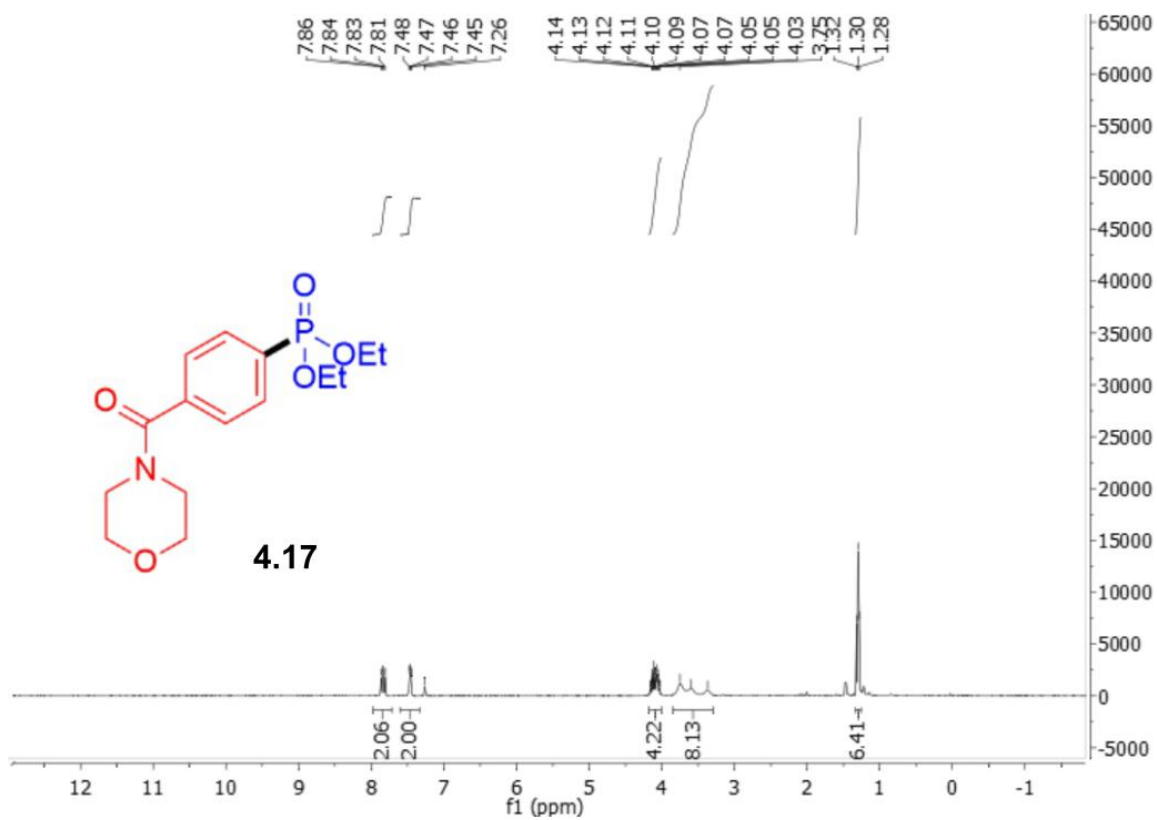


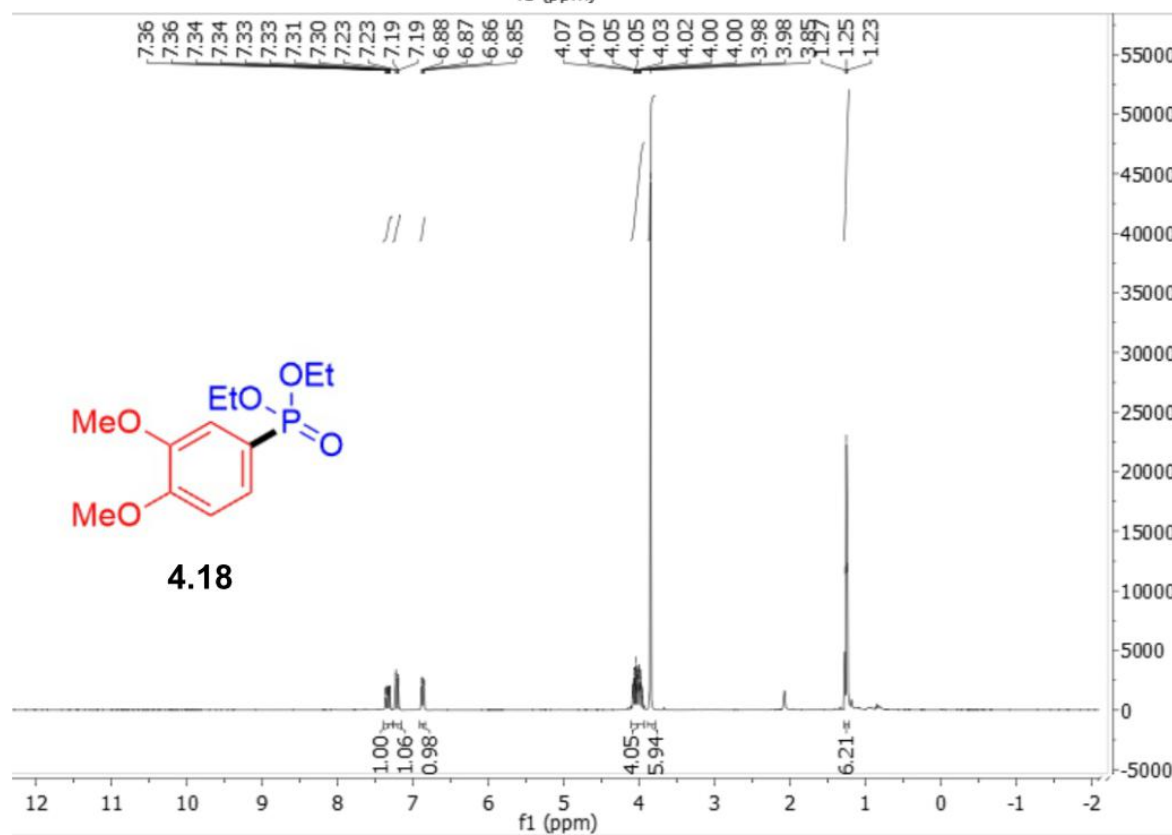
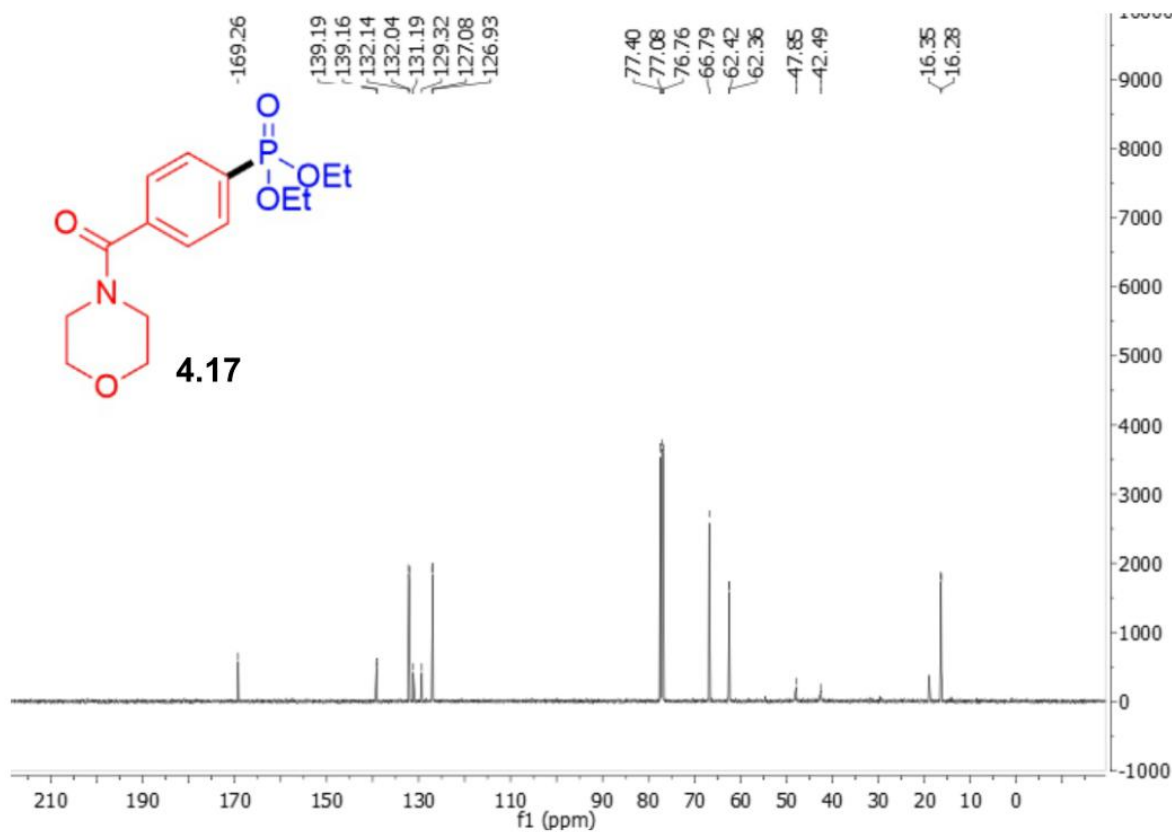


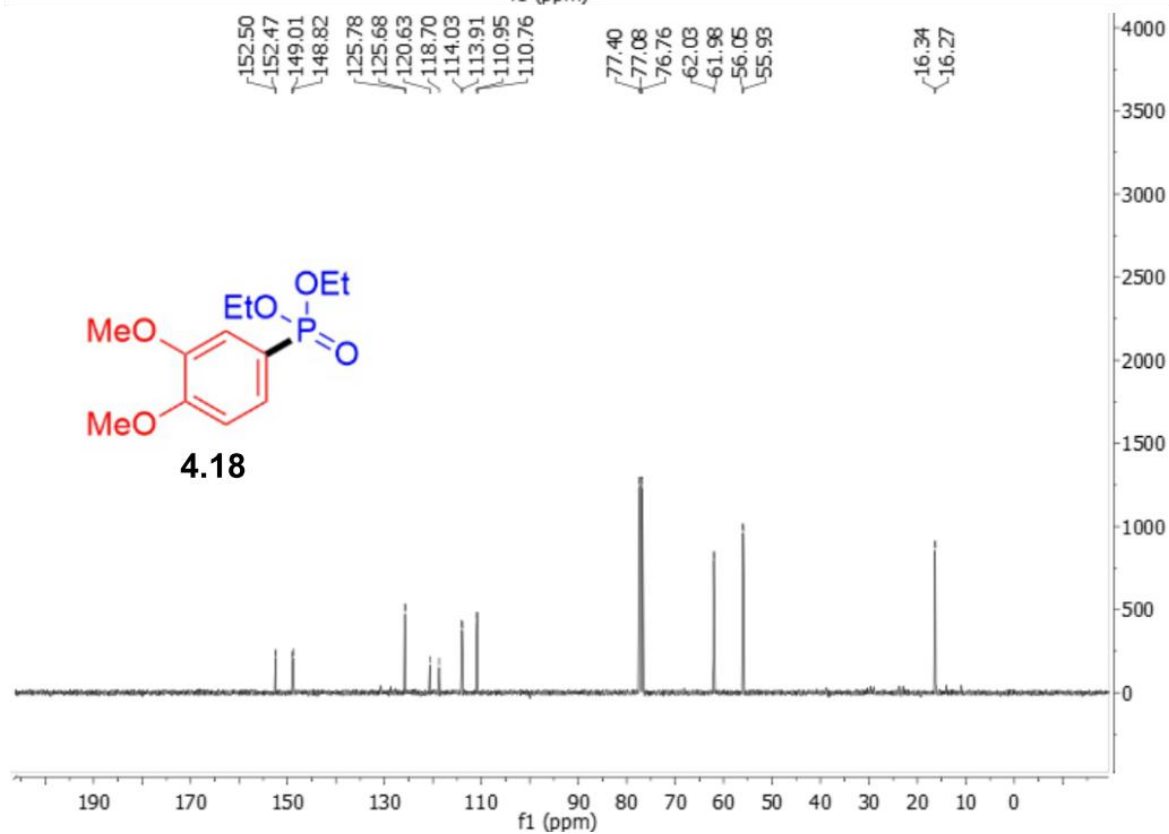
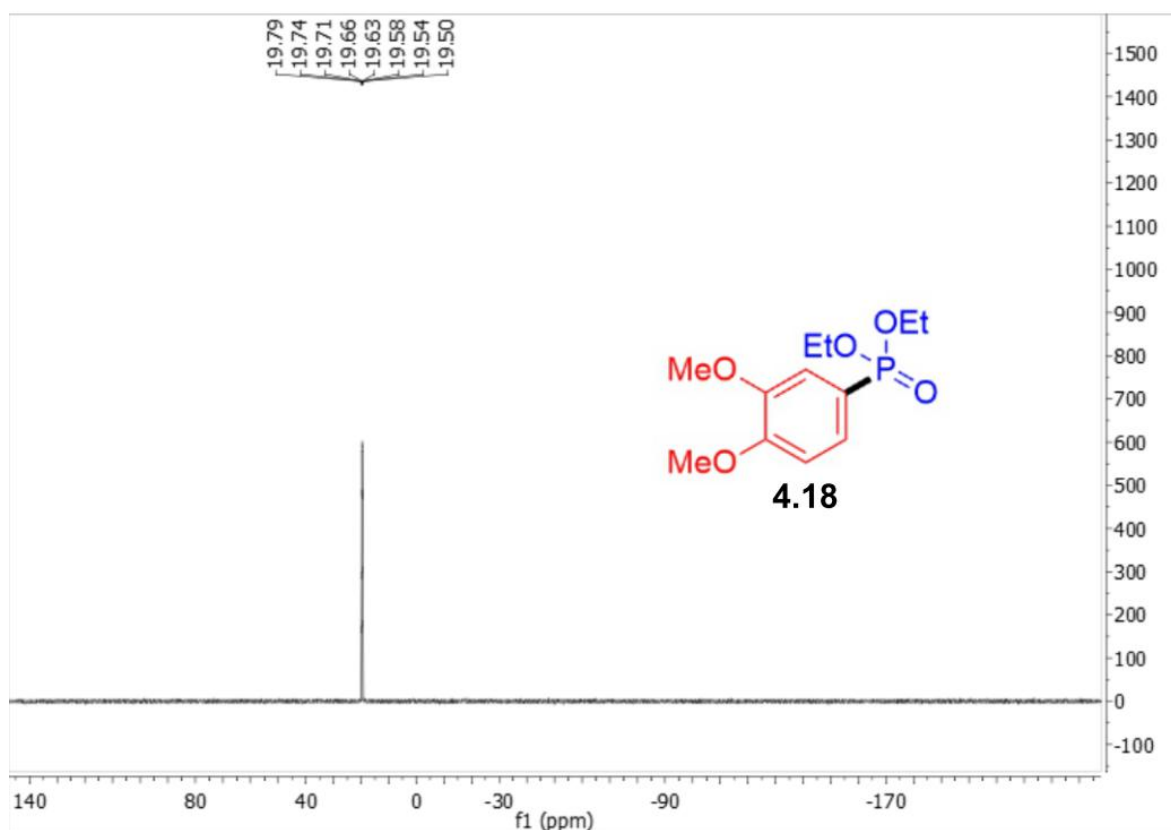


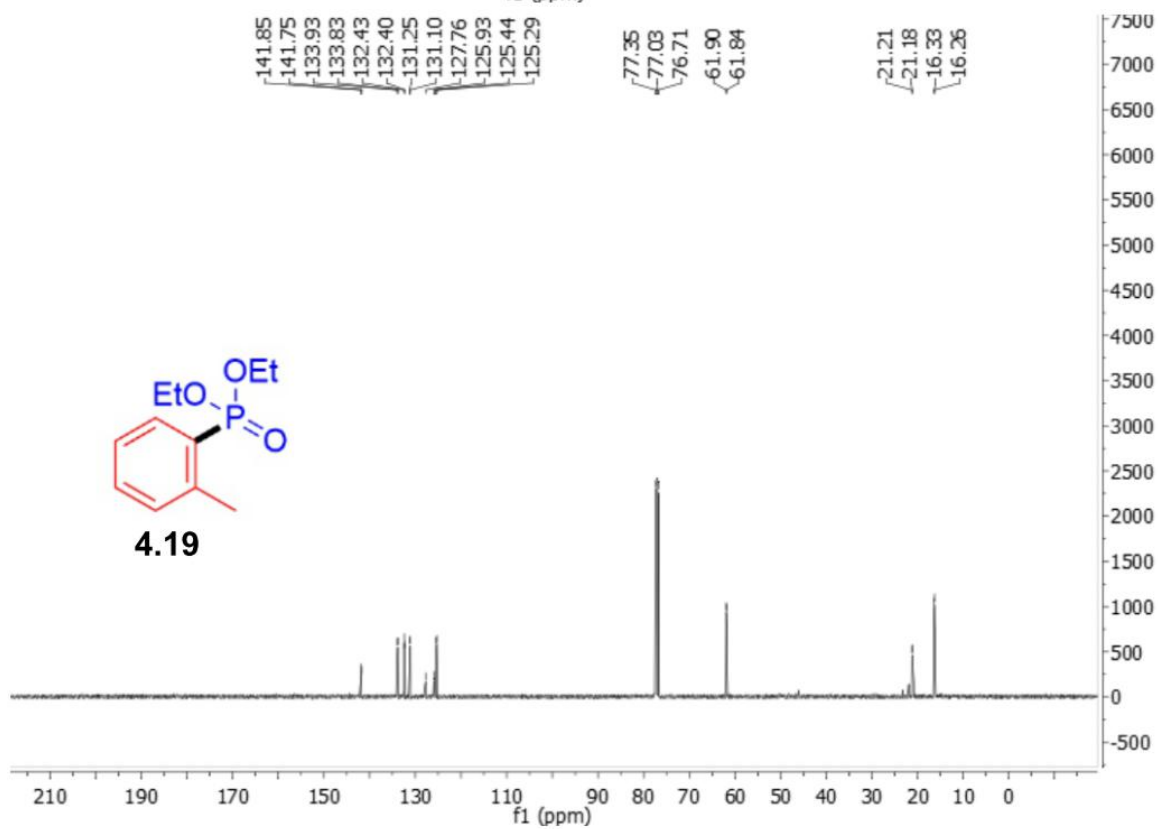
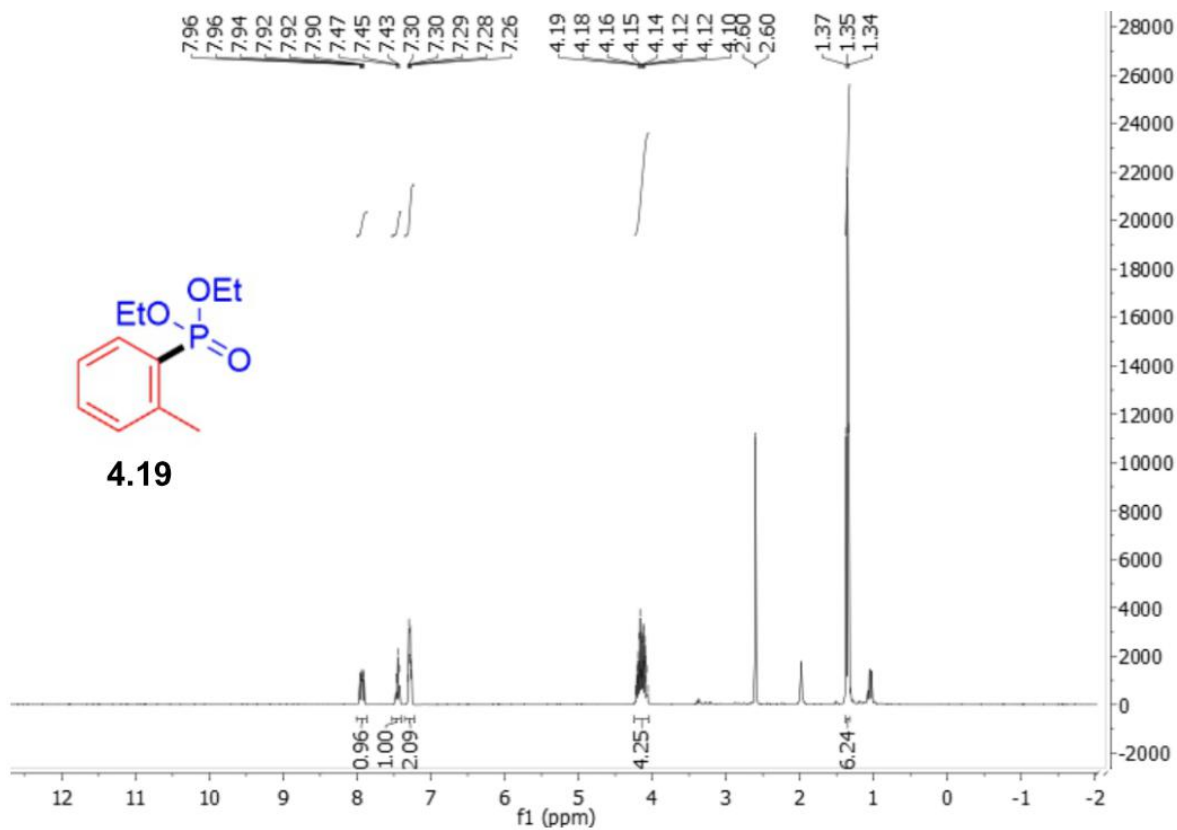


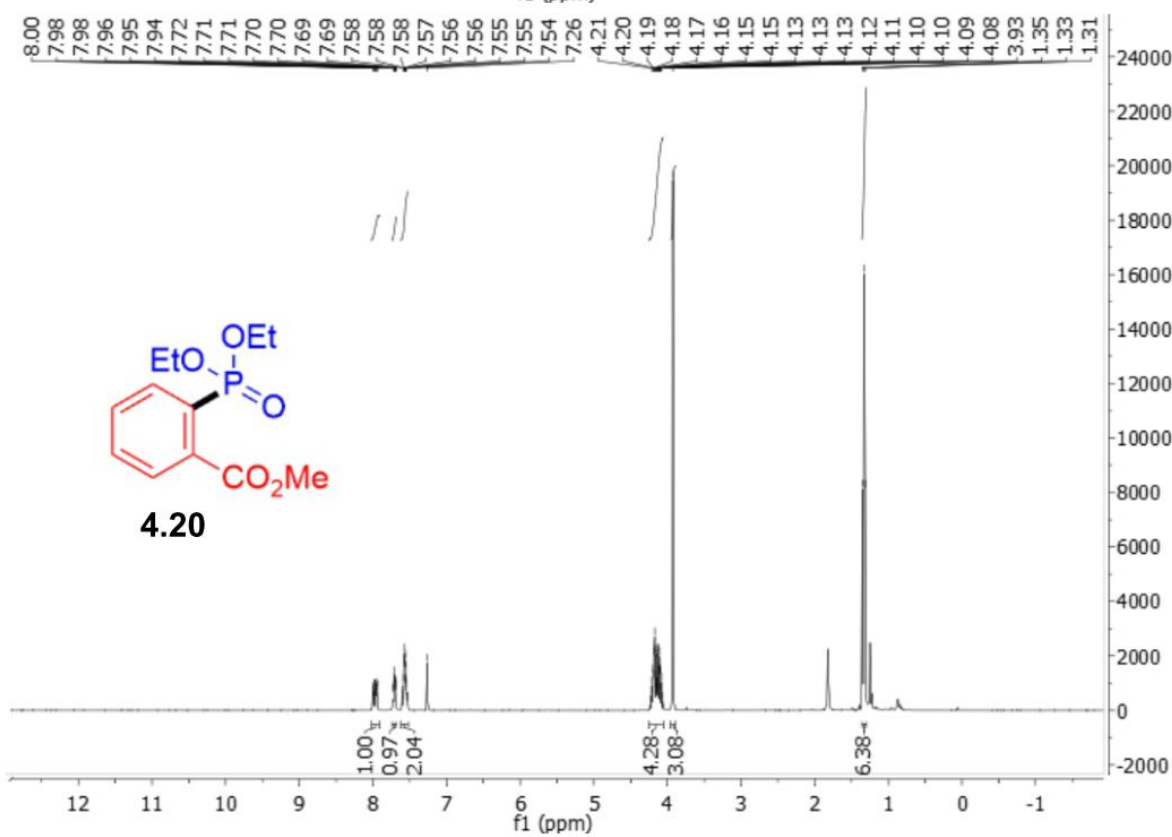
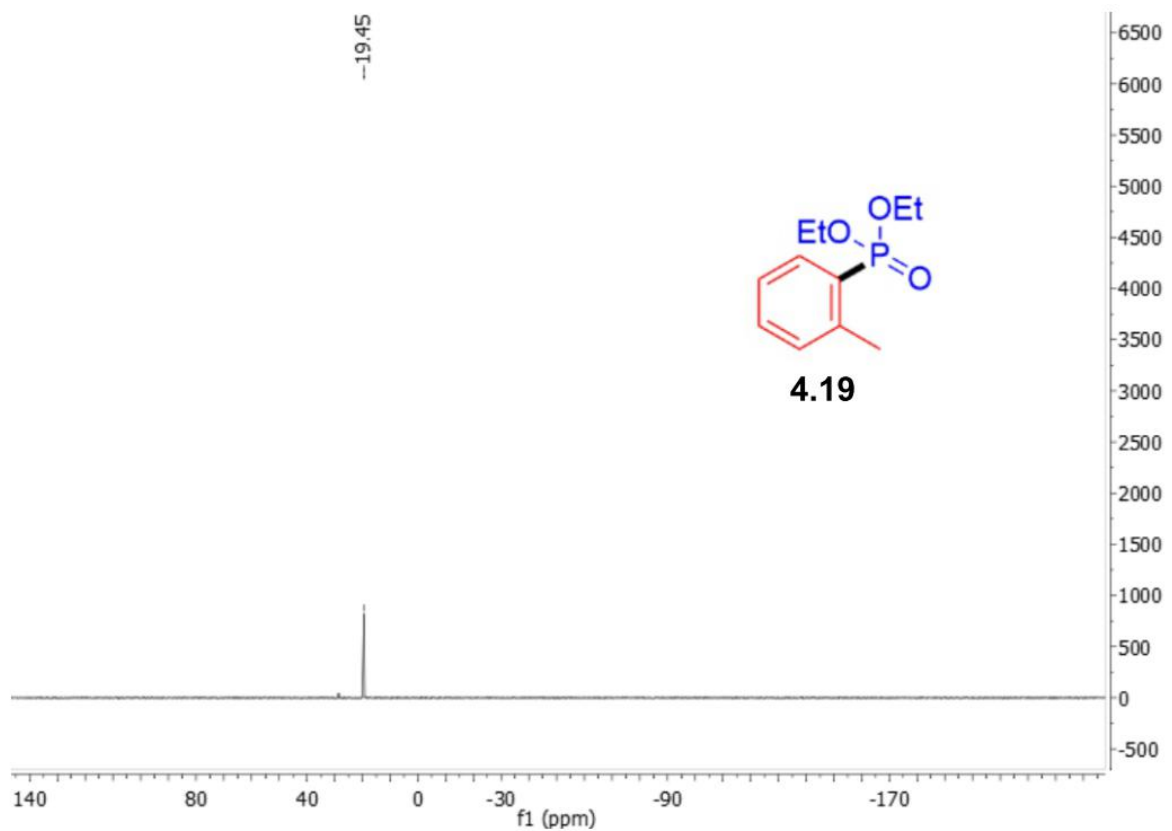


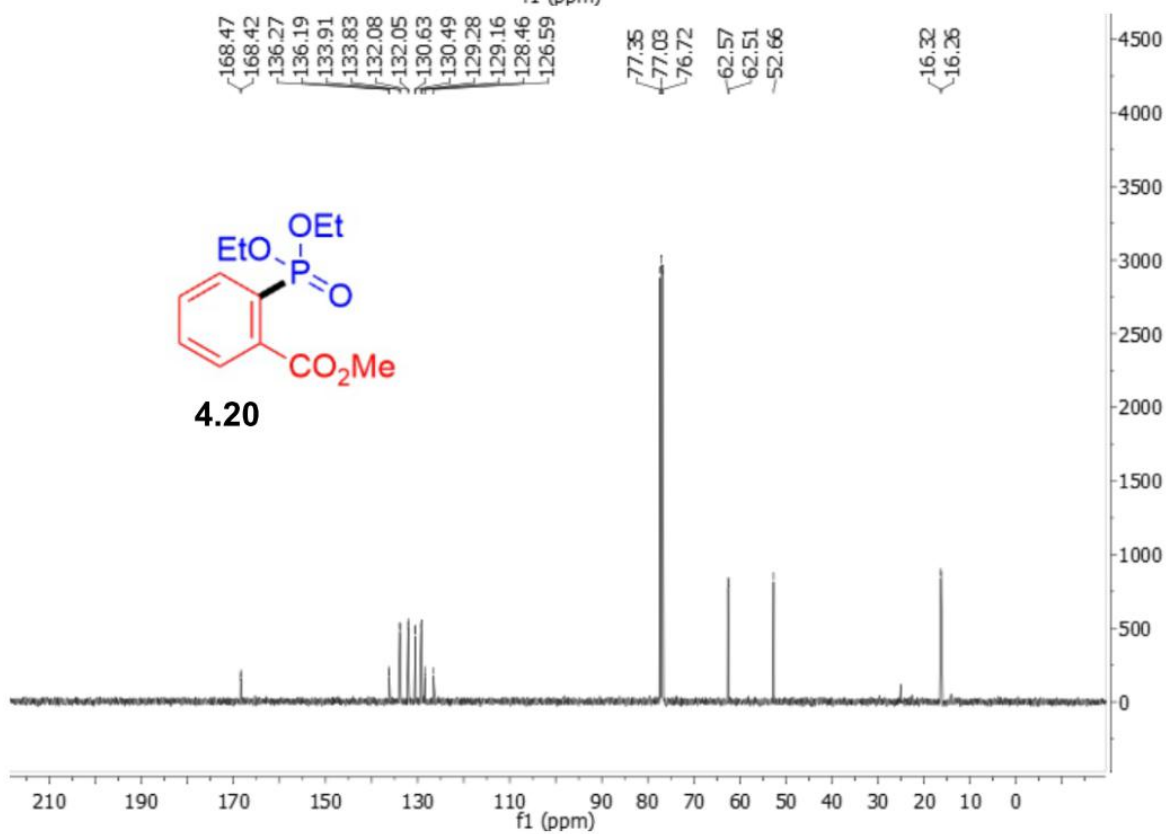
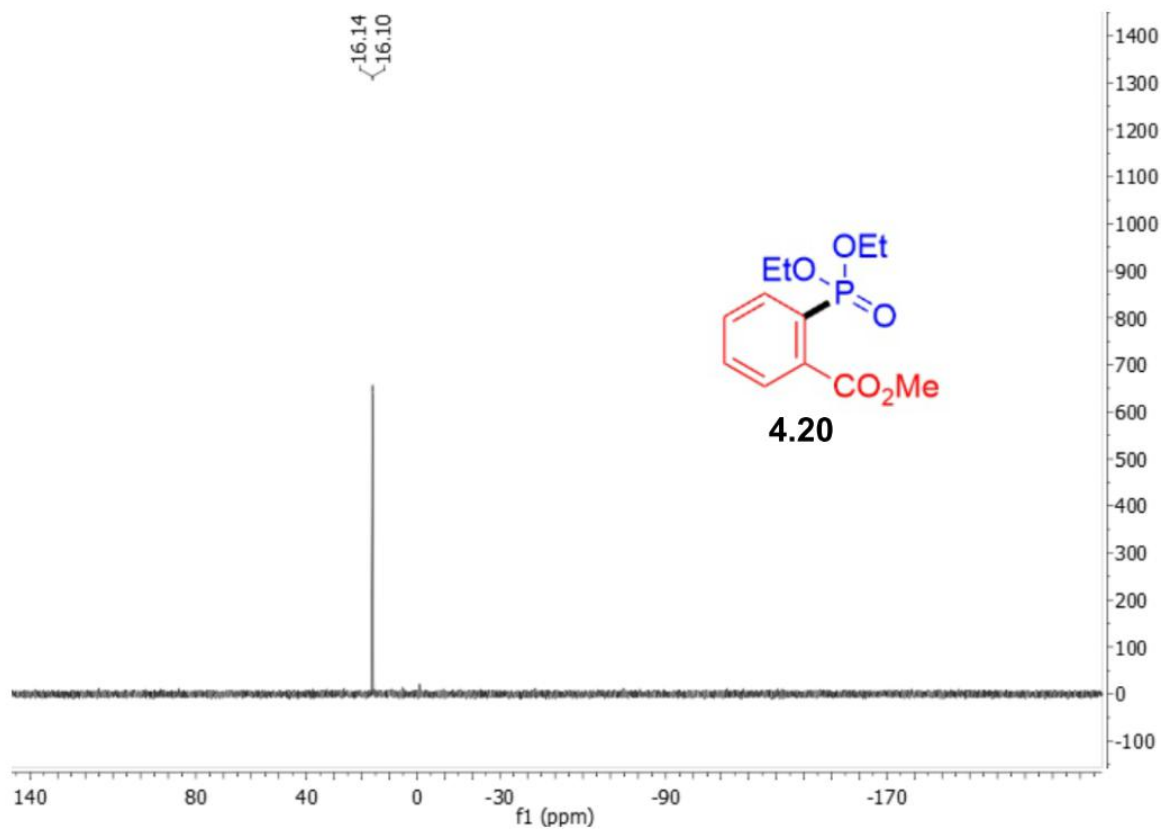


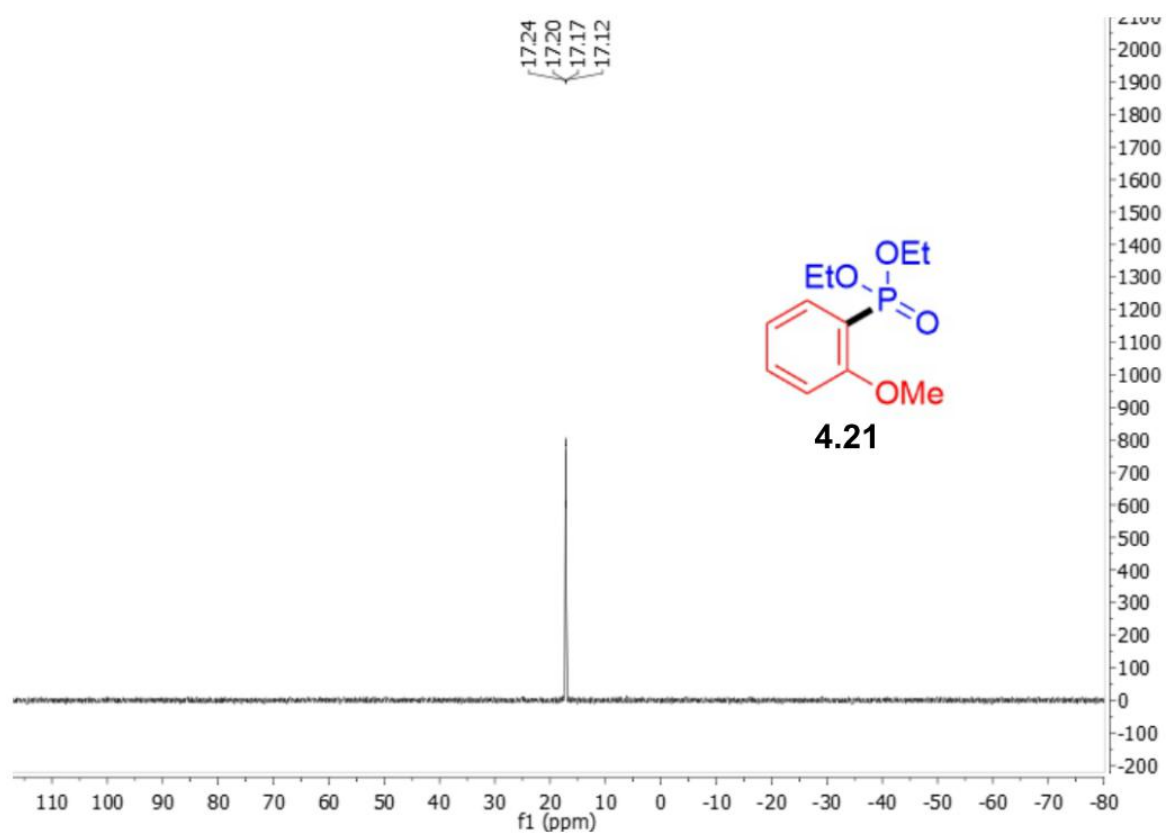
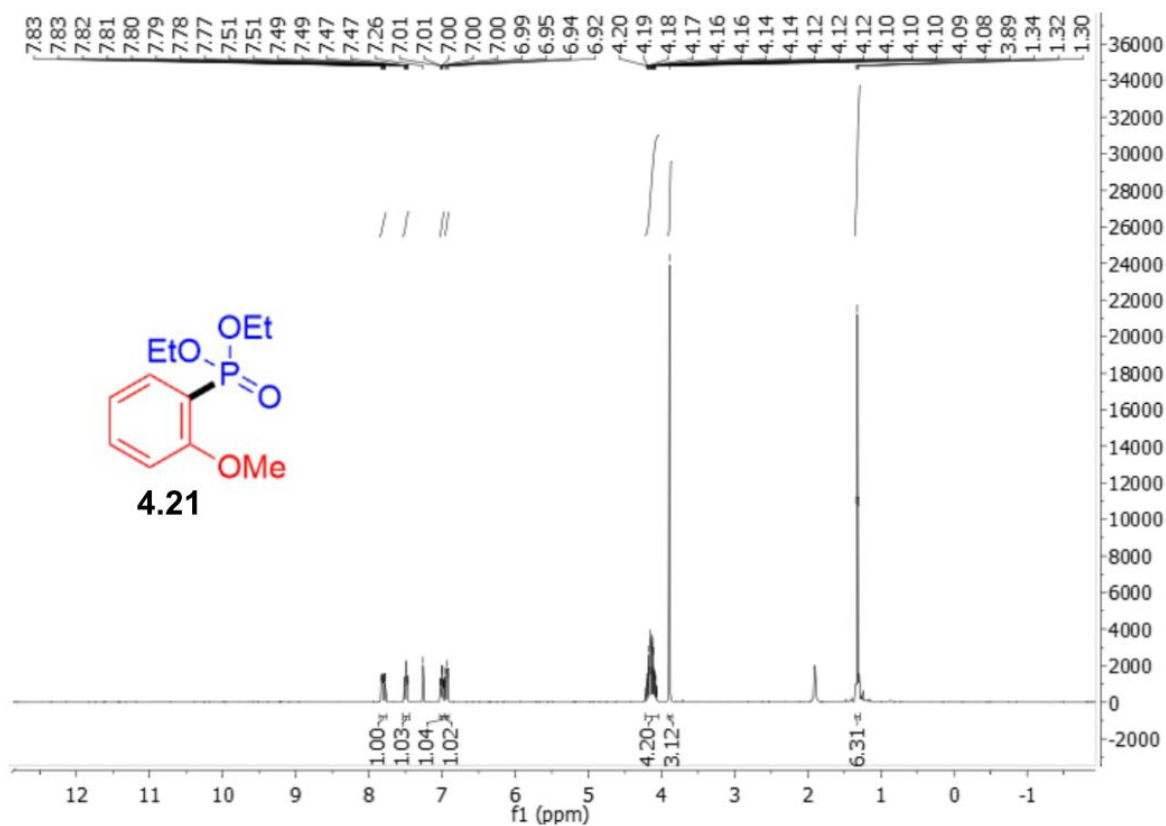


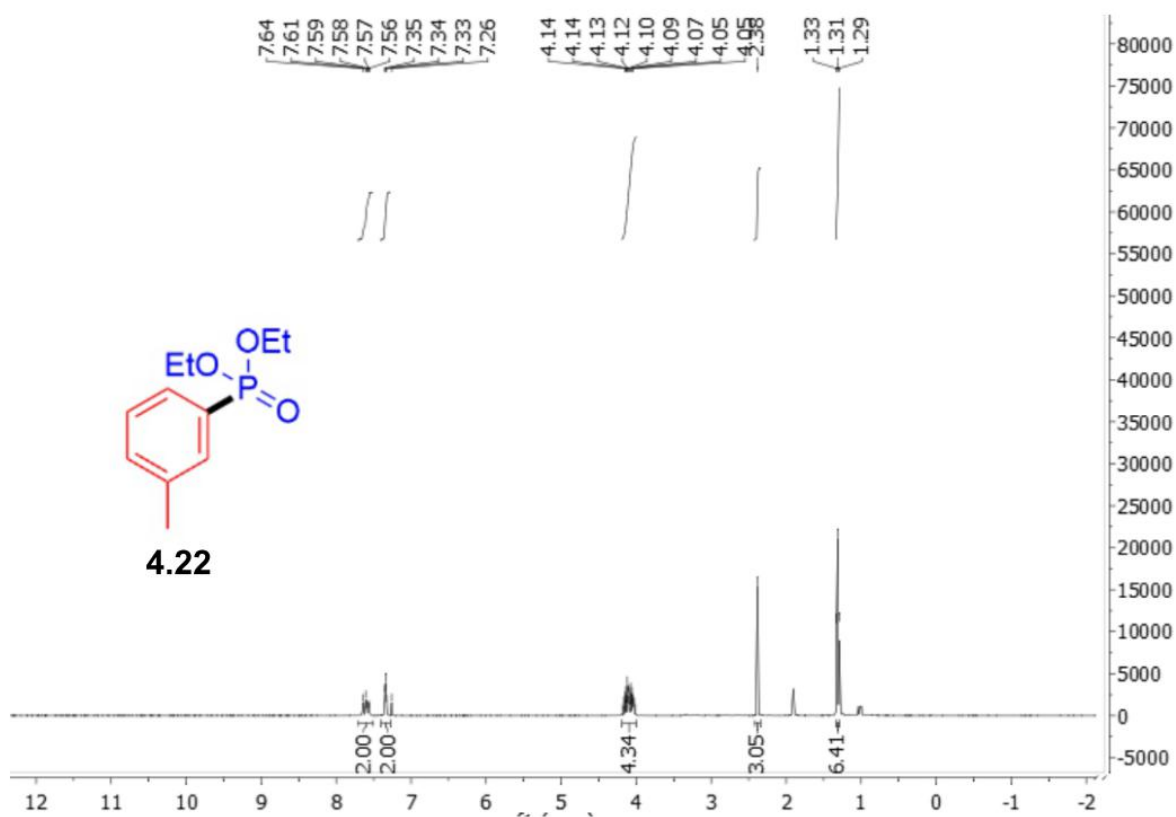
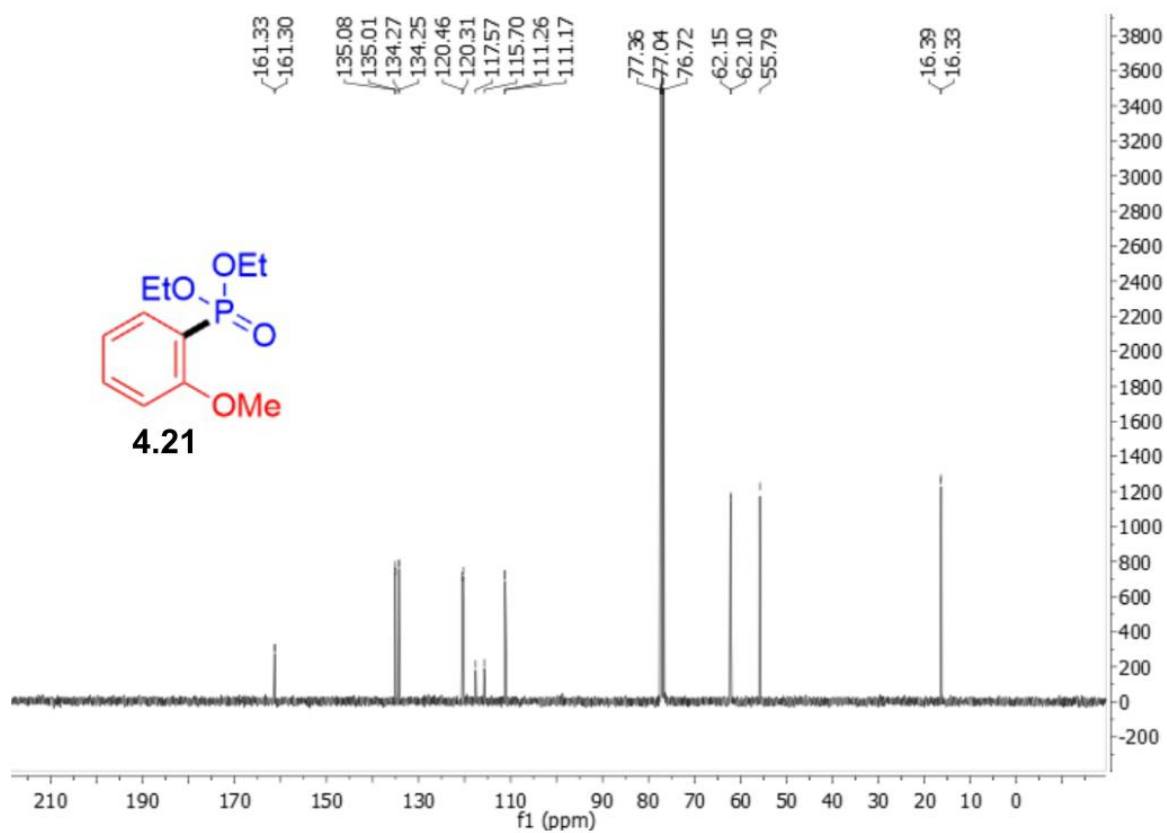


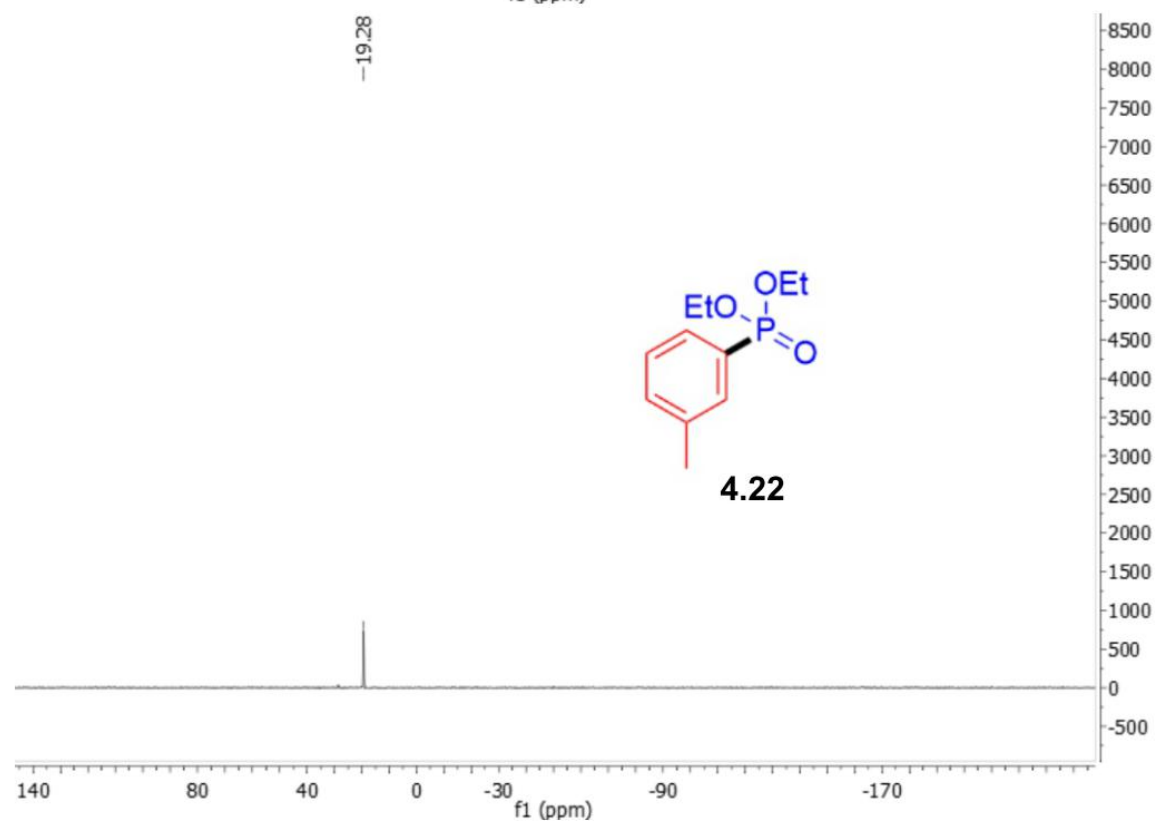
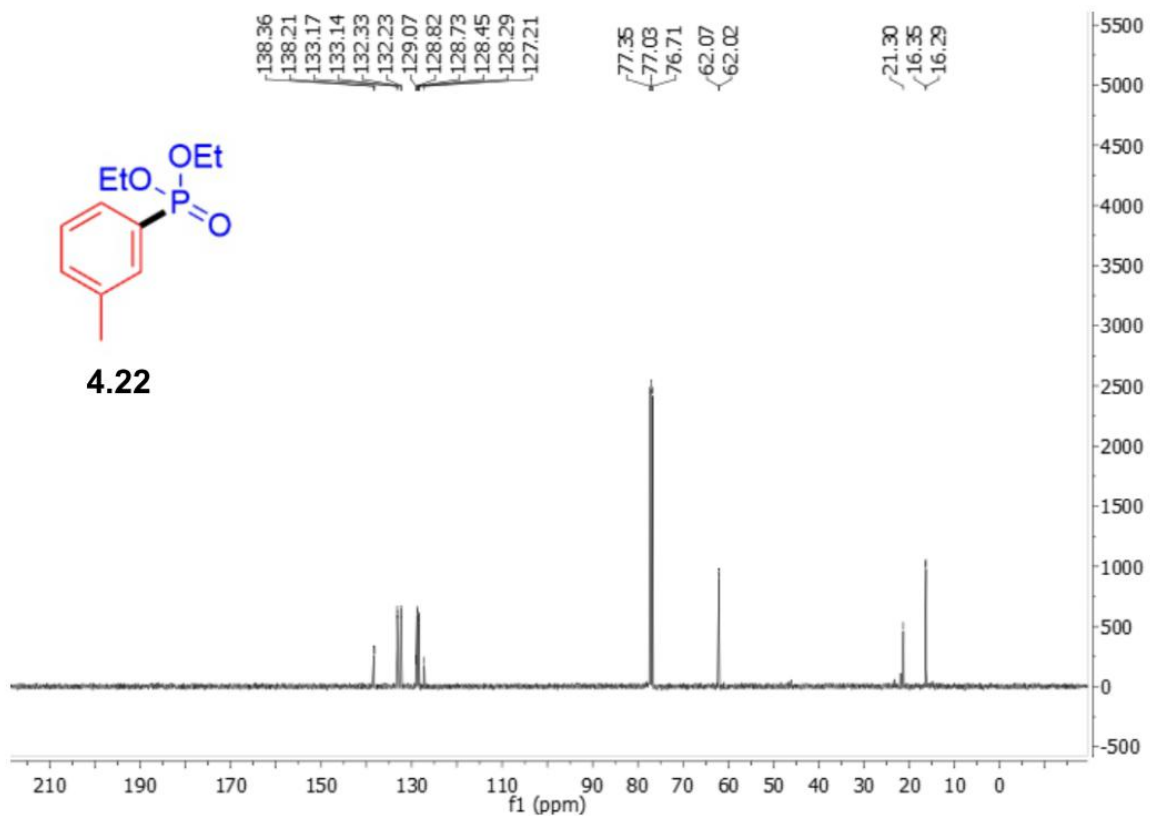


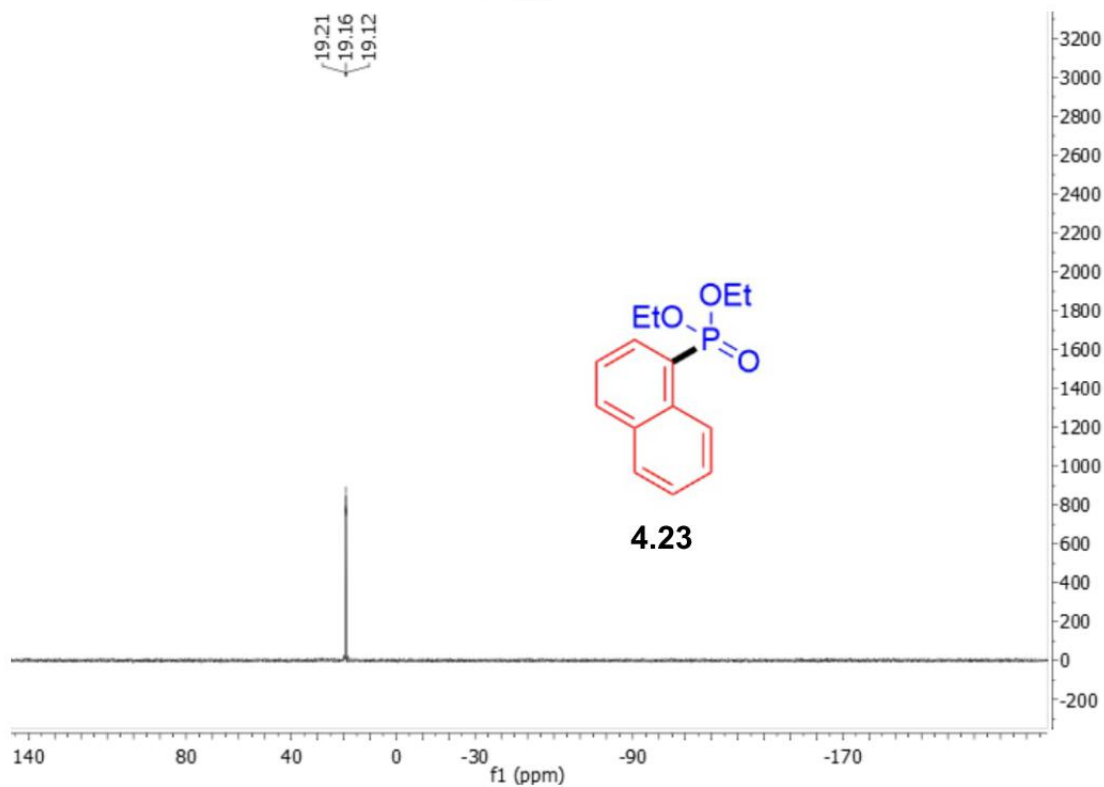
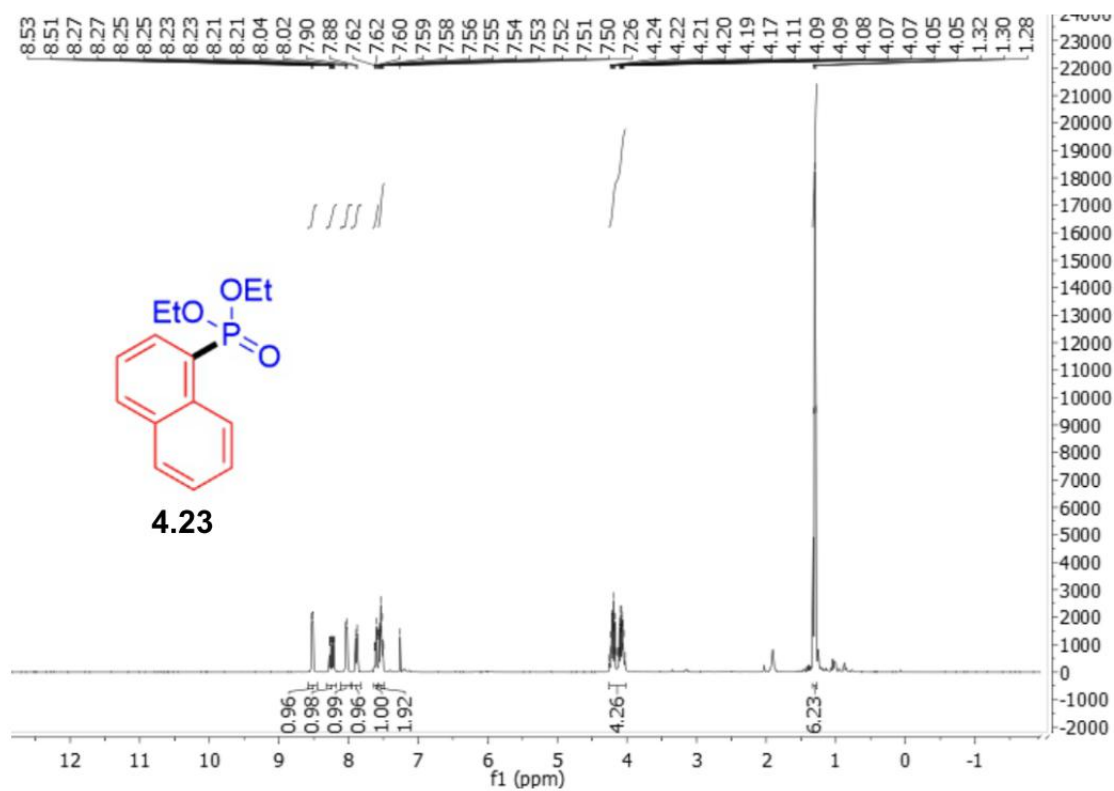


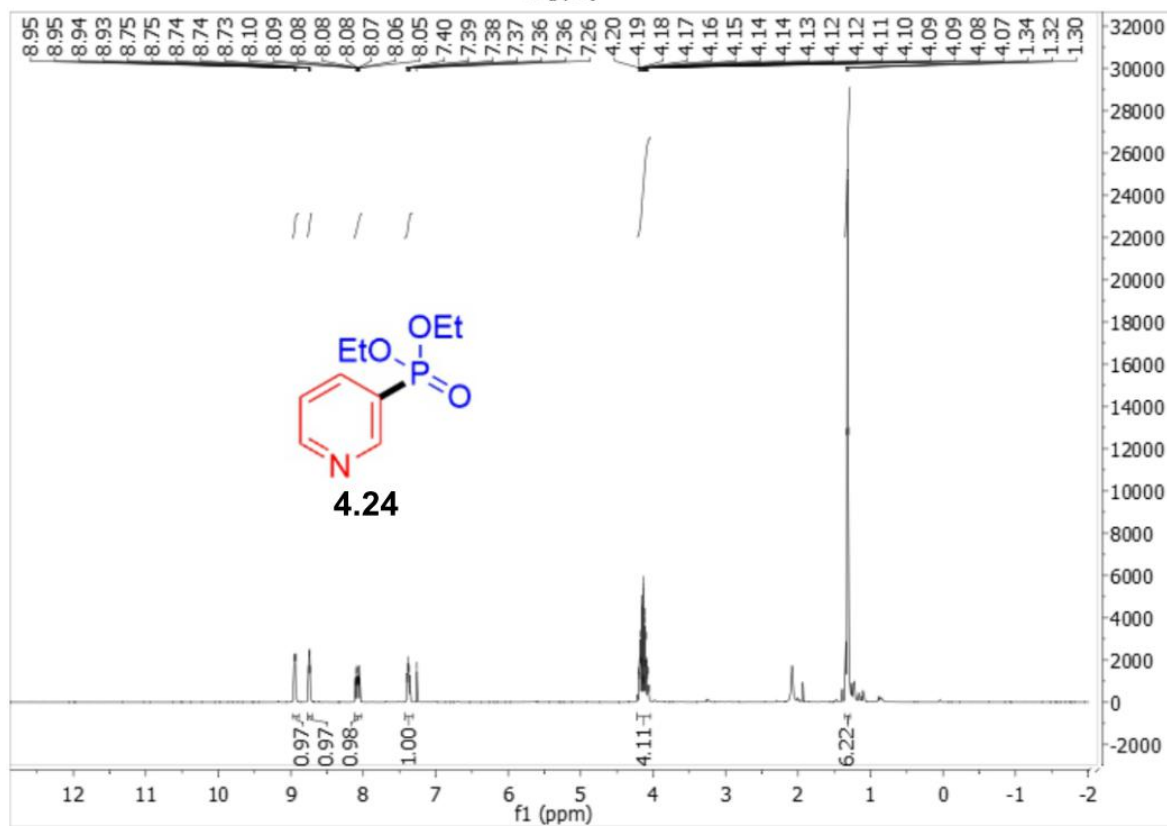
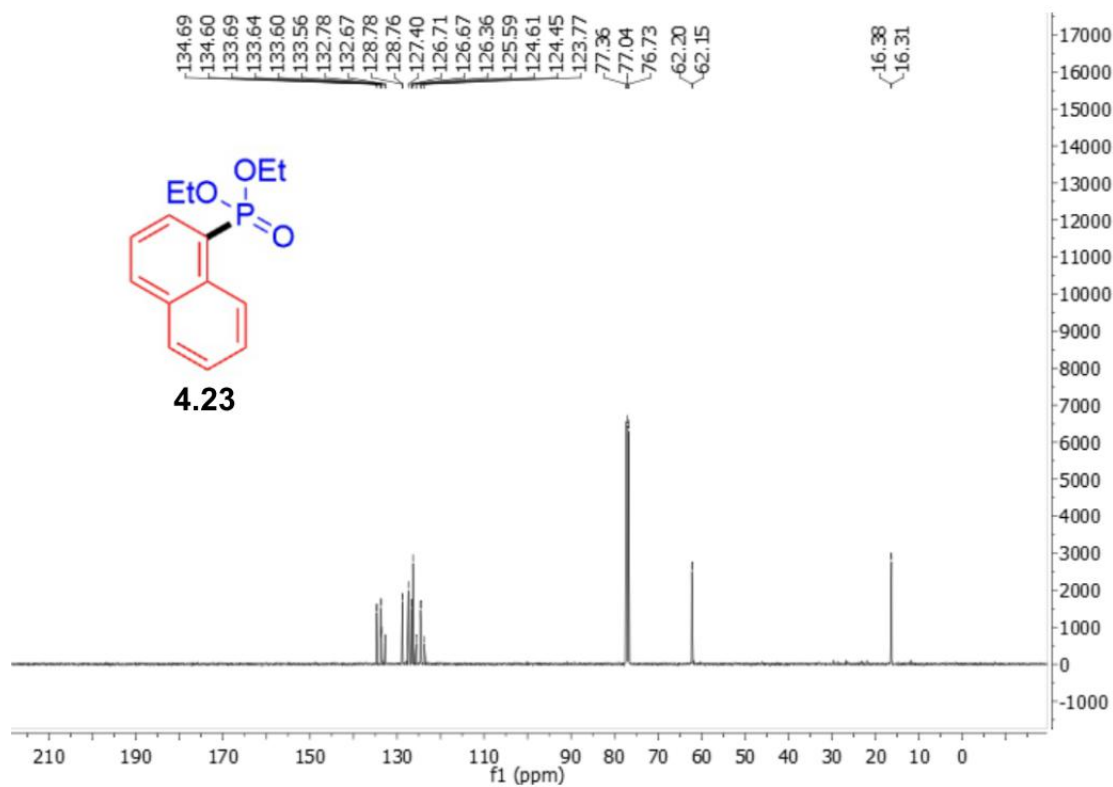


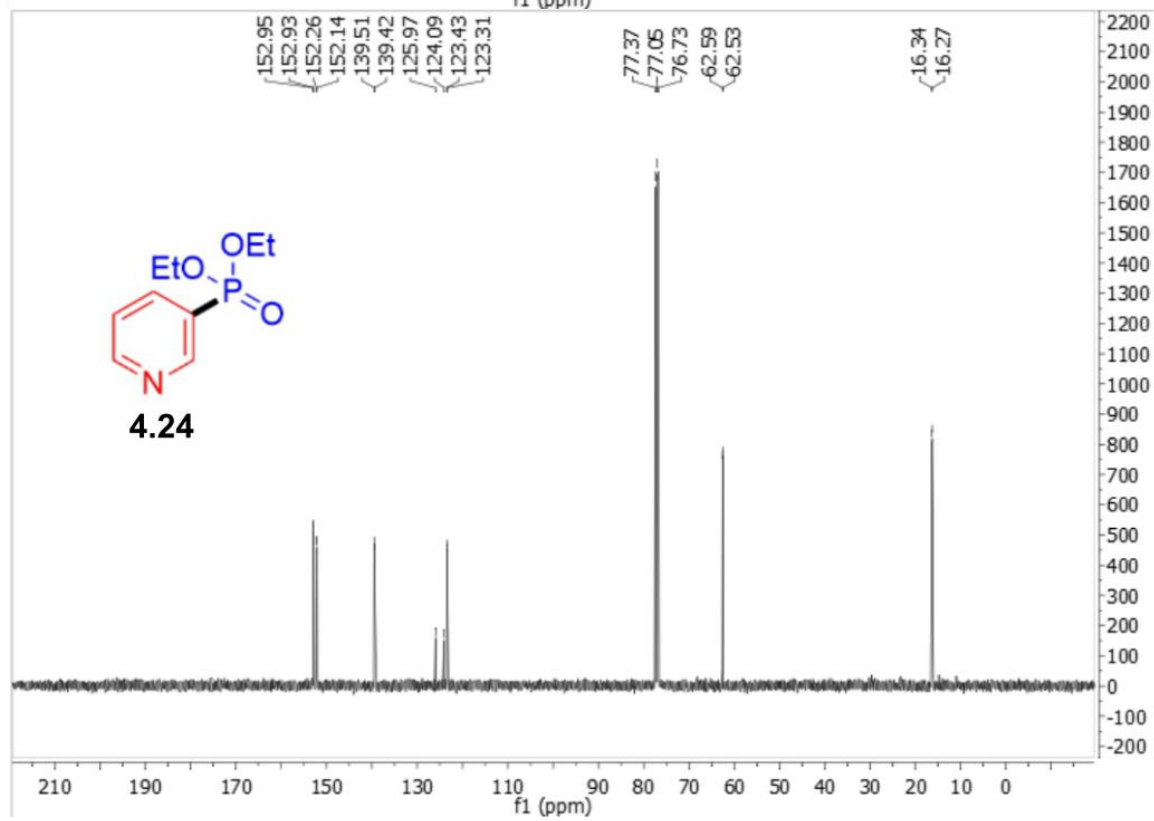
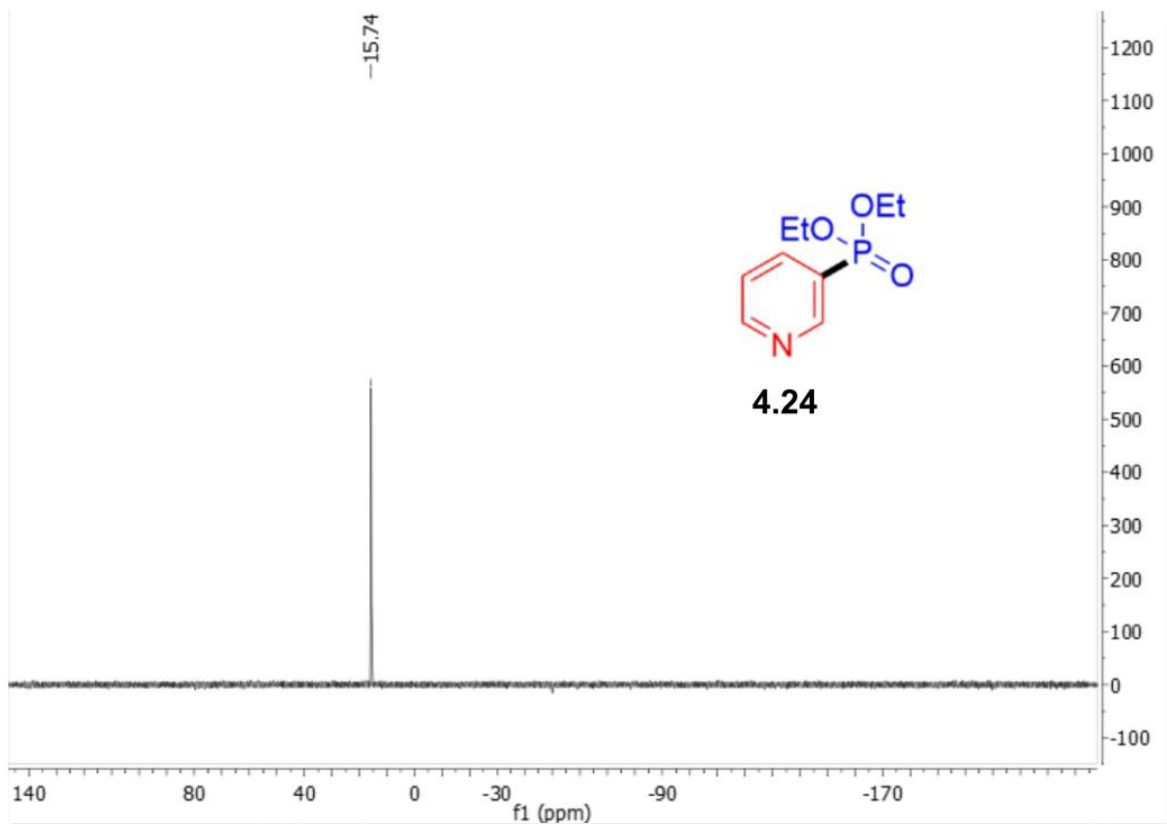


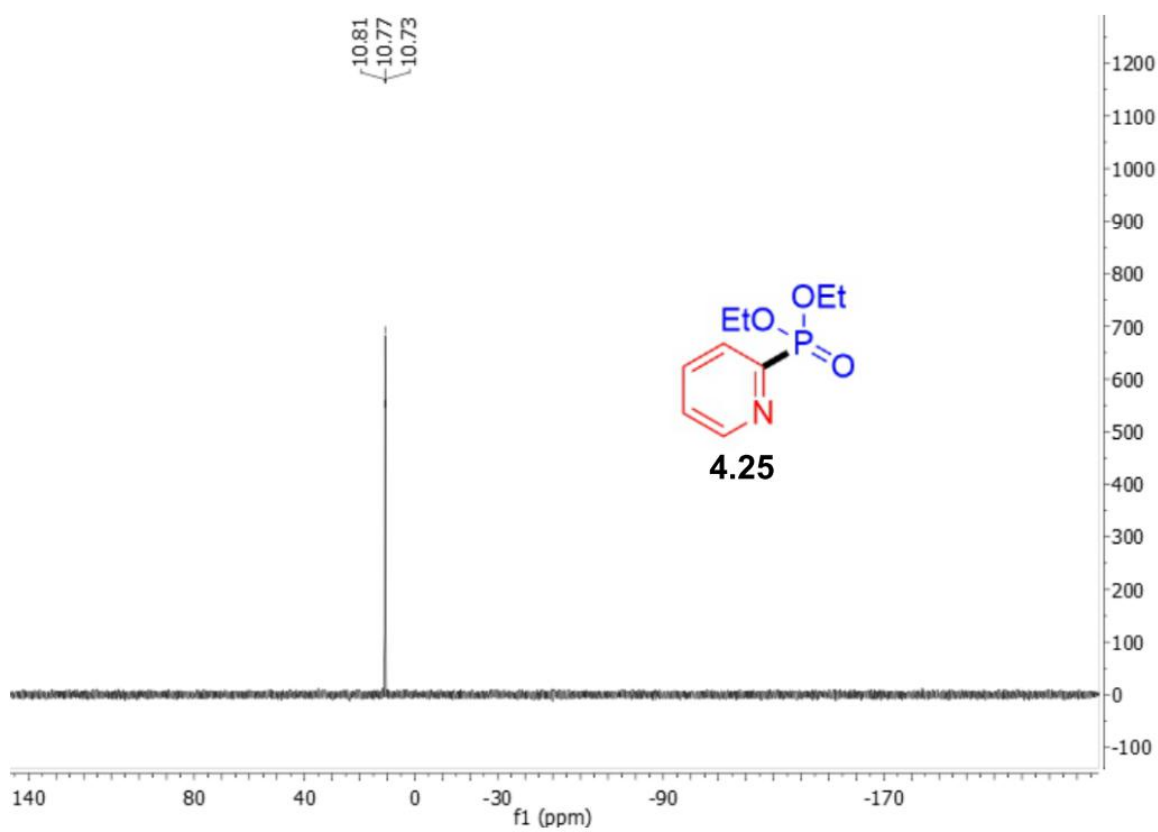
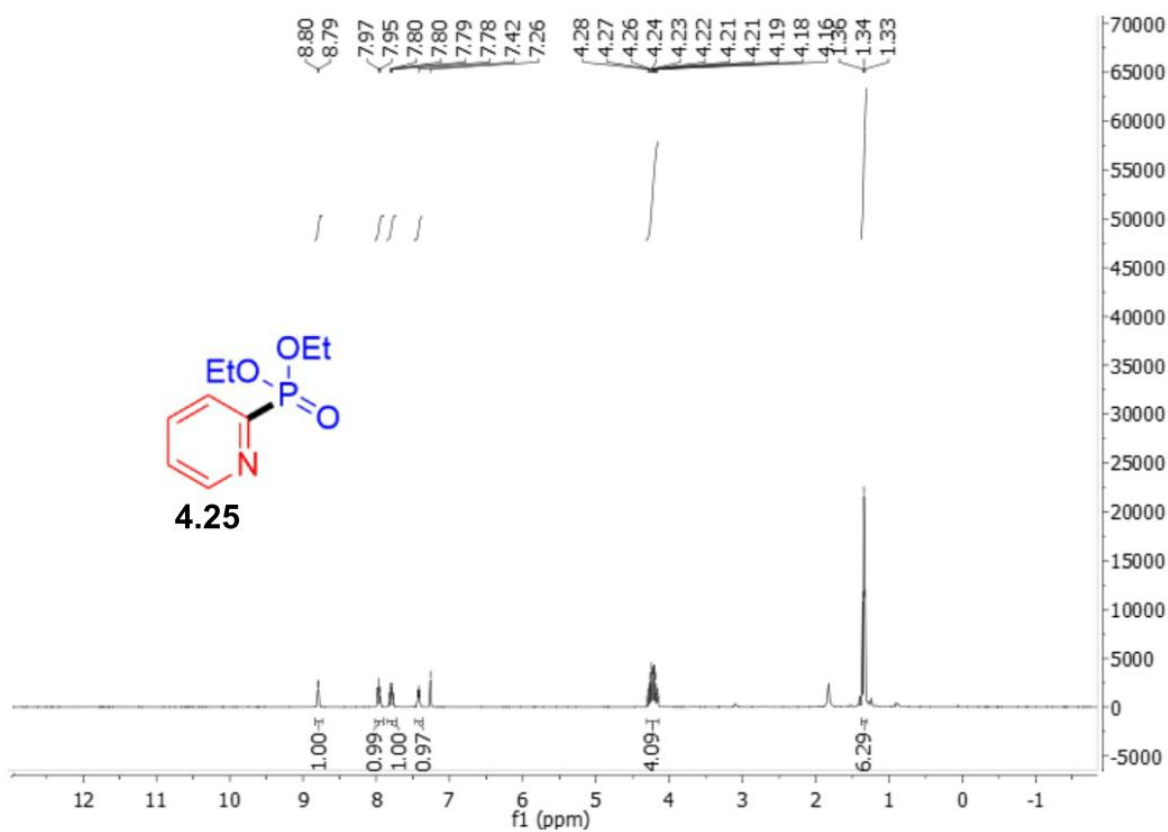


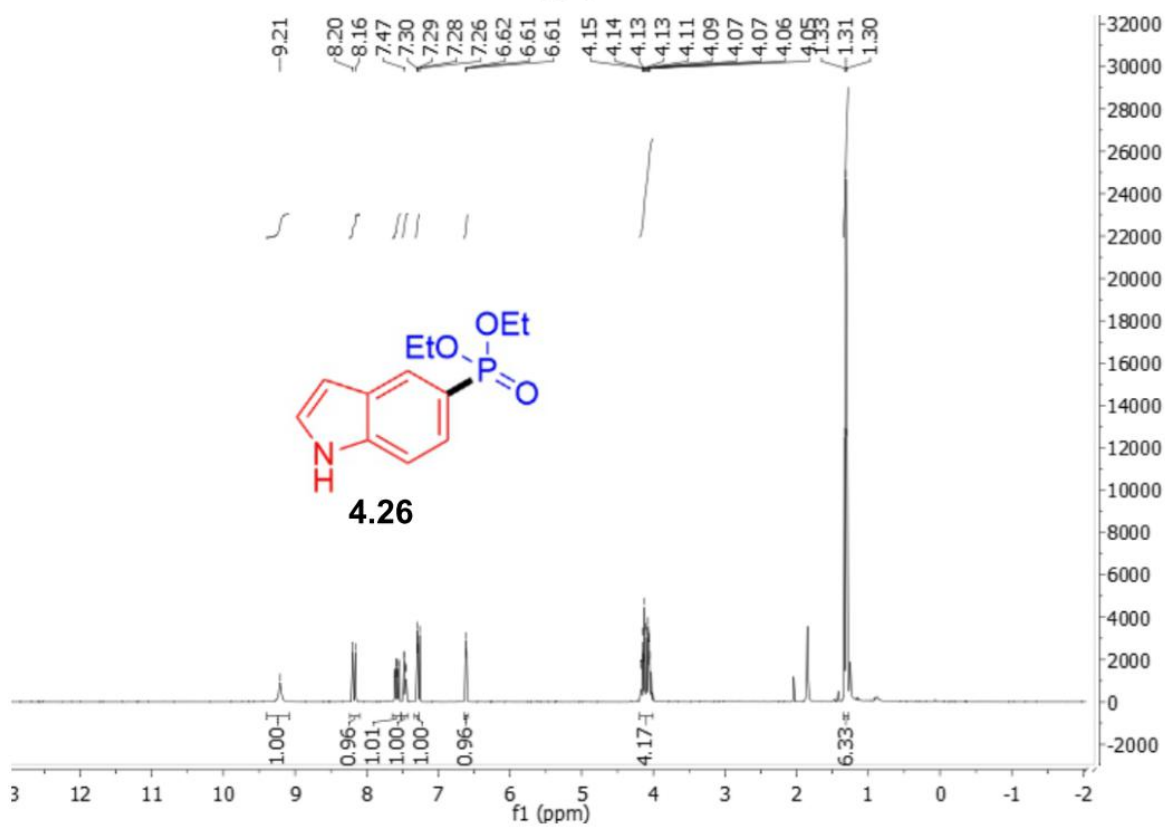
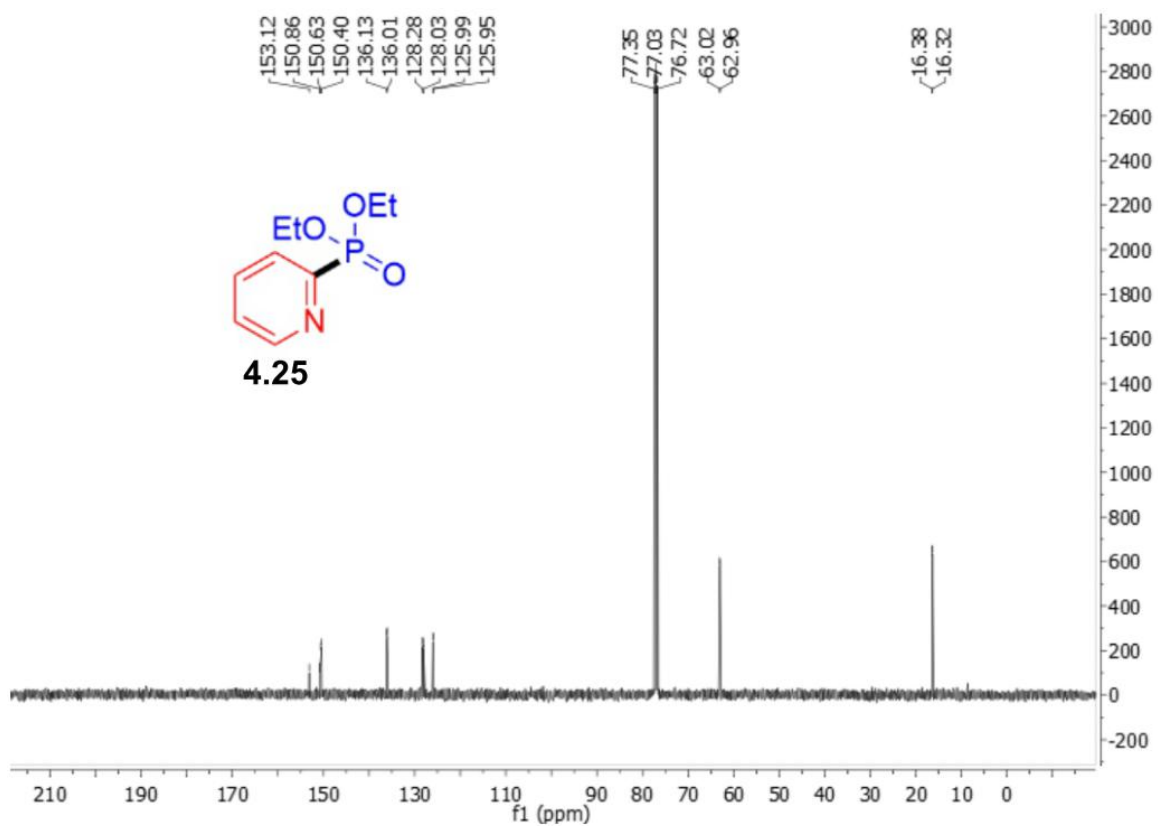


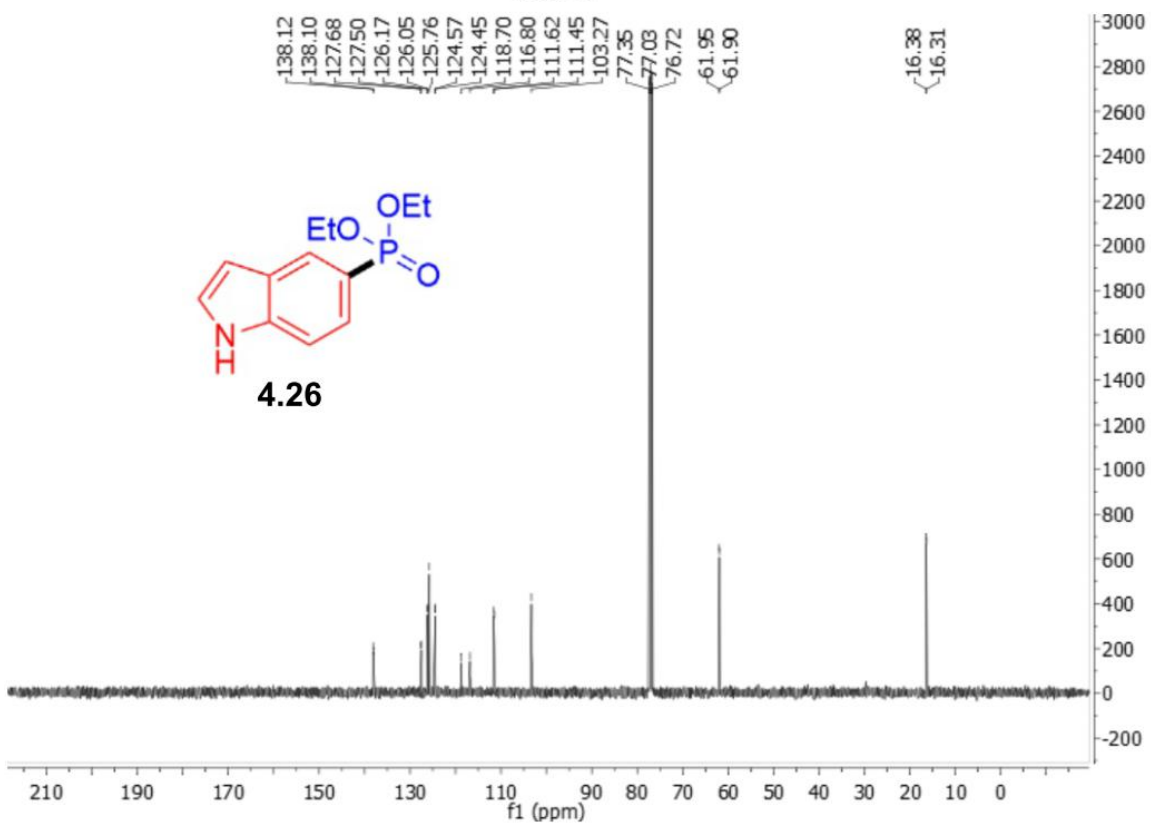
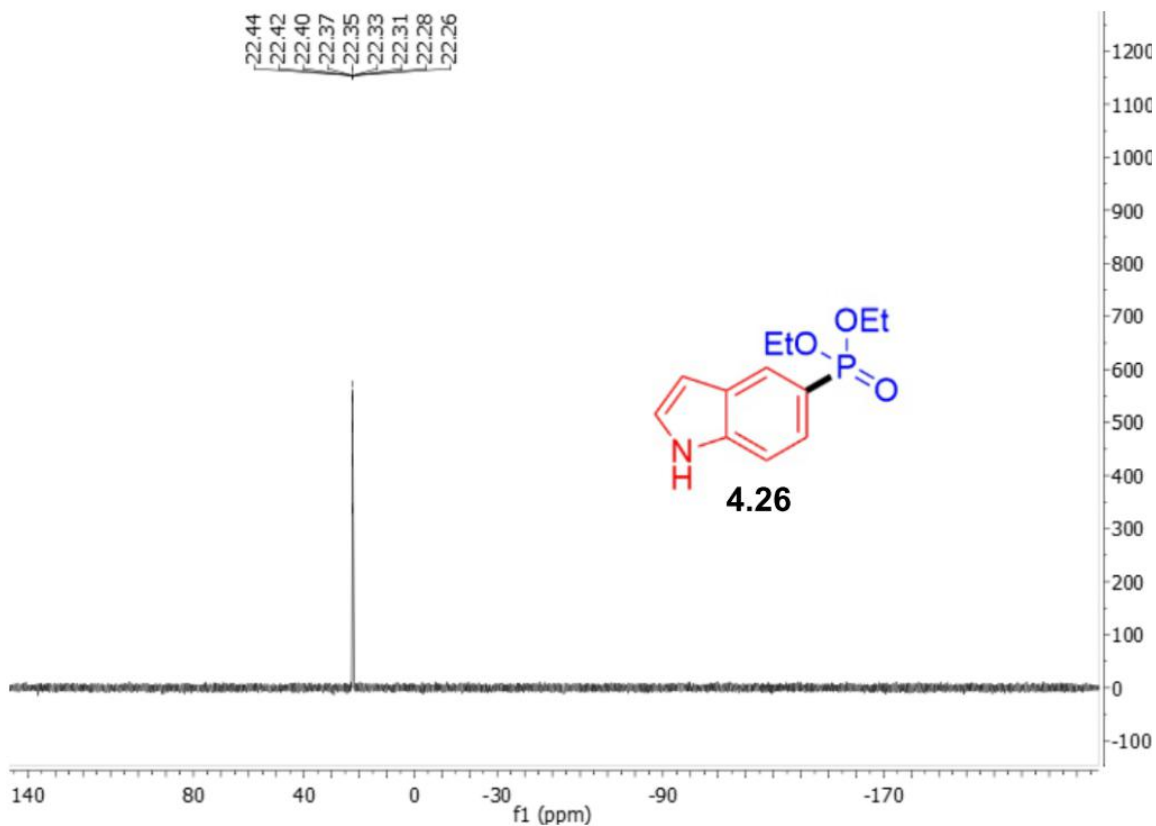


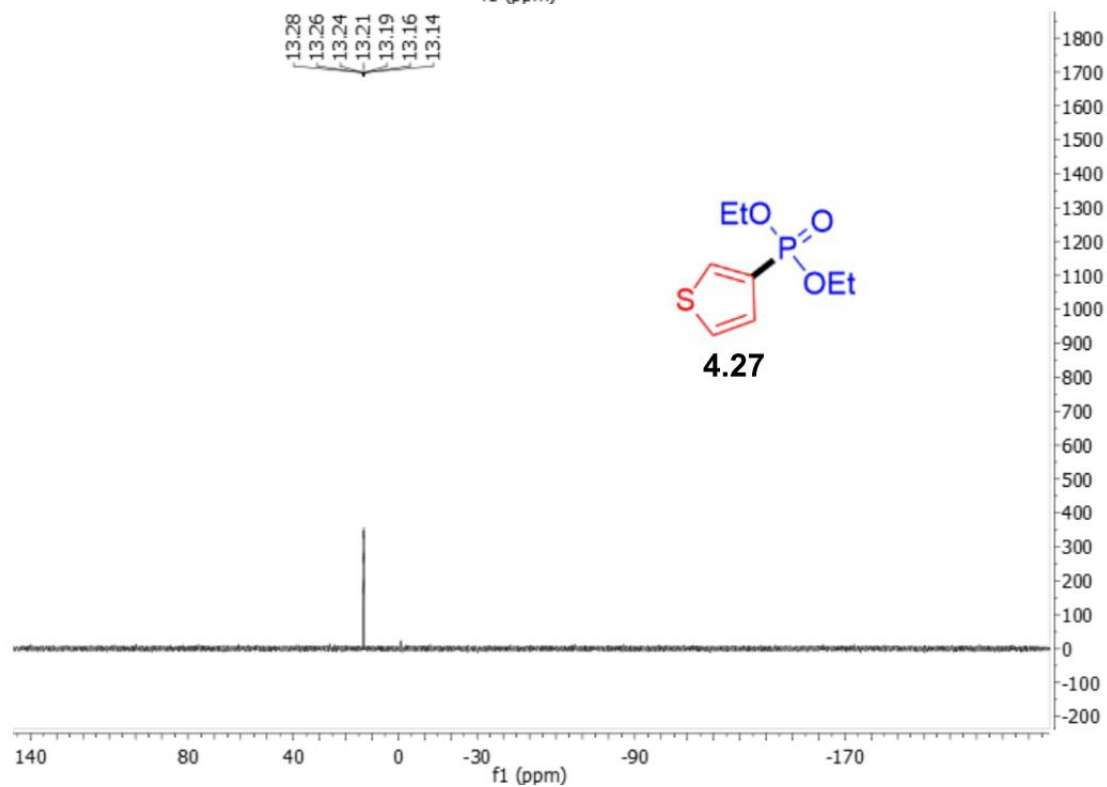
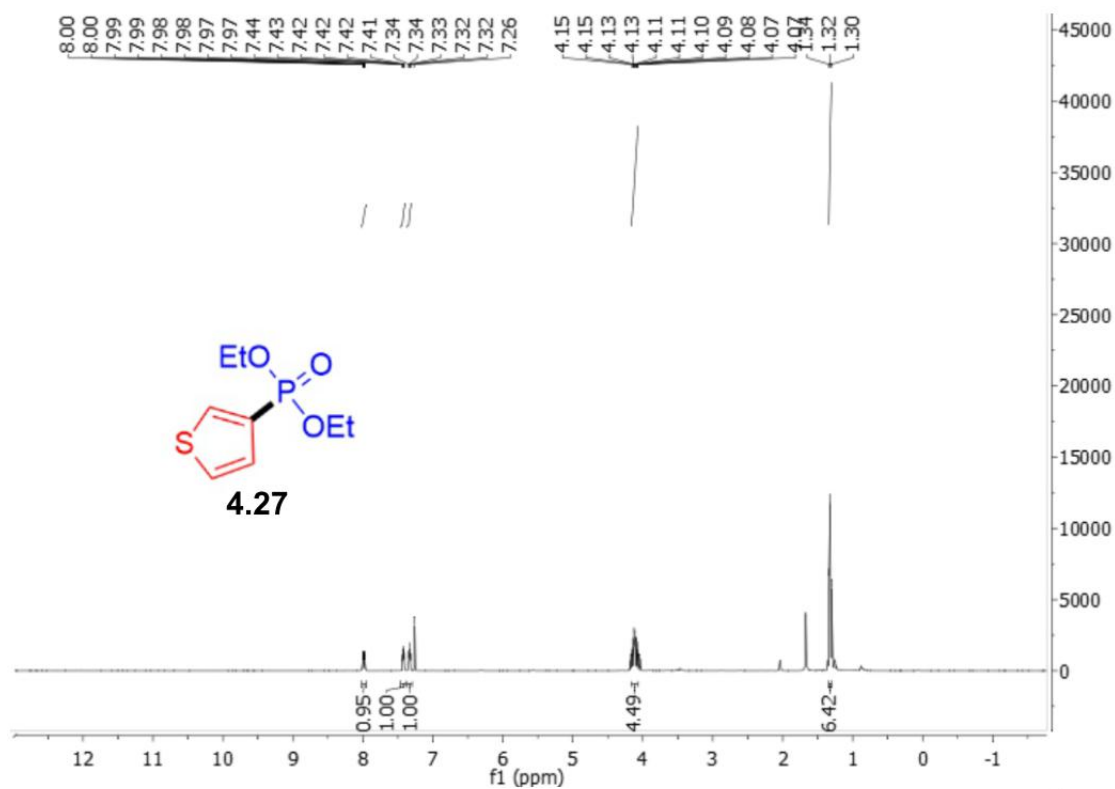


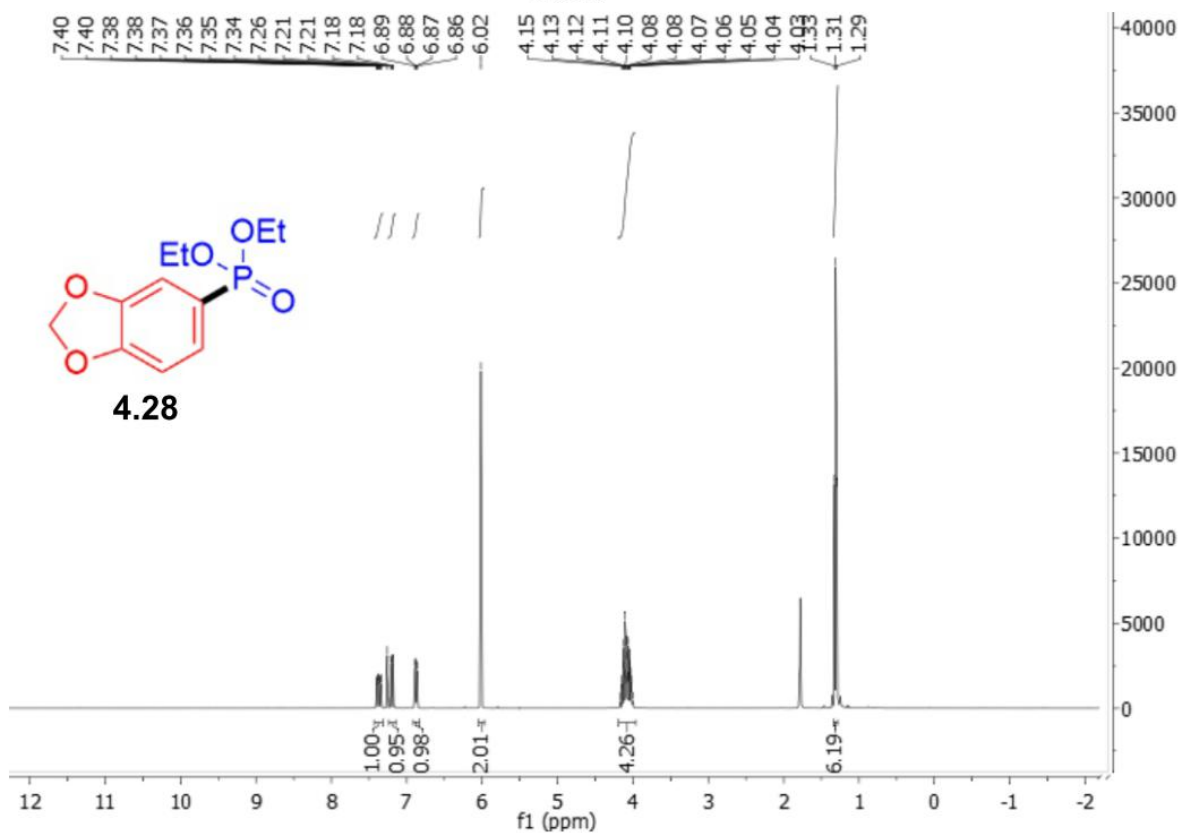
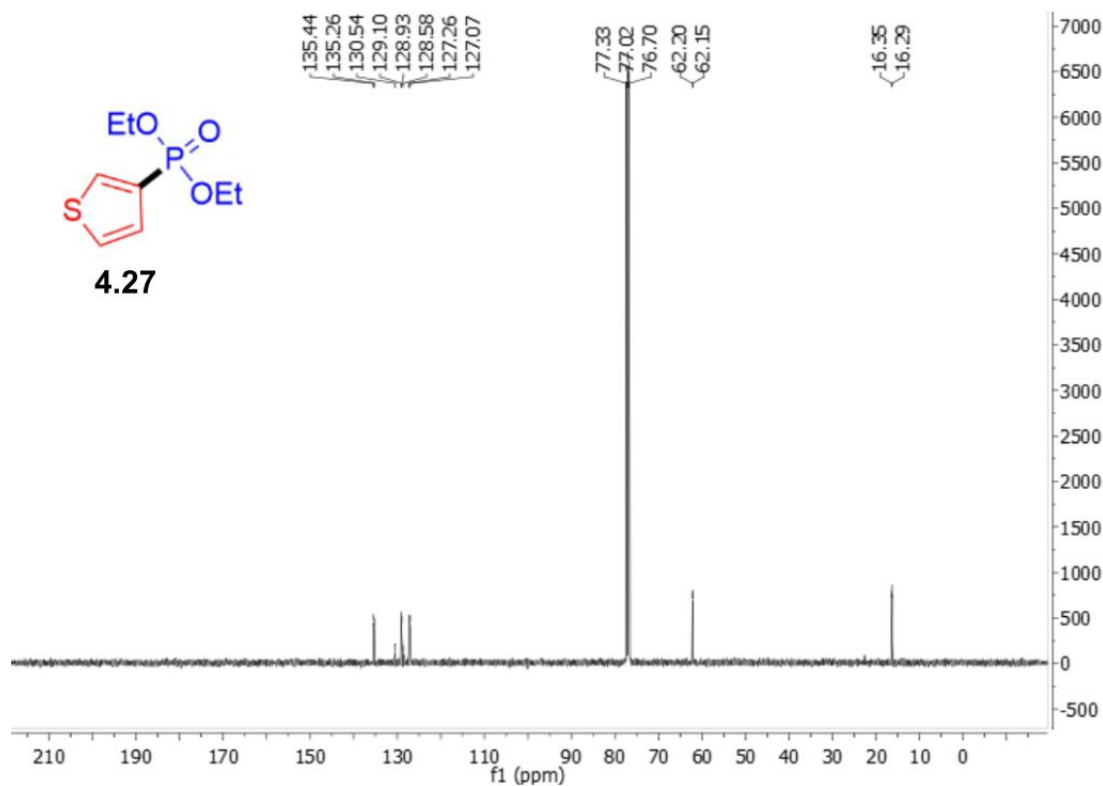


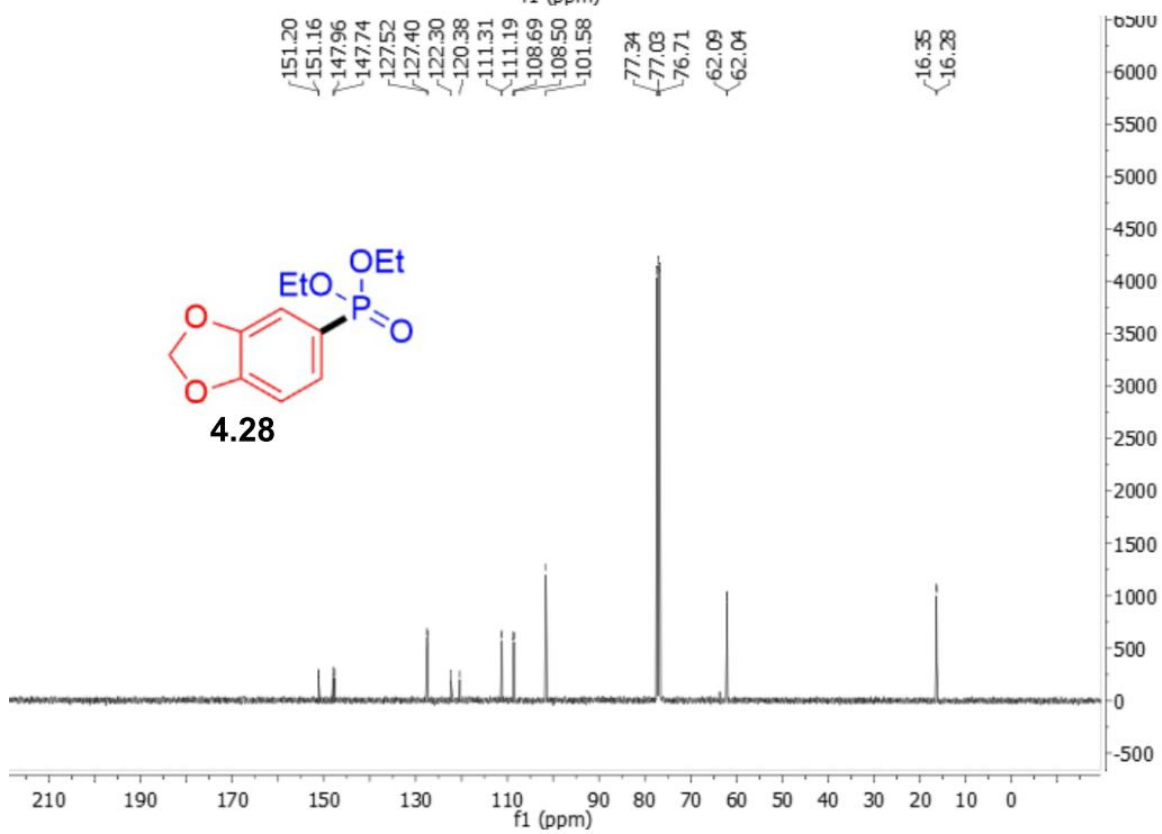
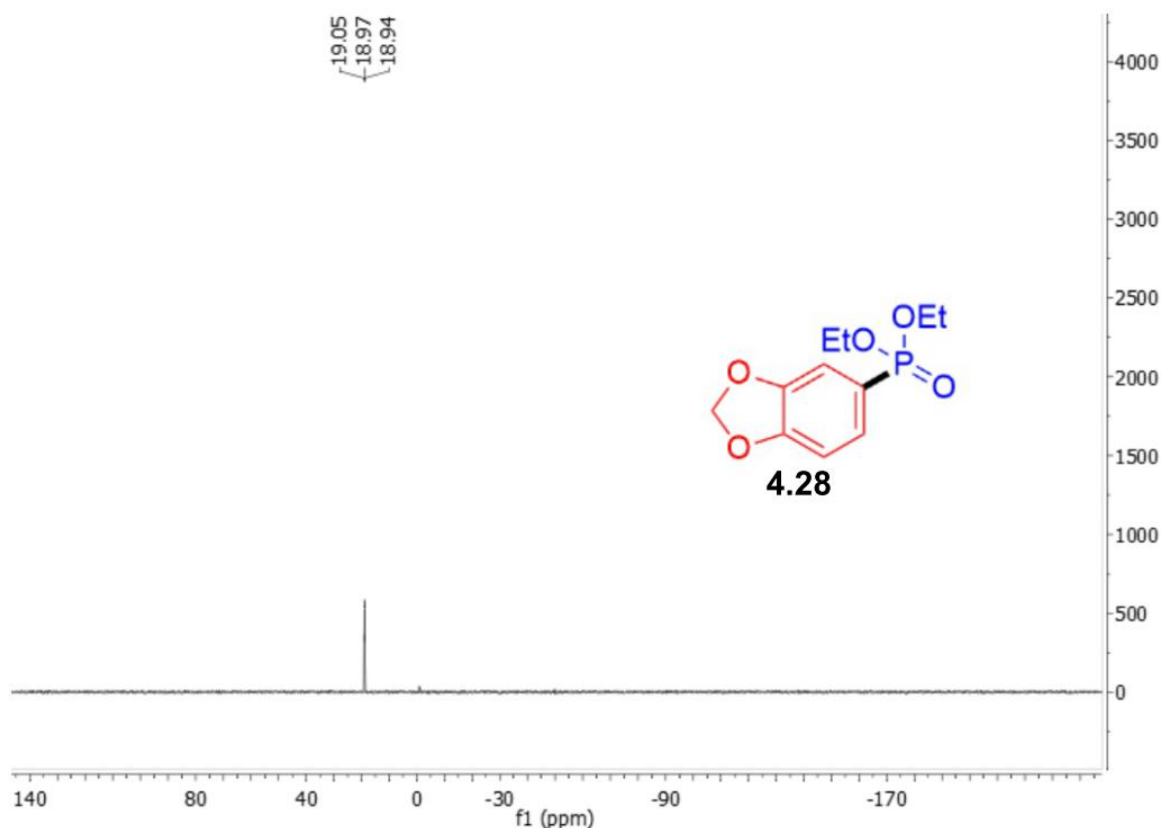


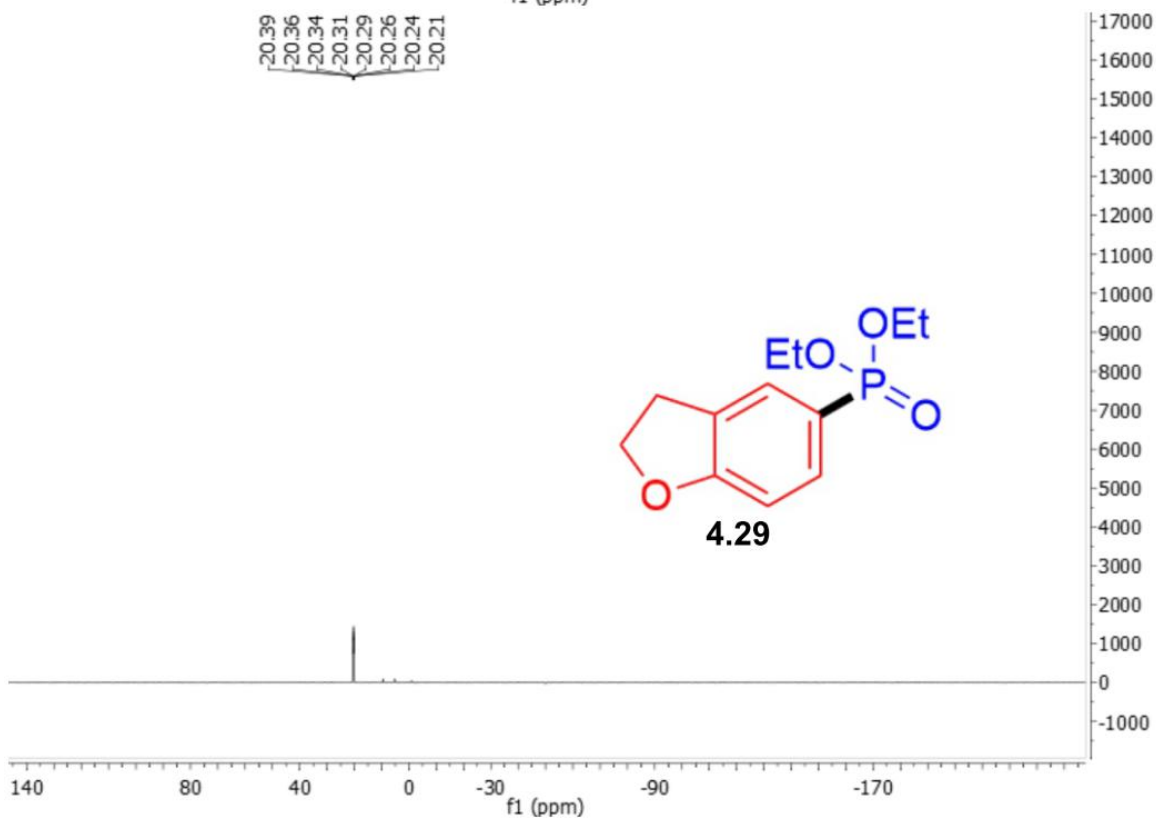
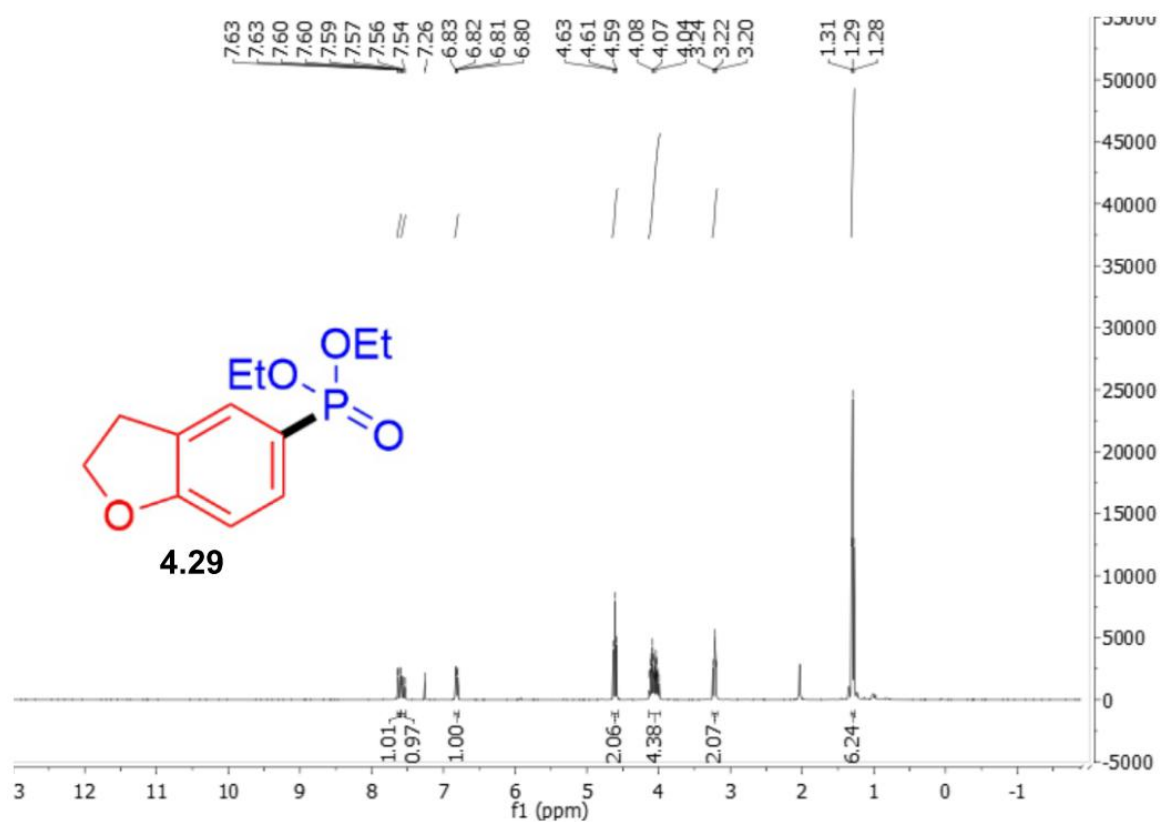


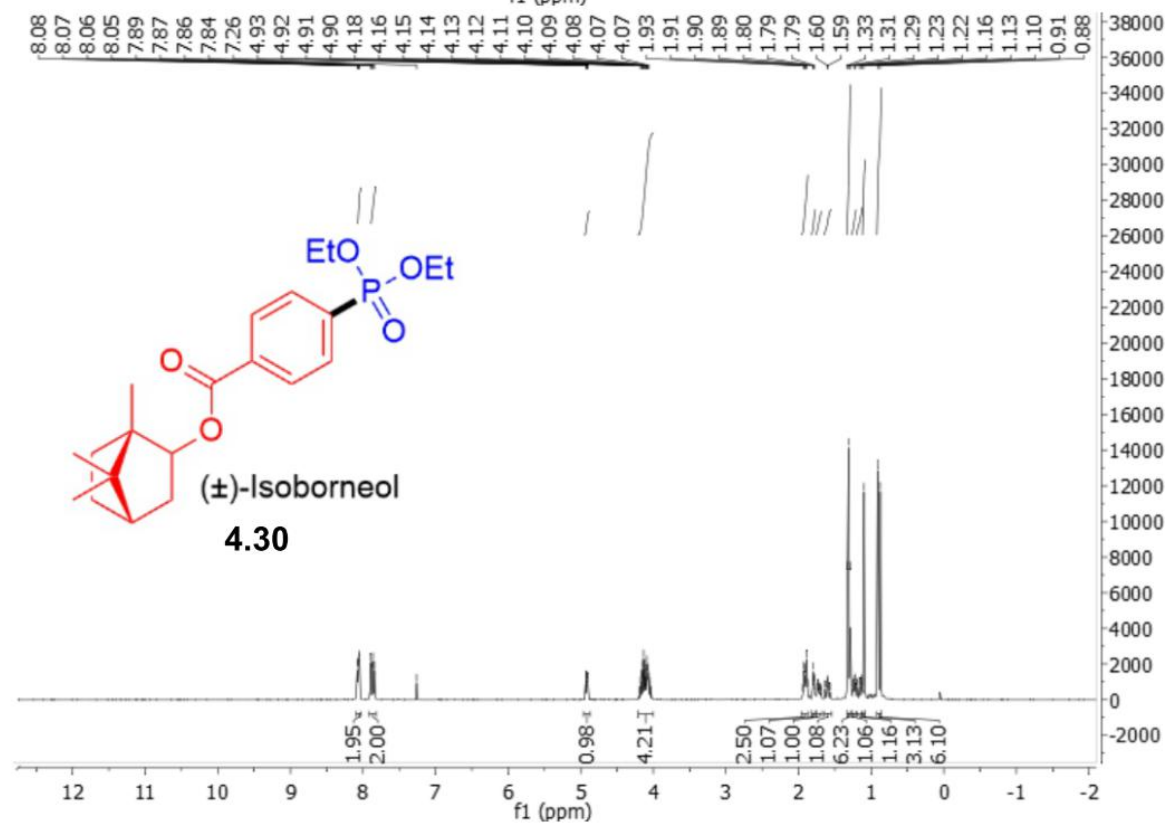
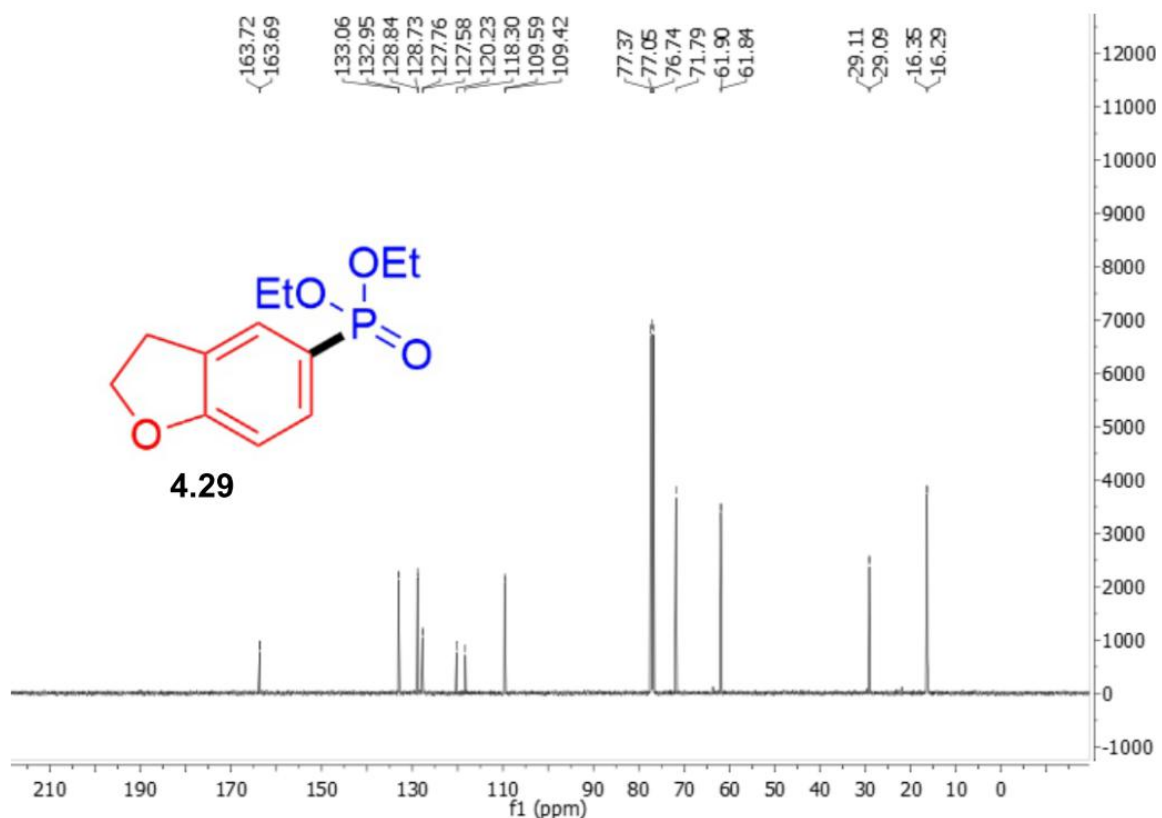


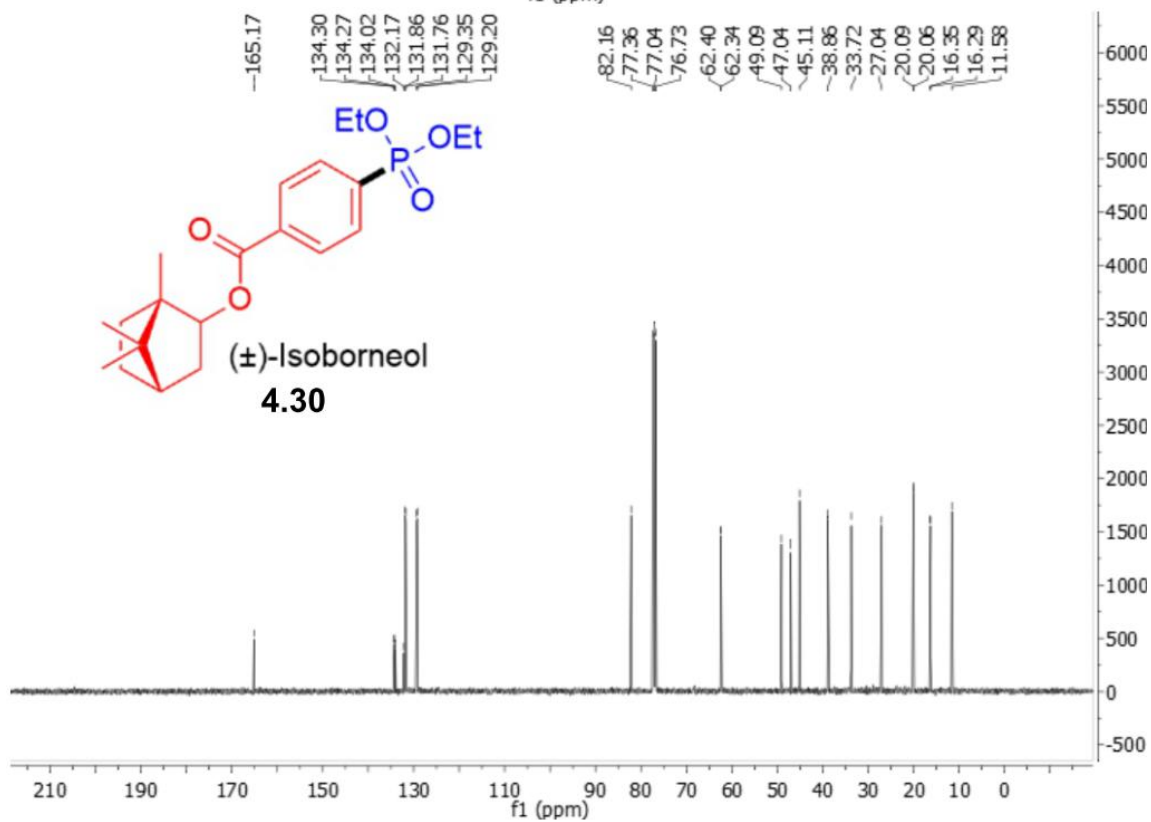
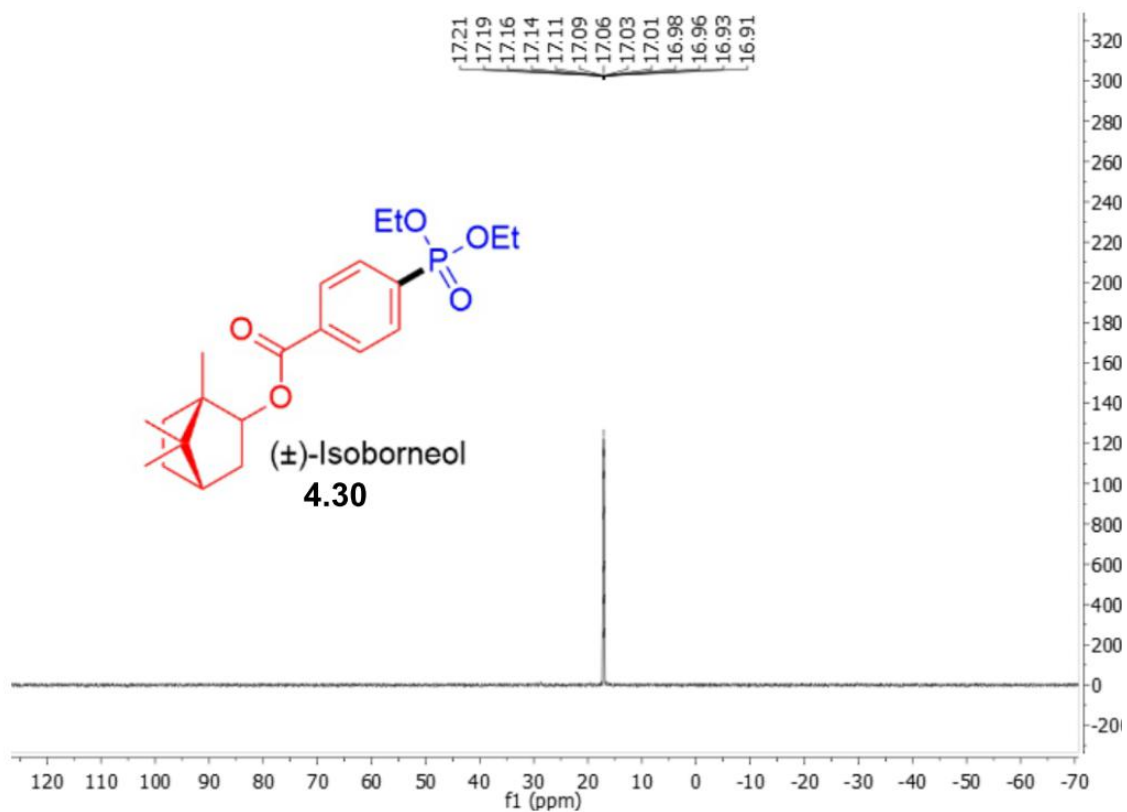


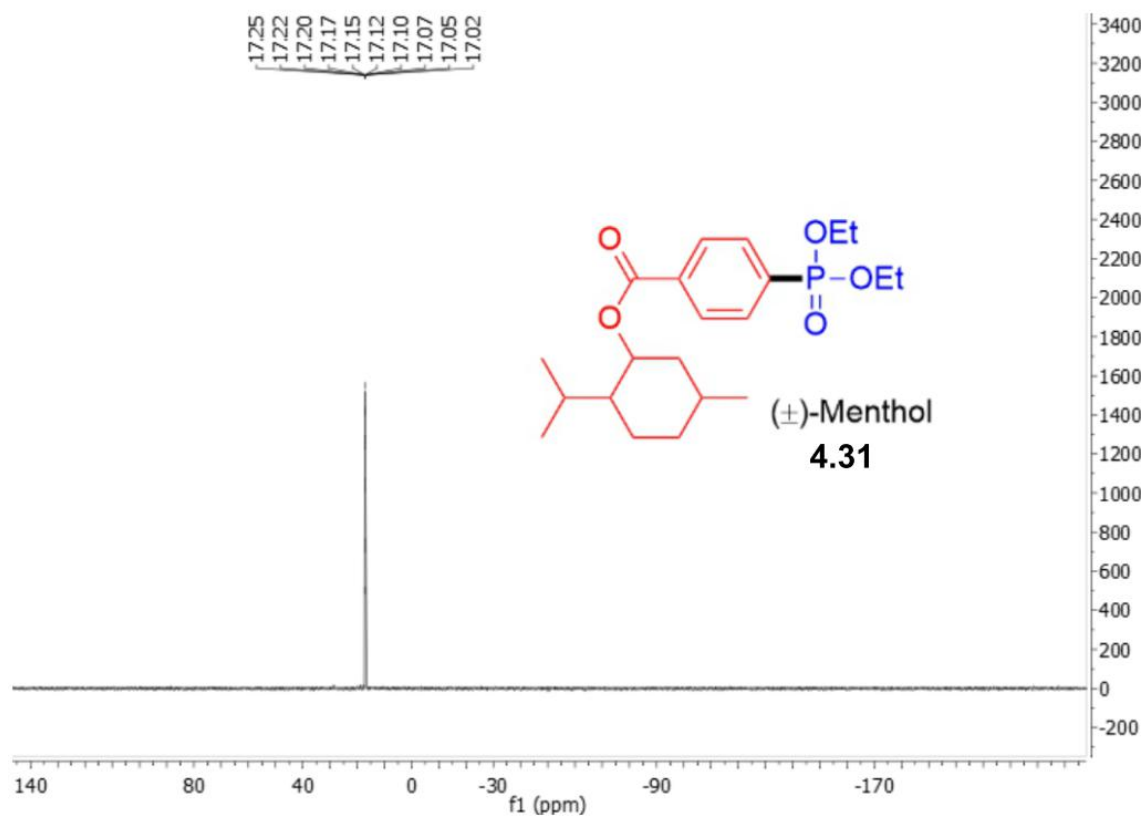
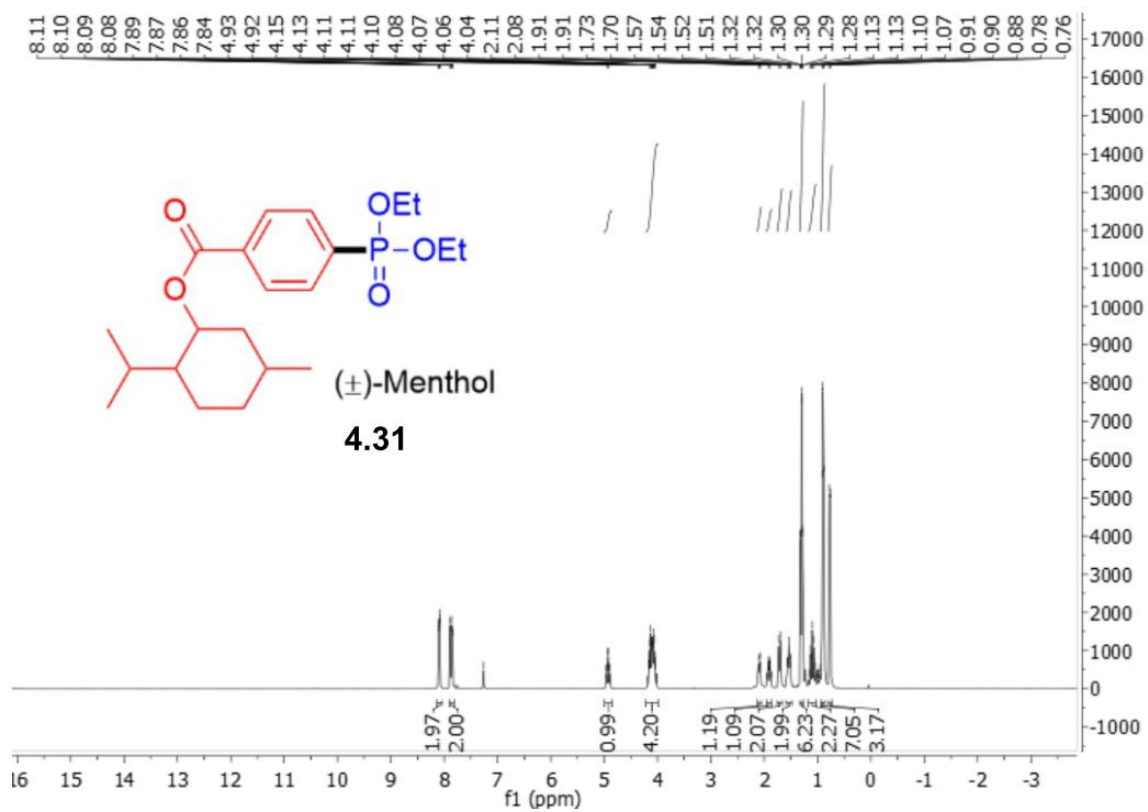


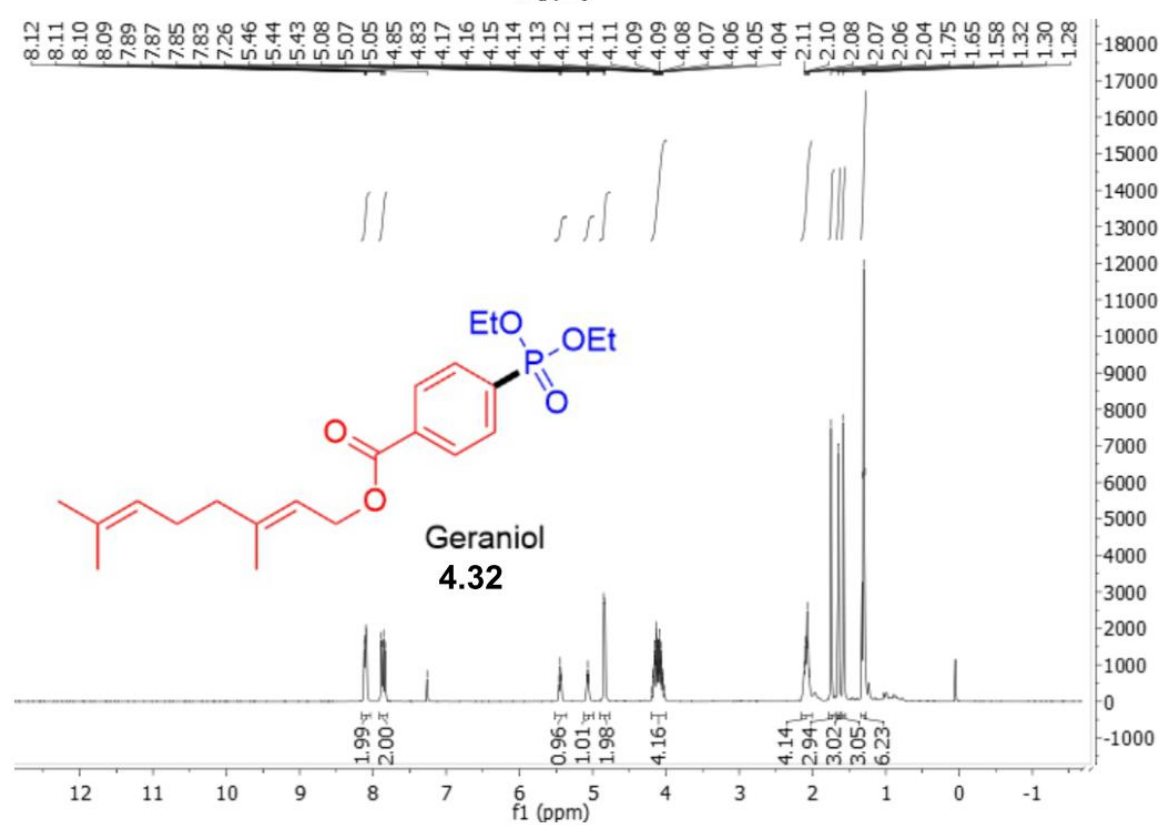
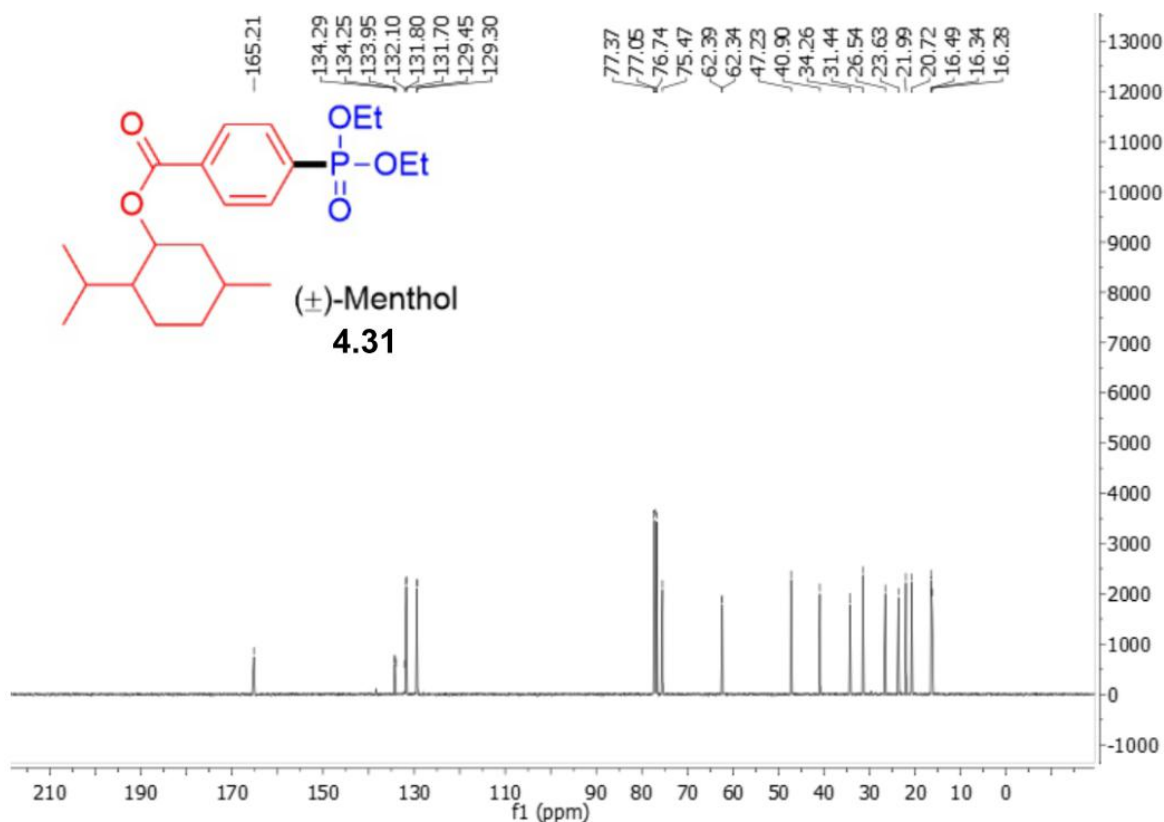


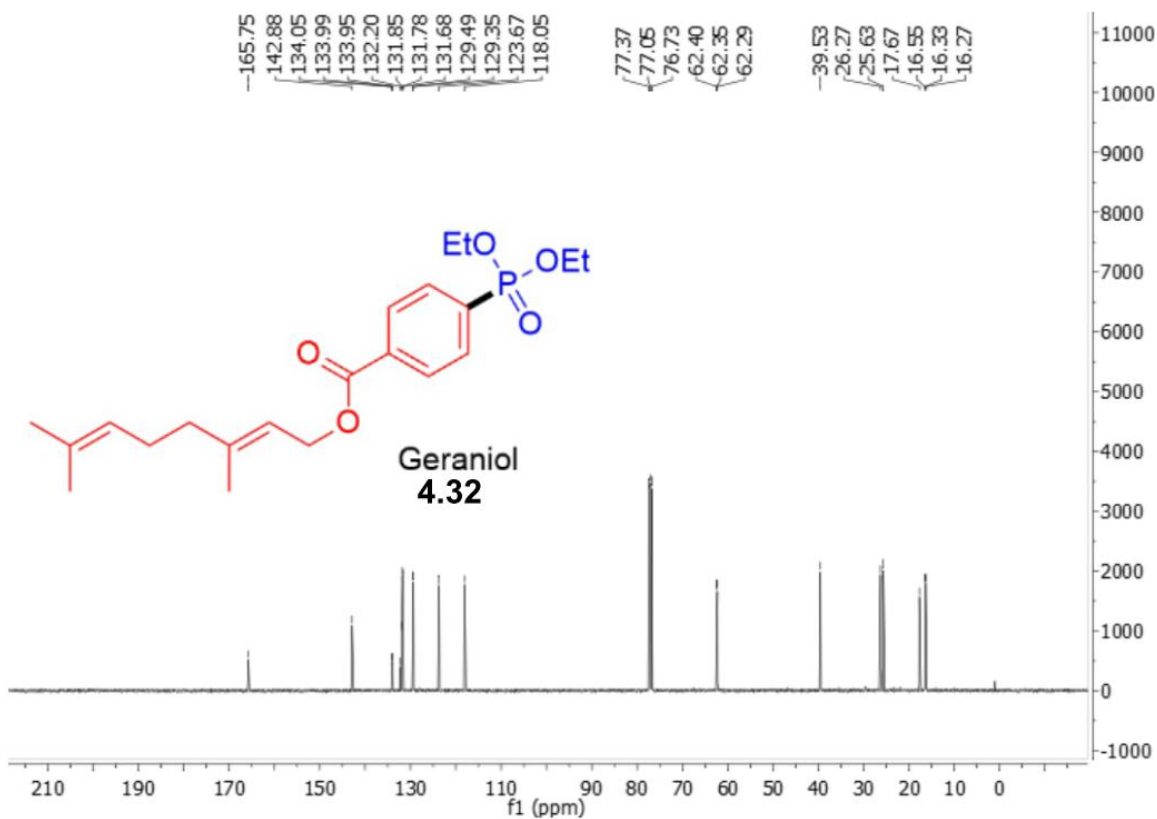
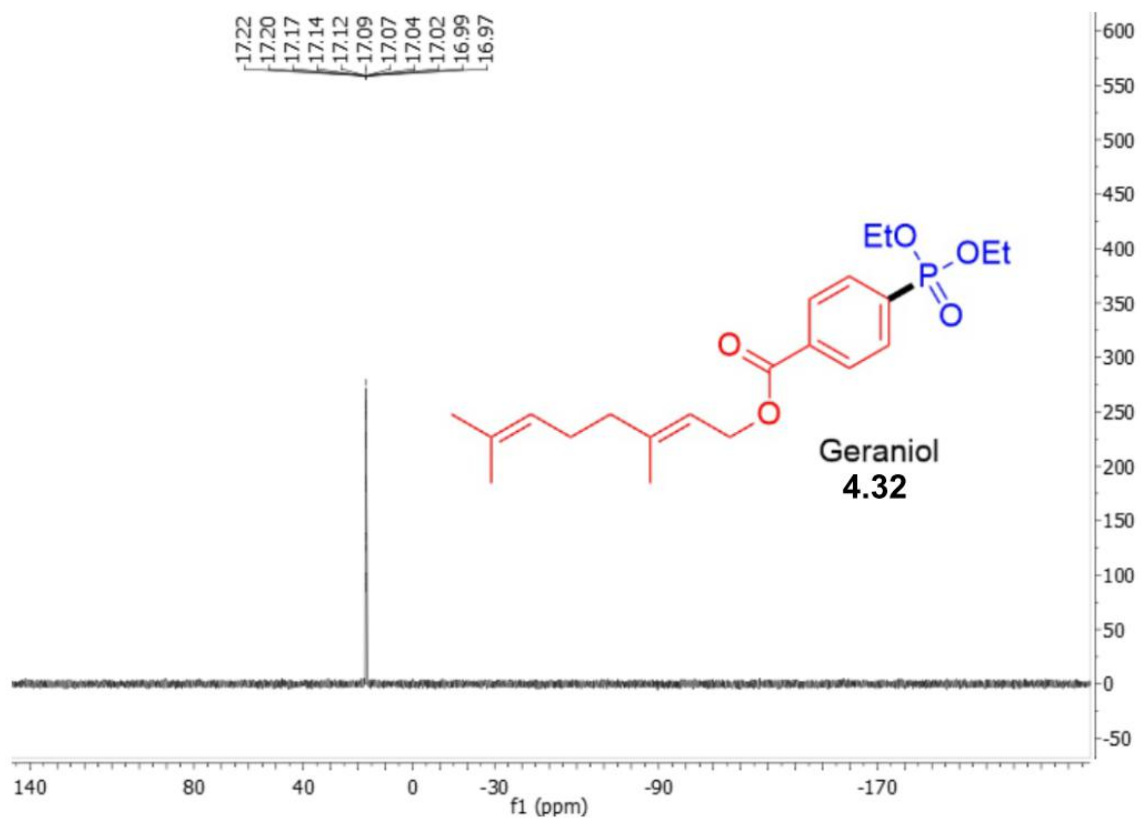


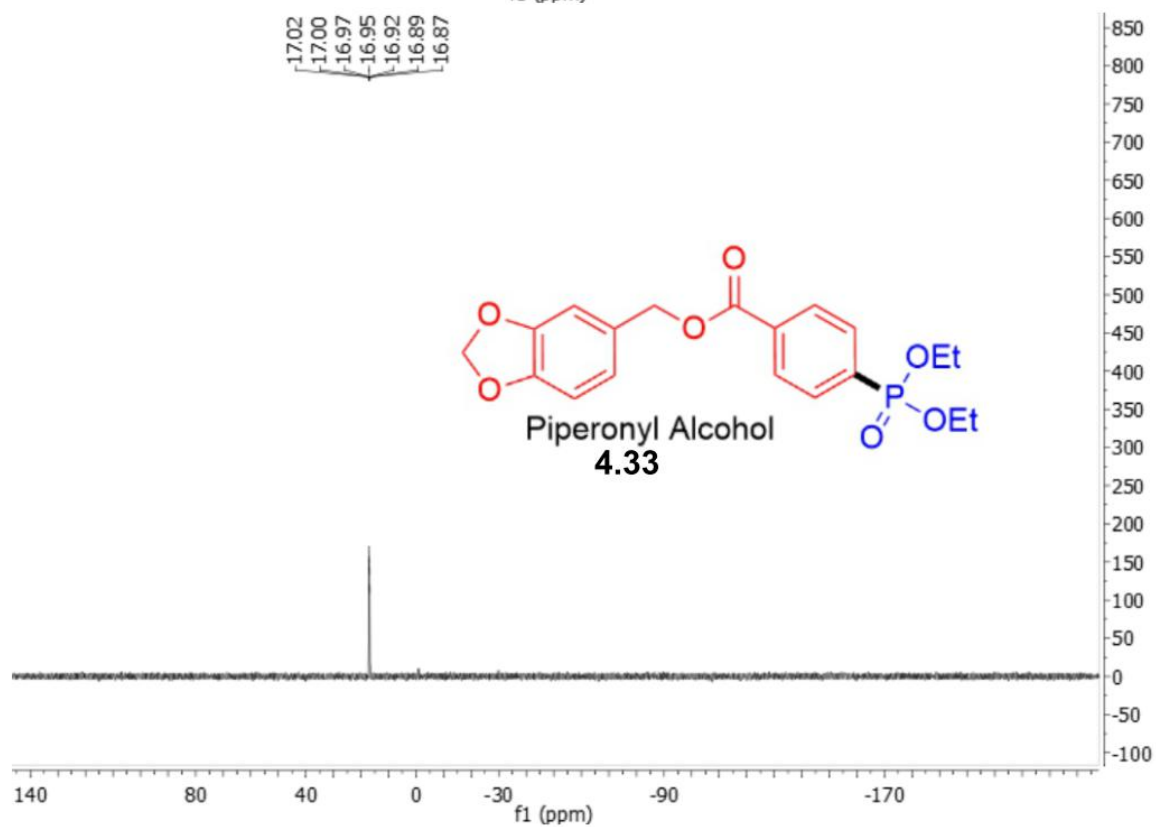
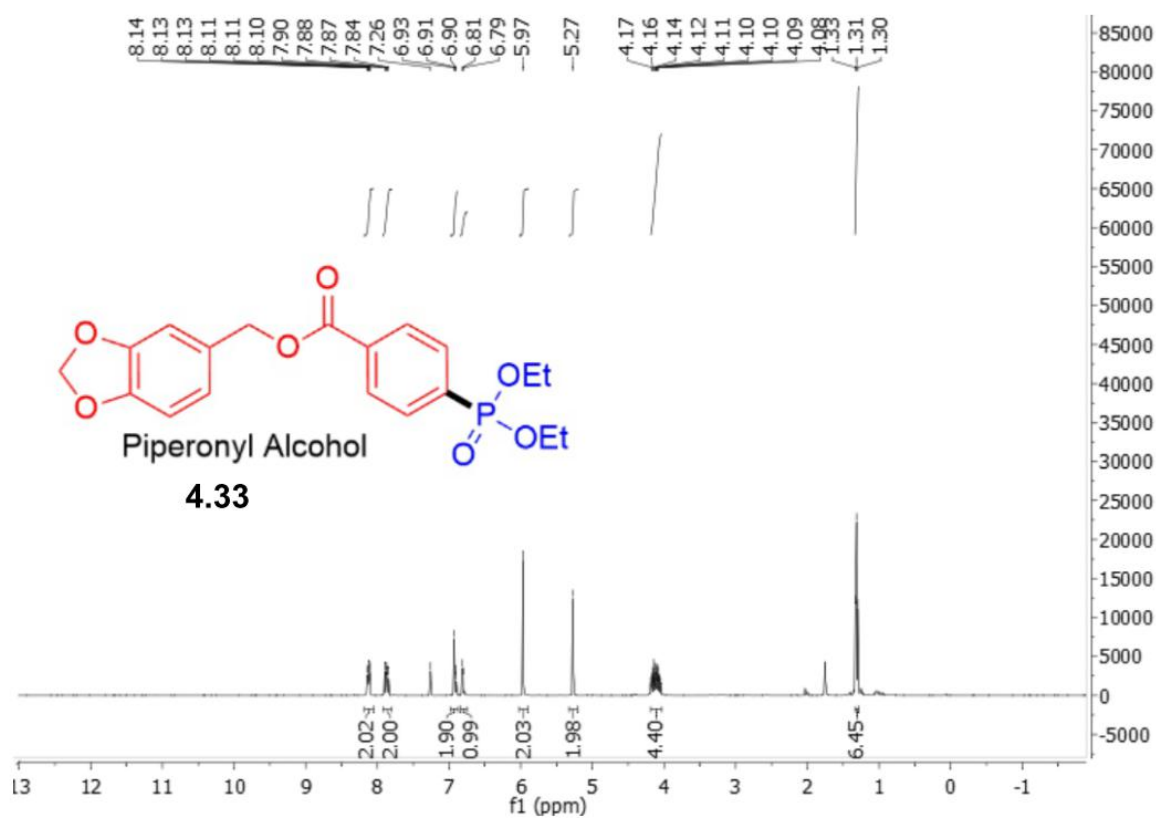


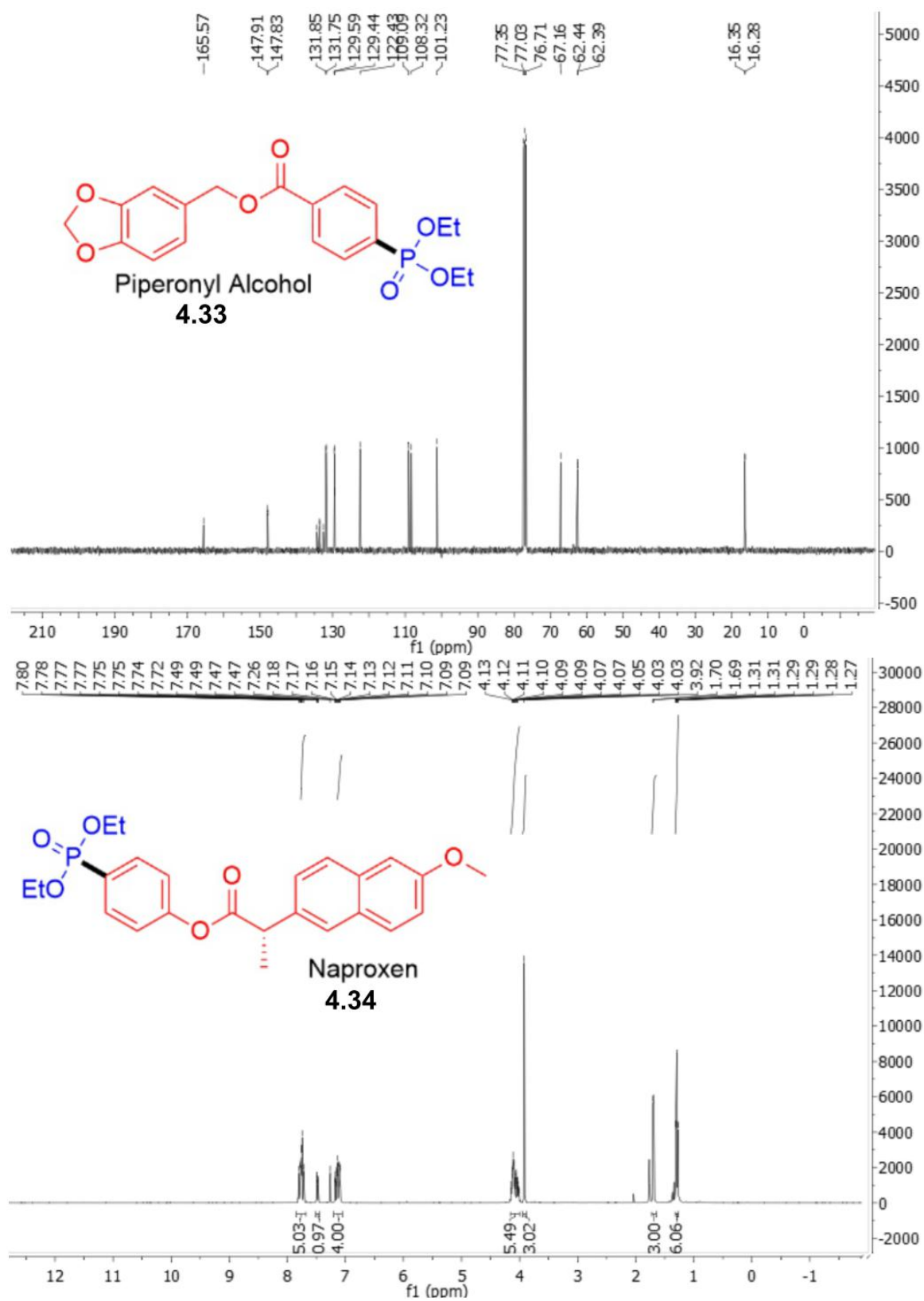


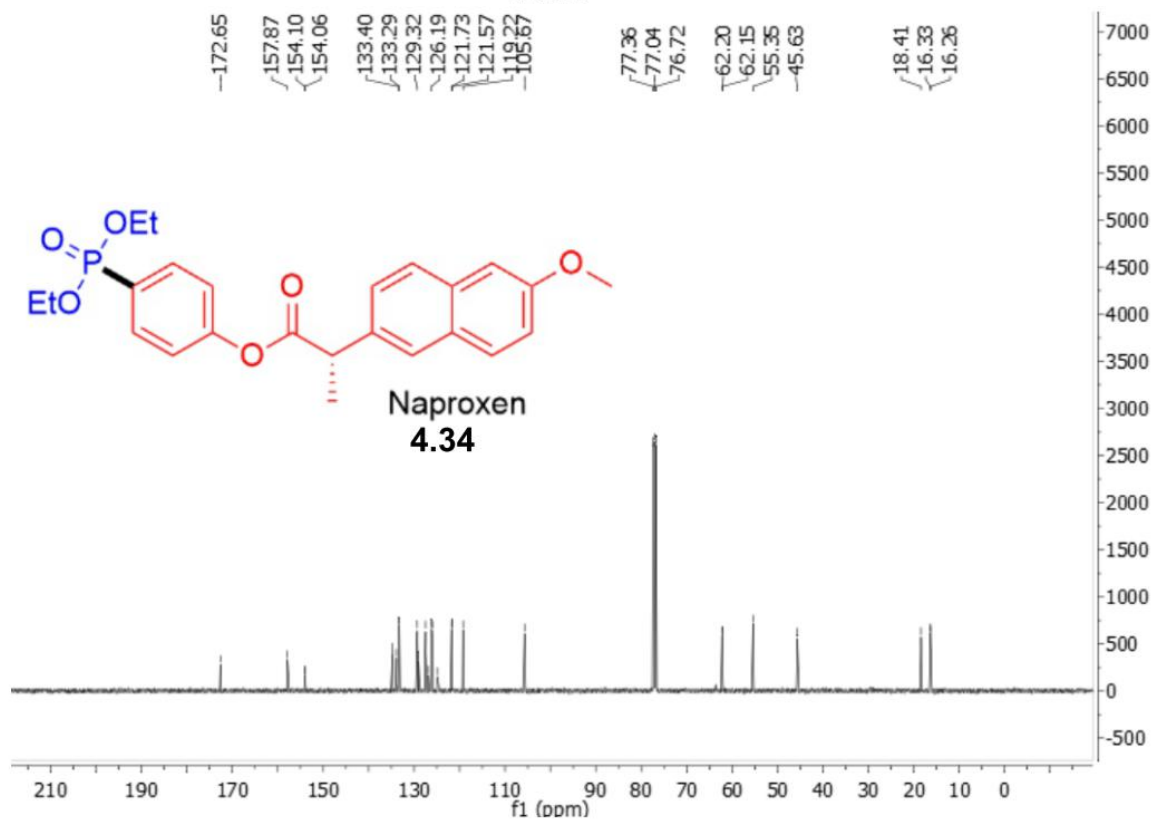
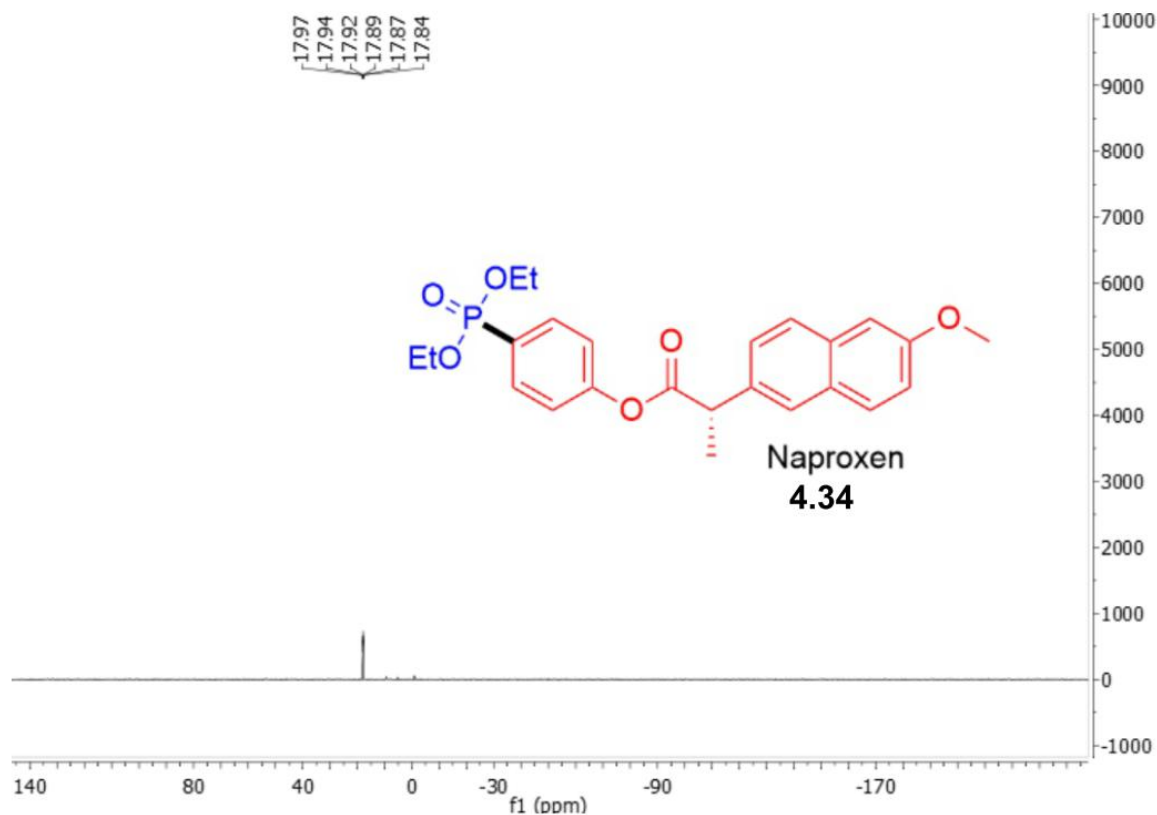


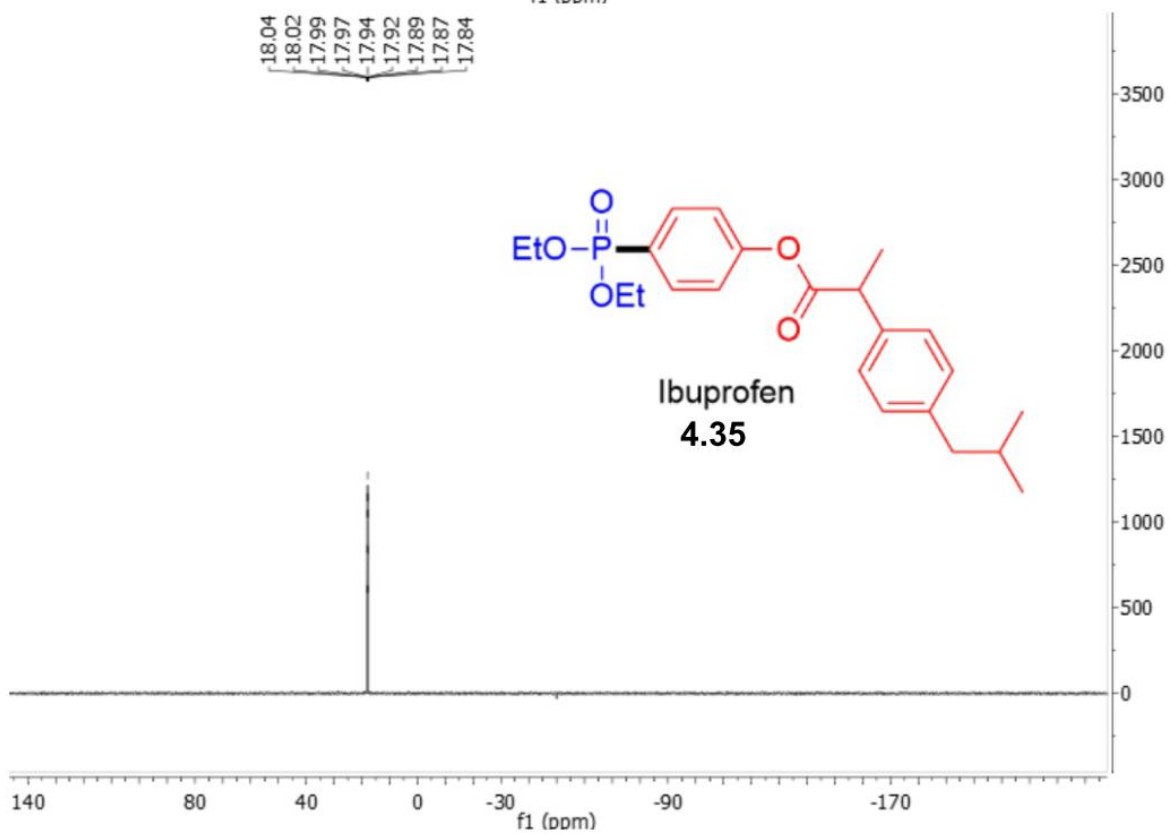
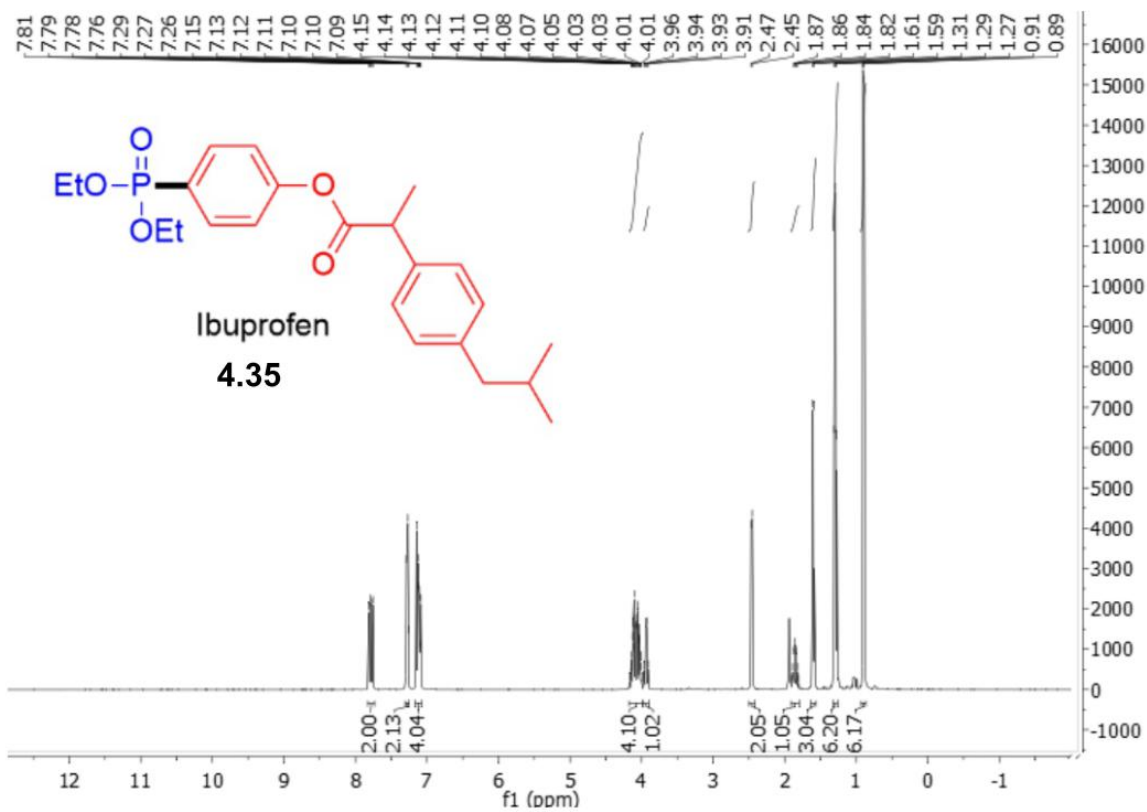


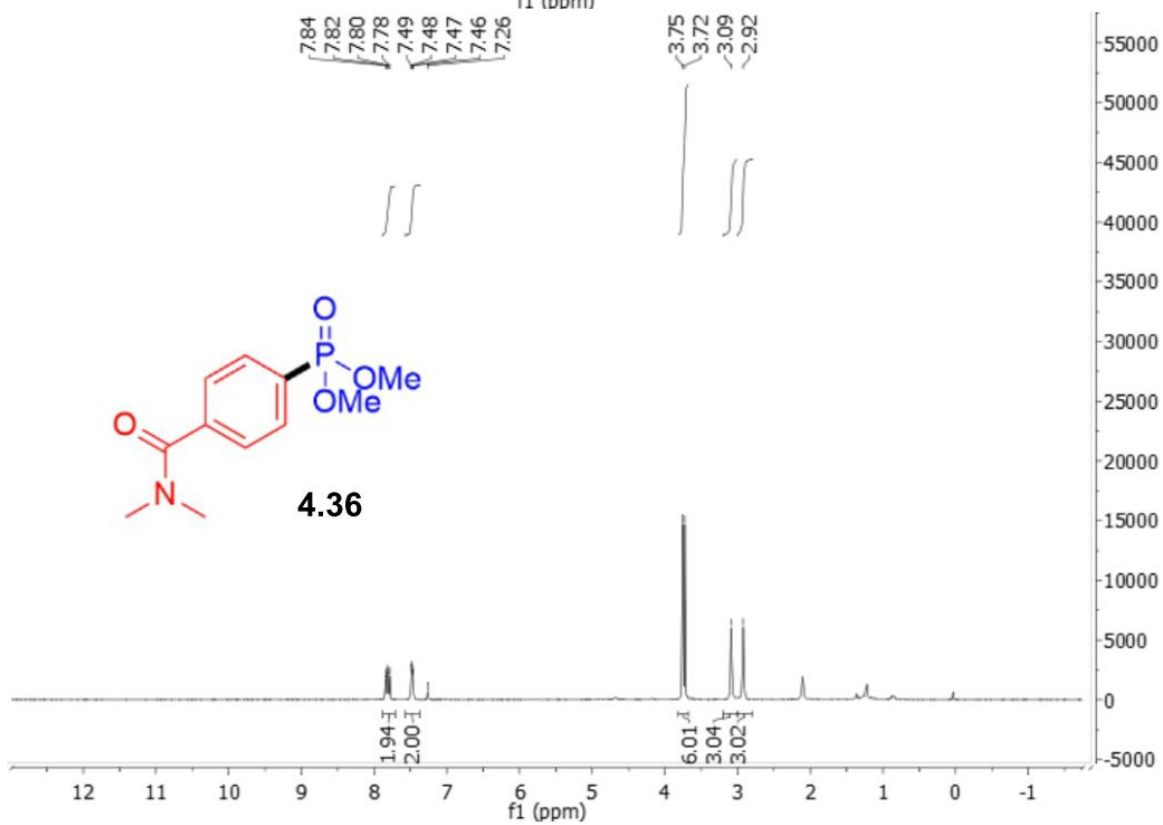
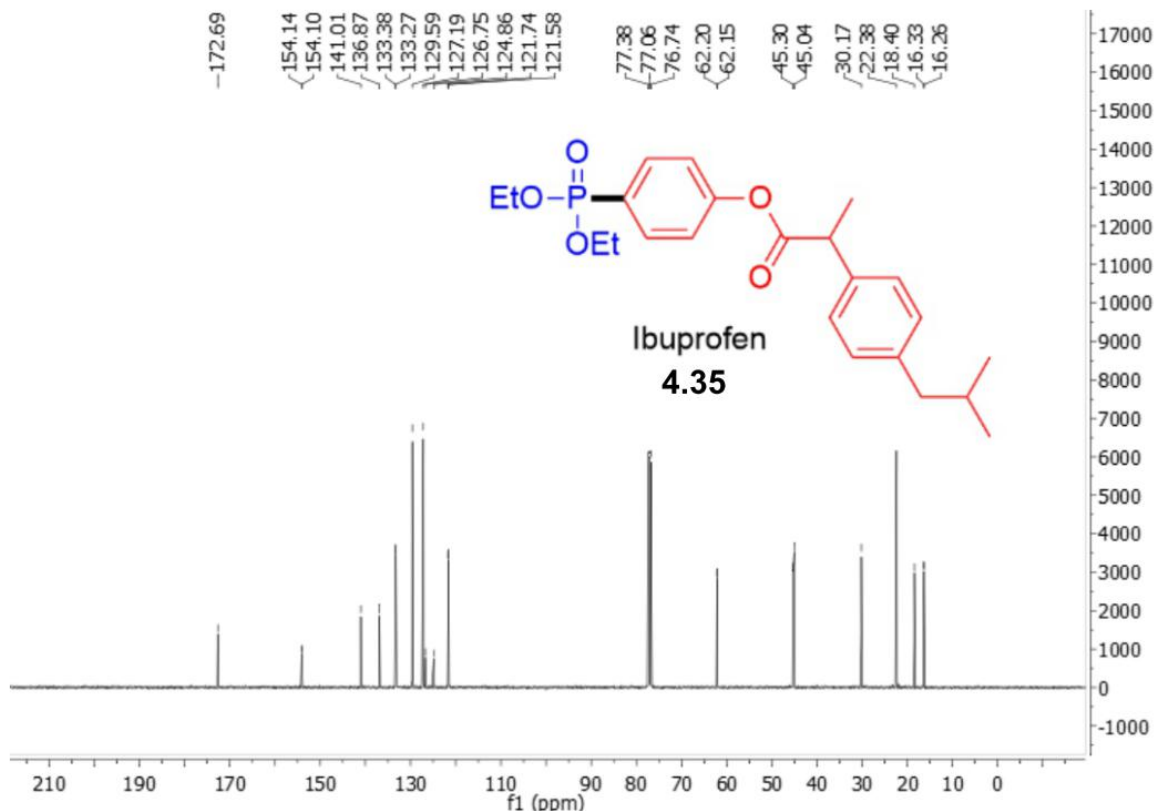


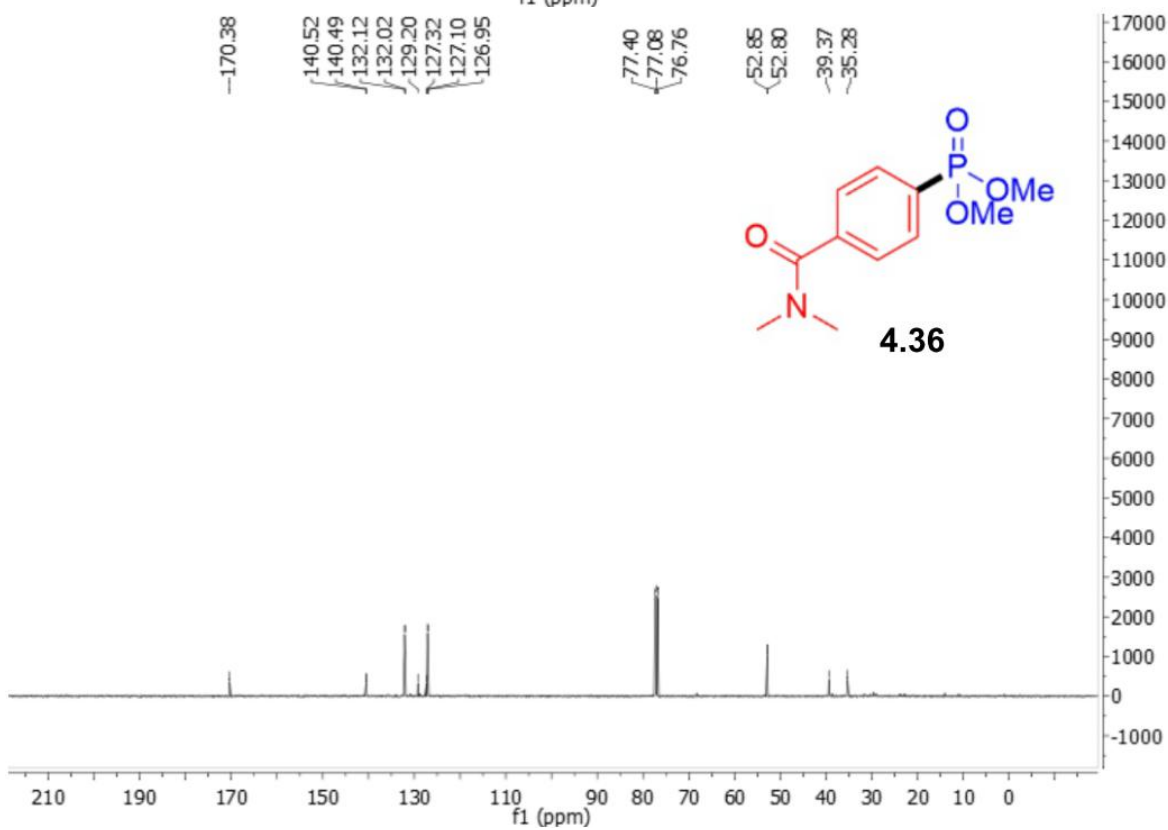
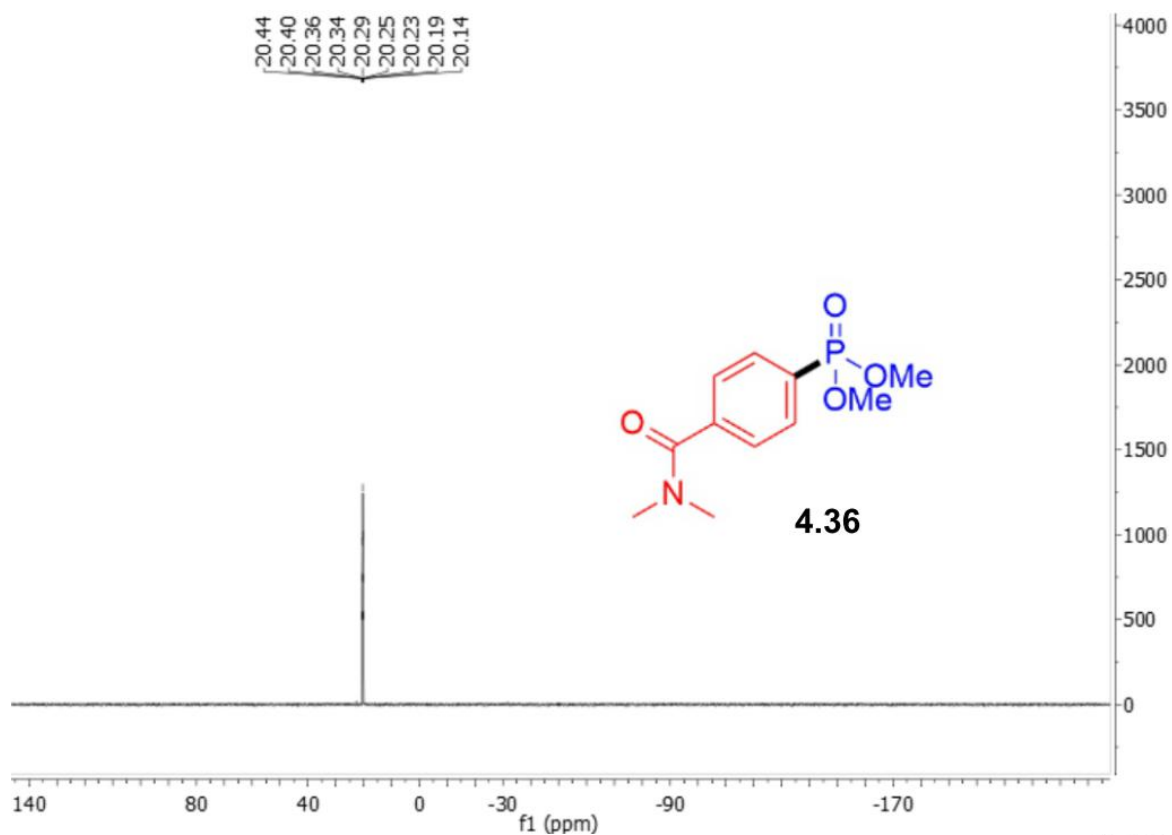


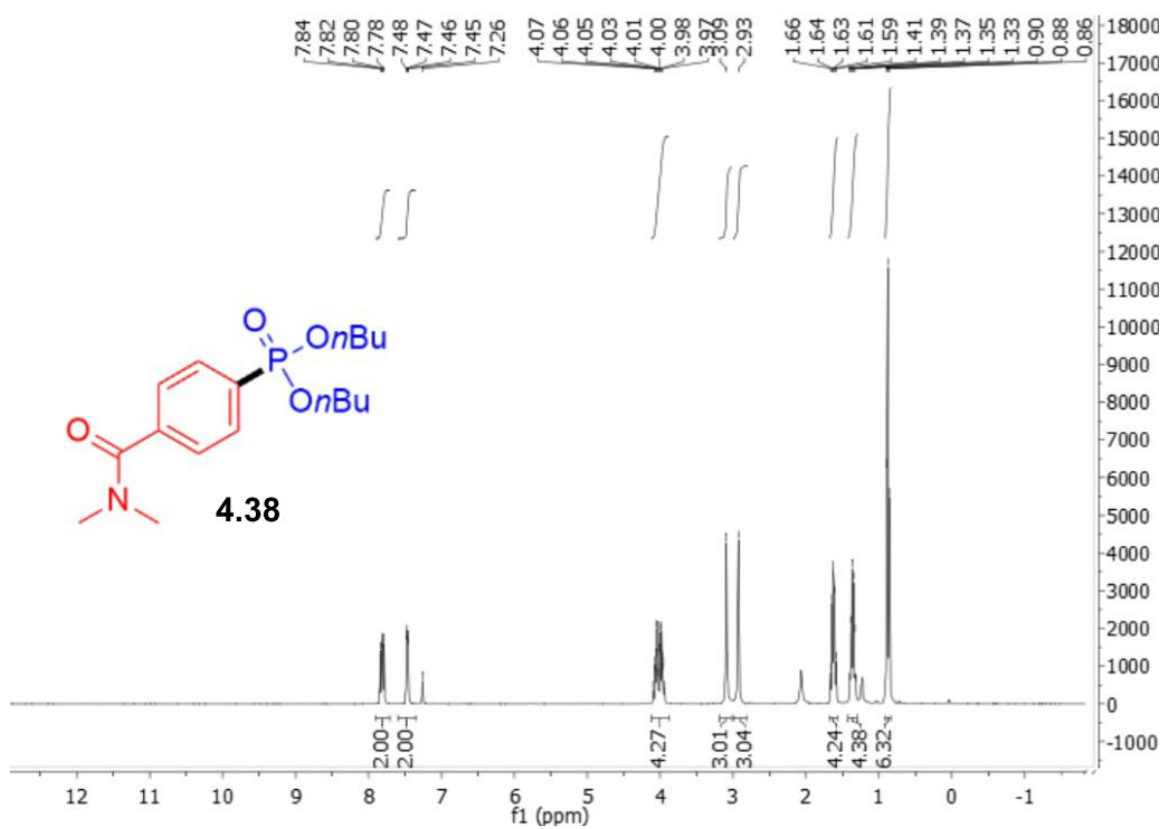


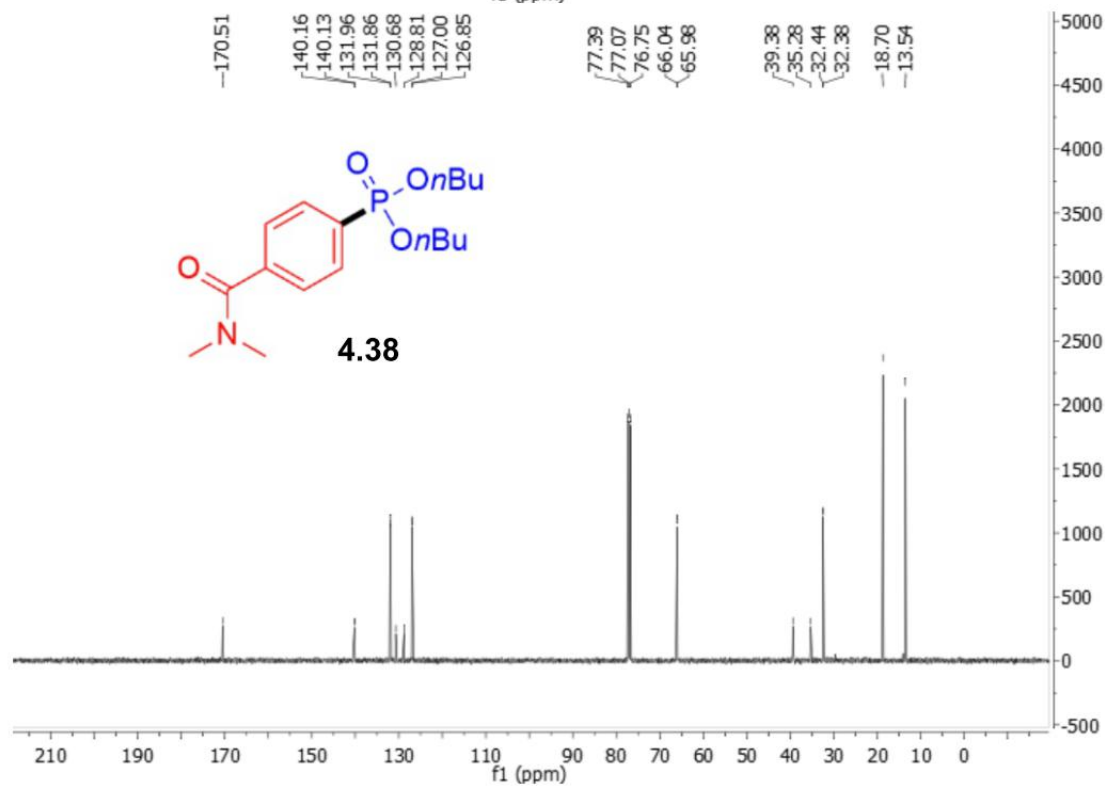
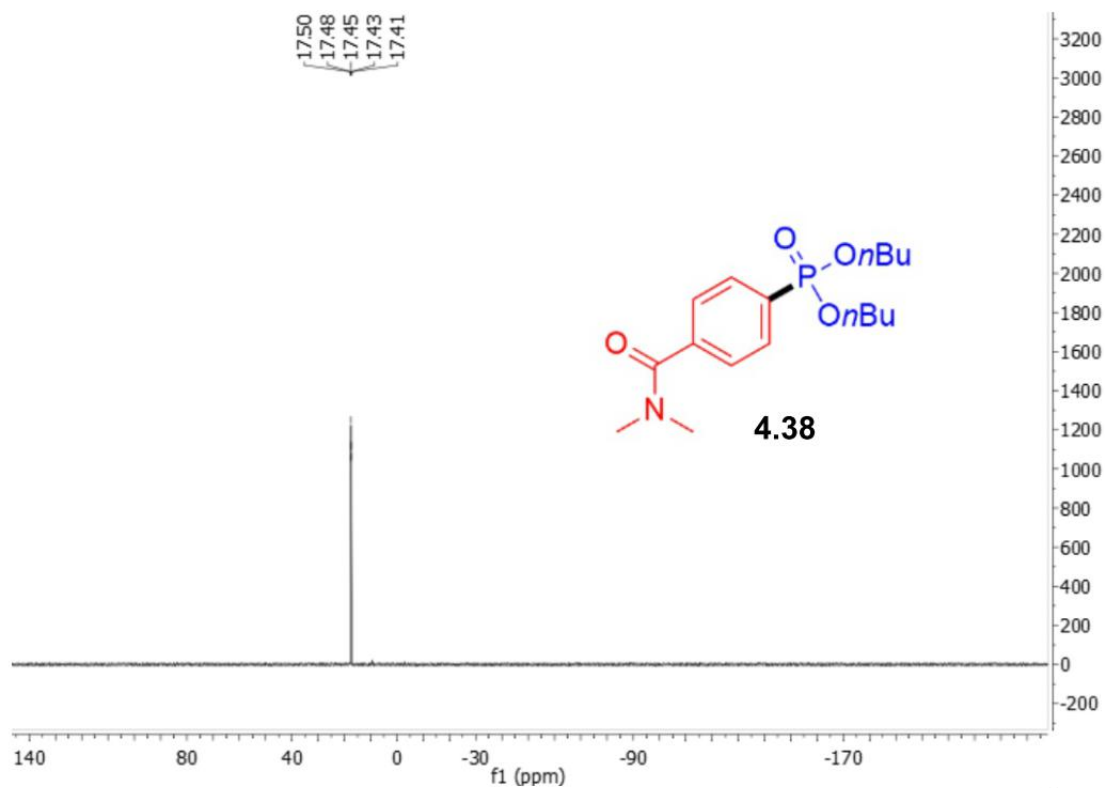


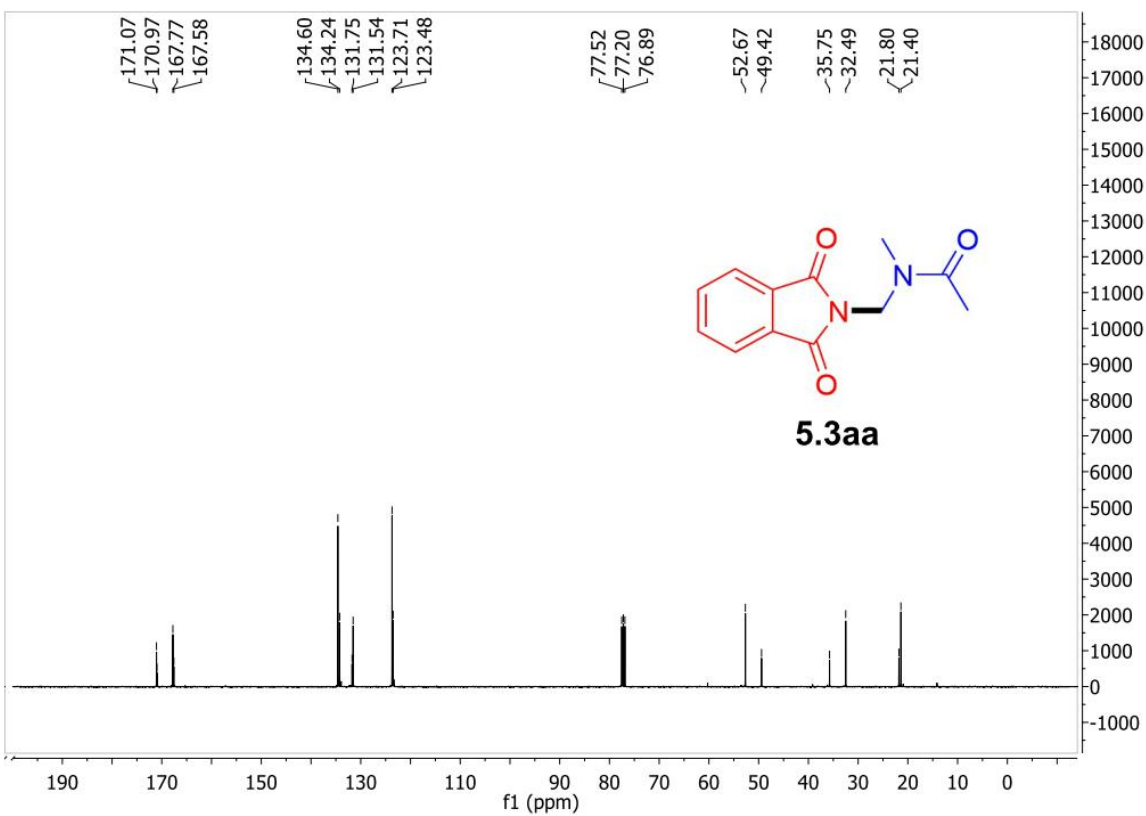
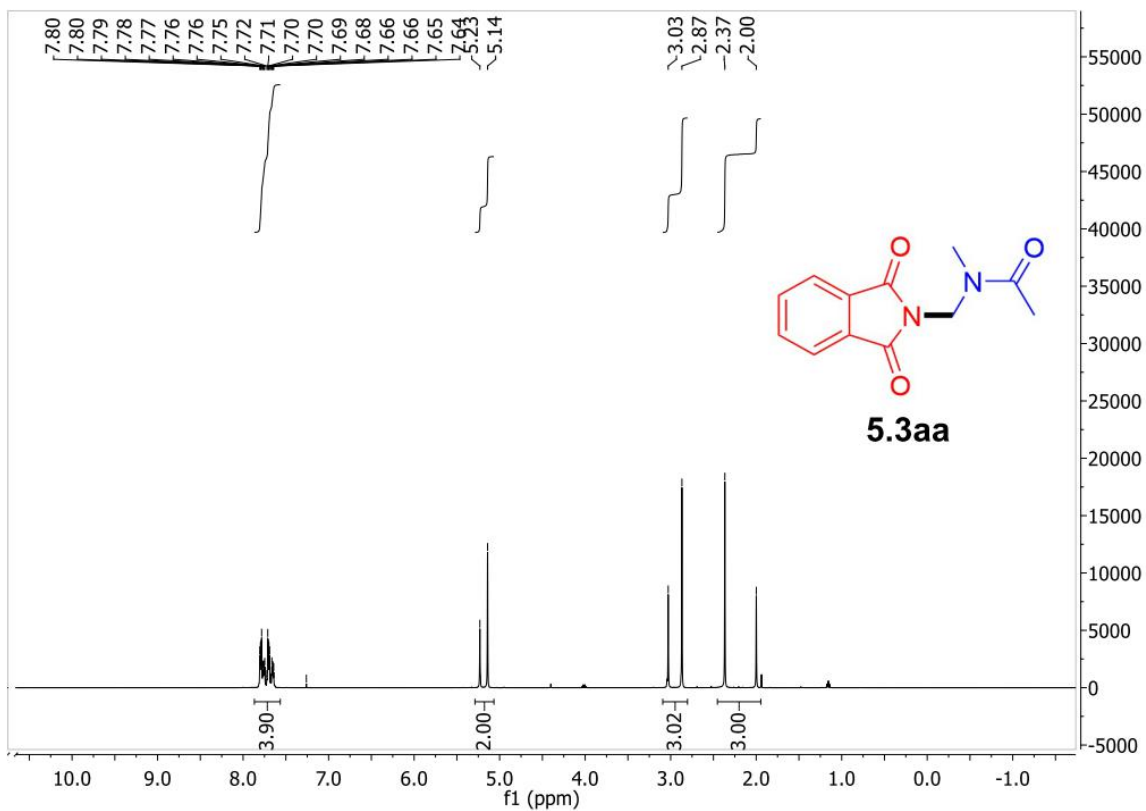


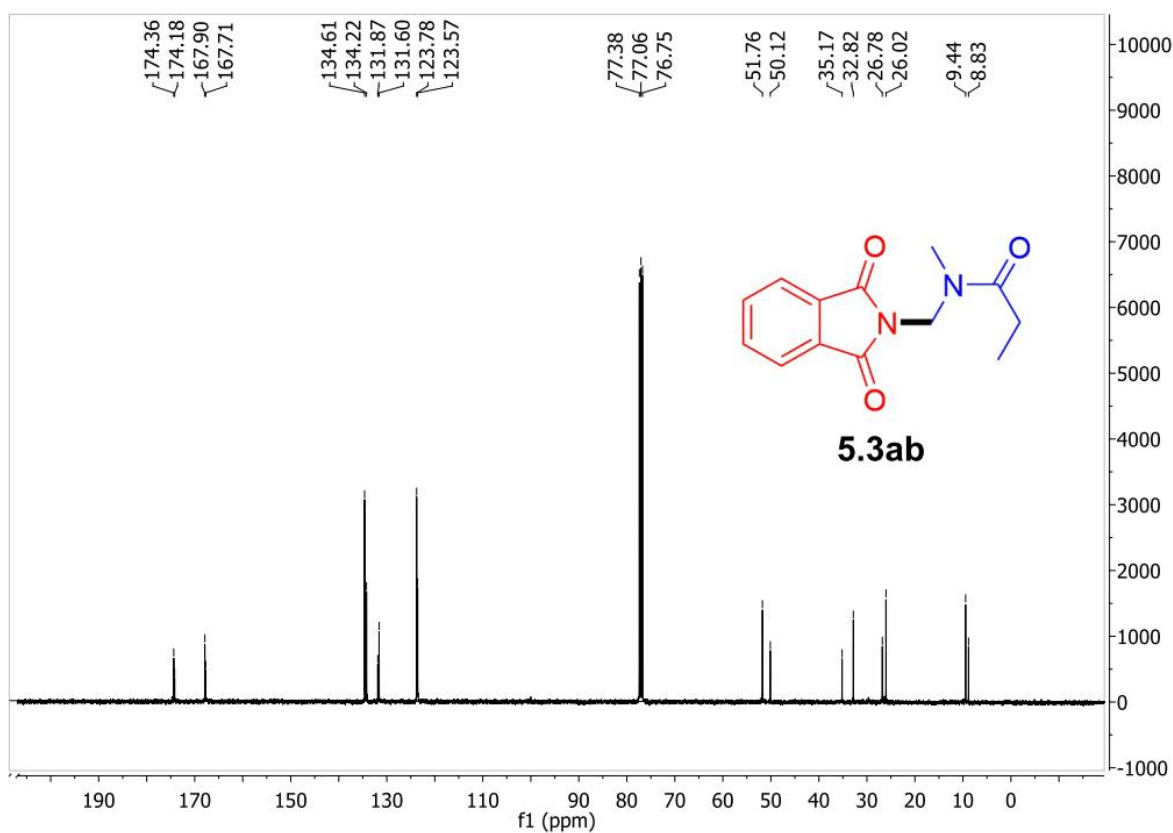
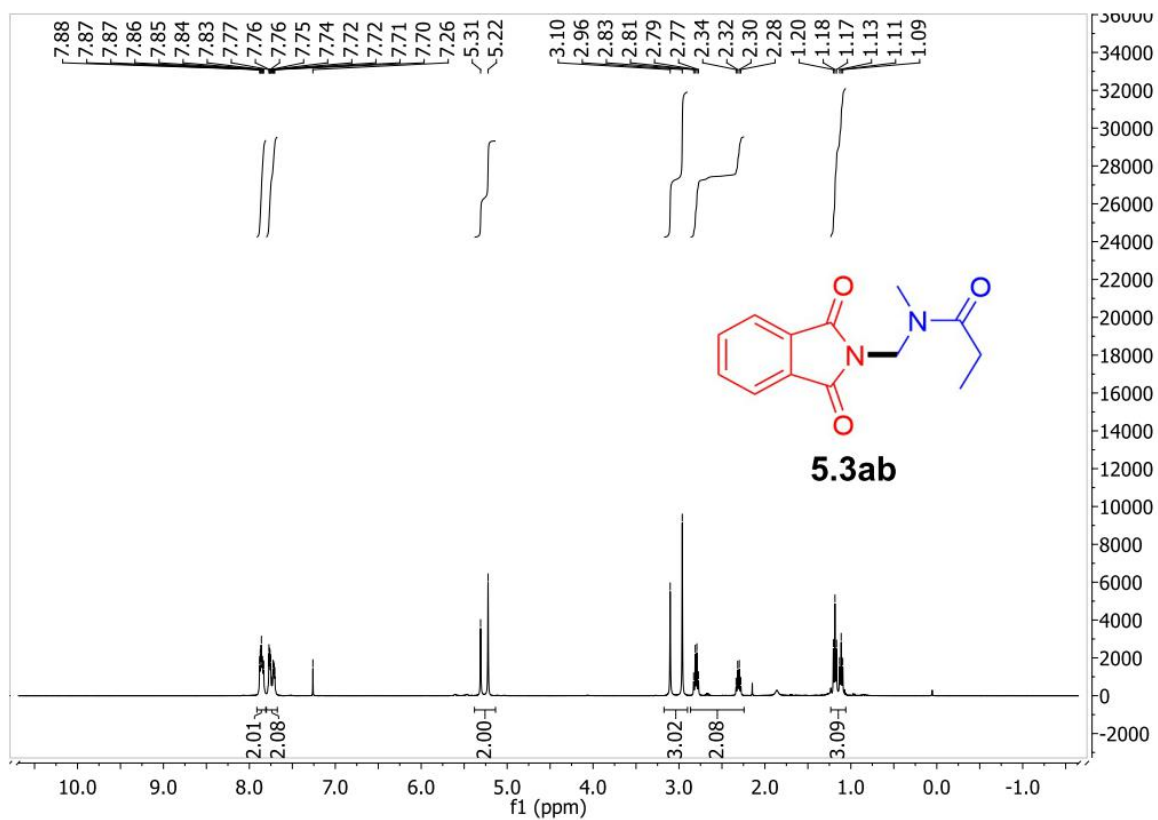


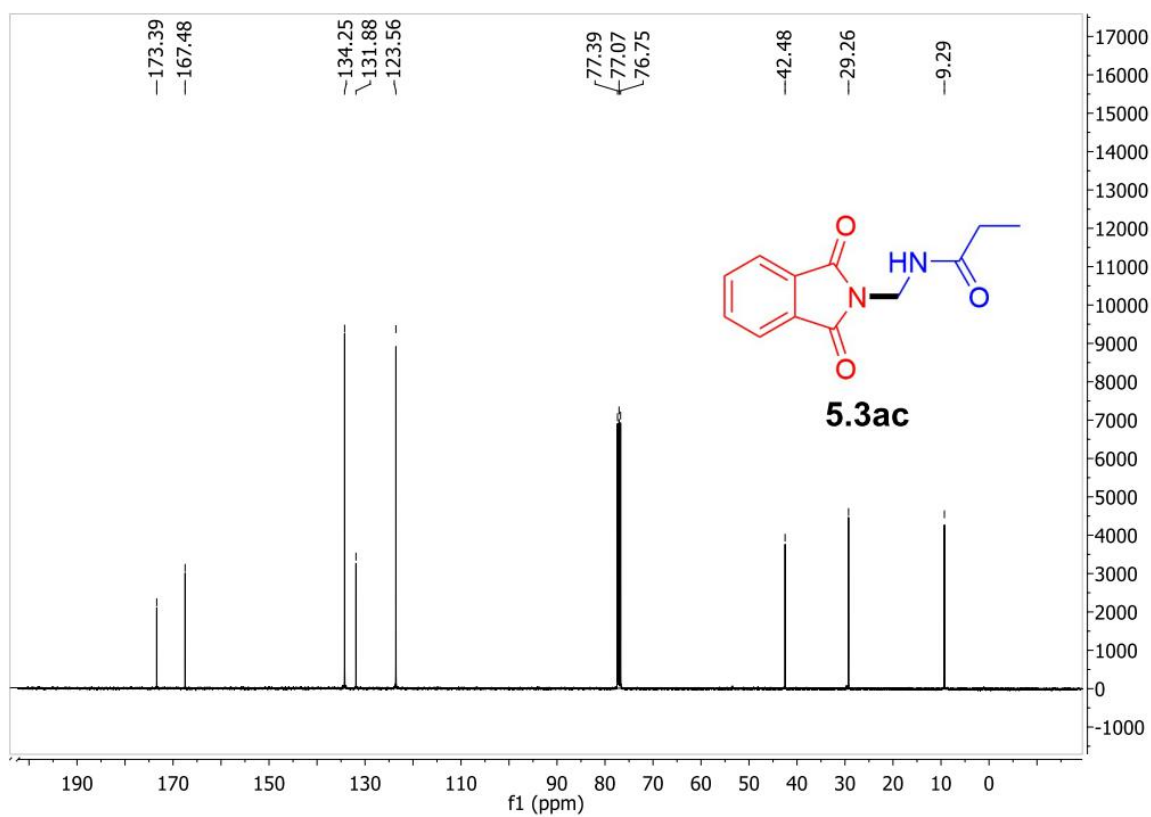
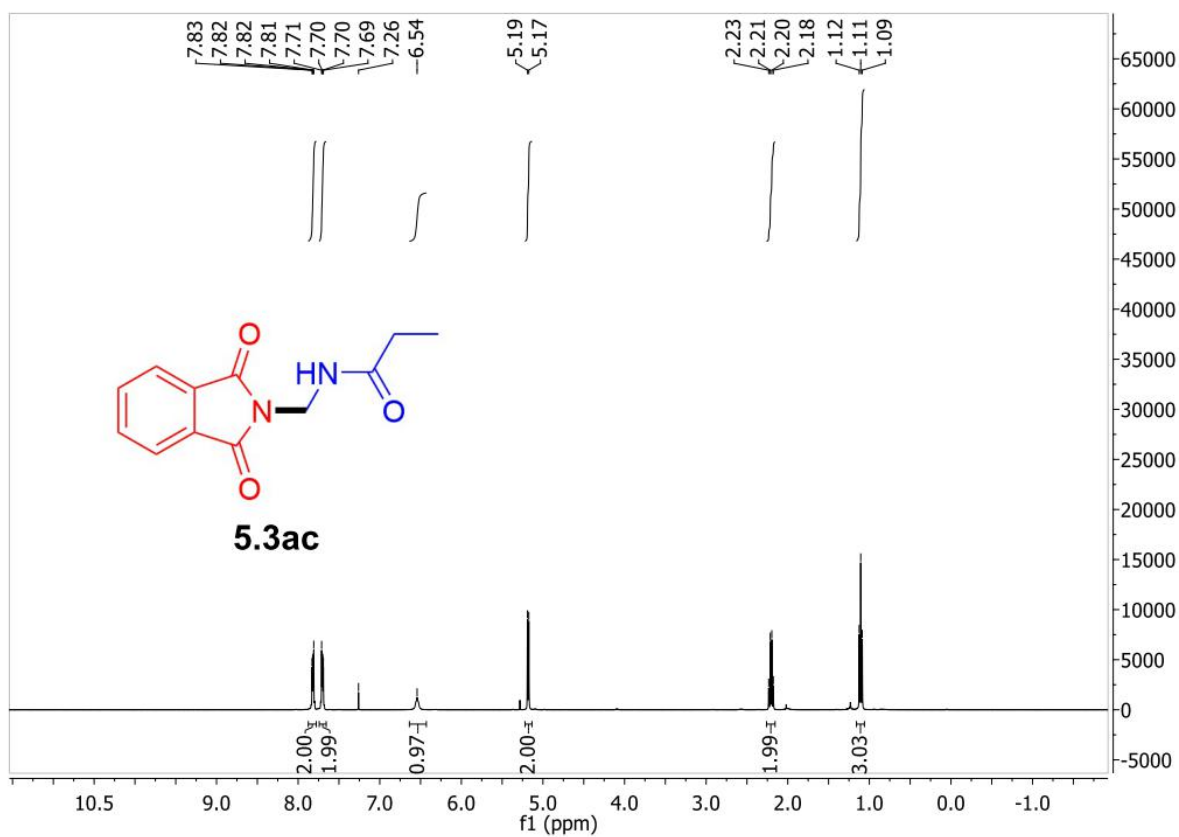


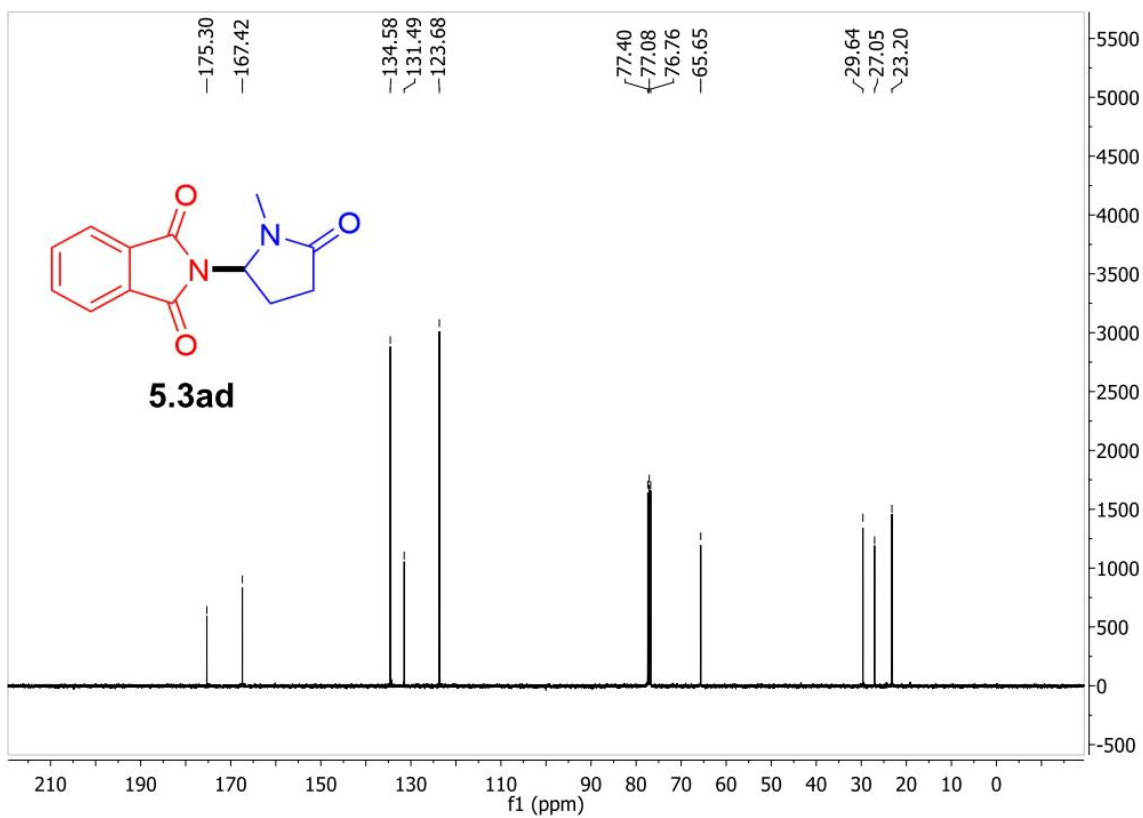
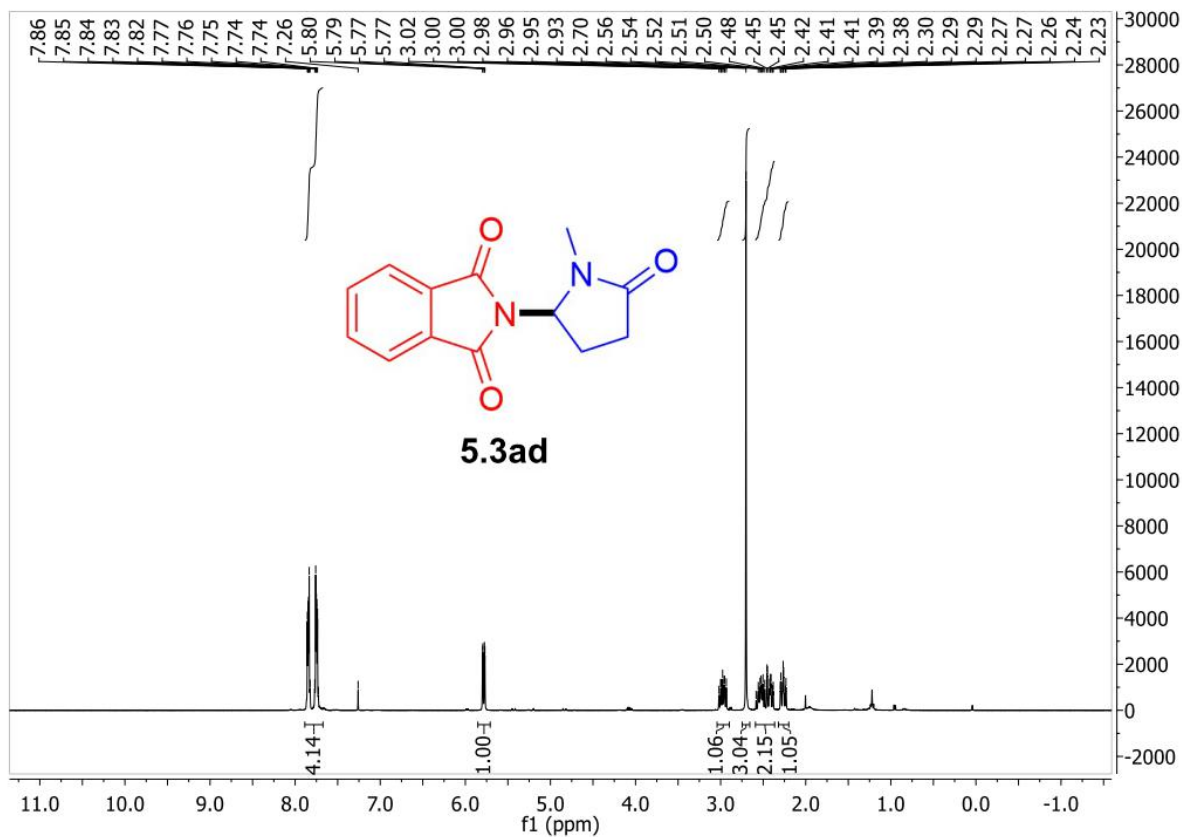


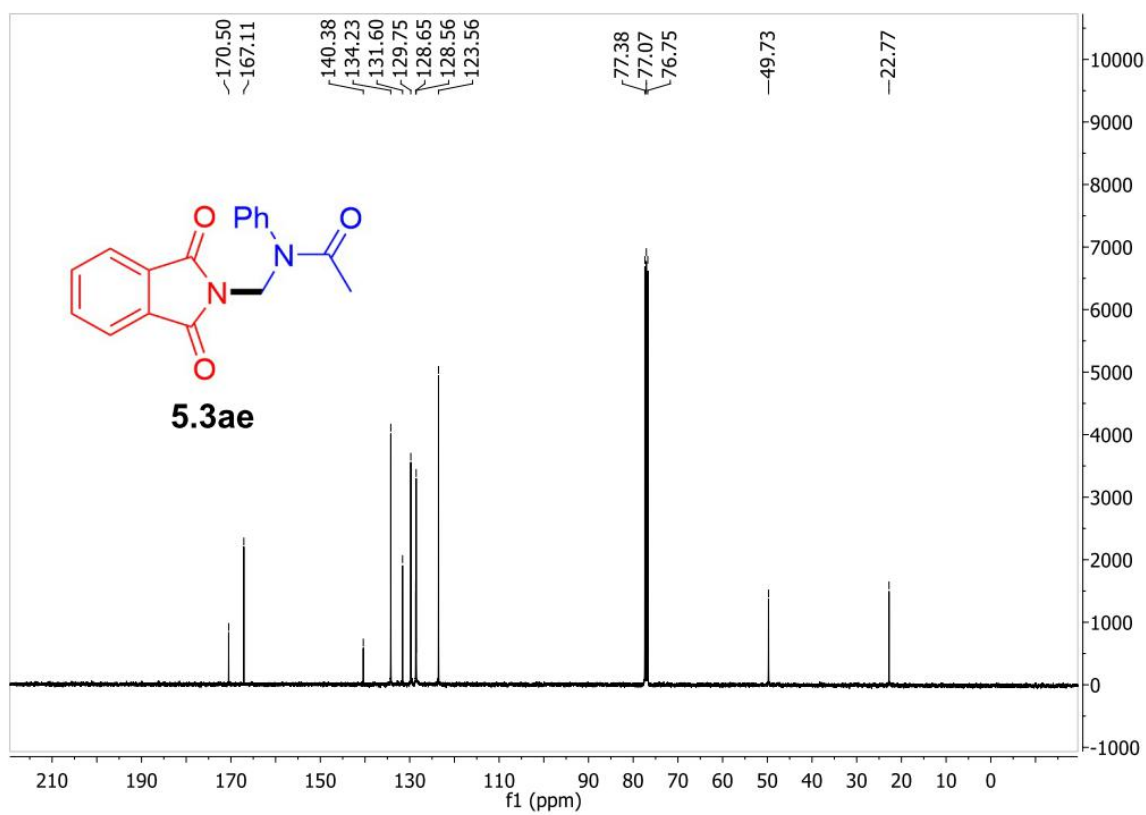
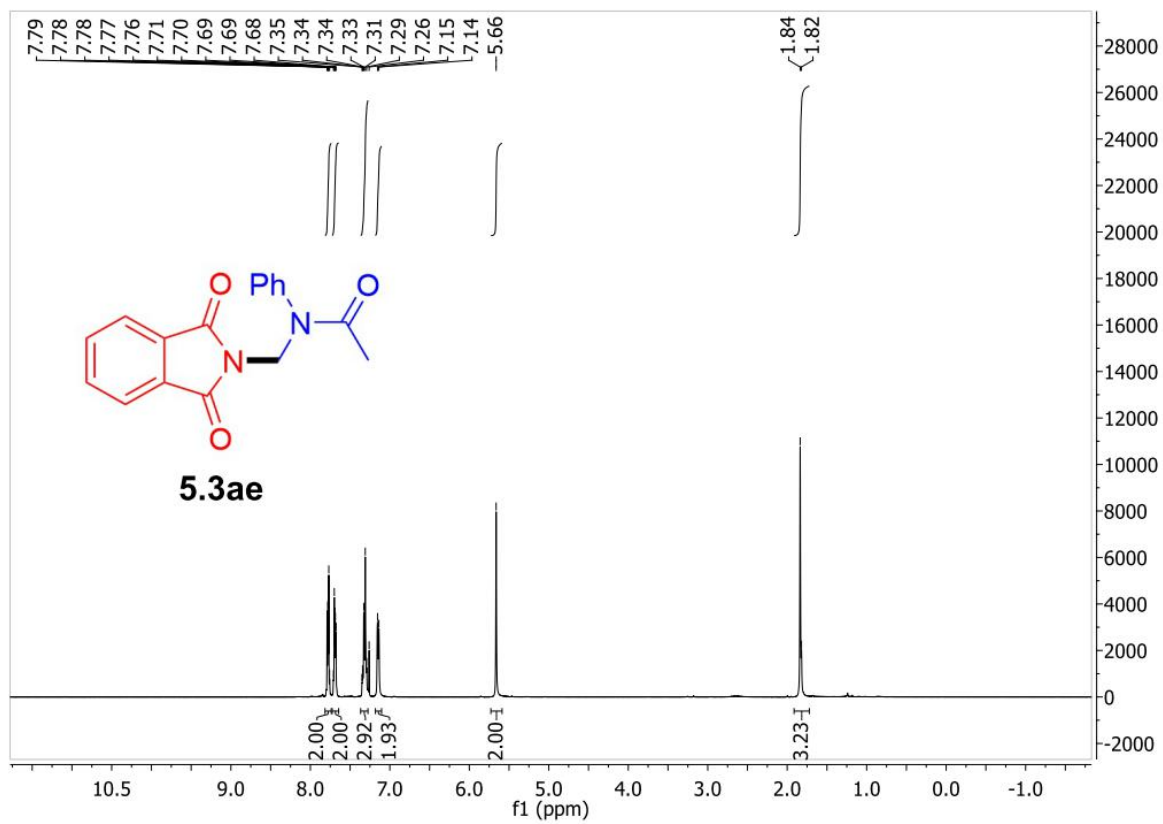


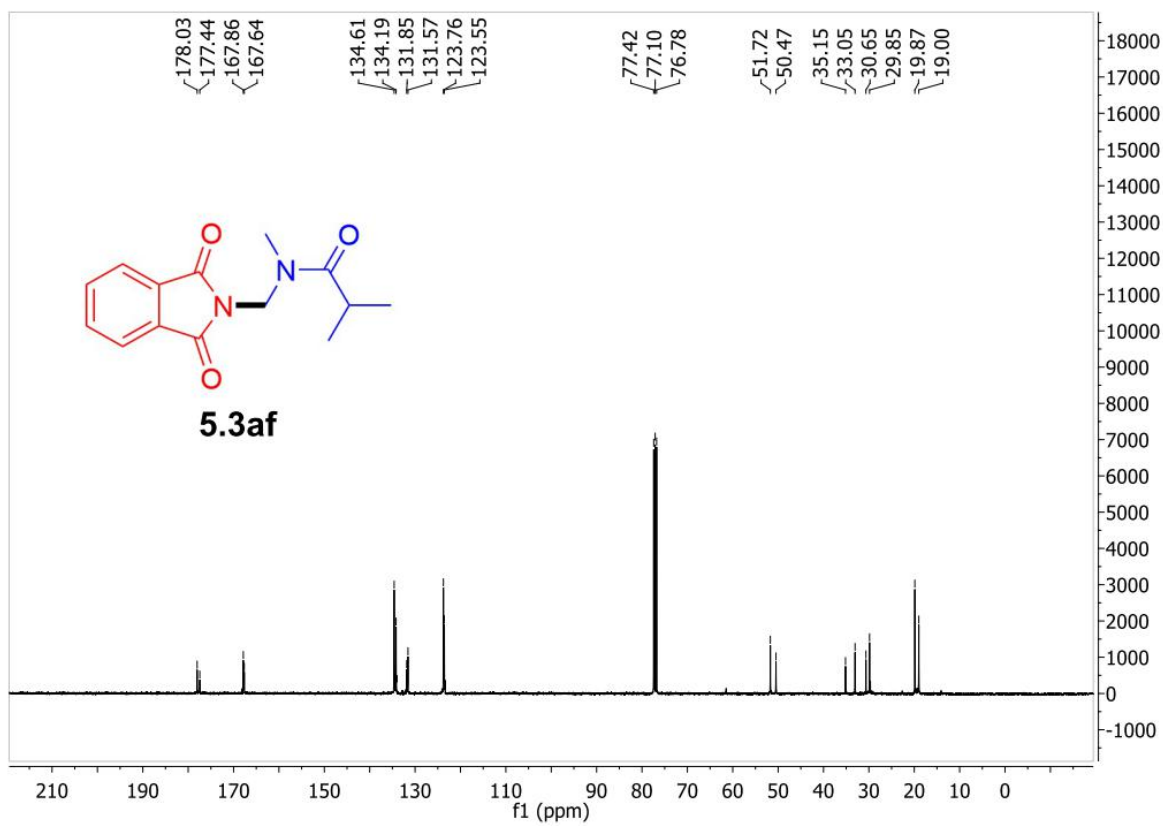
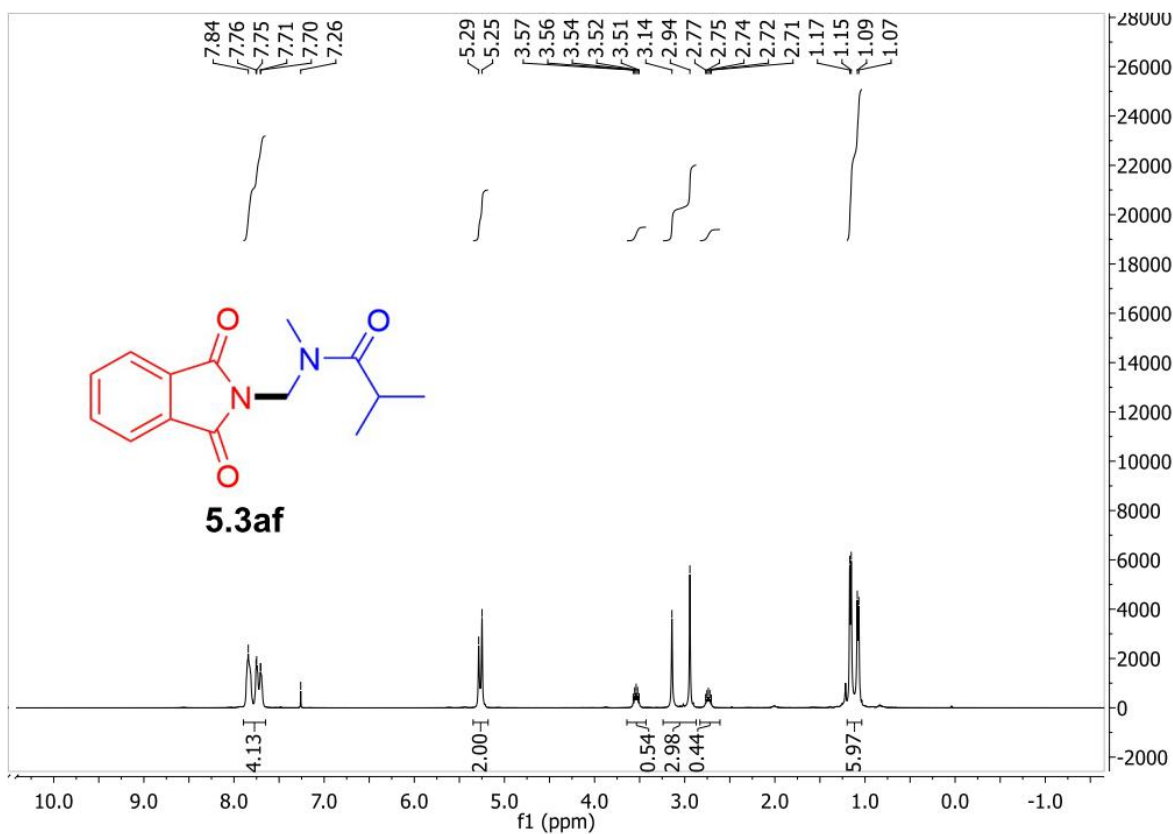


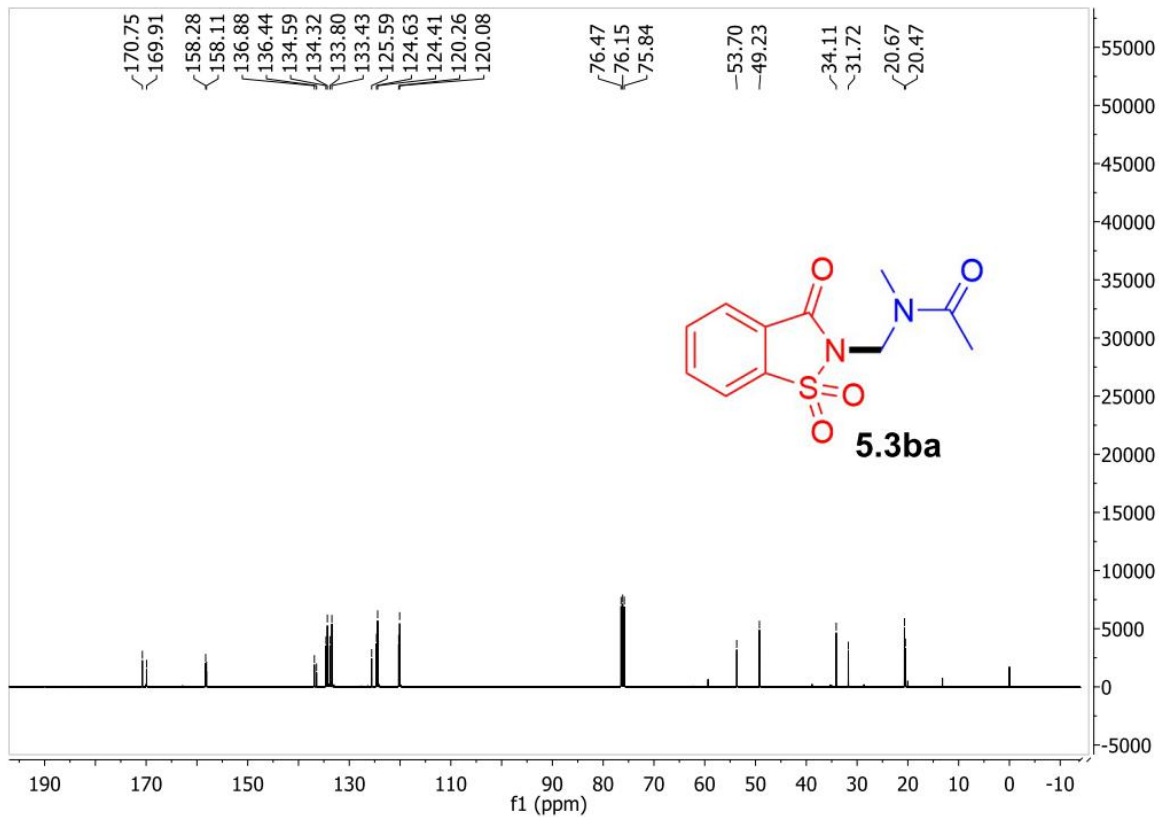
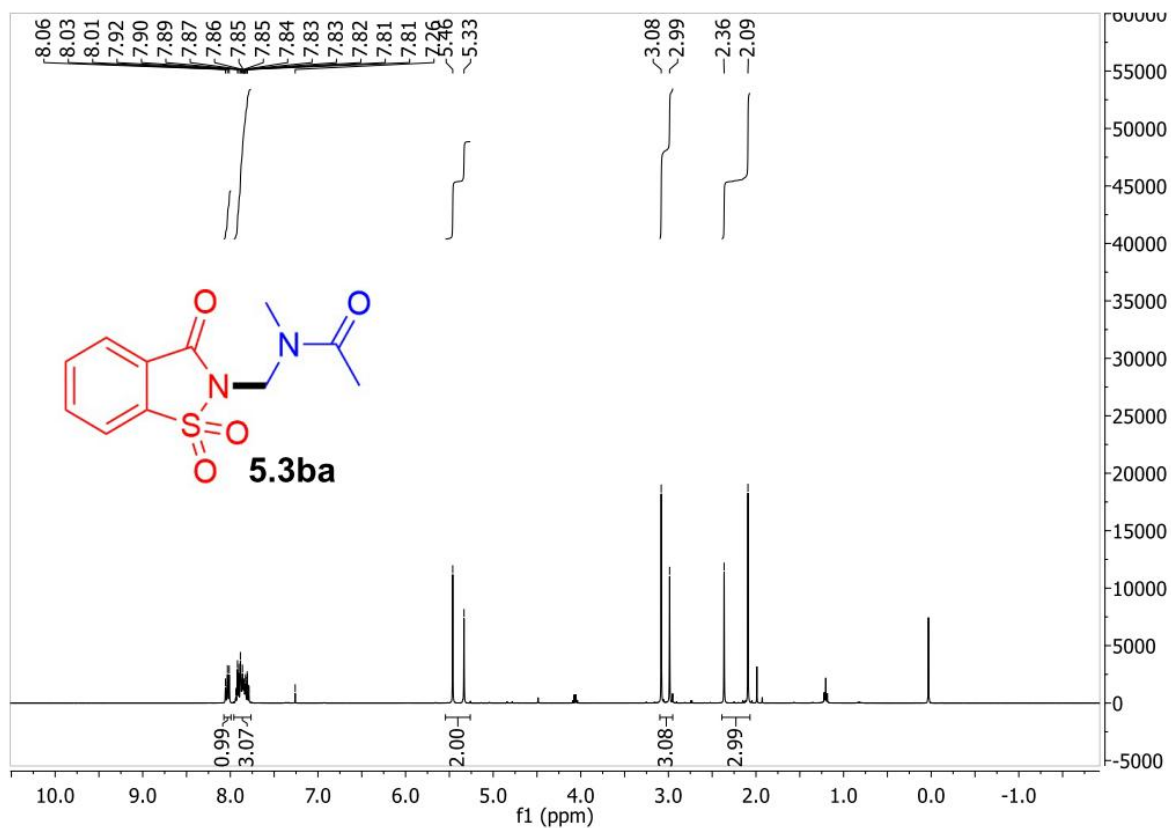


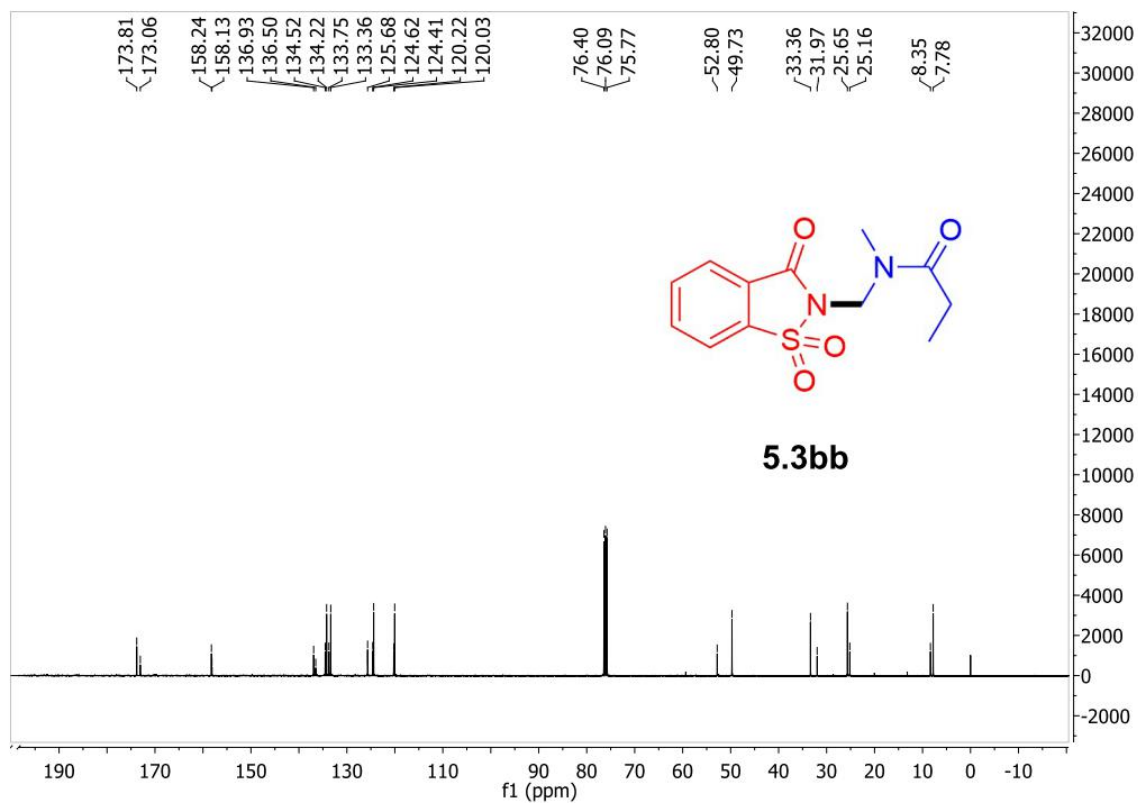
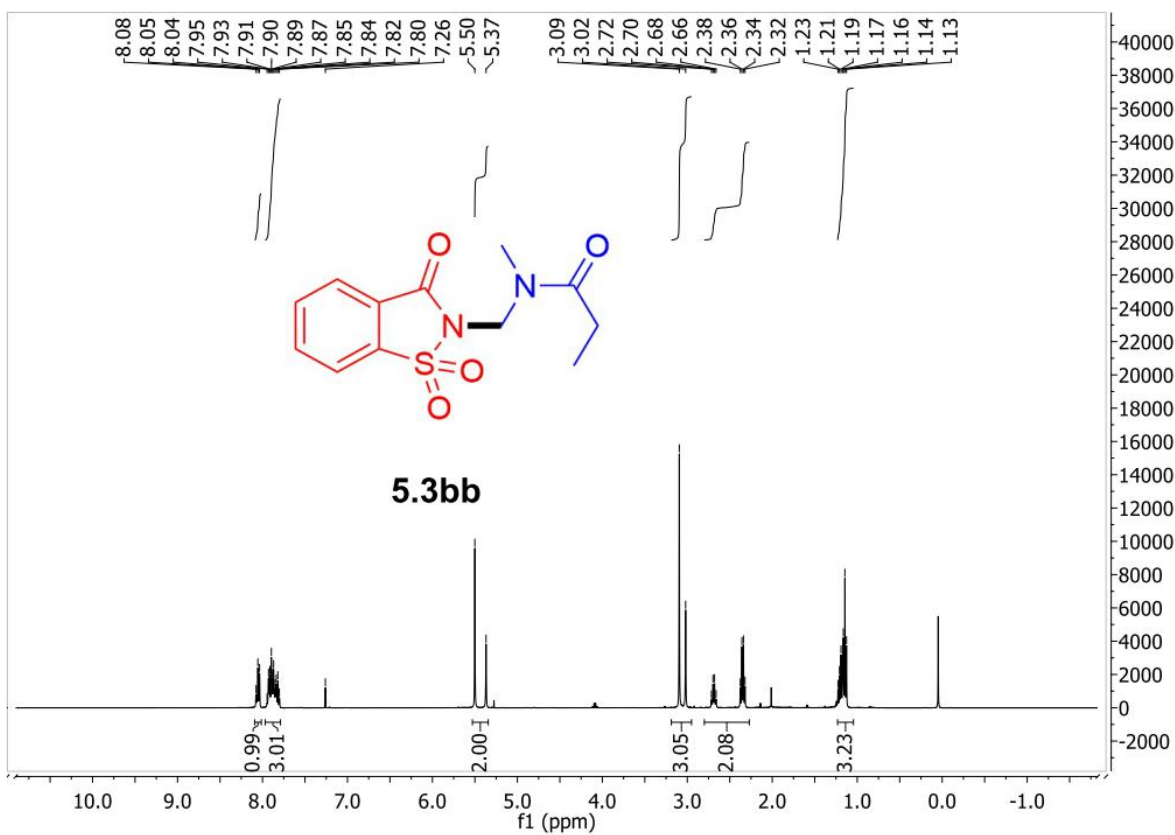


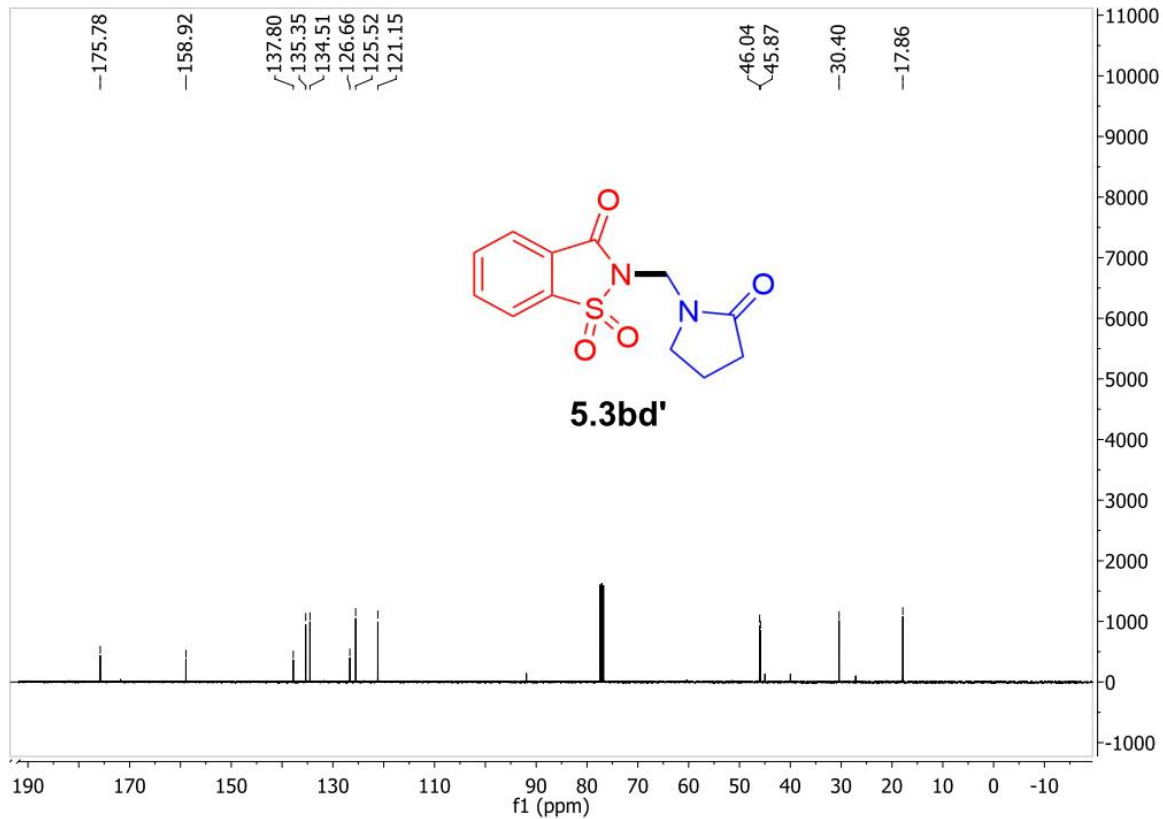
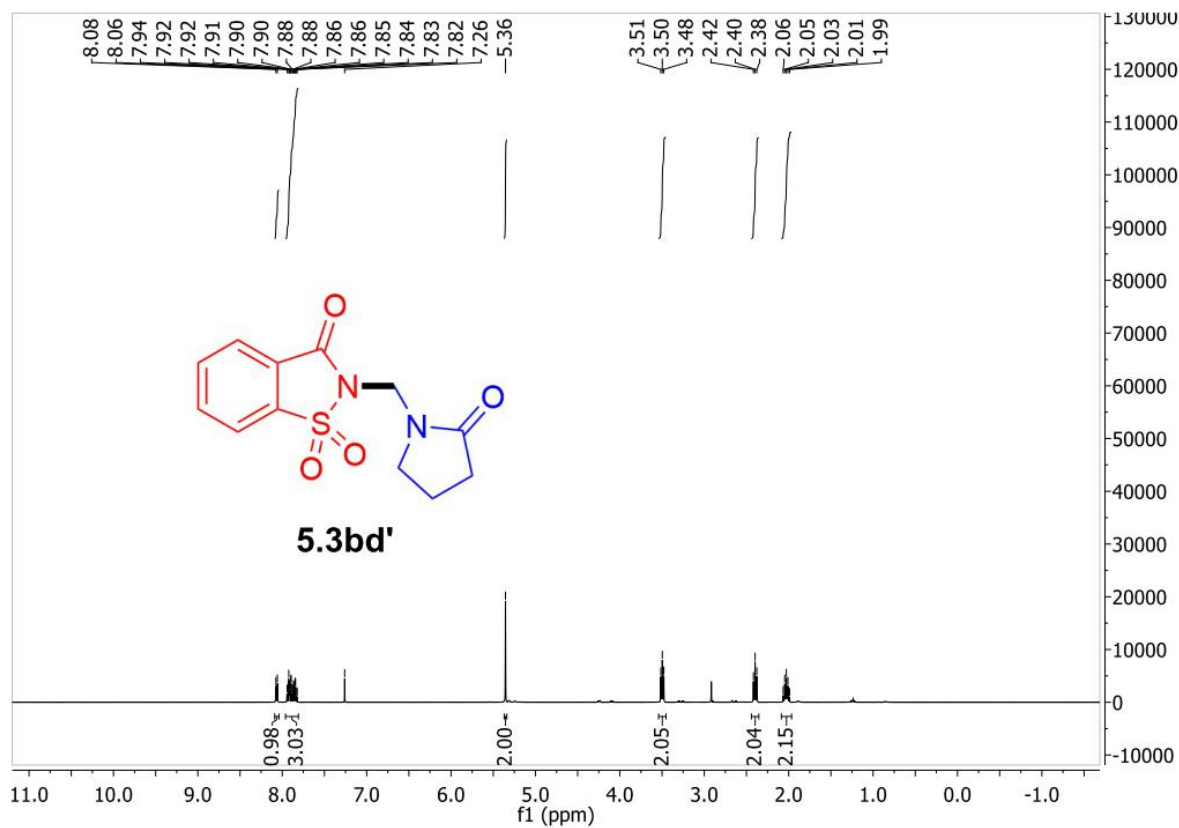


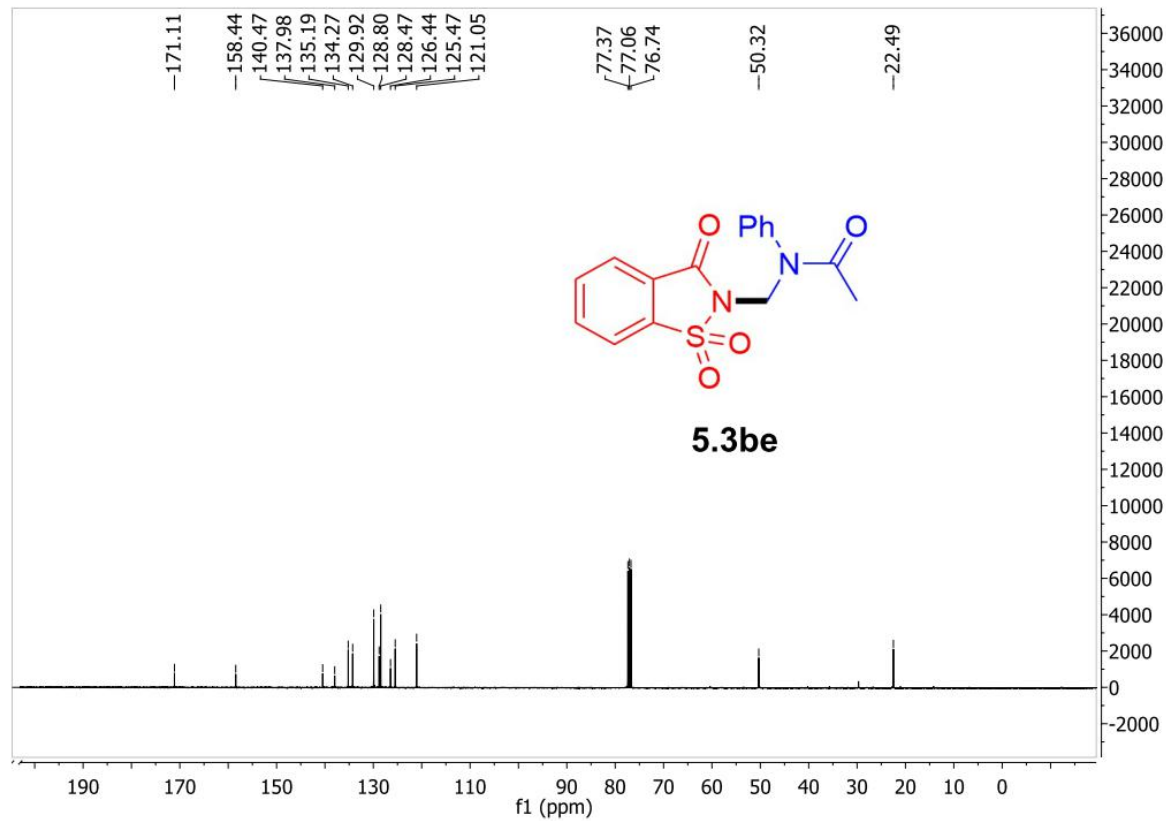
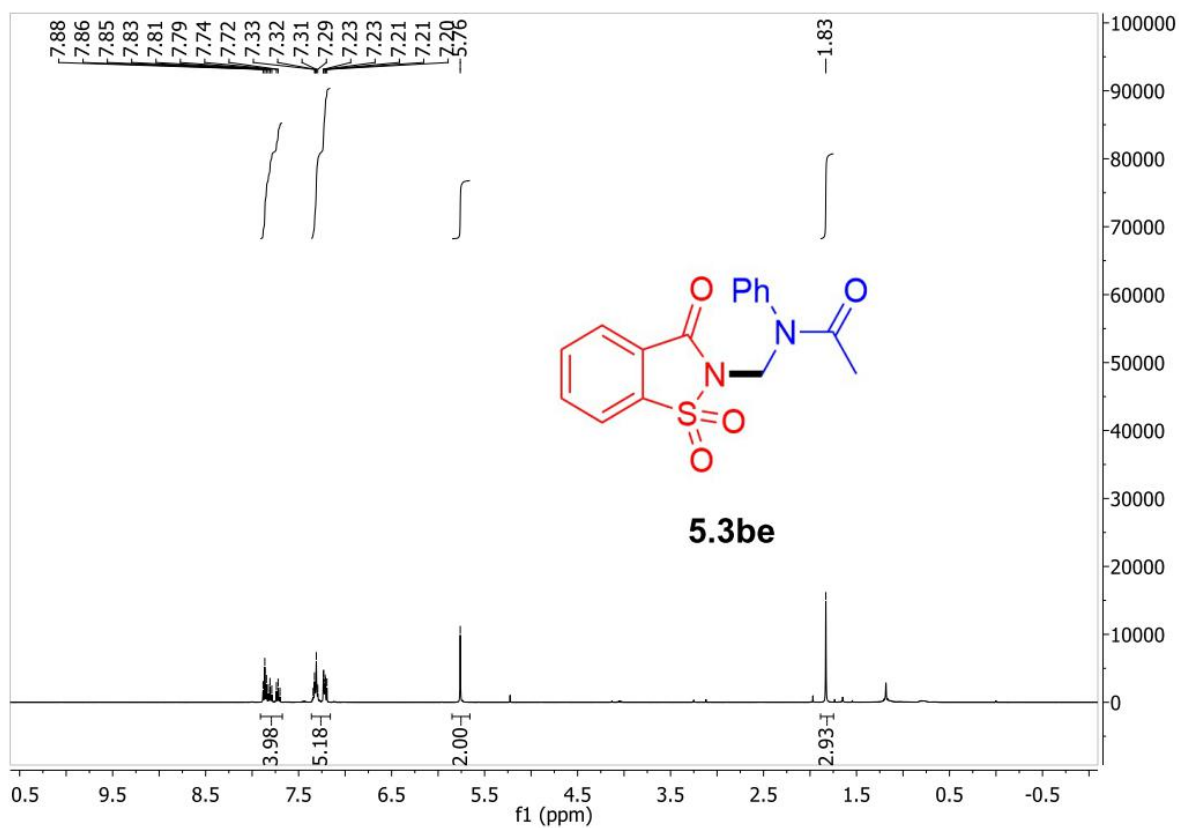


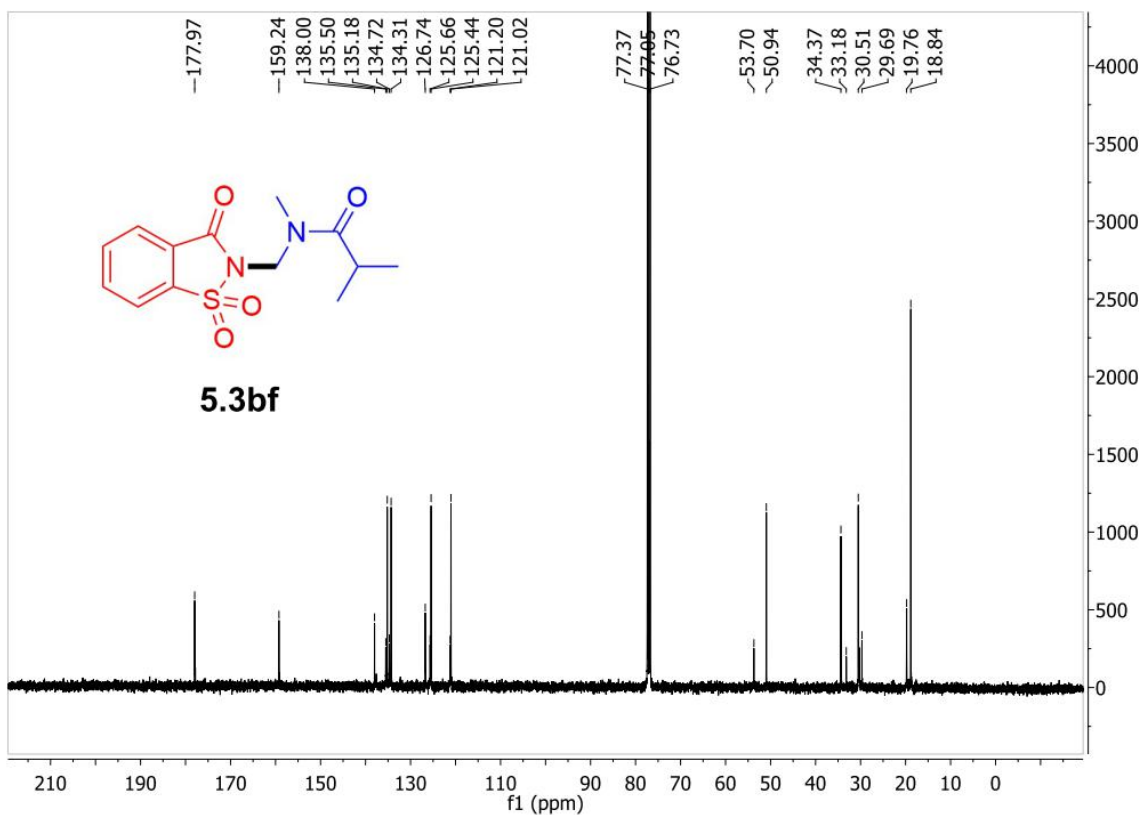
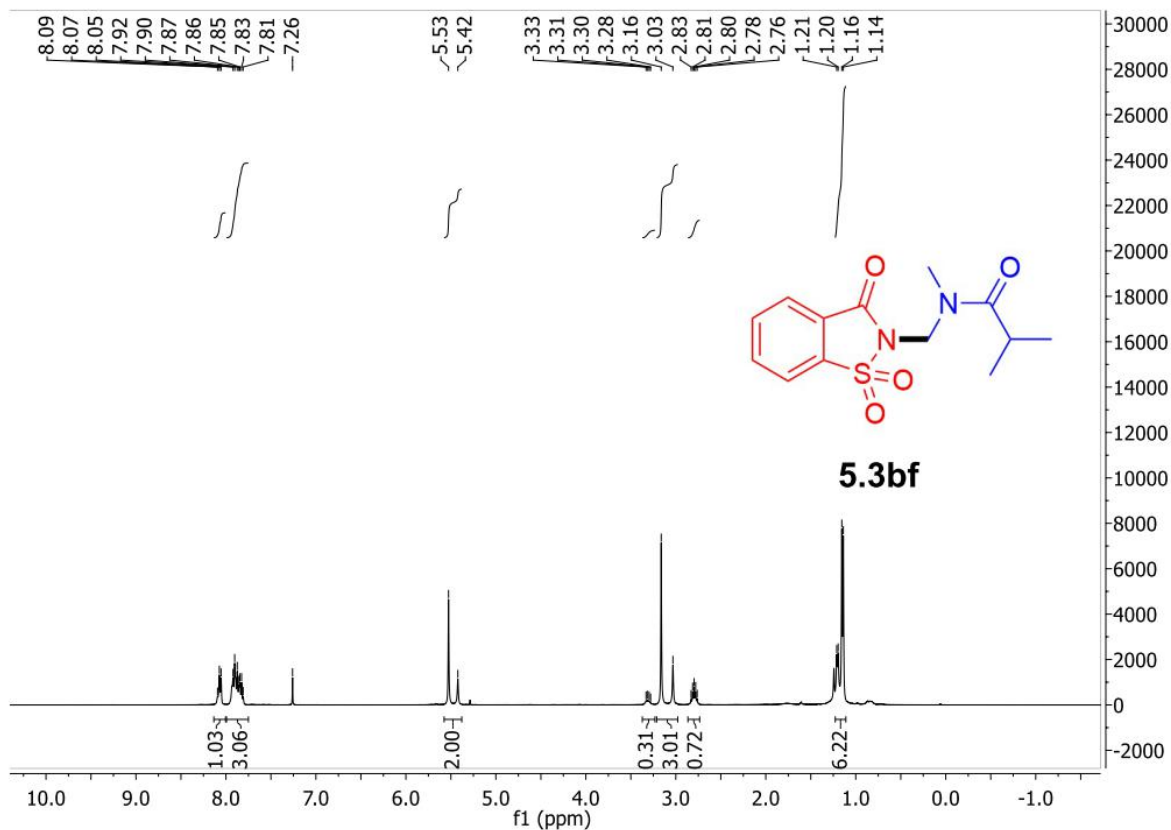


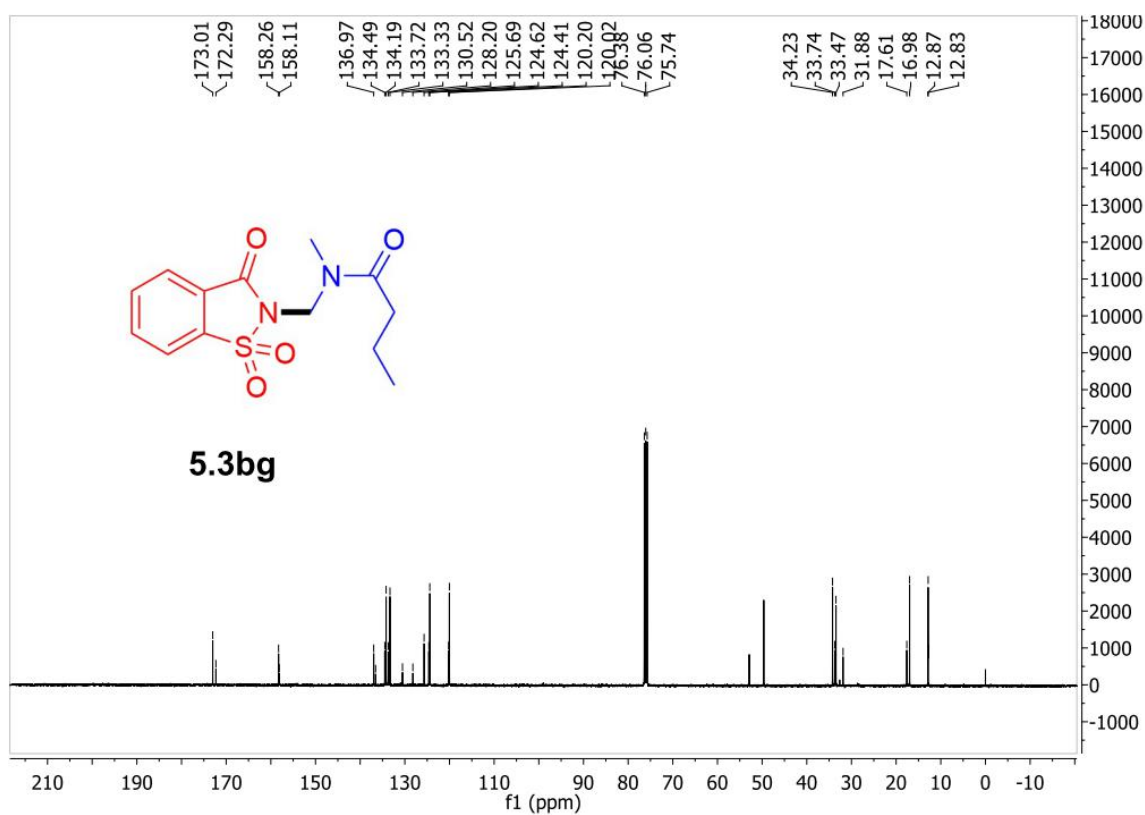
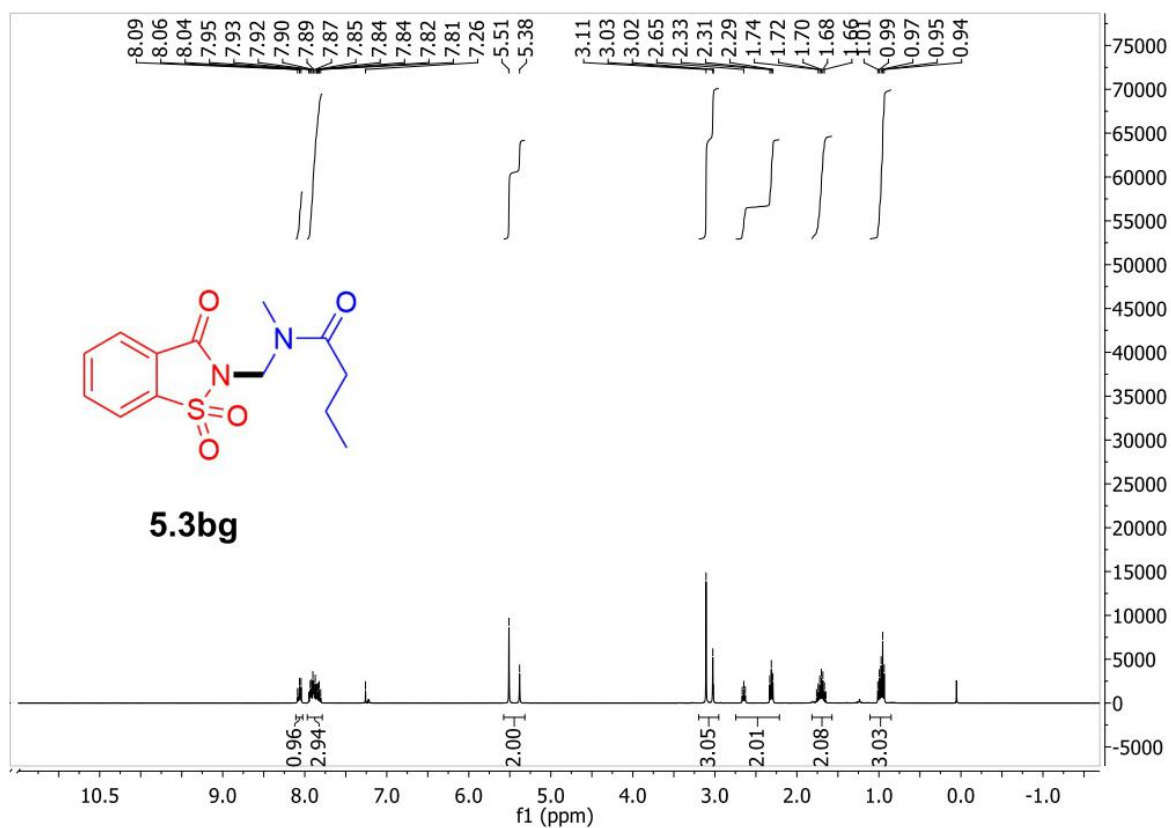


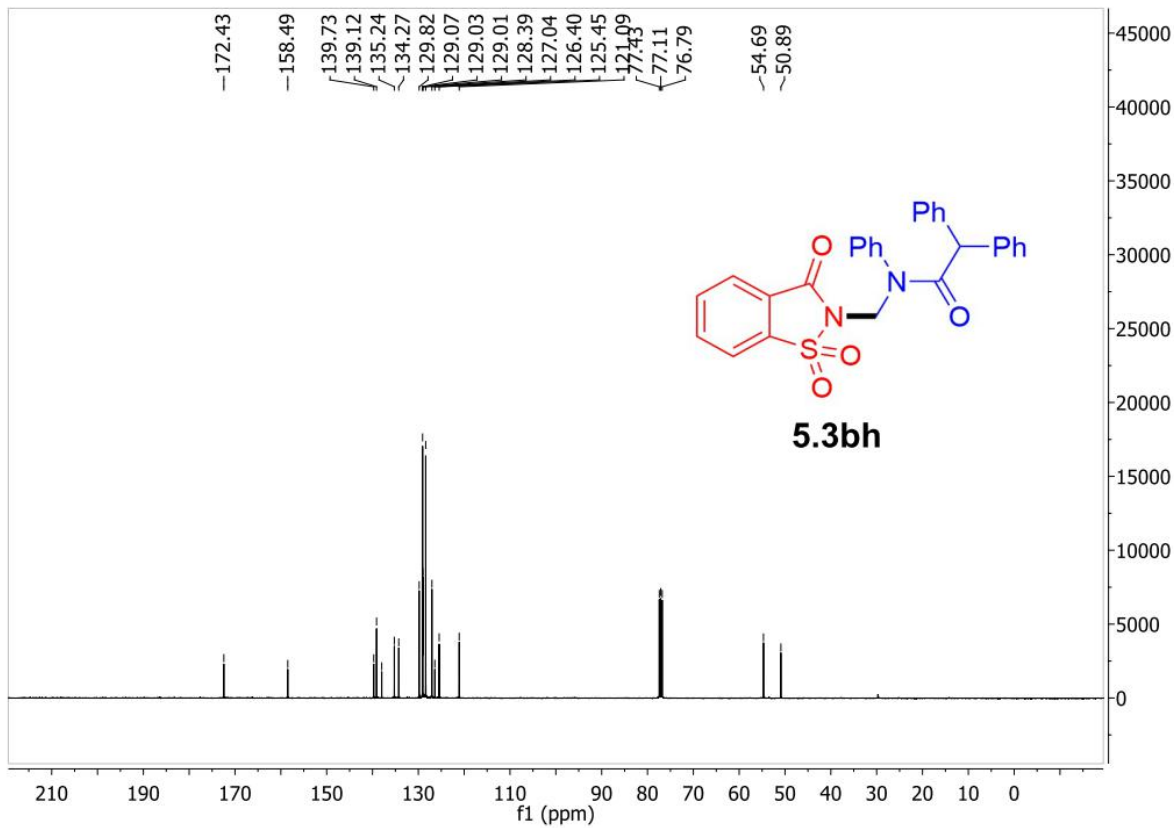
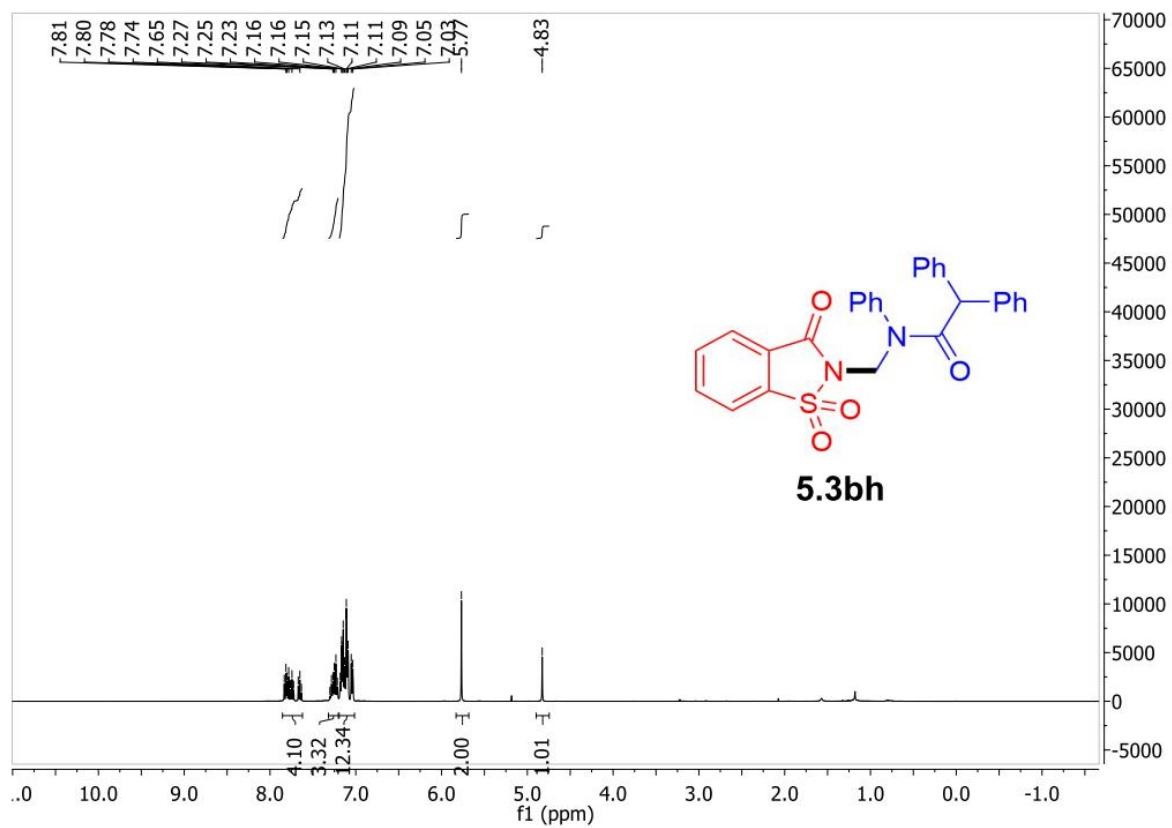


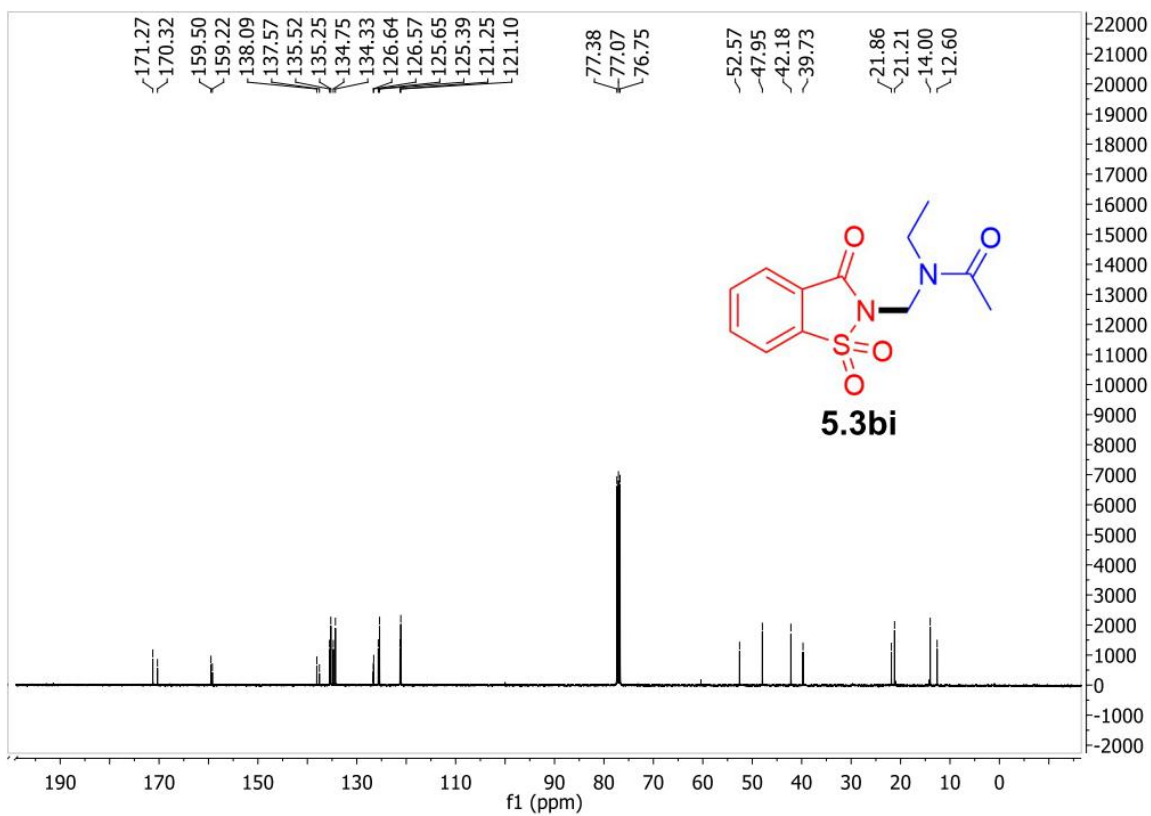
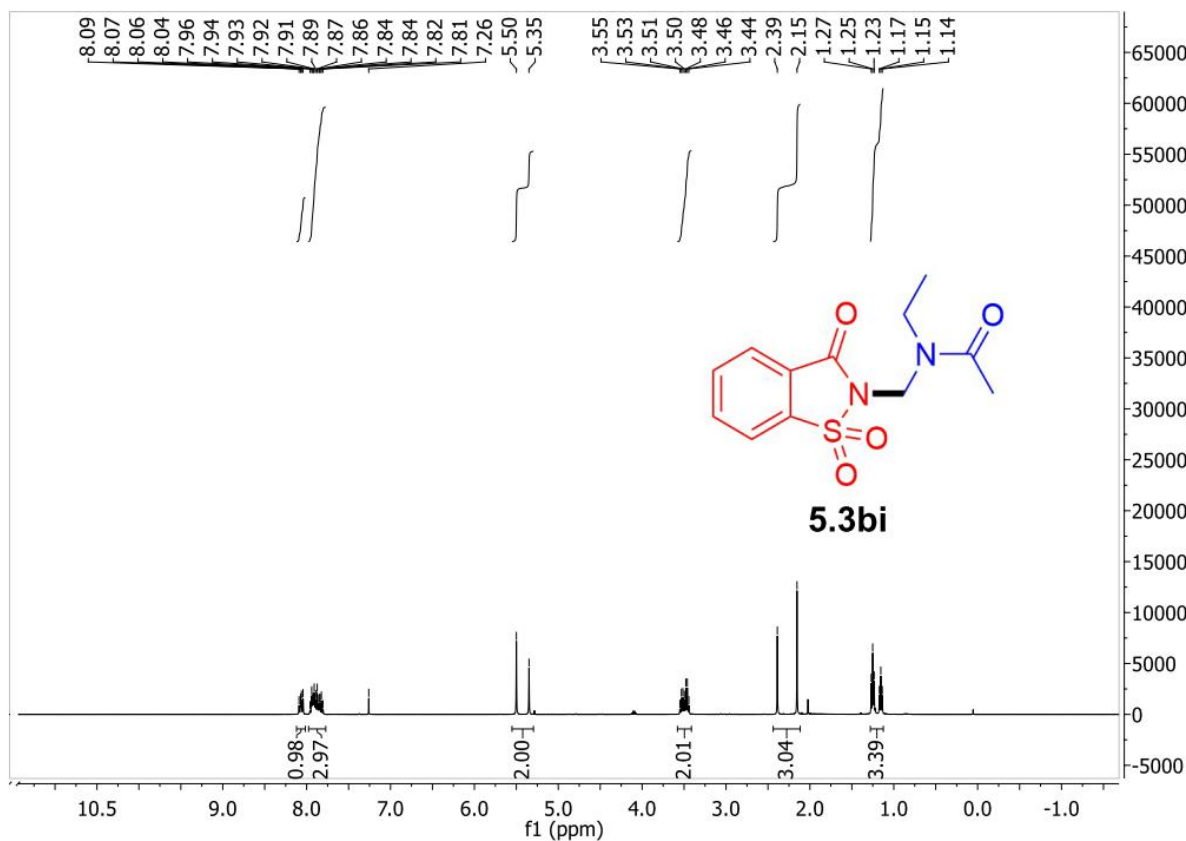


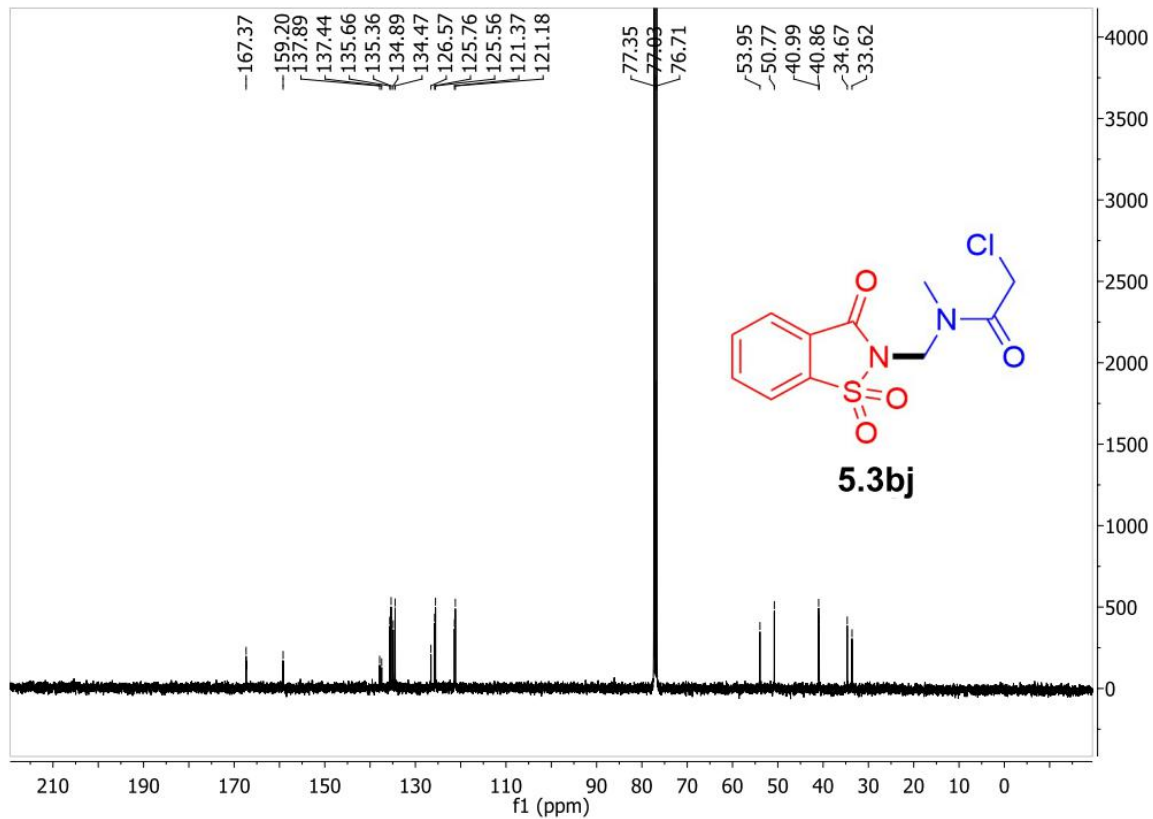
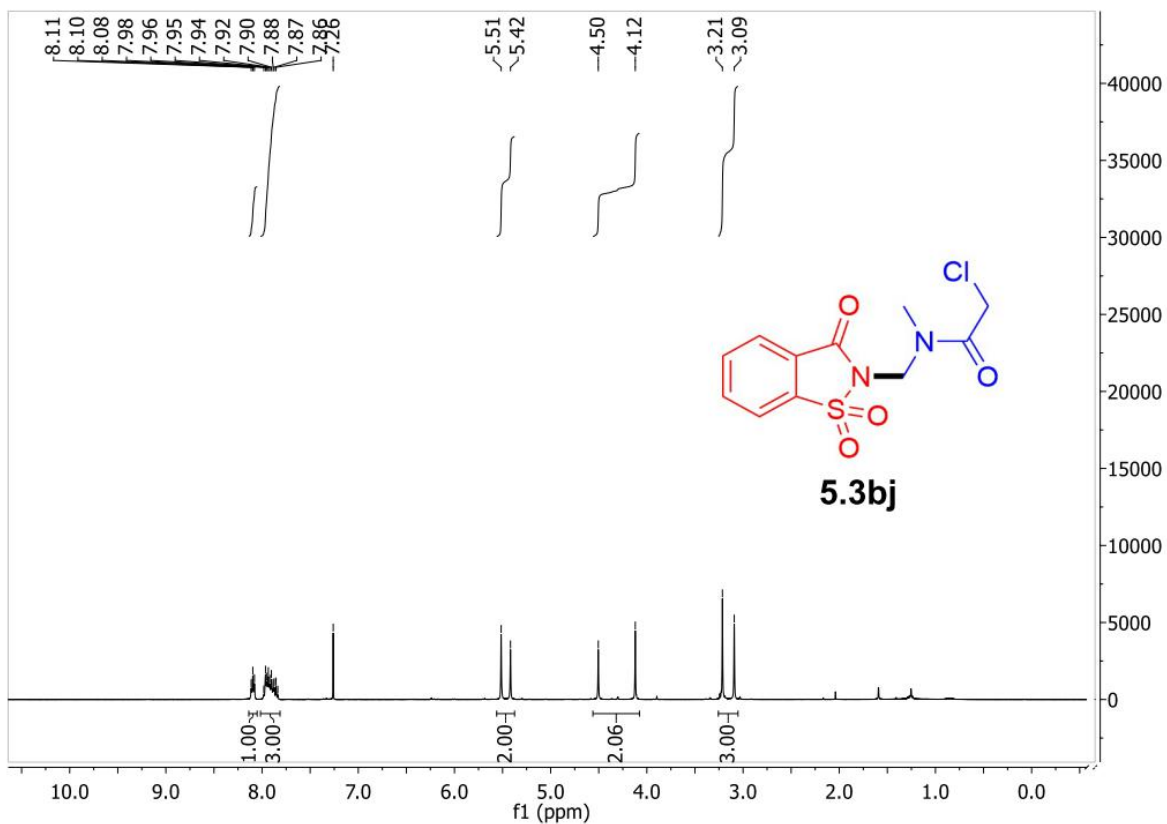


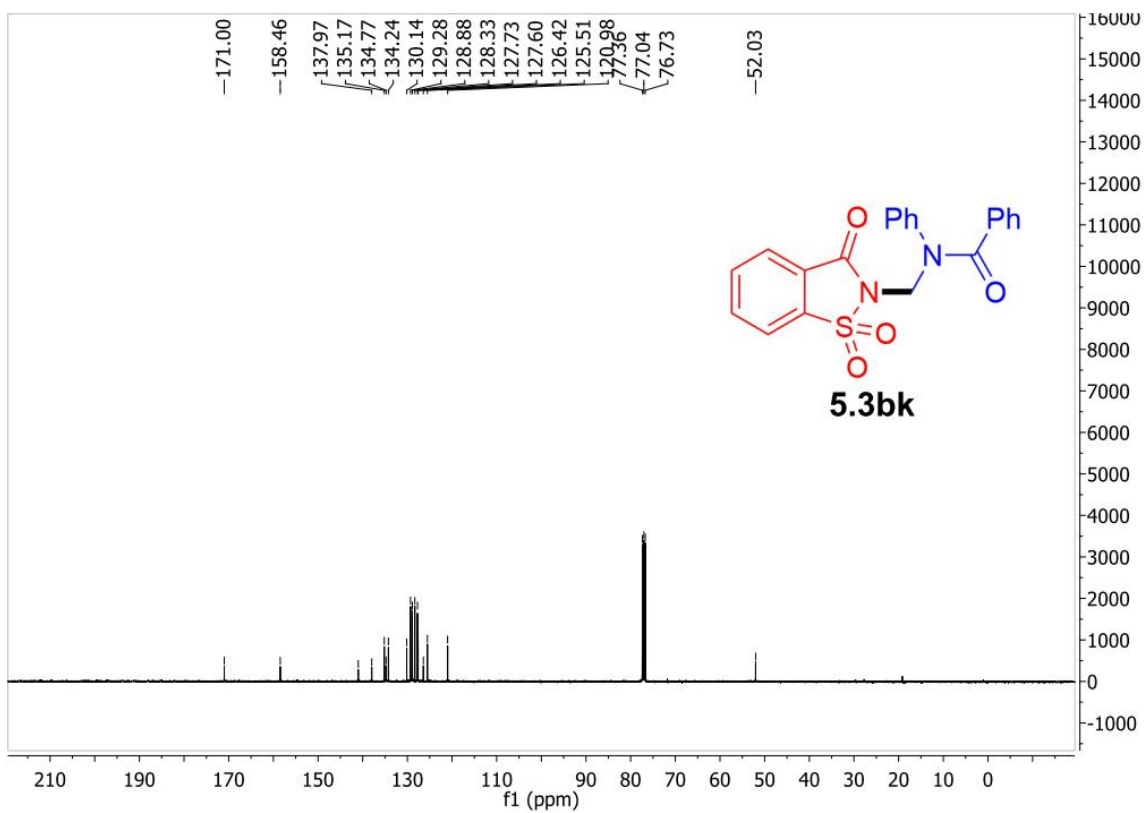
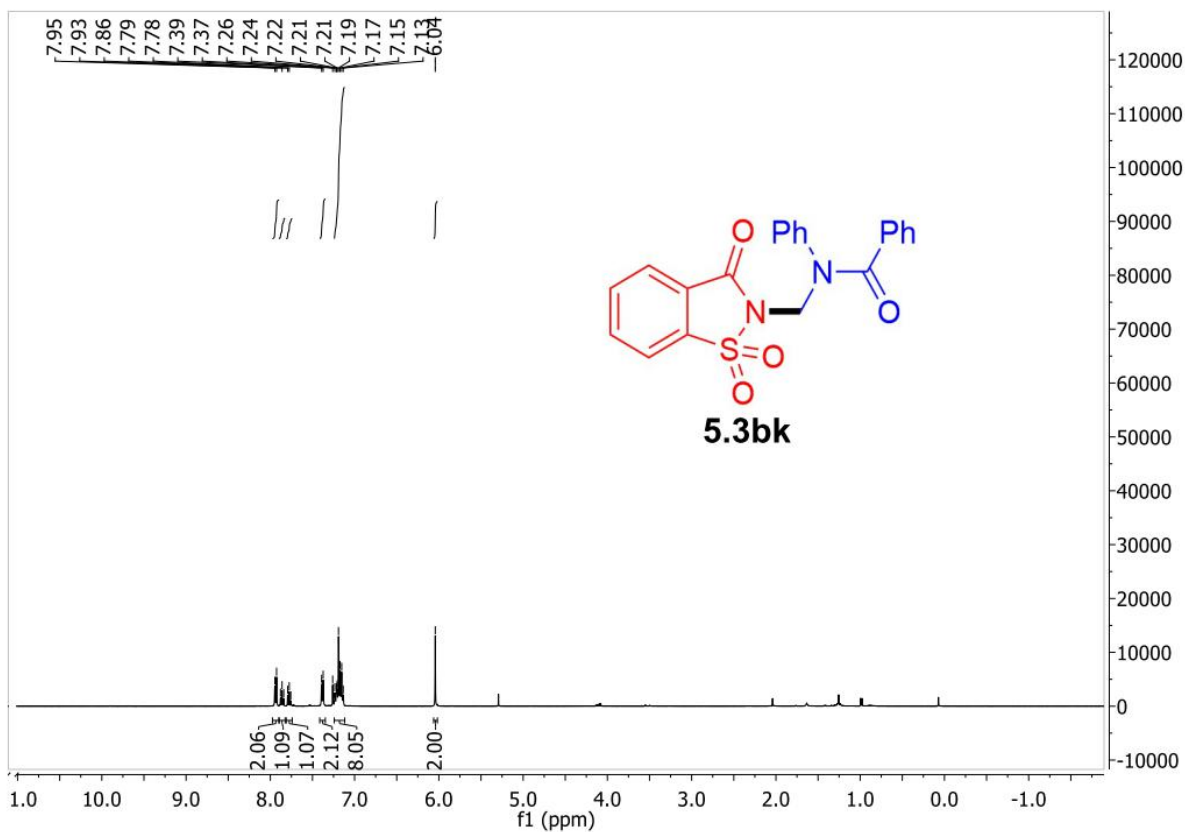


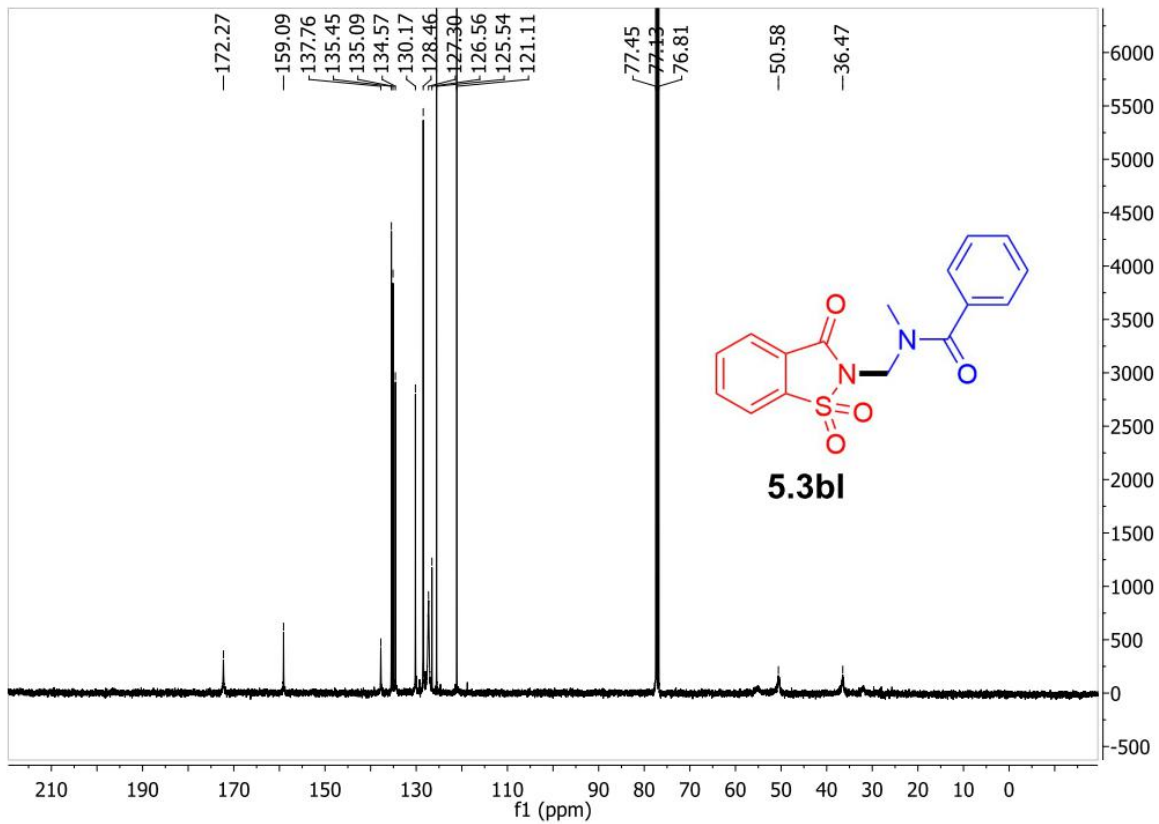
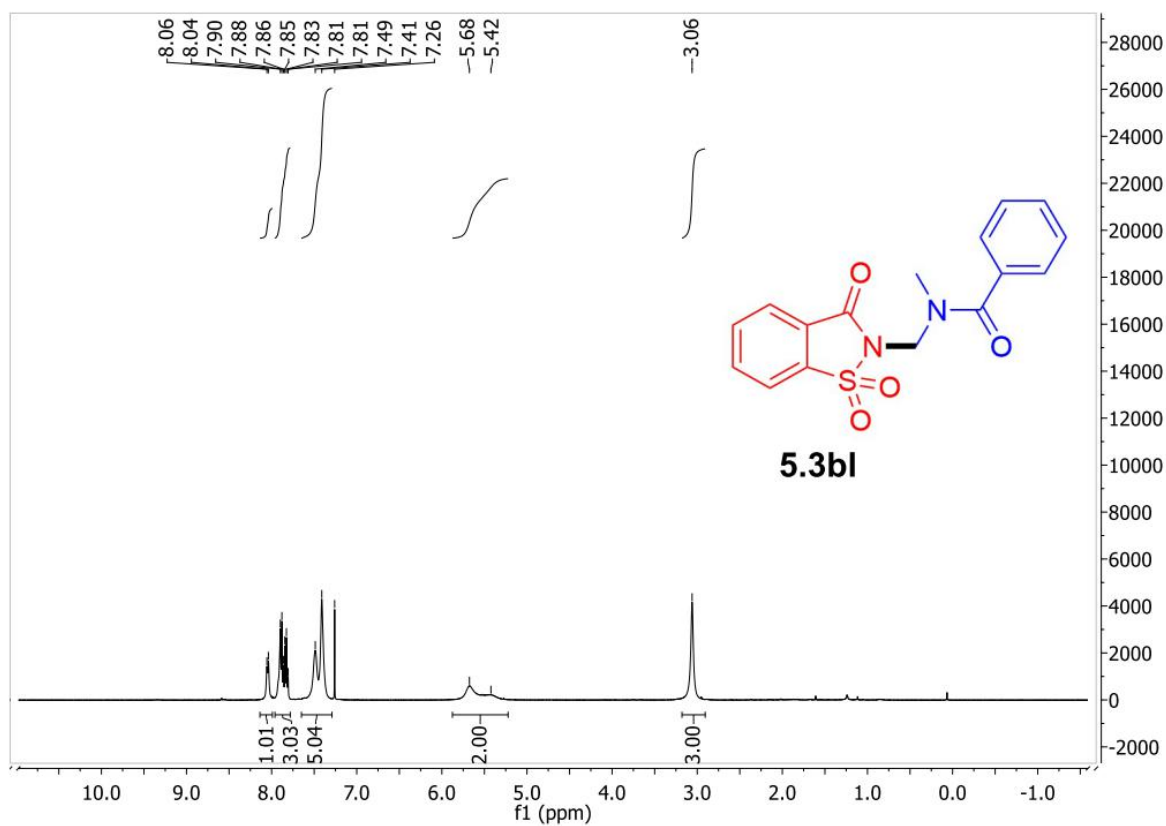


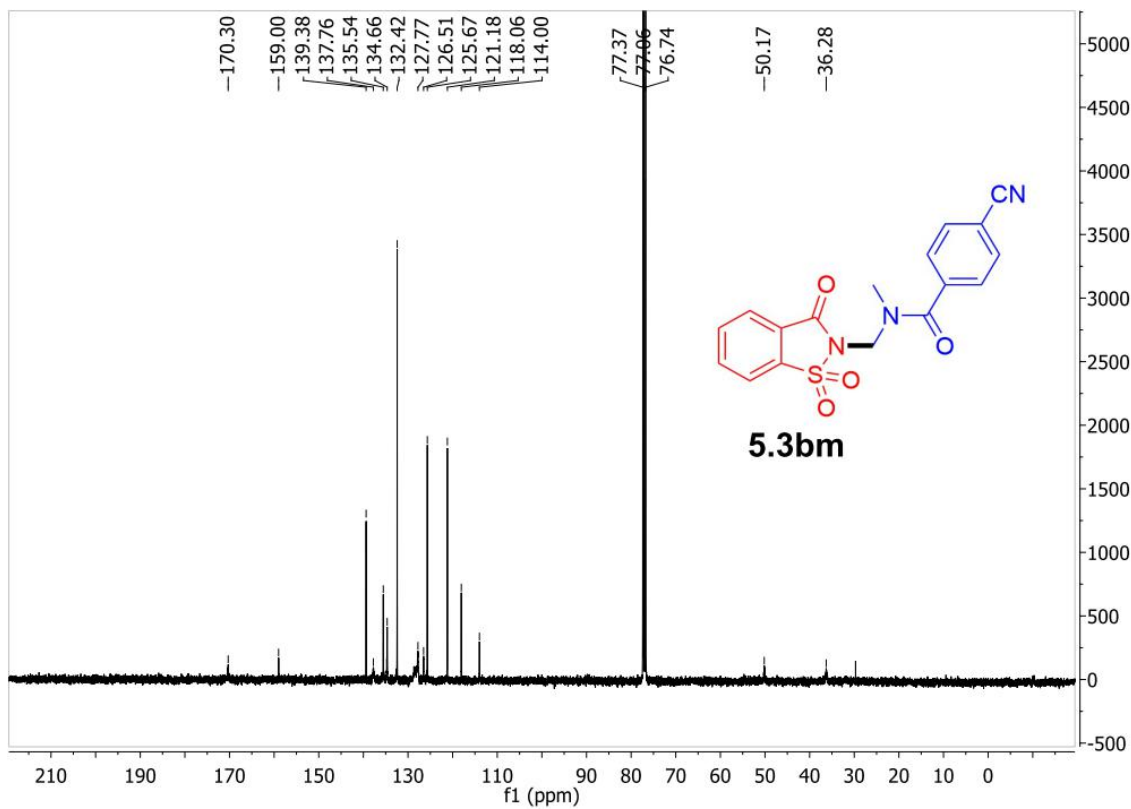
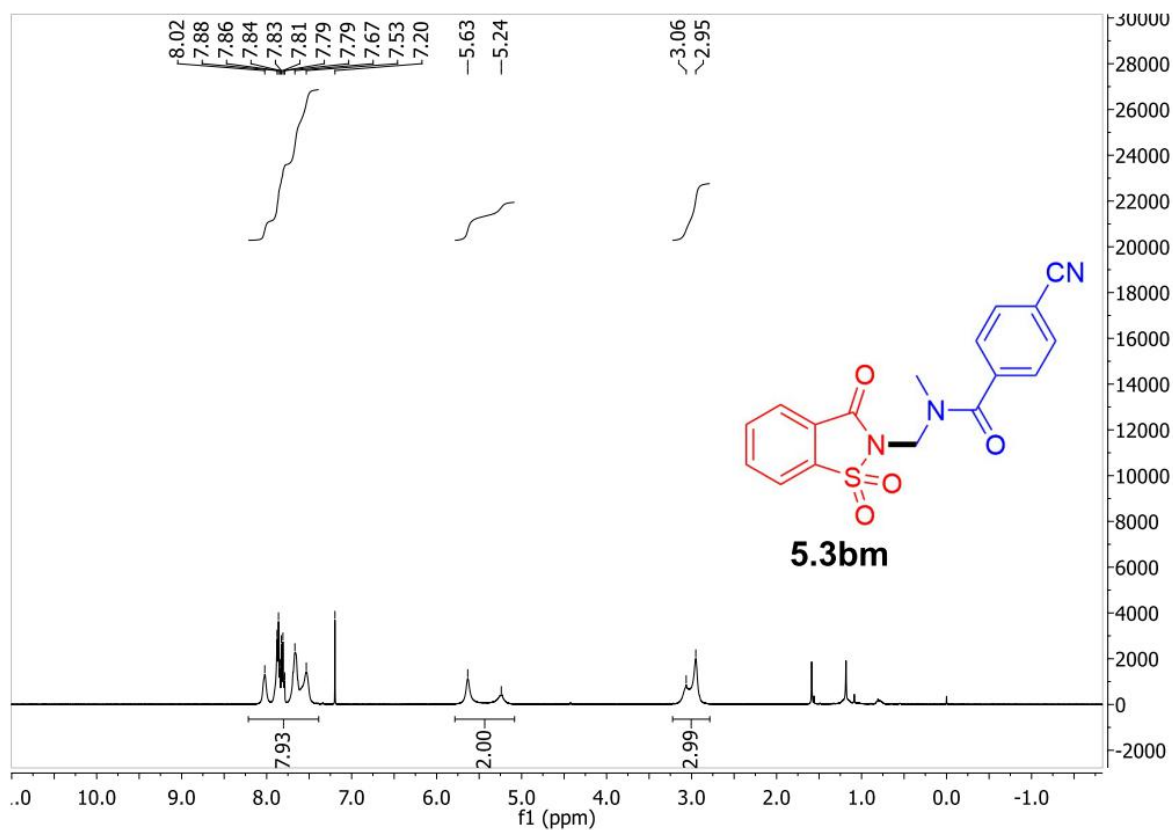


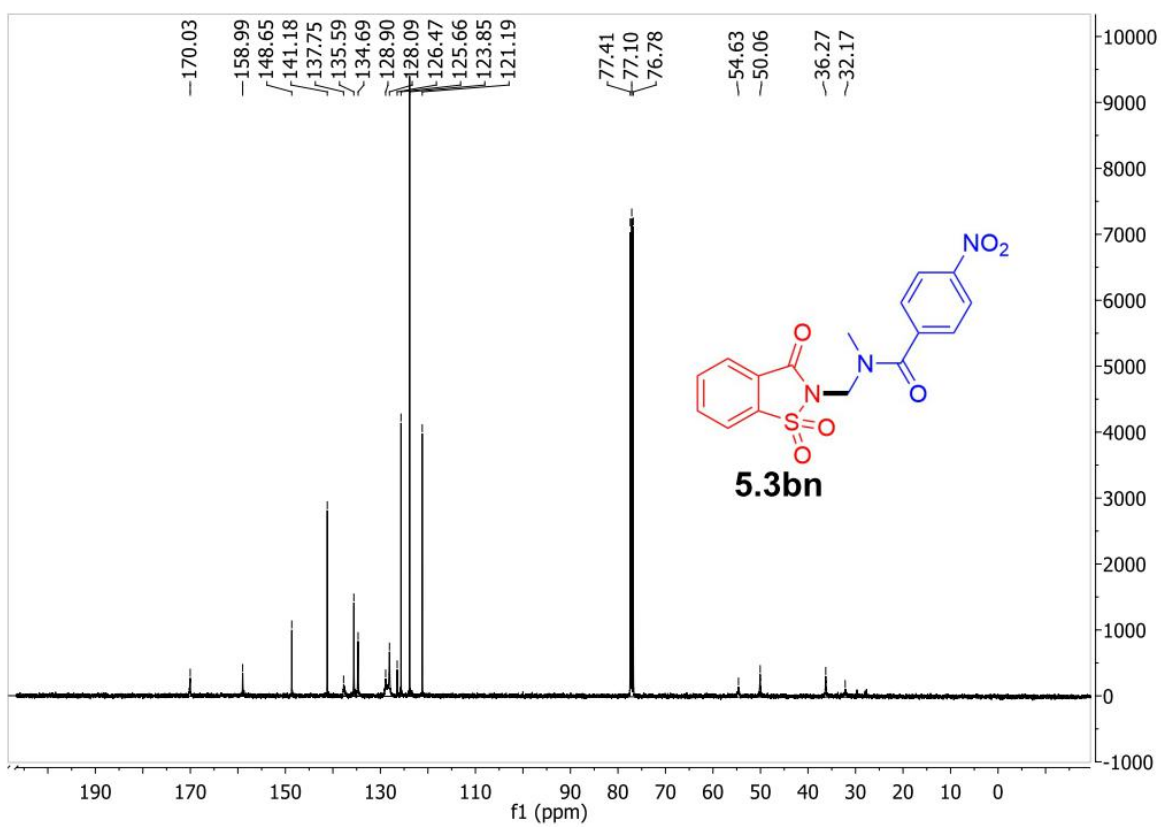
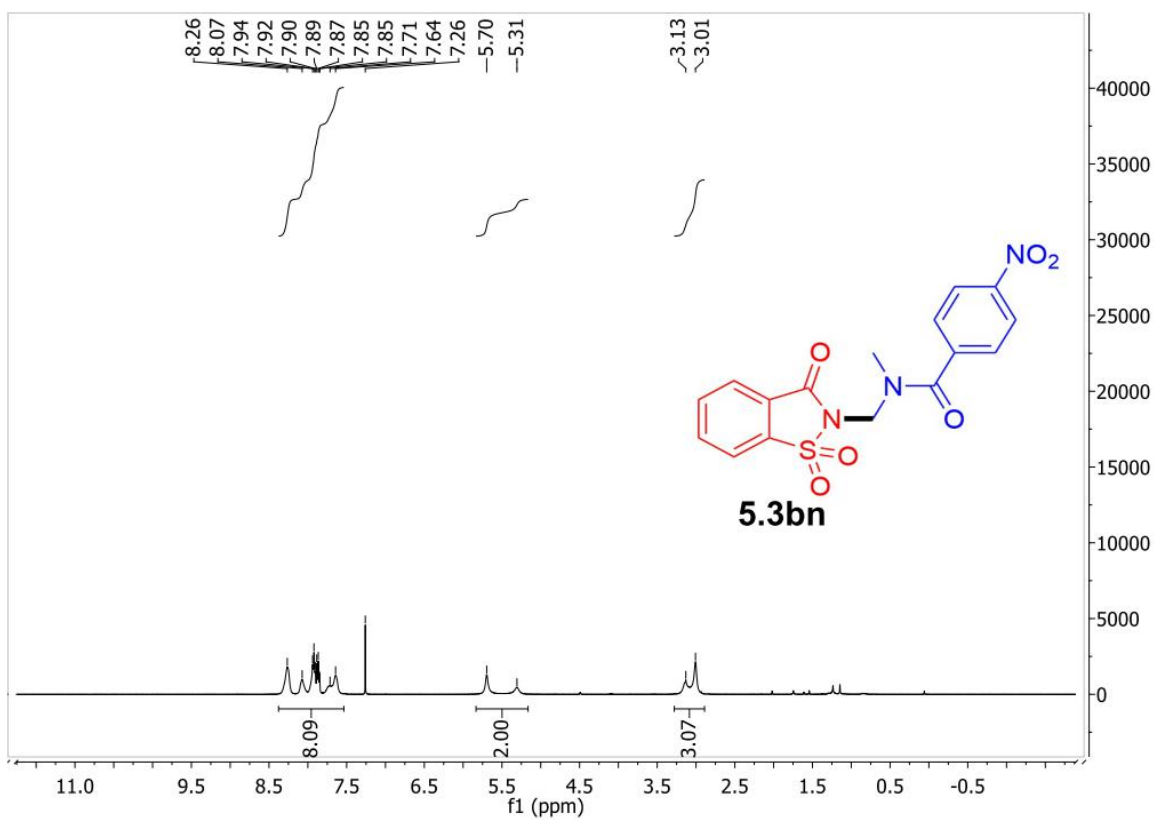


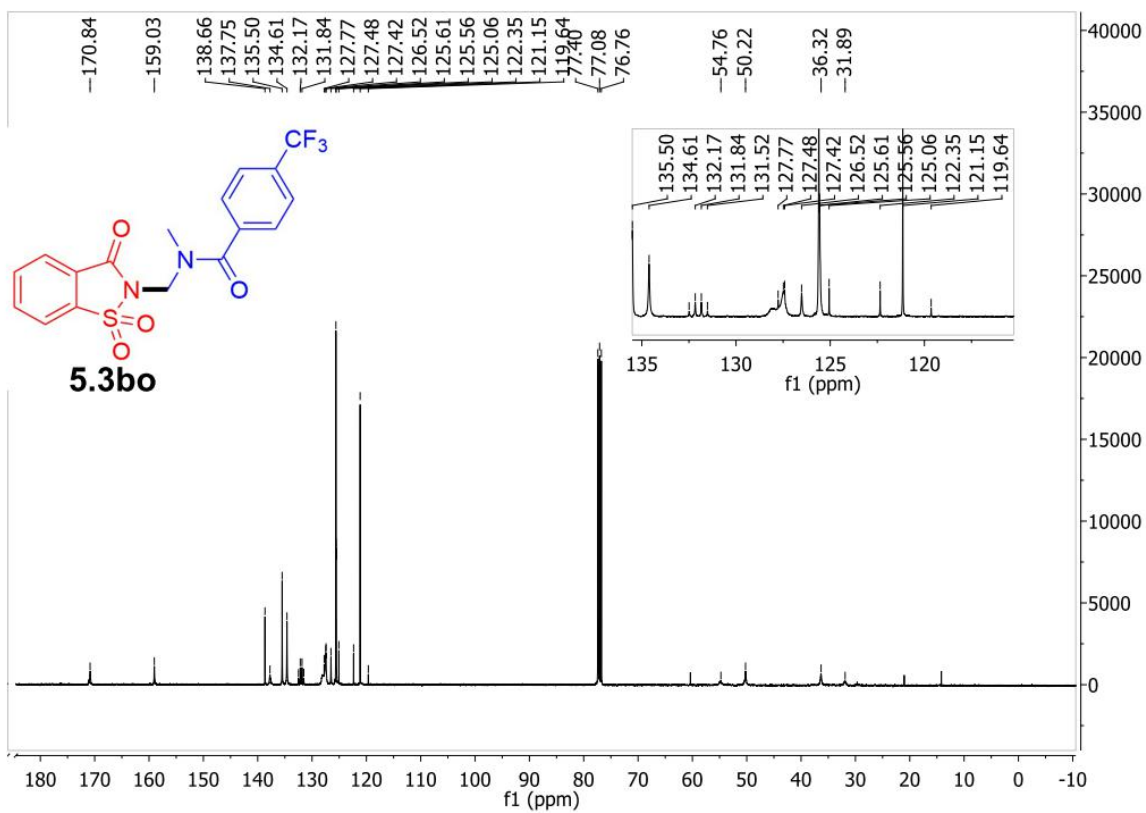
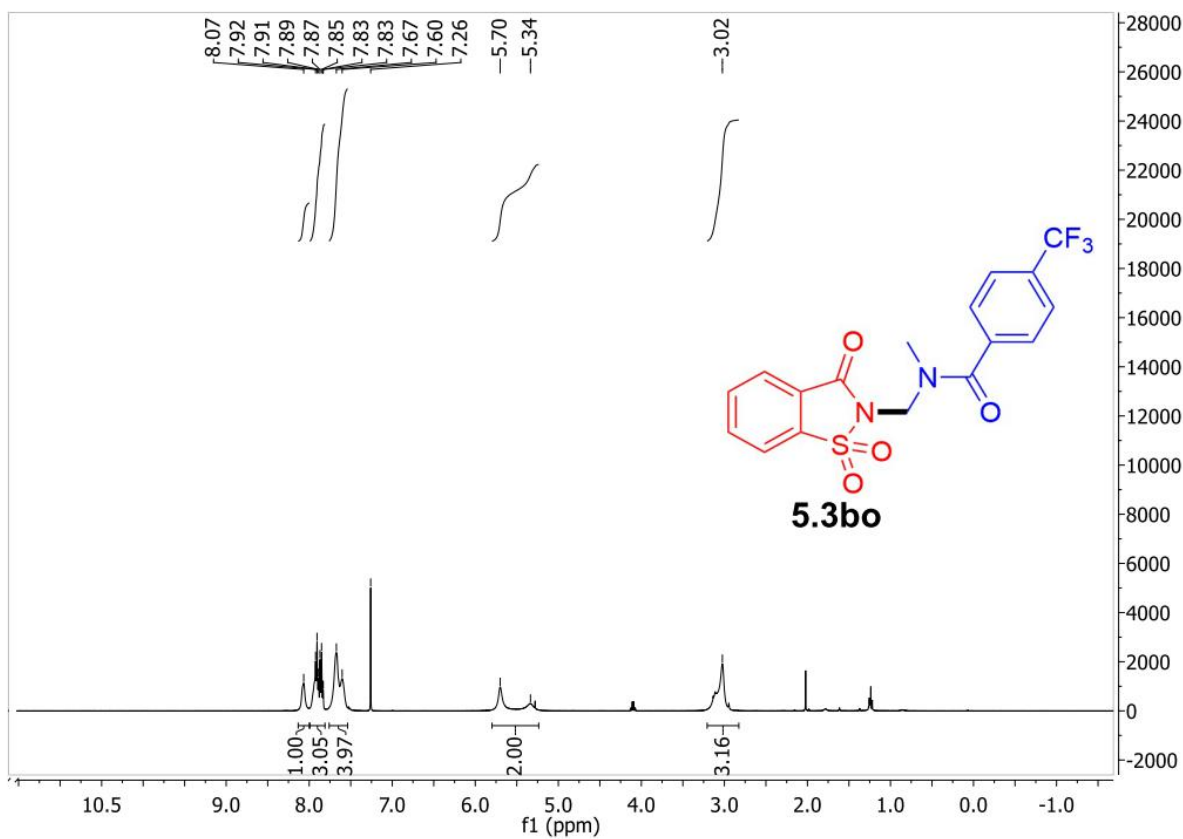


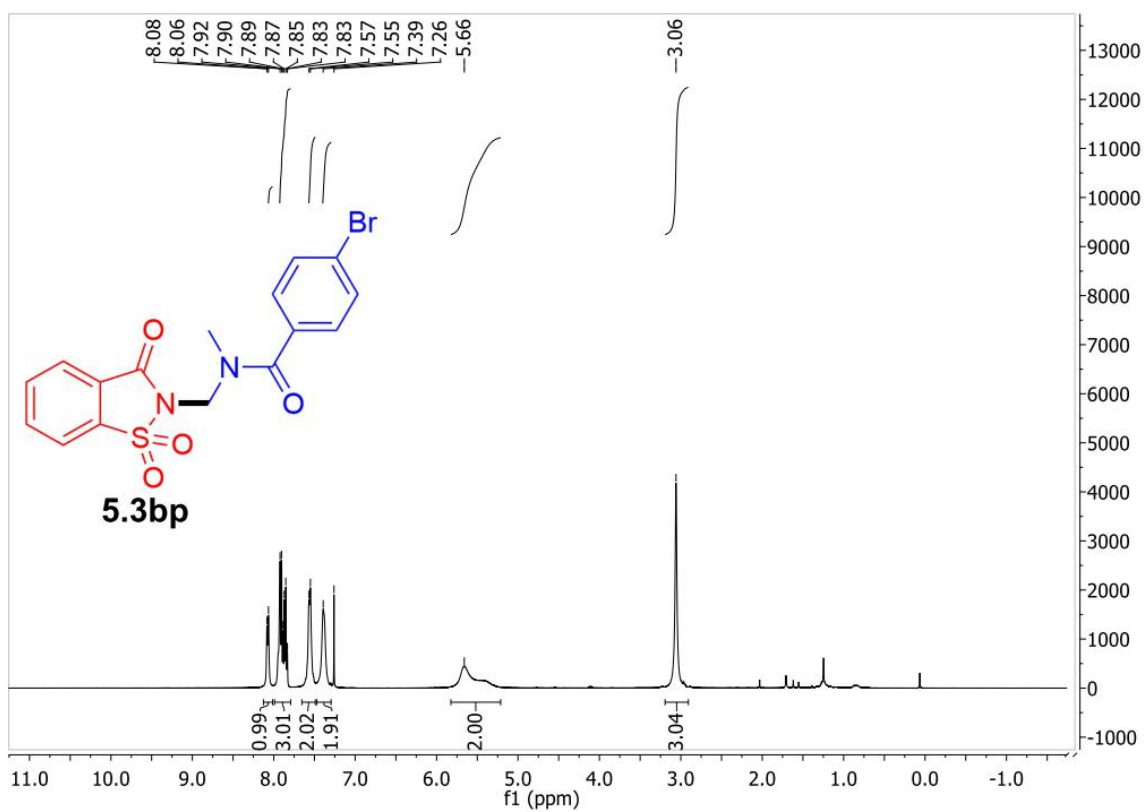
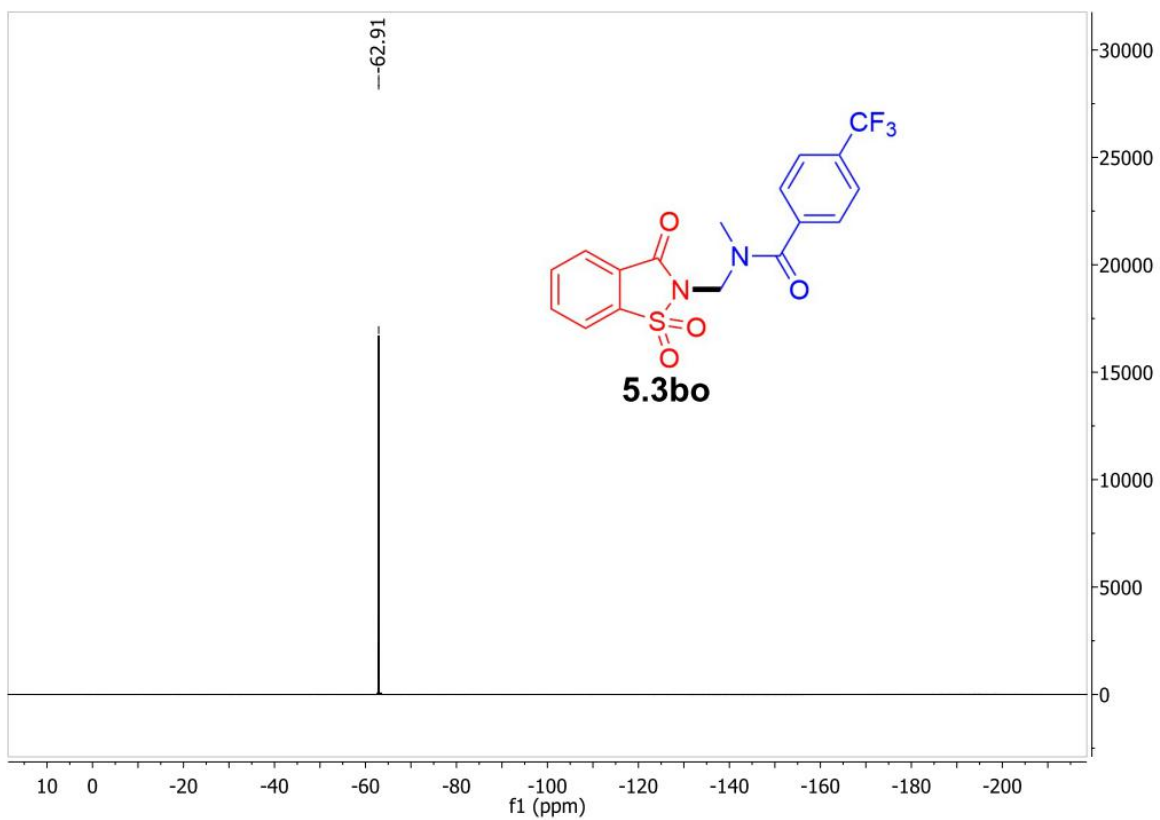


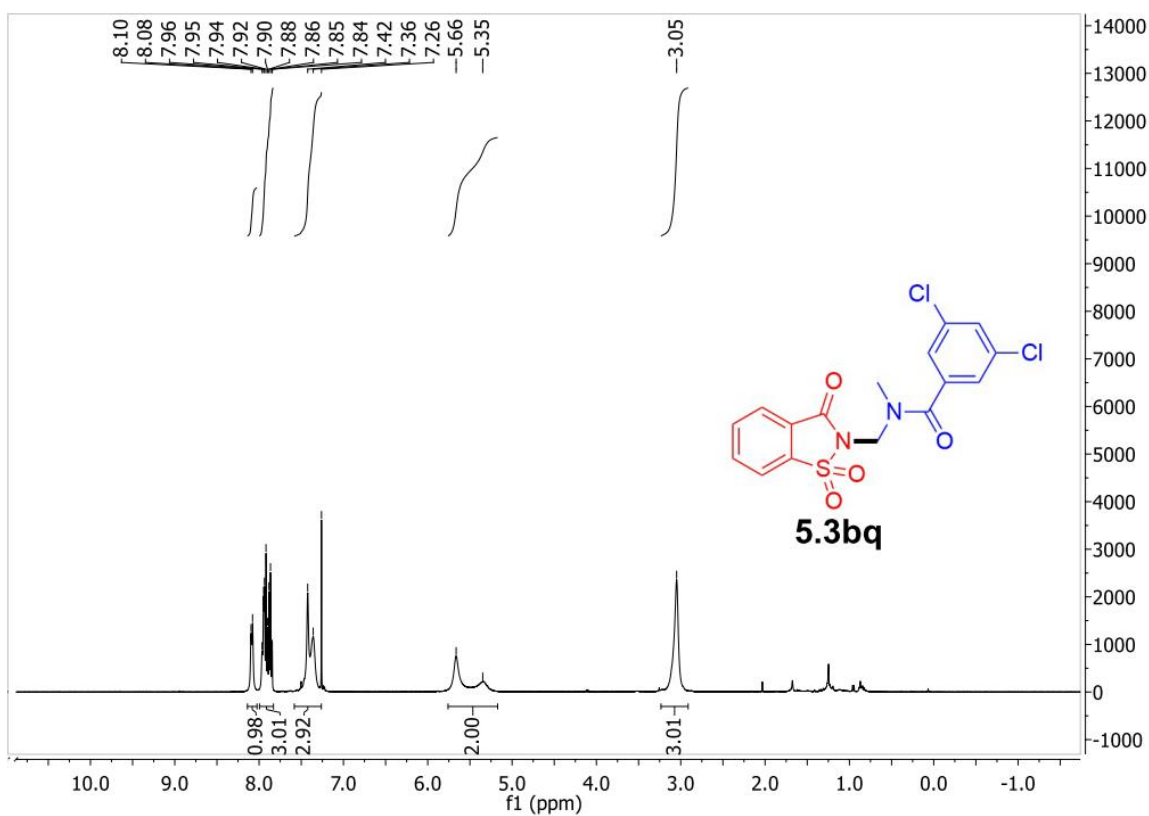
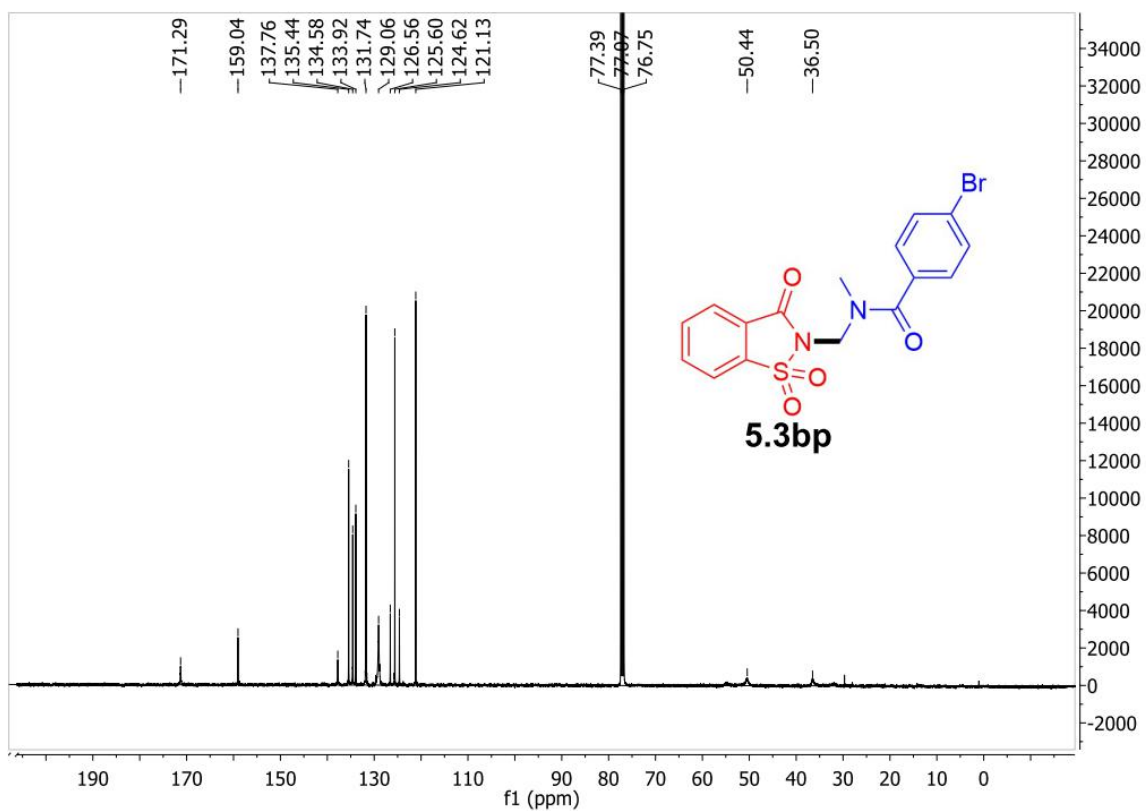


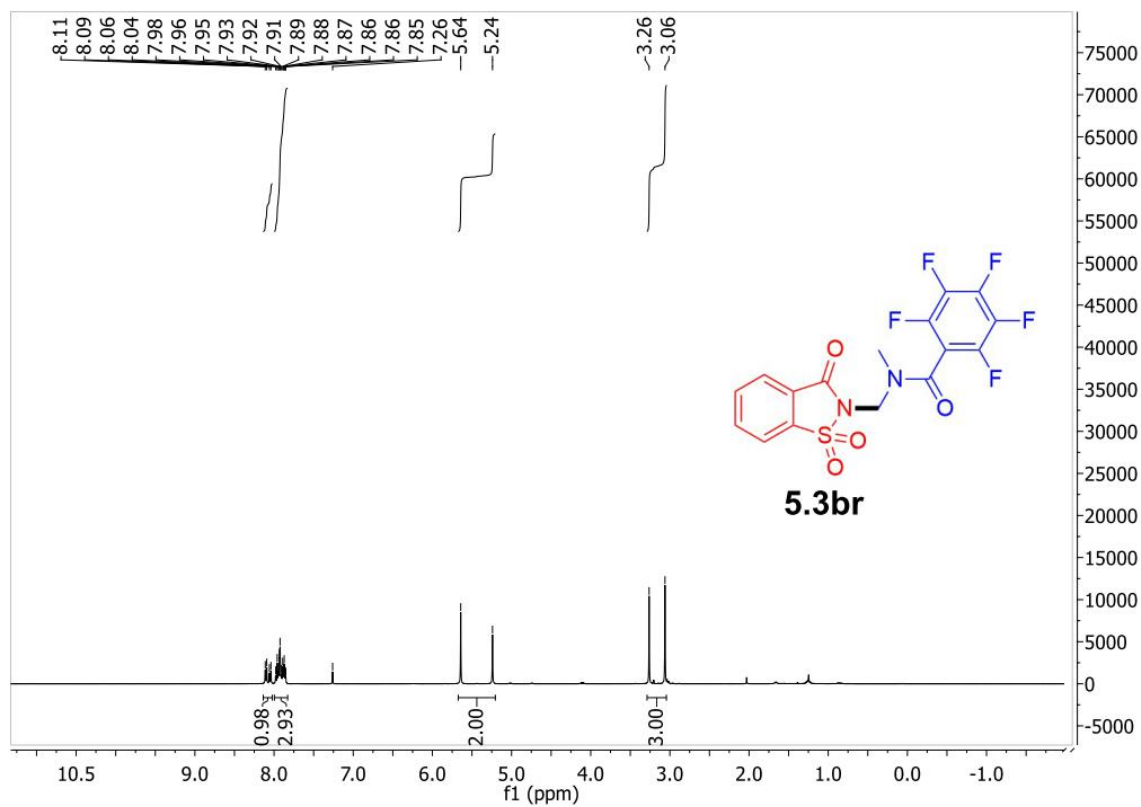
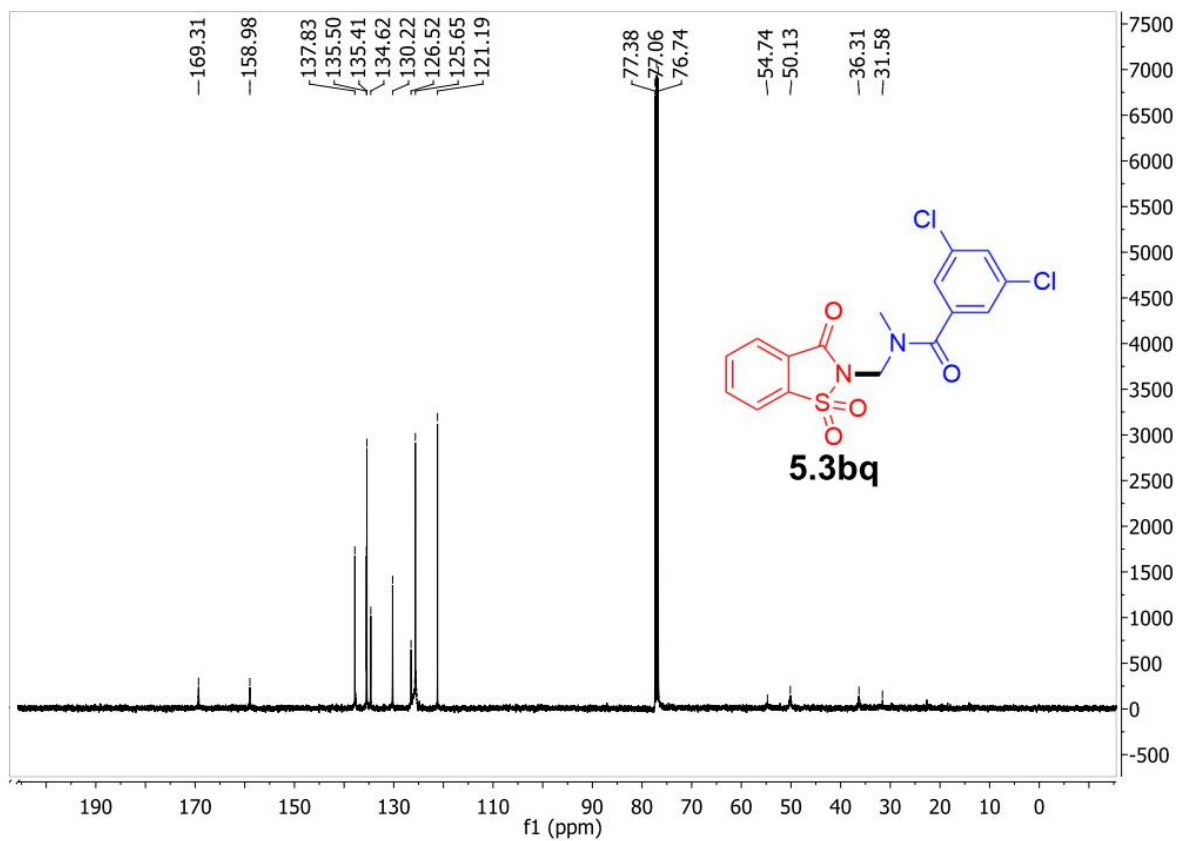


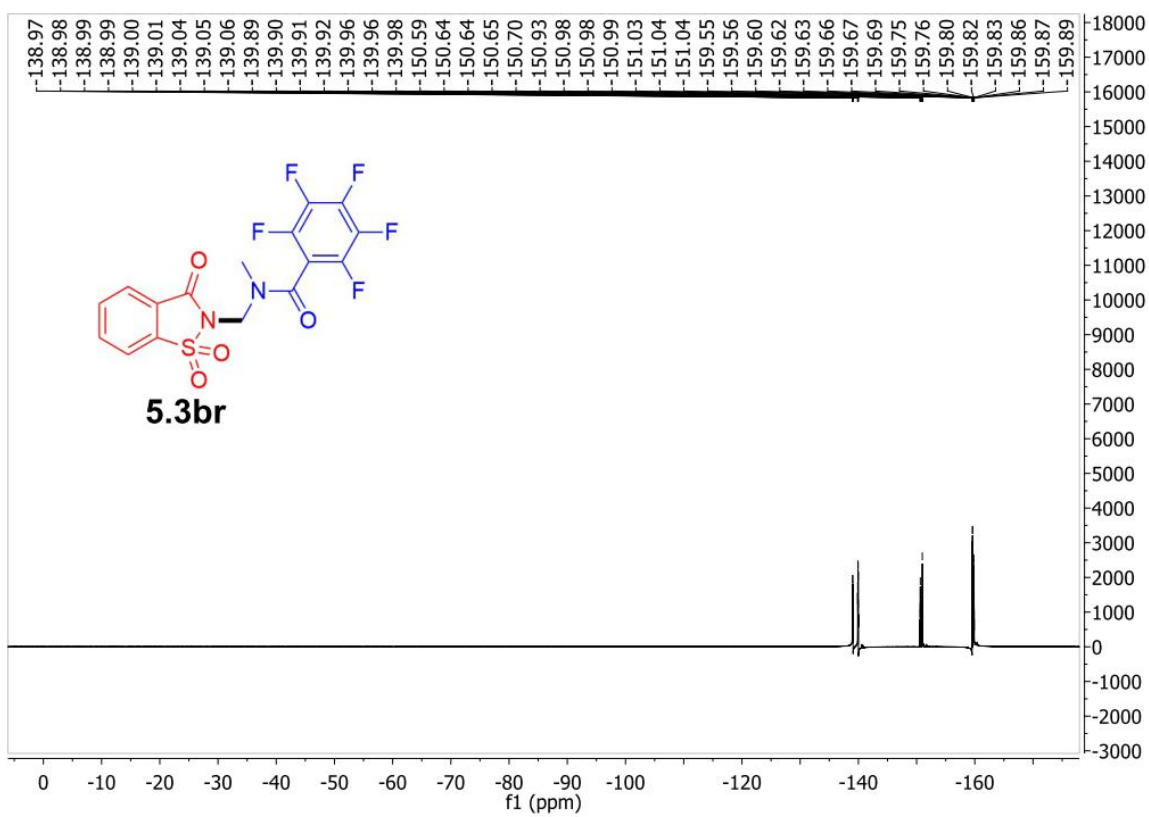
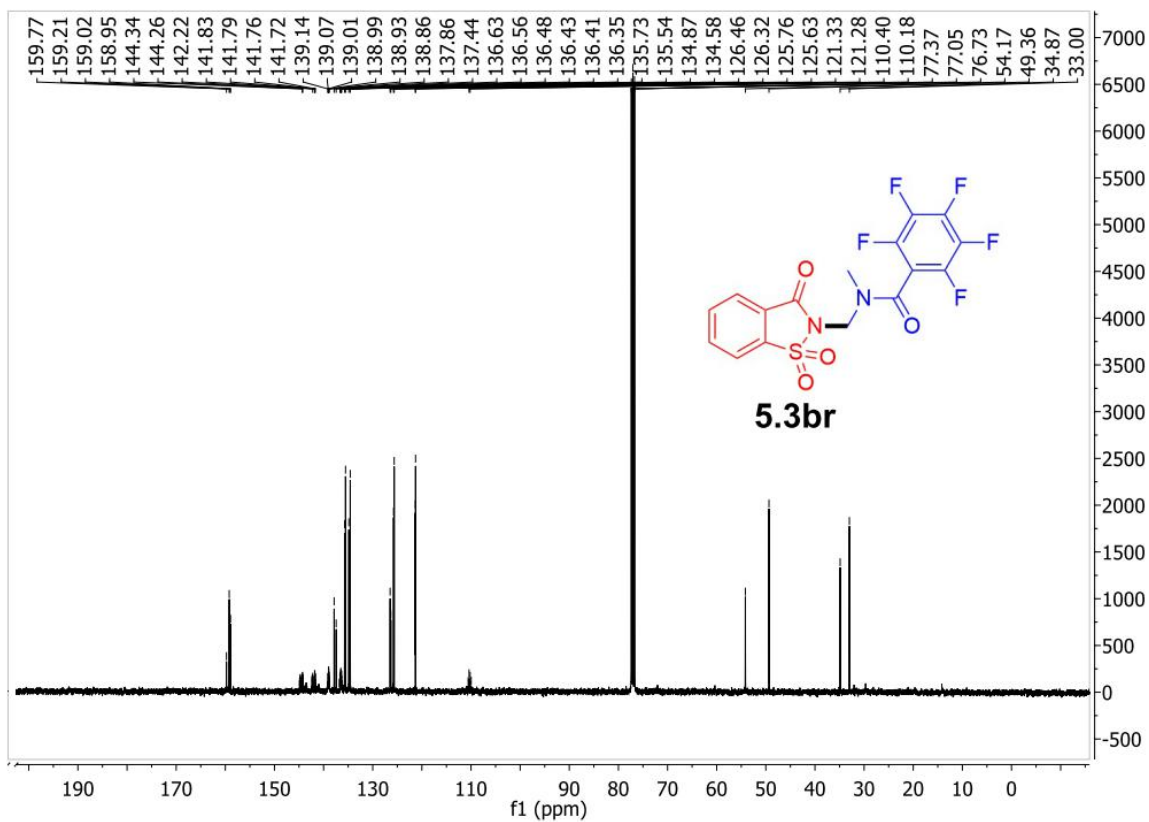


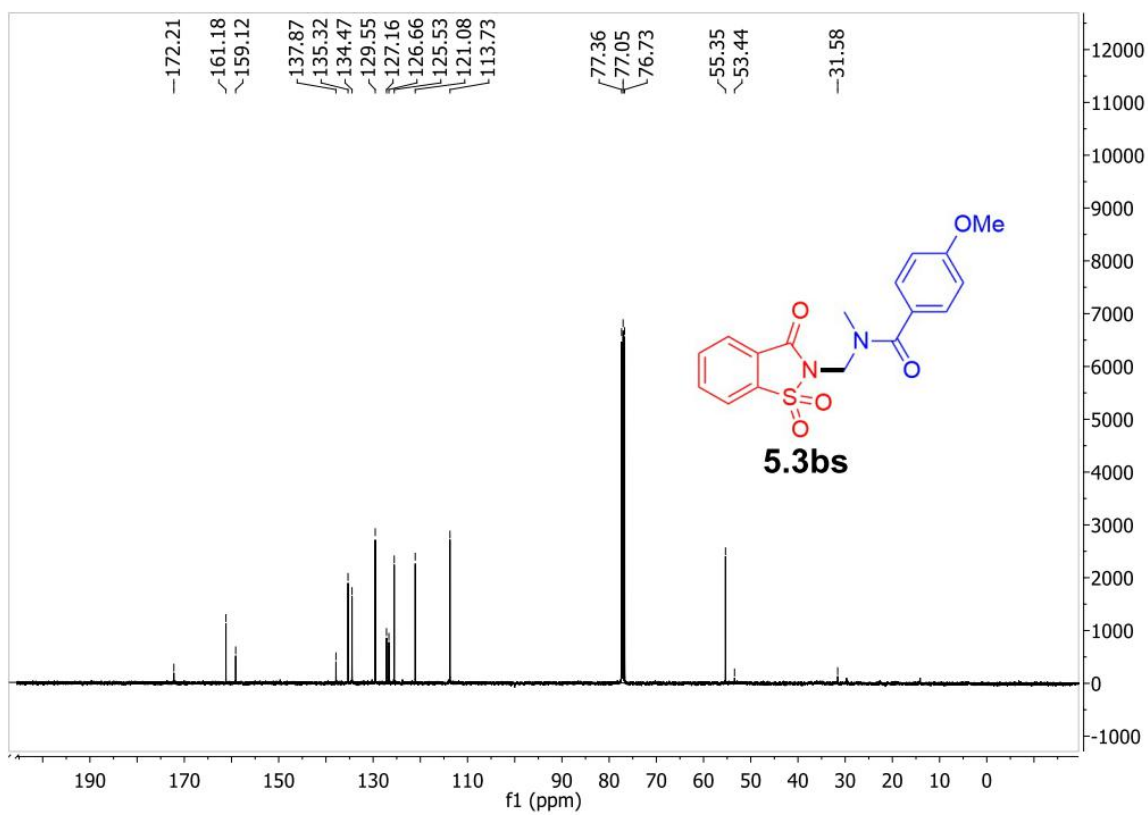
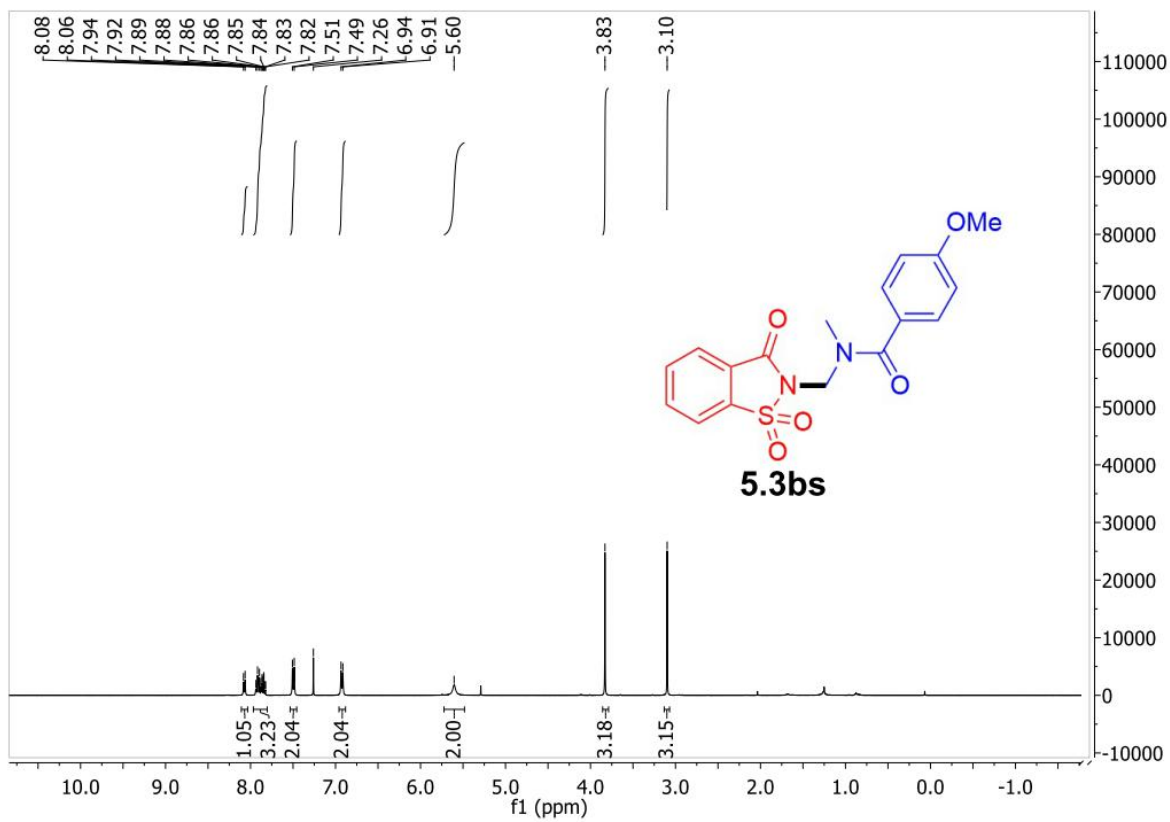


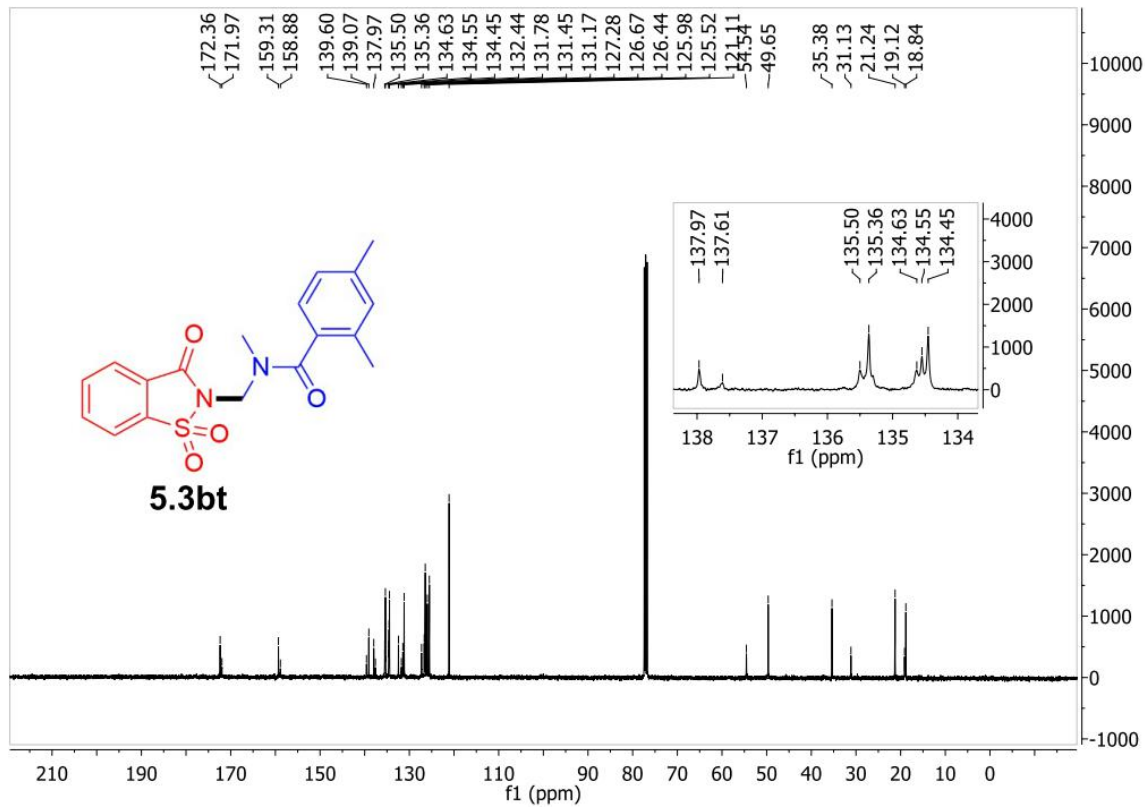
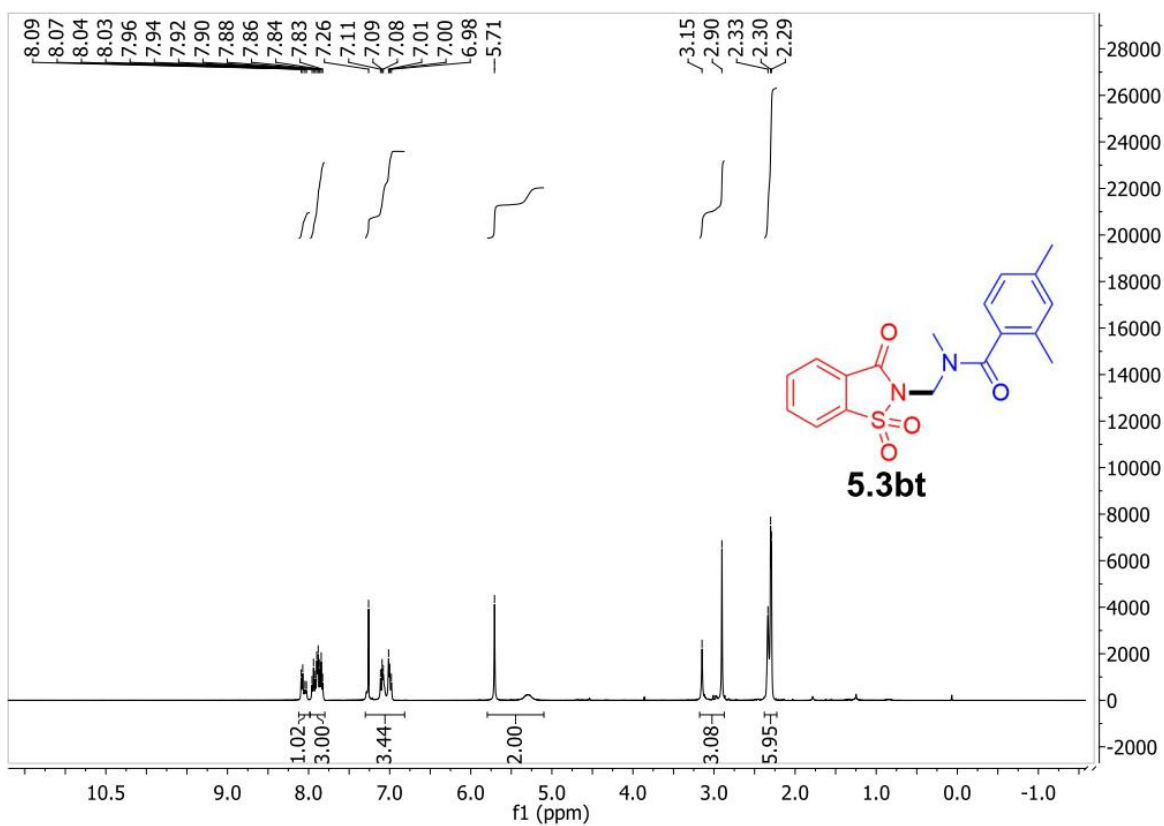


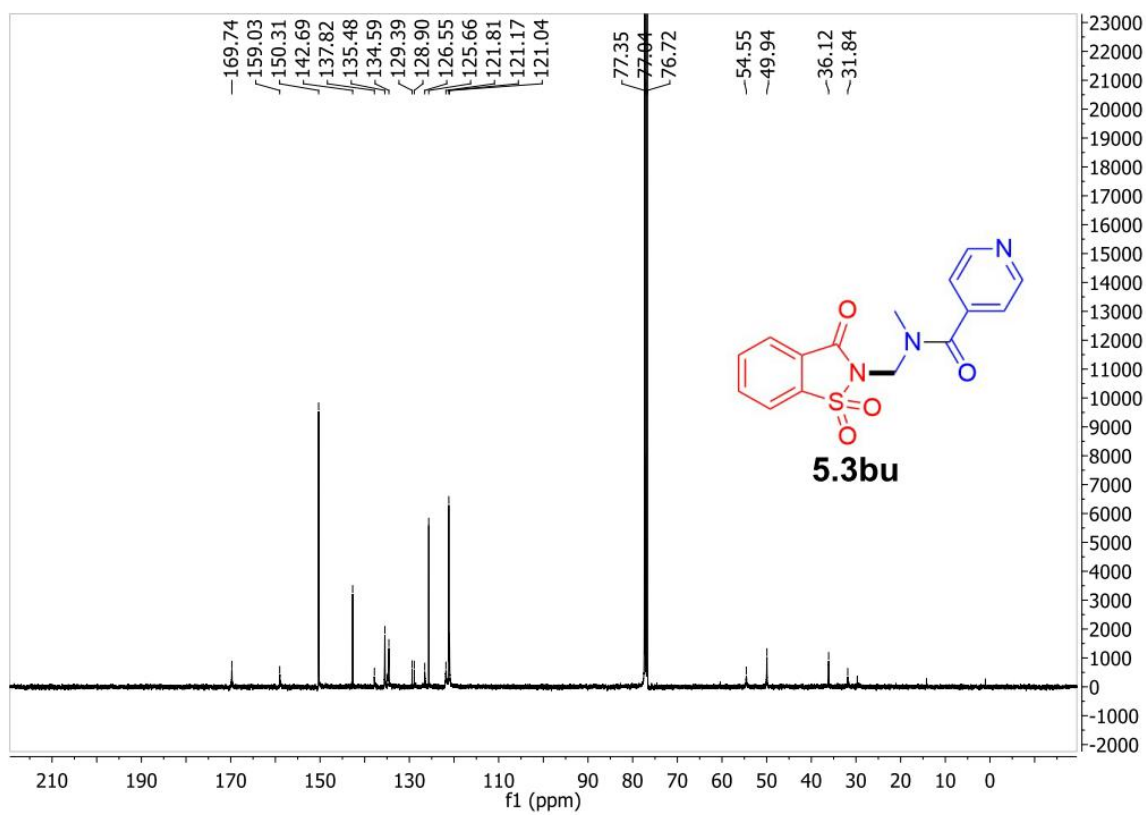
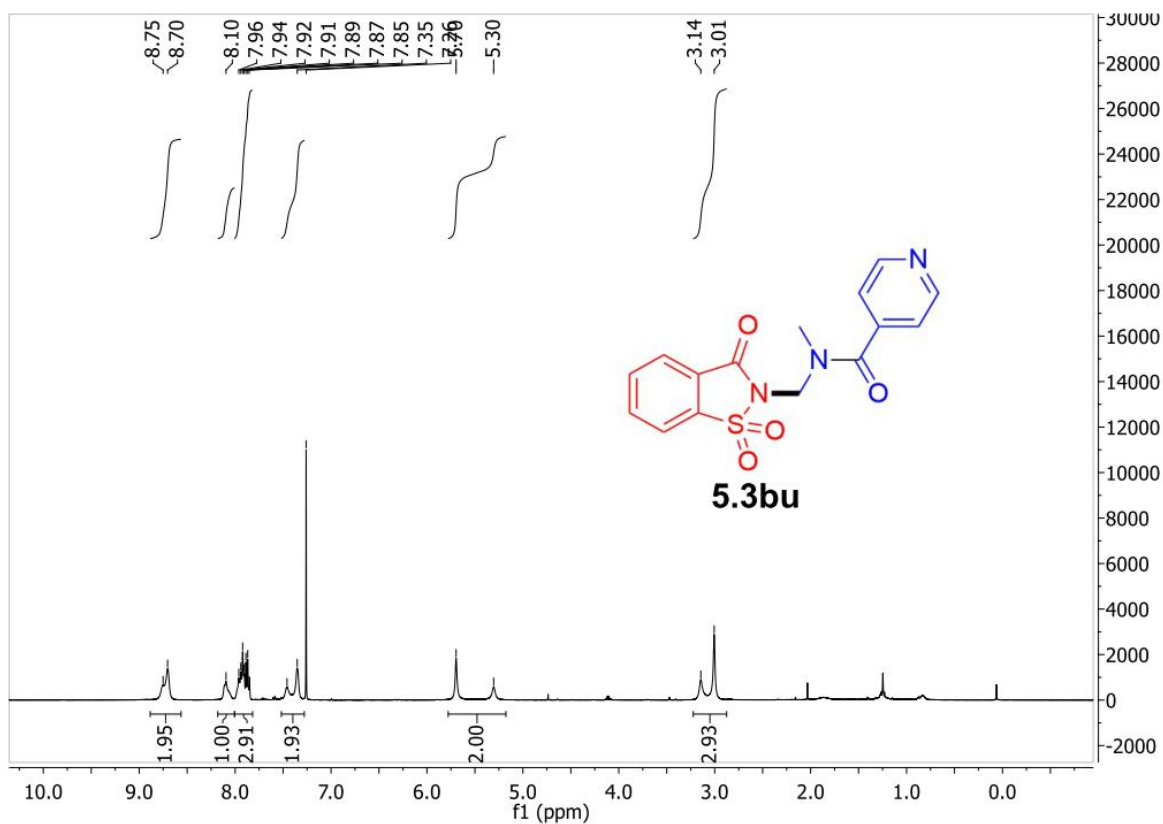


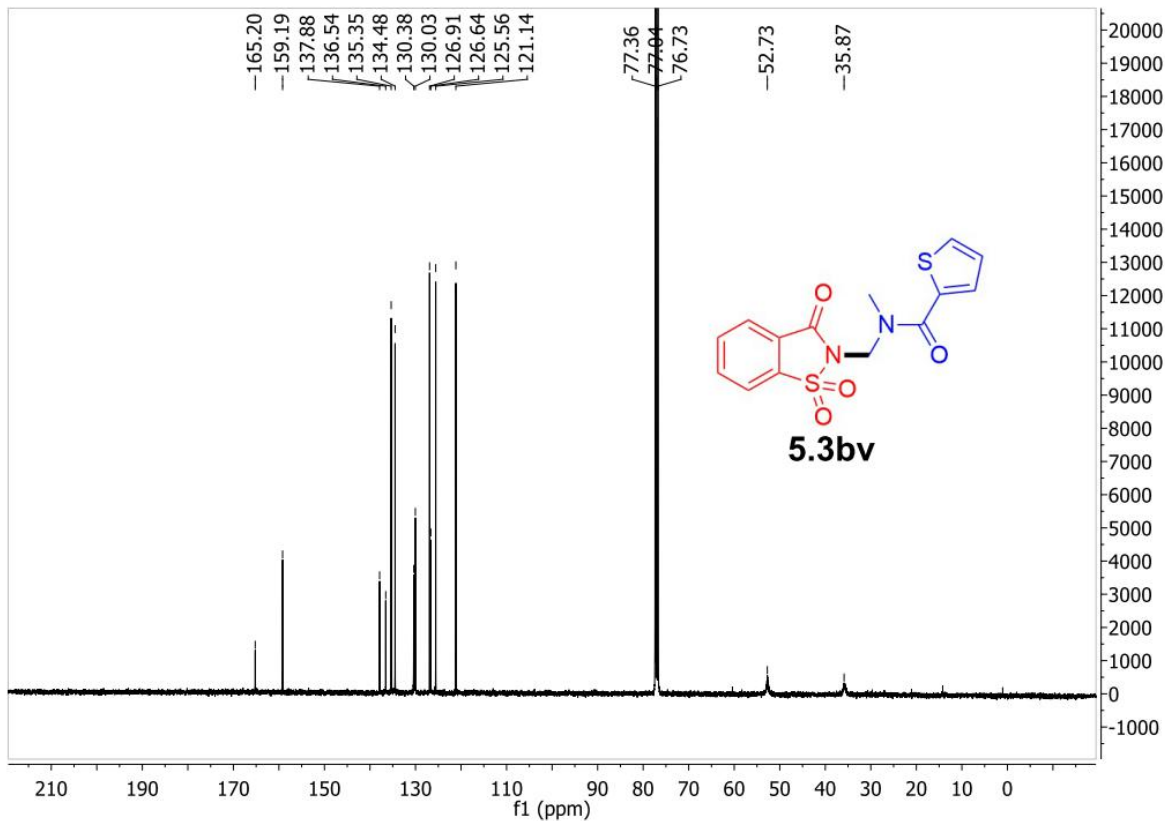
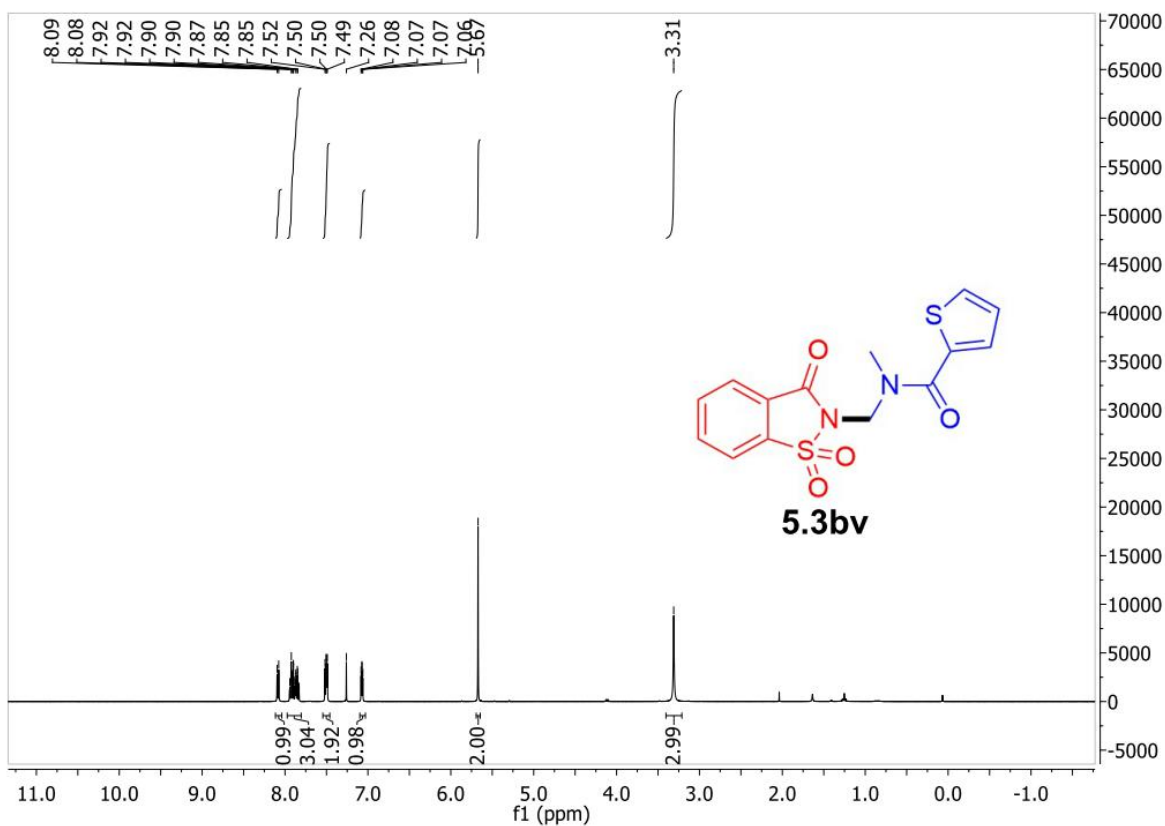


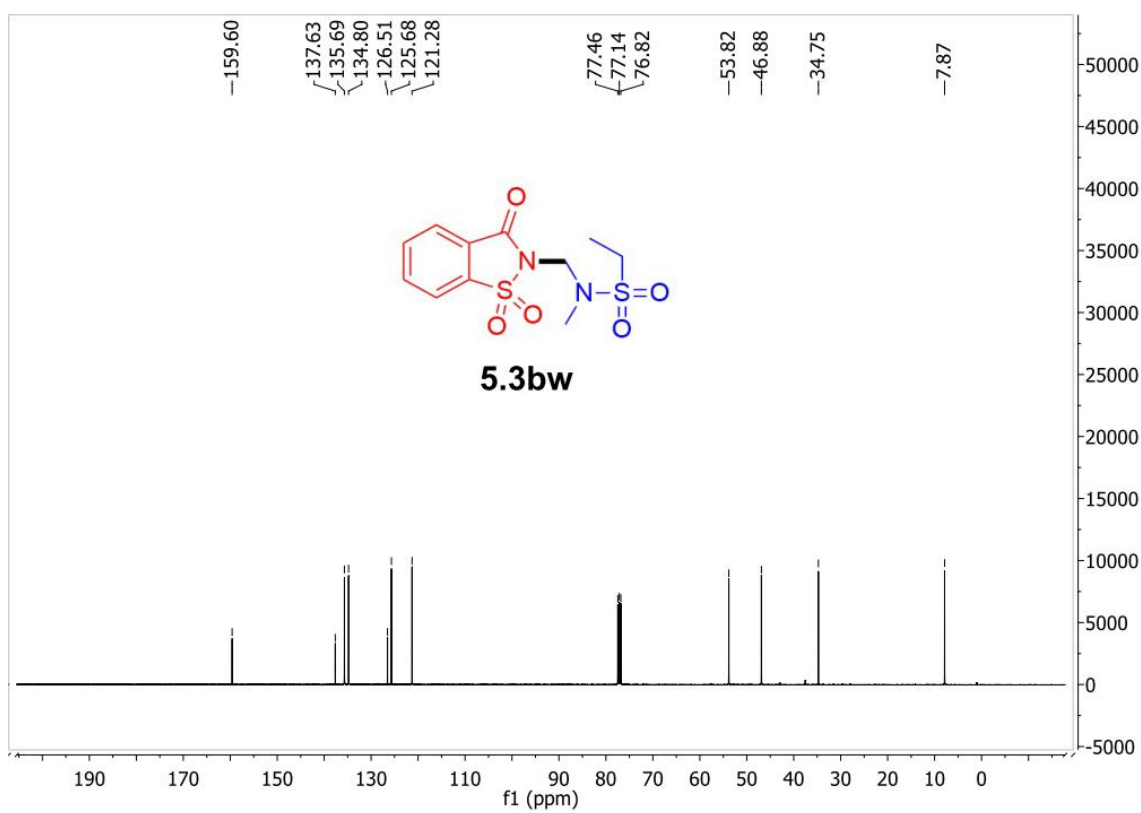
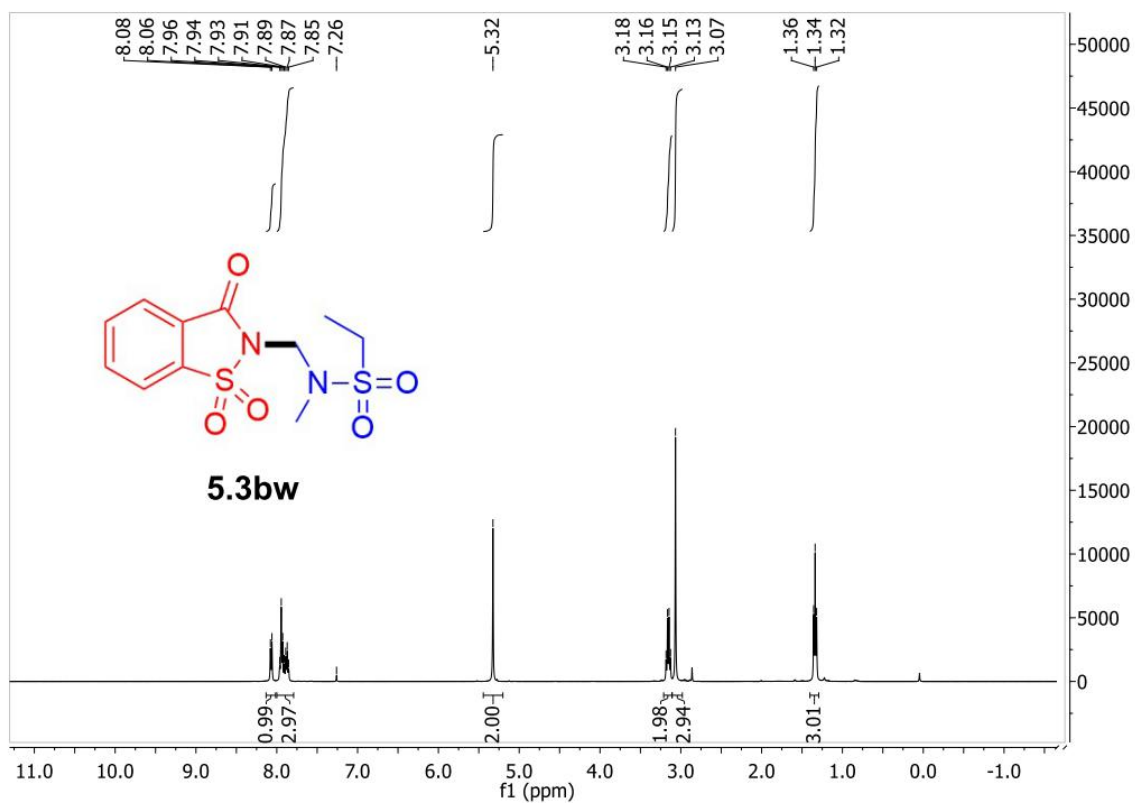


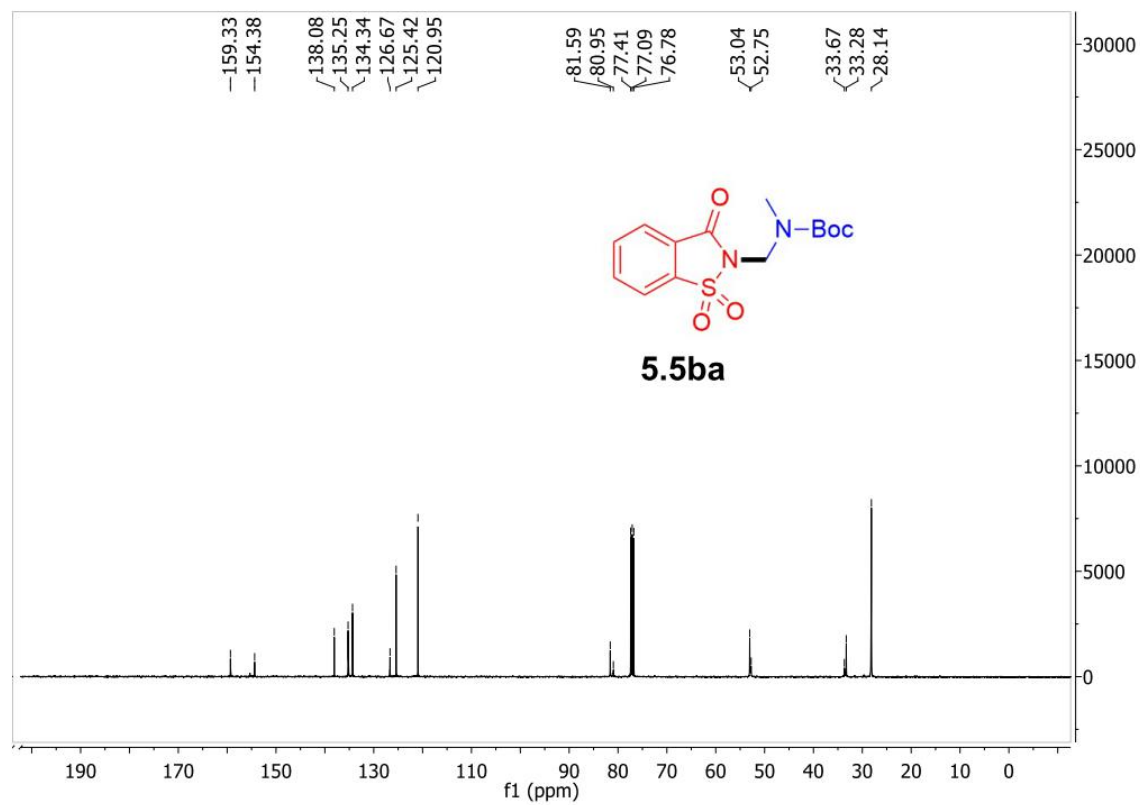
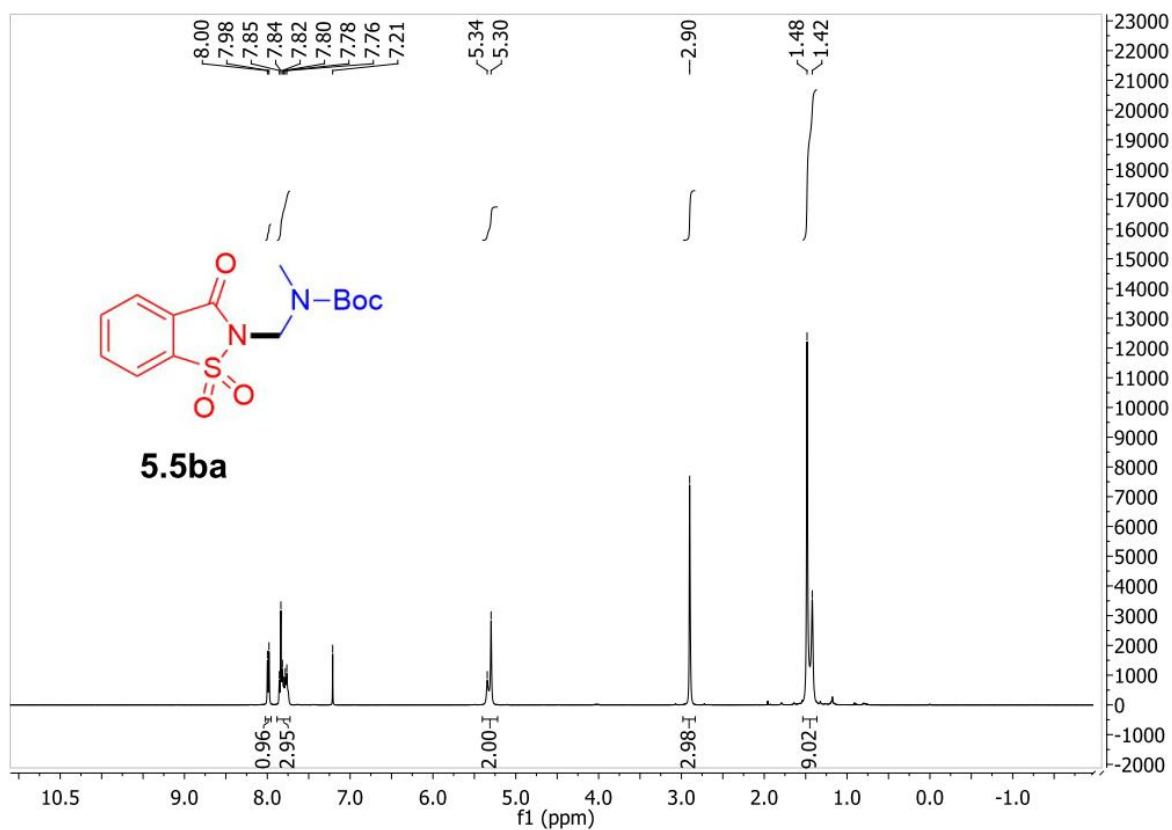


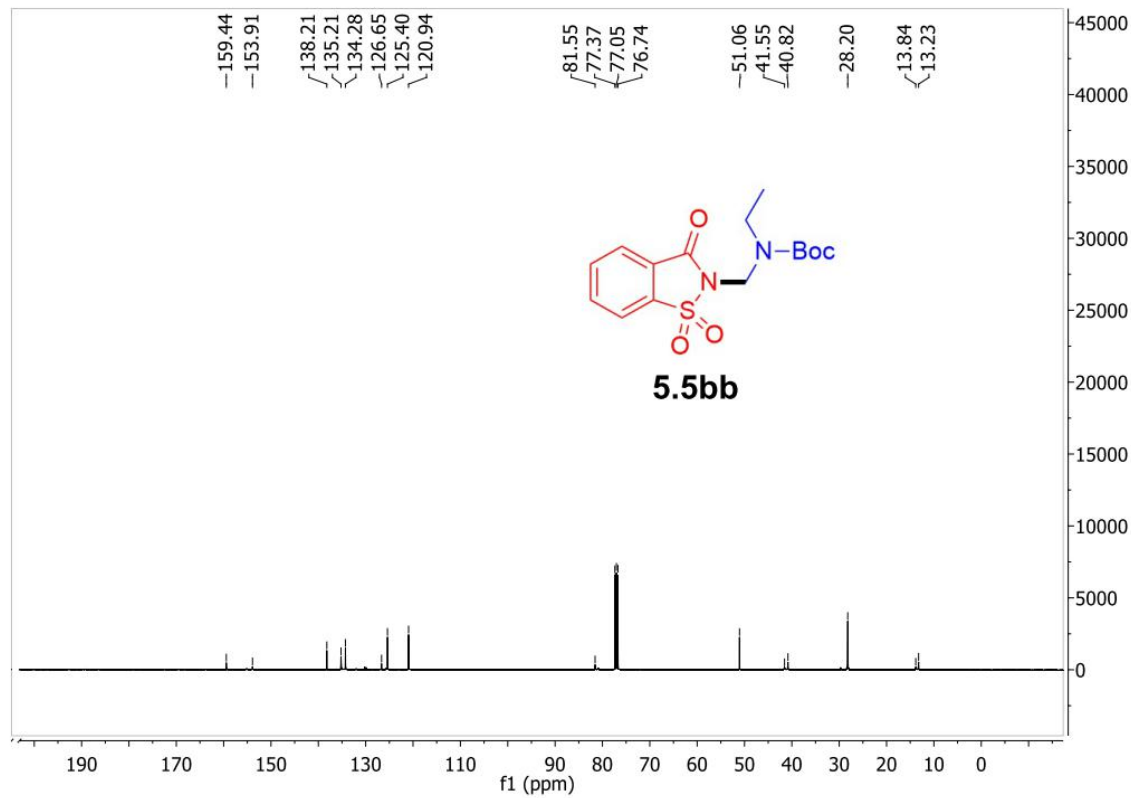
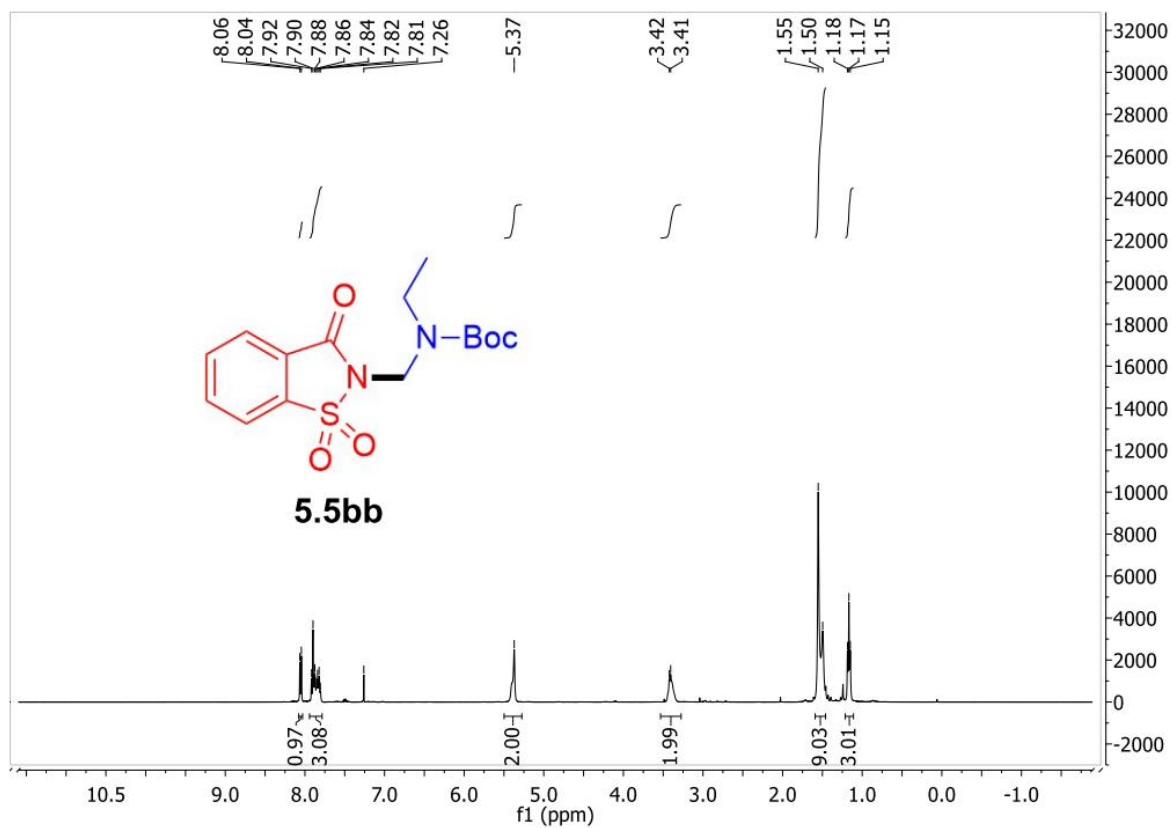


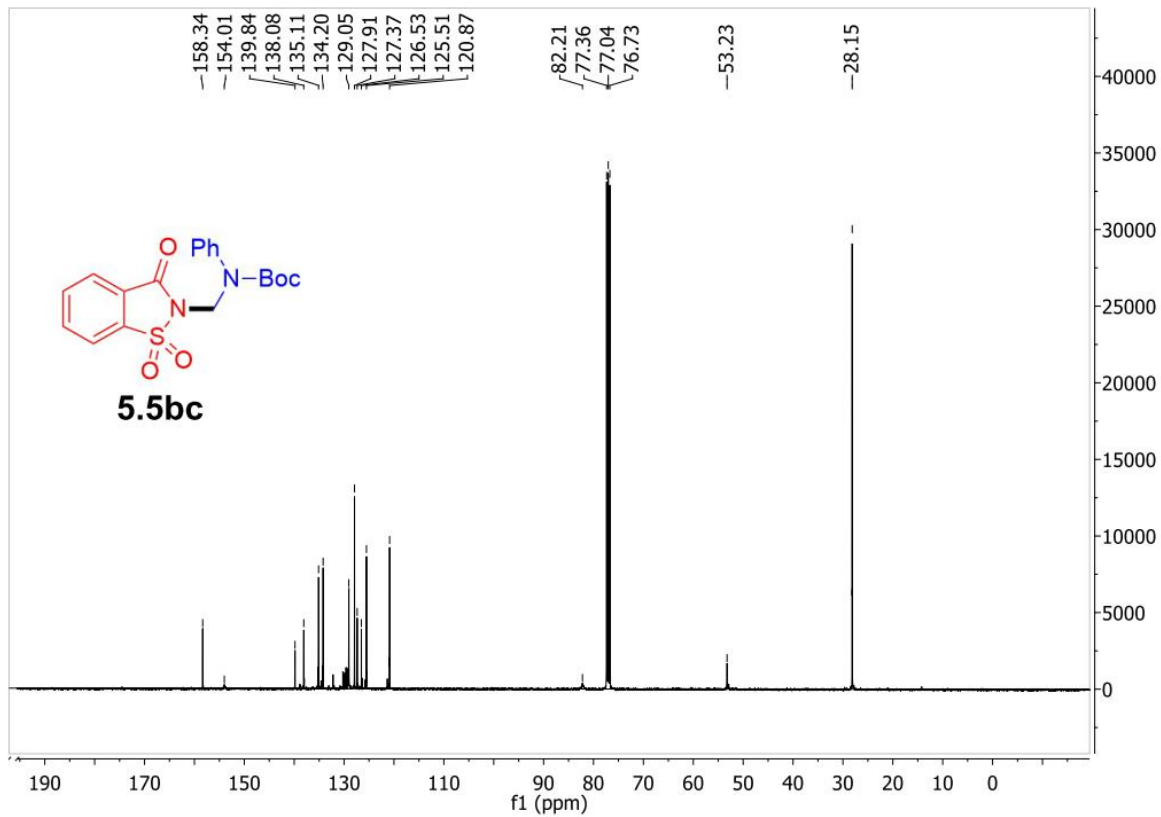
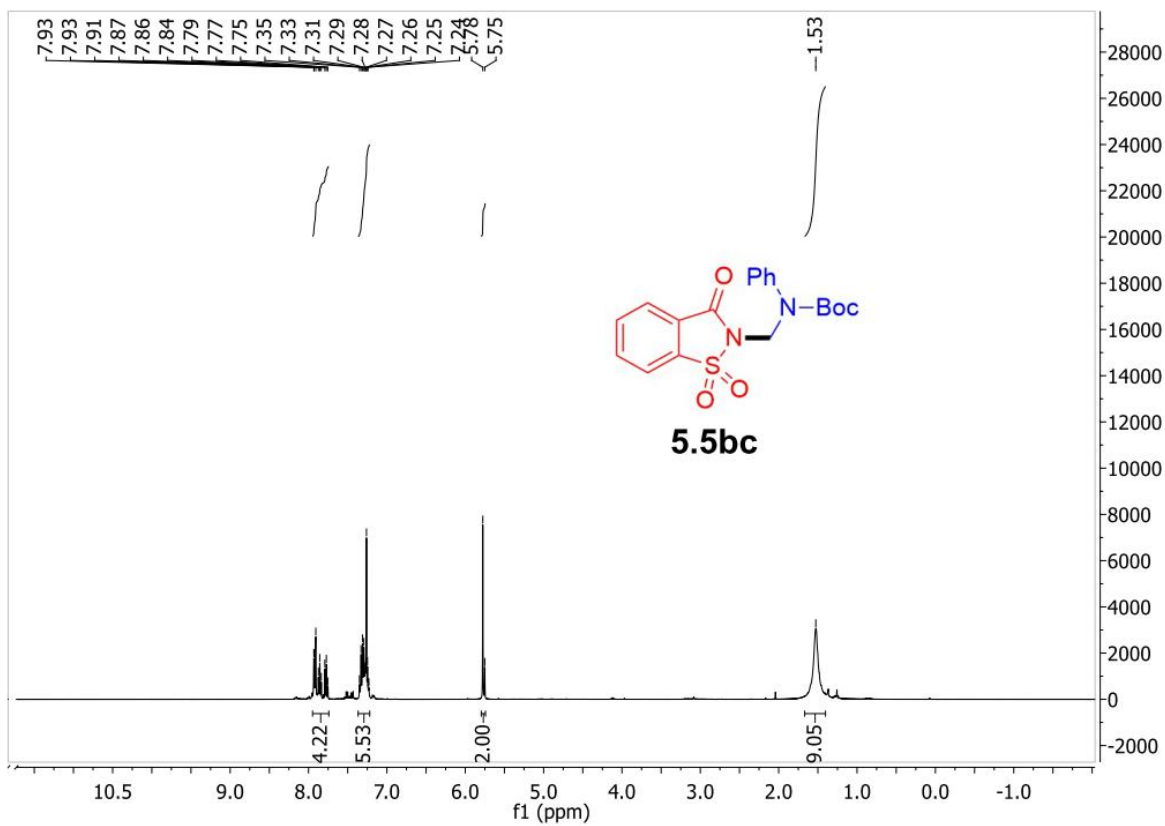


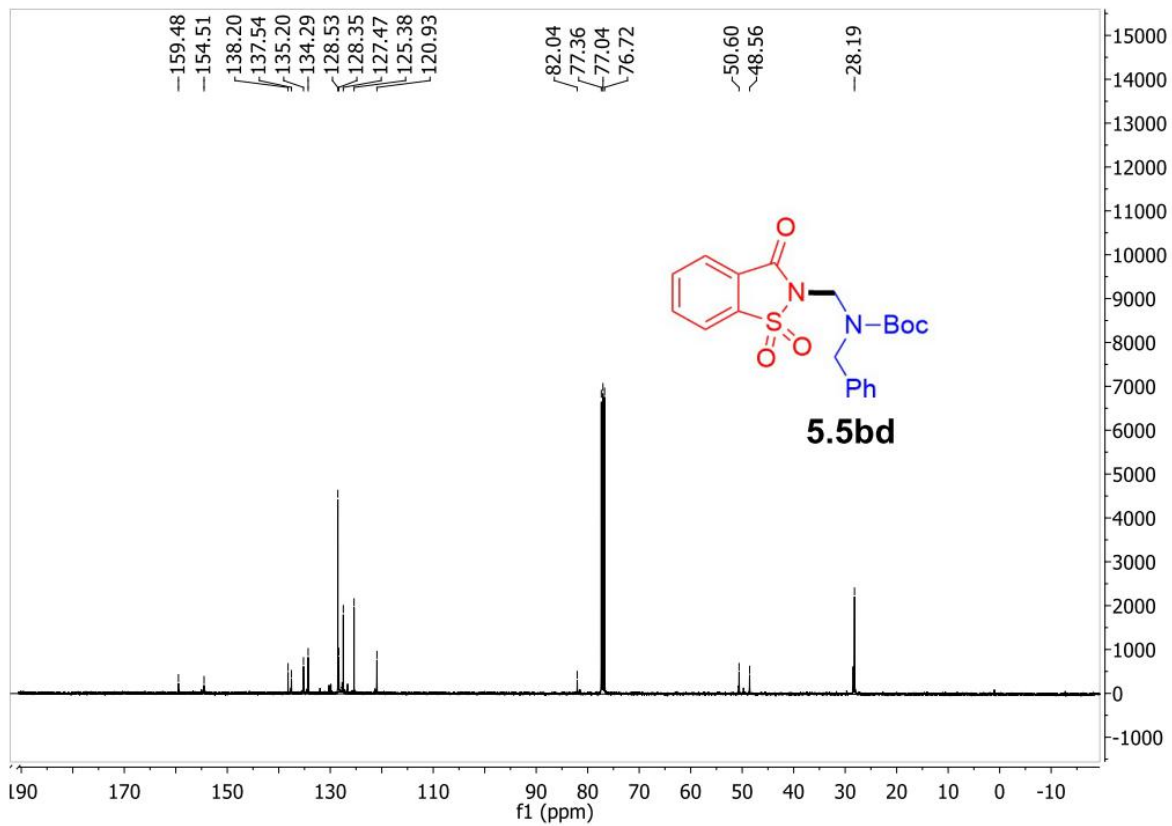
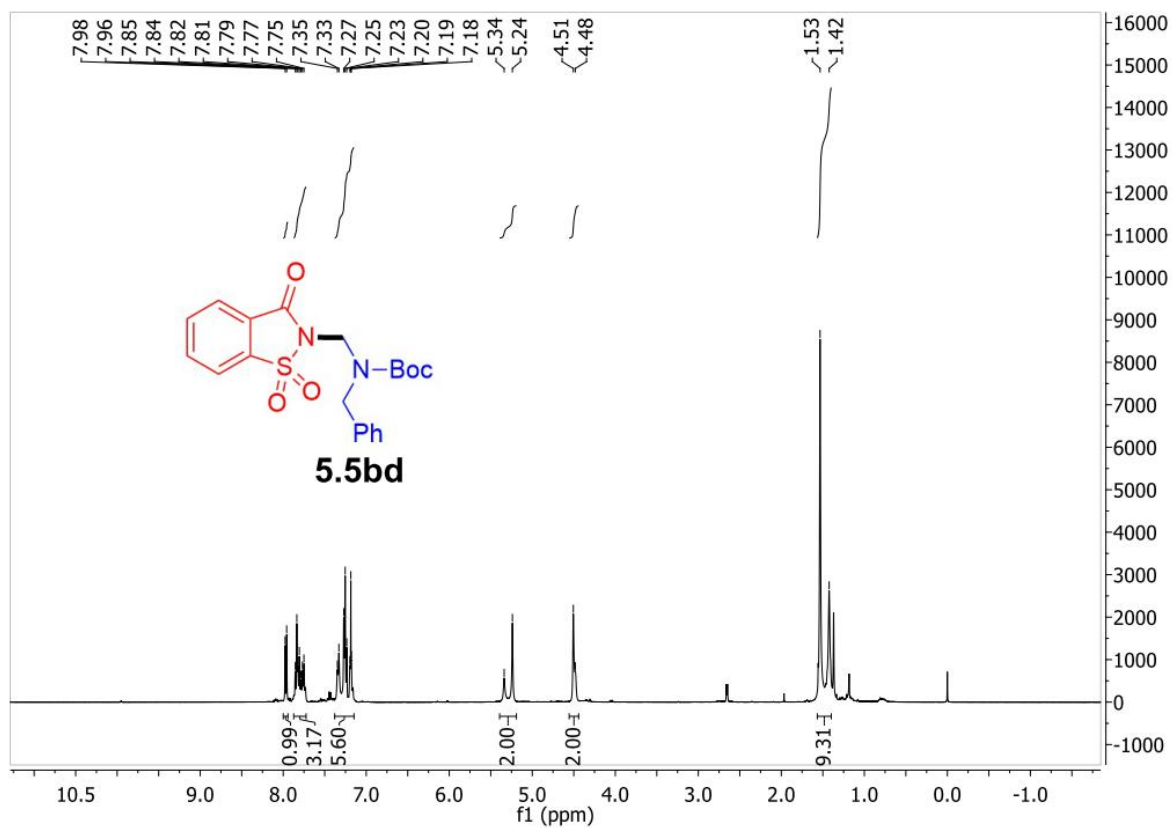


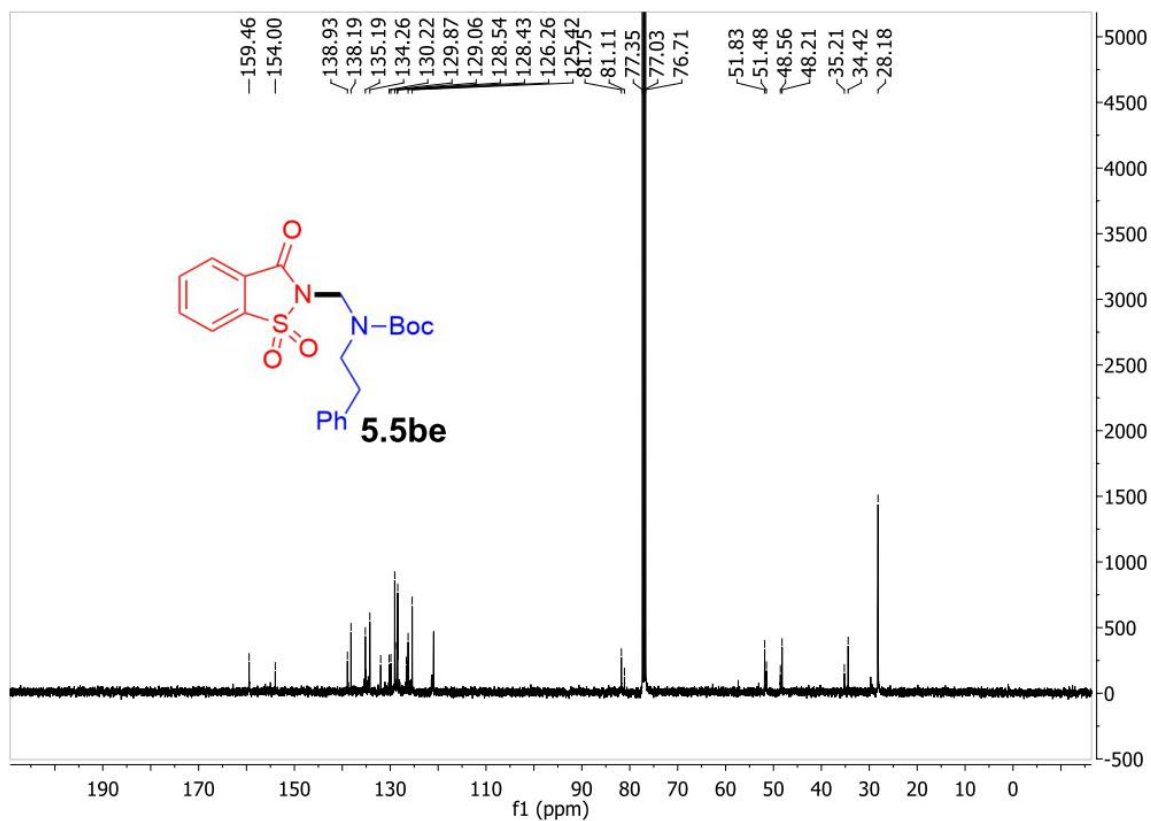
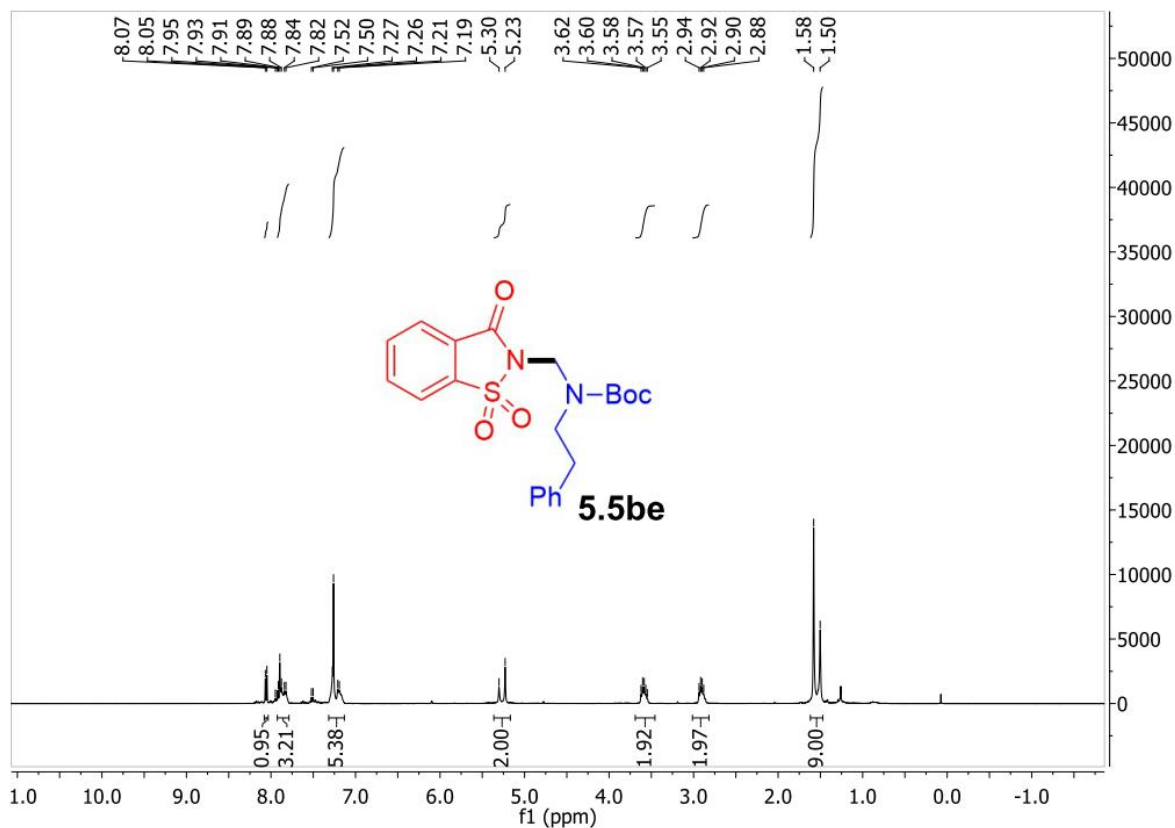


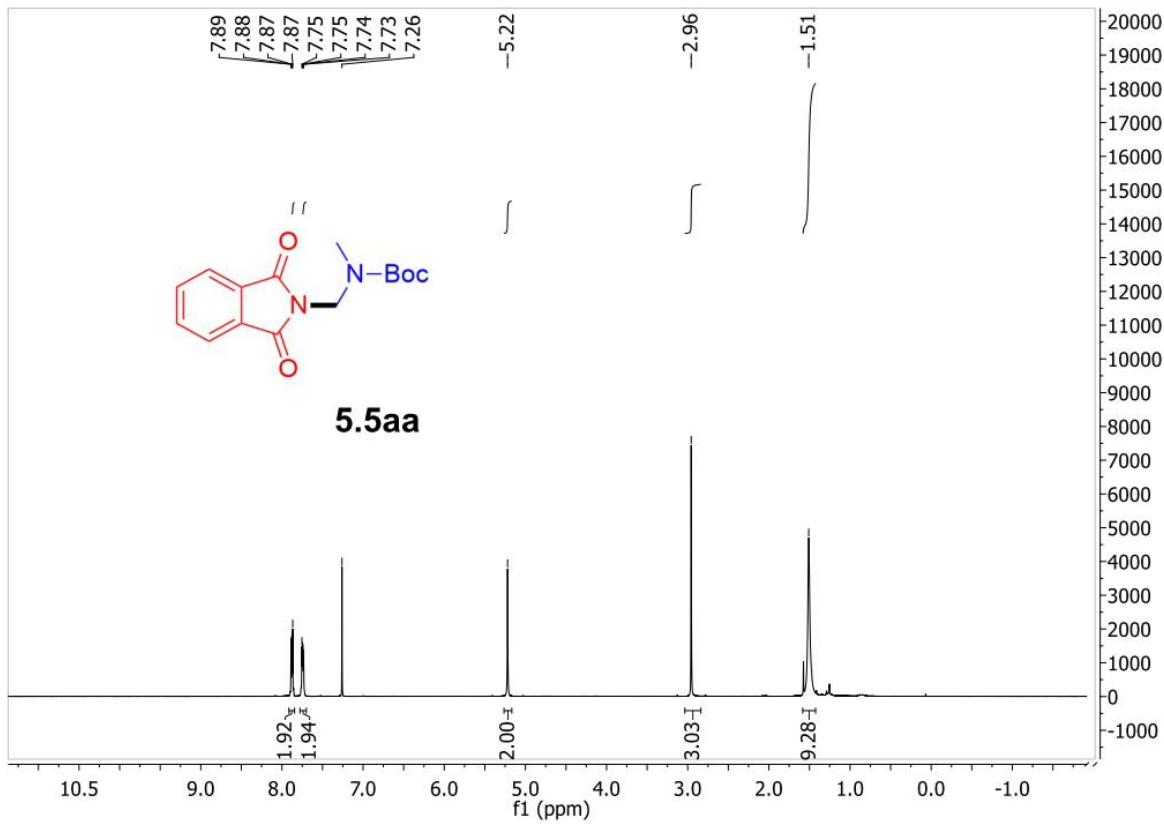
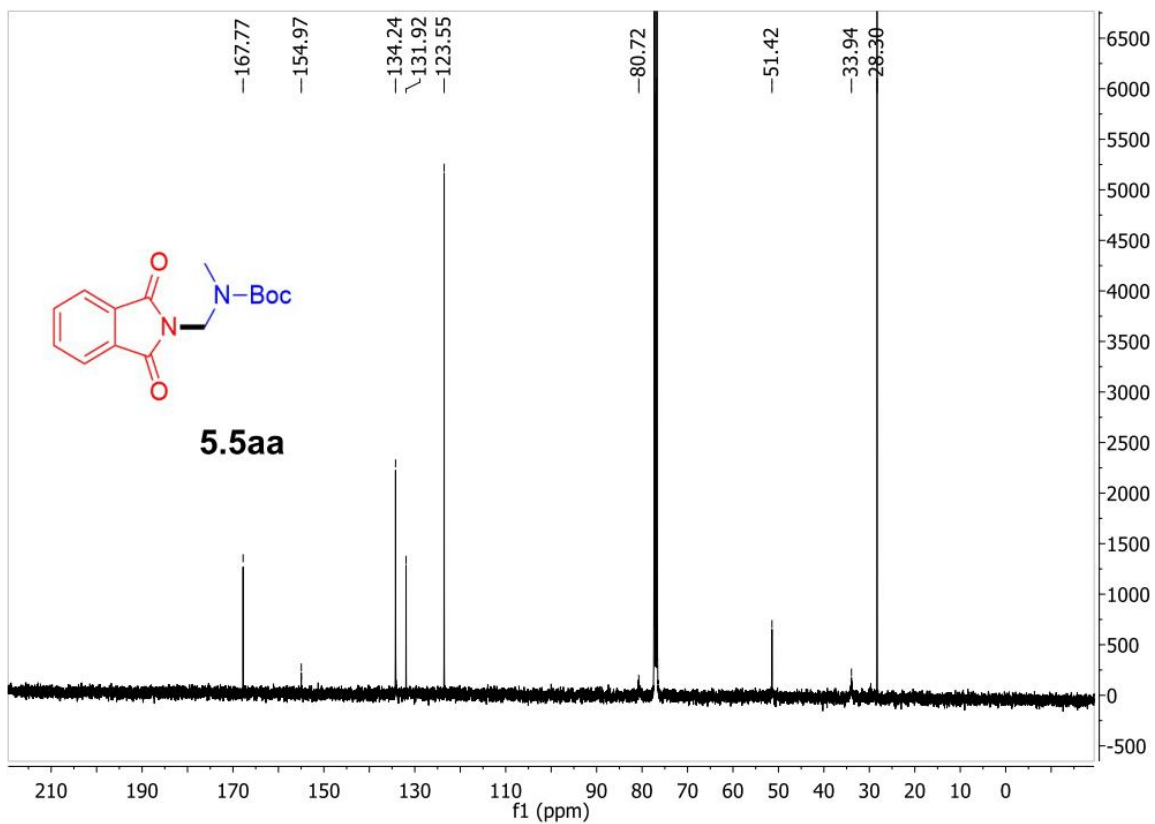


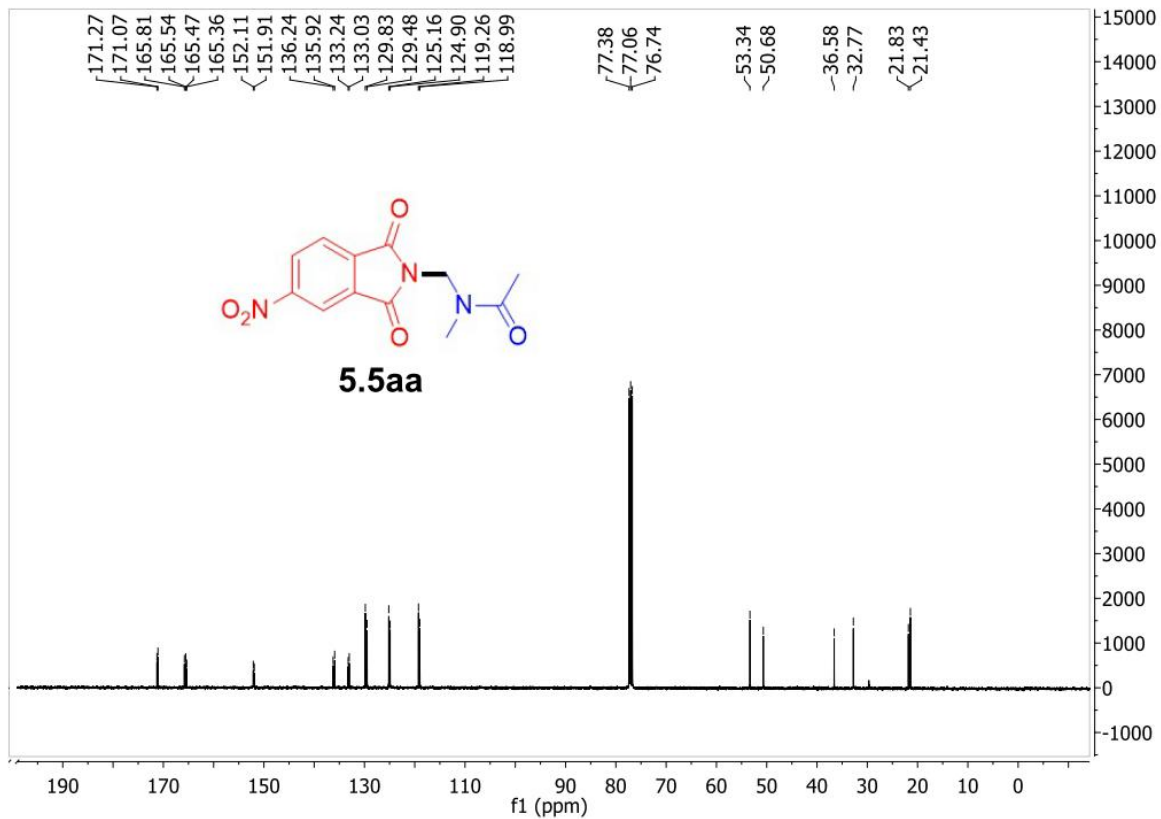
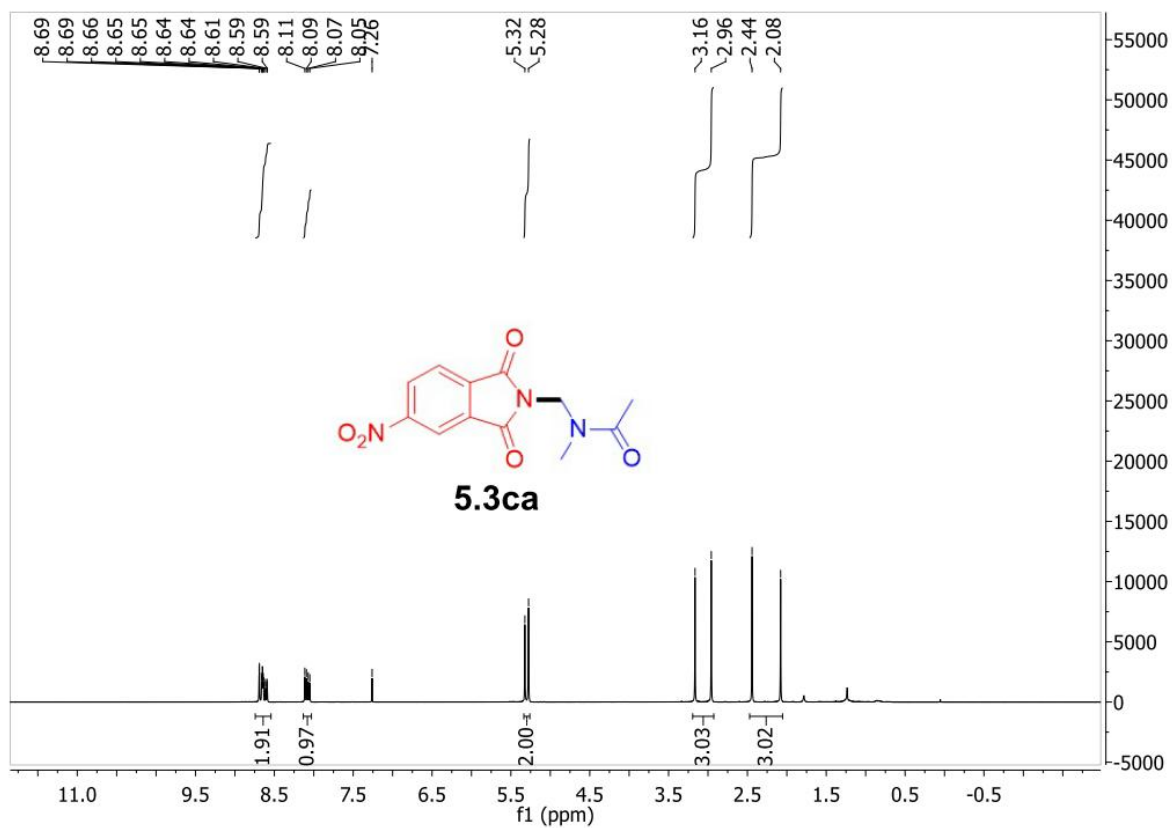




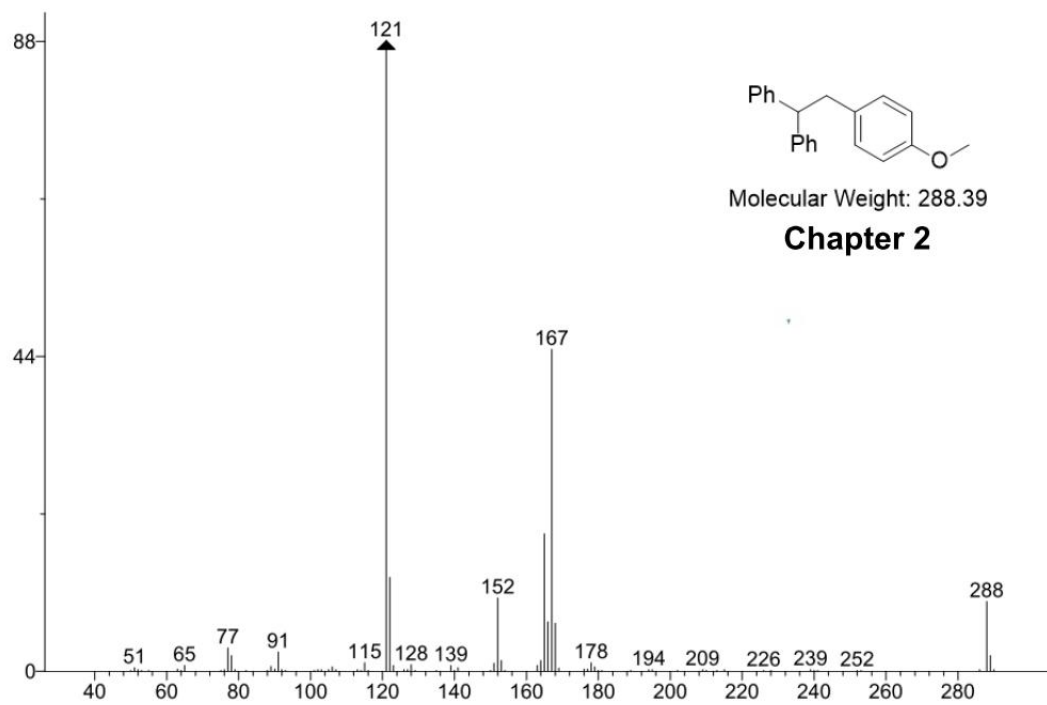
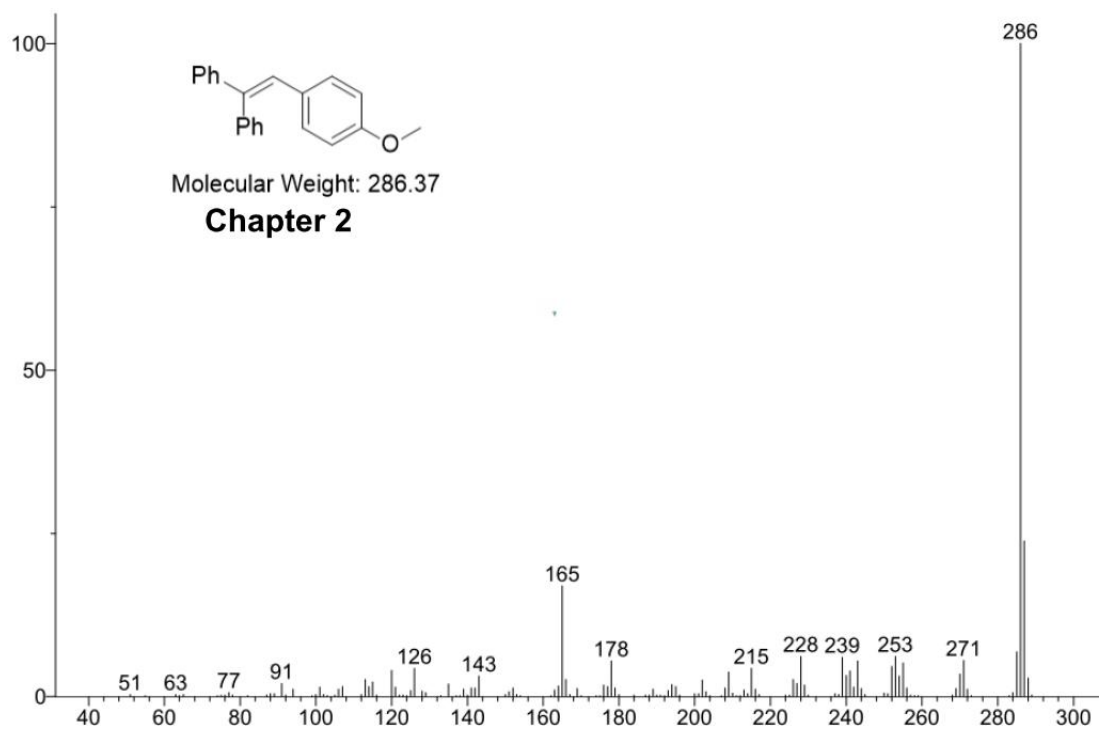


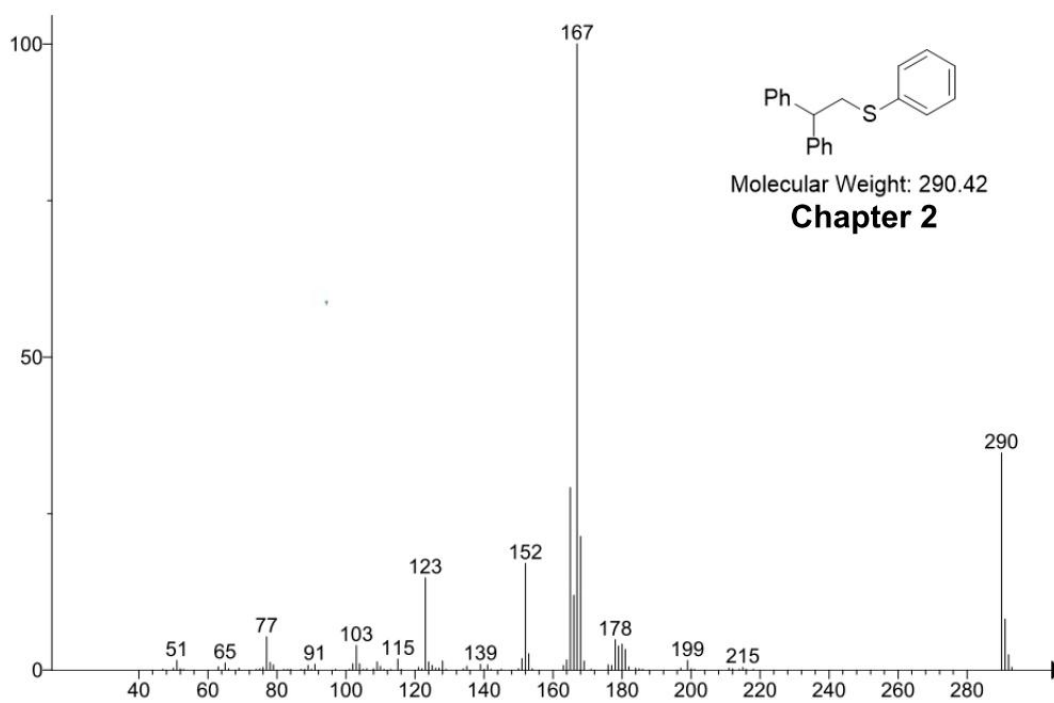
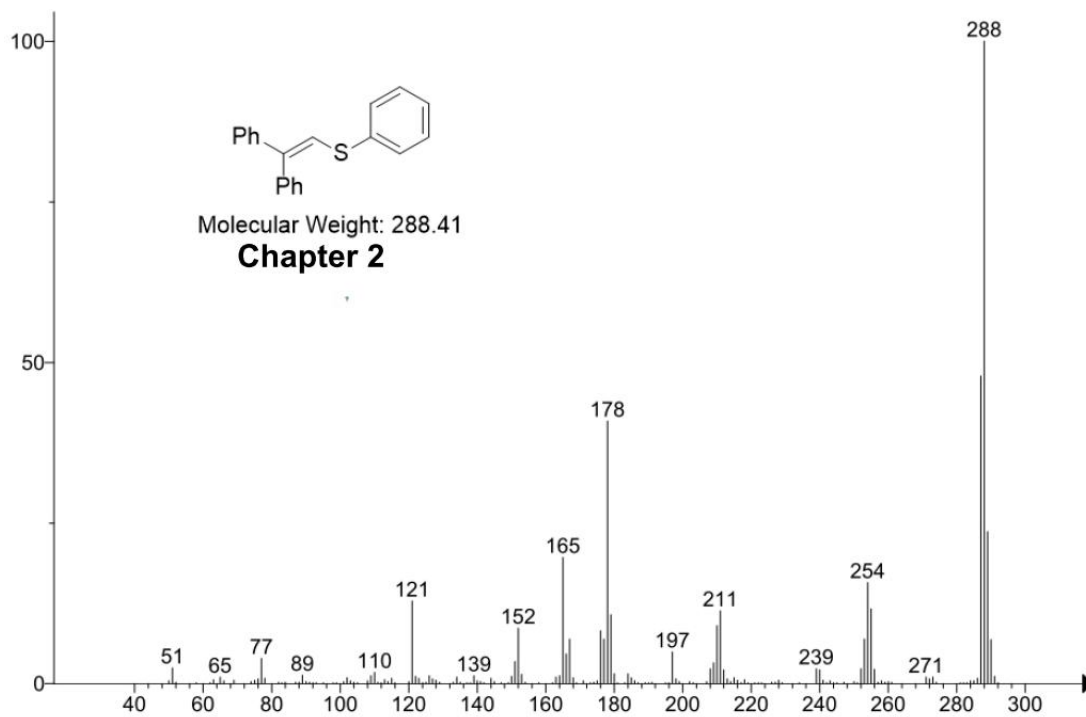


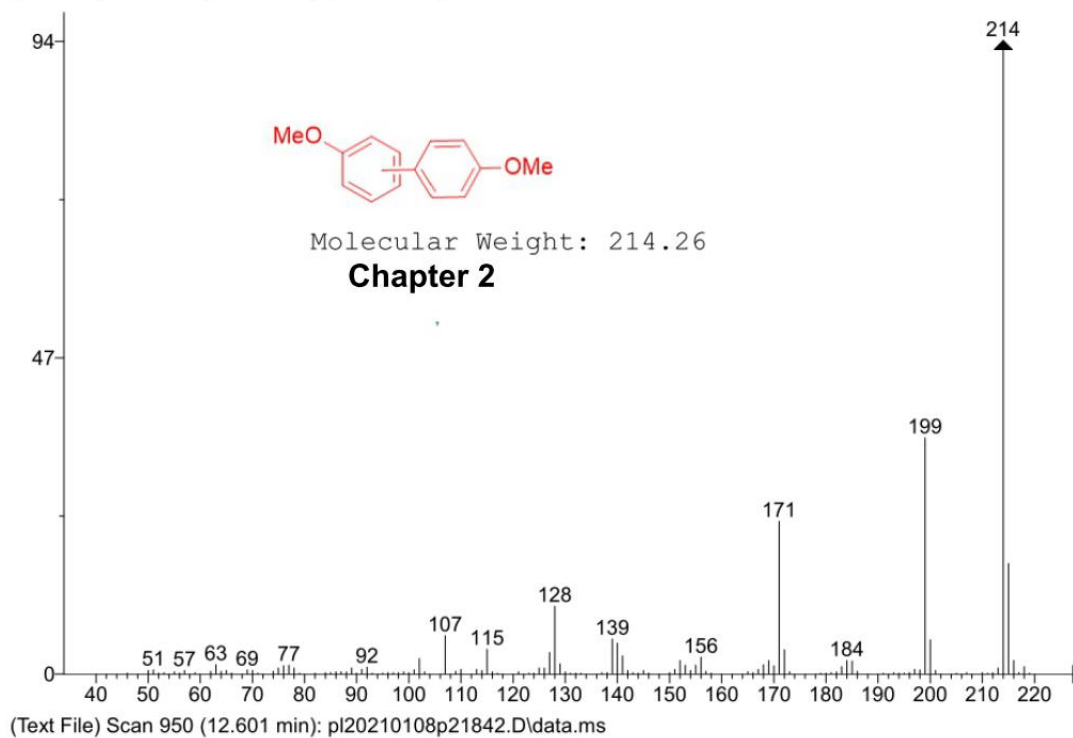
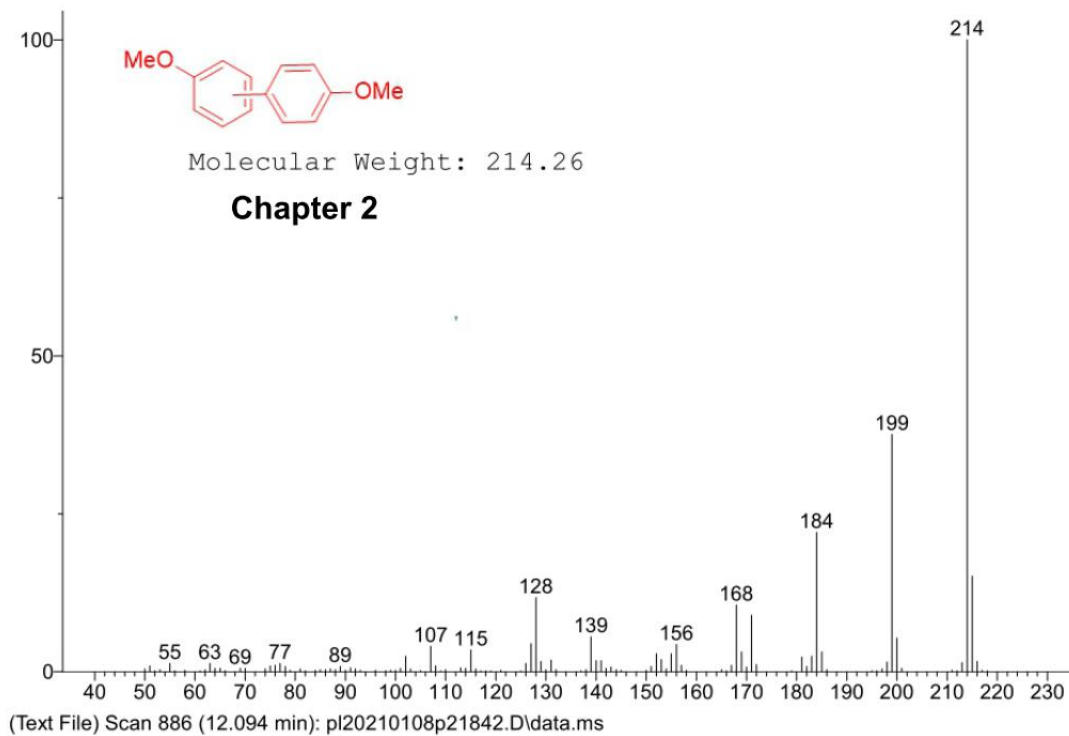


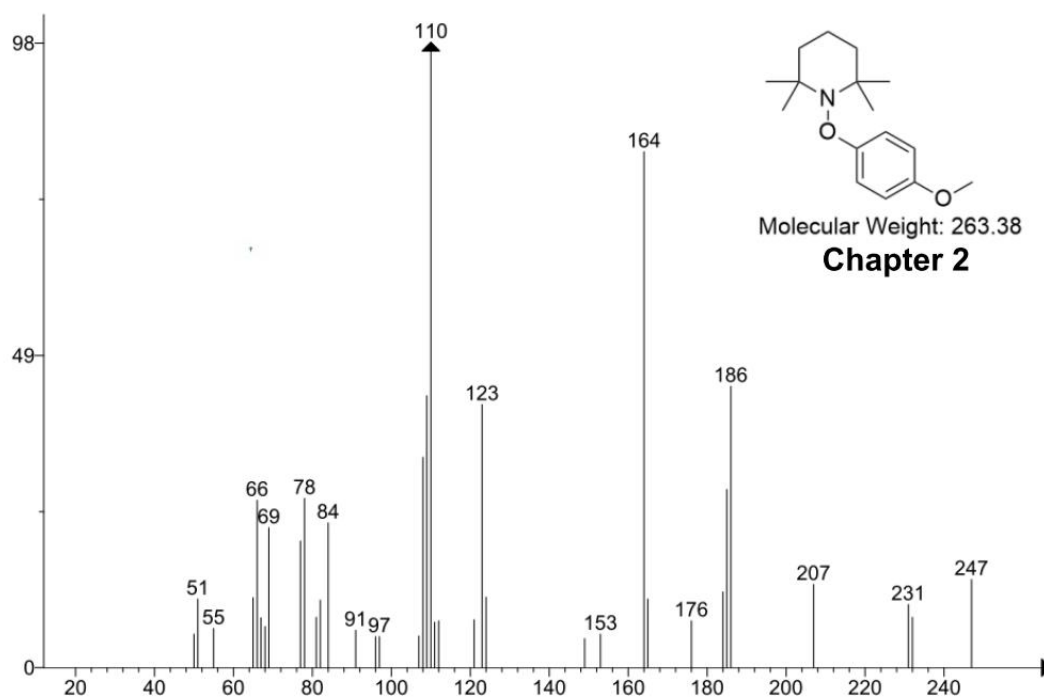
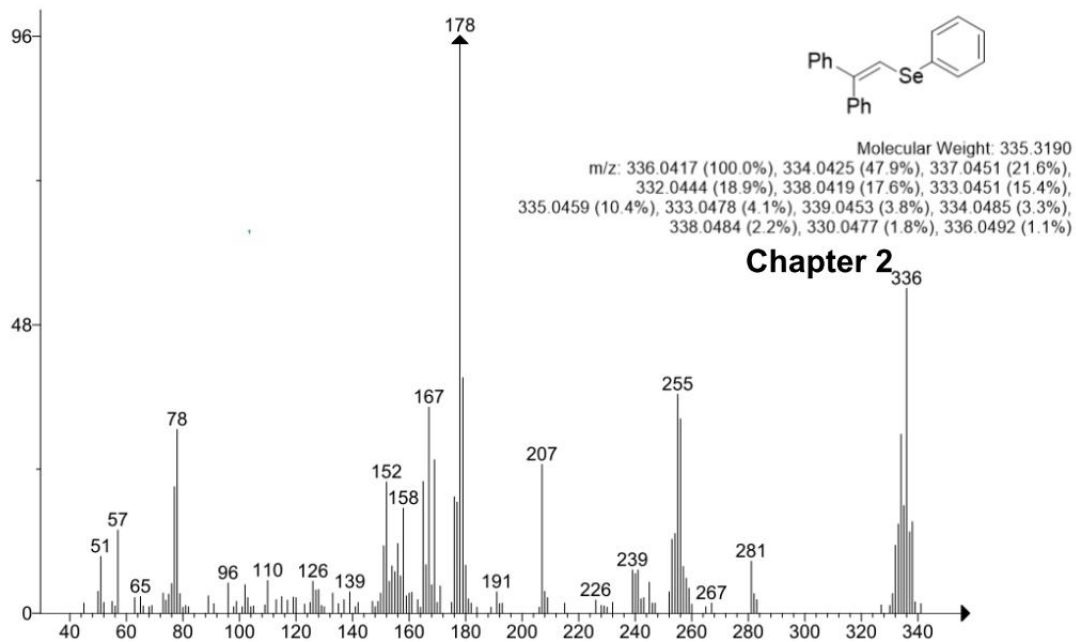


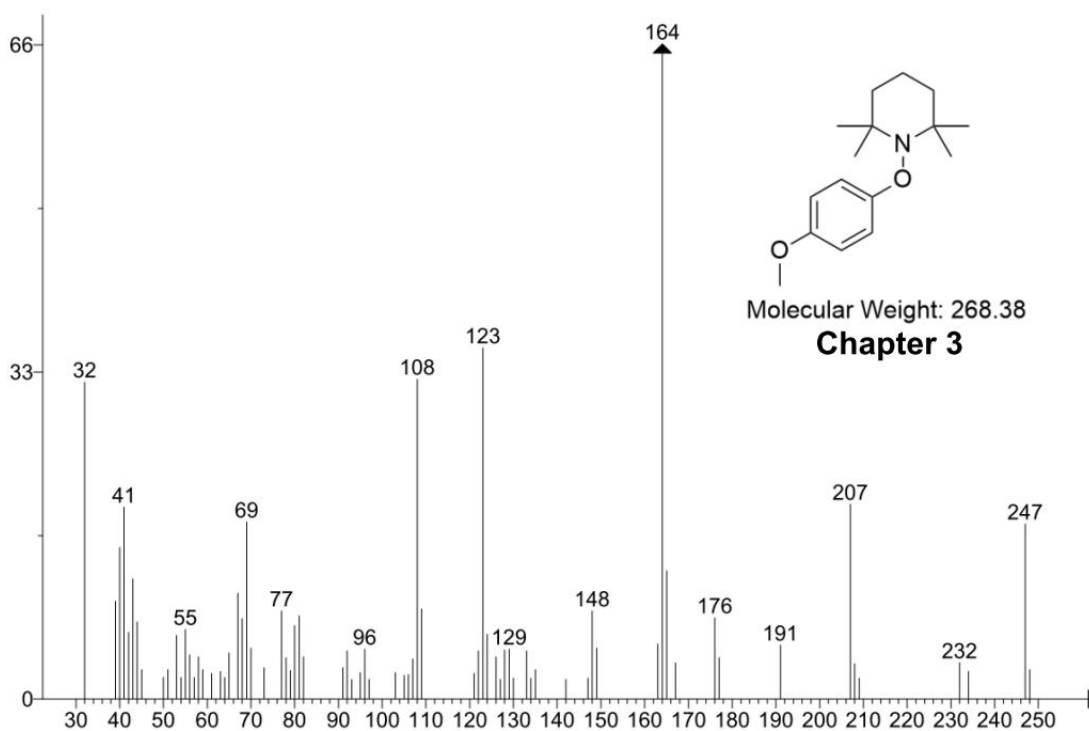
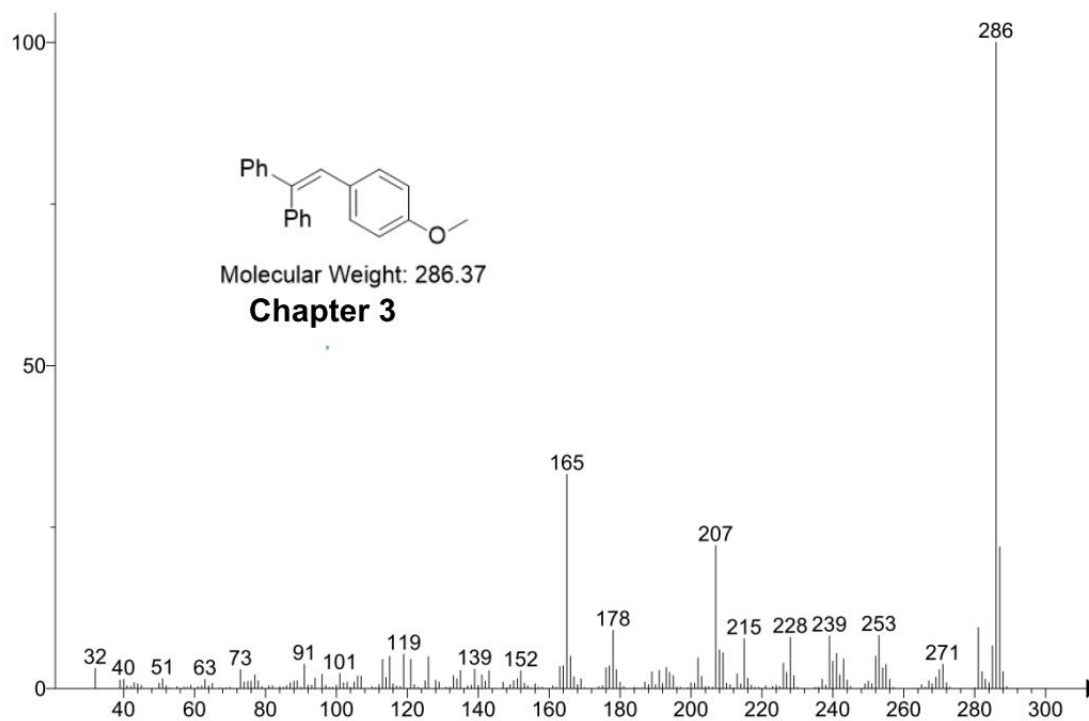
APPENDIX B. GC-MS SPECTRA

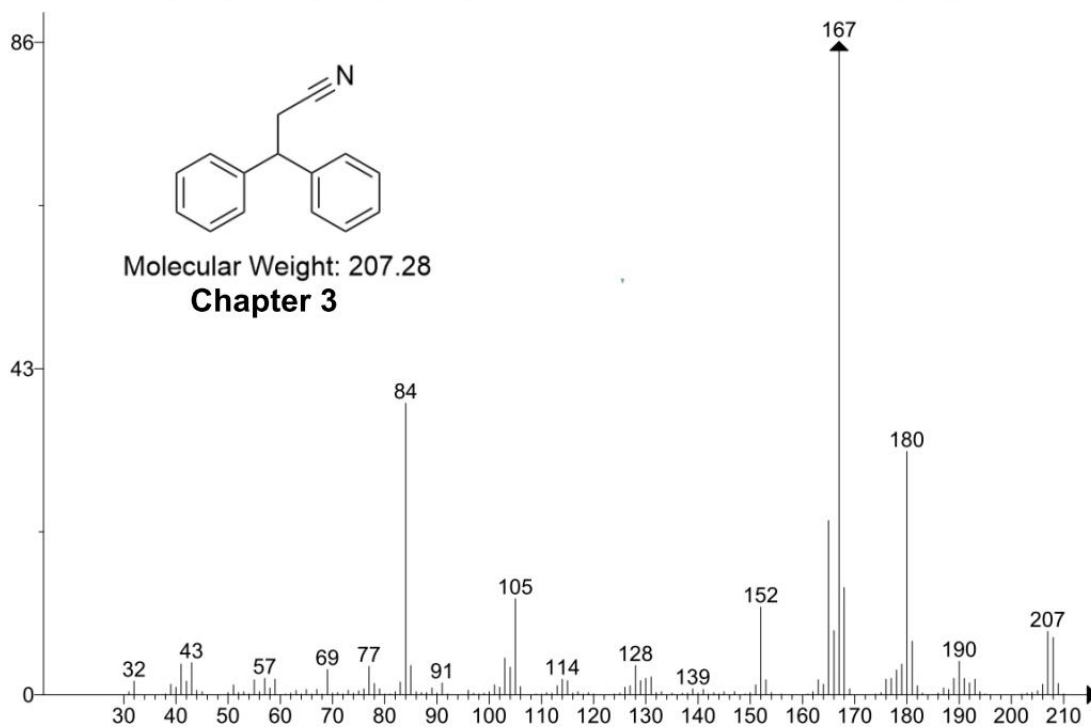
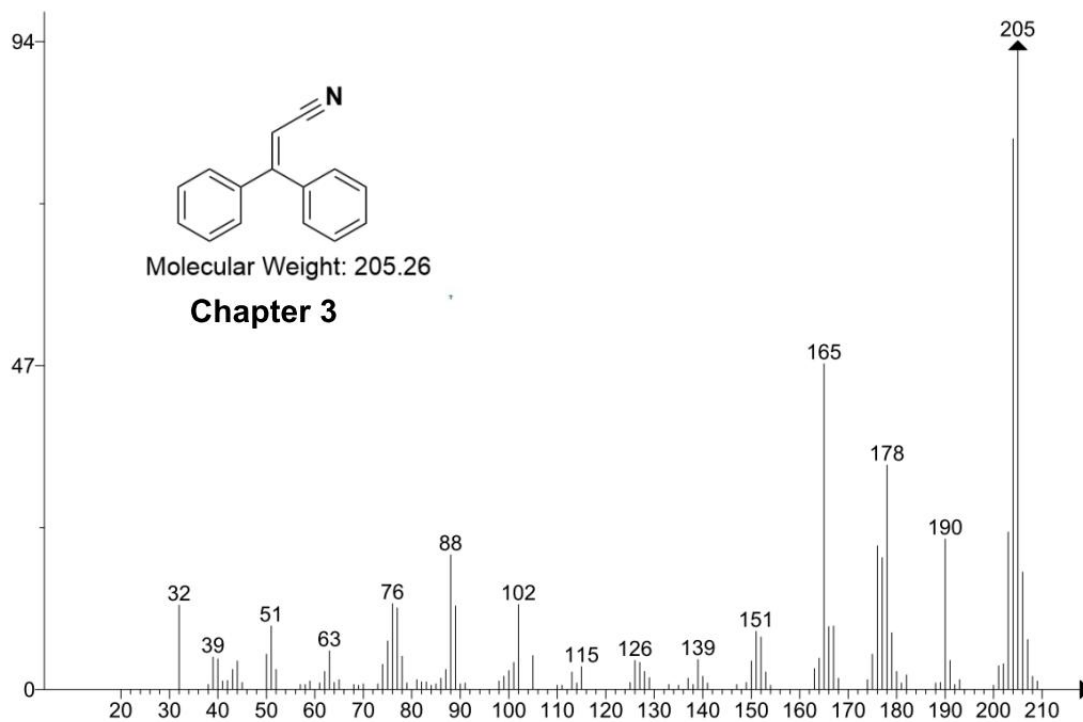


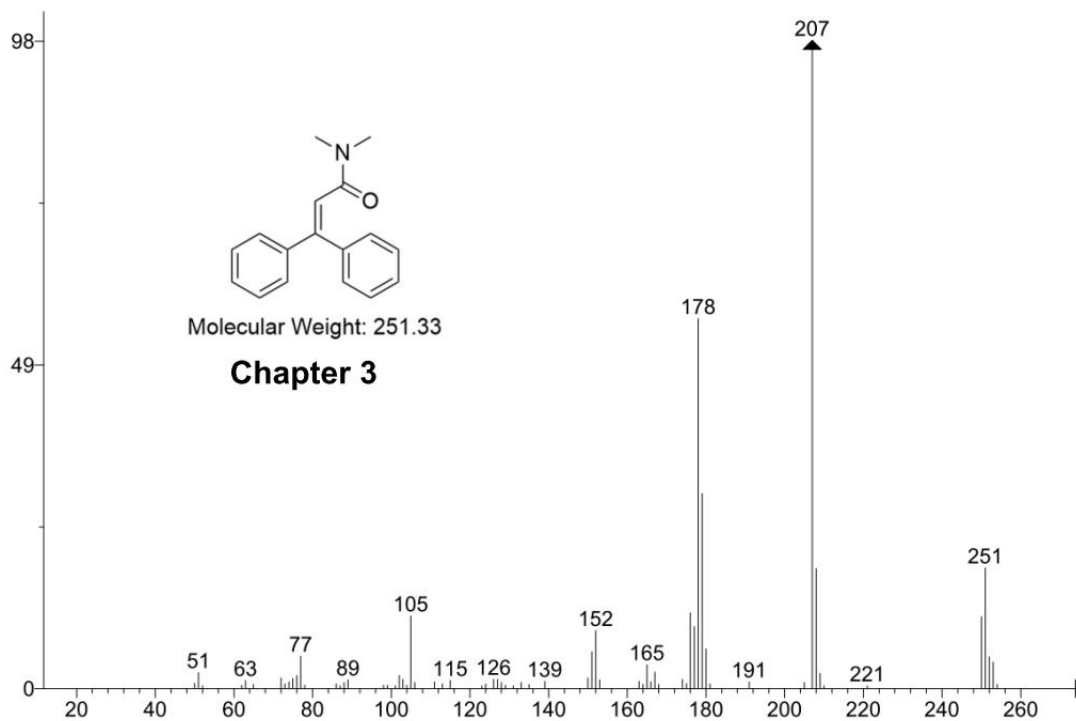
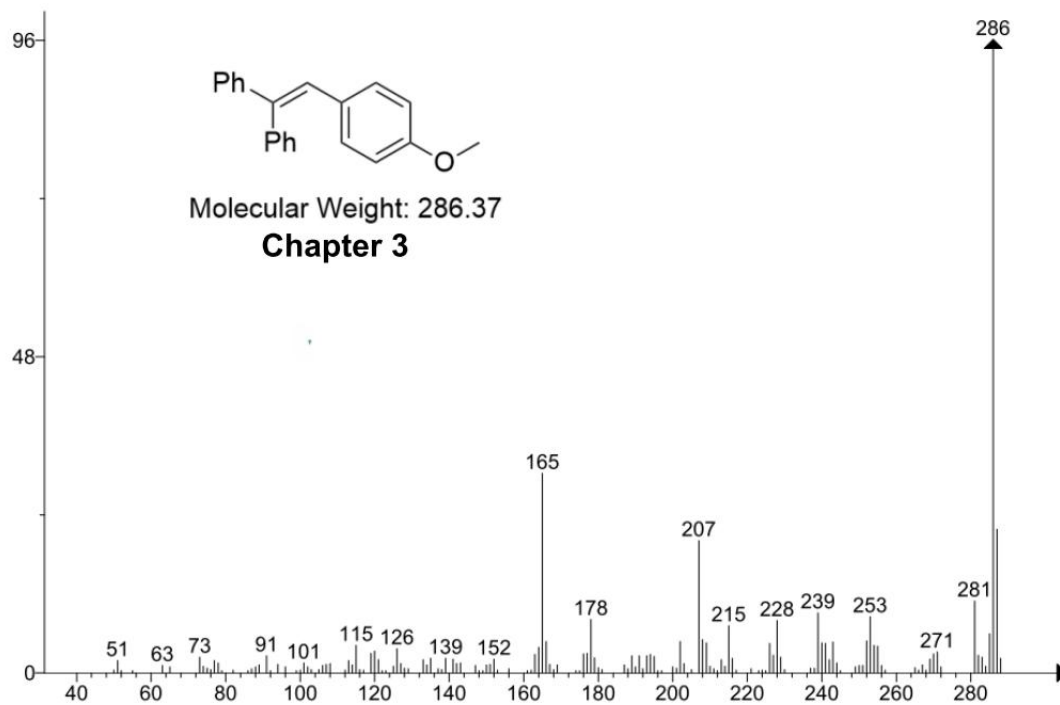


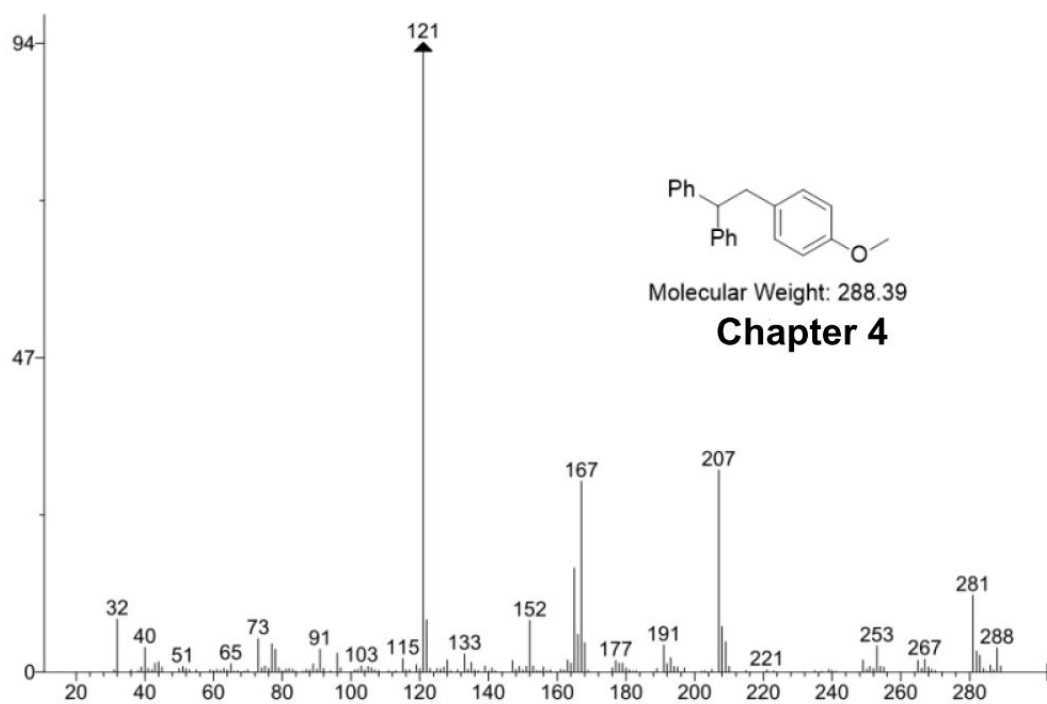
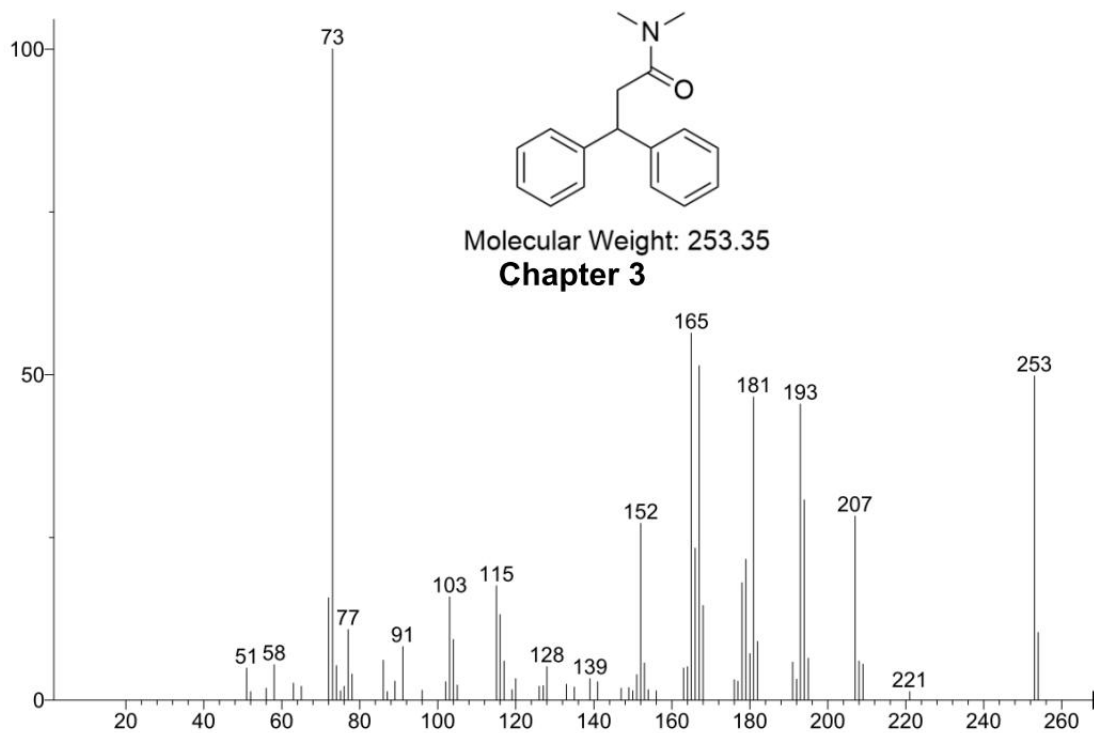


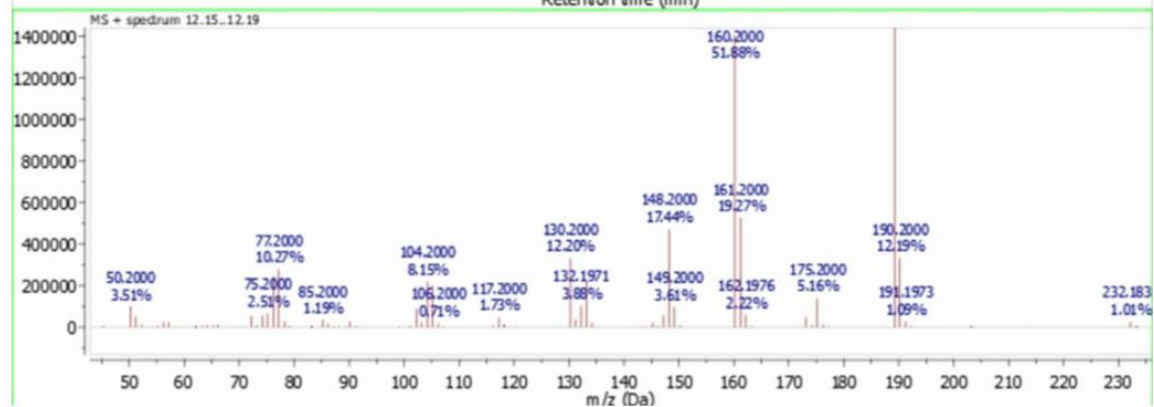
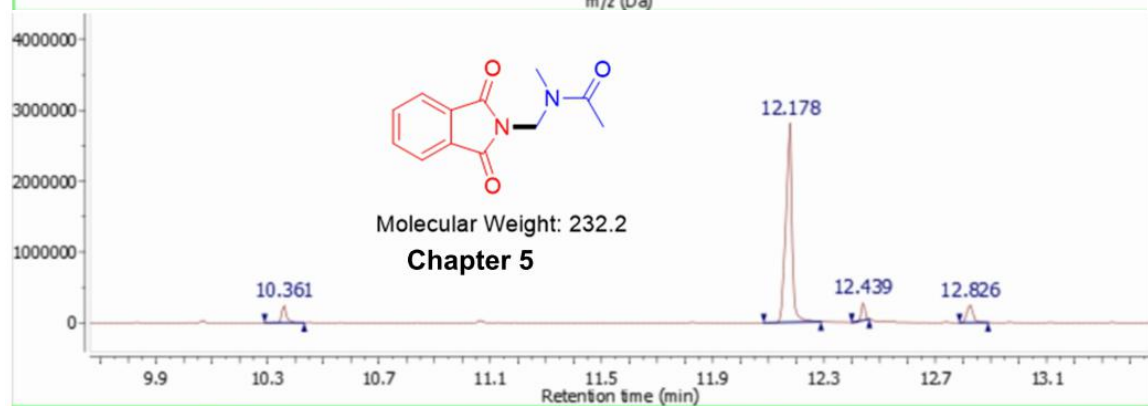
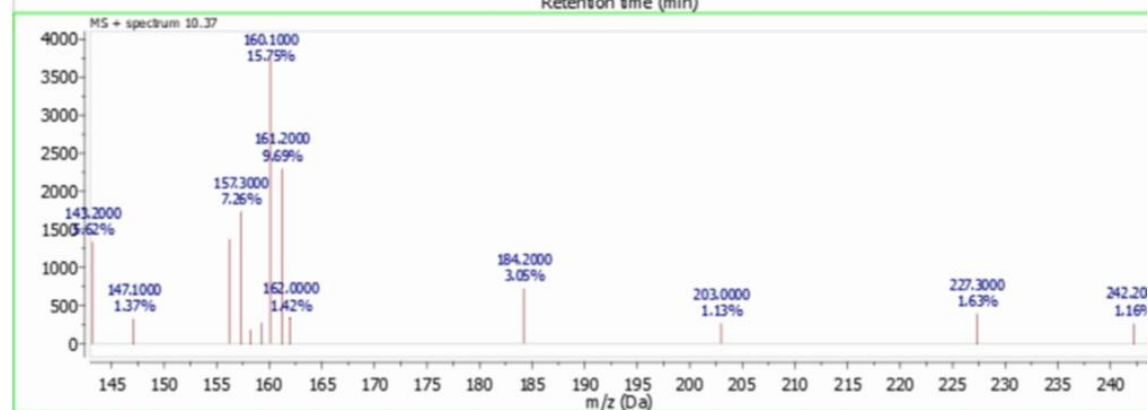
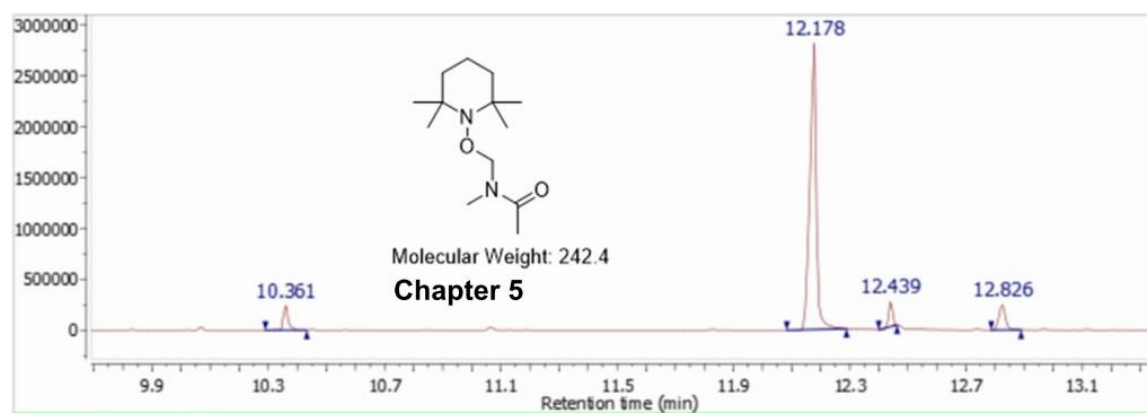


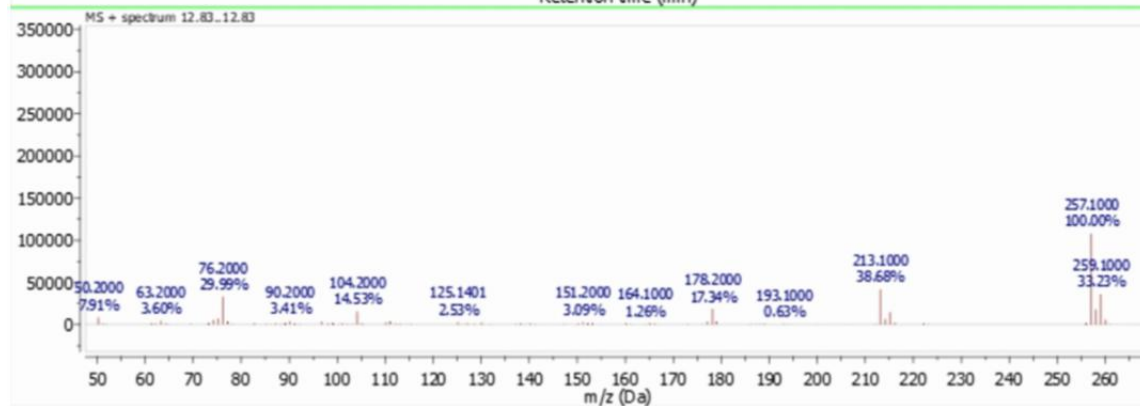
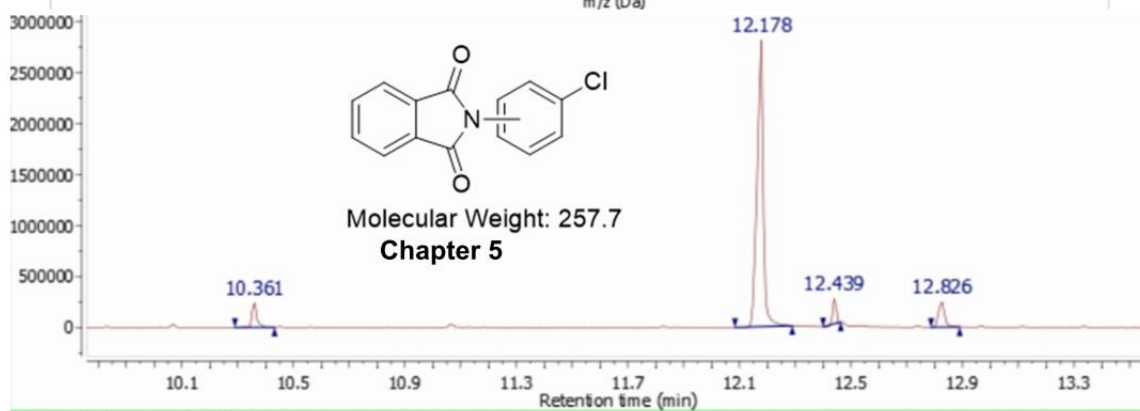
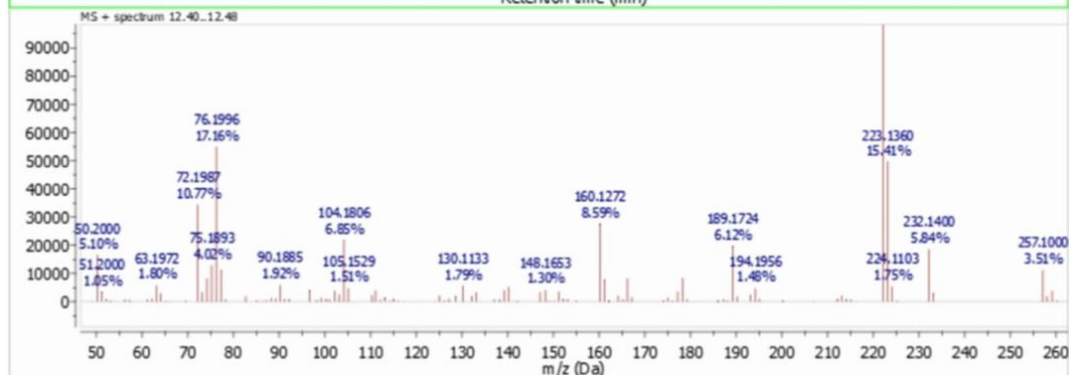
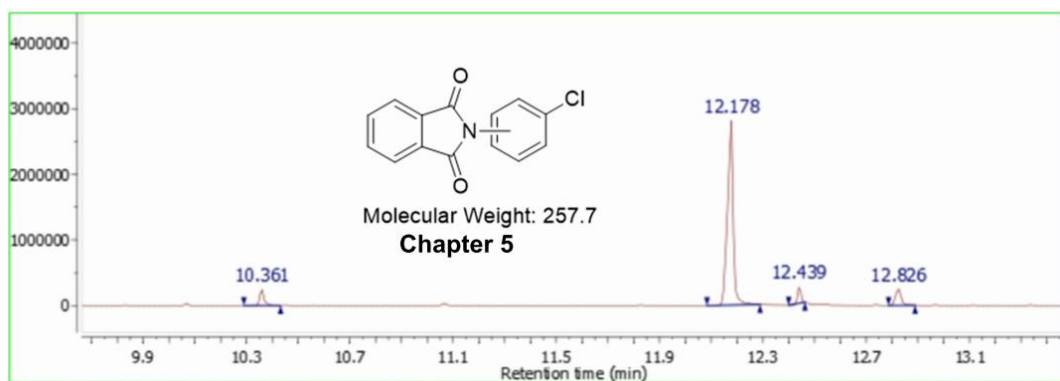










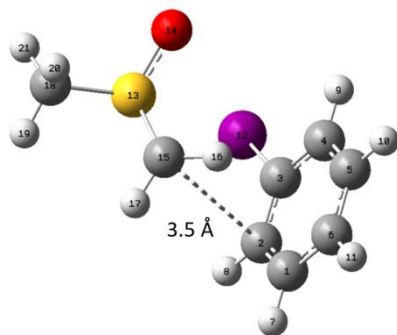


APPENDIX C. COMPUTATIONAL CALCULATIONS

Computational Calculations for Chapter 2

The optimization of the electron donor acceptor (EDA) complex was performed at the density functional theory level using the program suite Gaussian 09.¹ The wb97XD method² was employed for all calculations along with the 6-311+G(d,p) basis set for all atoms with the exception of I, which was treated with the MWB46 relativistic Stuttgart-Dresden pseudopotential. For the exploration of the EDA complex with *t*-butoxide, the potassium counter ion was not considered in the calculations. The gradient threshold used for all geometry optimization was 4.5×10^{-4} Hartree/Bohr. DMSO was used as an implicit solvent for all calculations and the method employed was the polarizable conductor calculation model (CPCM).^{3,4} Frequency calculations were conducted to determine if each optimization was a minimum in the potential energy surface. The excited state properties of the EDA complex were obtained with the time-dependent density functional (TD-DFT) formalism.^{5,6} The structure of all EDA complexes were obtained from the optimization of different initial structures of interaction along the double bonds of the aromatic ring with the dymstil anion and the *t*-butoxide followed by analysis of the energies of the first excited state.

Dimstyl anion-Aryl iodide EDA complex



Center Number	Atomic Number	Atomic Type	Coordinates (Angstroms)		
			X	Y	Z
1	6	0	-0.369737	2.786442	-1.154958
2	6	0	-0.826474	1.472791	-1.196291

3	6	0	-1.018739	0.789249	-0.002219
4	6	0	-0.756491	1.386148	1.224287
5	6	0	-0.298678	2.700691	1.248874
6	6	0	-0.107783	3.402394	0.063543
7	1	0	-0.217005	3.323086	-2.084122
8	1	0	-1.027644	0.996777	-2.147580
9	1	0	-0.904970	0.845641	2.150595
10	1	0	-0.093394	3.172804	2.202622
11	1	0	0.249330	4.425197	0.089763
12	53	0	-1.753217	-1.206756	-0.055748
13	16	0	2.409239	-0.763899	-0.004003
14	8	0	2.454196	-0.856227	1.509159
15	6	0	2.574289	0.896225	-0.477139
16	1	0	2.094633	1.629116	0.159973
17	1	0	2.764134	1.100668	-1.524177
18	6	0	3.981351	-1.408284	-0.641981
19	1	0	4.015223	-1.233431	-1.717568
20	1	0	4.803577	-0.905876	-0.133454
21	1	0	3.988808	-2.477635	-0.435350

```

-----
Zero-point correction=                0.157411 (Hartree/Particle)
Thermal correction to Energy=         0.170907
Thermal correction to Enthalpy=       0.171851
Thermal correction to Gibbs Free Energy= 0.112279
Sum of electronic and zero-point Energies= -795.421362
Sum of electronic and thermal Energies= -795.407866
Sum of electronic and thermal Enthalpies= -795.406922
Sum of electronic and thermal Free Energies= -795.466494

```

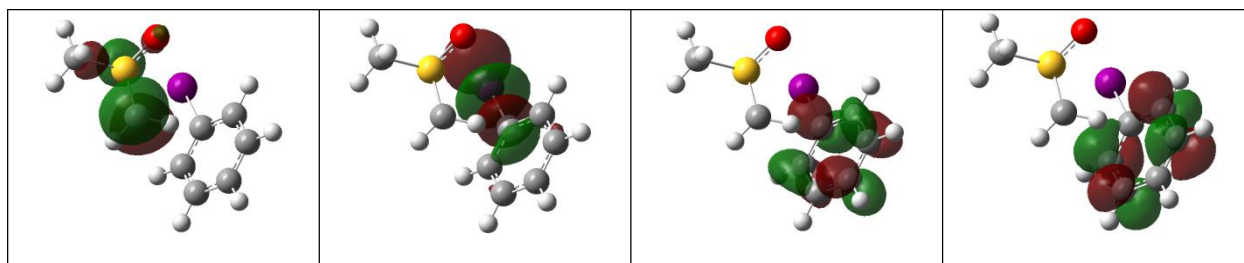
Excited State 1: 1.000-A 3.1623 eV 392.07 nm f=0.0093 <S2>=0.000**

```

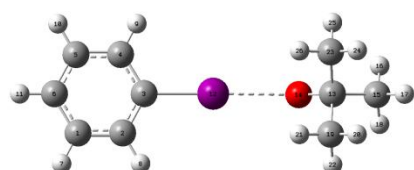
45A -> 46A      0.26642 (HOMO -> LUMO, 14% contribution = 2*0.26642^2*100)
45A -> 47A      0.60366 (HOMO -> LUMO+1, 73% contribution = 2*0.60366^2*100)
45A -> 48A      0.20308 (HOMO -> LUMO+2, 8% contribution = 2*0.20308^2*100)
45A -> 49A      0.10346
45B -> 46B      0.26642
45B -> 47B      0.60366
45B -> 48B      0.20308
45B -> 49B      0.10346

```

HOMO (π_{anion})	LUMO ($\sigma^*_{\text{aryl halide}}$)	LUMO+1 ($\pi^*_{\text{aryl halide}}$)	LUMO+2 ($\pi^*_{\text{aryl halide}}$)
-0.55 eV	0.85 eV	1.17 eV	1.21 eV



*t*BuO⁻-aryl halide complex (conformer 1)



Center Number	Atomic Number	Atomic Type	Coordinates (Angstroms)		
			X	Y	Z
1	6	0	4.234343	1.243953	0.220713
2	6	0	2.853176	1.215495	0.047083
3	6	0	2.181620	-0.002819	-0.021437
4	6	0	2.900546	-1.190849	0.084689
5	6	0	4.281754	-1.159199	0.258239
6	6	0	4.952497	0.057447	0.326355
7	1	0	4.747434	2.198125	0.272549
8	1	0	2.304607	2.147315	-0.034294
9	1	0	2.389257	-2.145677	0.032892
10	1	0	4.832231	-2.090164	0.339609
11	1	0	6.027908	0.080849	0.461264
12	53	0	0.042670	-0.045787	-0.291817
13	6	0	-3.593920	0.019616	0.132162
14	8	0	-2.618381	-0.102768	-0.834040
15	6	0	-5.000429	-0.058851	-0.502977
16	1	0	-5.123912	-1.019003	-1.015910
17	1	0	-5.803446	0.039591	0.238513
18	1	0	-5.117831	0.739659	-1.243696
19	6	0	-3.479372	1.372855	0.871940
20	1	0	-4.246300	1.496241	1.646718
21	1	0	-2.495590	1.453784	1.345949
22	1	0	-3.579675	2.196173	0.156101
23	6	0	-3.482778	-1.107812	1.185202
24	1	0	-4.254320	-1.037183	1.961948
25	1	0	-3.577547	-2.082972	0.694773
26	1	0	-2.501923	-1.066918	1.670412

```

-----
Zero-point correction=                0.213687 (Hartree/Particle)
Thermal correction to Energy=         0.227660
Thermal correction to Enthalpy=       0.228604
Thermal correction to Gibbs Free Energy= 0.169899
Sum of electronic and zero-point Energies= -476.000675
Sum of electronic and thermal Energies= -475.986702
Sum of electronic and thermal Enthalpies= -475.985757
Sum of electronic and thermal Free Energies= -476.044463

```

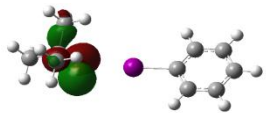
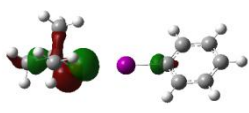
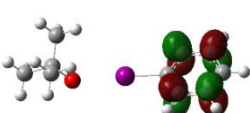
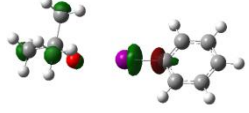
Excitation energies and oscillator strengths:

Excited State 1: 1.000-A 4.8050 eV 258.03 nm f=0.0474 <S2>=0.000**

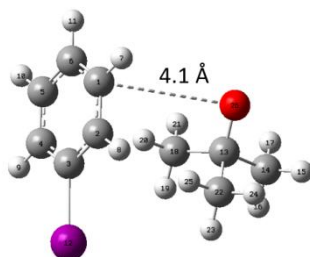
```

44A -> 48A      0.12775 (HOMO-1 -> LUMO+2, 3% contribution = 2*0.12775^2*100)
44A -> 49A      0.59921 (HOMO-1 -> LUMO+3, 72% contribution = 2*0.59921^2*100)
44A -> 51A     -0.15778 (HOMO-1 -> LUMO+5, 5% contribution = 2*0.15778^2*100)
44A -> 52A     -0.22191 (HOMO-1 -> LUMO+6, 10% contribution = 2*0.22191^2*100)
44B -> 48B      0.12775
44B -> 49B      0.59921
44B -> 51B     -0.15778
44B -> 52B     -0.22191

```

HOMO-1 -6.98 eV	HOMO -6.91 eV	LUMO 1.31 eV	LUMO+3 1.82 eV
			

*t*BuO⁻-aryl halide complex (conformer 2)



```

-----

```

Center Number	Atomic Number	Atomic Type	Coordinates (Angstroms)		
			X	Y	Z

1	6	0	-0.156296	2.476999	-1.249806
2	6	0	0.494651	1.247485	-1.227832
3	6	0	1.116214	0.838256	-0.055963

4	6	0	1.110716	1.630725	1.084244
5	6	0	0.458088	2.859188	1.045301
6	6	0	-0.177683	3.282151	-0.116648
7	1	0	-0.650493	2.799096	-2.159111
8	1	0	0.504017	0.621359	-2.110919
9	1	0	1.596487	1.301059	1.993923
10	1	0	0.445702	3.481594	1.932603
11	1	0	-0.689877	4.236901	-0.138813
12	53	0	2.065780	-1.066186	0.003477
13	6	0	-3.164561	-0.634603	0.008848
14	6	0	-4.293812	-1.536451	0.565364
15	1	0	-4.855923	-1.983527	-0.262365
16	1	0	-3.915049	-2.348643	1.199098
17	1	0	-4.989238	-0.934449	1.161315
18	6	0	-2.380491	-0.066442	1.216998
19	1	0	-1.966503	-0.852254	1.862460
20	1	0	-1.551397	0.553950	0.863260
21	1	0	-3.042071	0.561775	1.824558
22	6	0	-2.195919	-1.538717	-0.793107
23	1	0	-1.784375	-2.359352	-0.191406
24	1	0	-2.718707	-1.972784	-1.653266
25	1	0	-1.358462	-0.941425	-1.168736
26	8	0	-3.671984	0.374129	-0.775162

```

-----
Zero-point correction=                0.213804 (Hartree/Particle)
Thermal correction to Energy=         0.227729
Thermal correction to Enthalpy=       0.228673
Thermal correction to Gibbs Free Energy= 0.170158
Sum of electronic and zero-point Energies= -475.998949
Sum of electronic and thermal Energies= -475.985023
Sum of electronic and thermal Enthalpies= -475.984079
Sum of electronic and thermal Free Energies= -476.042594

```

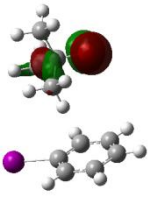
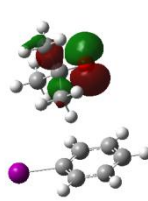
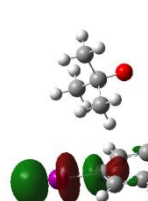
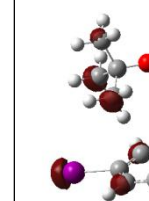
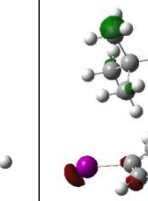
Excitation energies and oscillator strengths:

```

Excited State  1:  1.000-A      4.6567 eV  266.25 nm  f=0.0693  <S**2>=0.000
 44A -> 46A      -0.14927
 44A -> 47A       0.20690
 44A -> 48A       0.11886
 44A -> 49A       0.38266  (HOMO-1 -> LUMO+3,  29% contribution = 2*0.38266^2*100)
 44A -> 50A      -0.38252  (HOMO-1 -> LUMO+4,  29% contribution = 2*0.38252^2*100)
 44A -> 53A      -0.10849
 44A -> 57A       0.16931
 44A -> 58A       0.19256
 44B -> 46B      -0.14927

```

44B -> 47B 0.20690
 44B -> 48B 0.11886
 44B -> 49B 0.38266
 44B -> 50B -0.38252
 44B -> 53B -0.10849
 44B -> 57B 0.16931
 44B -> 58B 0.19256

HOMO-1 -6.83 eV	HOMO -6.83 eV	LUMO 0.78 eV	LUMO+3 1.62 eV	LUMO+4 2.08 eV
				

Reference:

1. Frisch, M. J.; Trucks, G. W.; Schlegel, H. B.; Scuseria, G. E.; Robb, M. A.; Cheeseman, J. R.; Scalmani, G.; Barone, V.; Mennucci, B.; Petersson, G. A.; Nakatsuji, H.; Caricato, M.; Li, X.; Hratchian, H. P.; Izmaylov, A. F.; Bloino, J.; Zheng, G.; Sonnenberg, J. L.; Hada, M.; Ehara, M.; Toyota, K.; Fukuda, R.; Hasegawa, J.; Ishida, M.; Nakajima, T.; Honda, Y.; Kitao, O.; Nakai, H.; Vreven, T.; Montgomery Jr., J. A.; Peralta, J. E.; Ogliaro, F.; Bearpark, M.; Heyd, J. J.; Brothers, E.; Kudin, K. N.; Staroverov, V. N.; Kobayashi, R.; Normand, J.; Raghavachari, K.; Rendell, A.; Burant, J. C.; Iyengar, S. S.; Tomasi, J.; Cossi, M.; Rega, N.; Millam, J. M.; Klene, M.; Knox, J. E.; Cross, J. B.; Bakken, V.; Adamo, C.; Jaramillo, J.; Gomperts, R.; Stratmann, R. E.; Yazyev, O.; Austin, A. J.; Cammi, R.; Pomelli, C.; Ochterski, J. W.; Martin, R. L.; Morokuma, K.; Zakrzewski, V. G.; Voth, G. A.; Salvador, P.; Dannenberg, J. J.; Dapprich, S.; Daniels, A. D.; Farkas, Ö.; Foresman, J. B.; Ortiz, J. V.; Cioslowski, J.; Fox, D. J. Gaussian 09 Revision E.01. Gaussian Inc. Wallingford CT 2009.
2. Chai, J.-D.; Head-Gordon, M. *Phys. Chem. Chem. Phys.*, **2008**, *10*, 6615-6620.
3. Barone, V.; Cossi, M. *J. Phys. Chem. A*, **1998**, *102*, 1995-2001.
4. Cossi, M.; Rega, N.; Scalmani, G.; Barone, V. *J. Comput. Chem.*, 2003, *24*, 669-681.
5. Scalmani, G.; Frisch, M. J.; Mennucci, B.; Tomasi, J.; Cammi, R.; Barone, V. *J. Phys. Chem.*, **2006**, *124*, 094107:1-15.
6. Laurent, A. D.; Adamo, C.; Jacquemin, D. *Phys. Chem. Chem. Phys.*, **2014**, *16*, 14334-14356.

Computational Methods for Chapter 5

The optimization of the reactants, products, intermediates and transition states was performed at the density functional theory level using the program suite Gaussian 09.¹ The B3LYP method² was employed for all calculations along with the 6-311+G(d,p) basis set for all

atoms with the exception of Br, which was treated with the MWB28 relativistic Stuttgart-Dresden pseudopotential. The lithium counter ion was not taken into account in the calculations. The gradient threshold used for all geometry optimization was 4.5×10^{-4} Hartree/Bohr. The implicit solvation method employed for all calculations was the polarizable conductor calculation model (CPCM).^{3,4} Frequency calculations were conducted to determine if each optimization was at a minimum (reactants, products and intermediates) or a maximum (transition states) in the potential energy surface. Furthermore, each transition state was confirmed via intrinsic reaction coordinate (IRC) calculations. The excited state properties of the Br-phthalimide-LiOtBu adduct were obtained with the time-dependent density functional (TD-DFT) formalism.^{5,6} The activation free energy for the single electron transfer (SET) was calculated through Marcus-Hush theory with equation S1,⁷

$$\Delta G_{SET}^{\ddagger} = \frac{\lambda}{4} \left(1 + \frac{\Delta G_{rel}}{\lambda} \right)^2 \quad (\text{eq. S1})$$

where ΔG_{rel} is the relative difference in free energies of the SET step and λ refers to the reorganization energy.

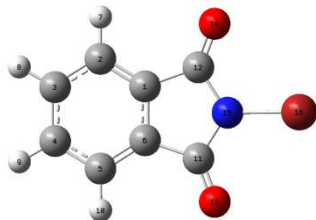
References:

1. M. J. Frisch, G. W. Trucks, H. B. Schlegel, G. E. Scuseria, M. A. Robb, J. R. Cheeseman, G. Scalmani, V. Barone, B. Mennucci, G. A. Petersson, H. Nakatsuji, M. Caricato, X. Li, H. P. Hratchian, A. F. Izmaylov, J. Bloino, G. Zheng, J. L. Sonnenberg, M. Hada, M. Ehara, K. Toyota, R. Fukuda, J. Hasegawa, M. Ishida, T. Nakajima, Y. Honda, O. Kitao, H. Nakai, T. Vreven, J. A. Montgomery Jr., J. E. Peralta, F. Ogliaro, M. Bearpark, J. J. Heyd, E. Brothers, K. N. Kudin, V. N. Staroverov, R. Kobayashi, J. Normand, K. Raghavachari, A. Rendell, J. C. Burant, S. S. Iyengar, J. Tomasi, M. Cossi, N. Rega, J. M. Millam, M. Klene, J. E. Knox, J. B. Cross, V. Bakken, C. Adamo, J. Jaramillo, R. Gomperts, R. E. Stratmann, O. Yazyev, A. J. Austin, R. Cammi, C. Pomelli, J. W. Ochterski, R. L. Martin, K. Morokuma, V. G. Zakrzewski, G. A. Voth, P. Salvador, J. J. Dannenberg, S. Dapprich, A. D. Daniels, Ö. Farkas, J. B. Foresman, J. V. Ortiz, J. Cioslowski and D. J. Fox, Gaussian 09 Revision E.01. Gaussian Inc. Wallingford CT 2009.
2. A. D. Becke, *J. Chem. Phys.*, **1993**, 98, 5648-5652.; C. Lee, W. Yang and R. G. Parr, *Phys. Rev. B*, **1988**, 37, 785-789.
3. V. Barone and M. Cossi, *J. Phys. Chem. A*, **1998**, **102**, 1995-2001.
4. M. Cossi, N. Rega, G. Scalmani and V. Barone, *J. Comput. Chem.*, **2003**, 24, 669-681.
5. G. Scalmani, M. J. Frisch, B. Mennucci, J. Tomaso, R. Cammi, V. Barone, *J. Phys. Chem.*, **2006**, 124, 094107:1-15.
6. A. D. Laurent, C. Adamo, D. Jacquemin, *Phys. Chem. Chem. Phys.*, **2014**, 16, 14334-14356.
7. C. Adouama, M. E. Budén, W. D. Guerra, M. Puiatti, B. Joseph, S. M. Barolo, R. A. Rossi, M. Médebielle, *Org. Lett.*, **2019**, 21, 320-324.

Computational Data

Cartesian coordinates

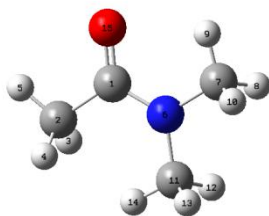
N-bromophthalimide



Center Number	Atomic Number	Atomic Type	Coordinates (Angstroms)		
			X	Y	Z
1	6	0	-0.000116	1.388291	0.698062
2	6	0	0.000079	2.568095	1.422786
3	6	0	0.000297	3.766652	0.698758
4	6	0	0.000297	3.766652	-0.698758
5	6	0	0.000079	2.568095	-1.422786
6	6	0	-0.000116	1.388291	-0.698062
7	1	0	0.000094	2.563320	2.505628
8	1	0	0.000495	4.710635	1.230453
9	1	0	0.000495	4.710635	-1.230453
10	1	0	0.000094	2.563320	-2.505628
11	6	0	-0.000367	-0.022389	-1.181666
12	6	0	-0.000367	-0.022389	1.181666
13	8	0	-0.000141	-0.452973	-2.307655
14	8	0	-0.000141	-0.452973	2.307655
15	7	0	-0.001039	-0.792835	0.000000
16	35	0	0.000276	-2.690236	0.000000

Zero-point correction=	0.104357 (Hartree/Particle)
Thermal correction to Energy=	0.113865
Thermal correction to Enthalpy=	0.114810
Thermal correction to Gibbs Free Energy=	0.067932
Sum of electronic and zero-point Energies=	-525.867773
Sum of electronic and thermal Energies=	-525.858265
Sum of electronic and thermal Enthalpies=	-525.857321
Sum of electronic and thermal Free Energies=	-525.904199

N,N-dimethylacetamide

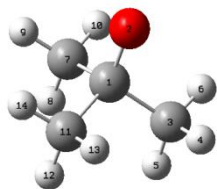


Center Number	Atomic Number	Atomic Type	Coordinates (Angstroms)		
			X	Y	Z
1	6	0	-0.723894	-0.291345	-0.000089
2	6	0	-1.774516	0.806918	-0.000110
3	1	0	-1.692941	1.444551	0.883495
4	1	0	-1.693003	1.444543	-0.883722
5	1	0	-2.751956	0.329288	-0.000065
6	7	0	0.587769	0.078553	-0.000732
7	6	0	1.634749	-0.937685	-0.000046
8	1	0	2.264017	-0.830604	0.889298
9	1	0	1.177741	-1.922938	-0.002441
10	1	0	2.267500	-0.827776	-0.886520
11	6	0	1.069770	1.454748	0.000341
12	1	0	1.683170	1.638042	0.888690
13	1	0	1.687802	1.637417	-0.884874
14	1	0	0.248576	2.164249	-0.002137
15	8	0	-1.067743	-1.477807	0.000353

Zero-point correction= 0.129189 (Hartree/Particle)
 Thermal correction to Energy= 0.137153
 Thermal correction to Enthalpy= 0.138097
 Thermal correction to Gibbs Free Energy= 0.095417
 Sum of electronic and zero-point Energies= -287.797106
 Sum of electronic and thermal Energies= -287.789142
 Sum of electronic and thermal Enthalpies= -287.788197
 Sum of electronic and thermal Free Energies= -287.830877

Recommended a0 for SCRF calculation = 4.18 angstrom

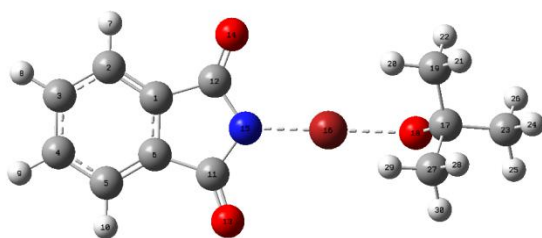
t-butoxide anion



Center Number	Atomic Number	Atomic Type	Coordinates (Angstroms)		
			X	Y	Z
1	6	0	-0.000030	-0.000049	0.132247
2	8	0	-0.000882	0.000187	1.504169
3	6	0	0.891635	-1.145588	-0.432979
4	1	0	0.520717	-2.110769	-0.071025
5	1	0	0.915297	-1.175680	-1.530995
6	1	0	1.918322	-1.022983	-0.070956
7	6	0	0.546749	1.344531	-0.433406
8	1	0	0.561718	1.379618	-1.531410
9	1	0	-0.072576	2.172772	-0.071794
10	1	0	1.567996	1.505826	-0.070847
11	6	0	-1.437645	-0.199111	-0.434124
12	1	0	-1.475223	-0.204094	-1.532192
13	1	0	-1.845273	-1.149573	-0.072454
14	1	0	-2.088175	0.604687	-0.072107

Zero-point correction= 0.120428 (Hartree/Particle)
 Thermal correction to Energy= 0.126753
 Thermal correction to Enthalpy= 0.127697
 Thermal correction to Gibbs Free Energy= 0.091777
 Sum of electronic and zero-point Energies= -233.107250
 Sum of electronic and thermal Energies= -233.100925
 Sum of electronic and thermal Enthalpies= -233.099981
 Sum of electronic and thermal Free Energies= -233.135901

t-butoxide *N*-bromophthalimide complex (S₀)



Center Number	Atomic Number	Atomic Type	Coordinates (Angstroms)		
			X	Y	Z

1	6	0	-3.024903	0.706088	0.044589
2	6	0	-4.184708	1.450390	0.184205
3	6	0	-5.387410	0.748856	0.340738
4	6	0	-5.408818	-0.649085	0.354521
5	6	0	-4.228277	-1.390237	0.212085
6	6	0	-3.046137	-0.684866	0.058224
7	1	0	-4.163223	2.533758	0.173004
8	1	0	-6.316333	1.296267	0.453234
9	1	0	-6.354093	-1.165361	0.477548
10	1	0	-4.240160	-2.473772	0.222076
11	6	0	-1.628911	-1.154842	-0.116107
12	6	0	-1.594194	1.129305	-0.138161
13	8	0	-1.250389	-2.314247	-0.153225
14	8	0	-1.181004	2.275958	-0.196897
15	7	0	-0.833029	-0.025526	-0.226210
16	35	0	1.197691	-0.059382	-0.462528
17	6	0	4.200941	0.028154	0.275216
18	8	0	3.327996	-0.110369	-0.826044
19	6	0	4.017953	1.392367	0.973369
20	1	0	3.007949	1.483640	1.381130
21	1	0	4.730033	1.522615	1.795704
22	1	0	4.168979	2.203620	0.254877
23	6	0	5.629043	-0.055146	-0.302029
24	1	0	6.385503	0.035425	0.485474
25	1	0	5.772850	-1.012301	-0.811328
26	1	0	5.788703	0.746385	-1.028897
27	6	0	4.005260	-1.109449	1.299950
28	1	0	4.724069	-1.036476	2.123392
29	1	0	2.998375	-1.077142	1.723996
30	1	0	4.137519	-2.079552	0.811456

```

Zero-point correction=                0.227512 (Hartree/Particle)
Thermal correction to Energy=          0.244878
Thermal correction to Enthalpy=        0.245822
Thermal correction to Gibbs Free Energy= 0.179765
Sum of electronic and zero-point Energies= -759.015660
Sum of electronic and thermal Energies=   -758.998294
Sum of electronic and thermal Enthalpies=  -758.997350
Sum of electronic and thermal Free Energies= -759.063408

```

```

Excited State  1:  3.000-A      2.9816 eV  415.82 nm  f=0.0000  <S**2>=2.000
  60A -> 63A      -0.24449
  61A -> 63A      -0.24700
  62A -> 63A      -0.59867
  60B -> 63B       0.24449

```

61B -> 63B 0.24700
 62B -> 63B 0.59867

This state for optimization and/or second-order correction.

Total Energy, E(TD-HF/TD-KS) = -759.133598719

Copying the excited state density for this state as the 1-particle RhoCI density.

Excited State 2: 1.000-A 3.0008 eV 413.17 nm f=0.0001 <S**2>=0.000
 62A -> 63A 0.70557
 62B -> 63B 0.70557

Excited State 3: 3.000-A 3.0343 eV 408.61 nm f=0.0000 <S**2>=2.000
 57A -> 63A -0.13212
 60A -> 63A 0.30839
 61A -> 63A 0.47915
 62A -> 63A -0.36652
 57B -> 63B 0.13212
 60B -> 63B -0.30839
 61B -> 63B -0.47915
 62B -> 63B 0.36652

Excited State 4: 1.000-A 3.1696 eV 391.16 nm f=0.0007 <S**2>=0.000
 61A -> 63A 0.70059
 61B -> 63B 0.70059

Excited State 5: 3.000-A 3.1955 eV 387.99 nm f=0.0000 <S**2>=2.000
 55A -> 63A 0.11989
 57A -> 63A -0.17302
 58A -> 64A 0.13197
 60A -> 63A 0.48343
 61A -> 63A -0.42634
 55B -> 63B -0.11989
 57B -> 63B 0.17302
 58B -> 64B -0.13197
 60B -> 63B -0.48343
 61B -> 63B 0.42634

Excited State 6: 3.000-A 3.3458 eV 370.57 nm f=0.0000 <S**2>=2.000
 61A -> 65A 0.67895
 61A -> 67A 0.14228
 61B -> 65B -0.67895
 61B -> 67B -0.14228

Excited State 7: 3.000-A 3.4077 eV 363.83 nm f=0.0000 <S**2>=2.000
 59A -> 63A 0.68700
 59B -> 63B -0.68700

Excited State 8: 3.000-A 3.4462 eV 359.77 nm f=0.0000 <S**2>=2.000
 62A -> 65A -0.68809

```

62A -> 67A      -0.12023
62B -> 65B       0.68809
62B -> 67B       0.12023

```

Excited State 9: 3.000-A 3.5362 eV 350.62 nm f=0.0000 <S**2>=2.000

```

54A -> 63A      -0.21742
55A -> 63A      -0.11422
57A -> 63A       0.53064
58A -> 64A      -0.25262
60A -> 63A       0.24861
60A -> 68A      -0.11694
54B -> 63B       0.21742
55B -> 63B       0.11422
57B -> 63B      -0.53064
58B -> 64B       0.25262
60B -> 63B      -0.24861
60B -> 68B       0.11694

```

Excited State 10: 1.000-A 3.7289 eV 332.49 nm f=0.0090 <S**2>=0.000

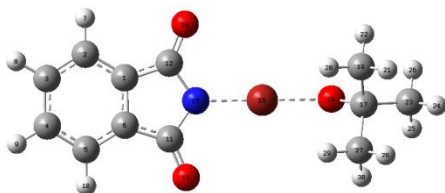
```

60A -> 63A       0.69762
60B -> 63B       0.69762

```

SavETr: write IOETrn= 770 NScale= 10 NData= 16 NLR=1 LETran= 190.

t-butoxide *N*-bromophthalimide complex (S₁)



Center Number	Atomic Number	Atomic Type	Coordinates (Angstroms)		
			X	Y	Z
1	6	0	3.023950	-0.697125	0.059072
2	6	0	4.232867	-1.390701	0.216948
3	6	0	5.397644	-0.651177	0.358378
4	6	0	5.372469	0.766489	0.342535
5	6	0	4.182069	1.460554	0.185060
6	6	0	2.999124	0.721037	0.040244
7	1	0	4.253289	-2.474649	0.229352
8	1	0	6.345150	-1.162813	0.484098
9	1	0	6.301278	1.314177	0.455093
10	1	0	4.163800	2.544546	0.172146
11	6	0	1.623216	1.119702	-0.139343

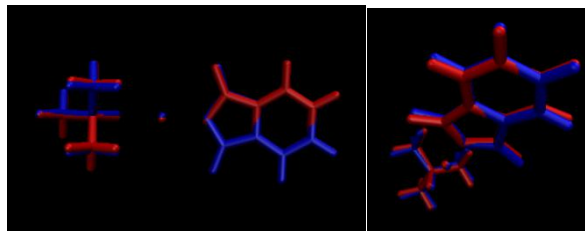
12	6	0	1.662844	-1.148031	-0.109323
13	8	0	1.112078	2.268434	-0.209648
14	8	0	1.193985	-2.315851	-0.161280
15	7	0	0.841187	-0.029700	-0.227383
16	35	0	-1.189546	-0.067141	-0.463045
17	6	0	-4.184729	0.032211	0.278703
18	8	0	-3.312375	-0.120917	-0.821900
19	6	0	-3.989168	-1.095512	1.314263
20	1	0	-2.982600	-1.060002	1.738425
21	1	0	-4.708389	-1.011725	2.135974
22	1	0	-4.123428	-2.070072	0.835662
23	6	0	-5.611829	-0.053407	-0.299048
24	1	0	-6.367515	0.048023	0.487519
25	1	0	-5.768937	0.740699	-1.034386
26	1	0	-5.758355	-1.015652	-0.797607
27	6	0	-3.995309	1.403575	0.961036
28	1	0	-4.708354	1.544072	1.780460
29	1	0	-2.985774	1.495035	1.369489
30	1	0	-4.142766	2.207192	0.233524

```

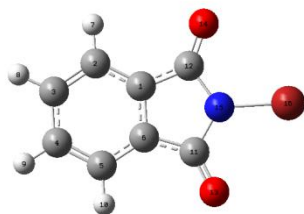
Zero-point correction=                                0.224176 (Hartree/Particle)
Thermal correction to Energy=                          0.241691
Thermal correction to Enthalpy=                       0.242636
Thermal correction to Gibbs Free Energy=              0.176292
Sum of electronic and zero-point Energies=            -758.902665
Sum of electronic and thermal Energies=               -758.885150
Sum of electronic and thermal Enthalpies=             -758.884206
Sum of electronic and thermal Free Energies=          -758.950549

```

Structure comparison of S0(blue) and S1(red). RMSD: 0.169



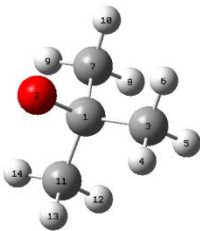
N-bromophthalimide radical anion



Center Number	Atomic Number	Atomic Type	Coordinates (Angstroms)		
			X	Y	Z
1	6	0	-0.000015	1.354431	0.717155
2	6	0	0.000011	2.568883	1.423669
3	6	0	0.000043	3.757271	0.711630
4	6	0	0.000043	3.757271	-0.711630
5	6	0	0.000011	2.568883	-1.423669
6	6	0	-0.000015	1.354431	-0.717155
7	1	0	0.000010	2.570834	2.508530
8	1	0	0.000069	4.703351	1.242054
9	1	0	0.000069	4.703351	-1.242054
10	1	0	0.000010	2.570834	-2.508530
11	6	0	-0.000049	-0.004763	-1.200298
12	6	0	-0.000049	-0.004763	1.200298
13	8	0	-0.000032	-0.482400	-2.347079
14	8	0	-0.000032	-0.482400	2.347079
15	7	0	-0.000130	-0.768045	0.000000
16	35	0	0.000039	-2.673243	0.000000

Zero-point correction=	0.101514 (Hartree/Particle)
Thermal correction to Energy=	0.111219
Thermal correction to Enthalpy=	0.112163
Thermal correction to Gibbs Free Energy=	0.064346
Sum of electronic and zero-point Energies=	-525.977509
Sum of electronic and thermal Energies=	-525.967803
Sum of electronic and thermal Enthalpies=	-525.966859
Sum of electronic and thermal Free Energies=	-526.014677

t-butoxide radical



Center Number	Atomic Number	Atomic Type	Coordinates (Angstroms)		
			X	Y	Z
1	6	0	0.022851	0.000179	0.078789
2	8	0	-0.158896	-0.002651	1.449323
3	6	0	1.510957	-0.002327	-0.301056
4	1	0	2.002187	-0.890228	0.104903
5	1	0	1.644441	-0.000827	-1.386032
6	1	0	2.005865	0.882234	0.107740
7	6	0	-0.696373	1.268567	-0.457782
8	1	0	-0.590993	1.300435	-1.544962
9	1	0	-1.755717	1.247142	-0.198646
10	1	0	-0.243070	2.167942	-0.036409
11	6	0	-0.701359	-1.264188	-0.461263
12	1	0	-0.596050	-1.292875	-1.548547
13	1	0	-0.251355	-2.166508	-0.042715
14	1	0	-1.760597	-1.239502	-0.202044

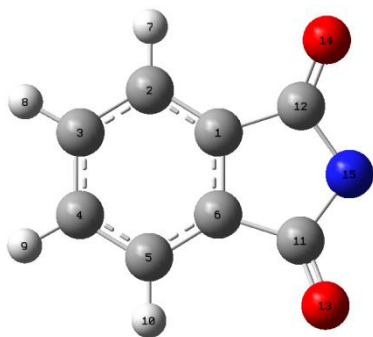
```

Zero-point correction=                0.120153 (Hartree/Particle)
Thermal correction to Energy=          0.126406
Thermal correction to Enthalpy=        0.127350
Thermal correction to Gibbs Free Energy= 0.090751
Sum of electronic and zero-point Energies= -232.961837
Sum of electronic and thermal Energies= -232.955584
Sum of electronic and thermal Enthalpies= -232.954640
Sum of electronic and thermal Free Energies= -232.991239

```

Recommended a0 for SCRF calculation = 4.06 angstrom

Phthalimide radical



Center Number	Atomic Number	Atomic Type	Coordinates (Angstroms)		
			X	Y	Z
1	6	0	0.005697	0.143289	0.701016
2	6	0	0.008087	1.327886	1.427831
3	6	0	0.001286	2.518789	0.703829
4	6	0	0.001286	2.518789	-0.703829
5	6	0	0.008087	1.327886	-1.427831
6	6	0	0.005697	0.143289	-0.701016
7	1	0	0.010775	1.324255	2.510532
8	1	0	-0.005814	3.465910	1.229816
9	1	0	-0.005814	3.465910	-1.229816
10	1	0	0.010775	1.324255	-2.510532
11	6	0	0.010888	-1.272686	-1.149464
12	6	0	0.010888	-1.272686	1.149464
13	8	0	-0.112315	-1.720310	-2.268322
14	8	0	-0.112315	-1.720310	2.268322
15	7	0	0.210804	-2.094673	0.000000

```

Zero-point correction=                                0.100994 (Hartree/Particle)
Thermal correction to Energy=                          0.109031
Thermal correction to Enthalpy=                       0.109975
Thermal correction to Gibbs Free Energy=              0.066815
Sum of electronic and zero-point Energies=            -512.446220
Sum of electronic and thermal Energies=               -512.438184
Sum of electronic and thermal Enthalpies=             -512.437240
Sum of electronic and thermal Free Energies=          -512.480400

```

Bromo anion



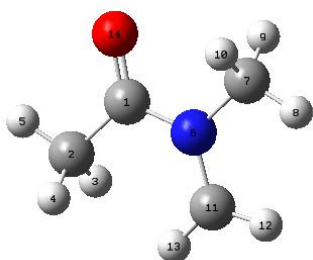
Center Number	Atomic Number	Atomic Type	Coordinates (Angstroms)		
			X	Y	Z
1	35	0	0.000000	0.000000	0.000000

```

Zero-point correction=          0.000000 (Hartree/Particle)
Thermal correction to Energy=    0.001416
Thermal correction to Enthalpy=  0.002360
Thermal correction to Gibbs Free Energy= -0.016176
Sum of electronic and zero-point Energies= -13.557361
Sum of electronic and thermal Energies= -13.555945
Sum of electronic and thermal Enthalpies= -13.555001
Sum of electronic and thermal Free Energies= -13.573537

```

N,N-dimethylacetamide radical



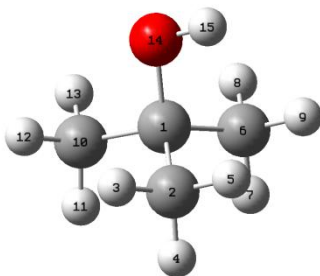
Center Number	Atomic Number	Atomic Type	Coordinates (Angstroms)		
			X	Y	Z
1	6	0	-0.664759	-0.323024	-0.000047
2	6	0	-1.834516	0.631561	0.000071
3	1	0	-1.821776	1.277216	0.882864
4	1	0	-1.822464	1.276877	-0.882966
5	1	0	-2.751318	0.045880	0.000457
6	7	0	0.606554	0.222876	-0.000097
7	6	0	1.730274	-0.725516	-0.000010
8	1	0	2.660449	-0.162624	-0.001826
9	1	0	1.687266	-1.359783	0.885823
10	1	0	1.685189	-1.362071	-0.884057
11	6	0	0.875187	1.572965	0.000236
12	1	0	1.905603	1.885903	0.000234
13	1	0	0.066408	2.281773	-0.001338
14	8	0	-0.811544	-1.547401	-0.000002

```

Zero-point correction=                0.115499 (Hartree/Particle)
Thermal correction to Energy=         0.123259
Thermal correction to Enthalpy=       0.124203
Thermal correction to Gibbs Free Energy= 0.082985
Sum of electronic and zero-point Energies= -287.154576
Sum of electronic and thermal Energies= -287.146816
Sum of electronic and thermal Enthalpies= -287.145872
Sum of electronic and thermal Free Energies= -287.187091

```

t-butanol



Center Number	Atomic Number	Atomic Type	Coordinates (Angstroms)		
			X	Y	Z
1	6	0	-0.006713	0.000003	0.009767
2	6	0	0.676866	-1.263408	-0.527333
3	1	0	0.200974	-2.157482	-0.116916
4	1	0	0.614388	-1.307901	-1.618186
5	1	0	1.736241	-1.279254	-0.251590
6	6	0	0.676093	1.263934	-0.527103
7	1	0	0.613540	1.308614	-1.617945
8	1	0	0.199685	2.157637	-0.116480
9	1	0	1.735469	1.280358	-0.251403
10	6	0	-1.498422	-0.000424	-0.322665
11	1	0	-1.650590	-0.000380	-1.404549
12	1	0	-1.982235	-0.887193	0.094473
13	1	0	-1.982778	0.885980	0.094619
14	8	0	0.055619	-0.000114	1.458739
15	1	0	0.983417	-0.000092	1.722070

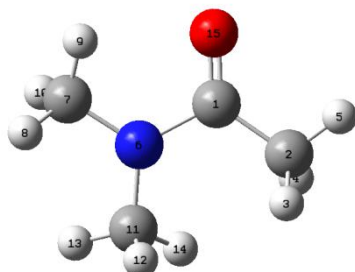
```

Zero-point correction=                0.134595 (Hartree/Particle)
Thermal correction to Energy=         0.141383
Thermal correction to Enthalpy=       0.142327
Thermal correction to Gibbs Free Energy= 0.105547
Sum of electronic and zero-point Energies= -233.622356
Sum of electronic and thermal Energies= -233.615568

```

Sum of electronic and thermal Enthalpies= -233.614624
Sum of electronic and thermal Free Energies= -233.651403

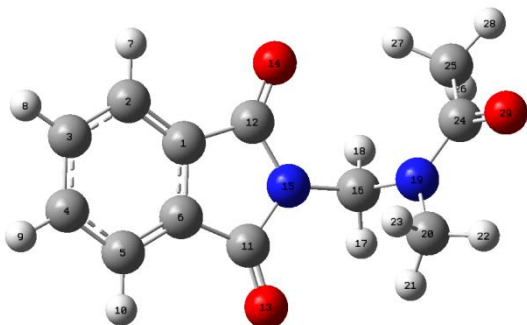
N,N-dimethylacetamide radical cation



Center Number	Atomic Number	Atomic Type	Coordinates (Angstroms)		
			X	Y	Z
1	6	0	0.785090	-0.320787	0.000689
2	6	0	1.814695	0.759079	-0.029004
3	1	0	1.633117	1.466370	-0.840293
4	1	0	1.814390	1.312423	0.914221
5	1	0	2.786263	0.288885	-0.161363
6	7	0	-0.635144	0.101689	-0.003952
7	6	0	-1.663016	-0.908388	-0.034644
8	1	0	-2.452310	-0.585208	-0.718047
9	1	0	-1.241594	-1.869921	-0.307822
10	1	0	-2.105656	-0.971272	0.971026
11	6	0	-1.022074	1.492470	0.034507
12	1	0	-0.969954	1.890162	-0.991128
13	1	0	-2.046232	1.579206	0.390182
14	1	0	-0.335841	2.067283	0.654608
15	8	0	0.984456	-1.502999	0.035875

Zero-point correction= 0.127326 (Hartree/Particle)
Thermal correction to Energy= 0.135234
Thermal correction to Enthalpy= 0.136178
Thermal correction to Gibbs Free Energy= 0.094665
Sum of electronic and zero-point Energies= -287.543283
Sum of electronic and thermal Energies= -287.535374
Sum of electronic and thermal Enthalpies= -287.534430
Sum of electronic and thermal Free Energies= -287.575943

Radical-radical coupling product

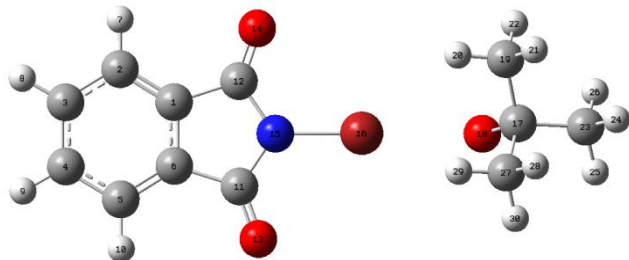


Center Number	Atomic Number	Atomic Type	Coordinates (Angstroms)		
			X	Y	Z
1	6	0	1.811709	-0.776915	-0.024080
2	6	0	2.794791	-1.688401	0.325519
3	6	0	4.073067	-1.185072	0.592893
4	6	0	4.342516	0.184492	0.507142
5	6	0	3.342836	1.097148	0.151293
6	6	0	2.080629	0.589146	-0.110283
7	1	0	2.582296	-2.748466	0.390071
8	1	0	4.868121	-1.866594	0.871022
9	1	0	5.342356	0.543604	0.720161
10	1	0	3.547833	2.158501	0.083596
11	6	0	0.826118	1.287602	-0.505263
12	6	0	0.378778	-0.992284	-0.367087
13	8	0	0.637006	2.467653	-0.703421
14	8	0	-0.244050	-2.029518	-0.437766
15	7	0	-0.152401	0.282821	-0.622767
16	6	0	-1.538562	0.534160	-1.021456
17	1	0	-1.535341	1.496328	-1.534878
18	1	0	-1.833451	-0.239537	-1.722498
19	7	0	-2.463205	0.578761	0.095121
20	6	0	-2.295841	1.679393	1.048210
21	1	0	-1.918959	2.553599	0.517357
22	1	0	-3.257091	1.911195	1.500683
23	1	0	-1.591904	1.419226	1.844781
24	6	0	-3.409992	-0.381384	0.357774
25	6	0	-3.615947	-1.493322	-0.652784
26	1	0	-3.922699	-1.097291	-1.624453
27	1	0	-2.704947	-2.078445	-0.791366
28	1	0	-4.404720	-2.139920	-0.274013
29	8	0	-4.093315	-0.321966	1.378910

Zero-point correction= 0.226319 (Hartree/Particle)
Thermal correction to Energy= 0.241767

Thermal correction to Enthalpy=	0.242711
Thermal correction to Gibbs Free Energy=	0.182213
Sum of electronic and zero-point Energies=	-799.735744
Sum of electronic and thermal Energies=	-799.720296
Sum of electronic and thermal Enthalpies=	-799.719352
Sum of electronic and thermal Free Energies=	-799.779850

EDA complex TS



Center Number	Atomic Number	Atomic Type	Coordinates (Angstroms)		
			X	Y	Z
1	6	0	-3.086344	0.707528	0.050614
2	6	0	-4.246117	1.452931	0.183539
3	6	0	-5.450255	0.752071	0.329820
4	6	0	-5.473355	-0.645761	0.340412
5	6	0	-4.293076	-1.388240	0.205237
6	6	0	-3.109290	-0.683735	0.061434
7	1	0	-4.223102	2.536112	0.174766
8	1	0	-6.379213	1.300277	0.436709
9	1	0	-6.419944	-1.161239	0.455248
10	1	0	-4.305853	-2.471610	0.212783
11	6	0	-1.698718	-1.161959	-0.102777
12	6	0	-1.660918	1.136380	-0.121144
13	8	0	-1.314492	-2.315977	-0.138322
14	8	0	-1.238862	2.276423	-0.174992
15	7	0	-0.896278	-0.026457	-0.207646
16	35	0	0.989285	-0.057569	-0.416948
17	6	0	4.492316	0.022766	0.214233
18	8	0	3.602876	-0.117627	-0.859356
19	6	0	4.317511	1.389204	0.919008
20	1	0	3.307850	1.480338	1.328912
21	1	0	5.032082	1.522519	1.739769
22	1	0	4.464992	2.200593	0.199298
23	6	0	5.926469	-0.059126	-0.355488
24	1	0	6.686269	0.034454	0.429665
25	1	0	6.071782	-1.017231	-0.863720
26	1	0	6.085121	0.740119	-1.085945

27	6	0	4.308602	-1.108455	1.254012
28	1	0	5.029804	-1.030956	2.076008
29	1	0	3.302011	-1.075463	1.679985
30	1	0	4.440061	-2.081979	0.771193

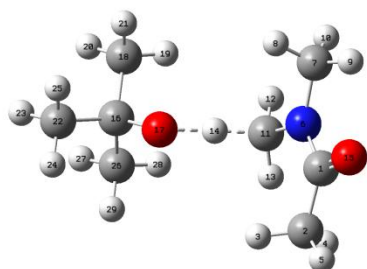
```

Zero-point correction=                0.226278 (Hartree/Particle)
Thermal correction to Energy=          0.243296
Thermal correction to Enthalpy=        0.244240
Thermal correction to Gibbs Free Energy= 0.178517
Sum of electronic and zero-point Energies= -758.997338
Sum of electronic and thermal Energies= -758.980321
Sum of electronic and thermal Enthalpies= -758.979376
Sum of electronic and thermal Free Energies= -759.045100

```

Imaginary frequency (1): -44.37

HAT TS



Center Number	Atomic Number	Atomic Type	Coordinates (Angstroms)		
			X	Y	Z
1	6	0	2.739827	-0.412638	0.182421
2	6	0	2.489249	-1.860245	-0.183157
3	1	0	1.488364	-2.181134	0.114249
4	1	0	2.587953	-2.020916	-1.259801
5	1	0	3.228576	-2.468222	0.333518
6	7	0	1.888461	0.539546	-0.349561
7	6	0	2.053479	1.938577	0.052257
8	1	0	1.348769	2.195879	0.848706
9	1	0	3.066680	2.088886	0.413038
10	1	0	1.867113	2.582201	-0.808343
11	6	0	0.719831	0.213567	-1.087751
12	1	0	0.419366	1.038290	-1.732669
13	1	0	0.804396	-0.716793	-1.642078
14	1	0	-0.216735	0.043586	-0.311237
15	8	0	3.671326	-0.088573	0.912537

16	6	0	-2.484793	-0.067999	0.127930
17	8	0	-1.168924	-0.178812	0.639804
18	6	0	-2.769979	1.365387	-0.351221
19	1	0	-2.123696	1.627594	-1.193368
20	1	0	-3.808201	1.470386	-0.678911
21	1	0	-2.587945	2.077827	0.457163
22	6	0	-3.385251	-0.407650	1.337772
23	1	0	-4.436525	-0.348918	1.041980
24	1	0	-3.177807	-1.417992	1.696576
25	1	0	-3.211585	0.297557	2.153350
26	6	0	-2.720881	-1.084141	-1.002281
27	1	0	-3.758072	-1.051369	-1.347565
28	1	0	-2.075091	-0.866839	-1.857861
29	1	0	-2.502894	-2.096906	-0.654368

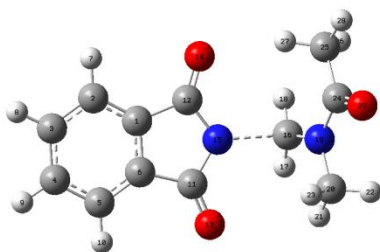
```

Zero-point correction=                0.247960 (Hartree/Particle)
Thermal correction to Energy=          0.262991
Thermal correction to Enthalpy=        0.263935
Thermal correction to Gibbs Free Energy= 0.203140
Sum of electronic and zero-point Energies= -520.753031
Sum of electronic and thermal Energies= -520.738001
Sum of electronic and thermal Enthalpies= -520.737057
Sum of electronic and thermal Free Energies= -520.797851

```

Imaginary frequency (1): -1050.53

Radical-radical coupling TS



Center Number	Atomic Number	Atomic Type	Coordinates (Angstroms)		
			X	Y	Z
1	6	0	1.993792	-0.736850	-0.043111
2	6	0	3.054067	-1.581815	0.237122

3	6	0	4.288958	-0.990026	0.533262
4	6	0	4.438611	0.399717	0.544368
5	6	0	3.358543	1.245278	0.259310
6	6	0	2.143245	0.649837	-0.032456
7	1	0	2.935085	-2.658706	0.227769
8	1	0	5.143194	-1.618277	0.757416
9	1	0	5.406579	0.828156	0.777034
10	1	0	3.471477	2.322854	0.266839
11	6	0	0.808465	1.244781	-0.378595
12	6	0	0.563430	-1.031404	-0.395608
13	8	0	0.527169	2.427352	-0.495165
14	8	0	0.042953	-2.129437	-0.526026
15	7	0	-0.063505	0.187505	-0.548223
16	6	0	-1.947894	0.454222	-1.185087
17	1	0	-1.703304	1.358876	-1.721956
18	1	0	-1.994461	-0.457093	-1.759655
19	7	0	-2.798091	0.586364	-0.143019
20	6	0	-2.891184	1.879943	0.553990
21	1	0	-2.441846	2.644025	-0.075210
22	1	0	-3.935632	2.116709	0.745285
23	1	0	-2.356818	1.834268	1.504339
24	6	0	-3.469384	-0.512766	0.444434
25	6	0	-3.355644	-1.854575	-0.229929
26	1	0	-3.761615	-1.818591	-1.244379
27	1	0	-2.313097	-2.179810	-0.291126
28	1	0	-3.929972	-2.569466	0.354996
29	8	0	-4.119927	-0.325174	1.452584

Zero-point correction=	0.223655 (Hartree/Particle)
Thermal correction to Energy=	0.238938
Thermal correction to Enthalpy=	0.239883
Thermal correction to Gibbs Free Energy=	0.179647
Sum of electronic and zero-point Energies=	-799.698534
Sum of electronic and thermal Energies=	-799.683251
Sum of electronic and thermal Enthalpies=	-799.682307
Sum of electronic and thermal Free Energies=	-799.742542

PUBLICATIONS

1. Pan, L.; Kelley, A.; Cooke, M.V.; Deckert, M.; Laulhé, S., Metal-Free Photoredox Phosphonation of C–N and C–X Bonds in Aqueous Solvent Mixtures. (DOI: 10.33774/chemrxiv-2021-xpwps)
2. Pan, L.; Elmasry, J.; Oscorima, T.; Cooke, M. V.; Laulhé, S. Photochemical Regioselective C(sp³)–H Amination of Amides Using *N*-haloimides. *Org. Lett.* **2021**, 23, 3389–3393.
3. Pan L.; Cooke MV.; Spencer A.; Laulhé S. Dimsyl Anion Enables Visible-Light-Promoted Charge Transfer in Cross-Coupling Reactions of Aryl Halides. *Adv. Synth. Catal.*, **2021** (DOI: 10.1002/adsc.202101052) (DOI:10.33774/chemrxiv-2021-sz1ww.)
4. Li, B.; Seth, K.; Niu, B.; Pan, L.; Yang, H.; Ge, H. Transient-liganden-enabled ortho-arylation of five-membered heterocycles: facile access to mechanochromic materials. *Angew. Chem., Int. Ed.* **2018**, 57, 3401–3405.
5. Pan, L.; Yang, K.; Li, G.; Ge, H. Palladium-Catalyzed Site-Selective Arylation of Aliphatic Ketones Enabled by a Transient Ligand. *Chem. Commun.* **2018**, 54, 2759–2762.
6. Pan, L.; Tang, P.; Yang, K.; Wang, M.; Wang, J.; Li, G.; Ge, H. Theoretical and experimental studies of palladium-catalyzed site-selective C (sp³)–H bond functionalization enabled by transient ligands. DOI: 10.26434/chemrxiv.5717950.v1.